

FINAL CONTRACTOR REPORT  
FOR  
NASA COOPERATIVE AGREEMENT  
NCC-2-313

*ADDCS*  
*SECRET*  
*134771*  
*2828*  
*TM*

A CORRELATION STUDY OF  
X-29A AIRCRAFT AND  
ASSOCIATED ANALYTICAL DEVELOPMENT

by

ALI AHMADI - PRINCIPAL RESEARCHER  
KAJAL GUPTA - NASA TECHNICAL ADVISOR  
PAUL FORTIN - KU PRINCIPAL INVESTIGATOR

UNIVERSITY OF KANSAS  
CENTER FOR RESEARCH

MARCH 1988

# A CORRELATION STUDY OF X-29A AIRCRAFT AND ASSOCIATED ANALYTICAL DEVELOPMENTS

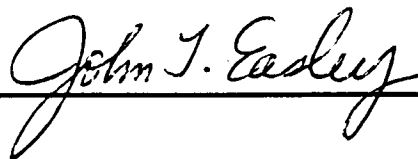
by

**Ali Reza Ahmadi**  
**B.S., U.S. International University, 1980**  
**M.S., University of California Irvine, 1982**

Submitted to the Department of Civil Engineering  
and The Faculty of the Graduate School of the  
University of Kansas  
In Partial Fulfillment of the Requirements for  
the Degree of Doctor of Engineering

## Dissertation Committee:

**Prof. J. T. Easley**  
Chair-Person



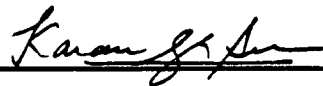
**Dr. P. E. Fortin**



**Dr. K. K. Gupta**



**Prof. K. S. Surana**



**Prof. F. M. Thomas**

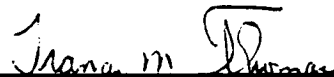


# ***TABLE OF CONTENTS***

## **ACKNOWLEDGEMENTS 1**

## **ABSTRACT 2**

## **INTRODUCTION 3**

- LI Overview 3**
- LII Objectives 5**
- LIH Scope and Tasks 5**
- LIV Contents 6**

## **CHAPTER 1**

### **X-29A AIRCRAFT CONCEPT 8**

- 1.1 Background 8**
- 1.2 Divergence Problem 9**
- 1.3 Special Features of the X-29A Aircraft 13**
  - 1.3.1 Variable-Incidence Close-Coupled Canard 14**
  - 1.3.2 Relaxed Static Stability 15**
  - 1.3.3 Thin Super-Critical Wing 16**
  - 1.3.4 Aeroelastically-Tailored Composite Wing 16**

1.3.5	Improved Pitch Control	16
1.3.6	Discrete Variable Camber	17
1.4	Advantages of the X-29A Aircraft	18
1.4.1	Less Drag and Less Weight	19
1.4.2	Improved Supersonic Performance	21
1.4.3	Better Maneuverability	21

## **CHAPTER 2**

### **THE STARS COMPUTER PROGRAM 23**

2.1	Background	23
2.2	Structural Analysis	24
2.2.1	Static Analysis	24
2.2.2	Undamped Free Vibration Analysis	25
2.2.3	Undamped Free Vibration Analysis of Spinning Structures	26
2.2.4	Damped Free Vibration Analysis	26
2.2.5	Dynamic Response Analysis	28
2.3	Aerodynamic Analysis	28
2.4	Tools Modification	31
2.4.1	Aerodynamic Analysis Program	32
2.4.1.1	History of the FASTEX Computer Program	33
2.4.1.2	FASTEX Modification	34
2.4.1.3	Incorporation of FASTEX into the STARS Package	35
2.4.1.4	Further Improvements of FASTEX	37
2.4.2	Graphics Program	40
2.4.3	PS300 Graphics System	40
2.4.3.1	Function Keys and Control Dials	44
2.4.3.1.1	Static Case	44
2.4.3.1.2	Free Vibration Case	49
2.4.3.1.3	Forced Vibration Case	50
2.4.3.1.4	Nodal Displacement	52
2.4.3.1.5	Line Element Forces	54
2.4.3.1.6	Shell Stress	56



2.4.3.1.7 Solid Stress 57

**CHAPTER 3**

**COMPARATIVE ANALYSIS OF X-29A AIRCRAFT 59**

3.1	Background	59
3.2	Free Vibration Analysis of the Canard	65
3.3	Free Vibration Analysis of the Wing	69
3.4	Analysis of the Entire Aircraft	74
3.4.1	Free Vibration Analysis ( Symmetric )	76
3.4.1.1	Wing First Bending ( W1B )	79
3.4.2	Free Vibration Analysis ( Anti-Symmetric )	84
3.4.2.1	Wing First Bending ( W1B )	87
3.4.2.2	Fuselage First Bending ( F1B )	92
3.4.3	Flutter/Divergence Analysis ( Symmetric )	97
3.4.3.1	Wing First Bending ( W1B )	101
3.4.3.2	Fuselage First Bending ( F1B )	102
3.4.3.3	Fuselage Second Bending ( F2B )	104
3.4.3.4	Canard Pitch ( CP )	105
3.4.3.5	Wing Second Bending ( W2B )	107
3.4.3.6	Wing First Torsion ( W1T )	108
3.4.3.7	Canard Bending Pitch ( CBP )	110
3.4.3.8	Wing Third Bending ( W3B )	111
3.4.4	Flutter/Divergence Analysis ( Anti-Symmetric )	113
3.4.4.1	Wing First Bending ( W1B )	117
3.4.4.2	Fuselage First Bending ( F1B )	119
3.4.4.3	Vertical Fin First Bending ( VF1B )	120
3.4.4.4	Canard Pitch ( CP )	122
3.4.4.5	Wing First Torsion ( W1T )	123
3.4.4.6	Wing Second Bending ( W2B )	125
3.4.4.7	Vertical Fin Second Bending ( VF2B )	126
3.4.4.8	Wing Third Bending ( W3B )	128
3.4.4.9	Vertical Fin First Torsion ( VF1T )	129
3.4.4.10	Inboard Flap Torsion ( IFT )	130

## **CHAPTER 4**

### **PROJECT MANAGEMENT 133**

- 4.1 Project Overview 133
- 4.2 Budget and Time-Schedule 134
- 4.3 Project's Tasks and Personell 136
- 4.4 Organization 138

## **CHAPTER 5**

### **CONCLUSIONS 140**

- C.1 General Conclusions 140
- C.2 Current and future developments 141

## **APPENDIX A**

### **FINITE DYNAMIC ELEMENT METHOD 143**

- A.1 Background 143
- A.2 Finite Dynamic Element Formulation 144
- A.3 Plane-Stress Triangular Element 146
- A.4 Numerical Example and Conclusion 153
- A.5 Listing of the MACSYMA Program 160
- A.6 Listing of the Subroutine TSHK0 168
- A.7 Listing of the Subroutine TSHK2 171
- A.8 Listing of the Subroutine TSHK4 184
- A.9 Listing of the Subroutine TSHM0 216
- A.10 Listing of the Subroutine TSHM2 218

## **APPENDIX B**

### **NATURAL MODE-SHAPES OF X-29A AIRCRAFT 223**

- B.1 Symmetric Mode-shapes 223
  - B.1.1 Fuselage First Bending ( F1B ) 224
  - B.1.2 Fuselage Second Bending ( F2B ) 226
  - B.1.3 Canard Pitch ( CP ) 229
  - B.1.4 Wing Second Bending ( W2B ) 231

B.1.5	Wing First Torsion ( W1T )	234
B.1.6	Canard Bending Pitch ( CBP )	236
B.1.7	Wing Third Bending ( W3B )	239
B.2	Anti-Symmetric Mode-shapes	241
B.2.1	Vertical Fin First Bending ( VF1B )	242
B.2.2	Canard Pitch ( CP )	244
B.2.3	Wing First Torsion ( W1T )	247
B.2.4	Wing Second Bending ( W2B )	249
B.2.5	Vertical Fin Second Bending ( VF2B )	252
B.2.6	Wing Third Bending ( W3B )	254
B.2.7	Vertical Fin First Torsion ( VF1T )	256
B.2.8	Inboard Flap Torsion ( IFT )	259

## REFERENCES 261

## ***LIST OF FIGURES***

1.2A	Structural Divergence Problem	10
1.2B	Structural Divergence Solution	12
1.3A	X-29A Aircraft	13
1.3.5A	Three-Surface Trimming	17
1.3.6A	Discrete Variable Camber	18
1.4.1A	Shock Position on FSW and a Comparable ASW	20
2.4A	Layout of the STARS Package with the Addition of Aerodynamic Analysis and Graphics Capabilities	32
2.4.1.3A	Linkage of the AERODYNAMICS Part of the STARS Program	36
2.4.1.4A	Improved Version of Aerodynamic Analysis Package	39
2.4.2A	STARS Post-Processor on MEGATEK	41
2.4.3A	Layout of the POST-PLOT Graphics Program	43
3.1A	Finite Element Model of the Canard Component	61
3.1B	Finite Element Model of the Wing Component	61
3.1C	Finite Element Model of the X-29A Aircraft	62
3.1D	Model Used for the Aerodynamic Analysis of the X-29A Aircraft	63

3.1E	Aerodynamic Verification Steps	64
3.1F	Structural Verification Steps	65
3.2A	Canard Component	66
3.2B-1	Canard's First Pitch Mode	67
3.2B-2	Canard's First Bending Mode	67
3.2B-3	Canard's Second Bending Mode	67
3.2B-4	Canard's Second Pitch Mode	68
3.2B-5	Canard's Third Bending Mode	68
3.2B-6	Canard's First Yaw Mode	68
3.3A	Wing Component	70
3.3B-1	Wing's First Bending Mode	71
3.3B-2	Wing's First Torsion Mode	71
3.3B-3	Wing's Second Bending Mode	72
3.3B-4	Wing's Third Bending Mode	72
3.3B-5	Wing's Inboard Flap Torsion Mode	73
3.3B-6	Wing's Flap First Bending Mode	73
3.4A	X-29A Aircraft	74
3.4.1A	Natural Frequency Difference with Respect to GVS Results	77
3.4.1B	Generalized Mass Difference with Respect to GVS Results	78
3.4.1.1A-1	STARS Wing First Bending Mode	80
3.4.1.1A-2	GAC Wing First Bending Mode	81
3.4.1.1A-3	GVS Wing First Bending Mode	82
3.4.1.1A-4	Wing First Bending Node Lines	83
3.4.2A	Natural Frequency Difference with Respect to GVS Results	85
3.4.2B	Generalized Mass Difference with Respect to GVS Results	86
3.4.2.1A-1	STARS Wing First Bending Mode	88
3.4.2.1A-2	GAC Wing First Bending Mode	89
3.4.2.1A-3	GVS Wing First Bending Mode	90
3.4.2.1A-4	Wing First Bending Node Lines	91
3.4.2.2A-1	STARS Fuselage First Bending Mode	93
3.4.2.2A-2	GAC Fuselage First Bending Mode	94

3.4.2.2A-3	GVS Fuselage First Bending Mode	95
3.4.2.2A-4	Fuselage First Bending Node Lines	96
3.4.3A-1.1	STARS Frequency Trend ( Symmetric )	98
3.4.3A-1.2	STARS Damping Trend ( Symmetric )	98
3.4.3A-2.1	GAC Frequency Trend ( Symmetric )	99
3.4.3A-2.2	GAC Damping Trend ( Symmetric )	99
3.4.3A-3.1	GVS Frequency Trend ( Symmetric )	100
3.4.3A-3.2	GVS Damping Trend ( Symmetric )	100
3.4.3.1A-1	Wing First Bending Frequency ( Symmetric )	101
3.4.3.1A-2	Wing First Bending Damping ( Symmetric )	102
3.4.3.2A-1	Fuselage First Bending Frequency ( Symmetric )	103
3.4.3.2A-2	Fuselage First Bending Damping ( Symmetric )	103
3.4.3.3A-1	Fuselage Second Bending Frequency ( Symmetric )	104
3.4.3.3A-2	Fuselage Second Bending Damping ( Symmetric )	105
3.4.3.4A-1	Canard Pitch Frequency ( Symmetric )	106
3.4.3.4A-2	Canard Pitch Damping ( Symmetric )	106
3.4.3.5A-1	Wing Second Bending Frequency ( Symmetric )	107
3.4.3.5A-2	Wing Second Bending Damping ( Symmetric )	108
3.4.3.6A-1	Wing First Torsion Frequency ( Symmetric )	109
3.4.3.6A-2	Wing First Torsion Damping ( Symmetric )	109
3.4.3.7A-1	Canard Bending Pitch Frequency ( Symmetric )	110
3.4.3.7A-2	Canard Bending Pitch Damping ( Symmetric )	111
3.4.3.8A-1	Wing Third Bending Frequency ( Symmetric )	112
3.4.3.8A-2	Wing Third Bending Damping ( Symmetric )	112
3.4.4A-1.1	STARS Frequency Trend ( Anti-Symmetric )	114
3.4.4A-1.2	STARS Damping Trend ( Anti-Symmetric )	115
3.4.4A-2.1	GAC Frequency Trend ( Anti-Symmetric )	115
3.4.4A-2.2	GAC Damping Trend ( Anti-Symmetric )	116
3.4.4A-3.1	GVS Frequency Trend ( Anti-Symmetric )	116
3.4.4A-3.2	GVS Damping Trend ( Anti-Symmetric )	117
3.4.4.1A-1	Wing First Bending Frequency ( Anti-Symmetric )	118
3.4.4.1A-2	Wing First Bending Damping ( Anti-Symmetric )	118
3.4.4.2A-1	Fuselage First Bending Frequency ( Anti-Symmetric )	119
3.4.4.2A-2	Fuselage First Bending Damping ( Anti-Symmetric )	120

3.4.4.3A-1	Vertical Fin First Bending Frequency ( Anti-Symmetric )	121
3.4.4.3A-2	Vertical Fin First Bending Damping ( Anti-Symmetric )	121
3.4.4.4A-1	Canard Pitch Frequency ( Anti-Symmetric )	122
3.4.4.4A-2	Canard Pitch Damping ( Anti-Symmetric )	123
3.4.4.5A-1	Wing First Torsion Frequency ( Anti-Symmetric )	124
3.4.4.5A-2	Wing First Torsion Damping ( Anti-Symmetric )	124
3.4.4.6A-1	Wing Second Bending Frequency ( Anti-Symmetric )	125
3.4.4.6A-2	Wing Second Bending Damping ( Anti-Symmetric )	126
3.4.4.7A-1	Vertical Fin Second Bending Frequency ( Anti-Symmetric )	127
3.4.4.7A-2	Vertical Fin Second Bending Damping ( Anti-Symmetric )	127
3.4.4.8A-1	Wing Third Bending Frequency ( Anti-Symmetric )	128
3.4.4.8A-2	Wing Third Bending Damping ( Anti-Symmetric )	129
3.4.4.9A-1	Vertical Fin First Torsion Frequency ( Anti-Symmetric )	130
3.4.4.9A-2	Vertical Fin First Torsion Damping ( Anti-Symmetric )	130
3.4.4.10A-1	Inboard Flap Torsion Frequency ( Anti-Symmetric )	131
3.4.4.10A-2	Inboard Flap Torsion Damping ( Anti-Symmetric )	132
4.2A	Grant Used for the Student Support at K.U.	135
4.2B	Author's Project Time-Schedule	136
4.4A	Overall Project Organization for X-29A Aircraft	138
4.4B	The Author's Project Team for Analytical Study of the X-29A Aircraft	139
A.3A	Six-Node Plane-Stress Triangular Element	147
A.4A	Square Plate, Thirty-Two-Elements Mesh	153
A.4B	Two-Elements Mesh Error Graphs	156
A.4C	Eight-Elements Mesh Error Graphs	157
A.4D	Thirty-Two-Elements Mesh Error Graphs	157
A.4E	Error for Mode Number 1	158
A.4F	Error for Mode Number 2	158
A.4G	Error for Mode Number 3	159
A.4H	Error for Mode Number 5	159

B.1.1A-1	STARS Fuselage First Bending Mode	224
B.1.1A-2	GAC Fuselage First Bending Mode	225
B.1.1A-3	GVS Fuselage First Bending Mode	225
B.1.1A-4	Fuselage First Bending Node Lines	226
B.1.2A-1	STARS Fuselage Second Bending Mode	227
B.1.2A-2	GAC Fuselage Second Bending Mode	227
B.1.2A-3	GVS Fuselage Second Bending Mode	228
B.1.2A-4	Fuselage Second Bending Node Lines	228
B.1.3A-1	STARS Canard Pitch Mode	229
B.1.3A-2	GAC Canard Pitch Mode	230
B.1.3A-3	GVS Canard Pitch Mode	230
B.1.3A-4	Canard Pitch Node Lines	231
B.1.4A-1	STARS Wing Second Bending Mode	232
B.1.4A-2	GAC Wing Second Bending Mode	232
B.1.4A-3	GVS Wing Second Bending Mode	233
B.1.4A-4	Wing Second Bending Node Lines	233
B.1.5A-1	STARS Wing First Torsion Mode	234
B.1.5A-2	GAC Wing First Torsion Mode	235
B.1.5A-3	GVS Wing First Torsion Mode	235
B.1.5A-4	Wing First Torsion Node Lines	236
B.1.6A-1	STARS Canard Bending Pitch Mode	237
B.1.6A-2	GAC Canard Bending Pitch Mode	237
B.1.6A-3	GVS Canard Bending Pitch Mode	238
B.1.6A-4	Canard Bending Pitch Node Lines	238
B.1.7A-1	STARS Wing Third Bending Mode	239
B.1.7A-2	GAC Wing Third Bending Mode	240
B.1.7A-3	GVS Wing Third Bending Mode	240
B.1.7A-4	Wing Third Bending Node Lines	241
B.2.1A-1	STARS Vertical Fin First Bending Mode	242
B.2.1A-2	GAC Vertical Fin First Bending Mode	243
B.2.1A-3	GVS Vertical Fin First Bending Mode	243
B.2.1A-4	Vertical Fin First Bending Node Lines	244
B.2.2A-1	STARS Canard Pitch Mode	245
B.2.2A-2	GAC Canard Pitch Mode	245



B.2.2A-3	GVS Canard Pitch Mode	246
B.2.2A-4	Canard Pitch Node Lines	246
B.2.3A-1	STARS Wing First Torsion Mode	247
B.2.3A-2	GAC Wing First Torsion Mode	248
B.2.3A-3	GVS Wing First Torsion Mode	248
B.2.3A-4	Wing First Torsion Node Lines	249
B.2.4A-1	STARS Wing Second Bending Mode	250
B.2.4A-2	GAC Wing Second Bending Mode	250
B.2.4A-3	GVS Wing Second Bending Mode	251
B.2.4A-4	Wing Second Bending Node Lines	251
B.2.5A-1	STARS Vertical Fin Second Bending Mode	252
B.2.5A-2	GAC Vertical Fin Second Bending Mode	253
B.2.5A-3	GVS Vertical Fin Second Bending Mode	253
B.2.5A-4	Vertical Fin Second Bending Node Lines	254
B.2.6A-1	STARS Wing Third Bending Mode	255
B.2.6A-2	GVS Wing Third Bending Mode	255
B.2.6A-3	Wing Third Bending Node Lines	256
B.2.7A-1	STARS Vertical Fin First Torsion Mode	257
B.2.7A-2	GAC Vertical Fin First Torsion Mode	257
B.2.7A-3	GVS Vertical Fin First Torsion Mode	258
B.2.7A-4	Vertical Fin First Torsion Node Lines	258
B.2.8A-1	STARS Inboard Flap Torsion Mode	259
B.2.8A-2	GVS Inboard Flap Torsion Mode	260
B.2.8A-3	Inboard Flap Torsion Node Lines	260

## ***LIST OF TABLES***

1.3A	X-29A Aircraft's Special Features	14
1.4A	X-29A Aircraft's Important Advantages	18
2.1A	Capabilities of the STARS Package	24
3.2A	Results of the Canard's Free Vibration Analysis	66
3.3A	Results of the Wing's Free Vibration Analysis	69
3.4.1A	Natural Frequencies of the X-29A Aircraft ( Symmetric )	77
3.4.1B	Generalized Mass Values of the X-29A Aircraft ( Symmetric )	78
3.4.2A	Natural Frequencies of the X-29A Aircraft ( Anti-Symmetric )	85
3.4.2B	Generalized Mass Values of the X-29A Aircraft ( Anti-Symmetric )	86
3.4.3A	Divergence Speeds ( Symmetric )	97
3.4.3B	Flutter Speeds ( Symmetric )	97
3.4.4A	Divergence Speeds ( Anti-Symmetric )	113
3.4.4B	Flutter Speeds ( Anti-Symmetric )	114

A.3A	Finite Displacement Boundary Conditions	150
A.4A	Natural Frequencies and Errors for Two-Elements Mesh	154
A.4B	Natural Frequencies and Errors for Eight-Elements Mesh	155
A.4C	Natural Frequencies and Errors for Thirty Two-Elements Mesh	155

## ***LIST OF SYMBOLS***

<b>AFDL</b>	Air Force Flight Dynamics Laboratory
<b>ASW</b>	Aft Swept Wing
<b>CBP</b>	Canard Bending Pitch
<b>CP</b>	Canard Pitch
<b>CRINC</b>	Center of Research Inc.
<b>DARPA</b>	Defence Advanced Research Project Agency
<b>DEM</b>	Dynamic Element Method
<b>F1B</b>	Fuselage First Bending
<b>F2B</b>	Fuselage Second Bending
<b>FASTEX</b>	FASTER EXecution
<b>FASTOP</b>	Flutter And STrength OPTimization
<b>FBW</b>	Fly By Wire
<b>FEM</b>	Finite Element Method
<b>FSW</b>	Forward Swept Wing
<b>GAC</b>	Grumman Aircraft Corporation
<b>GENMASS</b>	GENeralized MASS
<b>GRIDCHG</b>	GRID CHanGe

<b>GVS</b>	Ground Vibration Survey
<b>HMC</b>	Harvey Mudd College
<b>IFT</b>	Inboard Flap Torsion
<b>KU</b>	Kansas University
<b>NASA</b>	National Aeronautics and Space Administration
<b>STARS</b>	STructures, Aerodynamics, and Related Systems
<b>VF1B</b>	Vertical Fin First Bending
<b>VF2B</b>	Vertical Fin Second Bending
<b>VF1T</b>	Vertical Fin First Torsion
<b>W1B</b>	Wing First Bending
<b>W2B</b>	Wing Second Bending
<b>W3B</b>	Wing Third Bending

## ***ACKNOWLEDGEMENTS***

I would like to acknowledge and thank the following for their support and guidance. Dr. K. K. Gupta for his valuable input on every aspect of this project. Mr. Robin Mitra for his help on the structure and the grammar of the thesis. Mr. E. E. Hahn, Mr. R. A. Truax, Mr. G. Fuchs, and Mr. S. Ibrahim for their assistance in the analyses and the development of the supporting tools. Also, I would like to thank the members of the doctoral committee for reviewing the dissertation.

Also, I would like to extend my personal thanks to my brother Mehrdad and to my friends Lori and Pisci for their valuable support and understanding throughout this project.

## ***ABSTRACT***

This thesis is primarily concerned with verifying contractor results of the structural and aerodynamic analysis of the X-29A aircraft. A brief history and potential advantages of the X-29A aircraft are discussed. The NASA developed computer package, STARS (S**TR**uctures, A**E**rodynamics, and R**E**lated S**Y**stems), which is used in verifying contractor results is discussed. Enhancements of the STARS package are described, particularly the incorporation of the FASTEX computer program into STARS, and the development of a complete computer graphics system. A comparative study of free vibration and aerodynamic analysis of the X-29A aircraft is given. This study has shown that the natural frequencies and modeshapes determined analytically by STARS and the contractor compare relatively well with experimentally determined data. Also included in the study is the formulation and development of the higher-order plane-stress finite dynamic triangular element.

## ***INTRODUCTION***

### **II OVERVIEW**

The X-29A is the first forward swept wing (FSW) research aircraft developed in the United States. It was designed and fabricated by the Grumman Aircraft Corporation (GAC). The X-29A project was initiated by the Defence Advanced Research Project Agency (DARPA) to explore the high maneuverability and other potentials of the Forward Swept Wing (FSW) design. NASA-Dryden is currently performing flight tests on the aircraft. Determination of the aerodynamic instabilities of the X-29A aircraft is essential for its flight safety. Such instabilities are determined analytically by the contractor (GAC) using their in-house computer programs. However, such analyses must be verified by NASA as a precautionary measure. This verification was carried-out at NASA-Dryden in two ways, analytically and experimentally.



In the experimental approach the natural frequencies and natural modes-shapes of the aircraft are measured by Ground Vibration Survey (GVS). These characteristics are also determined analytically using the NASA developed computer package, STARS. In both cases the frequencies and modes-shapes are compared to those obtained by the contractor. The experimental and analytical results are then used as input to aerodynamic analysis packages based on Doublet-Lattice theory to determine the aerodynamic instabilities (flutter and divergence speeds) of the X-29A aircraft. The flutter and divergence speeds obtained by using GVS results are then compared to those calculated by the STARS program and the results obtained by the contractor.

The project presented here involves the analytical study of the X-29A aircraft using STARS package. The results obtained by the STARS program are compared to those of the GVS and the GAC. This was achieved by developing a complete finite element and aerodynamic models of the X-29A aircraft. These mathematical models were then solved by the STARS package to determine the analytical results. However, the STARS package had to be further developed in the areas of aerodynamics and computer graphics in order to accommodate these analyses. Furthermore, an illustrative study of the finite dynamic element method is also presented in this project as a more economical approach to obtain the natural frequencies and the natural modes-shapes of complex structures such as X-29A aircraft. However, this technique is still at research level, and it could not be applied directly to the study of the X-29A aircraft.

## **I.II OBJECTIVES**

The overall objectives of this project are:

- To determine the natural frequencies, natural modeshapes, flutter speeds, and divergence speeds of the X-29A aircraft and compare these results to those obtained by the GVS and the GAC.
- To present the finite dynamic element technique as an alternative to the finite element technique by developing and studying a higher-order plane-stress triangular element.

## **I.III SCOPE AND TASKS**

The scope of this project is as follows:

- Study of the X-29A aircraft,
- Study of the STARS computer package,
- Comparison of the contractor results to those obtained by the STARS package.
- Study of the finite dynamic element technique.

The tasks performed by the author with his team to complete this project are the following:

- Development of a complete computer graphics system for the STARS package. This feature was used to generate and modify the mathematical models required for the analysis.

This package is also capable of displaying the natural mode-shapes for better study of the results (team effort),

- Conversion of the FASTEX program from CDC computer to VAX computer. The conversion was made to make the program more versatile and transferable to other computers. (individual effort),
- Incorporation of the FASTEX program into the STARS package. The program was used to perform the aerodynamic analysis of the X-29A aircraft. (individual effort),
- Development of the finite element and aerodynamic models of the X-29A aircraft. The models were used to perform the free vibration and aerodynamic analyses of the X-29A aircraft. (team effort),
- Free vibration and aerodynamic analyses of the X-29A aircraft using the STARS package. (team effort),
- Interpretation of the results of free vibration and aerodynamic analyses of the X-29A aircraft. (team effort),
- Study and development of higher-order plane-stress finite dynamic triangular element (individual effort).

## **I.IV CONTENTS**

The project report presented here starts with the forward swept wing design concept in chapter 1. The special features and potential advantages of the aircraft are discussed here. Chapter 2 deals with the STARS

computer package. In this chapter the basic capabilities of the program are presented, the development of the aerodynamics and computer graphics packages are also discussed. Comparative analysis of the X-29A aircraft is presented in chapter 3. This covers a discussion of the analyses performed, the results obtained and a comparison of these results with those obtained by the contractor and the Ground Vibration Survey. In this chapter two typical modes are discussed in detail. The remaining modes are presented in Appendix-B. In chapter 4 the author's project team, project's time-schedule, and the project's cost are presented. Chapter 5 presents an overall conclusion of the X-29A analyses along with the current and future studies associated with the aircraft. Appendix-A presents the basic formulation and history of the finite dynamic element method. The advantage of this technique over the finite element method is illustrated by the development of a higher-order plane-stress triangular element. The computer programs which were developed to study the finite dynamic element discussed in chapter are also presented in this appendix.

## ***CHAPTER 1***

# **X-29A AIRCRAFT CONCEPT**

### **1.1 BACKGROUND**

The X-29A advanced technology demonstrator program was initiated by the Defence Advanced Research Projects Agency (DARPA). Grumman Aircraft Corporation (GAC) was awarded the contract to design and fabricate the X-29A aircraft, incorporating the forward swept wing (FSW) concept and other associated advanced technologies. NASA-Dryden is currently performing flight tests on the aircraft. The contract is being administered by the U.S. Air Force.

The unique feature of the X-29A aircraft is the forward swept wing. The first FSW aircraft, JU-287, was built by the Germans towards

the end of the second world war. It was also the first jet-powered bomber. The primary purpose was to design an aircraft which could carry one large bomb. It was necessary to store the bomb near the center of gravity of the aircraft so that, when released, the aircraft would not suffer from a significant trim change. The forward swept wing including the carry-through structure could be attached to the rear part of the fuselage. This would allow the bomb to be placed near the center of gravity of the aircraft. Other advantages of the FSW were the high angle of attack and delayed tip stall.

## 1.2 DIVERGENCE PROBLEM

The primary reason that more forward swept wing aircraft have not been developed subsequent to the JU-287 is a problem known as structural divergence. As a forward swept wing of conventional construction bends under load, it tends to twist with the leading edge up, as shown in Figure - 1.2A. Due to leading edge up twist, more instantaneous aerodynamic load will be added to the wing resulting in more twist. As the aircraft accelerates, it will eventually reach the critical air speed at which these quasi-static aeroelastic forces will exceed the structural restoring moment capacity, and the wing will literally be ripped off the aircraft. This critical speed is known as the structural divergence speed. Similar aeroelastic forces on aft swept wings tend to be restorative rather than destabilizing. Therefore, an aft swept wing aircraft generally does not have divergence

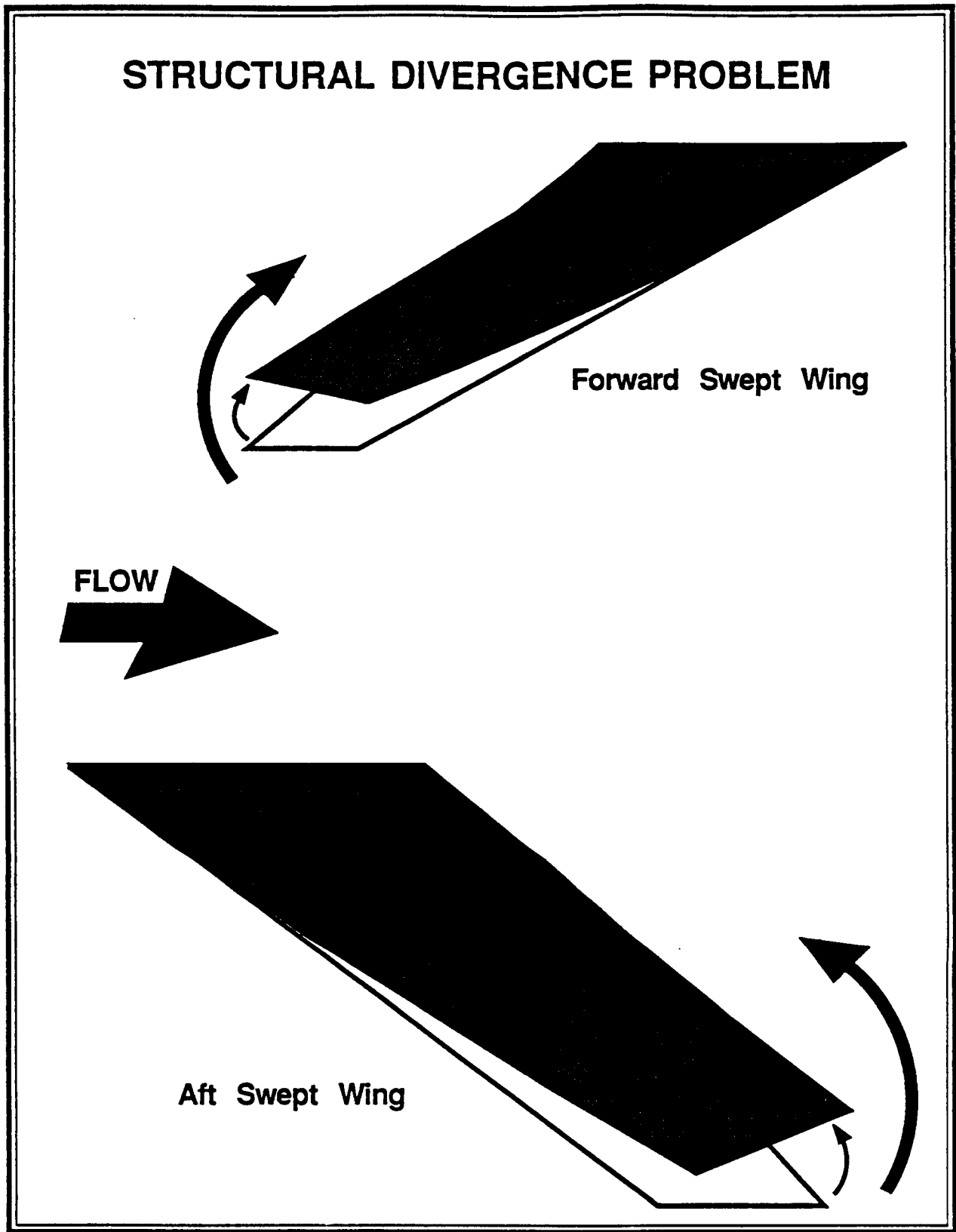


Figure 1.2A Structural Divergence Problem

problem. For forward swept wing aircraft, one possible solution for high divergence speed is to increase the wing stiffness, since the change in the divergence speed is directly proportional to the change in the wing stiffness. However, this results in such heavy wing structures that most performance benefits over aft swept wing aircraft are quickly lost. A more practical solution is to use composite materials. Composites are naturally stiffer than aluminum which tend to increase the divergence speed of the wing, but only by small amounts. A much more powerful effect can be achieved by the use of aeroelastically-tailored composite materials (Reference - 1). This technique orients the laminate ply direction of the composite wing skins in such a way as to produce a favorable bend-twist coupling of the wing. Properly done, the wing should tend to twist with leading edge down or at least stay chordwise level when the wing is bent upward, as shown in Figure - 1.2B. This significantly increases the divergence speed of the wing without increasing the weight.



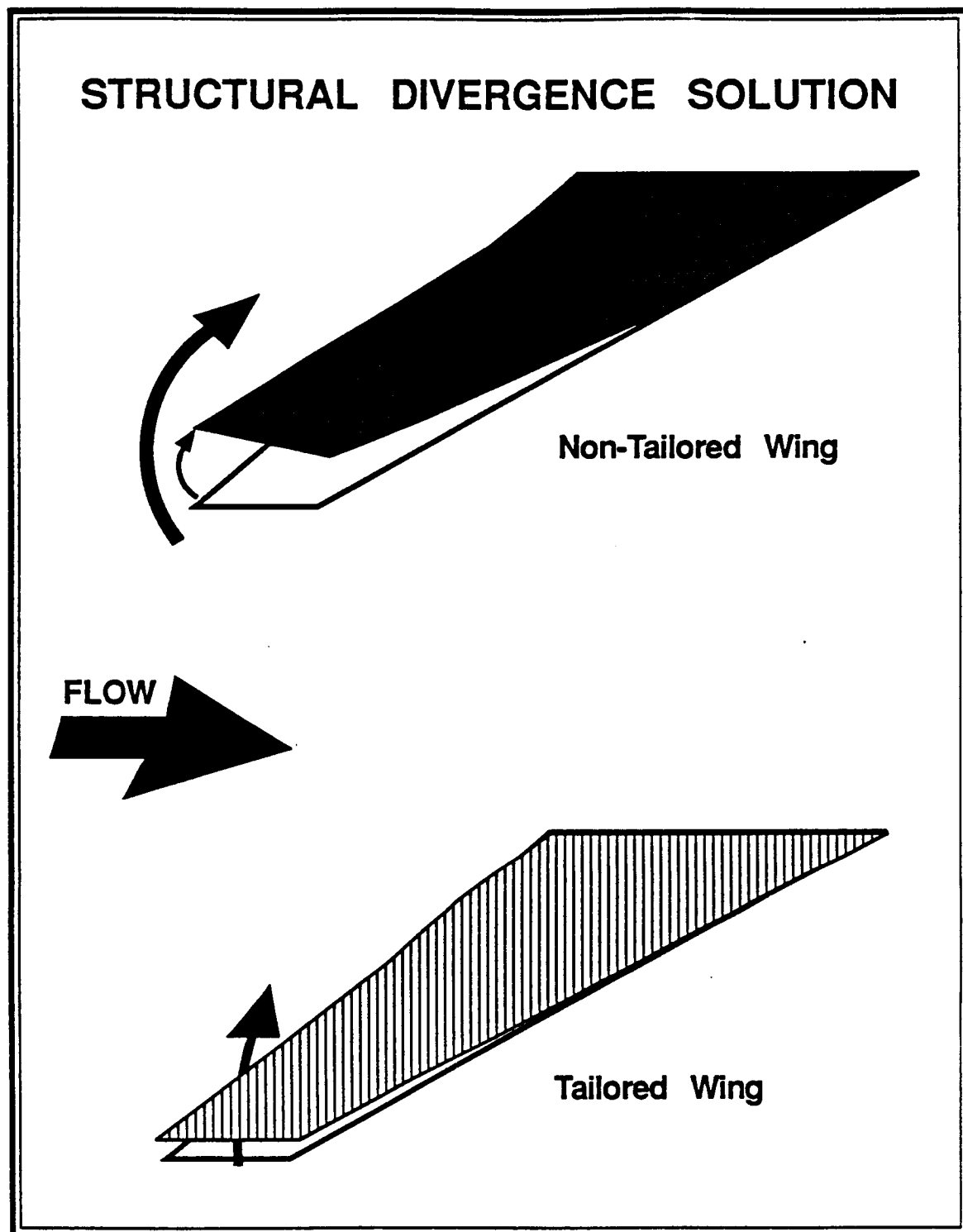


Figure 1.2B Structural Divergence Solution

### 1.3 SPECIAL FEATURES OF THE X-29A AIRCRAFT

The X-29A aircraft (Figure - 1.3A) employs an FSW with a leading edge sweep of 29.27 degrees. Other important features include a canard arrangement with F-5A forward fuselage module, two side mounted engine inlets, and an aft fuselage element of new design.

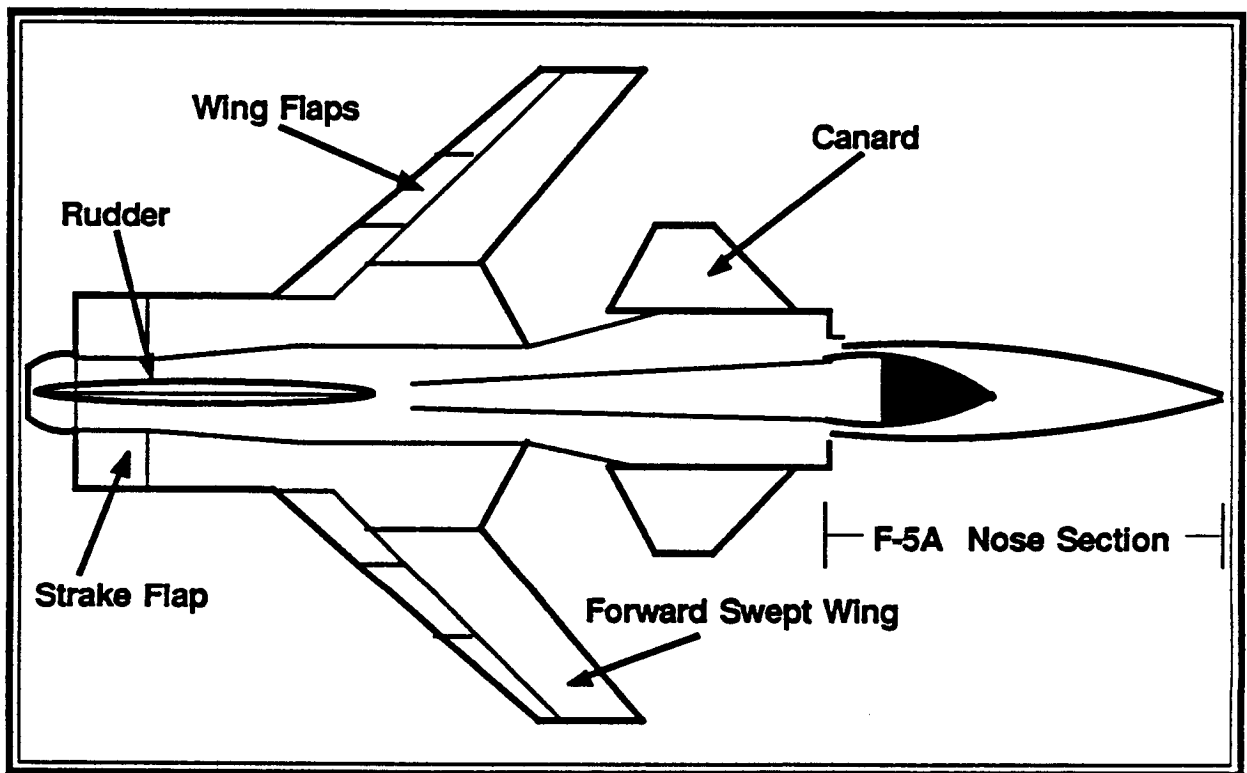


Figure 1.3A X-29A Aircraft

The X-29A aircraft has the following special features (Reference - 2).

- |   |   |   |
|---|---|---|
| 1 | — | VARIABLE-INCIDENCE CLOSE-COUPLED CANARD |
| 2 | — | RELAXED STATIC STABILITY                |
| 3 | — | THIN SUPER-CRITICAL WING                |
| 4 | — | AEROELASTICALLY-TAILORED COMPOSITE WING |
| 5 | — | IMPROVED PITCH CONTROL                  |
| 6 | — | DISCRETE VARIABLE CAMBER                |

**Table 1.3A** X-29A Aircraft's Special Features

### **1.3.1 Variable-Incidence Close-Coupled Canard**

The X-29A aircraft employs a variable-incidence close-coupled canard which was selected for its effectiveness in reducing the supersonic drag (Reference - 3). The canard deflects as much as  $30^\circ$  with leading edge up, and  $60^\circ$  with leading edge down. It is also the primary pitch control for the aircraft. It is designated a close-coupled canard because the aerodynamics of the canard and the aerodynamics of the wing are closely related. Close coupling of the canard and the wing allows beneficial interactions between their lifting surfaces. The wing up-wash of the canard produces a favorable increase of lift with high angle of attack, while the canard down-wash postpones the flow separation at the wing root.

One problem with a close-coupled design is that in subsonic flight

the aircraft tends to exhibit poor static pitch stability. In the extreme case, the aircraft's aerodynamic center of pressure will move in front of its center of gravity, and so the aircraft will be statically unstable. This problem is discussed in the next section.

### **1.3.2 Relaxed Static Stability**

An aircraft is highly stable during normal flight. Any change in flight position is resisted by the aircraft. However, such stability impairs maneuverability, and thus decreases the operational efficiency of a fighter aircraft. What is highly desirable or essential for such an aircraft (like the X-29A) is neutral stability, better known as relaxed static stability.

As mentioned earlier, the X-29A aircraft is statically unstable in pitch during subsonic flight because of the presence of the canard. This problem is corrected by the use of a triple channel digital fly-by-wire (FBW) feedback flight control system (Reference - 2). This system helps to synchronize the aircraft's movements with the pilot's commands by actuating the signals to the controls. The canards, trailing flaps on the wing, and strake flaps at the rear of the fuselage are moved forty times a second by the flight control system (FBW). This is done in order to maintain pitch stability, and minimize drag, and thereby optimize the performance of the aircraft.

### 1.3.3 Thin Super-Critical Wing

In general, the operating expenses of an aircraft can be substantially reduced by delaying the drag rise, associated with the development of local supersonic flow on the upper surface of the wing during transonic flight (Reference - 4). The objective is to delay the drag rise well beyond the critical Mach number by specially shaping the airfoil. The X-29A aircraft uses thin super-critical wing for this purpose (Reference - 4).

### 1.3.4 Aeroelastically-Tailored Composite Wing

The X-29A aircraft's wing is made of graphite-epoxy composite material. The composite material has stiffness coefficient higher than that of conventional aluminum; but more importantly, the direction of stiffness can be controlled by the orientation of the fibers. The composite wing not only resolves the problem of divergence, but also tailors aeroelastically the twist distribution at maneuver conditions (Reference - 3).

### 1.3.5 Improved Pitch Control

The X-29A aircraft utilizes the benefit of three-surface trimming by using canards, wing flaps, and strake flaps, shown in Figure - 1.3.5A, to produce optimum deflection combinations for minimum drag (Reference - 5). At high angles of attack, the strake flaps help to conserve the canard's power. In addition, the strake flaps assist the canard during takeoff.

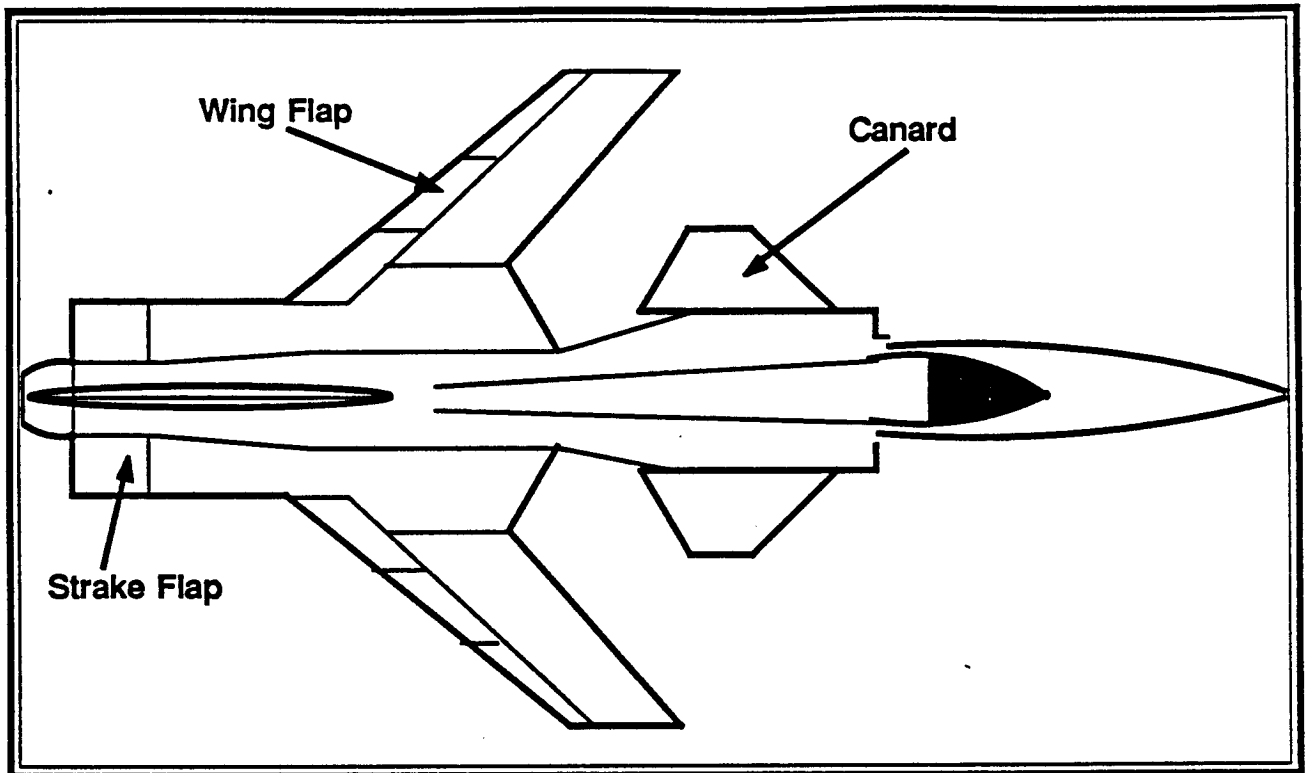


Figure 1.3.5A Three-Surface Trimming

### 1.3.6 Discrete Variable Camber

The trailing-edge control surfaces of the wing, which form the discrete variable camber system, as shown in Figure - 1.3.6A, consist of full-span, double-hinged flaperons. The double-hinged trailing-edge flaperons provide high lift during takeoff and landing, lateral control, and variable camber to increase aerodynamic efficiency. This system has a slight upper surface discontinuity in all positions except the transonic maneuver position; so it is an approximation of a smooth variable camber device. But it is much lighter and simpler to implement than other systems considered in Reference - 2.

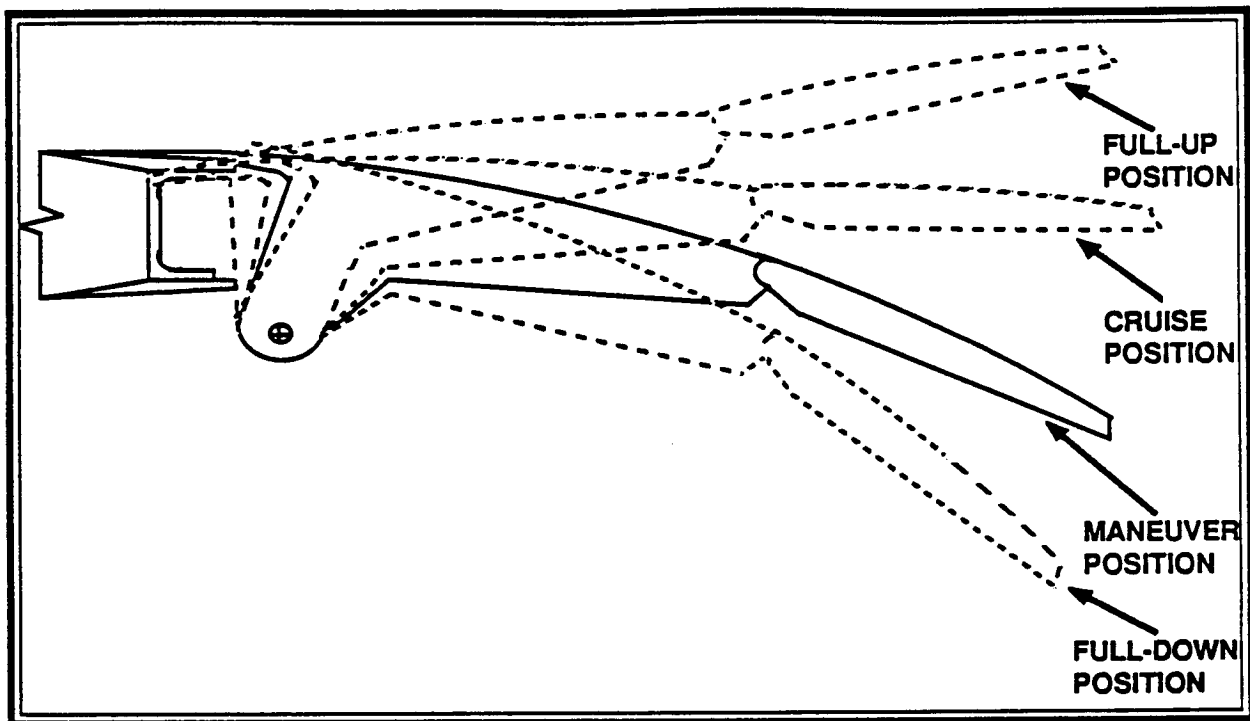


Figure 1.3.6A Discrete Variable Camber

## 1.4 ADVANTAGES OF THE X-29A AIRCRAFT

The most important advantages (Reference - 2) of the X-29A aircraft are as follows:

- |   |   |                                 |
|---|---|---------------------------------|
| 1 | — | LESS DRAG AND LESS WEIGHT       |
| 2 | — | IMPROVED SUPERSONIC PERFORMANCE |
| 3 | — | BETTER MANEUVERABILITY          |

Table 1.4A X-29A Aircraft's Important Advantages

### 1.4.1 Less Drag and Less Weight

In general, wing sweep tends to impair lift efficiency. However, for high subsonic, and supersonic flights, wing sweep is necessary to delay and reduce the otherwise prohibitive drag rise associated with shock formation. A forward swept wing requires less leading edge wing sweep than a comparable aft swept wing to achieve the same shock angle, and thus has better transonic and supersonic performance for the same design Mach number. For example (Reference - 3), given a design shock sweep angle of  $39^\circ$ , a forward swept wing needs to be swept (forward) only  $30^\circ$ , whereas a comparable aft swept wing (ASW) must be swept (aft)  $45^\circ$ , as shown in Figure - 1.4.1A. Hence the pressure on the lower surface of a forward swept wing is higher than that of a comparable aft swept wing. The higher pressure on the lower surface results in lower negative pressure on the upper surface. Therefore, the flow across the upper surface of an FSW is slightly slower than that of an ASW. As a result, there is less pressure drop as the aerodynamic flow exits through the shock wave which occurs in the transonic flight. Consequently, an FSW experiences less induced drag than a comparable ASW. Also, the shock-free area ahead of the shock wave is much greater for a forward swept wing than that for an aft swept wing. In effect, an FSW will have about ten to twenty percent less induced drag than a comparable ASW. This simply means better performance for the forward swept wing aircraft. In addition, drag benefit results in an aircraft which can employ a smaller engine. Hence, a forward swept wing aircraft (like X-29A)



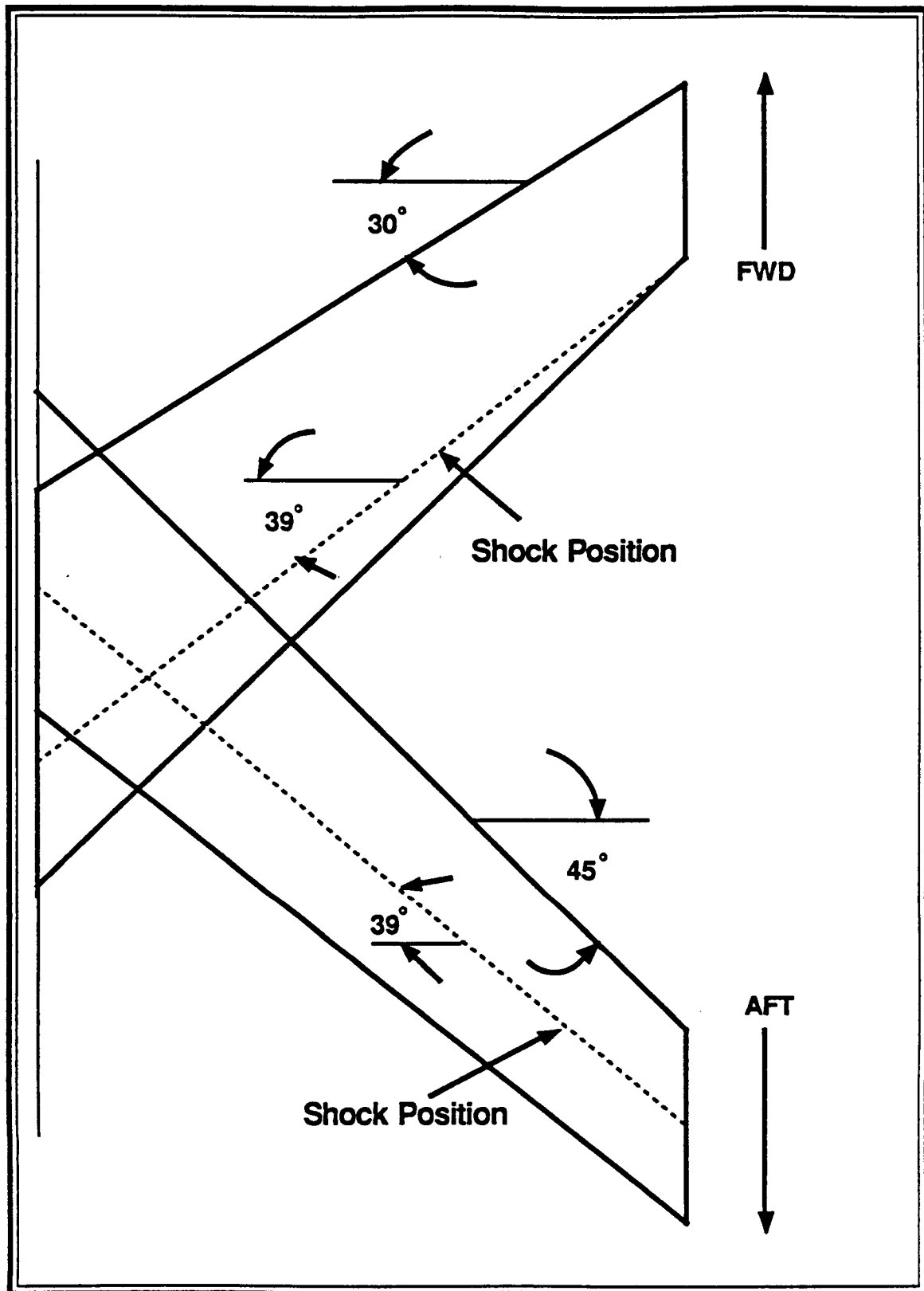


Figure 1.4.1A Shock Position on FSW and a Comparable ASW

will require less fuel than a comparable aft swept wing aircraft for a given flight range. Therefore, the overall weight is 5 to 25 percent lower for an FSW aircraft than for an ASW aircraft.

#### **1.4.2 Improved Supersonic Performance**

During the transition from subsonic to supersonic flight, the aerodynamic center of pressure of the aircraft shifts approximately from the quarter-chord to the half-chord of the wing. The resulting pitching moment on the wing must be counteracted by additional trim forces on other flight control surfaces. For an aft swept wing aircraft, this is done by increasing the downward load on the horizontal tail, located at the end of the aircraft. However, this requires additional wing lift in order to maintain the altitude, thereby increasing the induced trim forces on the wing. For the X-29A aircraft, the canard, being placed ahead of the wing, produces an upward load; this counteracts the pitching moment on the wing caused by the transition from subsonic to supersonic flight (Reference - 3). In effect, the canard shares the lift with the wing, and thus reduces the trim forces on the wing. Consequently, the forward swept wing aircraft gives better supersonic performance compared to an aft swept wing aircraft.

#### **1.4.3 Better Maneuverability**

Wind-tunnel tests have indicated improved high-angle-of-attack handling characteristics for a forward swept wing aircraft as compared to an aft swept wing aircraft. Comparison of the flow separation for FSW

and ASW shows that the flow separation for an FSW generally starts inboard, whereas in an ASW the flow separation starts at the wing tip; and this may cause roll control degradation. Also, Reference - 5 shows that even at very high angles of attack, the X-29A aircraft has a very impressive level of roll-control. All of these indicate that an FSW aircraft has better maneuverability than an ASW aircraft.

## ***CHAPTER 2***

# **THE STARS COMPUTER PROGRAM**

### **2.1 BACKGROUND**

In the development of advanced aircraft, it is essential to perform sufficient engineering analyses to ensure the safety of the aircraft. Therefore, it is necessary to verify that the major components of the X-29A aircraft, like the canards and the wings, have adequate strength and stiffness to withstand both static and dynamic loadings.

The STARS (STructures, Aerodynamics, and Related Systems) computer program (Reference - 6) is the integrated analysis tool designed to perform such calculations.

STARS package consists of three parts (Table - 2.1A).

1	—	STRUCTURAL ANALYSIS
2	—	AERODYNAMIC ANALYSIS
3	—	AEROSERVO-ELASTIC CONTROL ANALYSIS

**Table 2.1A** Capabilities of the STARS Package

In the analysis of the X-29A aircraft, only the first two parts of the program were used. Brief descriptions of these parts follow.

## **2.2 STRUCTURAL ANALYSIS**

In this part (Reference - 6, 7) the finite element method is used to perform a variety of structural analysis tasks. STARS has a library of basic one, two, and three dimensional elements. The "Structural Analysis" part of STARS is capable of solving the following types of problems.

### **2.2.1 Static Analysis**

In this case displacements and internal stresses induced by external loads are determined by solving the set of simultaneous equations

$$K_E U = P \quad (2.1)$$

where:

- $[K_E]$  — system elastic stiffness matrix,
- $\{U\}$  — nodal displacement vector,
- $\{P\}$  — external nodal load vector.

### 2.2.2 Undamped Free Vibration Analysis

In this case the governing differential equation of motion is

$$M \ddot{U} + K_E U = 0 \quad (2.2)$$

Where:

- $[M]$  — mass matrix,
- $\{\ddot{U}\}$  — nodal acceleration vector.

Assumption of harmonic motion results in an eigenvalue problem of the form

$$[K_E - \lambda M] \{\Phi\} = 0 \quad (2.3)$$

where:

- $\lambda = \omega^2$  — eigenvalue,
- $\{\Phi\}$  — eigenvector ( mode-shape ),
- $\omega$  — natural frequency.

The natural frequencies and natural mode-shapes are determined by using the combined Sturm Sequence and Inverse Iteration technique ( SS/II ) or the Lanczos procedure.

### 2.2.3 Undamped Free Vibration analysis of Spinning Structures

The differential equation of motion is

$$\mathbf{M} \ddot{\mathbf{U}} + \mathbf{C} \dot{\mathbf{U}} + \mathbf{K} \mathbf{U} = 0 \quad (2.4)$$

where:

- $\{\dot{\mathbf{U}}\}$  — nodal velocity vector,
- $[\mathbf{C}]$  — Coriolis effect matrix,
- $[\mathbf{K}']$  — equivalent stiffness matrix,  
 $= \mathbf{K}_E + \mathbf{K}_G + \mathbf{K}'$
- $[\mathbf{K}_G]$  — geometrical stiffness matrix,
- $[\mathbf{K}]$  — centrifugal force matrix,

The resulting quadratic eigenvalue problem

$$[\mathbf{K} + \omega \mathbf{C} + \omega^2 \mathbf{M}] [\Phi] = 0 \quad (2.5)$$

can be solved by using the Lanczos or the SS/II technique.

### 2.2.4 Damped Free Vibration Analysis

STARS is capable of handling three types of damping, structural, viscous, and proportional. The damping can be applied to the spinning or non-spinning structures. In the case of structural damping, the elastic stiffness matrix is modified as

$$[\mathbf{K}] = [\mathbf{K}_E] * (1 + i'g) \quad (2.6)$$

where:

$i$  — imaginary number,  $\sqrt{-1}$ ,

$g$  — structural damping parameter.

In the case of viscous damping, the damping matrix is defined by the user. The proportional damping matrix is determined by

$$C_p = \alpha K_E + \beta M \quad (2.7)$$

where:

$\alpha$ ,  $\beta$  — proportionality factors.

For non-spinning structures the differential equation of motion is

$$M \ddot{U} + C \dot{U} + K_E U = 0 \quad (2.8)$$

where:

$[C]$  — damping matrix.

For the spinning case the damping matrix is added to the Coriolis effect matrix.

STARS is also capable of handling any combination of viscous, structural and proportional damping. The resulting quadratic eigenvalue problem is solved by using the SS/II technique.



### 2.2.5 Dynamic Response Analysis

In the case of forced vibration the general differential equation of motion becomes

$$\mathbf{M} \ddot{\mathbf{U}} + \mathbf{C} \dot{\mathbf{U}} + \mathbf{K} \mathbf{U} = \mathbf{F}(t) \quad (2.9)$$

where:

$\mathbf{F}(t)$  — dynamic forcing function.

First, the natural frequencies and the associated natural mode-shapes of the structure are determined. Then modal superposition technique is used to determine the nodal displacements of the structure. From the displacements the induced stresses are computed.

## 2.3 AERODYNAMIC ANALYSIS

It is essential for the safety of an aircraft to predict its flutter and divergence speeds prior to its flight tests. The "Aero-Dynamic Analysis" part of the STARS computer program is designed to perform such calculations. The flutter solutions are obtained by the use of either the conventional K-method or the improved version of P-K method (Reference - 8).

The basic differential equation for a lifting surface in oscillatory motion (Reference - 9) is

$$M \ddot{q} + K q - Q q = 0 \quad (2.10)$$

where:

- [ M ] — generalized mass matrix,
- [ K ] — generalized stiffness matrix,
- [ Q ] — generalized aerodynamic force matrix,
- {  $\ddot{q}$  } — generalized coordinate acceleration vector,
- { q } — generalized coordinate displacement vector.

The generalized aerodynamic matrix is determined by using the conventional Doublet Lattice (Reference - 9) method.

The [ Q ] matrix can be expressed as

$$Q = 1/2 \rho v^2 A \quad (2.11)$$

where:

- [ A ] — aerodynamic matrix,
- $\rho$  — air density at sea level,
- $v$  — free stream velocity.

The elements of the aerodynamic matrix (Reference - 9) is defined by

$$A_{ij} = \iint_S W_i(x, y) C_{pj}(x, y) dS \quad (2.12)$$

where:

- $W_i$  — modal distribution of the  $i^{\text{th}}$  mode,  
 $C_{pj}$  — pressure coefficient distribution of the  $j^{\text{th}}$  mode,  
 $S$  — surface area of the lifting surface.

Therefore, equation 2.10 becomes

$$M \ddot{q} + K q - \frac{1}{2} \rho v^2 A q = 0 \quad (2.13)$$

Assumption of harmonic motion and hysteretic damping results in the eigenvalue problem

$$[ \omega^2 M + K^* - \frac{1}{2} \rho v^2 A ] [ \Phi ] = 0 \quad (2.14)$$

where:

$$[ K^* ] = [ I + i G ] [ K ] \quad (2.15)$$

where:

- $[ I ]$  — identity matrix,  
 $[ G ]$  — diagonal damping matrix.

This eigenproblem is solved by using the QR algorithm (Reference - 10). The eigenvalues are then interpreted to determine the frequency and the damping of the system. A positive value of the damping means that structural damping must be added to the system in order to achieve neutral stability; that is the system is unstable. A negative value of damping indicates the amount of damping to be removed from the system for neutral stability; this means

that the system is highly stable.

STARS also performs a divergence analysis using the aerodynamic forces derived from a non-oscillatory condition. In this case equation 2.13 becomes

$$[K] q - \frac{1}{2} \rho v^2 [A] q = 0 \quad (2.16)$$

Both  $[A]$  and  $[K]$  matrices are real and the eigenvalue to be determined by QR algorithm is  $v^2$ . The surface will not diverge if all the computed eigenvalues are negative; otherwise, the divergence speed will be the square root of the lowest positive eigenvalue.

## 2.4 TOOLS MODIFICATION

The STARS computer program had to be developed further so that it can be used for the analysis of X-29A aircraft. The complete layout of the STARS package is shown in Figure - 2.4A. As shown in this figure, the STARS package was capable of determining the response of a structure subjected to static or dynamic loading.

The developments made to the STARS package are

- 1 — addition of an aerodynamic analysis program,
- 2 — development of post-processing graphics package.

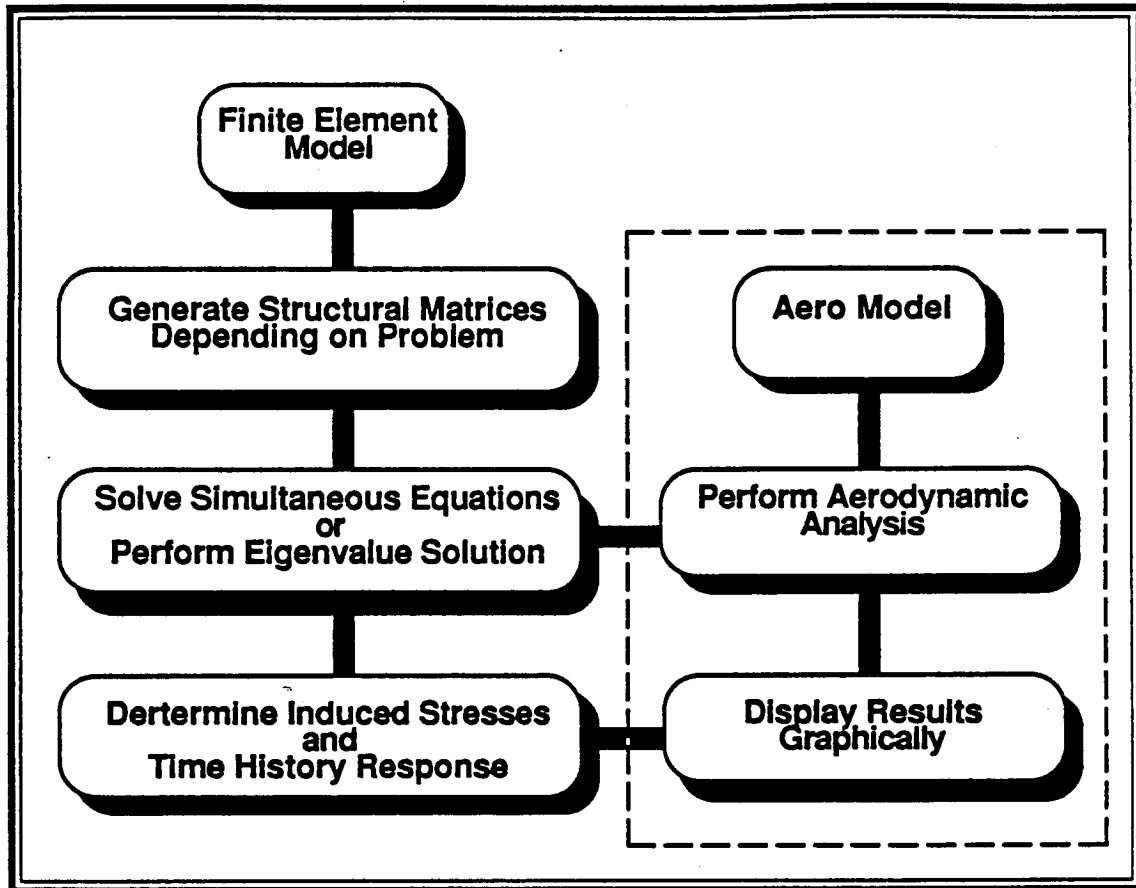


**Figure 2.4A** Layout of the STARS Package With the Addition of Aerodynamic Analysis and Graphics Capabilities

### 2.4.1 Aerodynamic Analysis Program

The aerodynamic analysis program was incorporated into the STARS package in 1983. The code was originally developed by Grumman Aircraft Corporation (GAC). The program was converted from CYBER-175 computer to VAX 11/780. During this conversion certain machine-dependent features of the original code were removed. The converted program is now in standard Fortran-77 language and it is operational on several VAX, CYBER, and IBM computers. A brief

history of the program and its incorporation into the STARS package is given in the following sections.

#### **2.4.1.1 History of The FASTEX Computer Program**

The primary objective in the design of an aircraft is to make the lifting surfaces aeroelastically stable, and yet light enough to achieve overall performance requirements. The FASTOP (Flutter And STrength OPTimization Program) computer program (Reference - 11) was developed for that purpose. With this program first, the strength and flutter analyses are performed on the initial design of a structure. The structure is then re-sized and re-analyzed iteratively until the minimum weight is achieved without exceeding the specified stresses, deflections, flutter speeds, and other design limitations.

The FASTOP program was further developed by the University of Dayton (References - 12, 13, 14) and the Grumman Aircraft Corporation (Reference - 15). A number of state-of-the-art features were included in the aerodynamic analysis part of the program. Consequently, the FASTOP program was mainly used to calculate the flutter and divergence speeds of advanced aircraft like the X-29A.

In 1980, AFDL (Air Force Flight Dynamics Laboratory) awarded a contract to the University of Dayton to enhance the aerodynamic capabilities of the FASTOP package. The primary objective was to update the program so that it would perform only aerodynamic analysis without the optimization capabilities. The FASTOP program

was then reorganized on CYBER-175 computer system at Wright Patterson Air Force Base for faster execution time. Additional features such as a more general modal interpolation procedure were also included. The resulting computer program, FASTEX (FASTER EXecution) (Reference - 16), has since been extensively used by both the government and the industry for the analysis of advanced flight vehicles such as the X-29A aircraft.

The FASTEX program was written in Fortran-4 programming language. In order to increase the time efficiency of the program, many machine-dependent features were incorporated into the coding for Input/Output (I/O) of the external files. A copy of the program was transferred to NASA-Dryden in 1981. However, because of the considerable machine-dependence, the FASTEX program could not be installed on the CYBER computer system at NASA-Dryden.

#### **2.4.1.2 FASTEX Modification**

Prior to the incorporation of the FASTEX program into the STARS package, it was necessary to remove the machine-dependent codings from FASTEX. As mentioned earlier, the machine-dependence of the program was in the external file I/O routines. These routines were designed to pack the arrays before writing them into the external file. This action reduces the storage requirements of the arrays, thereby reducing the I/O buffer usage of the computer. As a result, the program runs faster and uses less external storage.

The first attempt was to convert all the machine-dependent routines to the VAX-Fortran language. However, it was soon realized that such conversion will be expensive and time consuming. Also, the dependence on the VAX-Fortran language will restrict the transfer of the program to other computers.

Next the machine-dependent I/O routines were replaced by standard Fortran-77 sequential file I/O procedure. The validity of the change was then checked using standard FASTEX test data (Reference - 17).

#### **2.4.1.3 Incorporation of FASTEX into the STARS Package**

Here the main problem was the conversion of the mode-shapes (modal data) from the finite element grid used by structural analysis part of STARS (STRUCTURES) to the aerodynamic grid used by FASTEX. The modeshapes had to be specified on straight lines for the aerodynamic model. This problem was resolved by using a program called GRIDCHG (GRID CHanGe) (Reference - 18).

The GRIDCHG program was originally designed to interpolate modal amplitudes defined at arbitrary points on a grid, to a specified number of points along a straight line on the same grid using beam spline interpolation technique. Thus, the GRIDCHG program was modified to determine the modal data on the aerodynamic grid points, using the mode-shapes determined from the free vibration analysis by the STRUCTURES part of STARS.



The other required input to the FASTEX program is the generalized mass values of the structure. A small program called GENMASS (GENeralized MASS) was written to determine these values.

The final layout of the linkage of the AERODYNAMICS part of the STARS package is shown in Figure - 2.4.1.3A.

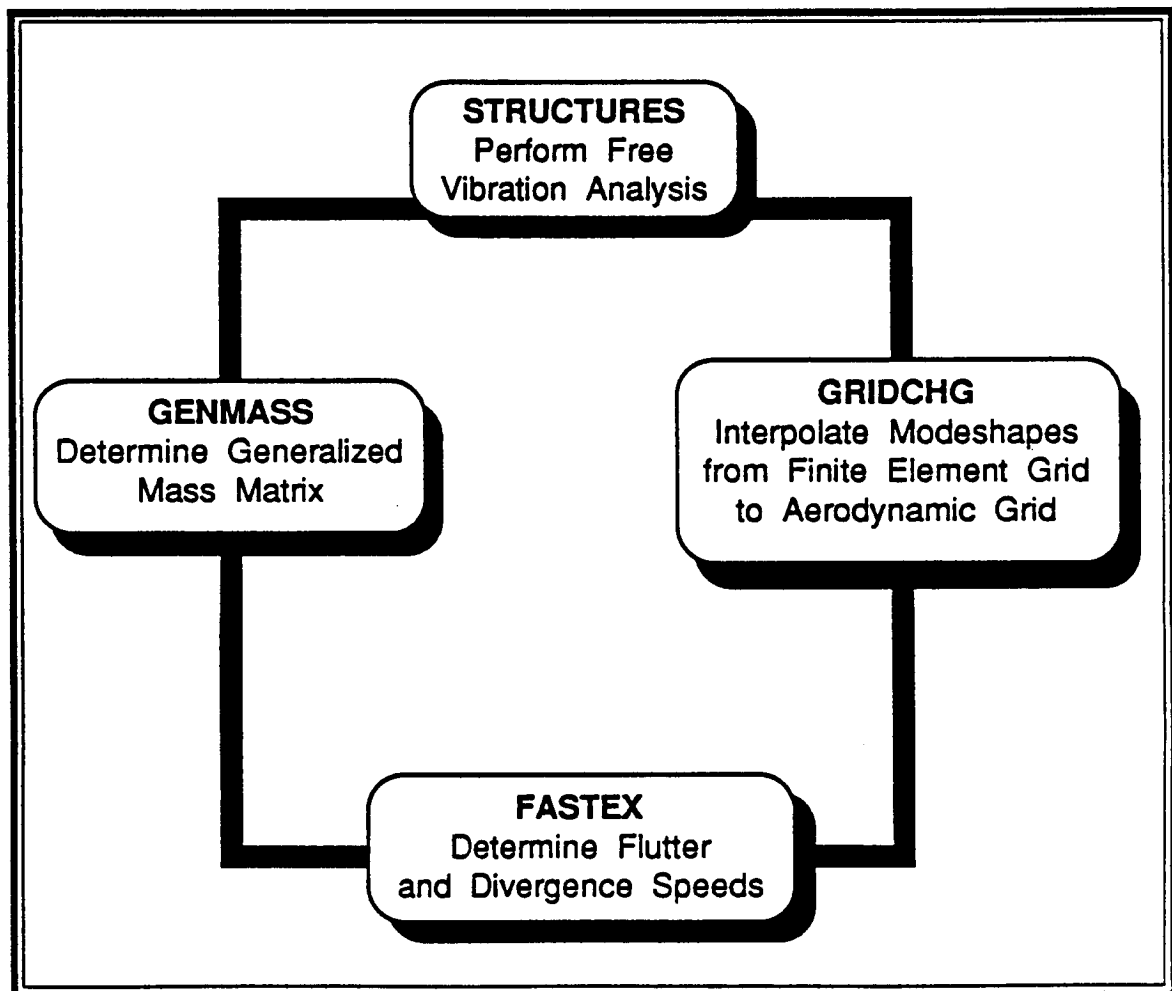


Figure 2.4.1.3A Linkage of the AERODYNAMICS Part of the STARS Program

#### **2.4.1.4 Further Improvements of FASTEX**

FASTEX was further improved by the University of Dayton (Reference - 19). The main objective of the project was:

- 1 — to increase the storage capacity of the program,
- 2 — to improve the interpolation method used by FASTEX.

Limitation on the problem size was one of the inherent deficiencies of the FASTEX computer program. The program was written with fixed dimensioned arrays. Such limitations were removed for the improved version of the FASTEX.

The other improvement done by the University of Dayton was to replace the beam spline interpolation technique by two dimensional surface spline method. The original version of the FASTEX performed modal interpolation to determine the amplitude at 3/4 and 1/4 points within an aerodynamic box. As it was mentioned earlier, the modal data used inside FASTEX was interpolated once before. Therefore, it was feasible to combine the two interpolation steps into one. As a result the interpolation routines were removed from the FASTEX module and a separate program called MODE\_INTERPOLATION was written to interpolate the modal data given on an arbitrary grid (finite element grid) to the 3/4 and 1/4 points of the aerodynamic boxes.

The new version of the aerodynamic analysis package was then linked to the structural analysis part of the STARS by a program

called SURFACE. The SURFACE computer program is designed to extract data from the results of the free vibration analysis and prepare appropriate data required by the MODE\_INTERPOLATION program.

Other computer programs (Figure - 2.4.1.4A) involved are GENMASS and AERO\_BOX. The GENMASS program, as mentioned earlier determines the generalized mass matrix. The AERO\_BOX program, is an extracted part of the old version of FASTEX. This program determines the 3/4 and 1/4 points of the aerodynamic boxes. This data is then used as input to the MODE\_INTERPOLATION program.

The programs recieved from the the University of Dayton were AERO\_BOX, MODE\_INTERPOLATION, and the revised version of FASTEX. SURFACE program was then developed to complete the link.

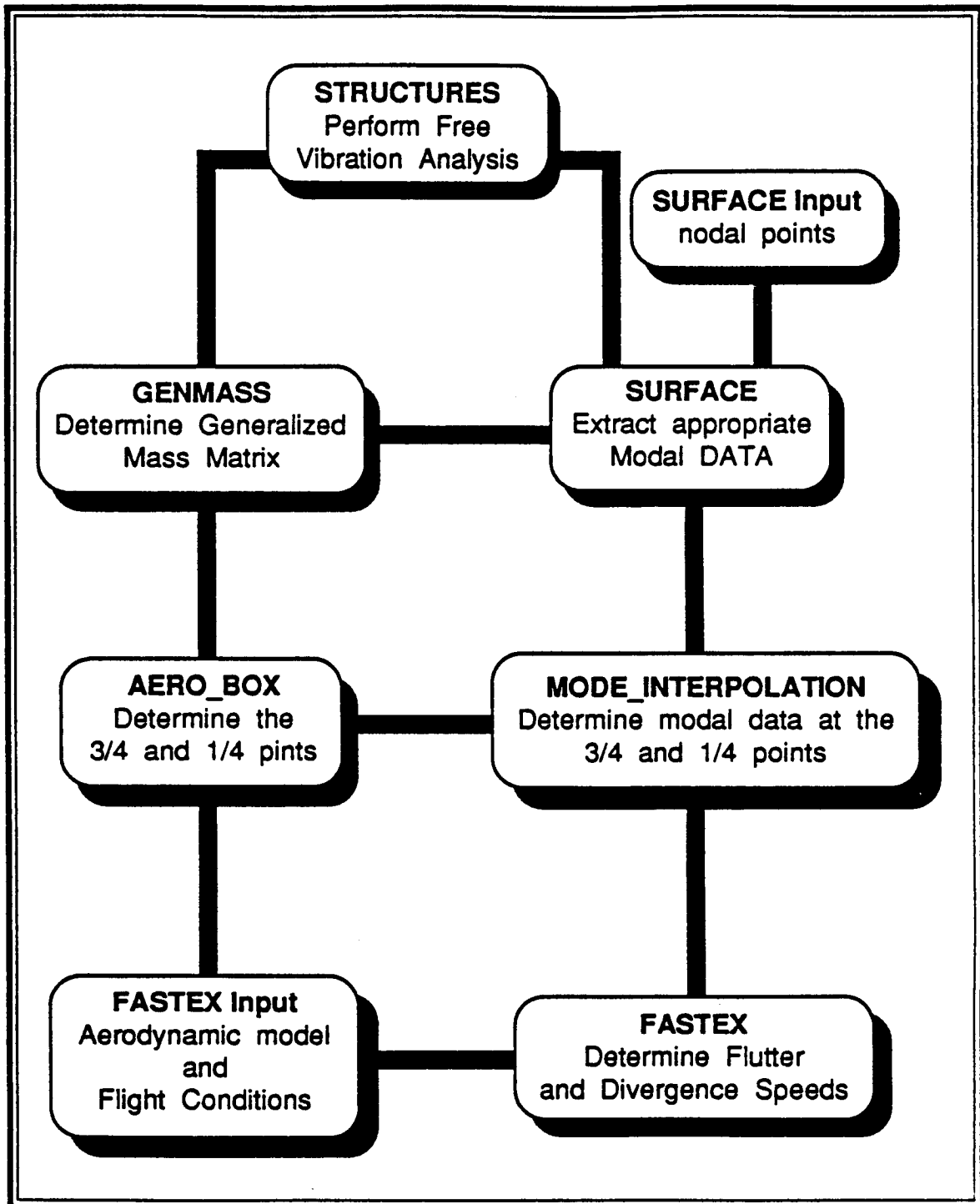


Figure 2.4.1.4A Improved Version of Aerodynamic Analysis Package

### **2.4.2 Graphics Program**

The graphics program for the STARS package was initially developed on the MEGATEK graphic system. The program was designed (Figure -2.4.2A) to take advantage of the graphics capabilities of the MATLIB (Reference - 20) computer program.

The program's capabilities were:

- 1 — to display the natural modeshapes for all dynamic cases,
- 2 — to display the deformed shape of the structures under static loading.

MATLIB package is capable of performing basic manipulation of the displayed structure, such as translation and rotation, in three dimensions. This was achieved by re-drawing the structure every time, which is very time consuming for large models.

Because of the complexity of the finite element model of the X-29A aircraft, it was necessary to have a more powerful graphics system. One of the capabilities required for this system was the manipulation of the structure in real time. After proper survey, the PS300 system by Evans & Sutherland was found to be the most suitable.

### **2.4.3 PS300 Graphics System**

The PS300 graphics system has some special capabilities. It is capable of real time translation and rotation of an object in three

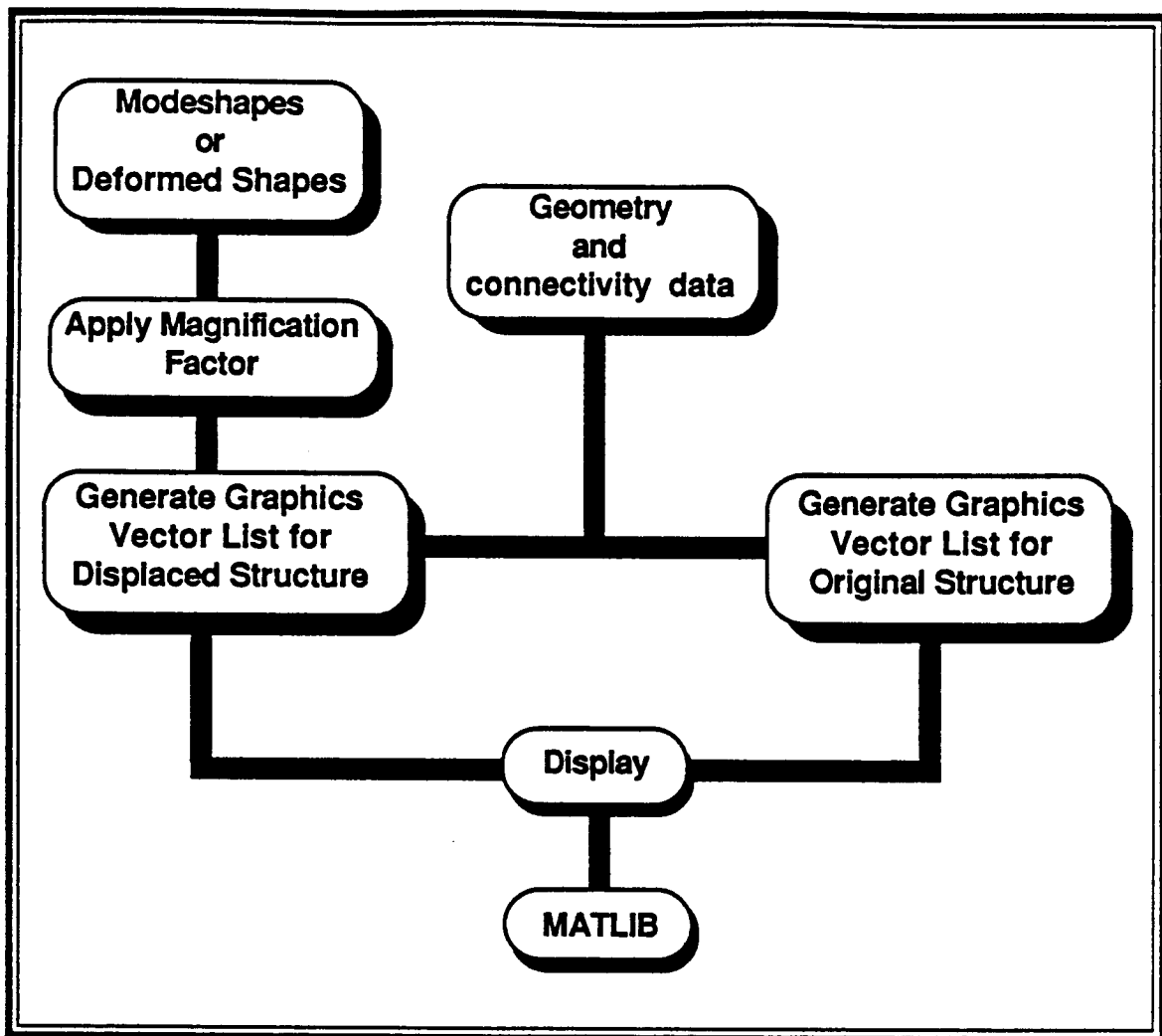


**Figure 2.4.2A** STARS Post-Processor on MEGATEK

dimensions. Scaling and re-sizing of an object are also done in real time.

The PS300 system has its own language. For this reason, the original graphics program for the STARS package had to be rewritten to suit the new graphics system. The objectives of the new graphics package called POST\_PLOT are as follows:

- 1 — to display the original structure,
- 2 — to display the deformed shape of the structure,
- 3 — to display the node numbers,
- 4 — to display the element numbers,
- 5 — to rotate and translate the structure,
- 6 — to scale the structure,
- 7 — to scale the node numbers,
- 8 — to scale the element numbers,
- 9 — to change the color intensity of the original structure, deformed shape, node numbers, element numbers, and other displays independently,
- 10 — to alter the perspective of the structure,
- 11 — to animate the natural mode-shapes,
- 12 — to animate the total time history response of a structure subjected to dynamic loading,
- 13 — to plot the displacements at a node with respect to time,
- 14 — to plot the internal stresses in an element with respect to time.

All of the above objectives are satisfied in the latest version of the POST\_PLOT. Function keys and the control dials of the PS300 system are programmed to create a user-friendly graphics environment. A summarized overview of the POST\_PLOT package is shown in Figure - 2.4.3A. Brief explanations of the function keys and the control dials follow.

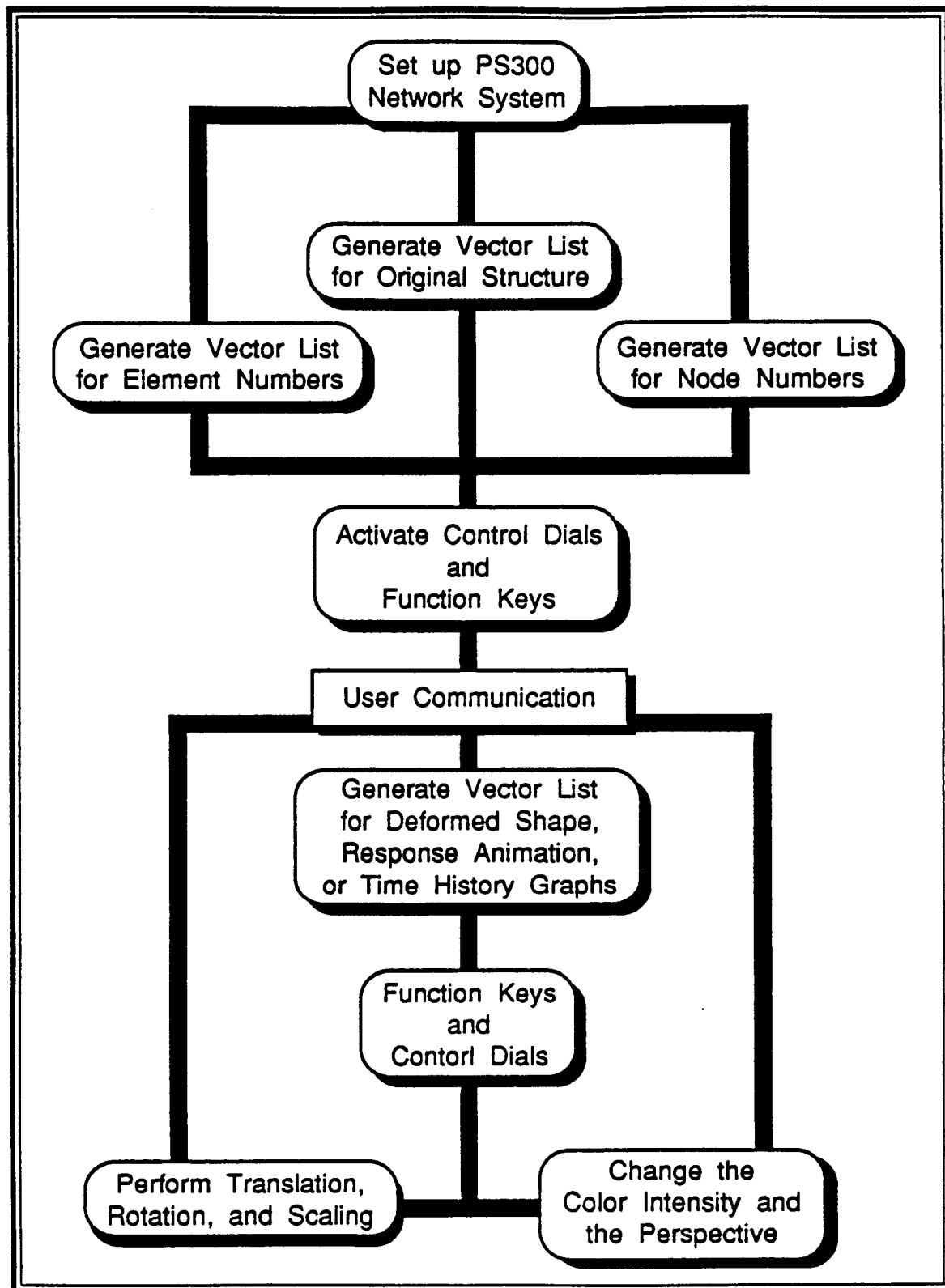


Figure 2.4.3A Layout of the POST\_PLOT Graphics Program



### 2.4.3.1 Function Keys and Control Dials

The PS300 graphics system has twelve function keys (F1 - F12) which can be operated in three different modes resulting in a total of thirty six functions. The twelve function keys have an eight character digital display which can be used as a status identification. Each function key, when operated, outputs an integer pertaining to its identification number (1 - 36) and a .TRUE. boolean. These parameters are used in the design of the function network to control the status of the display.

The PS300 system has eight control dials (D1 - D8). Each dial outputs real numbers in the range of 1 to -1. This output is used to control the rotation, translation, distortion, scaling, and coloring of the displayed objects.

The current POST\_PLOT program handles seven different cases. Description of each case and its function network follows.

#### 2.4.3.1.1 Static Case

Here the user can display the deformed shape of a structure subjected to static loading. In the case of multiple loadings (Reference - 6) all of the deformed shapes are loaded into the local memory of PS300. Each loading case can be put on display by using the assigned function key. Other function keys are used to control the display status of the node and element numbers.

The assignment for the function keys are as follows:

- F1** — controls the display state of the original structure,  
          <digital display> **ORG\_STRC**   (Original Structure)
- F2** — controls the display state of the deformed structure,  
          <digital display> **DEF\_STRC**   (Deformed Structure)
- F3** — Not Used,
- F4** — Not Used,
- F5** — controls the display state of the user input title,  
          <digital display> **TITLE**
- F6** — controls the display state of the node numbers,  
          <digital display> **NODE\_NUM**   (Node Numbers)
- F7** — controls the display state of the element numbers,  
          <digital display> **ELEM\_NUM**   (Element Numbers)
- F8** — controls the display state of the axes,  
          <digital display> **AXES**
- F9** — controls the clipping box,  
          <digital display> **CLIP\_ON**  
                              **CLIP\_OFF**
- F10** — controls the state of the control dials,  
          <digital display> **TRANSFER**  
                              **SCALE**  
                              **COLOR**  
                              **FOV**       (Field of View)
- F11** — controls the display of the load cases generated,  
          <digital display> **CASE xxx**
- F12** — Not Used.

The state of the control dials is controlled by the function key F10.

The explanation for each state follows.

**TRANSFER:**

- D1 — transfers the image along the X-axis,  
<digital display> X-TRAN**
- D2 — transfers the image along the Y-axis,  
<digital display> Y-TRAN**
- D3 — transfers the image along the Z-axis,  
<digital display> Z-TRAN**
- D4 — translation speed level,  
<digital display> LEVEL 1  
LEVEL 2  
LEVEL 3**
- D5 — rotates the image about the X-axis,  
<digital display> X-ROT**
- D6 — rotates the image about the Y-axis,  
<digital display> Y-ROT**
- D7 — rotates the image about the Z-axis,  
<digital display> Z-ROT**
- D8 — rotation speed level,  
<digital display> LEVEL 1  
LEVEL 2  
LEVEL 3**

**SCALE:**

- D1** — scales the original structure,  
    <digital display> **ORG\_STRC** (Original Structure)
- D2** — scales the defomed structure,  
    <digital display> **DEF\_STRC** (Deformed Structure)
- D3** — scales the node numbers,  
    <digital display> **NODE\_NUM** (Node Numbers)
- D4** — scales the element numbers,  
    <digital display> **ELEM\_NUM** (Element Numbers)
- D5** — scales the axes labels,  
    <digital display> **AXES**
- D6** — Not Used,
- D7** — Not Used,
- D8** — scaling speed level,  
    <digital display> **LEVEL 1**  
                          **LEVEL 2**  
                          **LEVEL 3**

**COLOR:**

- D1** — colors the original structure,  
    <digital display> **ORG\_STRC** (Original Structure)
- D2** — colors the defomed structure,  
    <digital display> **DEF\_STRC** (Deformed Structure)
- D3** — colors the node numbers,  
    <digital display> **NODE\_NUM** (Node Numbers)

- D4 — colors the element numbers,  
    <digital display> **ELEM\_NUM** (Element Numbers)
- D5 — colors the axes,  
    <digital display> **AXES**
- D6 — colors the title,  
    <digital display> **TITLE**
- D7 — Not Used,
- D8 — coloring speed level,  
    <digital display> **LEVEL 1**  
                          **LEVEL 2**  
                          **LEVEL 3**

**FOV:**

- D1 — moves the front window,  
    <digital display> **FRONT**
- D2 — moves the back window,  
    <digital display> **BACK**
- D3 — changes the view angle,  
    <digital display> **ANGLE**
- D4 — resets to the default view parameters,  
    <digital display> **RESET**
- D5 — front window speed level,  
    <digital display> **LEVEL 1**  
                          **LEVEL 2**  
                          **LEVEL 3**

**D6** — back window speed level,  
    <digital display> **LEVEL 1**  
                          **LEVEL 2**  
                          **LEVEL 3**

**D7** — view angle speed level,  
    <digital display> **LEVEL 1**  
                          **LEVEL 2**  
                          **LEVEL 3**

**D8** — Not Used.

#### **2.4.3.1.2 Free Vibration Case**

The calculated mode-shapes are displayed on top of the original form of the structure. The graphics package exploits the real time framing capability of the PS300 system to animate the modeshapes. This is done by first generating the data for the mirror image of the mode-shape and eight intermediate frames on the host computer. The data is then transferred to the PS300's memory banks. Each frame is displayed using a controlled timer to animate motion.

The assignment for the function keys are as follows:

- F1** — same as section 2.4.3.1.1,
- F2** — controls the display state of the modeshape,  
    <digital display> **DEF\_STRC** (Deformed Structure)
- F3** — controls the state of modeshape animation,  
    <digital display> **ANIMATE**

- F4** — performs manual display of the vibration steps,  
          <digital display> **STEP**
- F5** — same as section 2.4.3.1.1,
- F6** — same as section 2.4.3.1.1,
- F7** — same as section 2.4.3.1.1,
- F8** — same as section 2.4.3.1.1,
- F9** — same as section 2.4.3.1.1,
- F10** — same as section 2.4.3.1.1,
- F11** — controls the display of the mode-shapes generated,  
          <digital display> **MODE xxx**
- F12** — controls the state of the problem, only in the case of  
dynamic response analysis, **NAT\_MODE** for this case,  
          <digital display> **NAT\_MODE**   (Natural Mode-shapes)  
                              **RESPONSE**   (Dynamic Response)  
                              **DIS\_VS\_T**   (Displacement vs. Time)  
                              **STS\_VS\_T**   (Stress vs. Time)

The control dials controlled by the function key F10 are the same as in section 2.4.3.1.1.

#### 2.4.3.1.3 Forced Vibration Case

In this case the user can animate the total displacement time history. This is achieved by generating the vector lists for the displaced shape at each time steps (Reference - 6) defined by the user. The data from all the steps are transferred to the PS300 memory banks. The animation is then performed by the use of a

controlled timer.

The function keys assignments are as follows:

- F1** — same as section 2.4.3.1.1,
- F2** — controls the display state of the deformed structure,  
           <digital display> **DEF\_STRC**   (Deformed Structure)
- F3** — controls the state of dynamic response animation,  
           <digital display> **ANIMATE**
- F4** — performs manual display of the dynamic response steps,  
           <digital display> **STEP**
- F5** — same as section 2.4.3.1.1,
- F6** — same as section 2.4.3.1.1,
- F7** — same as section 2.4.3.1.1,
- F8** — same as section 2.4.3.1.1,
- F9** — same as section 2.4.3.1.1,
- F10** — same as section 2.4.3.1.1,
- F11** — controls the display of the individual frames with the  
           display of the actual time,  
           <digital display> **T=xxxxxx**
- F12** — controls the state of the problem, **RESPONSE** for this  
           case,  
           <digital display> **NAT\_MODE**   (Natural Mode-shapes)  
                               **RESPONSE**   (Dynamic Response)  
                               **DIS\_VS\_T**   (Displacement vs. Time)  
                               **STS\_VS\_T**   (Stress vs. Time)



The control dials controlled by the function key F10 are the same as in section 2.4.3.1.1.

#### **2.4.3.1.4 Nodal Displacement**

In this case the user can display the graph of displacement versus time for a particular node.

The assignment for the function keys are as follows:

- F1** — controls the display state of translation along X-axis,  
    <digital display> **X-TRAN**
- F2** — controls the display state of translation along Y-axis,  
    <digital display> **Y-TRAN**
- F3** — controls the display state of translation along Z-axis,  
    <digital display> **Z-TRAN**
- F4** — controls the display state of rotation about X-axis,  
    <digital display> **X-ROT**
- F5** — controls the display state of rotation about Y-axis,  
    <digital display> **Y-ROT**
- F6** — controls the display state of rotation about Z-axis,  
    <digital display> **Z-ROT**
- F7** — displays one of the three available grids,  
    <digital display> **GRID 1**  
                            **GRID 2**  
                            **GRID 3**  
                            **GRID OFF**

- F8** — same as section 2.4.3.1.1,
- F9** — Not Used,
- F10** — Not Used,
- F11** — controls the display of the graphs generated,  
<digital display> **NODExxxx**
- F12** — controls the state of the problem, **DIS\_VS\_T** for this case,  
<digital display>   **NAT\_MODE**   (Natural Modeshapes)  
                          **RESPONSE**   (Dynamic Response)  
                          **DIS\_VS\_T**   (Displacement vs. Time)  
                          **STS\_VS\_T**   (Stress vs. Time)

The control dials are used to control the color intensity of the graphs. The explanation for each state follows.

- D1** — colors the X-TRAN graph,  
<digital display> **X-TRAN**
- D2** — colors the Y-TRAN graph,  
<digital display> **Y-TRAN**
- D3** — colors the Z-TRAN graph,  
<digital display> **Z-TRAN**
- D4** — color speed level for dials D1 - D3,  
<digital display>   **LEVEL 1**  
                          **LEVEL 2**  
                          **LEVEL 3**
- D5** — colors the X-ROT graph,  
<digital display> **X-ROT**

- D6** — colors the Y-ROT graph,  
          <digital display> **Y-ROT**
- D7** — colors the Z-ROT graph,  
          <digital display> **Z-ROT**
- D8** — colors speed level for dials D5 - D7,  
          <digital display> **LEVEL 1**  
                              **LEVEL 2**  
                              **LEVEL 3**

#### 2.4.3.1.5 Line Element Forces

In this case the user can display the graph of forces versus time for a particular line element (Reference - 8).

The assignment for the function keys are as follows:

- F1** — controls the display state of force along local x-axis,  
          <digital display> **PX1**        (Force at node 1)  
                              **PX2**        (Force at node 2)
- F2** — controls the display state of force along local y-axis,  
          <digital display> **PY1**        (Force at node 1)  
                              **PY2**        (Force at node 2)
- F3** — controls the display state of force along local z-axis,  
          <digital display> **PZ1**        (Force at node 1)  
                              **PZ2**        (Force at node 2)
- F4** — controls the display state of moment about local x-axis,  
          <digital display> **MX1**        (Moment at node 1)  
                              **MX2**        (Moment at node 2)

- F5** — controls the display state of moment about local y-axis,  
    <digital display> **MY1**      (Moment at node 1)  
                         **MY2**      (Moment at node 2)
- F6** — controls the display state of moment about local z-axis,  
    <digital display> **MZ1**      (Moment at node 1)  
                         **MZ2**      (Moment at node 2)
- F7** — same as section 2.4.3.1.4,
- F8** — same as section 2.4.3.1.1,
- F9** — controls the state of the control dials used to color the  
    graphs for each end of the element,  
    <digital display> **END - 1**  
                         **END - 2**
- F10** — Not Used,
- F11** — controls the display of the graphs generated,  
    <digital display> **ELEMxxx**
- F12** — controls the state of the problem, **STS\_VS\_T** for this  
    case,  
    <digital display> **NAT\_MODE**    (Natural Mode-shapes)  
                         **RESPONSE**    (Dynamic Response)  
                         **DIS\_VS\_T**    (Displacement vs. Time)  
                         **STS\_VS\_T**    (Stress vs. Time)

The control dials are used to control the color intensity of the graphs. There are two modes controlled by the function key F9. The explanations for each state are the same as in section 2.4.3.1.4; the only difference is in the digital display of the dials.

### 2.4.3.1.6 Shell Stress

In this case the user can display the graph of stresses versus time for a particular shell element (Reference - 6).

The assignment for the function keys are as follows:

- F1** — controls the display state of normal stress on the top layer, in the direction of the local x-axis,  
<digital display>     **SXT**
- F2** — controls the display state of normal stress on the top layer, in the direction of the local y-axis,  
<digital display>     **SYT**
- F3** — controls the display state of shear stress on the top layer,  
<digital display>     **SXYT**
- F4** — controls the display state of element stress on the bottom layer, in the direction of the local x-axis,  
<digital display>     **SXB**
- F5** — controls the display state of element stress on the bottom layer, in the direction of the local y-axis,  
<digital display>     **SYB**
- F6** — controls the display state of shear stress on the bottom layer,  
<digital display>     **SXYB**
- F7** — same as section 2.4.3.1.4,
- F8** — same as section 2.4.3.1.1,
- F9** — Not Used,

- F10** — Not Used,
- F11** — same as 2.4.3.1.5
- F12** — same as 2.4.3.1.5

The control dials are used to control the color intensity of the graphs. The explanations for the dials are the same as in section 2.4.3.1.4; the only difference is in the digital display of the dials.

#### **2.4.3.1.7 Solid Stress**

In this case the user can display the graph of stresses versus time for a particular solid element (Reference - 6).

The assignment for the function keys are as follows:

- F1** — controls the display state of normal stress, in the direction of the local x-axis,  
    <digital display>     **SXX**
- F2** — controls the display state of normal stress, in the direction of the local y-axis,  
    <digital display>     **SYX**
- F3** — controls the display state of normal stress, in the direction of the local z-axis,  
    <digital display>     **SZZ**
- F4** — controls the display state of shear stress, in the local xy-plane,  
    <digital display>     **SXY**

- F5** — controls the display state of shear stress, in the  
local yz-plane,  
    <digital display>      **SYZ**
- F6** — controls the display state of shear stress, in the  
local xz-plane,  
    <digital display>      **SXZ**
- F7** — same as section 2.4.3.1.4,
- F8** — same as section 2.4.3.1.1,
- F9** — Not Used,
- F10** — Not Used,
- F11** — same as section 2.4.3.1.5
- F12** — same as section 2.4.3.1.5

The control dials are used to control the color intensity of the graphs. The explanations for the dials are the same as in section 2.4.3.1.4; the only difference is in the digital display of the dials.

## ***CHAPTER 3***

# **COMPARATIVE ANALYSIS OF X-29A AIRCRAFT**

### **3.1 BACKGROUND**

At NASA-Dryden, flight tests are being performed on the X-29A aircraft to ensure its air-worthiness. Prior to the flight tests, structural and aerodynamic analyses were performed to predict the potential instabilities such as the flutter and divergence speeds of the aircraft. The STARS computer program was the main analytical tool used for this task.

The analyses can be divided into two parts. The first part is the free vibration analysis; the second part is the aerodynamic analysis. The free vibration analysis is performed by the "Structural Analysis" part of the



STARS computer program to obtain the natural frequencies and the natural mode-shapes of the structure. The results from free vibration analysis are then used to determine the flutter and divergence speeds of the aircraft.

The finite element models used for the free vibration analyses are derived mostly from large order finite element stress models provided by the contractor, Grumman Aircraft Corporation (GAC). Model simplification is done so that the eigen-solution process suits the available computer resources.

Because of the complexity of the finite element model of the entire aircraft, it was decided to construct the finite element models of the canard and the wing components (these two being the most important features of the X-29A aircraft) first, in order to minimize accumulation of modelling errors. The finite element models for these components used by the STARS program are shown in Figures - 3.1A and 3.1B. Free vibration analyses were then performed on these components to verify and to modify the models, as required.

After the verification of the finite element models for the canard and the wing components, the model of the entire aircraft is constructed (Figure - 3.1C). For a complete solution, the analysis of the aircraft is performed in two phases, symmetric and anti-symmetric. The same finite element model is used in both cases, with different boundary conditions along the fuselage and the vertical tail. In the symmetric case, out of the

ORIGINAL PAGE IS  
OF POOR QUALITY

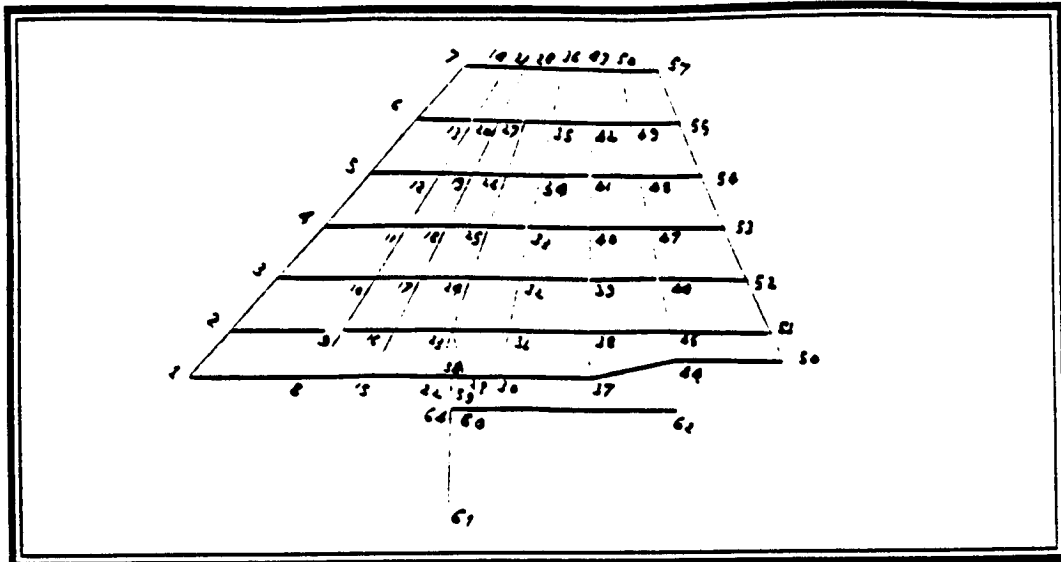


Figure 3.1A Finite Element Model of the Canard Component

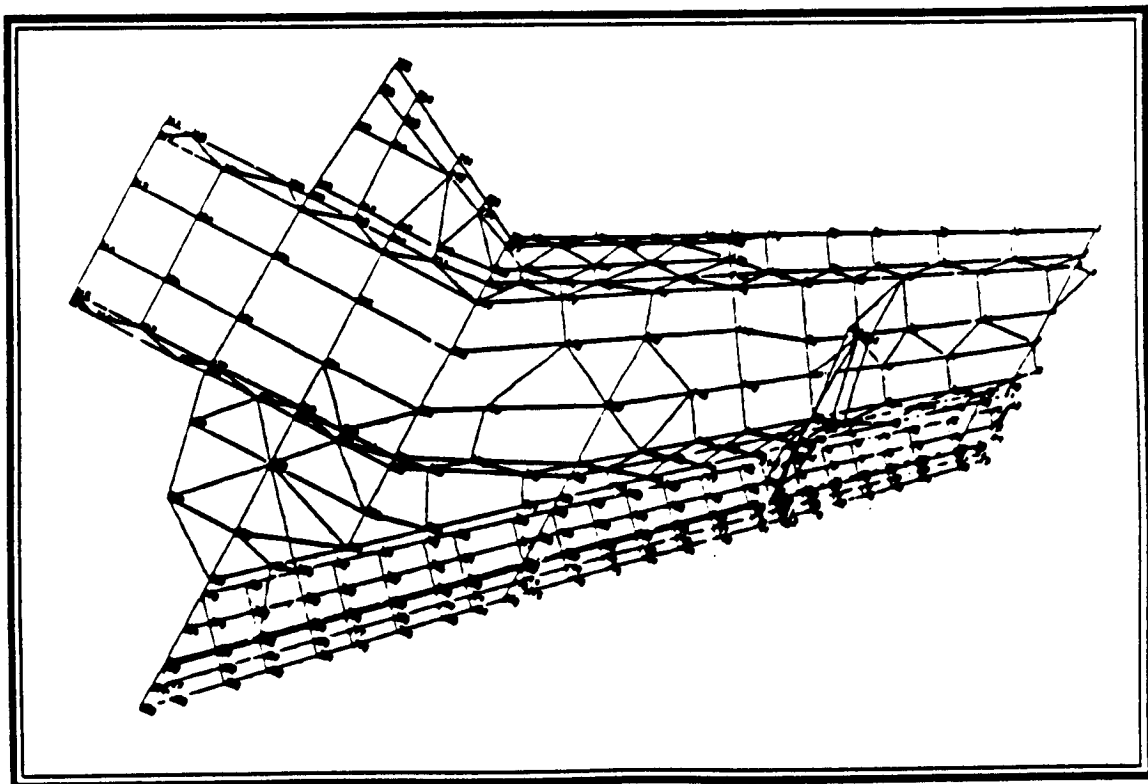
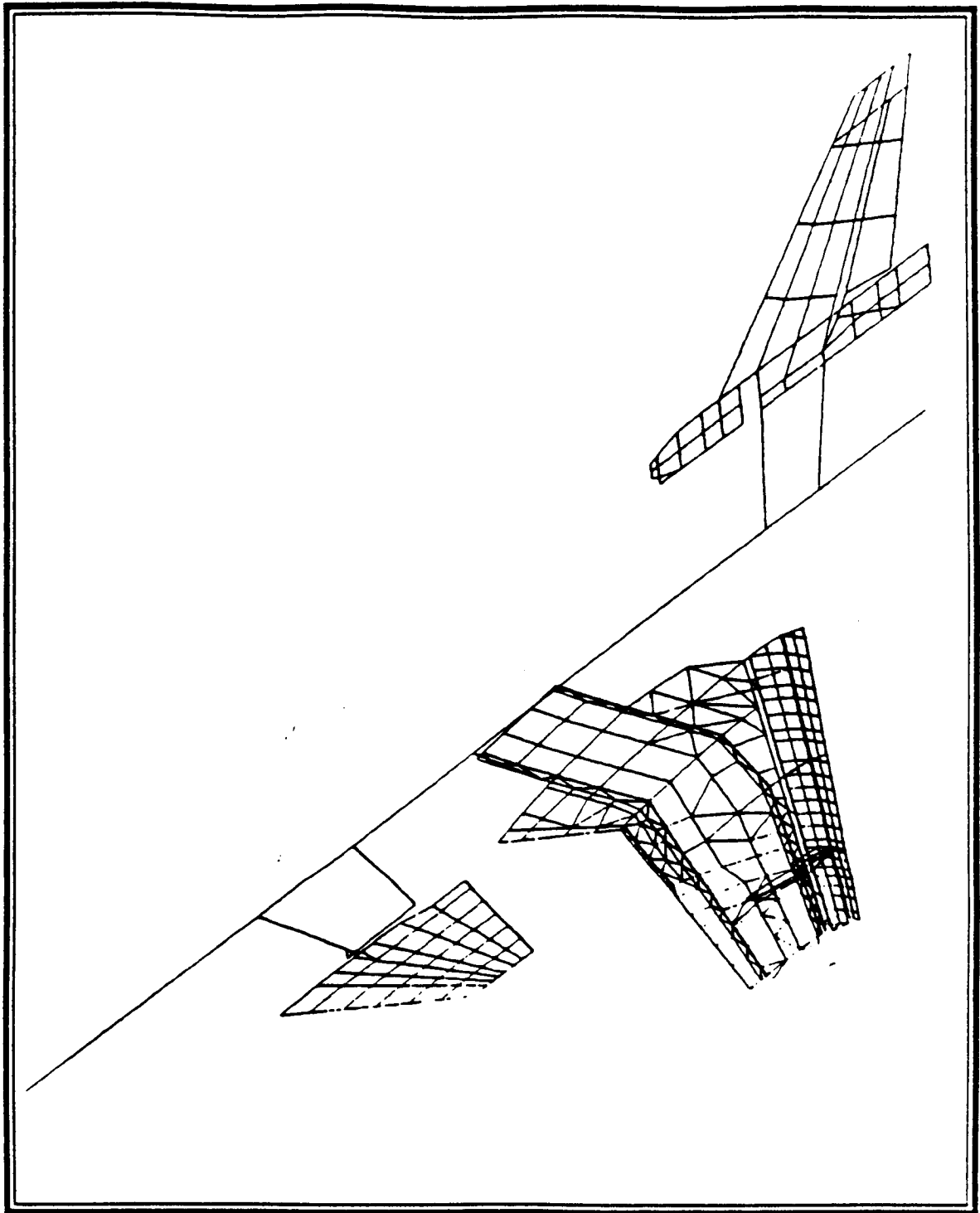


Figure 3.1B Finite Element Model of the Wing Component



**Figure 3.1C** Finite Element Model of the X-29A Aircraft

three translations (degrees of freedom) and the three rotations (degrees of freedom) at each node, the Y translation and the X and Z rotations are suppressed; this generated the symmetric natural modes of the aircraft. In the anti-symmetric case, the X and Z translations and the Y rotation are suppressed; this generated the anti-symmetric natural modes of the aircraft.

The "Aero-Dynamic Analysis" part of the STARS package is based on the Doublet Lattice method (Reference - 9). This technique requires the aircraft to be modeled in a two-dimensional panel form (Figure - 3.1D), and the natural mode-shapes to be defined in the out-of-plane direction (perpendicular to the surface). Therefore, only the out-of-plane components of the mode-shapes obtained for each case are interpolated using

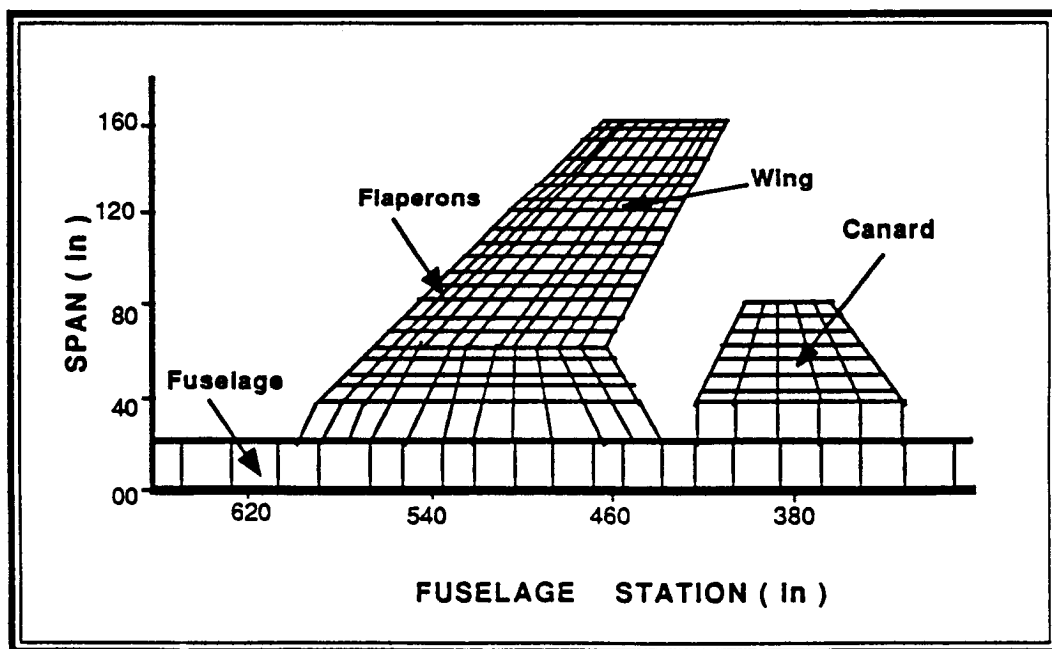


Figure 3.1D Model Used for the Aerodynamic Analysis of the X-29A Aircraft

surface spline algorithm to determine the modal amplitudes at the aerodynamic grid points of the model.

The natural frequencies, interpolated natural mode-shapes, and the associated generalized mass matrix along with the prescribed flight conditions are used as input to the "Aero-Dynamic Analysis" part of the STARS program, to predict the flutter and divergence speeds of the aircraft.

The Ground Vibration Survey (GVS) results are compared with the analytical results obtained by the STARS and GAC analyses. Figure - 3.1F demonstrates the interrelation of these three sources for the verification of structural models. Aerodynamic verification steps are shown in Figure - 3.1E.

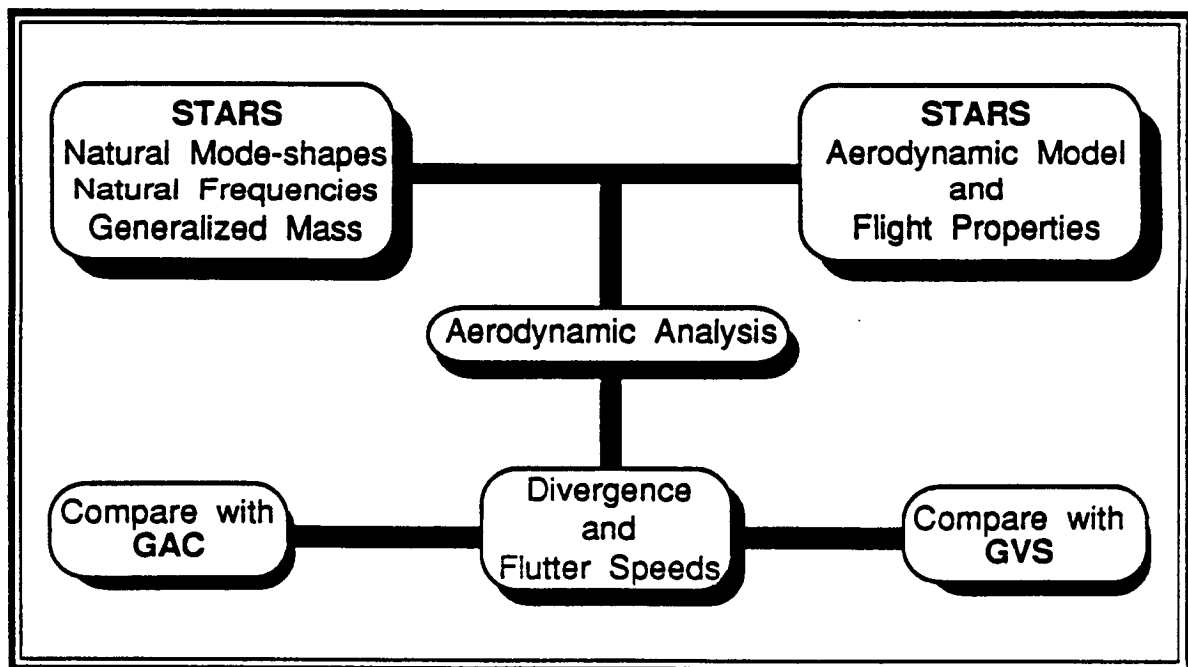


Figure 3.1E Aerodynamic Verification Steps

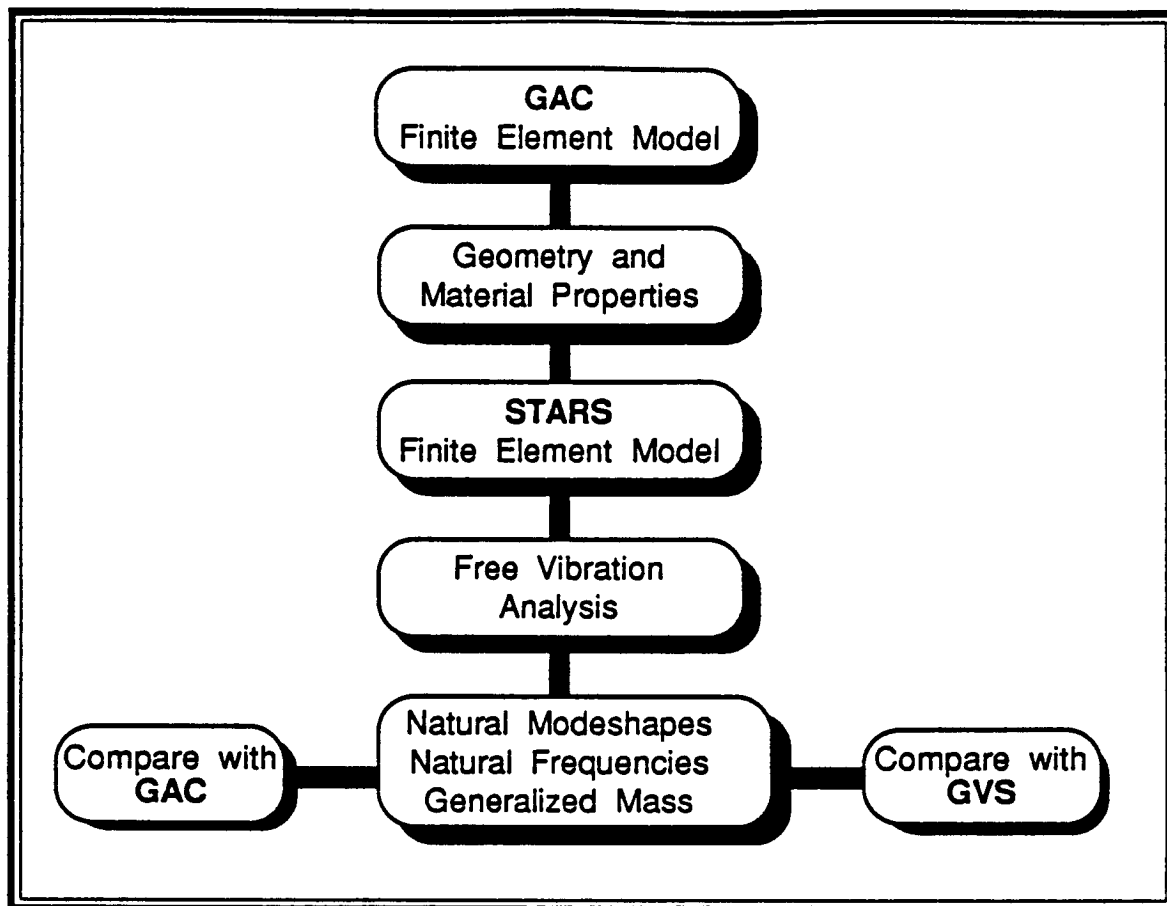


Figure 3.1F Structural Verification Steps

## 3.2 FREE VIBRATION ANALYSIS OF THE CANARD

The canard component (Figure - 3.2A) is made of aluminum. The finite element model used for the free vibration analysis is an equivalent shell model of the canard. It is constructed by collapsing the top and bottom skins of the canard and determining the equivalent stiffness and mass properties. The natural frequencies of the first six natural modes of the cantilevered canard component, determined by the STARS program, are

given in Table - 3.2A. The corresponding natural mode-shapes are presented in Figures - 3.2B-1 through 3.2B-6.

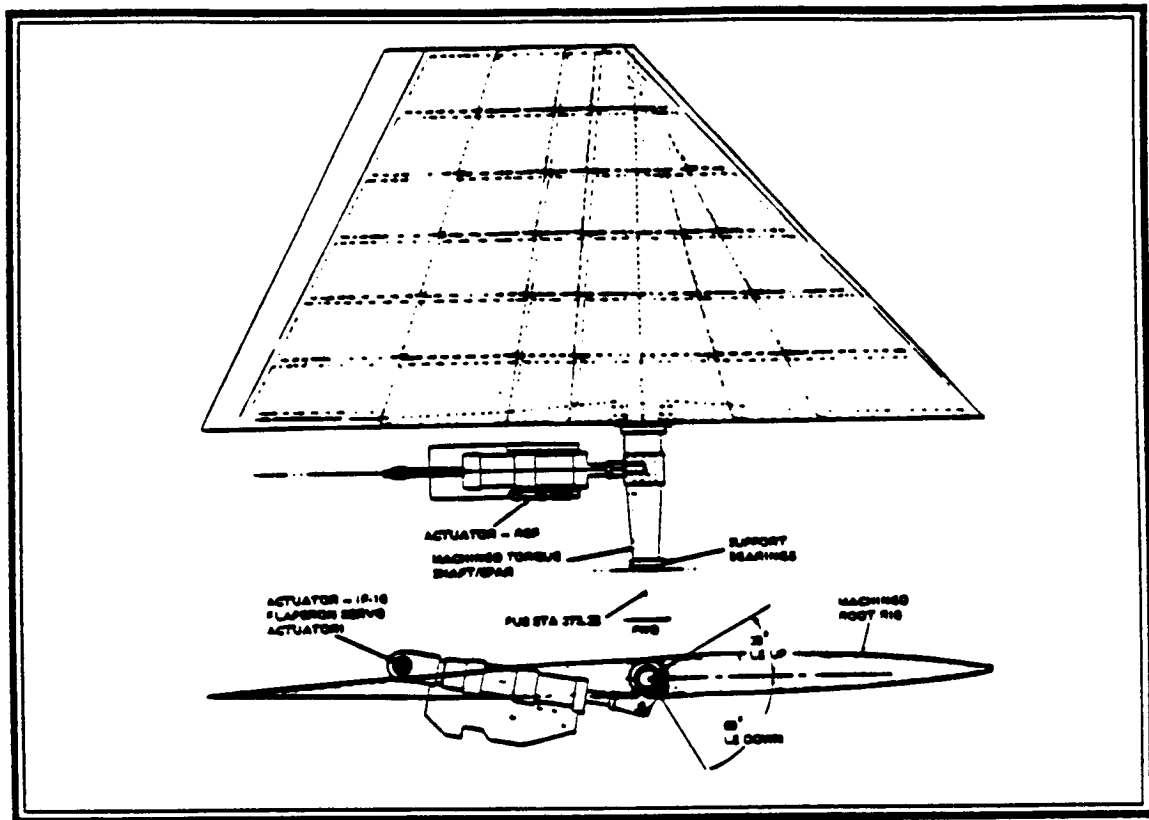
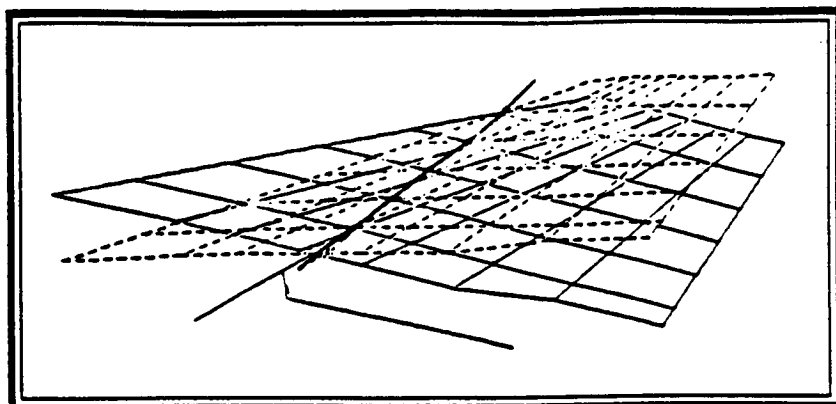


Figure 3.2A Canard Component

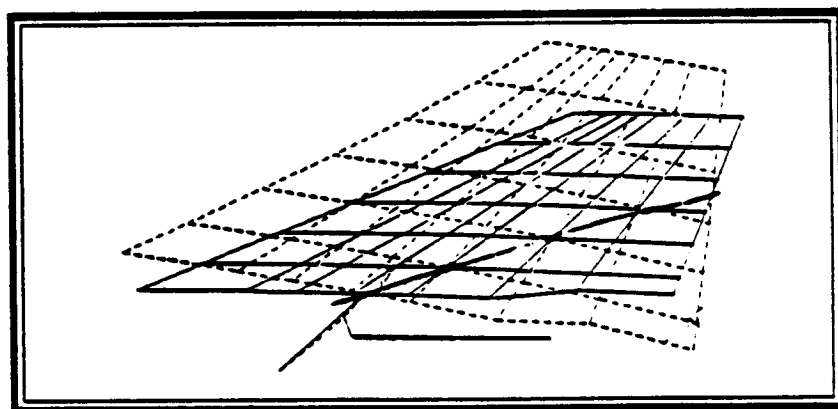
MODE No.	DESCRIPTION	FREQUENCY (Hz)	FIGURE No.
1	First Pitch	17.94	3.2B-1
2	First Bending	52.30	3.2B-2
3	Second Bending	98.22	3.2B-3
4	Second Pitch	116.1	3.2B-4
5	Third Bending	167.5	3.2B-5
6	First Yaw	184.2	3.2B-6

Table 3.2A Results of the Canard's Free Vibration Analysis

ORIGINAL PAGE IS  
OF POOR QUALITY



**Figure 3.2B-1** Canard's First Pitch Mode



**Figure 3.2B-2** Canard's First Bending Mode

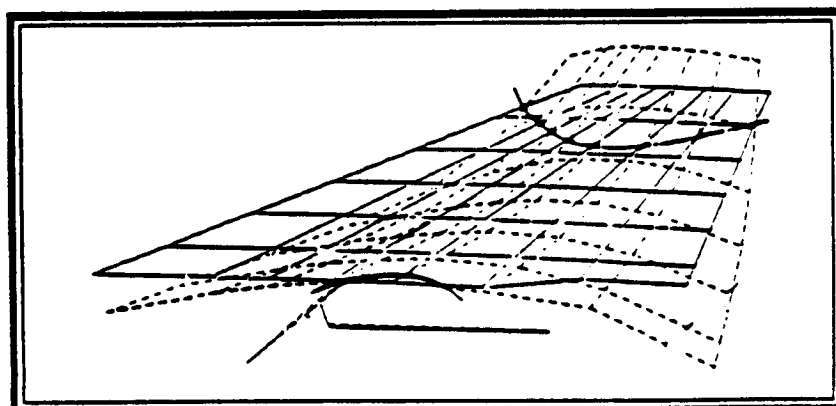


**Figure 3.2B-3** Canard's Second Bending Mode



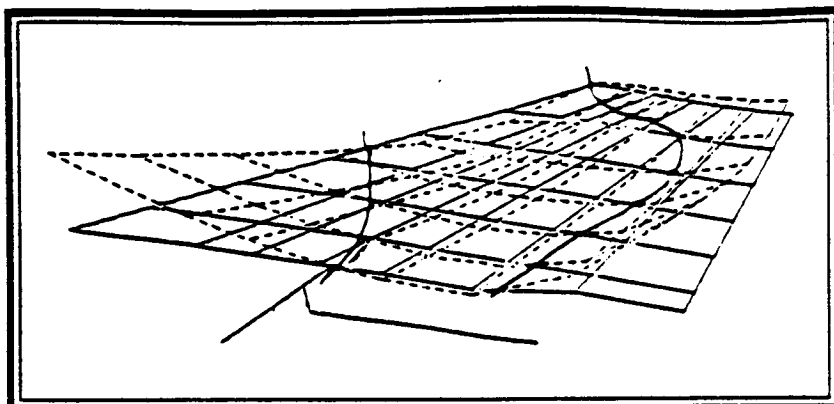


Figure 3.2B-4 Canard's Second Pitch Mode

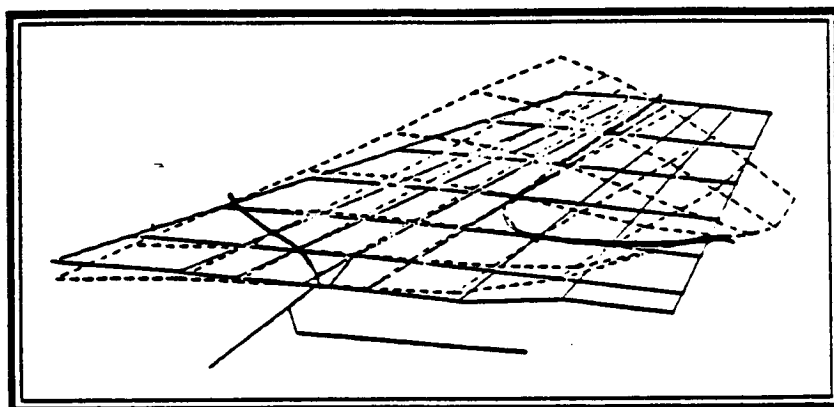


Figure 3.2B-5 Canard's Third Bending Mode

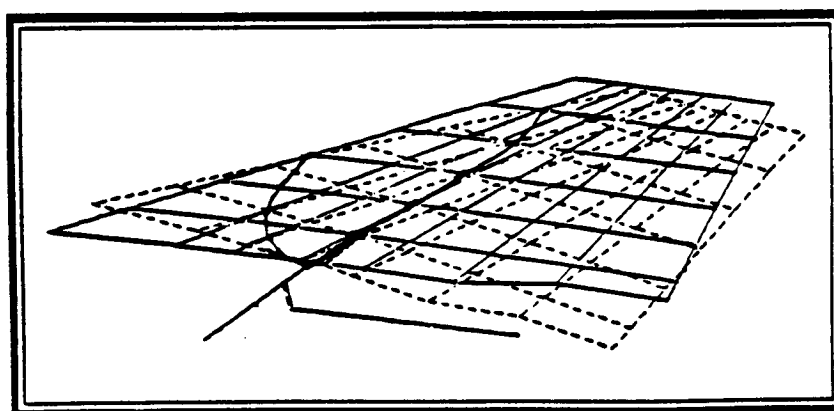


Figure 3.2B-6 Canard's First Yaw Mode

### 3.3 FREE VIBRATION ANALYSIS OF THE WING

The wing component (Figure - 3.3A) is primarily a box made of aeroelastically-tailored graphite-epoxy composite skin, bolted to titanium and aluminum spars. The wing skin consists of several layers of material with different material properties and material axes. The finite element model used for the free vibration analysis is an equivalent shell model of the wing. It is constructed by collapsing the top and bottom skins of the wing and determining the equivalent stiffness and mass properties. The natural frequencies of the first six natural modes of the cantilevered wing, determined by the STARS program, are given in Table - 3.3A. The corresponding natural mode-shapes are presented in Figures - 3.3B-1 through 3.3B-6.

<b>MODE No.</b>	<b>DESCRIPTION</b>	<b>FREQUENCY (Hz)</b>	<b>FIGURE No.</b>
<b>1</b>	<b>First Bending</b>	<b>10.31</b>	<b>3.3B-1</b>
<b>2</b>	<b>First Torsion</b>	<b>25.50</b>	<b>3.3B-2</b>
<b>3</b>	<b>Second Bending</b>	<b>33.40</b>	<b>3.3B-3</b>
<b>4</b>	<b>Third Bending</b>	<b>46.75</b>	<b>3.3B-4</b>
<b>5</b>	<b>Inboard Flap Torsion</b>	<b>54.50</b>	<b>3.3B-5</b>
<b>6</b>	<b>Flap First Bending</b>	<b>68.40</b>	<b>3.3B-6</b>

**Table 3.3A** Results of the Wing's Free Vibration Analysis

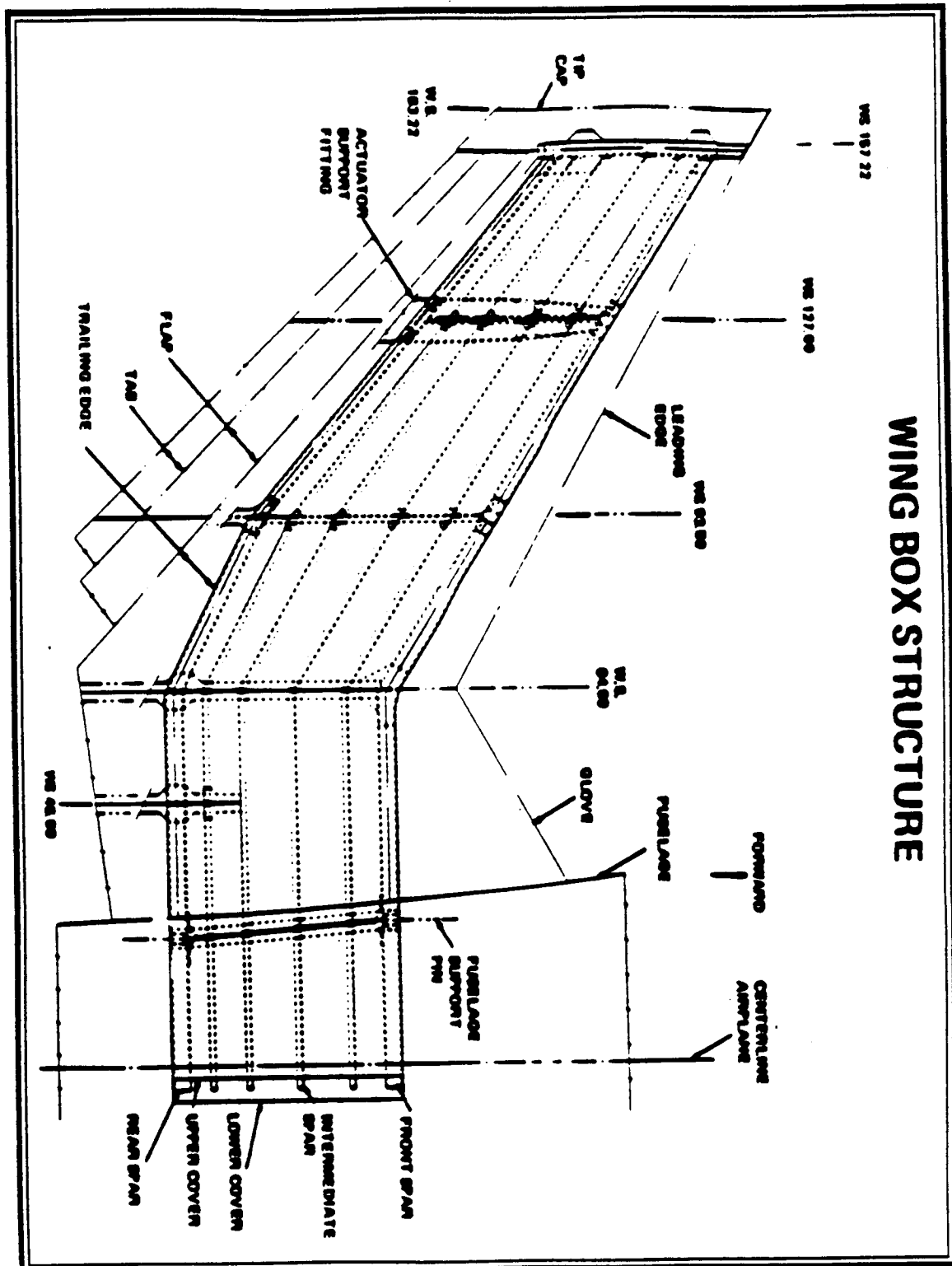


**Figure 3.3A Wing Component**

ORIGINAL PAGE IS  
OF POOR QUALITY

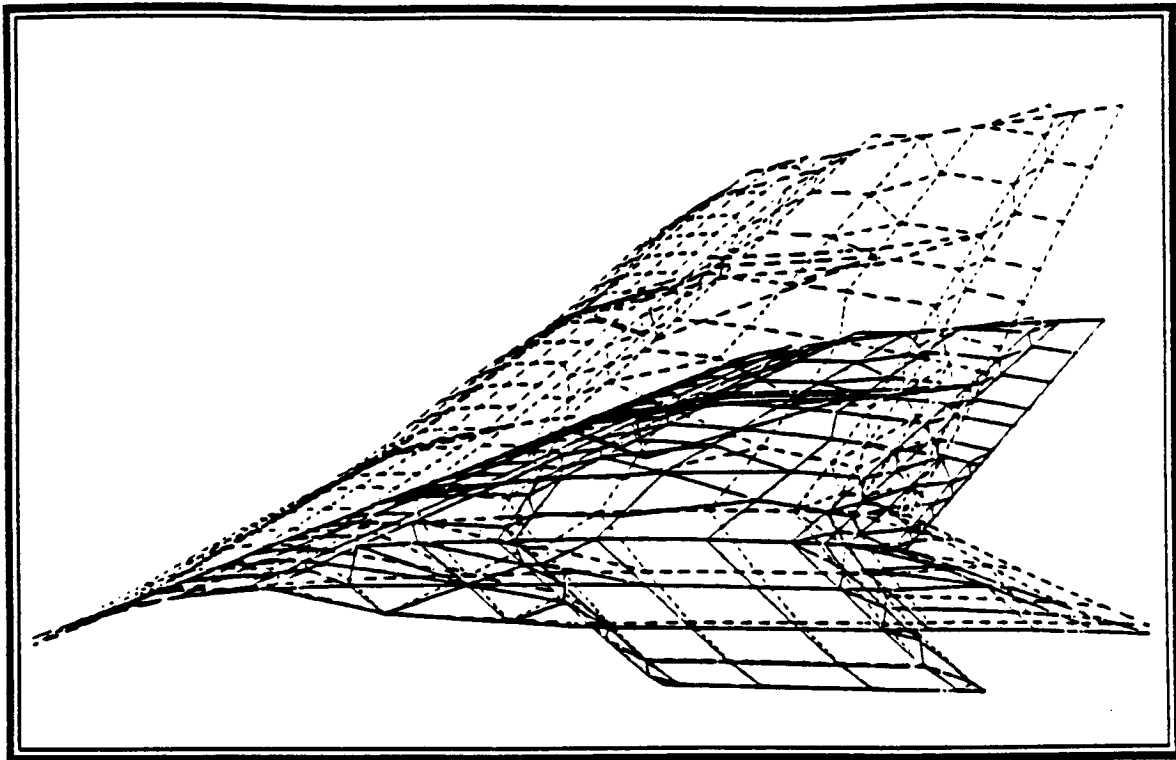


Figure 3.3B-1 Wing's First Bending Mode

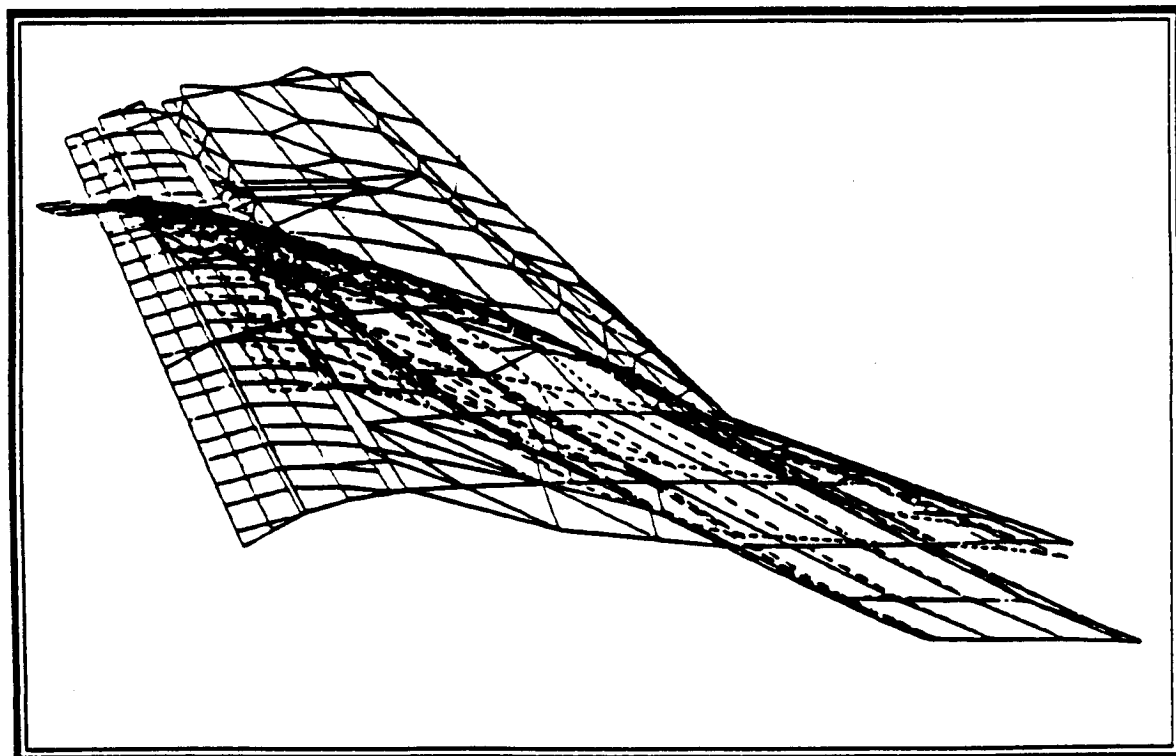


Figure 3.3B-2 Wing's First Torsion Mode

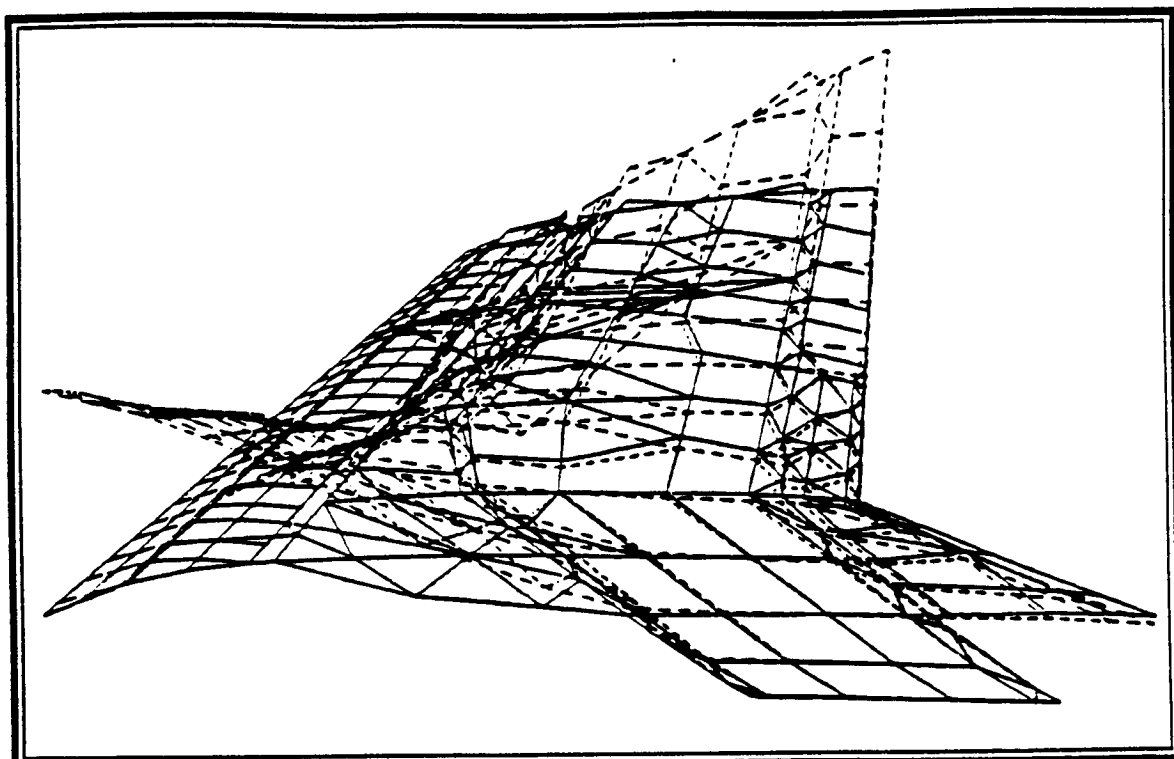


Figure 3.3B-3 Wing's Second Bending Mode

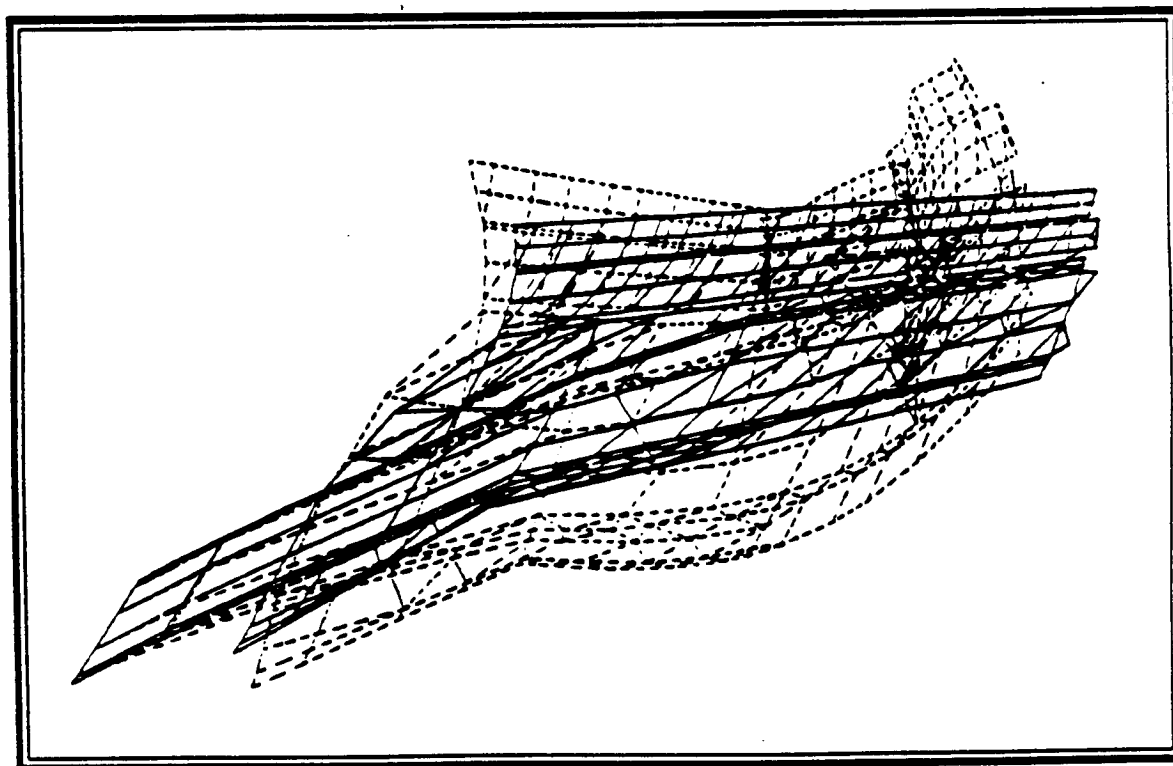
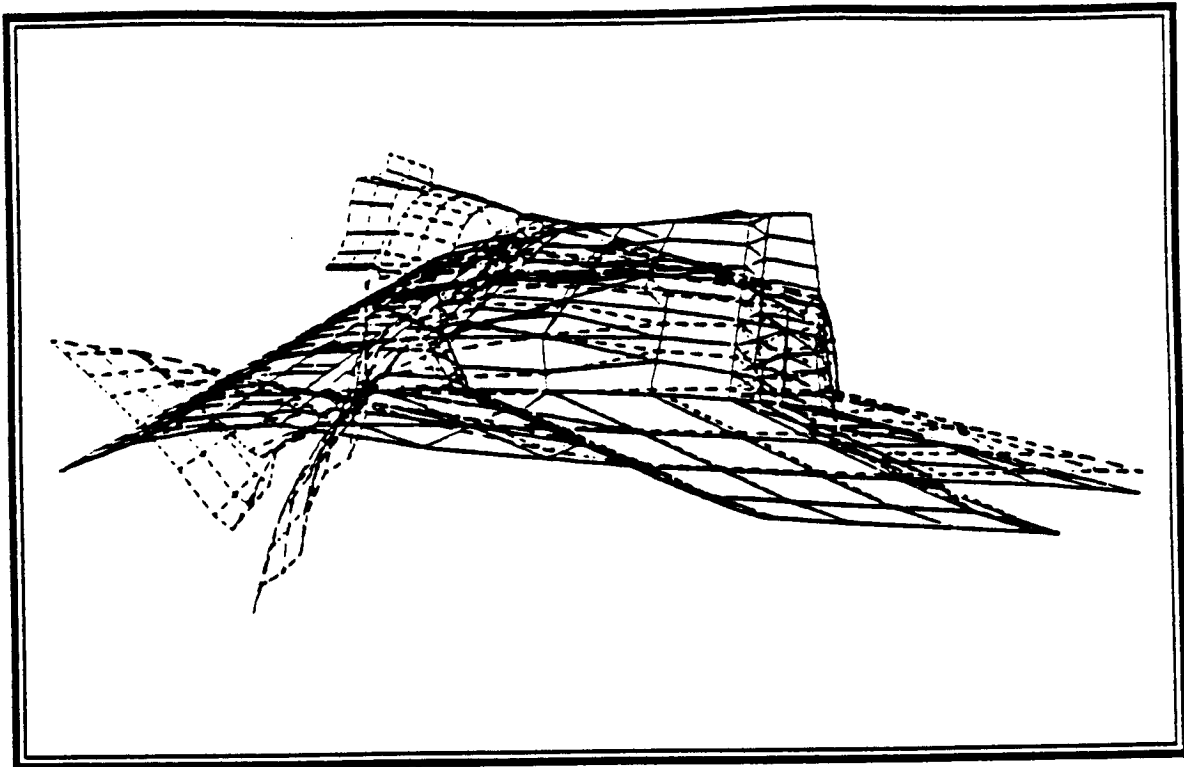
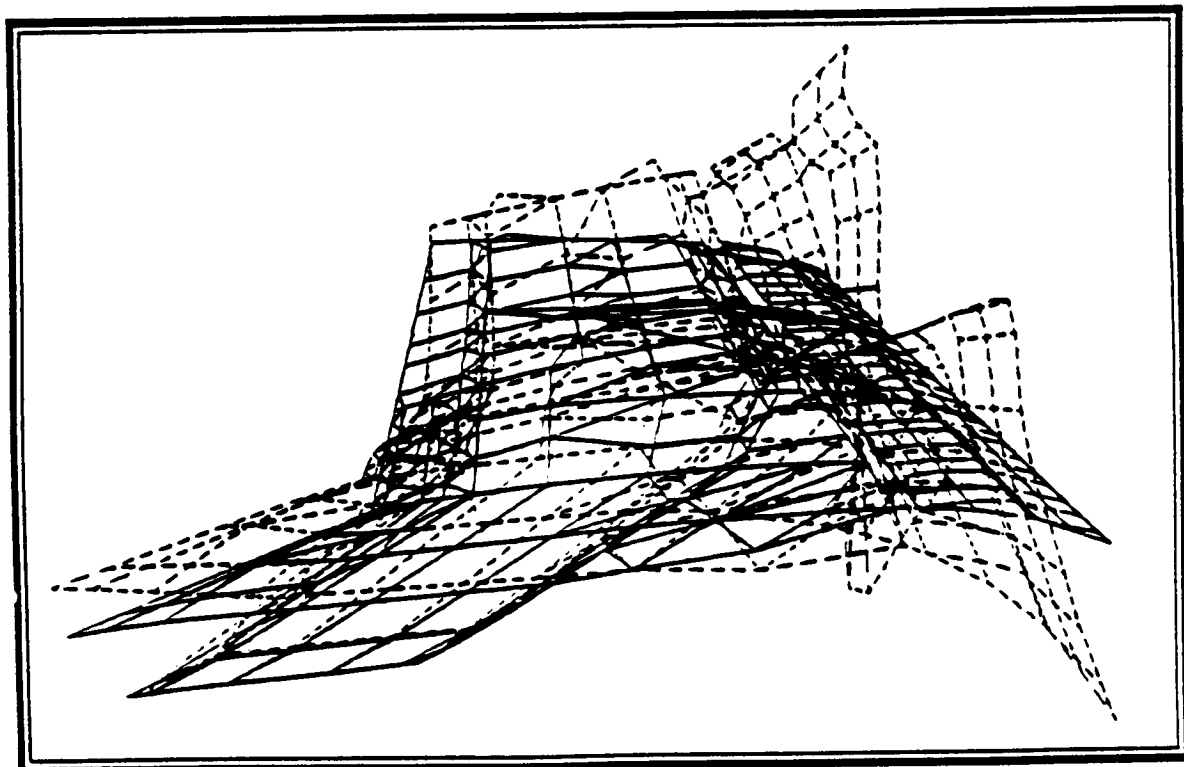


Figure 3.3B-4 Wing's Third Bending Mode



**Figure 3.3B-5** Wing's Inboard Flap Torsion Mode



**Figure 3.3B-6** Wing's Flap First Bending Mode

### **3.4 ANALYSIS OF THE ENTIRE AIRCRAFT**

The fuselage finite element model used in the STARS analysis is made of regular beam elements. The stiffness and mass properties of the elements of the fuselage model are one-half of the actual values. The finite element models of the wing, the canard, and the vertical tail are connected to the fuselage model by infinitely rigid beams.

As mentioned earlier, the analyses performed on the X-29A aircraft (Figure - 3.4A) are divided into the symmetric and anti-symmetric phases. The analytical results obtained by the STARS computer program are compared with those obtained by the contractor (GAC) and the experimental results obtained from the Ground Vibration Survey (GVS).

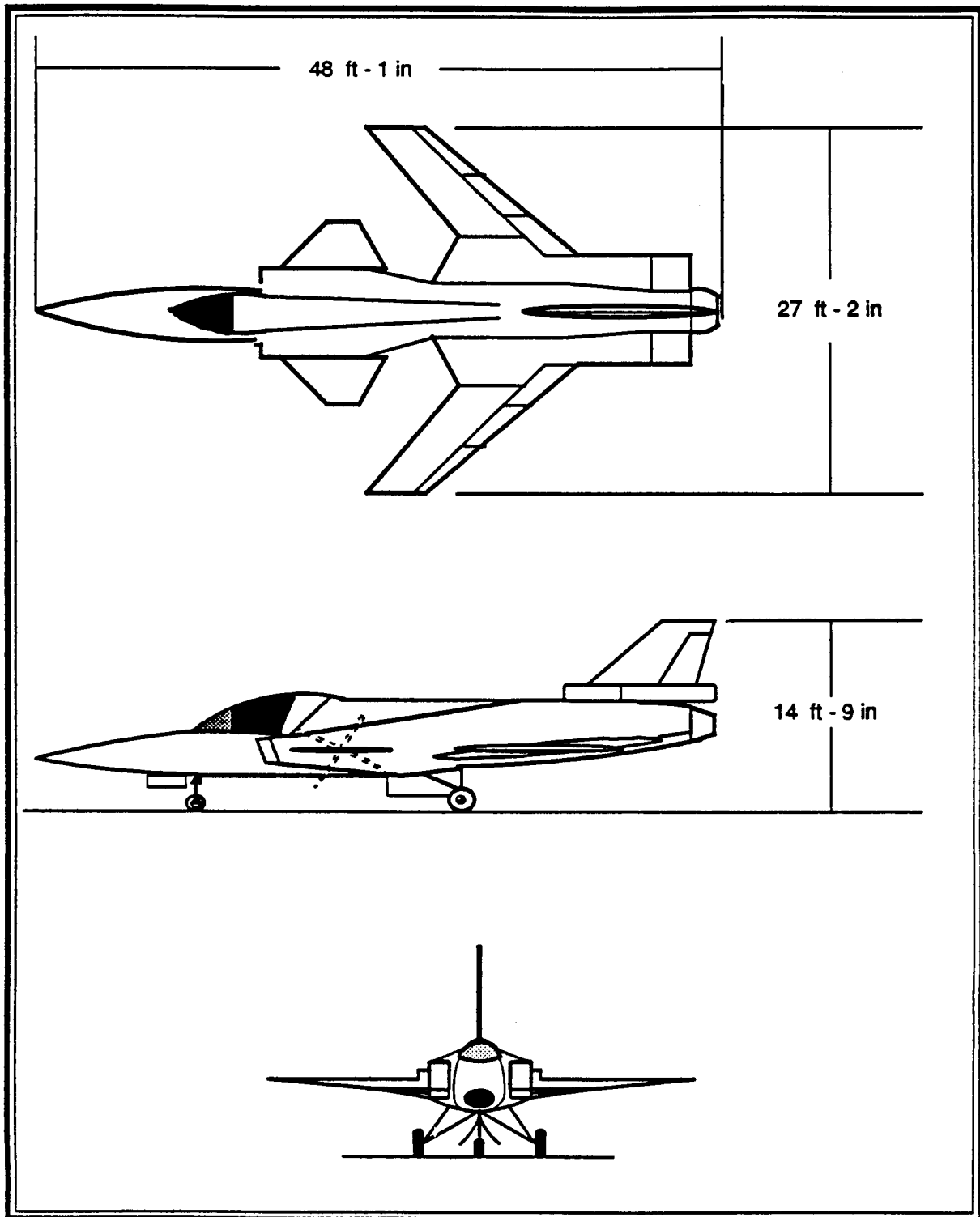


Figure 3.4A X-29A Aircraft



### 3.4.1 Free Vibration Analysis ( Symmetric )

Table - 3.4.1A presents a summary of the natural frequencies for eight representative symmetric natural modes determined by the three sources. The bar-graph shown in Figure - 3.4.1A presents the difference in natural frequencies with respect to the GVS results. The associated generalized mass values are given in Table - 3.4.1B. The difference in the generalized mass values is given in Figure - 3.4.1B.

The bar-graphs shown in Figures - 3.4.1A and 3.4.1B are presented for quick reference on the relative discrepancies in the natural frequencies and generalized mass values. As it is shown in the Figure 3.4.1B the relative difference in the generalized mass values are quite high. Such discrepancy is due to the difference in the natural mode-shapes obtained by three sources.

The STARS and the GAC analytical values are compared with the experimental values of the GVS. The analytically and experimentally obtained modal data for wing first bending mode are presented in the next section. The remaining symmetric modes are discussed in Appendix-B.

MODE	STARS Freq. (Hz)	GAC Freq. (Hz)	GVS Freq. (Hz)
W1B	8.96	8.11	8.61
F1B	12.87	10.02	11.65
F2B	19.03	19.62	24.30
CP	21.02	22.51	21.70
W2B	26.20	26.36	26.30
W1T	30.30	37.09	36.70
CBP	47.70	41.91	42.20
W3B	49.52	45.86	51.50

Table 3.4.1A Natural Frequencies of the X-29A Aircraft (Symmetric)

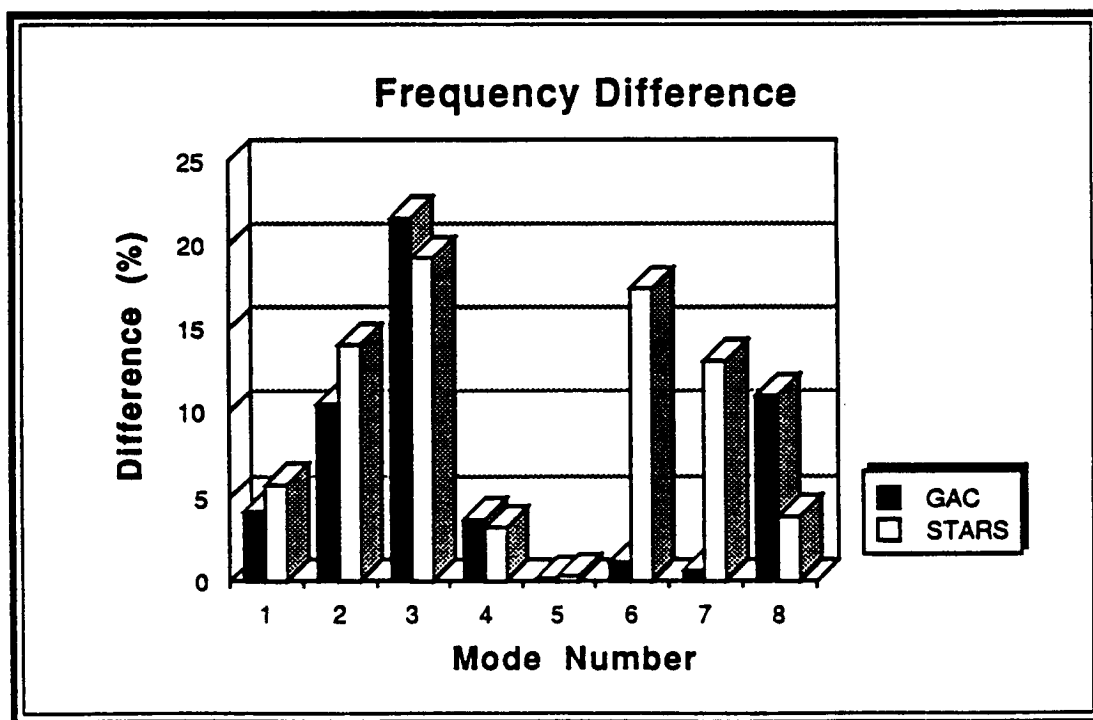


Figure 3.4.1A Natural Frequency Difference With Respect to GVS Results

MODE	STARS Gen.Mass(lb)	GAC Gen.Mass(lb)	GVS Gen.Mass(lb)
W1B	246.8	146.0	140.3
F1B	954.5	610.0	617.8
F2B	104.6	1034.0	281.2
CP	16.70	18.00	14.20
W2B	132.6	67.00	23.10
W1T	134.4	65.00	14.90
CBP	35.90	21.00	17.30
W3B	104.0	87.00	4.89

Table 3.4.1B Generalized Mass Values of the X-29A Aircraft (Symmetric)

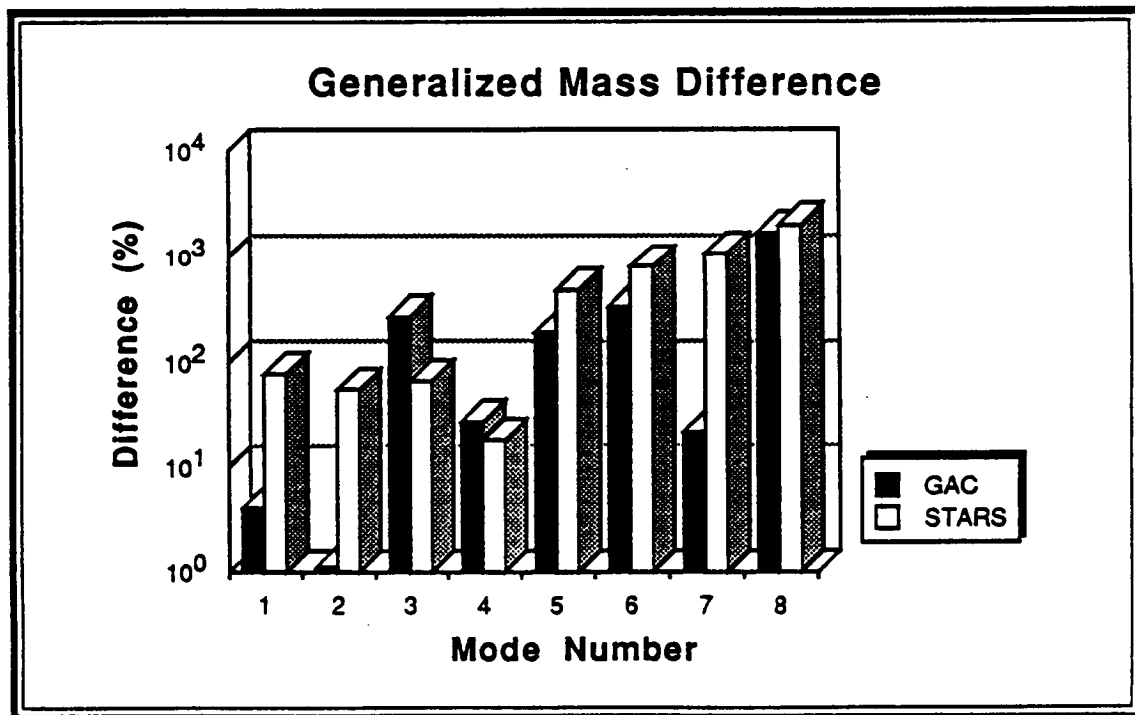


Figure 3.4.1B Generalized Mass Difference With Respect to GVS Results

#### **3.4.1.1 Wing First Bending (W1B)**

In general, the natural mode-shapes and natural frequencies from all three sources (STARS, GAC, and GVS) agree quite well (Figures 3.4.1.1A-1 through 3.4.1.1A-4). However, some discrepancy in the natural mode-shapes is evident in the central fuselage area. This is because the relative amplitude in this region is very small. Consequently, an accurate location of the node line becomes very difficult. However, the overall effect of this discrepancy on the aerodynamic analysis is negligible.

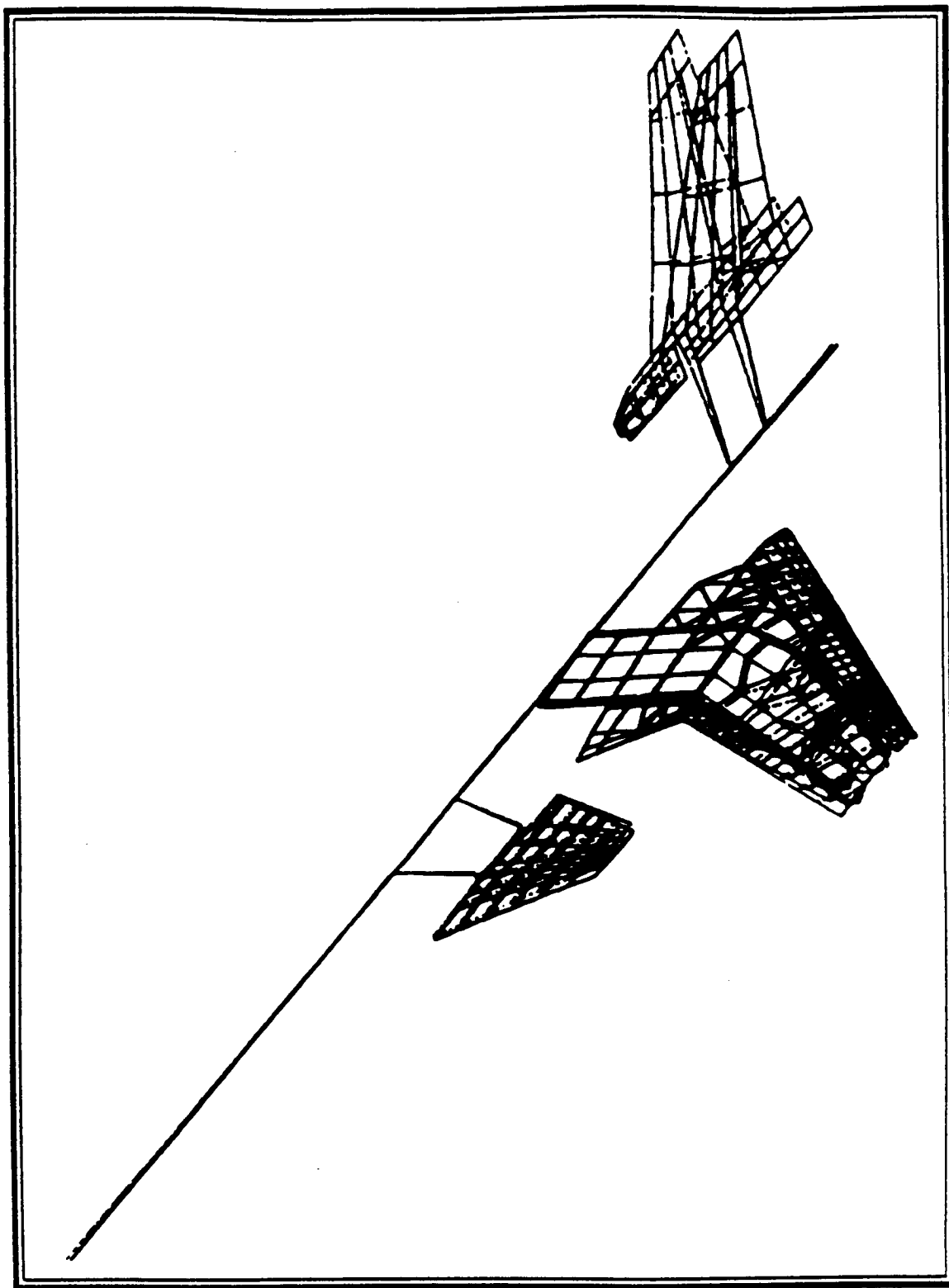


Figure 3.4.1.1A-1 STARS Wing First Bending Mode

C-2

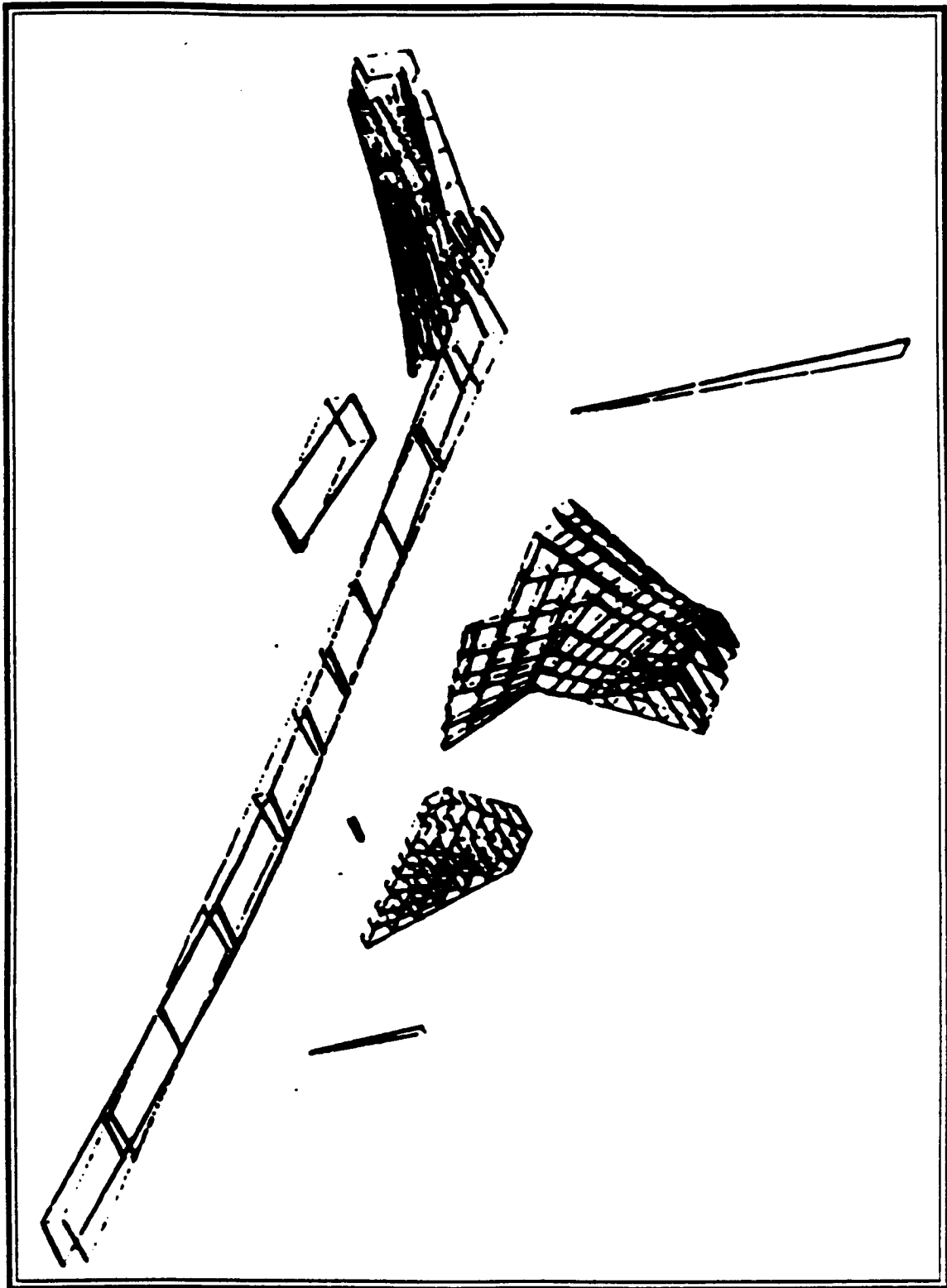


Figure 3.4.1.1A-2 GAC Wing First Bending Mode

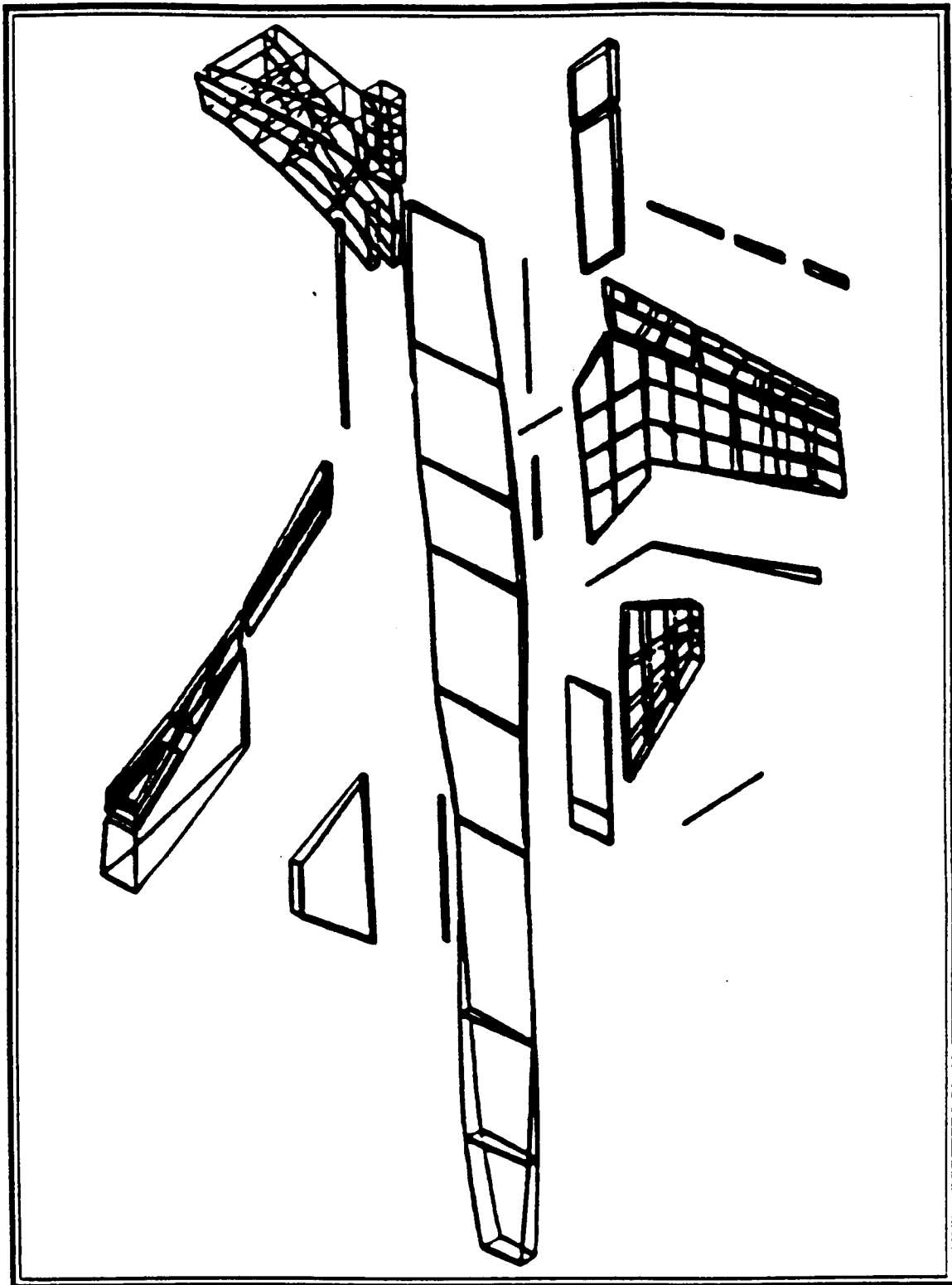
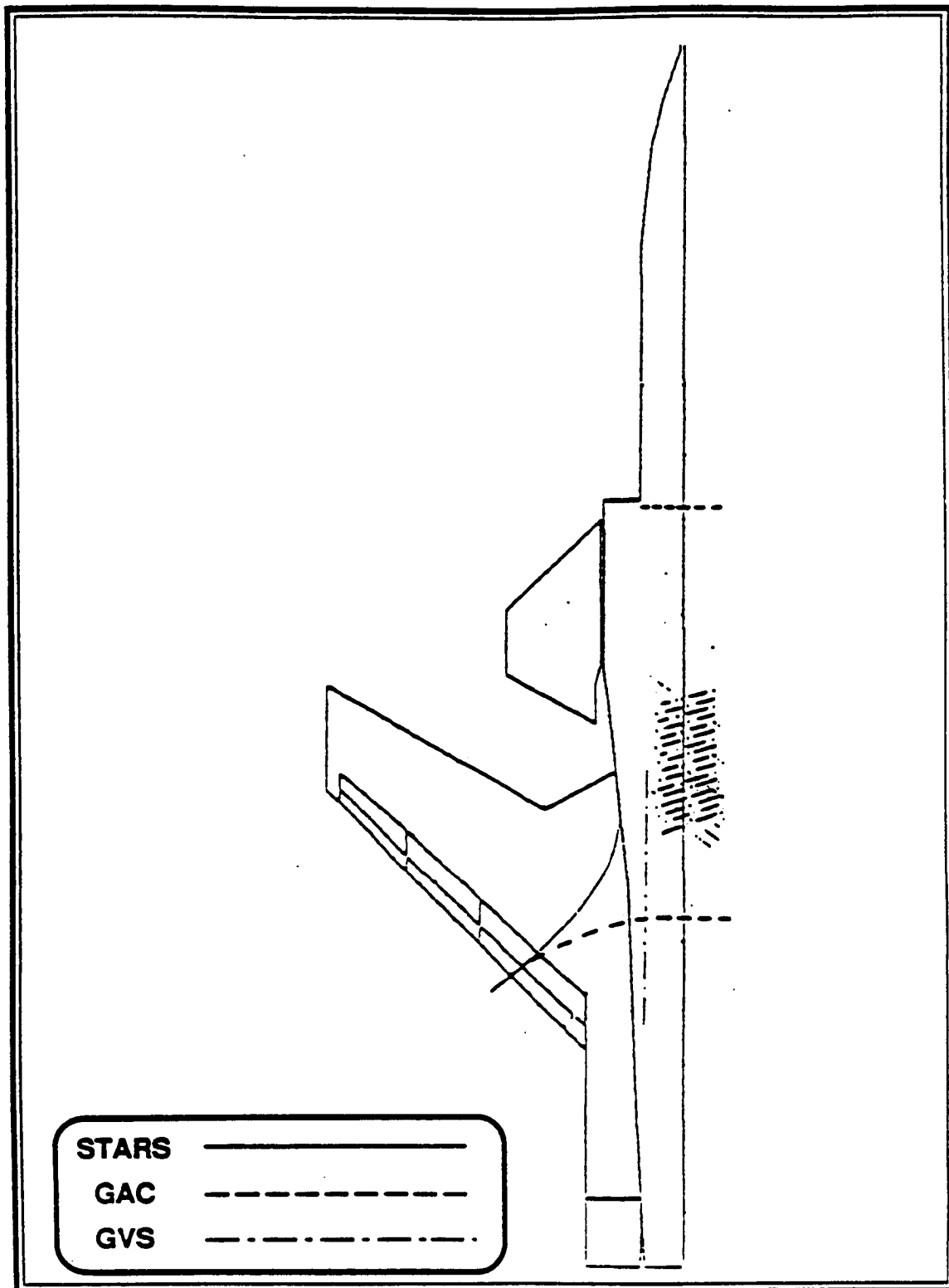


Figure 3.4.1.1A-3 GVS Wing First Bending Mode



**Figure 3.4.1.1A-4 Wing First Bending Node Lines**



### **3.4.2 Free Vibration Analysis ( Anti-Symmetric )**

Table - 3.4.2A presents a comparison of the natural frequencies for ten representative anti-symmetric modes as determined by the STARS, the GAC, and the GVS. The difference in natural frequencies is shown in Figure - 3.4.2A. The associated generalized mass values are given in Table - 3.4.2B. Figure - 3.4.2B shows the difference in the generalized mass values.

The STARS and the GAC analytical values are compared with the experimental values of the GVS. The analytically and experimentally obtained modal data for the wing first bending and the fuselage first bending modes are presented in the following sections. The remaining anti-symmetric modes are discussed in Appendix-B.

MODE	STARS Freq. (Hz)	GAC Freq. (Hz)	GVS Freq. (Hz)
W1B	10.08	13.11	11.30
F1B	12.35	9.22	12.50
VF1B	17.18	16.12	15.20
CP	21.52	22.07	21.90
W1T	27.15	24.85	26.80
W2B	32.88	35.95	34.80
VF2B	41.58	50.23	45.20
W3B	45.85	52.80	51.70
VF1T	48.95	44.09	50.00
IFT	50.83	61.00	51.00

Table 3.4.2A Natural Frequencies of the X-29A Aircraft (Anti-Symmetric)

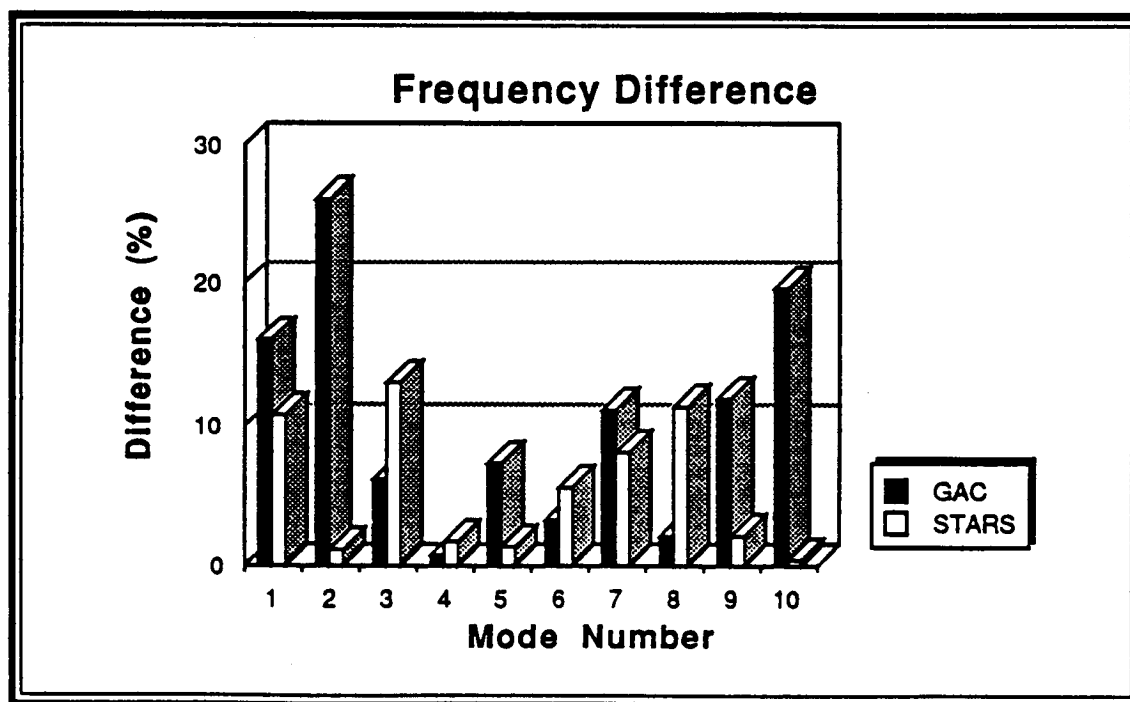


Figure 3.4.2A Natural Frequency Difference With Respect to GVS Results

MODE	STARS Gen. Mass (lb)	GAC Gen. Mass (lb)	GVS Gen. Mass (lb)
W1B	57.60	483.7	75.10
F1B	757.7	688.5	426.1
VF1B	47.60	16.30	18.60
CP	21.50	34.10	14.00
W1T	84.60	116.7	41.10
W2B	51.00	49.90	31.10
VF2B	7.10	9.80	6.80
W3B	275.4	—	11.10
VF1T	21.60	39.10	4.60
IFT	39.50	—	4.60

Table 3.4.2B Generalized Mass Values of the X-29A Aircraft (Anti-Symmetric)

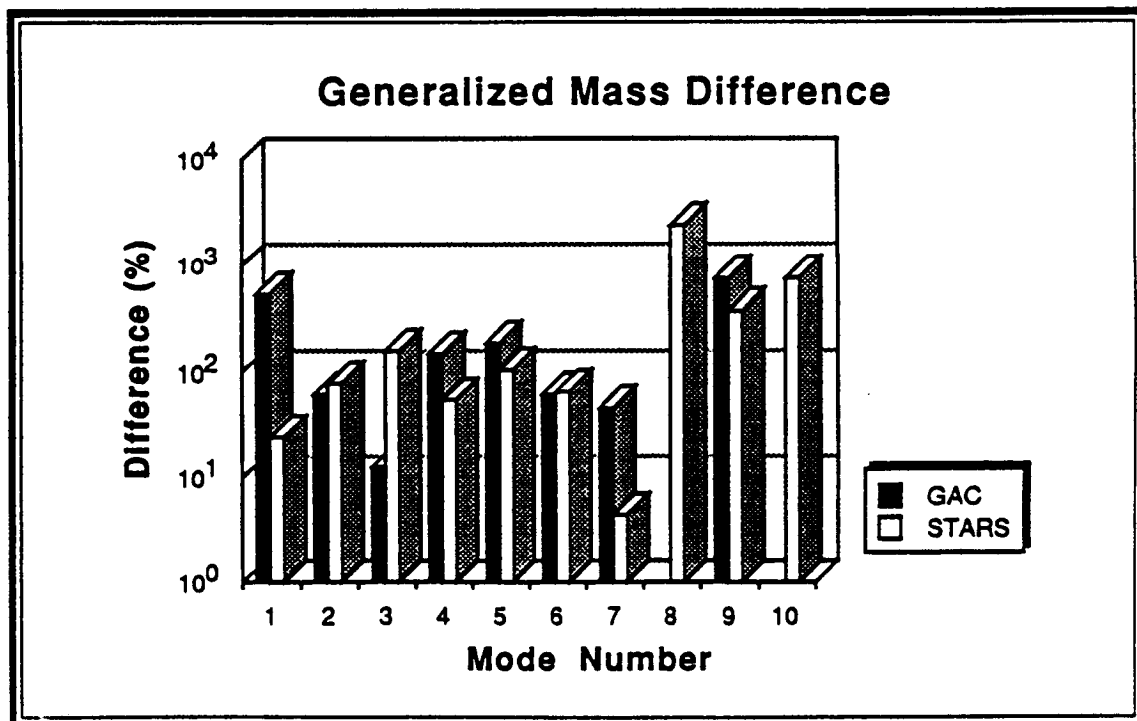


Figure 3.4.2B Generalized Mass Difference With Respect to GVS Results

### **3.4.2.1 Wing First Bending (W1B)**

The natural frequency calculated by the STARS is 10.8% lower while that calculated by the GAC is 16.0% higher than the measured value. Such discrepancy can be better understood by examining the next natural mode, the fuselage first bending (Figures - 3.4.2.2A-1 through 3.4.2.2A-4). Both modes are quite similar in natural mode-shape and close in natural frequency, indicating a high degree of structural coupling. Under such circumstances, relatively small errors in the analytical modelling can result in disproportionately large differences in the modal amplitude. For the wing first bending mode, the generalized mass from the STARS agrees reasonably well with that from the GVS, but the generalized mass from the GAC does not. Also, reasonably good agreement exists among the three sources in terms of the natural mode-shape and the node lines (Figures - 3.4.2.1A-1 through 3.4.2.1A-4).

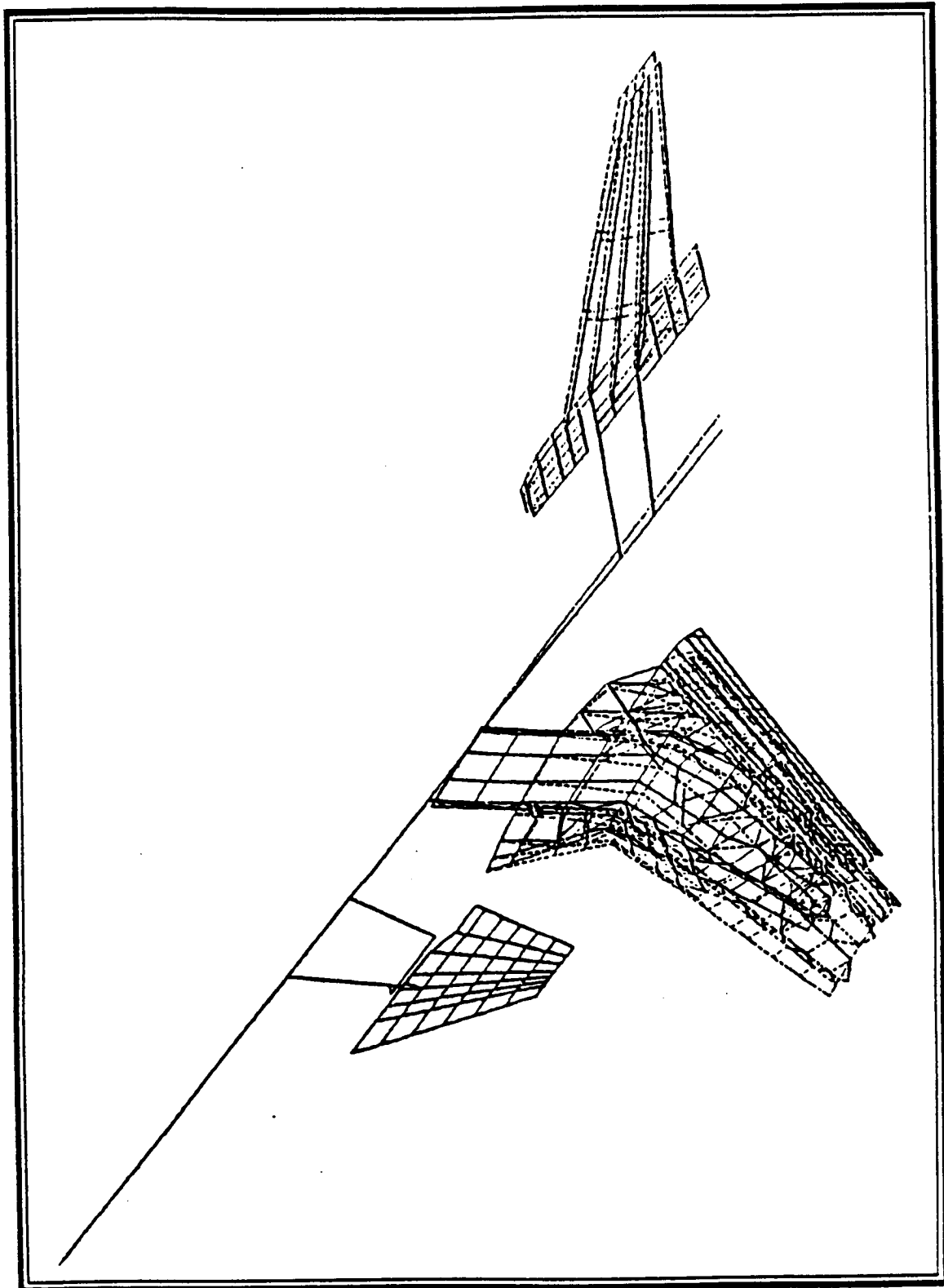


Figure 3.4.2.1A-1 STARS Wing First Bending Mode

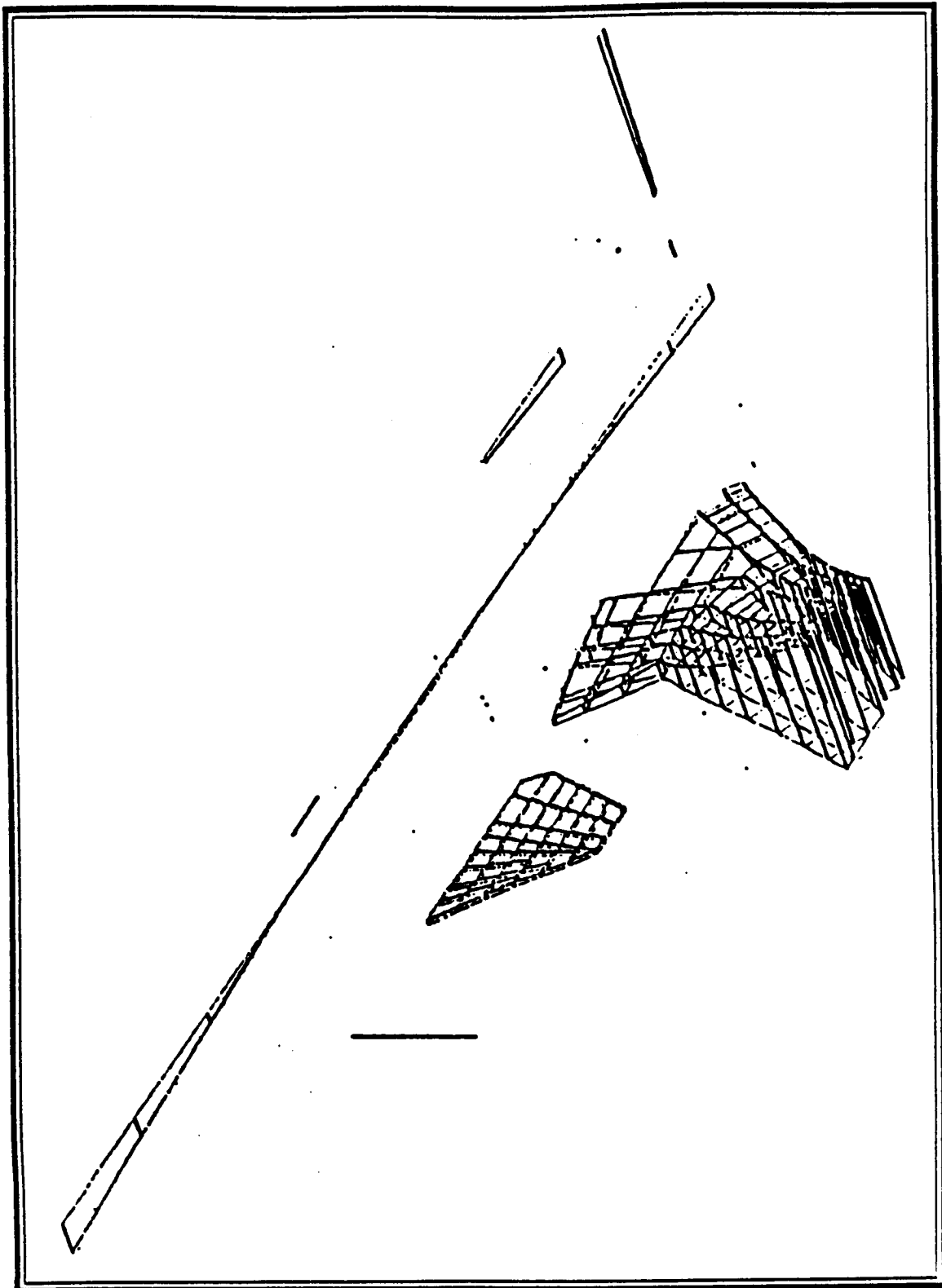


Figure 3.4.2.1A-2 GAC Wing First Bending Mode

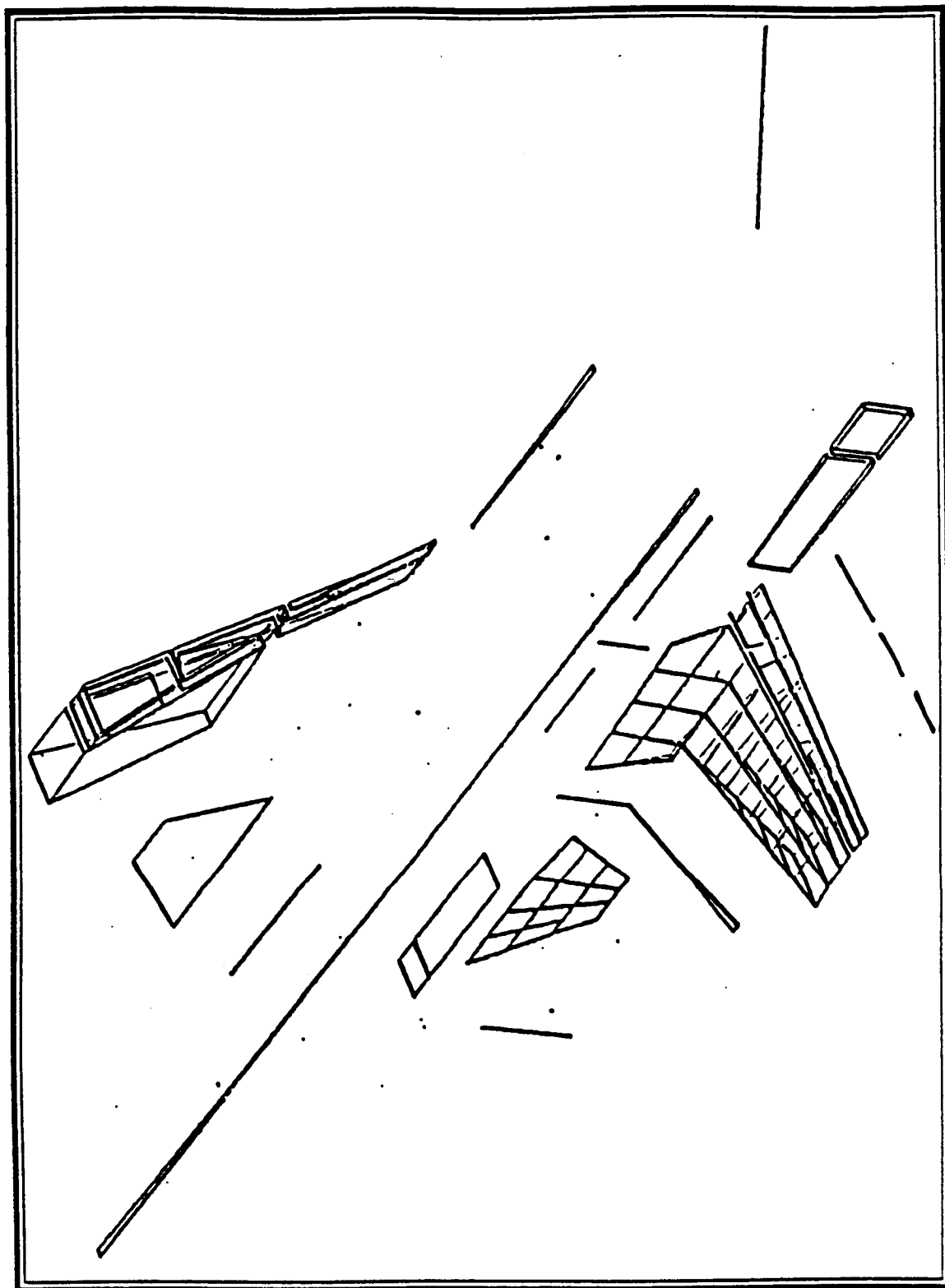


Figure 3.4.2.1A-3 GVS Wing First Bending Mode

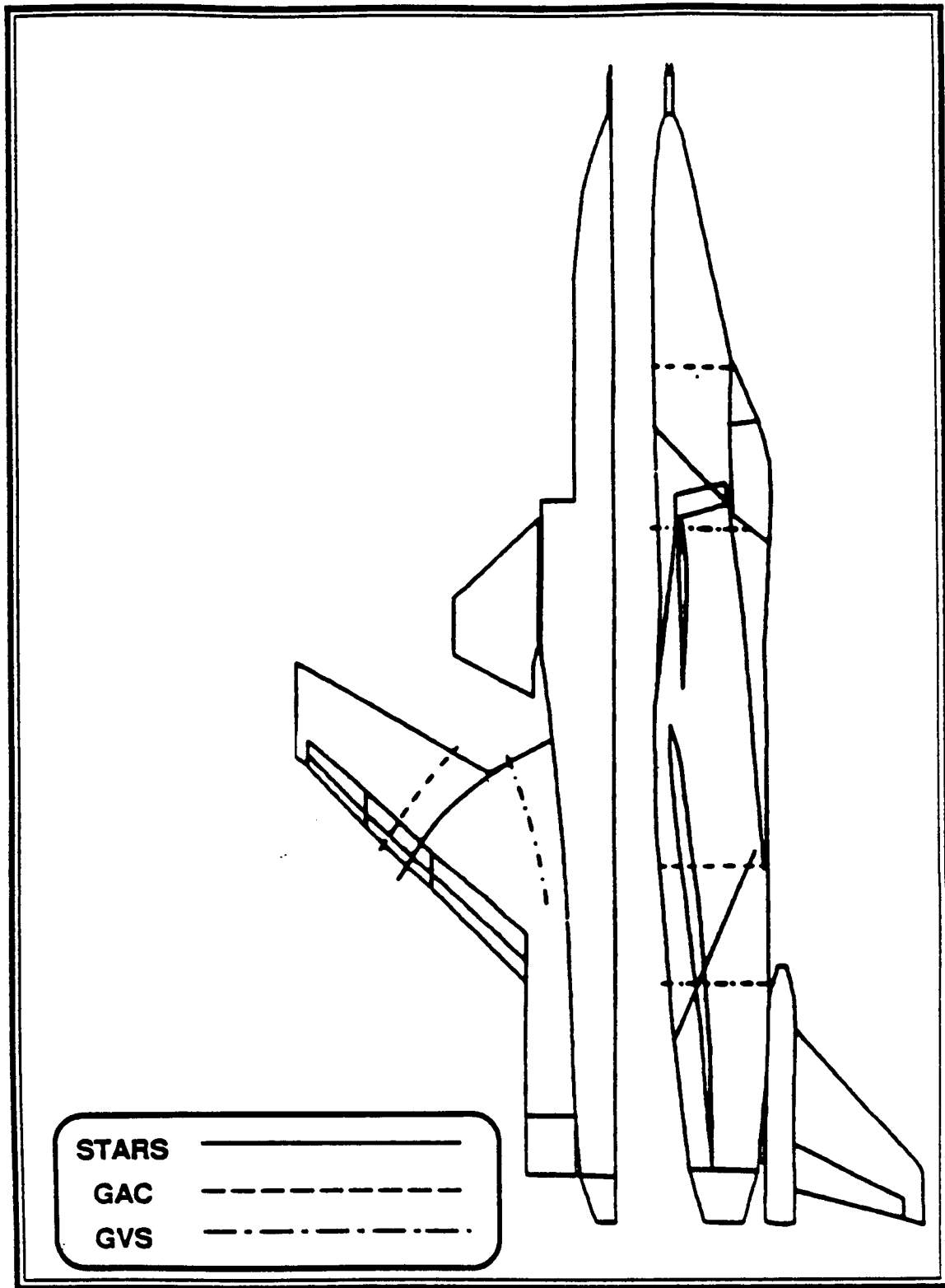


Figure 3.4.2.1A-4 Wing First Bending Node Lines



#### **3.4.2.2 Fuselage First Bending (F1B)**

There is good agreement in the natural frequency between the STARS and the GVS. However, the natural frequency obtained by GAC is on the low side. The natural mode-shapes and node lines (Figures - 3.4.2.2A-1 through 3.4.2.2A-4) obtained from the three sources are in good agreement.

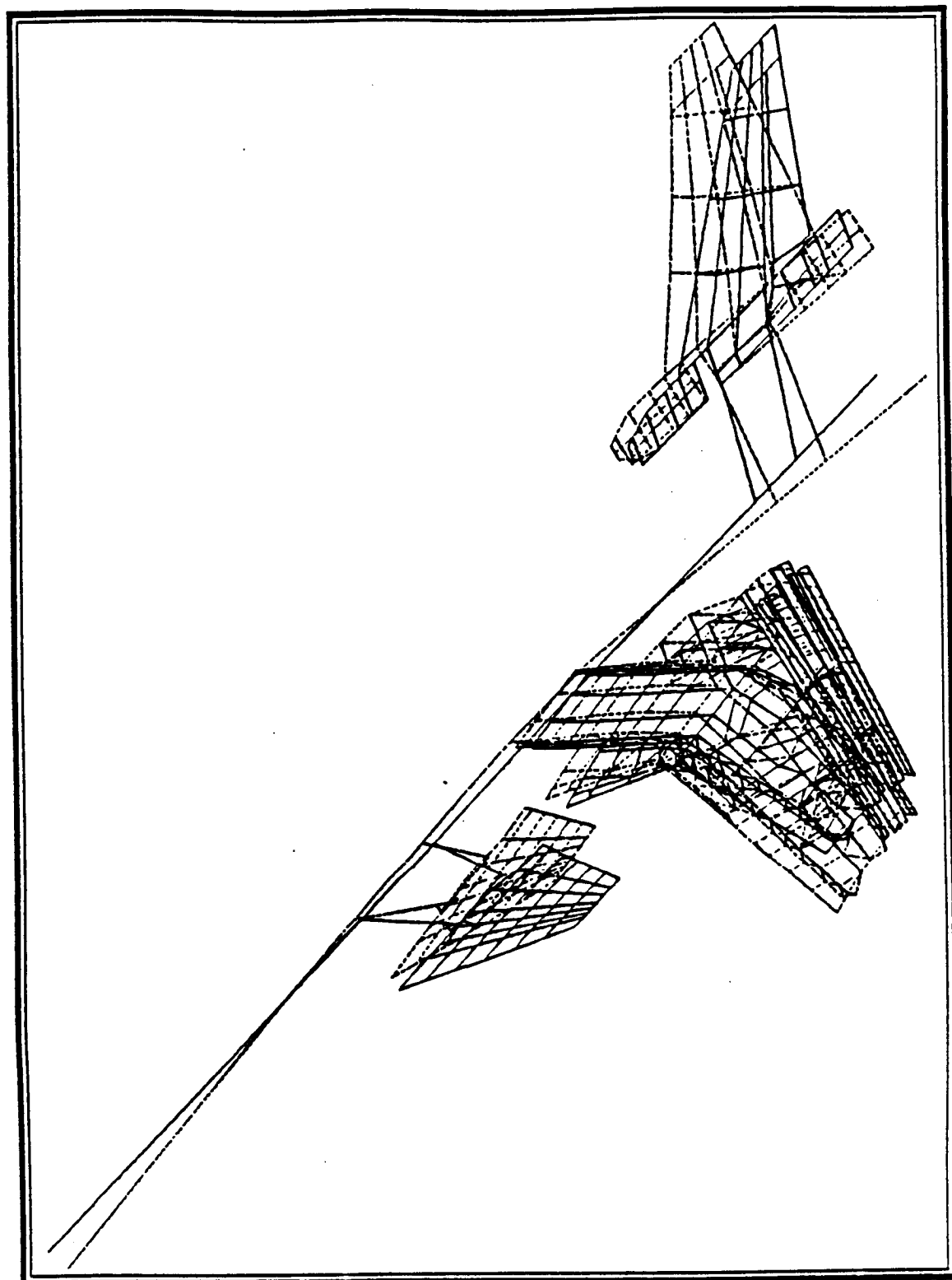


Figure 3.4.2.2A-1 STARS Fuselage First Bending Mode

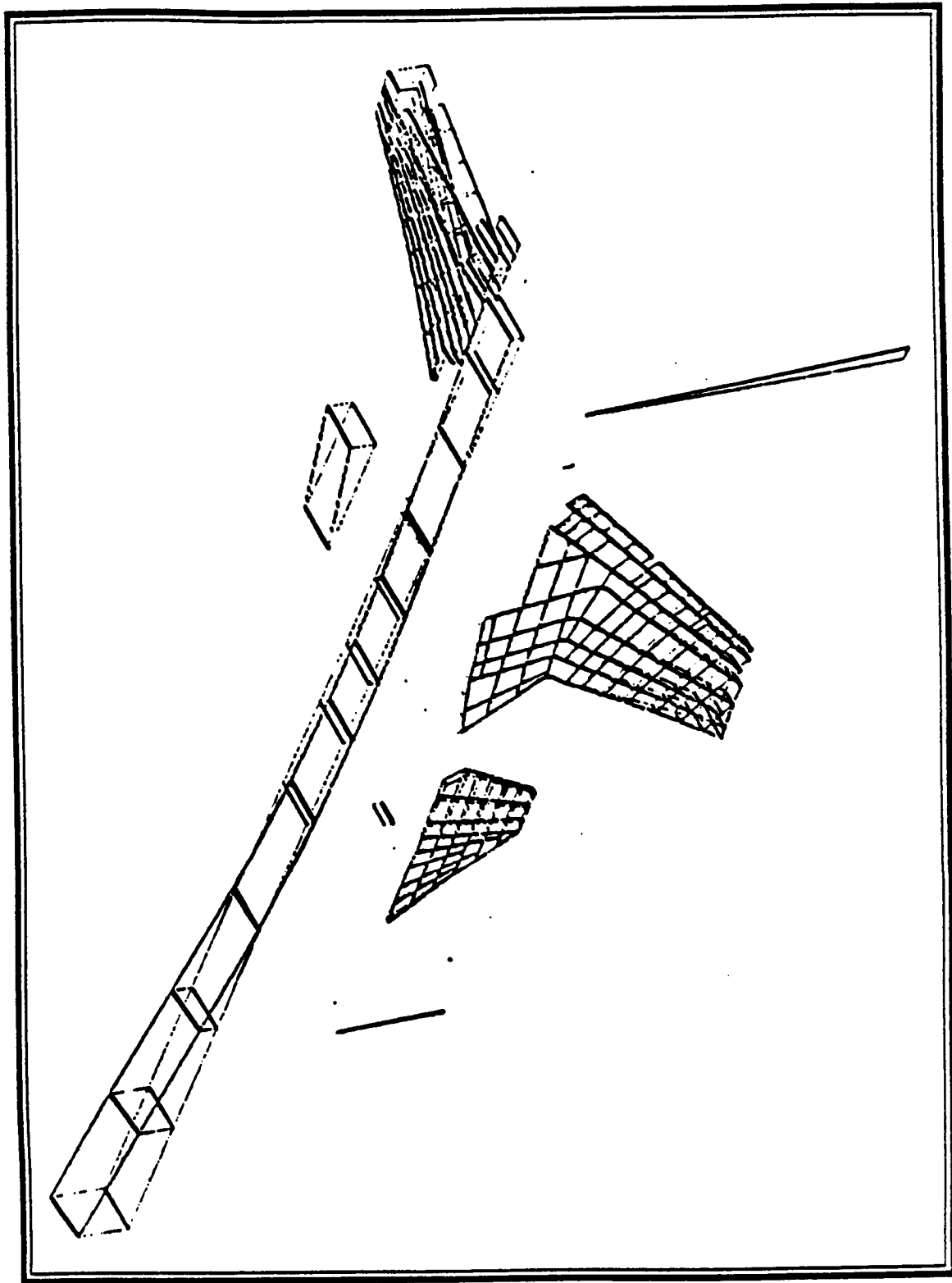


Figure 3.4.2.2A-2 GAC Fuselage First Bending Mode

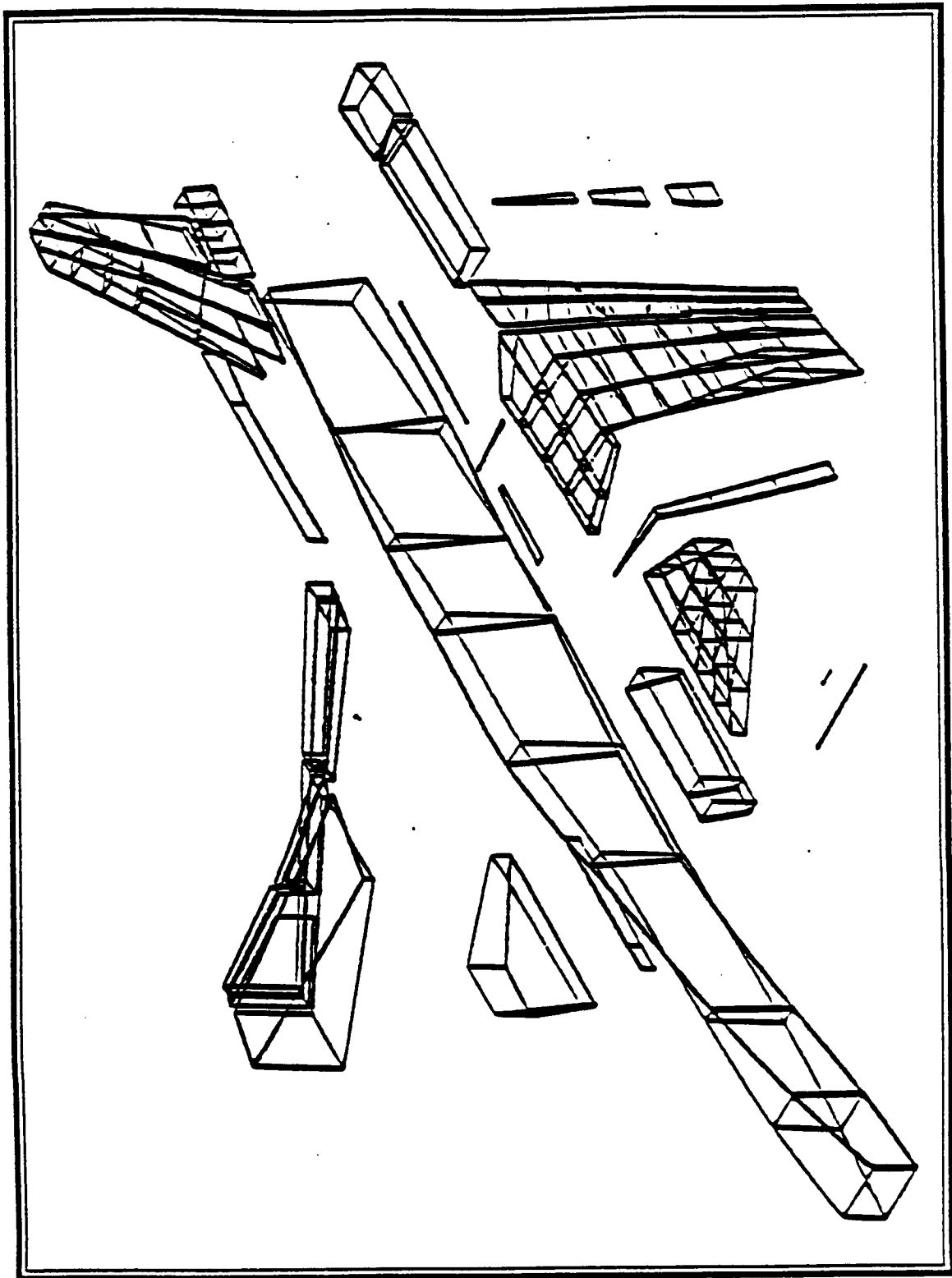


Figure 3.4.2.2A-3 GVS Fuselage First Bending Mode

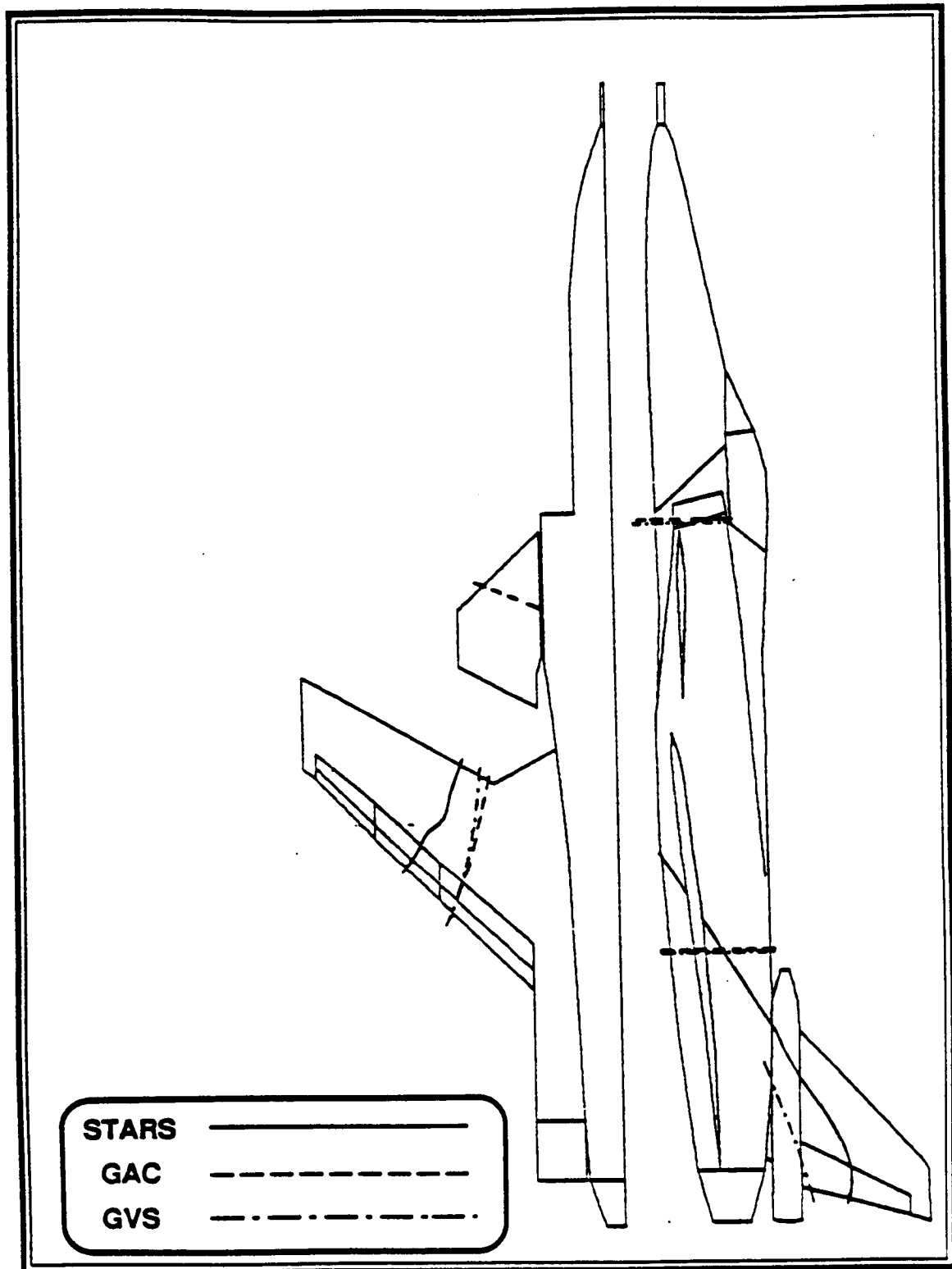


Figure 3.4.2.2A-4 Fuselage First Bending Node Lines

### 3.4.3 Flutter / Divergence Analysis ( Symmetric )

The free vibration analysis results obtained by the three sources, (STARS, GAC, and GVS) are used in the flutter/divergence analyses of the X-29A aircraft. A summary of the divergence and flutter speeds are given in Tables - 3.4.3A and 3.4.3B. The plots of the change in natural frequency versus the flight speed, and the change in damping versus the flight speed, are shown in Figures - 3.4.3A-1.1 through 3.4.3A-3.2. A review of the three sets of results for each mode follows.

MODE	STARS Speed (KTS)	GAC Speed (KTS)	GVS Speed (KTS)
W1B	806	820	808
CP	1082	1160	980

Table 3.4.3A Divergence Speeds (Symmetric)

MODE	STARS Speed (KTS)	GAC Speed (KTS)	GVS Speed (KTS)
F1B	848	—	924
F2B	—	1162	—
W2B	1058	—	1315
CBP	—	—	677

Table 3.4.3B Flutter Speeds (Symmetric)

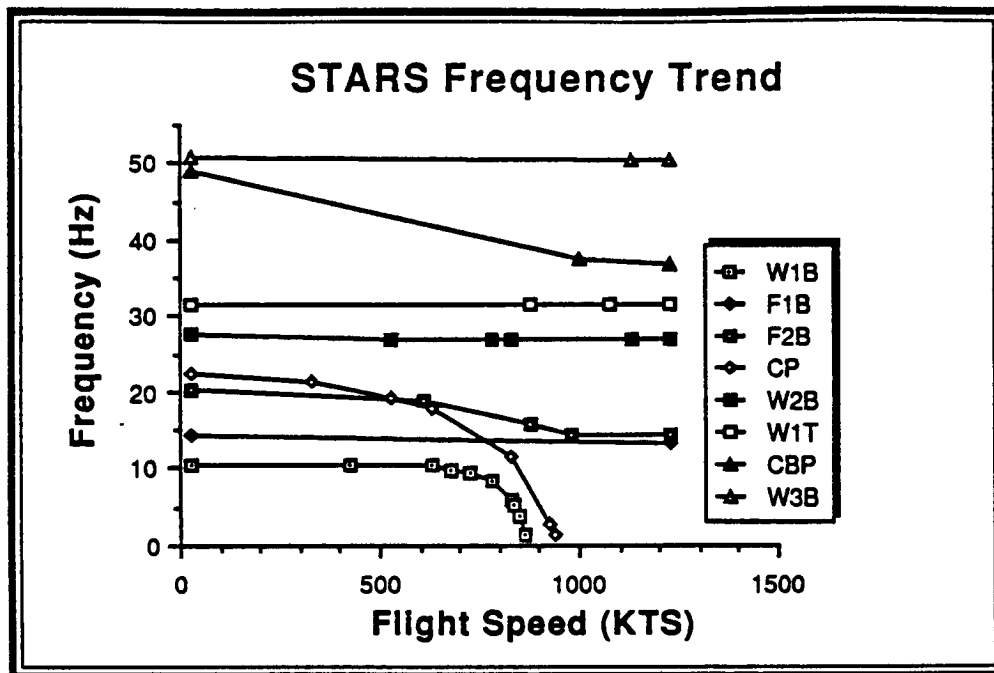


Figure 3.4.3A-1.1 STARS Frequency Trend (Symmetric)

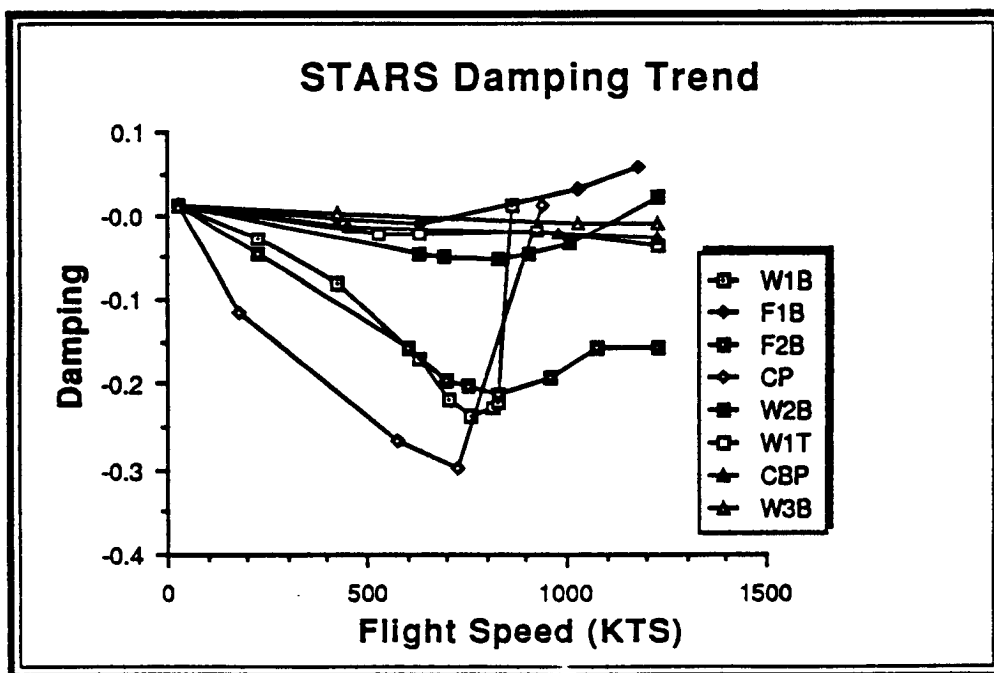


Figure 3.4.3A-1.2 STARS Damping Trend (Symmetric)

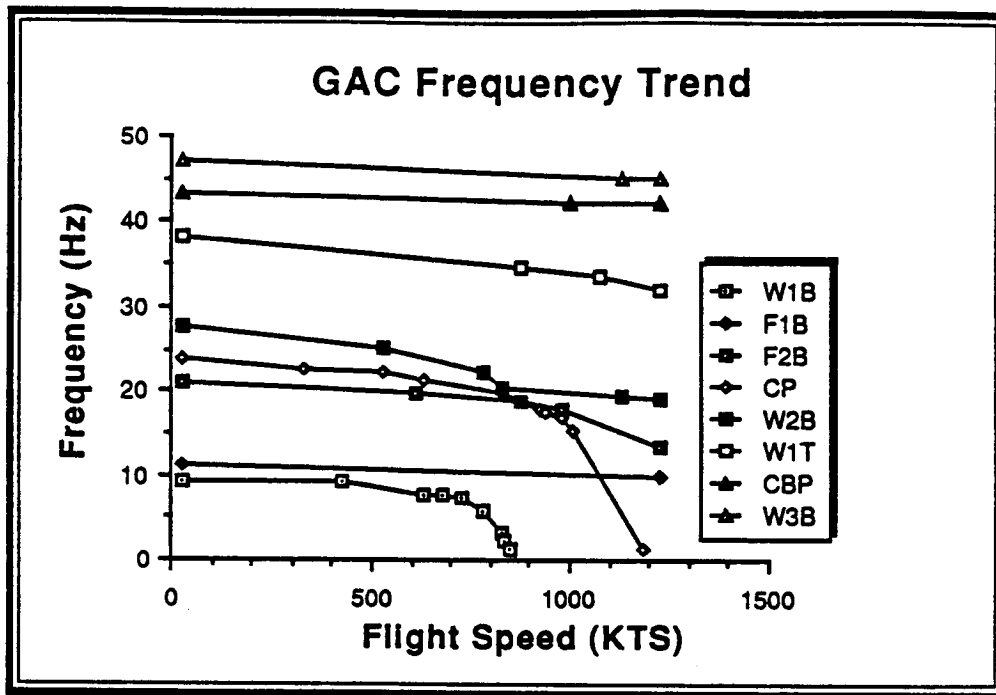


Figure 3.4.3A-2.1 GAC Frequency Trend (Symmetric)

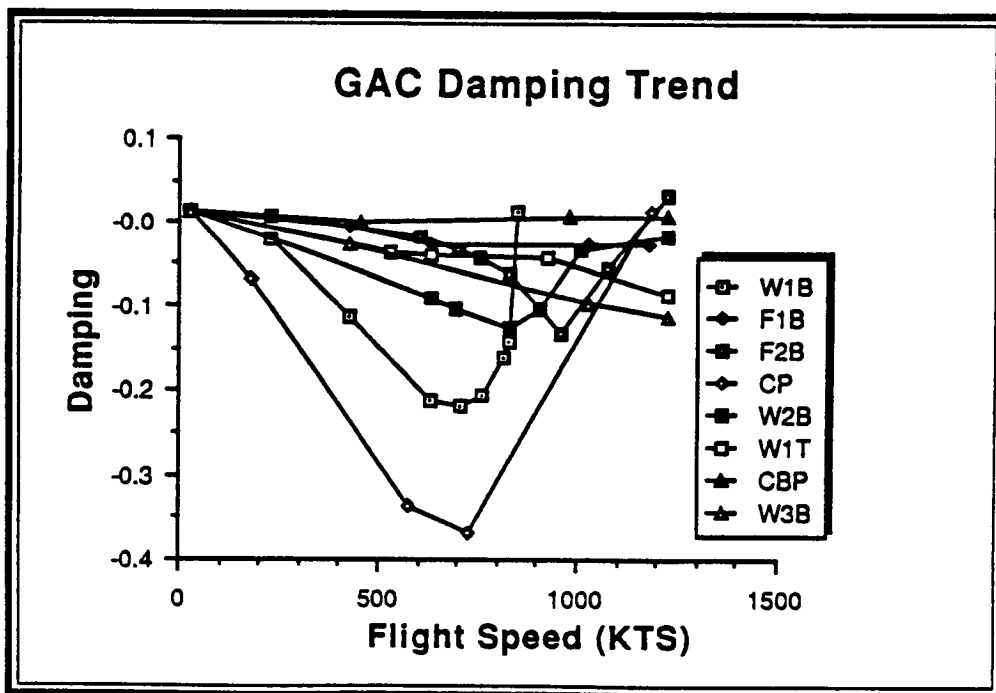


Figure 3.4.3A-2.2 GAC Damping Trend (Symmetric)



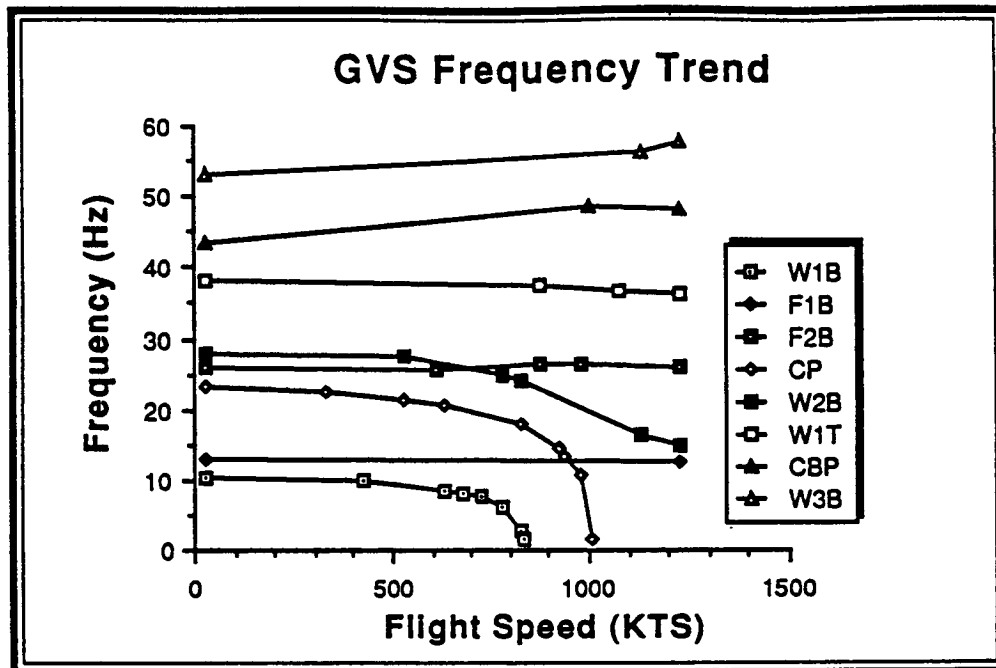


Figure 3.4.3A-3.1 GVS Frequency Trend (Symmetric)

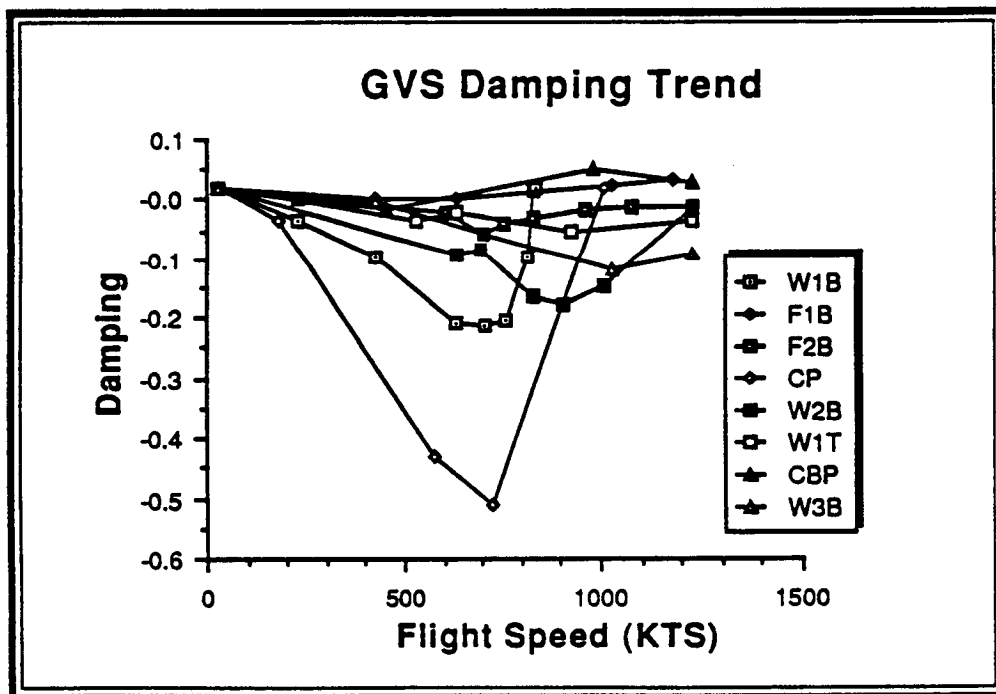


Figure 3.4.3A-3.2 GVS Damping Trend (Symmetric)

### 3.4.3.1 Wing First Bending (W1B)

This is the primary mode leading to the wing divergence (Figures - 3.4.3.1A-1 and 3.4.3.1A-2). There is good agreement in the divergence speed of the wing among the three sources.

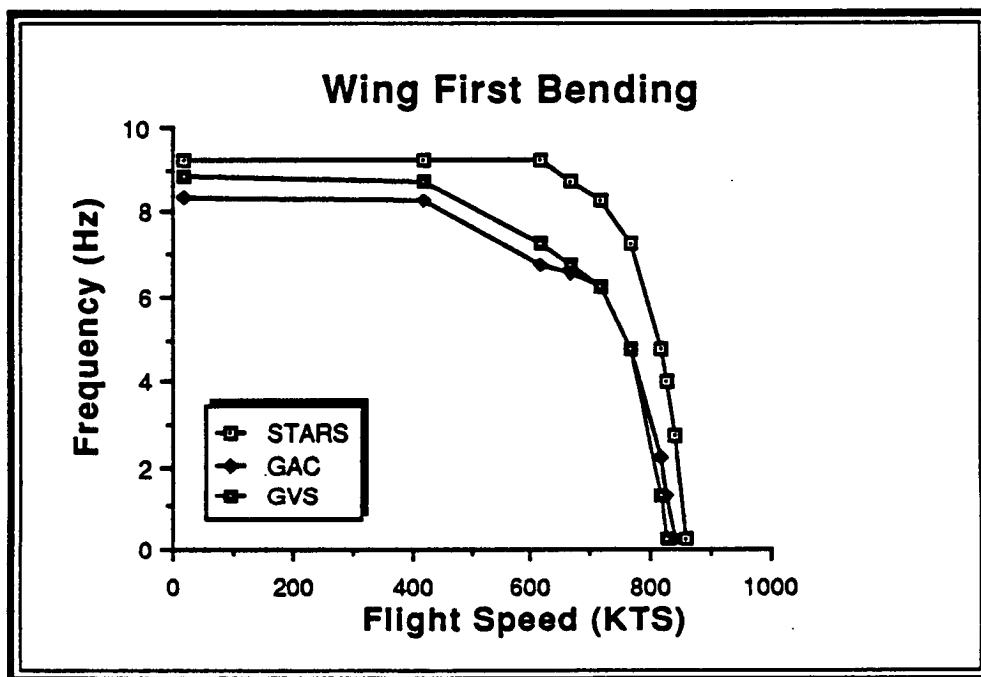


Figure 3.4.3.1A-1 Wing First Bending Frequency (Symmetric)

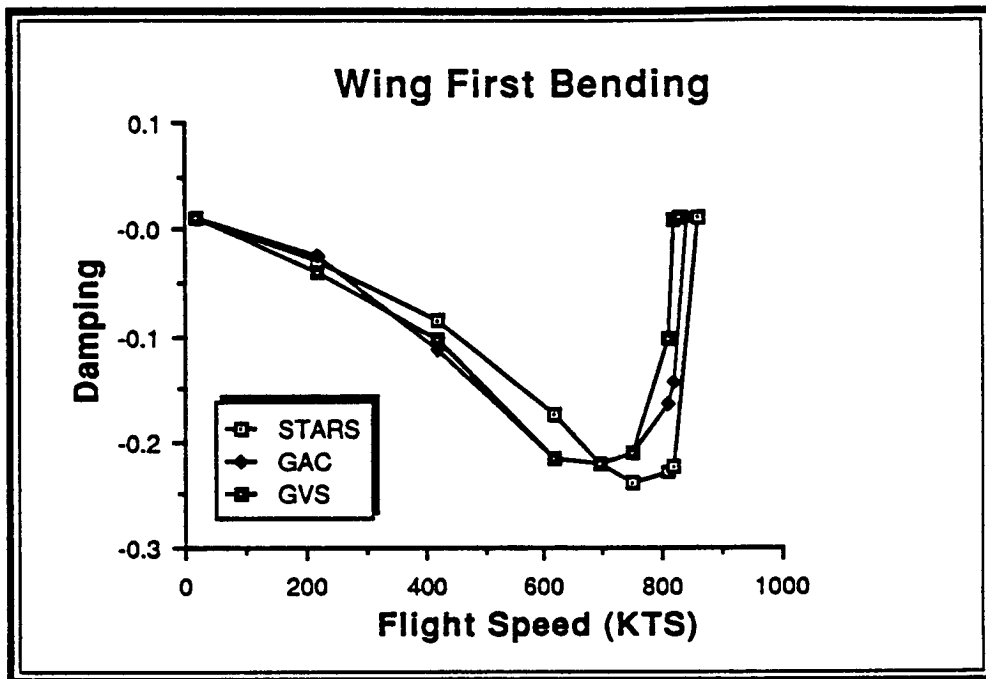


Figure 3.4.3.1A-2 Wing First Bending Damping (Symmetric)

### 3.4.3.2 Fuselage First Bending (F1B)

The STARS and the GVS analyses predict very shallow crossings (Figure - 3.4.3.2A-2) not evidenced by the GAC analysis. A shallow crossing is known as a mild form of flutter. This is a very important factor during flight test, for it gives advance warning of a flutter situation. The close agreement in the flutter speed between the STARS and the GVS results is remarkable for such a shallow crossing because with this condition, small variations in the modal input data can produce large discrepancies in results.

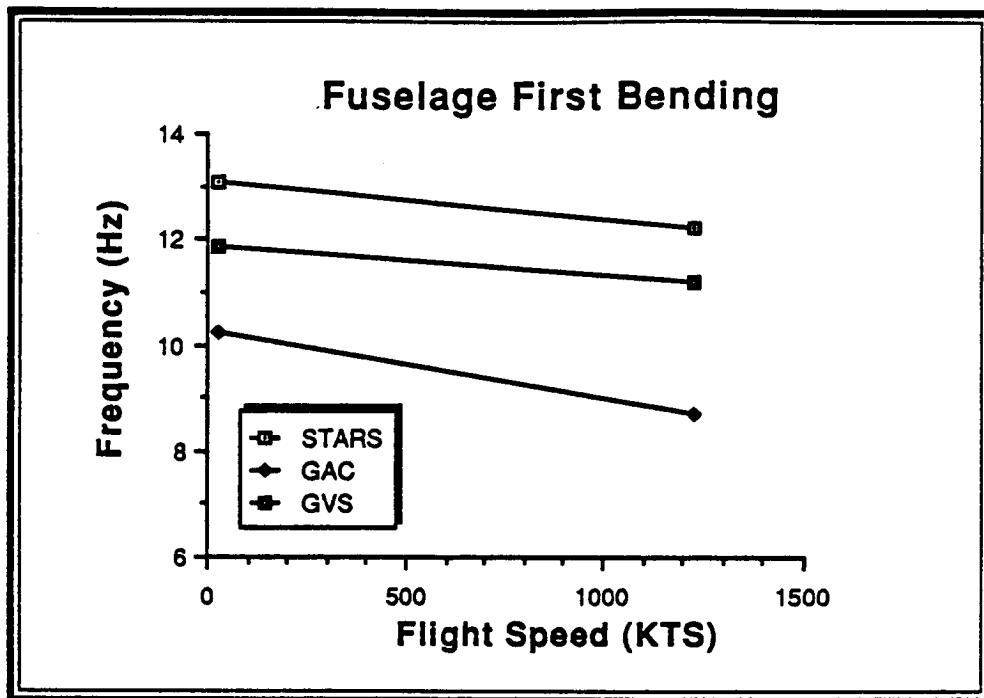


Figure 3.4.3.2A-1 Fuselage First Bending Frequency (Symmetric)

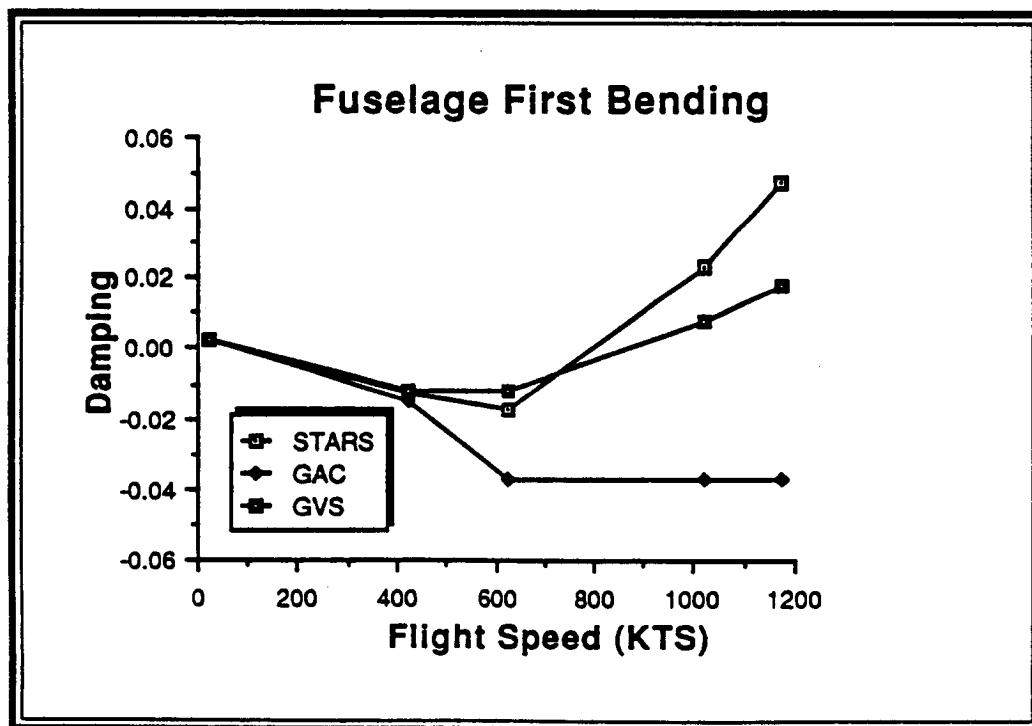


Figure 3.4.3.2A-2 Fuselage First Bending Damping (Symmetric)

### 3.4.3.3 Fuselage Second Bending (F2B)

The agreement in natural frequency and damping (Figures - 3.4.3.3A-1 and 3.4.3.3A-2) is not very close among the three sources. The GAC analysis predicts a flutter instability crossing not evidenced by either the GVS or the STARS analyses.

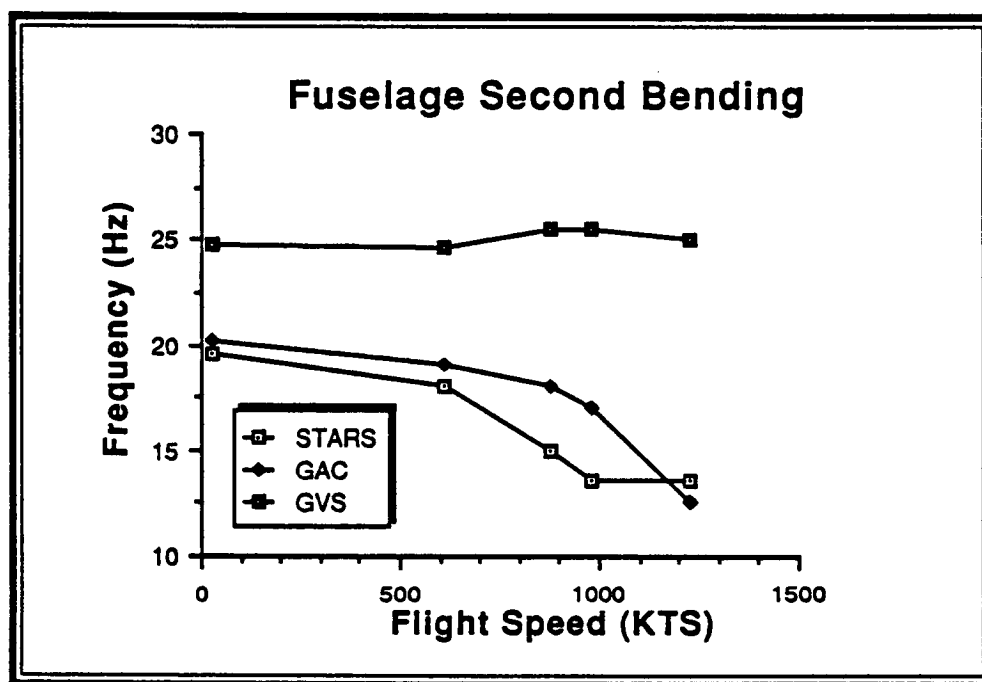


Figure 3.4.3.3A-1 Fuselage Second Bending Frequency (Symmetric)

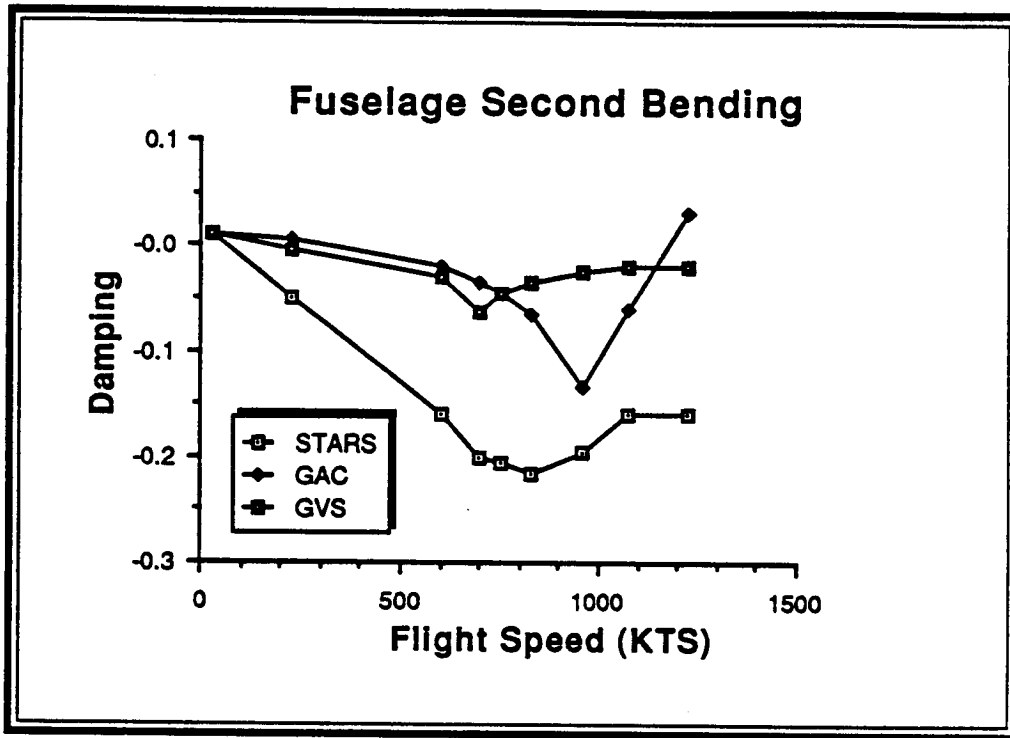


Figure 3.4.3.3A-2 Fuselage Second Bending Damping (Symmetric)

#### 3.4.3.4 Canard Pitch (CP)

This is the primary mode leading to the canard divergence (Figures - 3.4.3.4A-1 and 3.4.3.4A-2). There is good agreement between the STARS and the GVS results in all respects, but the GAC result does not agree well.

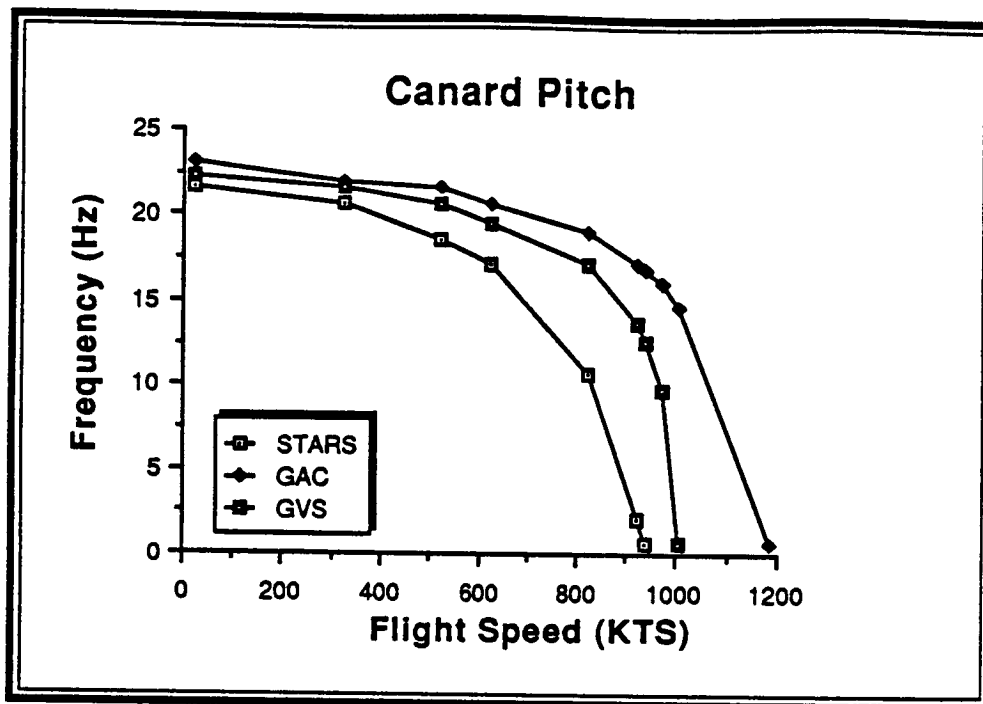


Figure 3.4.3.4A-1 Canard Pitch Frequency (Symmetric)

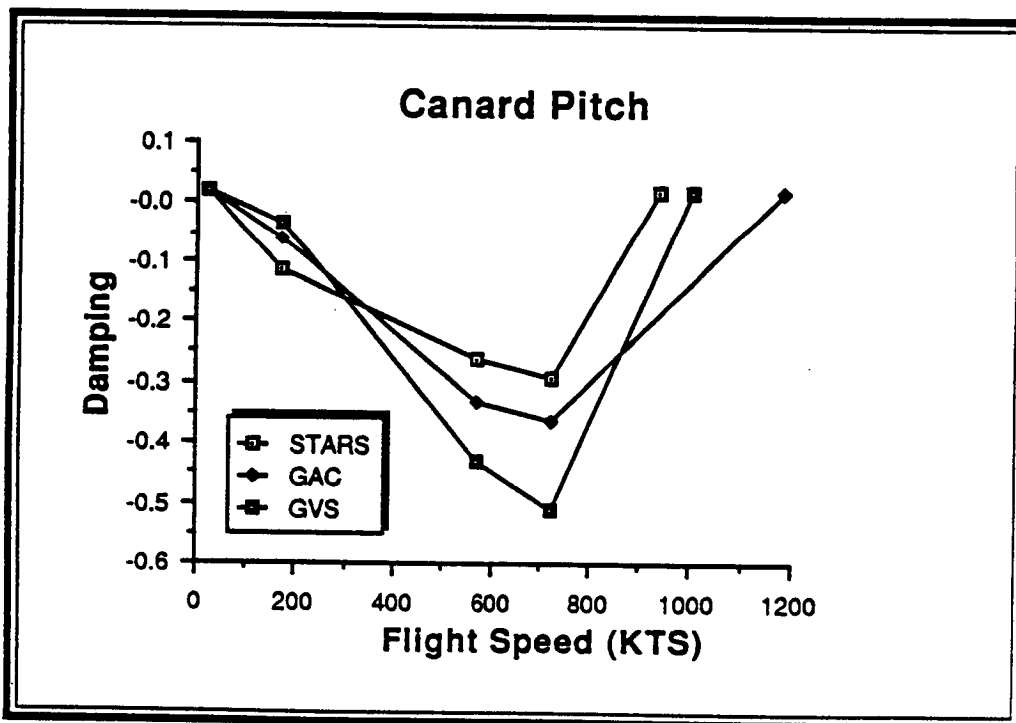


Figure 3.4.3.4A-2 Canard Pitch Damping (Symmetric)

### 3.4.3.5 Wing Second Bending (W2B)

Both the STARS and the GVS analysis predict somewhat similar crossings (Figure - 3.4.3.5A-2) with fairly close flutter speeds. However, the predicted flutter frequencies (Figure - 3.4.3.5A-1) do not agree well. The GAC analysis does not predict an instability crossing.

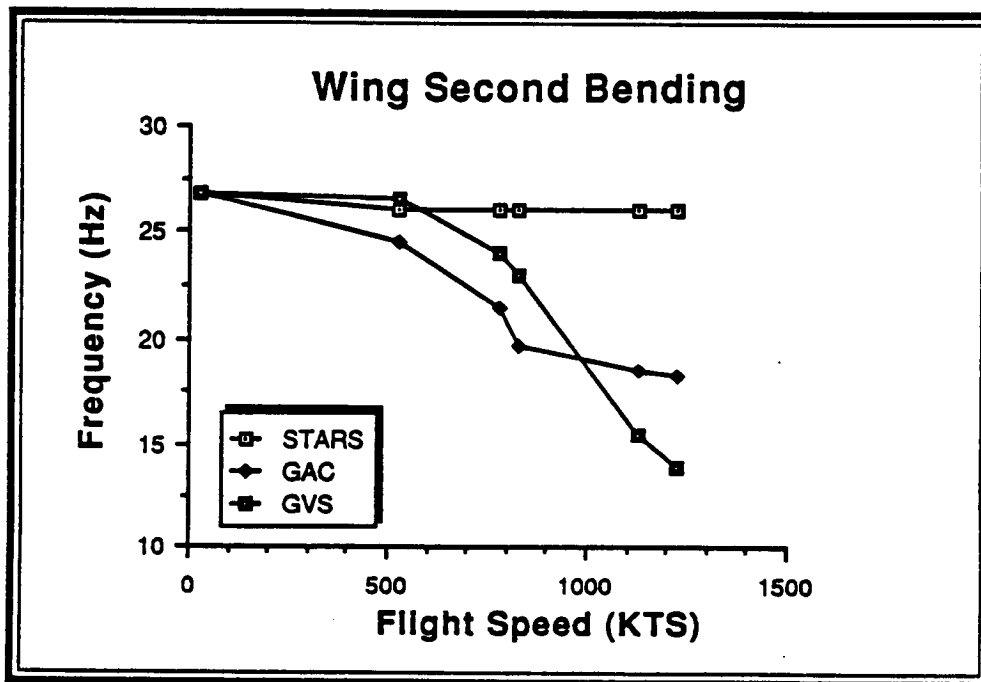


Figure 3.4.3.5A-1 Wing Second Bending Frequency (SYMMETRIC)



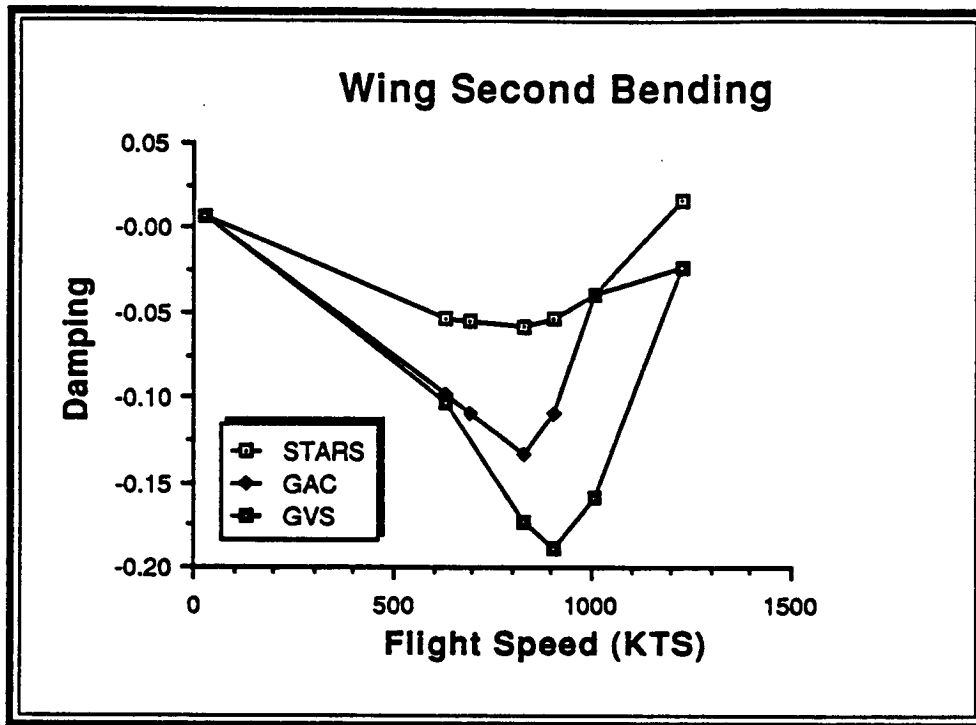


Figure 3.4.3.5A-2 Wing Second Bending Damping (Symmetric)

### 3.4.3.6 Wing First Torsion (W1T)

The three results seem to agree well in damping trends, which are fairly flat and without crossing (Figures - 3.4.3.6A-1 and 3.4.3.6A-2).

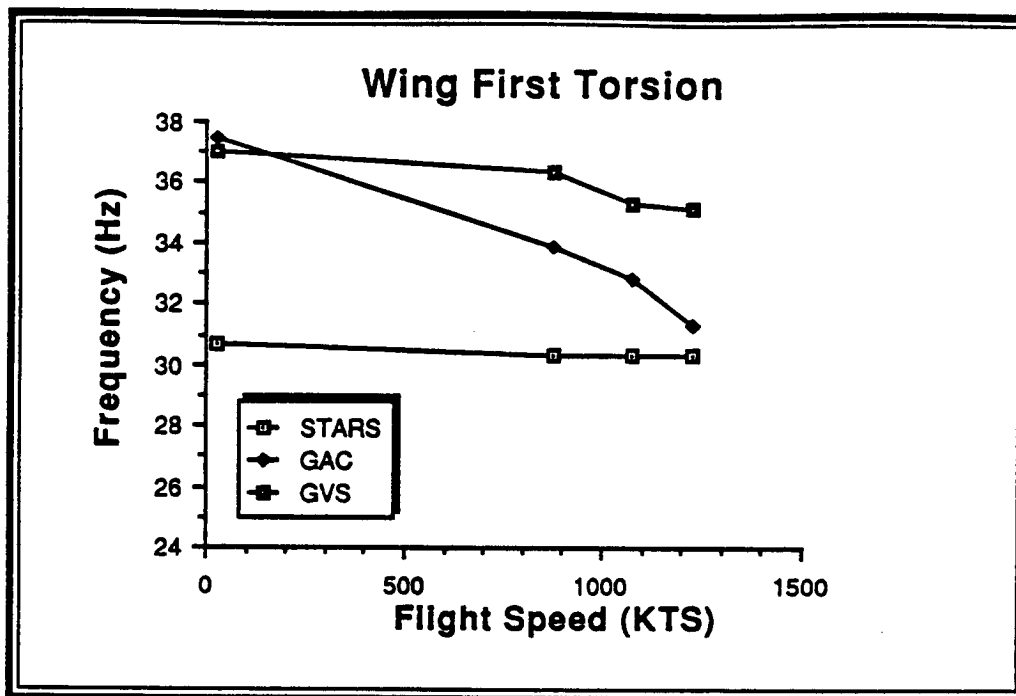


Figure 3.4.3.6A-1 Wing First Torsion Frequency (Symmetric)

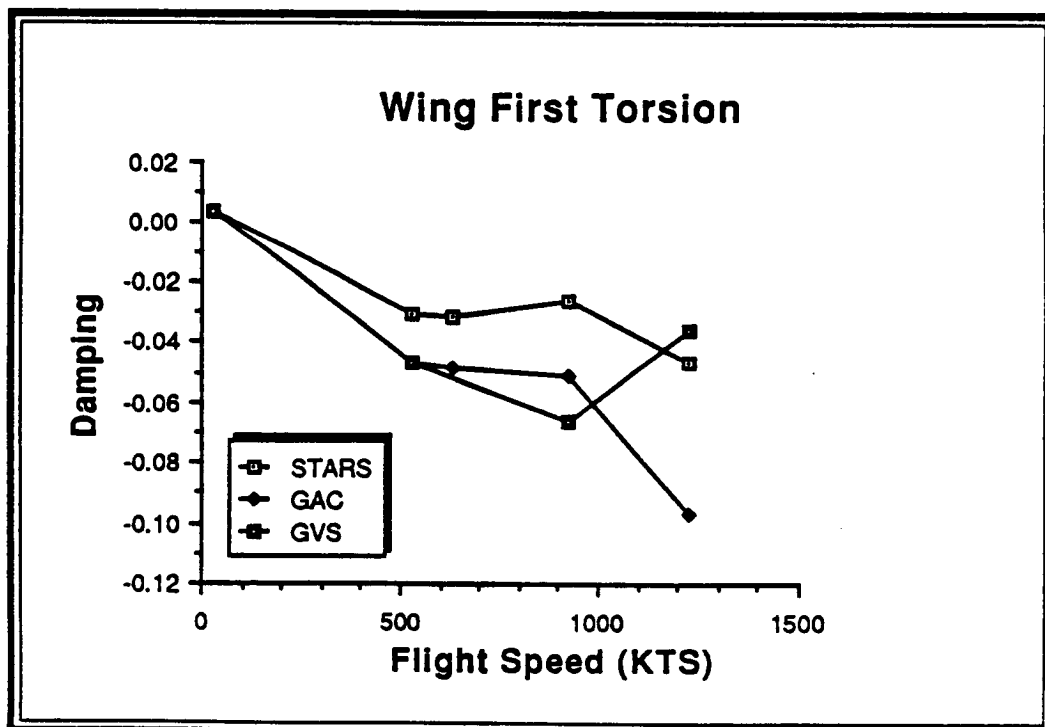


Figure 3.4.3.6A-2 Wing First Torsion Damping (Symmetric)

### 3.4.3.7 Canard Bending-Pitch (CBP)

There is poor agreement between the STARS and the GVS results and also between the GAC and the GVS results (Figures - 3.4.3.7A-1 and 3.4.3.7A-2). The GVS results show a canard flutter instability which is not present in the other two cases.

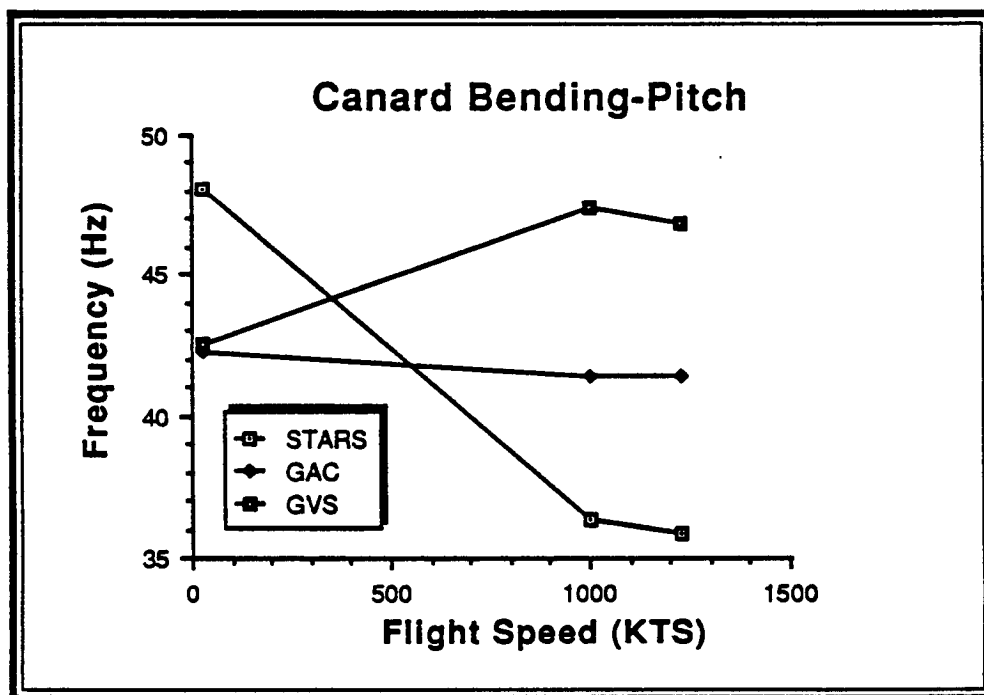
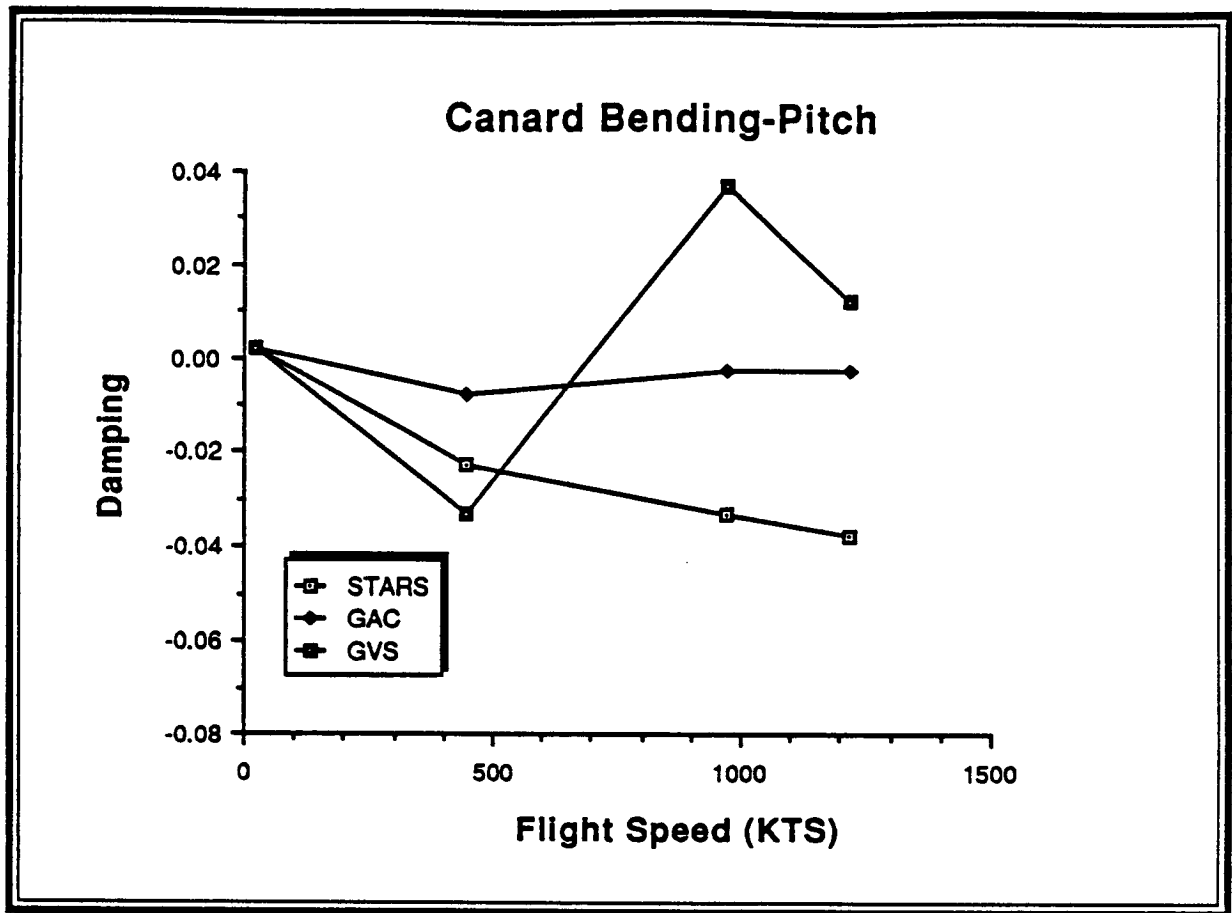


Figure 3.4.3.7A-1 Canard Bending Pitch Frequency (Symmetric)



**Figure 3.4.3.7A-2** Canard Bending Pitch Damping (Symmetric)

### 3.4.3.8 Wing Third Bending ( W3B )

None of the three analyses predicts a crossing of this mode within the speed range considered (Figures - 3.4.3.8A-1 and 3.4.3.8A-2).

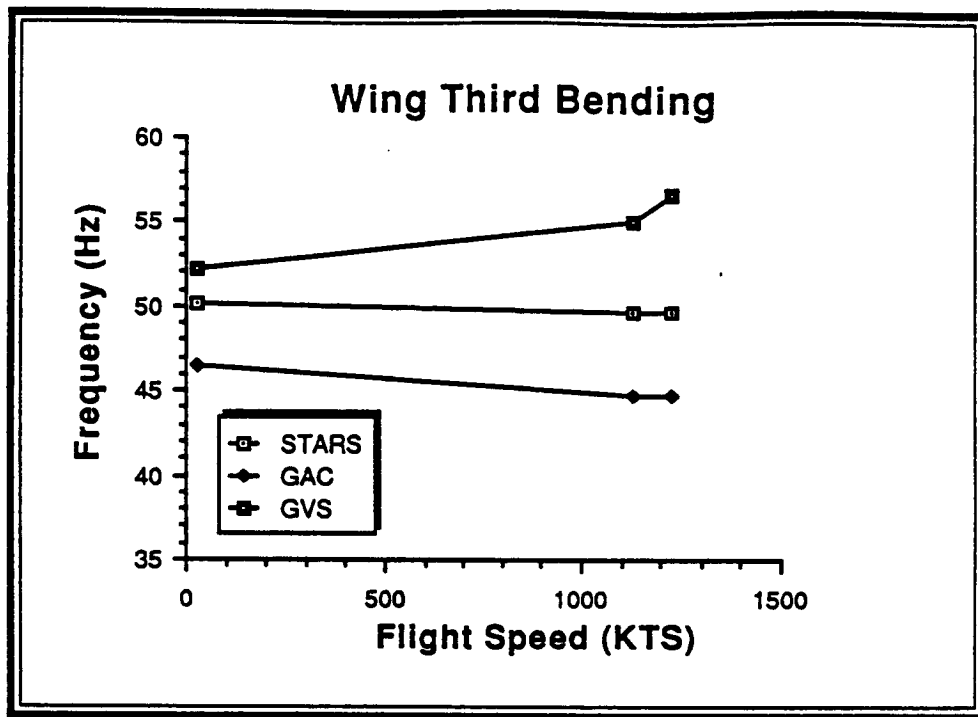


Figure 3.4.3.8A-1 Wing Third Bending Frequency (Symmetric)

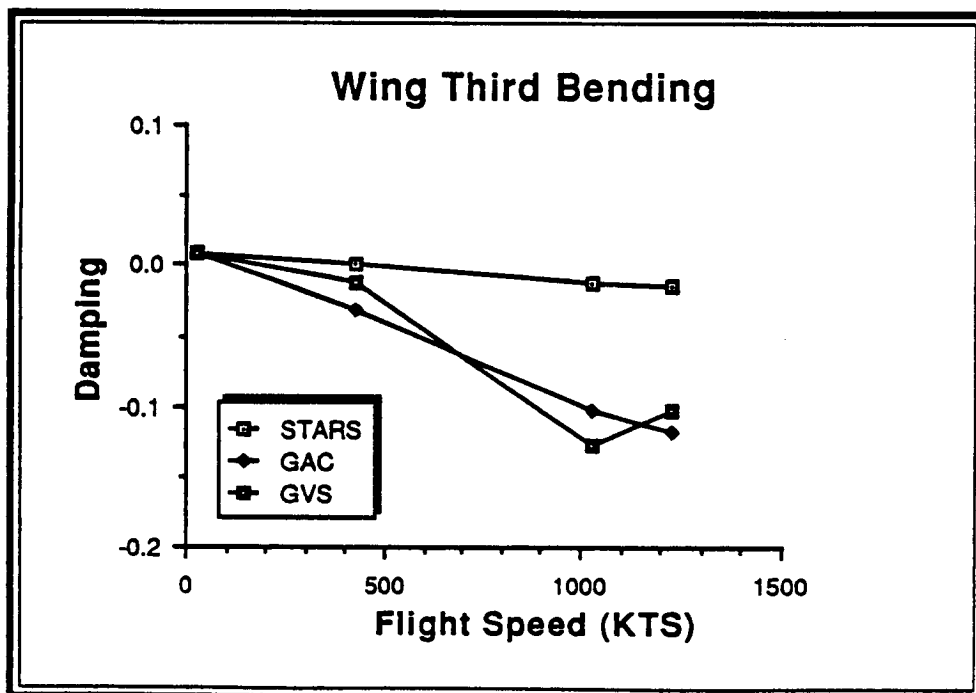


Figure 3.4.3.8A-2 Wing Third Bending Damping (Symmetric)

### 3.4.4 Flutter / Divergence Analysis ( Anti-Symmetric )

A summary of the predicted divergence and flutter speeds from the three sources is listed in Tables - 3.4.4A and 3.4.4B. The major differences are evident in the wing and the canard divergence speeds. The STARS wing divergence speed is 3.7% lower and the GAC wing divergence speed is 15.6% higher than the GVS wing divergence speed. The STARS canard divergence speed is 10.3% lower than the GVS canard divergence speed. The GAC analysis does not predict a canard divergence within the speed range considered. The STARS analysis predicts a flutter mechanism involving wing third bending, which agrees closely (+4.3%) in flutter speed with the GVS analysis. The GAC analysis was not available for the wing third bending mode. Plots of the change in natural frequency versus flight speed, and the change in damping versus flight speed, are shown in Figures 3.4.4A-1.1 through 3.4.4A-3.2. A critical review of the three sets of results for each mode follows.

MODE	STARS Speed(KTS)	GAC Speed(KTS)	GVS Speed(KTS)
W1B	833	1000	865
CP	912	—	1017

Table 3.4.4A Divergence Speeds (Anti-Symmetric)

MODE	STARS Speed (KTS)	GAC Speed (KTS)	GVS Speed (KTS)
CBP	—	765	694
W3B	1275	—	1222

Table 3.4.4B Flutter Speeds (Anti-Symmetric)

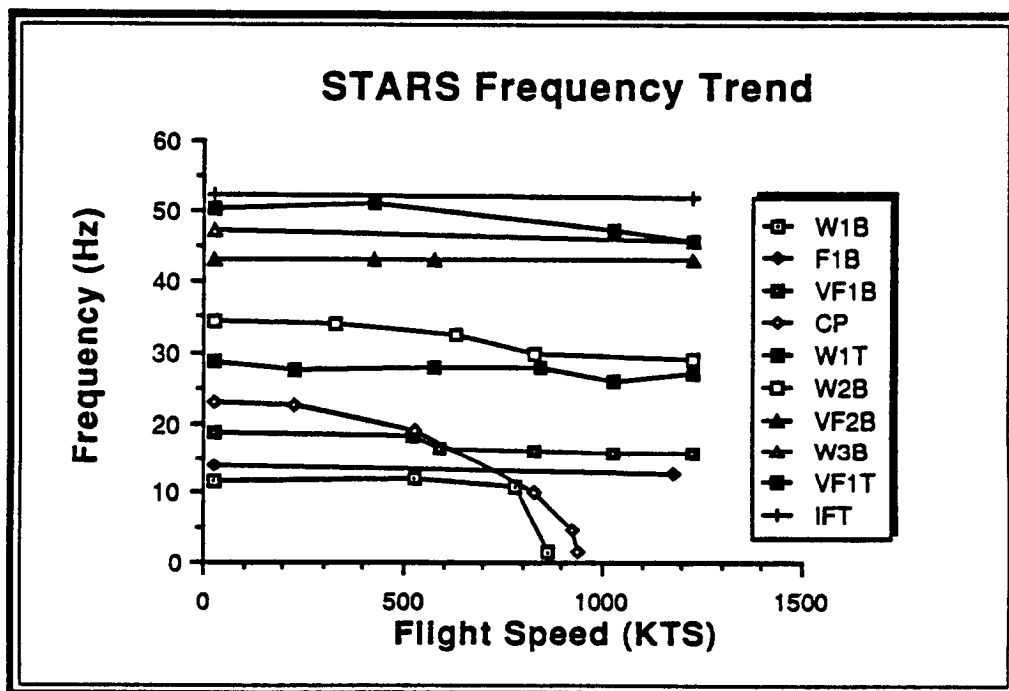


Figure 3.4.4A-1.1 STARS Frequency Trend (Anti-Symmetric)

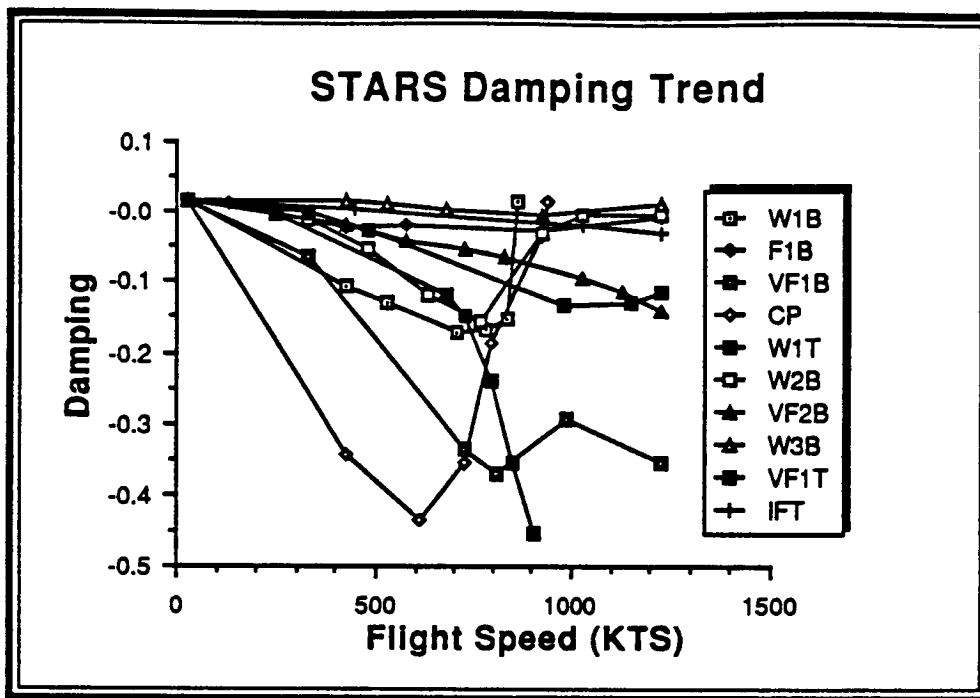


Figure 3.4.4A-1.2 STARS Damping Trend (Anti-Symmetric)

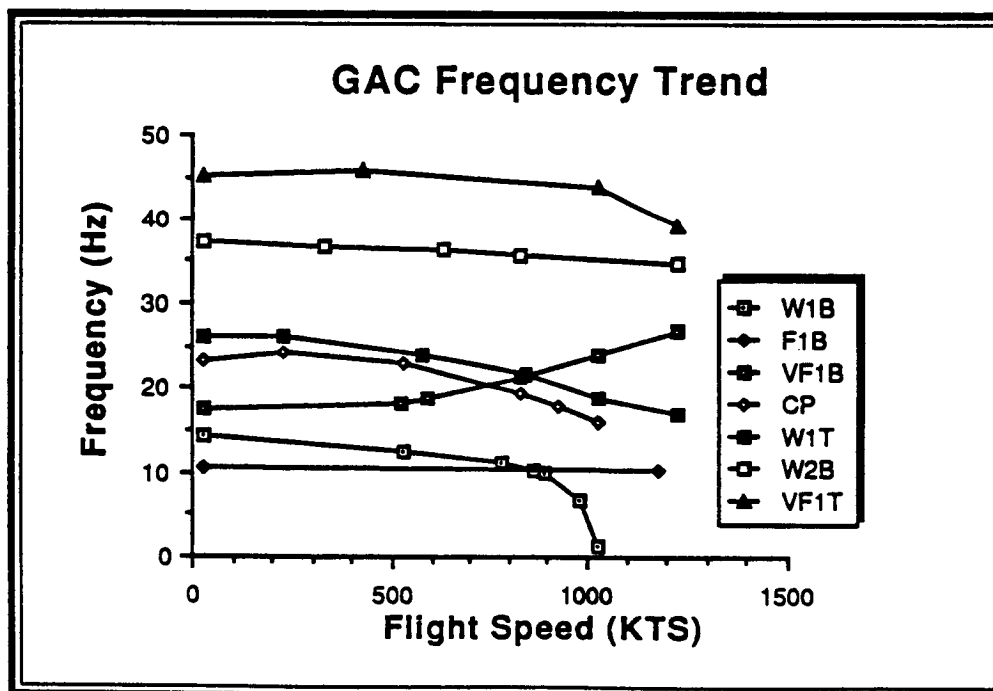


Figure 3.4.4A-2.1 GAC Frequency Trend (Anti-Symmetric)



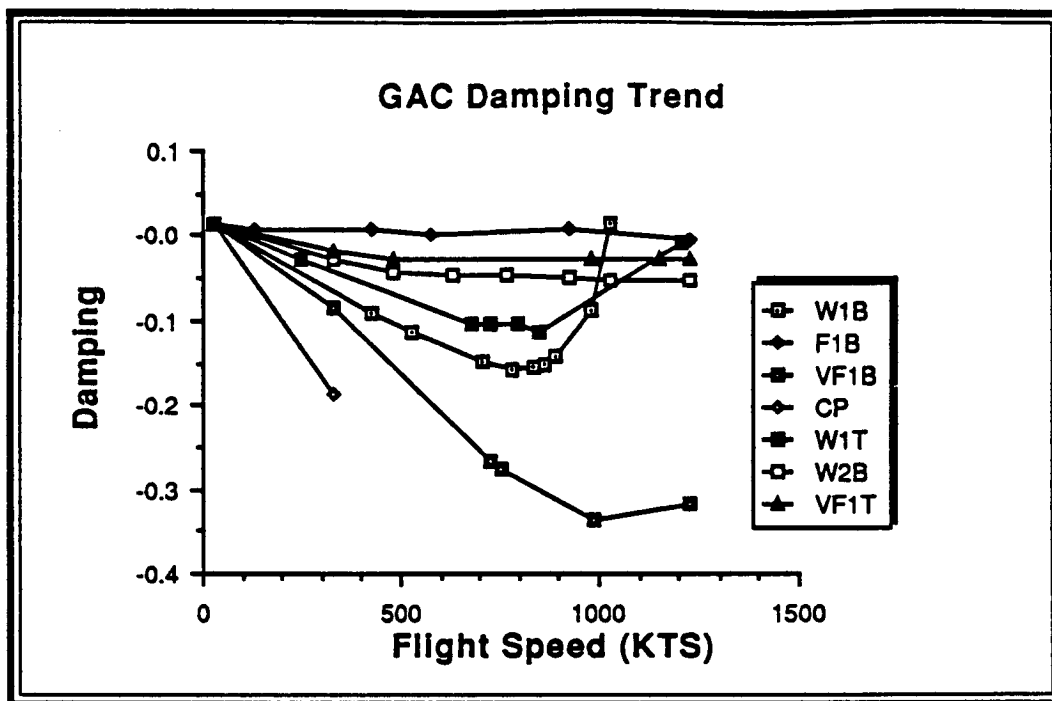


Figure 3.4.4A-2.2 GAC Damping Trend(Anti-Symmetric)

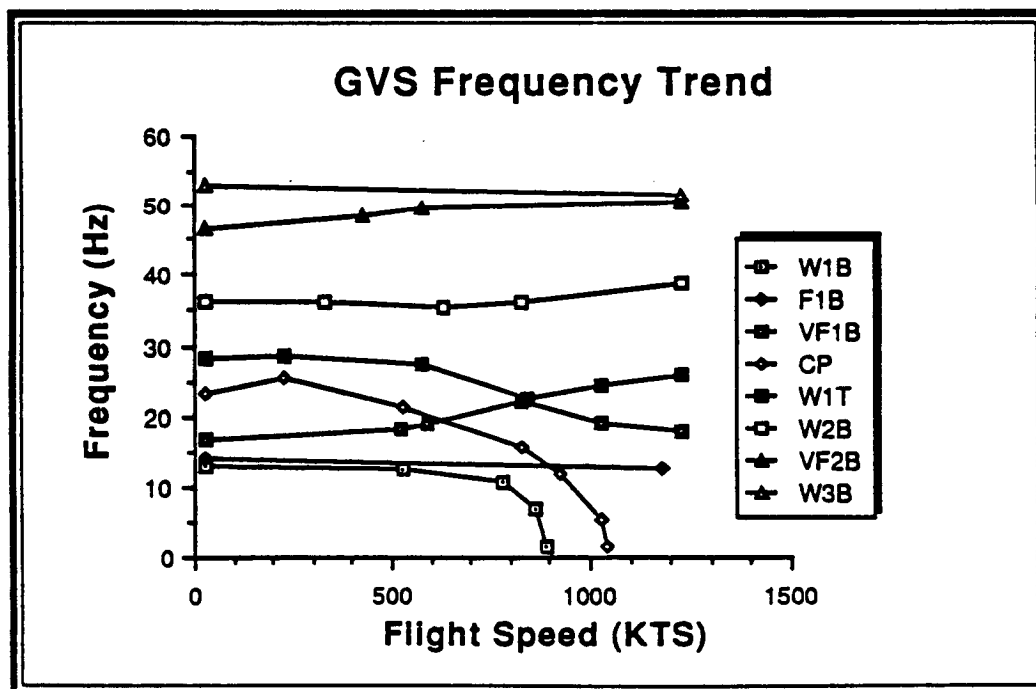


Figure 3.4.4A-3.1 GVS Frequency Trend (Anti-Symmetric)

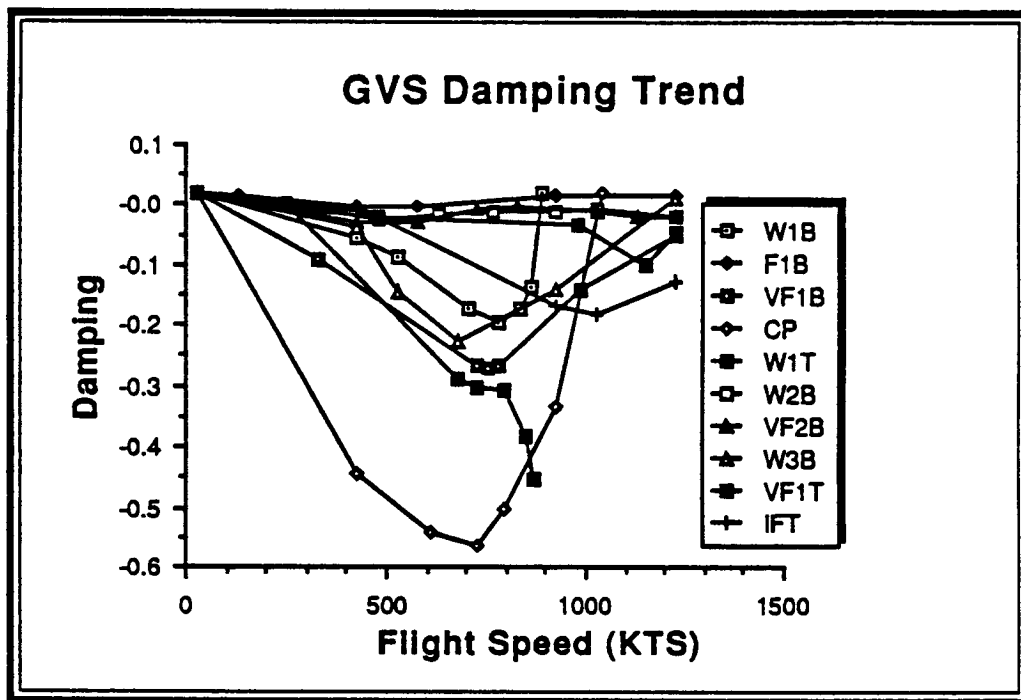


Figure 3.4.4A-3.2 GVS Damping Trend (Anti-Symmetric)

#### 3.4.4.1 Wing First Bending (W1B)

This is the fundamental anti-symmetric wing divergence mode (Figure - 3.4.4.1A-1 and 3.4.4.1A-2). The STARS result show good agreement in divergence speed with the GVS value, but the GAC's predicted value is unconservatively high.

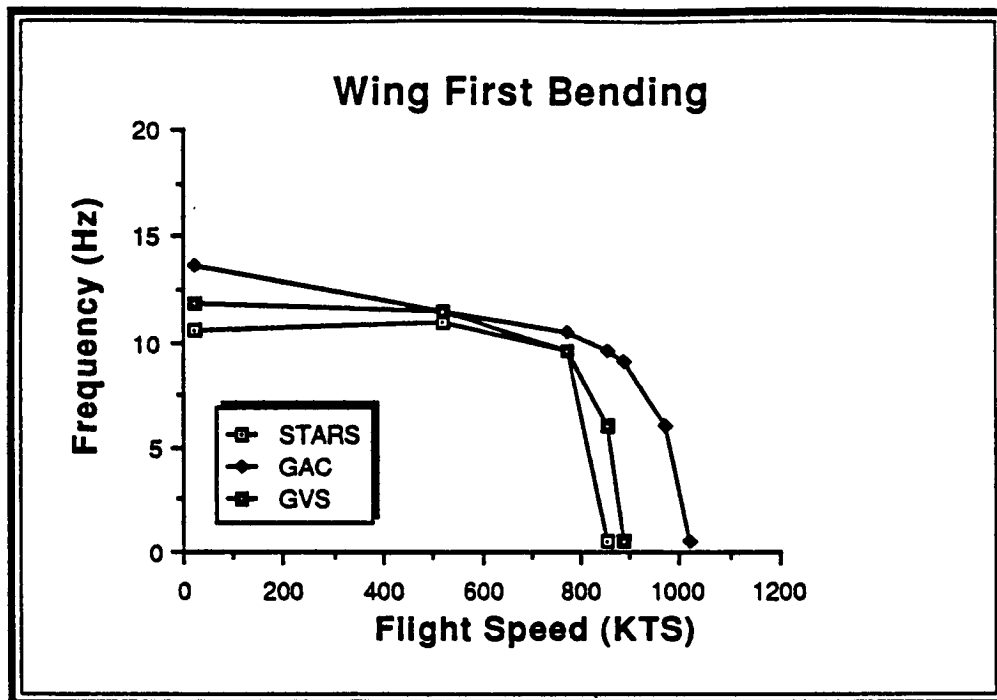


Figure 3.4.4.1A-1 Wing First Bending Frequency (Anti-Symmetric)

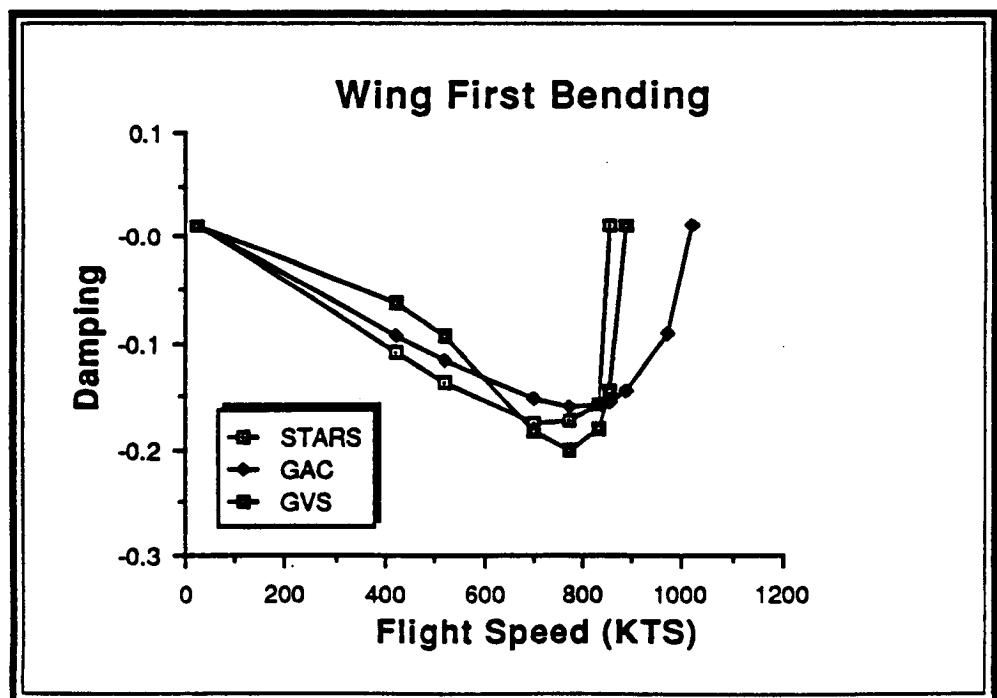


Figure 3.4.4.1A-2 Wing First Bending Damping (Anti-Symmetric)

### 3.4.4.2 Fuselage First Bending (F1B)

Reasonably good aeroelastic agreement exists among the three results, although the GAC natural frequency is very much lower than the STARS and the GVS values (Figure - 3.4.4.2A-1). The damping trends (Figure - 3.4.4.2A-2) are generally flat and the damping levels small, indicating relatively little aerodynamic coupling. The STARS damping levels are little higher than those of the other two analyses.

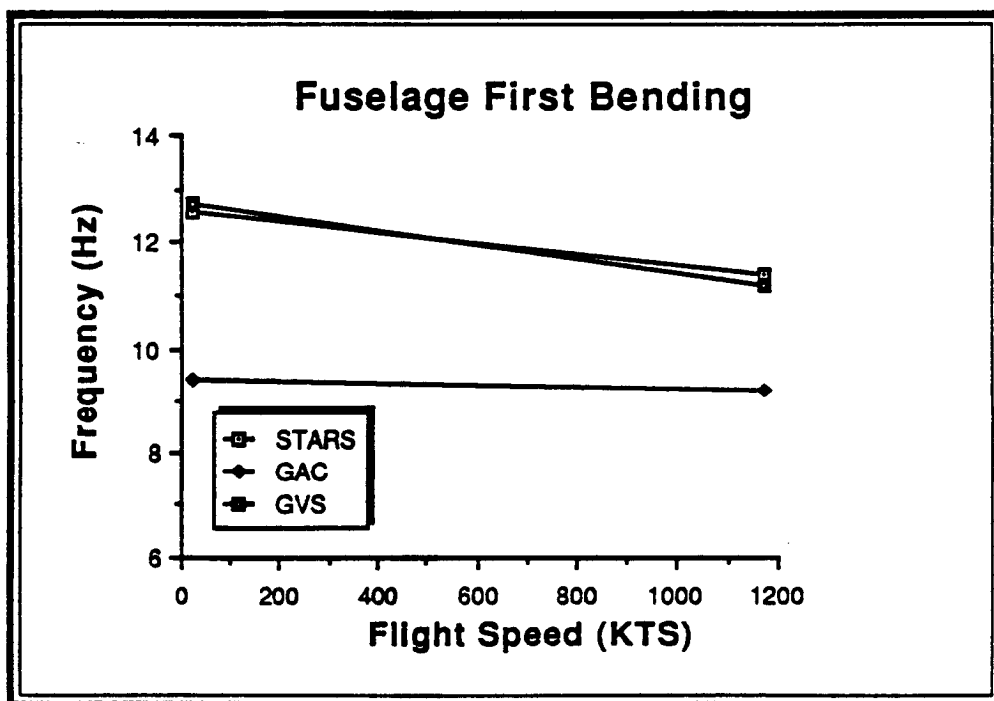


Figure 3.4.4.2A-1 Fuselage First Bending Frequency (Anti-Symmetric)

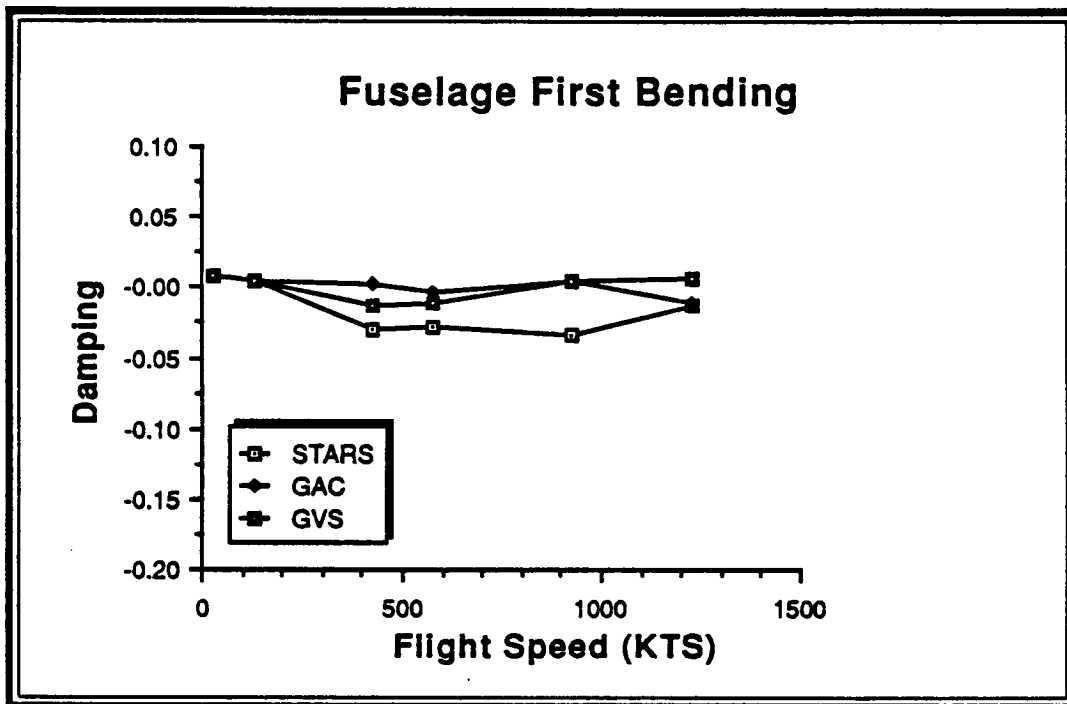


Figure 3.4.4.2A-2 Fuselage First Bending Damping (Anti-Symmetric)

### 3.4.4.3 Vertical Fin First Bending (VF1B)

At lower speeds, all three results agree well in frequency and damping trends, as shown in Figures - 3.4.4.3A-1 and 3.4.4.3A-2, with fairly flat frequency trends and rapid increases in damping. However, at higher speeds, the GVS result shows a significant decrease in damping, which is not evident in either the GAC or the STARS result.

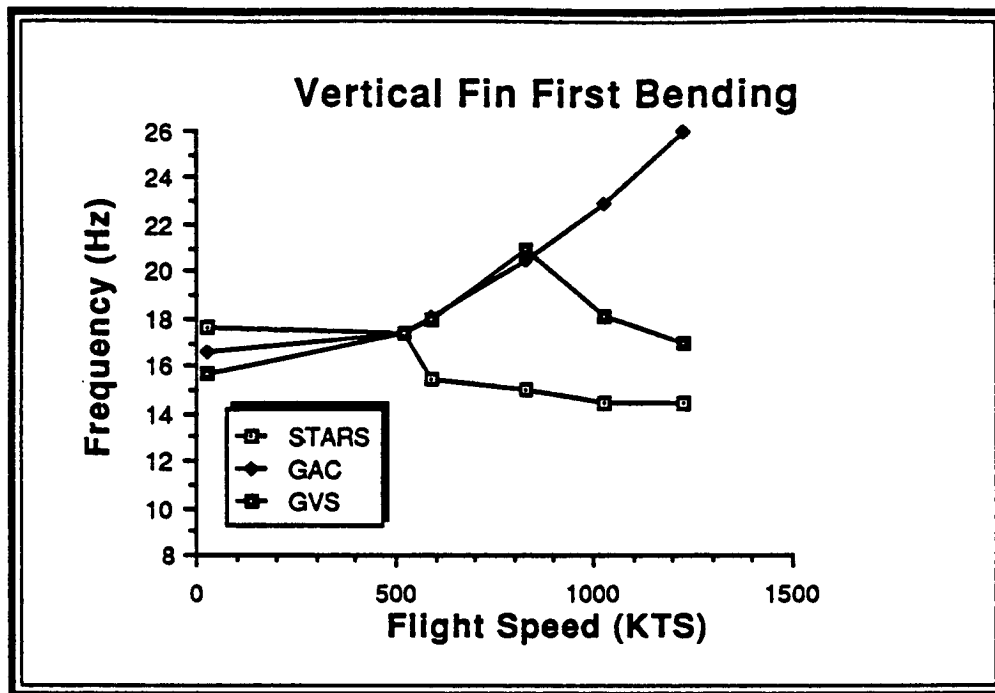


Figure 3.4.4.3A-1 Vertical Fin First Bending Frequency (Anti-Symmetric)

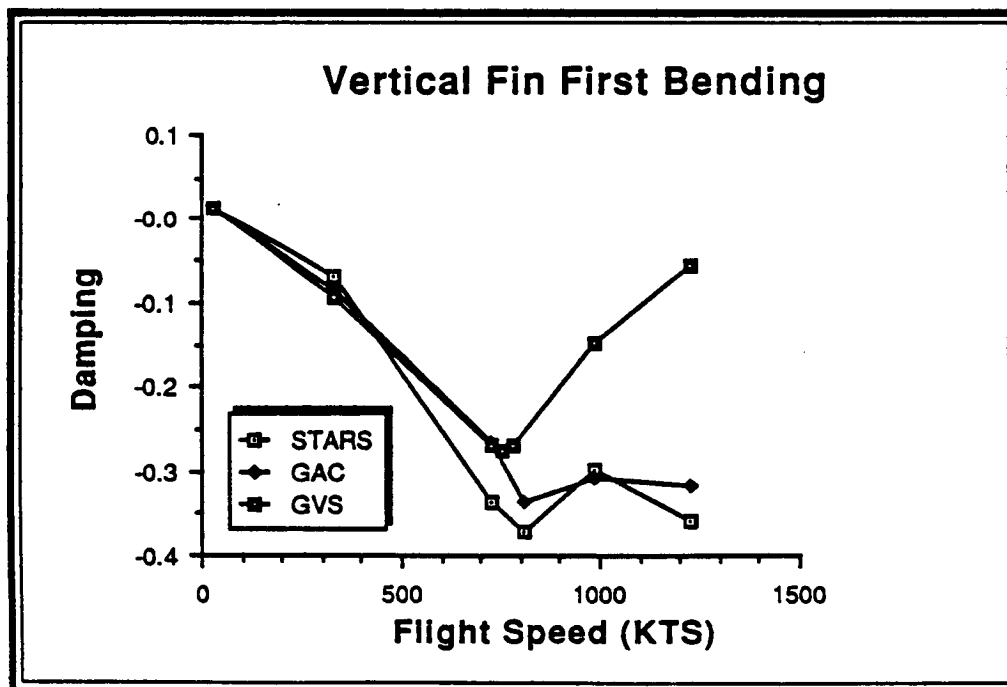


Figure 3.4.4.3A-2 Vertical Fin First Bending Damping (Anti-Symmetric)

#### 3.4.4.4 Canard Pitch (CP)

As in the symmetric case, this is the fundamental mode leading to canard divergence (Figures - 3.4.4.4A-1 and 3.4.4.4A-2). There is very little structural dynamic coupling between the canard and the rest of the aircraft. The STARS divergence speed shows much better agreement than the GAC value with the GVS result. The GAC result, when its frequency trend is extrapolated to zero, would indicate the occurrence of canard divergence well outside the speed range considered.

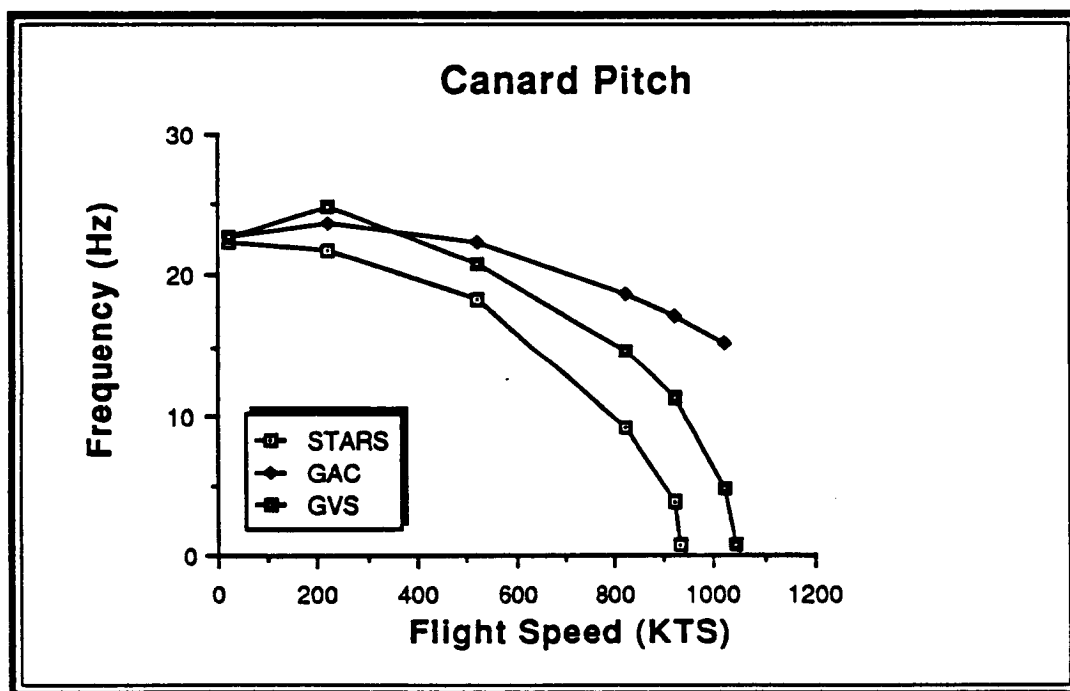


Figure 3.4.4.4A-1 Canard Pitch Frequency (Anti-Symmetric)

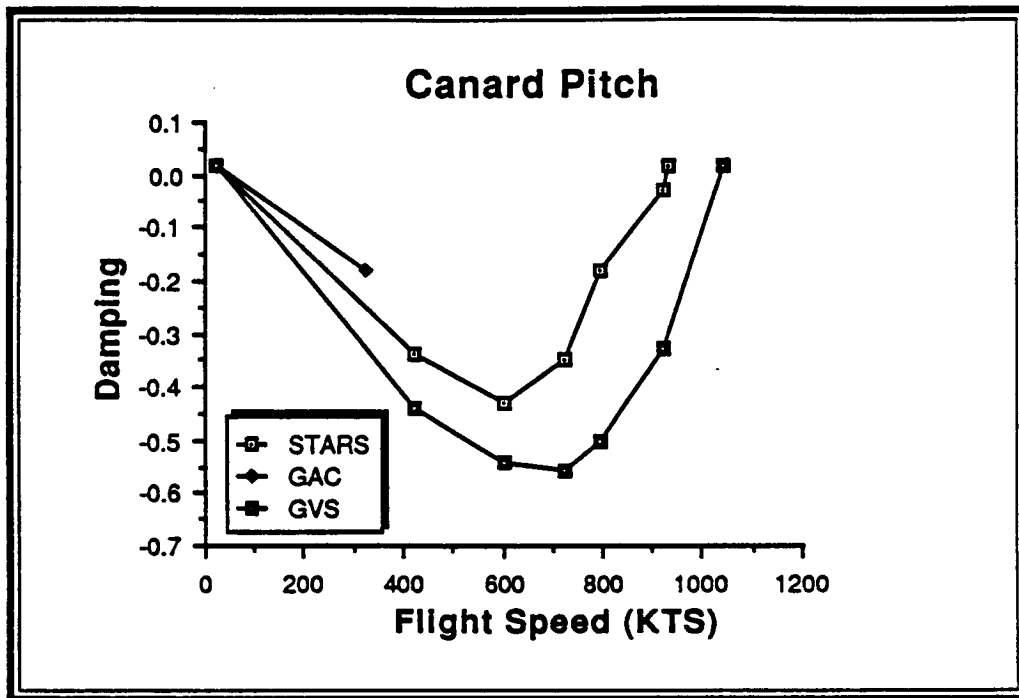


Figure 3.4.4.4A-2 Canard Pitch Damping (Anti-Symmetric)

#### 3.4.4.5 Wing First Torsion (W1T)

There is not very good agreement among the three results in either damping or frequency trends (Figures - 3.4.4.5A-1 and 3.4.4.5A-2). In particular, the STARS result show stronger coupling with the wing second bending mode (Figure - 3.4.4A-1.2) than either the GVS or the GAC results would indicate. This strong coupling is due to close frequency separation. In all three analyses no aeroelastic instability is predicted within the speed range considered.



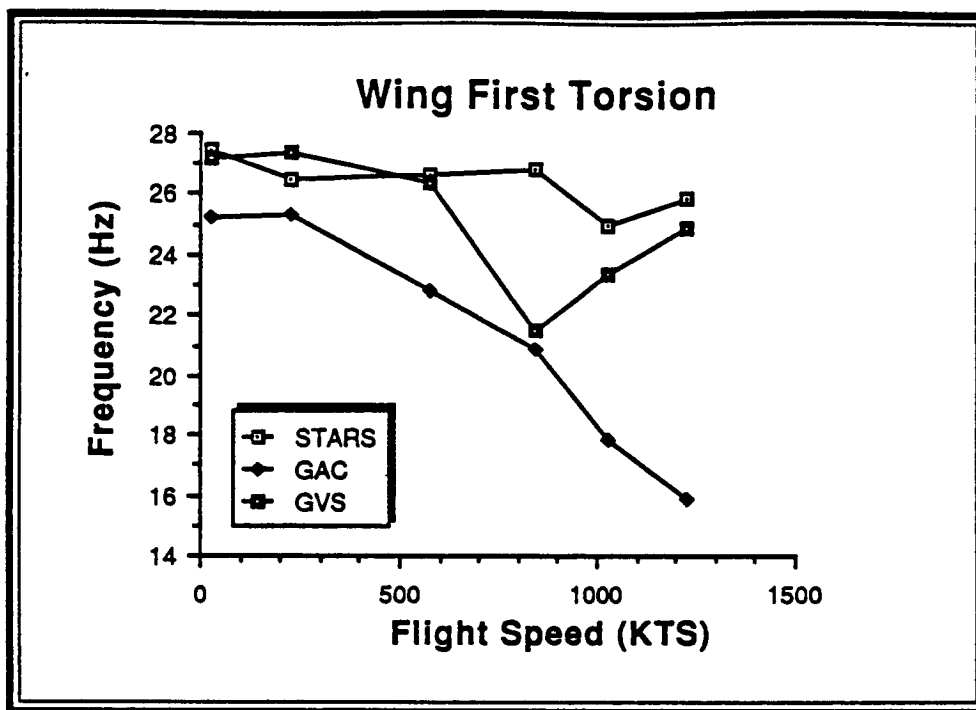


Figure 3.4.4.5A-1 Wing First Torsion Frequency (Anti-Symmetric)

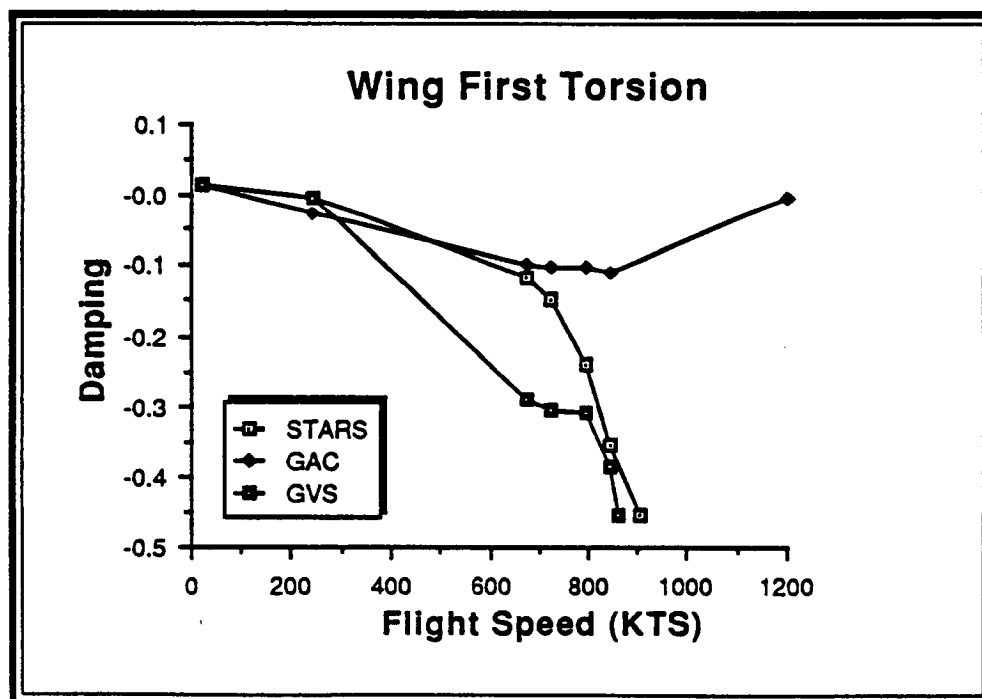


Figure 3.4.4.5A-2 Wing First Torsion Damping (Anti-Symmetric)

#### 3.4.4.6 Wing Second Bending (W2B)

Because of the coupling mentioned earlier, the STARS frequency and damping trends do not agree well with the GVS and the GAC frequency and damping trends (Figures - 3.4.4.6A-1 and 3.4.4.6A-2). No aeroelastic instability is predicted by any of the analyses.

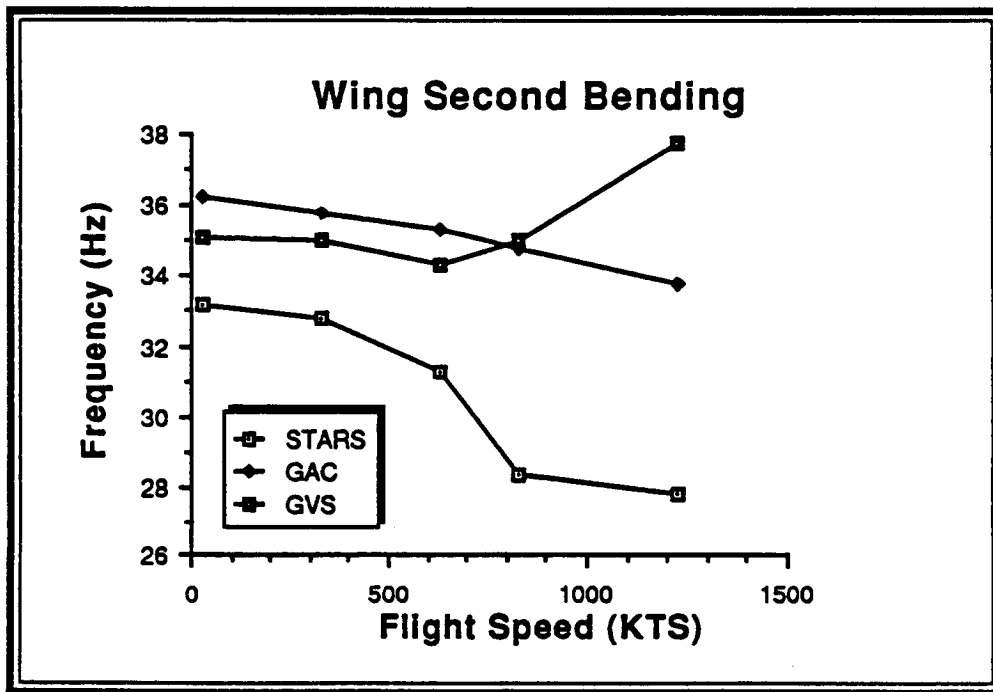


Figure 3.4.4.6A-1 Wing Second Bending Frequency (Anti-Symmetric)

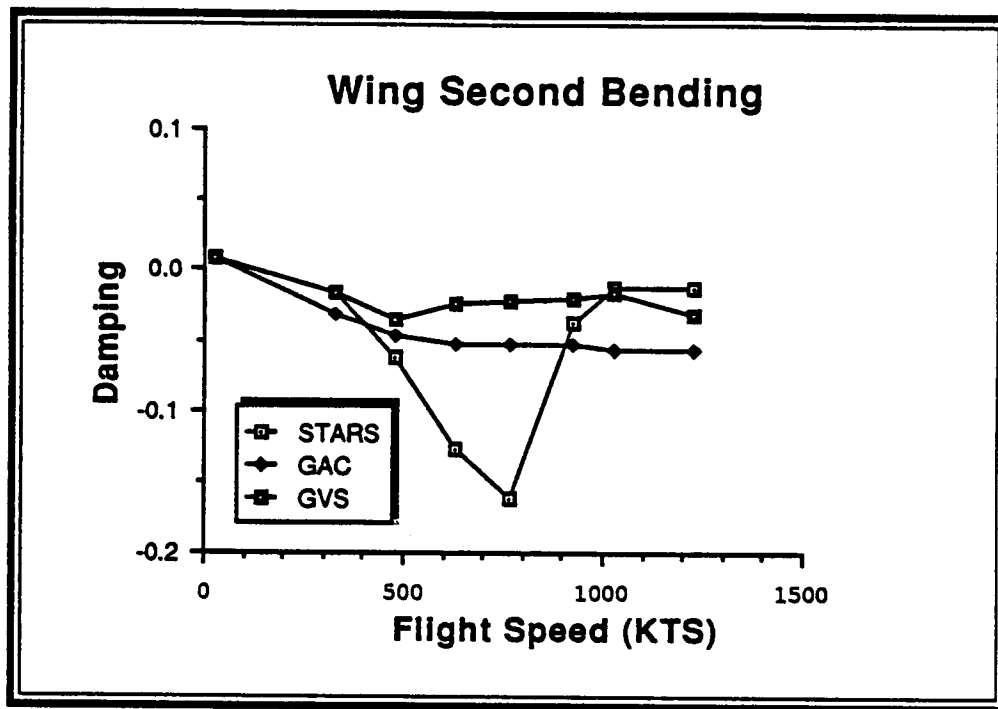


Figure 3.4.4.6A-2 Wing Second Bending Damping (Anti-Symmetric)

#### 3.4.4.7 Vertical Fin Second Bending (VF2B)

The aeroelastic responses of the GVS and the STARS analyses are shown in Figures -3.4.4.7A-1 and 3.4.4.7A-2. There are variations in the damping and frequency trends but no instability is predicted by either analysis. The result of the GAC analysis for this mode was not available.

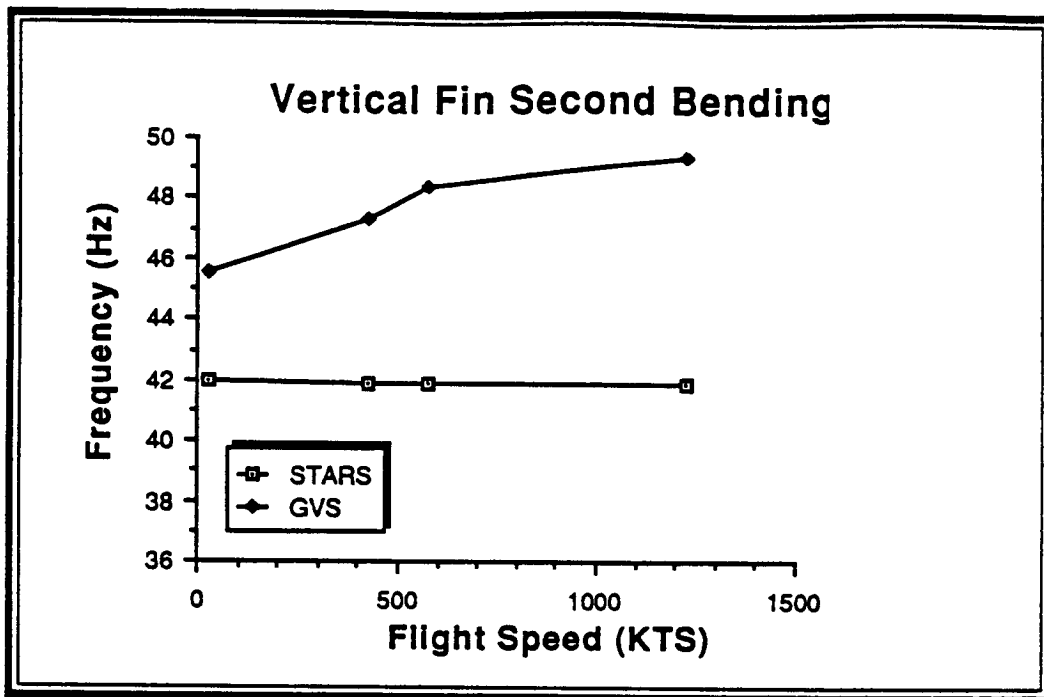


Figure 3.4.4.7A-1 Vertical Fin Second Bending Frequency (Anti-Symmetric)

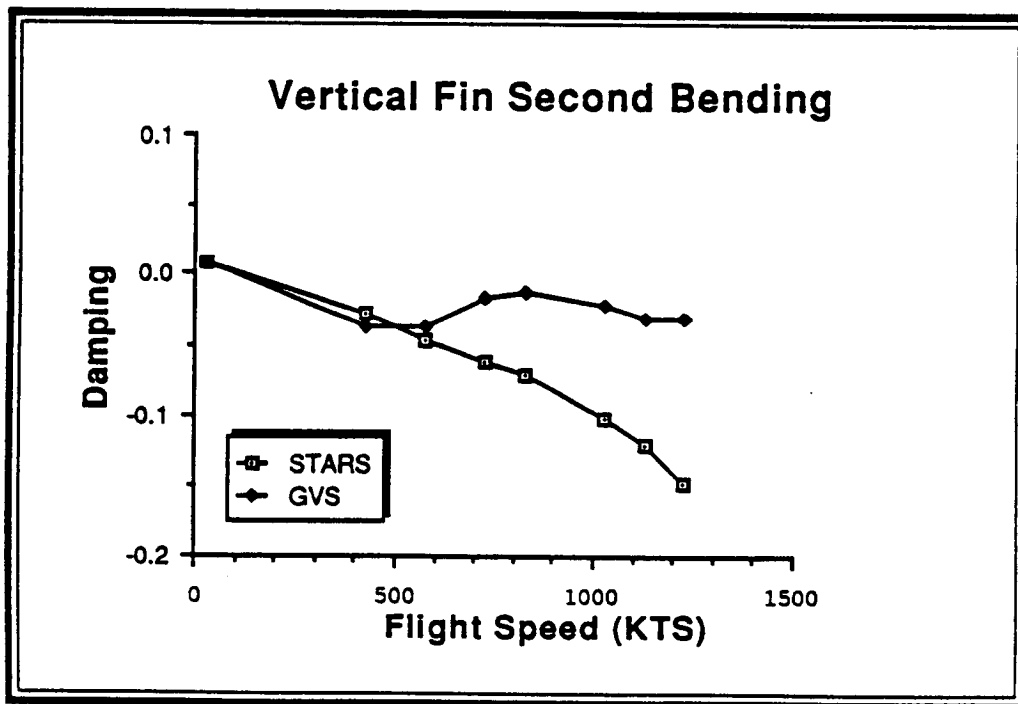


Figure 3.4.4.7A-2 Vertical Fin Second Bending Damping (Anti-Symmetric)

### 3.4.4.8 Wing Third Bending (W3B)

The aeroelastic response of the STARS analysis shows weak aeroelastic coupling. However, the aeroelastic response of the GVS analysis indicates a very strong coupling with other modes (Figure - 3.4.4A-3.2). Regardless of the differences in the damping trends at subcritical speeds (Figure - 3.4.4.8A-2), there is very good agreement in the predicted flutter speeds (Figure - 3.4.4.8A-2), there is very good agreement in the predicted flutter speeds. The result of the GAC analysis for this mode was not available.

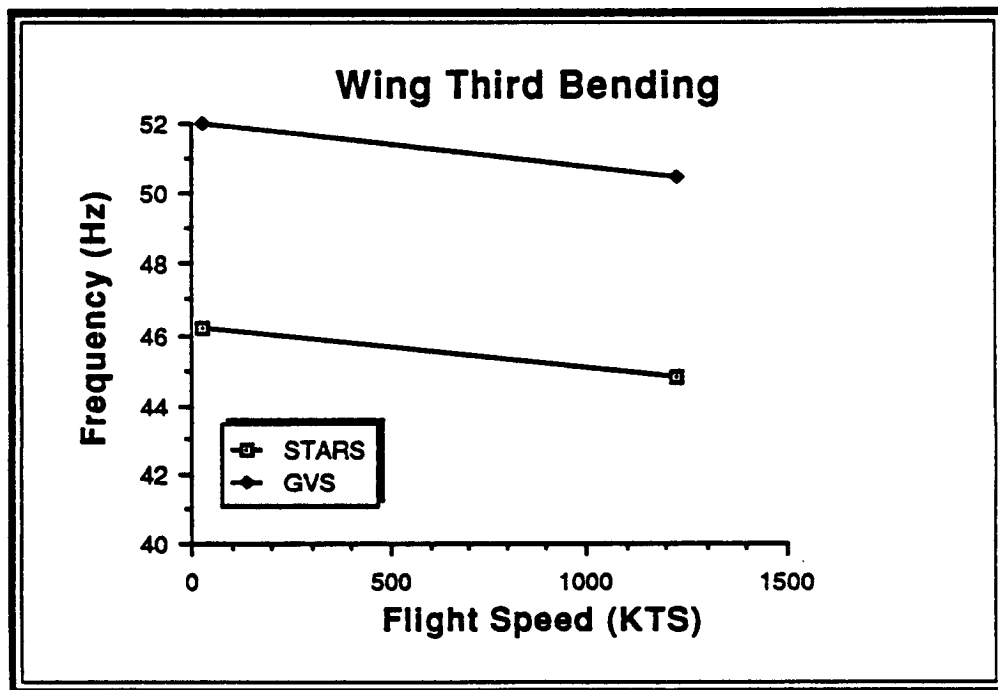


Figure 3.4.4.8A-1 Wing Third Bending Frequency (Anti-Symmetric)

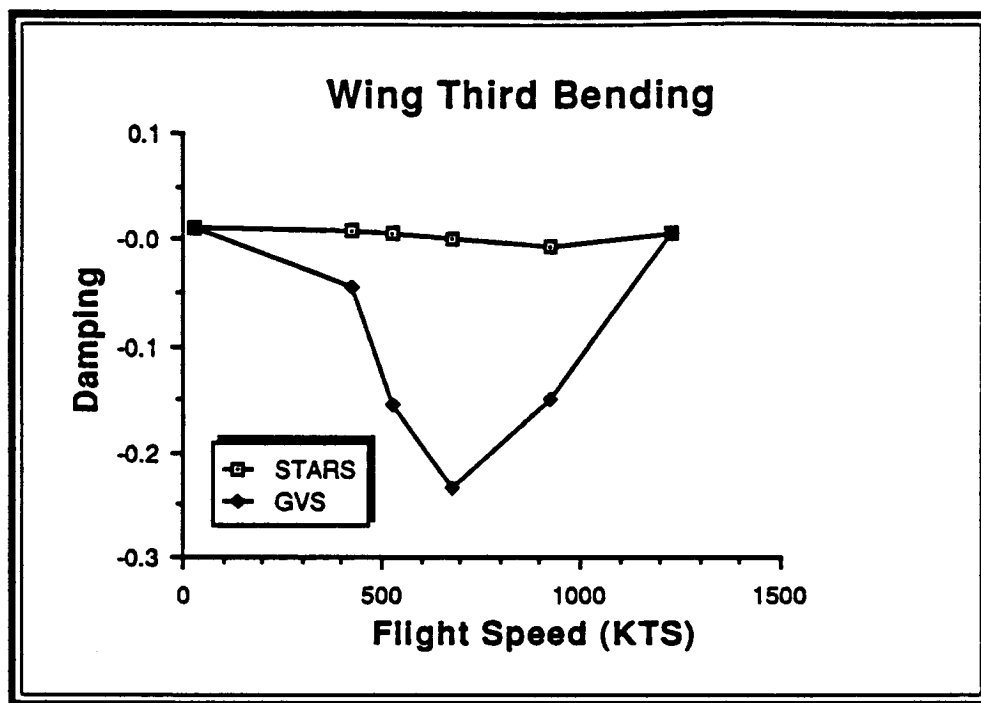


Figure 3.4.4.8A-2 Wing Third Bending Damping (Anti-Symmetric)

#### 3.4.4.9 Vertical Fin First Torsion (VF1T)

Aeroelastic response trends for all three results (Figures - 3.4.4.9A-1 and 3.4.4.9A-2) are fairly similar, with generally mild aeroelastic coupling (Figures - 3.4.4A-1.2, 3.4.4A-2.2, and, 3.4.4A-3.2); however, the GVS result displays a sharper but still stable aeroelastic interaction at high speeds. No aeroelastic instability is predicted by any of the analyses.

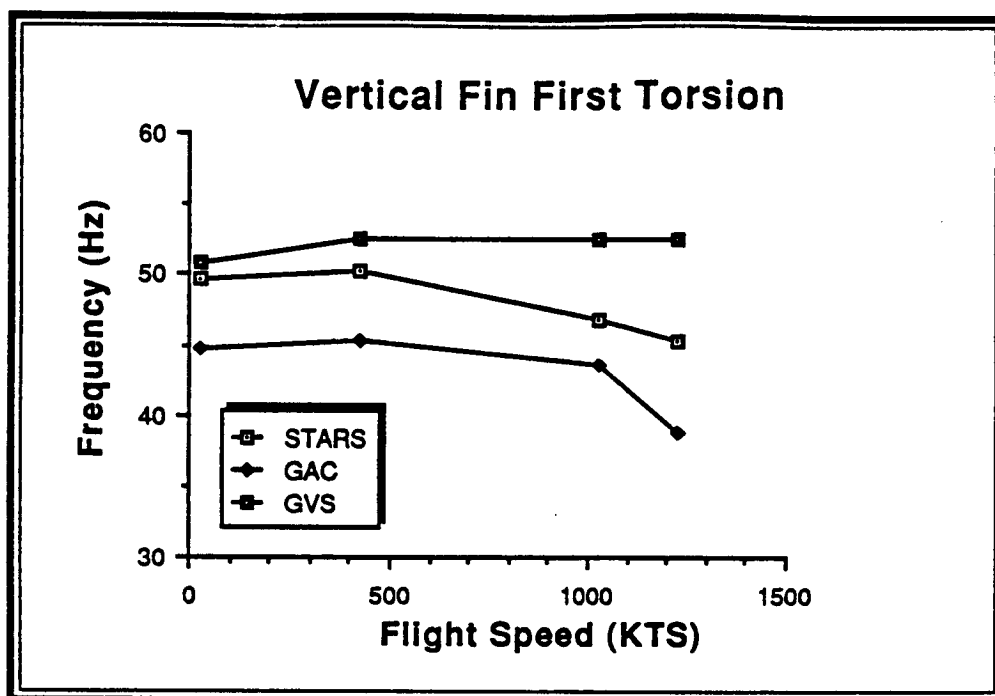


Figure 3.4.4.9A-1 Vertical Fin First Torsion Frequency (Anti-Symmetric)

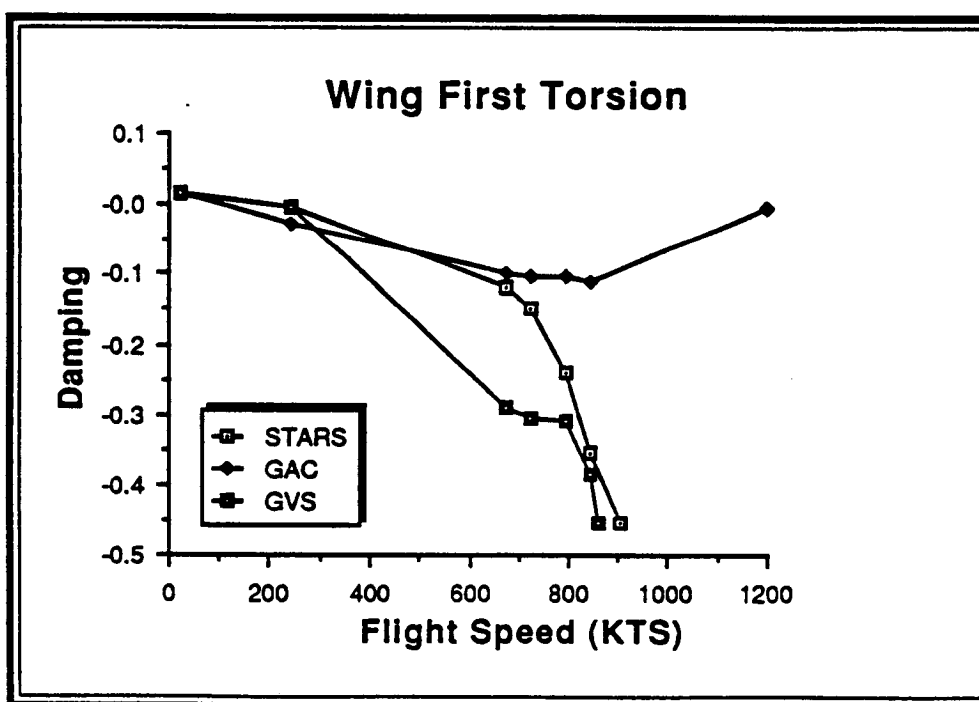


Figure 3.4.4.9A-2 Vertical Fin First Torsion Damping (Anti-Symmetric)

#### 3.4.4.10 Inboard Flap Torsion ( IFT )

The GVS result shows a strong aeroelastic coupling with some other mode whereas the STARS result does not show similar trend (Figures - 3.4.4A-1.2 and 3.4.4A-3.2). Neither of the analyses predict an aeroelastic instability (Figures - 3.4.4.10A-1 and 3.4.4.10A-2). The result of the GAC analysis for this mode was not available.

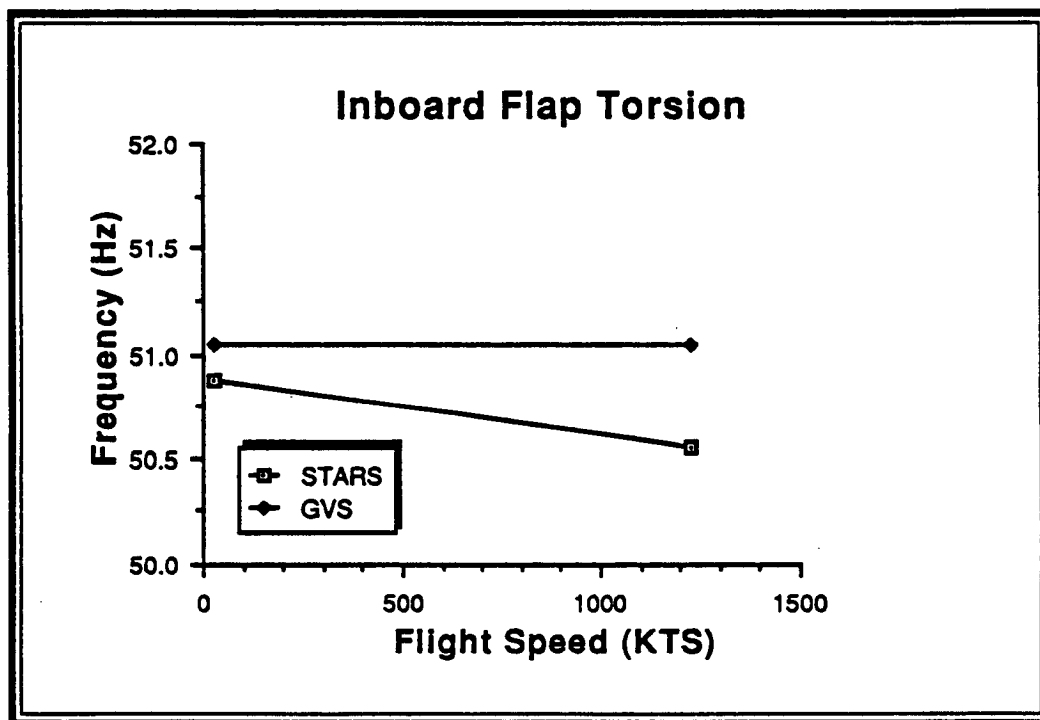


Figure 3.4.4.10A-1 Inboard Flap Torsion Frequency (Anti-Symmetric)



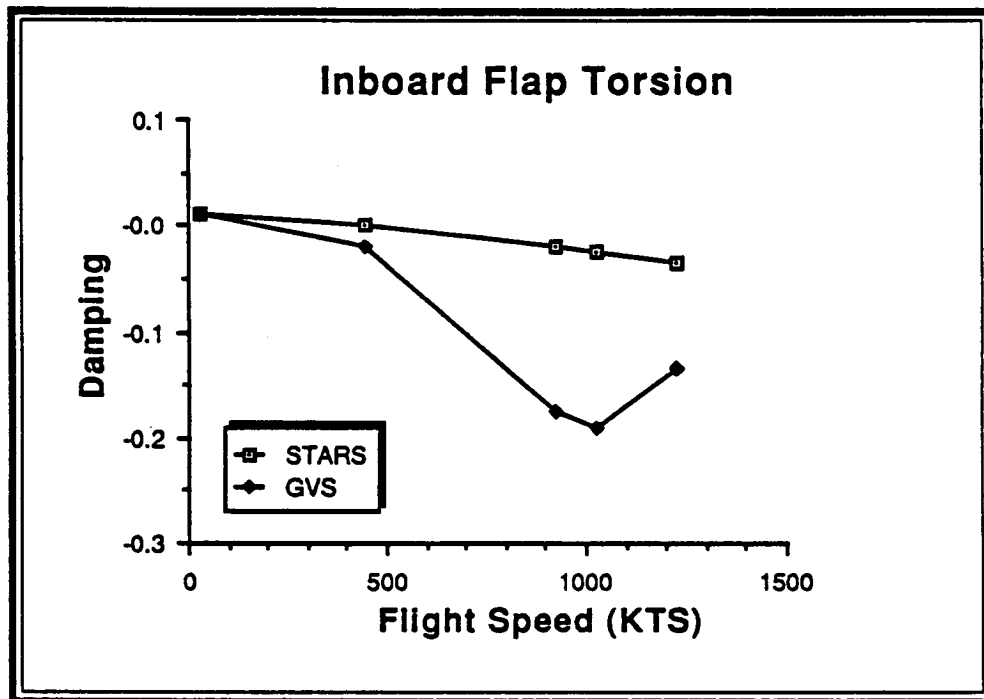


Figure 3.4.4.10A-2 Inboard Flap Torsion Damping (Anti-Symmetric)

## ***CHAPTER 4***

# **PROJECT MANAGEMENT**

### **4.1 PROJECT OVERVIEW**

NASA-Ames Research Center has embarked on the design and testing of the X-29A aircraft. The flight tests are currently being performed at NASA-Dryden. In addition, analytical and experimental studies such as finite element analysis and ground vibration surveys are conducted at NASA-Dryden to support the flight tests.

The structural dynamics group at NASA-Dryden is responsible for performing vibration and flutter analyses of the X-29A aircraft and its various components. The author worked as a research engineer responsible for these analyses. The report presented here is a

combination of analytical work performed for the comparative analysis of the X-29A aircraft, and research and development work done in formulating a finite dynamic element as an example for more economical approach to free vibration analysis.

This project was partly funded as a joint effort between NASA-Ames and the University of Kansas Center of Research, Inc (KU-CRINC). The remaining part of the project was funded through Harvey Mudd College (HMC). A more detailed explanation of the project's budget and time-schedule is given next.

## **4.2 BUDGET AND TIME-SCHEDULE**

A part of the project was funded by NASA-Ames through a grant to the University of Kansas (KU). The original proposal of the project budget made by the university is shown in Figure - 4.2A. As it is shown in the figure, the budget was designed to support the author through one school year at the KU. The rest of the project was funded through HMC by NASA-Ames through other grants.

The time-schedule of the project covers forty four months. Figure - 4.2B shows the schedule.

**DIRECT COSTS****Salaries and Stipends**

Student	\$6650
Faculty/Administration Support	\$2700
Total Salaries and Stipends	<u>\$9350</u>

**Fringe Benefit Costs**

18% Administration	\$486
8% Student	\$532

**Other Direct Costs**

Student Travel Costs	\$2500
Tuition	\$3500
Equipment	\$600
Faculty Travel	\$744
Publications	\$300
Total Direct Costs	<u>\$18,012</u>

**INDIRECT COSTS**

22.5% of Direct Costs	\$3918
Grand Total	<u>\$21,930</u>

**Figure 4.2A** Grant Used for the Student Support at KU

<b>Jan 01, 84 - Aug 15, 84</b>	Starting the Internship Requirement at NASA, Funded Through HMC
<b>Aug 16, 84 - May 31, 85</b>	Starting Course Requirements at the University of Kansas, Funded Through KU-CRINC
<b>Jun 01, 85 - Aug 15, 85</b>	Completion of Internship at NASA, Funded Through HMC
<b>Aug 16, 85 - Dec 15, 85</b>	Completion of Course Requirements at the University of Kansas, Funded Through KU-CRINC
<b>Dec 16, 85 - Oct 31, 87</b>	Completion of The X-29A Analyses, and Other Parts of the Project, Funded Through HMC

**Figure 4.2B** Author's Project Time-Schedule

### **4.3 PROJECT'S TASKS AND PERSONELL**

The tasks carried-out by the author are listed below.

- 1 —** Incorporation of the FASTEX computer program into the STARS package.
- 2 —** Development of a post-processor program on PS300 graphics system for the STARS package.
- 3 —** Generation of the finite element and aerodynamic models of X-29A aircraft.

- 4 — Free vibration analysis of the X-29A.
- 5 — Aerodynamic analysis of the X-29A.
- 6 — Interpretation of the free vibration and aerodynamic analyses of the X-29A.
- 7 — Developement of a higher-order plane-stress finite dynamic triangular element.

The team which the author worked with to carry-out the free vibration and aerodynamic analysis of the X-29A aircraft at NASA and the development of the STARS graphics package at HMC is listed below.

- 1 — **Dr. K. K. Gupta**; Head of Structural Dynamics group at NASA-Dryden; overall supervision of the author's project.
- 2 — **Leonard S. Voelker**; Senior Aero-Space Engineer at NASA-Dryden; development of the aerodynamic model of the X-29A aircraft, interpretation of the results from aerodynamic analysis.
- 3 — **Roger A. Truax**; Aero-Space Engineer at NASA-Dryden, Through HMC; assistance in modification and analysis of the X-29A's finite element and aerodynamic models.
- 4 — **Edward E. Hahn**; Aero-Space Engineer at NASA-Dryden, Through HMC; assistance in preparation, modification and analysis of the X-29A's models.
- 5 — **Gill Fuchs**; Research Assistant at HMC; assistance in developement of the STARS graphics package.

- 6 — Sharil Ibrahim; Research Assistant at HMC; assistance in development of the STARS graphics package.

## 4.4 ORGANIZATION

The overall project organization for the X-29A aircraft is shown in Figure - 4.4A. The figure shows the interaction between the different agencies (NASA, DARPA, USAF, and Grumman).

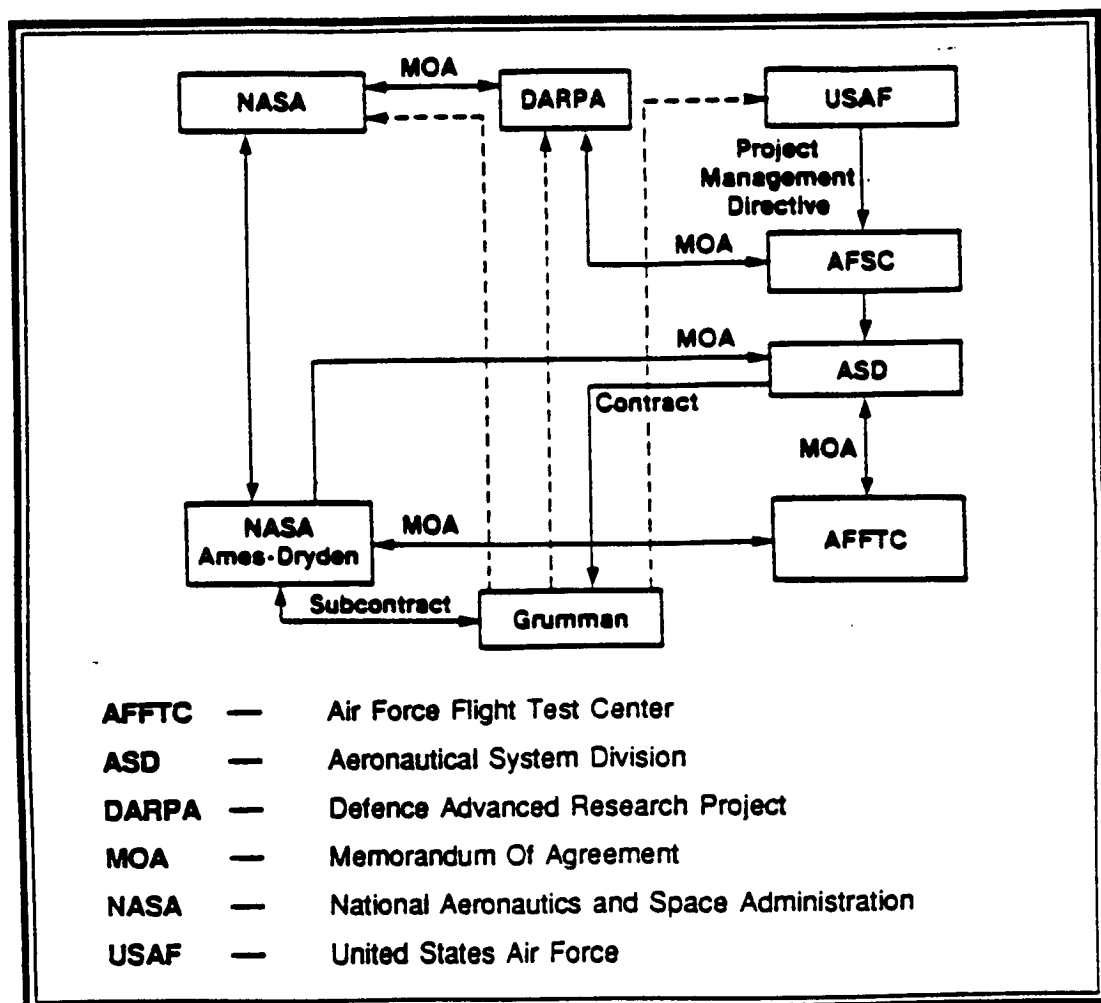
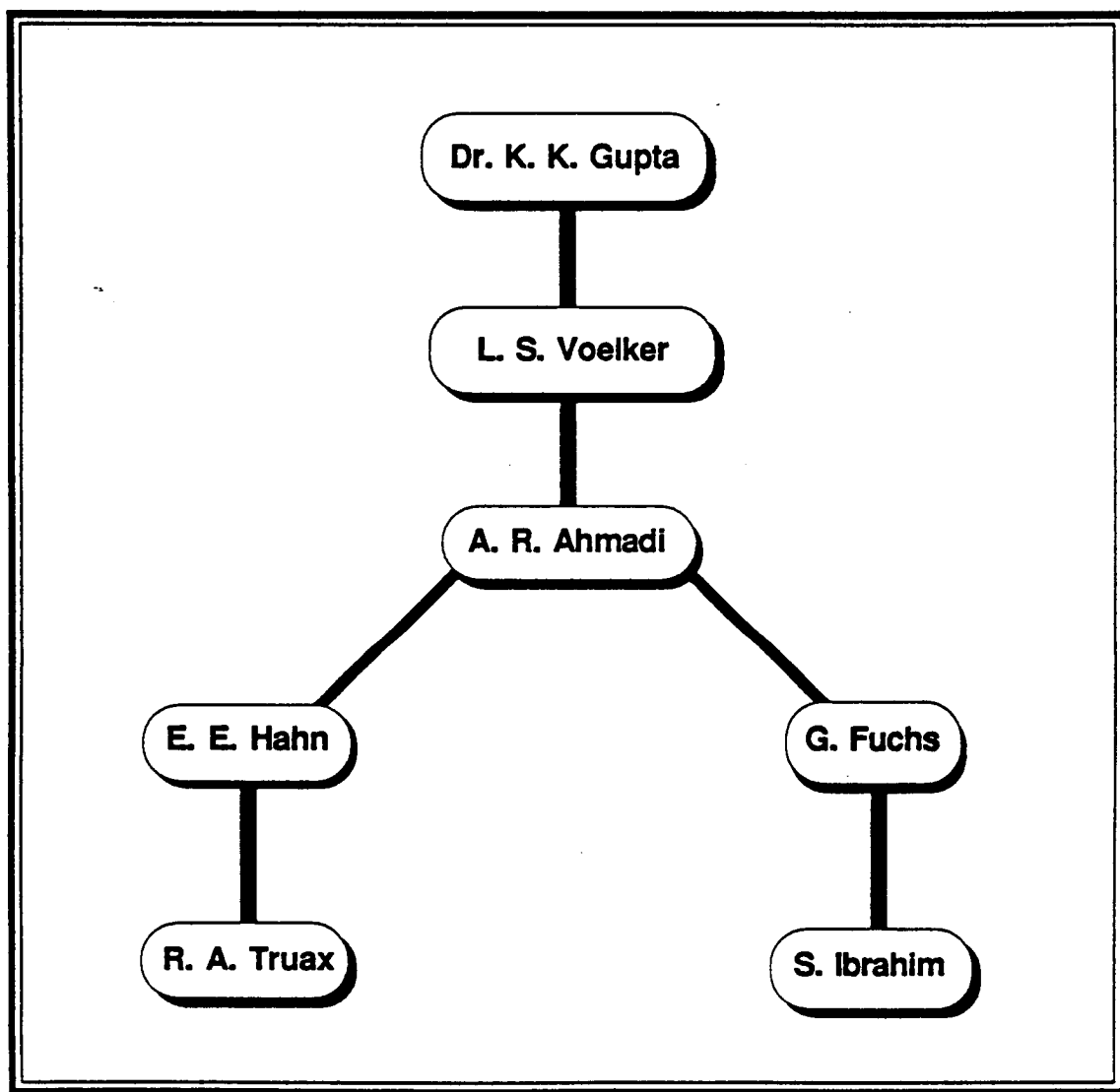


Figure 4.4A Overall Project Organization for X-29A Aircraft

The doctor of engineering program at the university of Kansas requires the doctoral candidate to function in a team environment and also have some supervisory responsibilities. The project team responsible for the analytical study of the X-29A aircraft is shown in Figure - 4.4B



**Figure 4.4B** The Author's Project Team for Analytical Study of the X-29A Aircraft



## ***CHAPTER 5***

# **CONCLUSIONS**

### **5.1 GENERAL CONCLUSIONS**

This thesis has shown the results of the free vibration and aerodynamic analyses of the X-29A aircraft carried out at NASA-Dryden. These results are compared to those submitted by the Grumman Aircraft Corporation (GAC) and the Ground Vibration Survey (GVS) results. The natural frequencies and mode-shapes of the X-29A aircraft determined analytically by STARS and GAC compare relatively well to the actual values obtained experimentally by GVS. The analytical results have least correlation to the experimental results in the areas of the fuselage and the vertical tail. This problem is due to the simplicity of

the fuselage model. However, on the results of the aero-servoelastic analysis of the X-29A aircraft, which is currently being carried out at NASA-Dryden, agrees very well with the flight test data. This simply suggests that the modal data for the fuselage and the vertical tail have minor contribution to the overall analysis.

The flutter and divergence speeds predicted using the analytical results of the STARS compare better to the GVS results than the GAC. However, the predicted instability speeds are well beyond the subsonic flight test speed. Therefore, the X-29A aircraft would not encounter any aerodynamic instability during its flight in the subsonic region.

## **5.2 CURRENT AND FUTURE DEVELOPMENTS**

As mentioned earlier the X-29A aircraft is undergoing flight tests at NASA-Dryden. The STARS computer package is currently being used to perform aero-servoelastic analysis to support the flight testings.

A trial and error modification of the finite element model of the fuselage and the vertical tail will be performed in the near future. This will help to reduce the propagation of the modal data error in the subsequent analyses.

The supersonic flutter and divergence analyses of the X-29A are currently being held for the completion of a new supersonic aerodynamic

analysis program based on the potential gradient method.

Development of more finite dynamic elements (Appendix - A) to complete a library of the basic elements is in the future plans. Also, research is currently being carried out under NASA grants to utilize Lanczos algorithm to solve the quadratic eigenvalue problem generated in the case of finite dynamic element method. This advancement in the eigenvalue solution procedure will give a clear edge to the finite dynamic element method over the finite element method.

## ***APPENDIX A***

# **FINITE DYNAMIC ELEMENT METHOD**

### **A.1 BACKGROUND**

Free vibration analysis is essential for the design of structures subjected to dynamic loading. A majority of practical structures such as the X-29A aircraft, when discretized by the usual finite element method, often yield rather large order matrices. The computer time required to solve the resulting eigenvalue problem is dependent on the order of the problem. Reference - 21 shows that the order of a problem can be reduced without the loss of accuracy by employing the finite dynamic element technique. This is achieved by the addition of higher order dynamic correction terms to the mass and the

stiffness matrices. However, the addition of these higher order terms will result in a quadratic eigenvalue problem. As a result, the decrease in the computer time achieved by the reduction in the size of the problem is negated by the increase in the computer time required to solve the quadratic eigenvalue problem.

An efficient algorithm based on the combined Sturm Sequence and Inverse Iteration technique for the solution of quadratic matrix eigenvalue problem is presented in References - 7 and 21. This eigenvalue solution technique coupled with the finite dynamic element method will result in a very efficient and economical free vibration analysis approach. The development of a higher order finite dynamic plane-stress triangular element is presented in the following sections.

## **A.2 FINITE DYNAMIC ELEMENT FORMULATION**

Matrix structural analysis deals with discrete quantities such as concentrated loads and displacements. Consequently, all equations of elasticity are re-formulated to suit the concept of discrete system.

The displacement at any point within a structure subjected to static loading can be related to a finite number of displacements on the structure. In the case of small displacements, this relationship is expressed as

$$u = aU \quad (A.1)$$

where:

$[u]$  — displacements within a continuum,

$[U]$  — nodal displacements,

$[a]$  — shape function.

However, in case of dynamic loading the shape function  $[a]$  is no longer unique. It is a function of the entire time history of the nodal displacements. In the case of harmonic motion,  $[a]$  can be represented as a function of the natural frequencies of the structure.

$$a = a(\omega) \quad (A.2)$$

Where:

$\omega$  — natural frequency.

But, the natural frequencies of a structure are unknown; therefore the shape function can not be determined. To avoid this complication, the solution for displacements  $[u]$  is assumed to be given by a series in ascending powers of the natural frequencies. Equation - A.1 (Reference - 22) becomes

$$u = \sum_{i=0}^{\infty} \omega^i a_i U \quad (A.3)$$

The stiffness and mass matrices are then expressed (References - 21, 22) as

$$\mathbf{K} = \mathbf{K}_0 + \omega^2 \mathbf{K}_2 + \omega^4 \mathbf{K}_4 + \dots \quad (\text{A.4})$$

$$\mathbf{M} = \mathbf{M}_0 + \omega^2 \mathbf{M}_2 + \omega^4 \mathbf{M}_4 + \dots \quad (\text{A.5})$$

Assumption of harmonic motion and truncation of the infinite series, result in the quadratic eigenvalue problem

$$[\mathbf{K}_0 - \omega^2 (\mathbf{M}_0 - \mathbf{K}_2) - \omega^4 (\mathbf{M}_2 - \mathbf{K}_4)] [\Phi] = 0 \quad (\text{A.6})$$

Where:

- $[\Phi]$  — natural mode-shapes matrix,
- $[\mathbf{K}_0]$  — elastic stiffness matrix,
- $[\mathbf{M}_0]$  — mass matrix,
- $[\mathbf{K}_2], [\mathbf{K}_4]$  — higher order stiffness correction matrices,
- $[\mathbf{M}_2]$  — higher order mass correction matrix.

### A.3 PLANE-STRESS TRIANGULAR ELEMENT

The governing differential equations of motion for the plane-stress triangular element, shown in Figure - A.3A, are

$$\frac{\partial^2 u_x}{\partial x^2} + \frac{\partial^2 u_x}{\partial y^2} + \frac{1}{(1-2\mu)} \cdot \frac{\partial}{\partial x} \left( \frac{\partial u_x}{\partial x} + \frac{\partial u_y}{\partial y} \right) = 2(1+\mu) \frac{\rho}{E} \frac{\partial^2 u_x}{\partial t^2} \quad (\text{A.7})$$

$$\frac{\partial^2 u_y}{\partial x^2} + \frac{\partial^2 u_y}{\partial y^2} + \frac{1}{(1-2\mu)} \cdot \frac{\partial}{\partial y} \left( \frac{\partial u_x}{\partial x} + \frac{\partial u_y}{\partial y} \right) = 2(1+\mu) \frac{\rho}{E} \frac{\partial^2 u_y}{\partial t^2} \quad (\text{A.8})$$

Where:

- $\rho$  — mass per unit volume,
- $\mu$  — poisson's ratio,
- $E$  — Young's modulus,
- $u_x$  — in-plane deformation in the  $x$  direction,
- $u_y$  — in-plane deformation in the  $y$  direction
- $t$  — time.

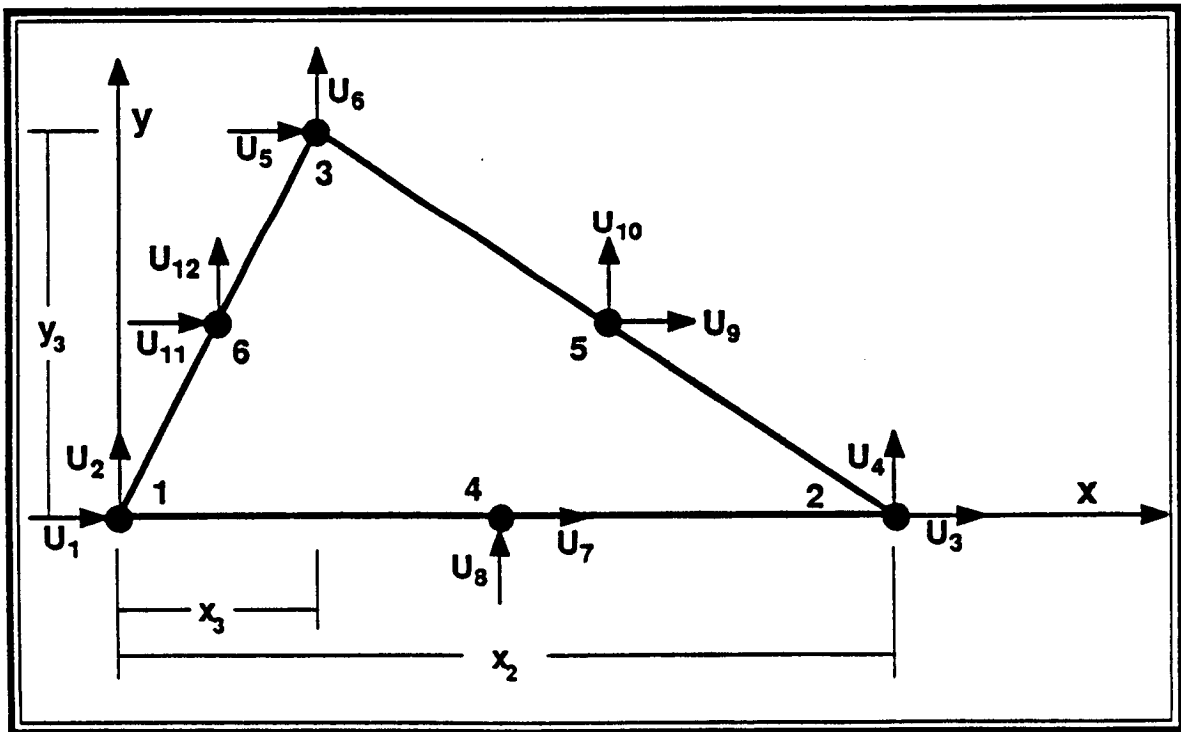


Figure A.3A Six-Node Plane-Stress Triangular Element



Solutions of the equations A.7 and A.8 can be given as

$$u_x = a(\omega)U = (a_{0x} + \omega a_{1x} + \omega^2 a_{2x} + \dots) U \quad (A.9)$$

$$u_y = a(\omega)U = (a_{0y} + \omega a_{1y} + \omega^2 a_{2y} + \dots) U \quad (A.10)$$

Truncation of the terms in equations A.9 and A.10 and substitution of them in the equations A.7 and A.8, result in

$$\frac{\partial^2 a_{0x}}{\partial x^2} + \frac{\partial^2 a_{0x}}{\partial y^2} + \alpha_2 \left( \frac{\partial^2 a_{0x}}{\partial x^2} + \frac{\partial^2 a_{0y}}{\partial x \partial y} \right) = 0 \quad (A.11)$$

$$\frac{\partial^2 a_{1x}}{\partial x^2} + \frac{\partial^2 a_{1x}}{\partial y^2} + \alpha_2 \left( \frac{\partial^2 a_{1x}}{\partial x^2} + \frac{\partial^2 a_{1y}}{\partial x \partial y} \right) = 0 \quad (A.12)$$

$$\alpha_1 \frac{\partial^2 a_{2x}}{\partial x^2} + \frac{\partial^2 a_{2x}}{\partial y^2} + \alpha_2 \frac{\partial^2 a_{1y}}{\partial x \partial y} = -\beta a_{0x} \quad (A.13)$$

$$\frac{\partial^2 a_{0y}}{\partial x^2} + \frac{\partial^2 a_{0y}}{\partial y^2} + \alpha_2 \left( \frac{\partial^2 a_{0y}}{\partial y^2} + \frac{\partial^2 a_{0x}}{\partial x \partial y} \right) = 0 \quad (A.14)$$

$$\frac{\partial^2 a_{1y}}{\partial x^2} + \frac{\partial^2 a_{1y}}{\partial y^2} + \alpha_2 \left( \frac{\partial^2 a_{1y}}{\partial y^2} + \frac{\partial^2 a_{1x}}{\partial x \partial y} \right) = 0 \quad (A.15)$$

$$\alpha_1 \frac{\partial^2 a_{2y}}{\partial y^2} + \frac{\partial^2 a_{2y}}{\partial x^2} + \alpha_2 \frac{\partial^2 a_{1x}}{\partial x \partial y} = -\beta a_{0y} \quad (A.16)$$

Where:

$$\alpha_1 = \frac{2(1-\mu)}{(1-2\mu)}$$

$$\alpha_2 = \frac{1}{(1-2\mu)}$$

$$\beta = \frac{2\rho}{E} (1+\mu)$$

The solutions of the differential equations A.11 through A.16 can be expressed in a polynomial form (Reference - 23)

$$a_{0x} = C_1 + C_2x + C_3y + C_4x^2 + C_5xy + C_6y^2 \quad (A.17)$$

$$a_{0y} = C_7 + C_8x + C_9y + C_{10}x^2 + C_{11}xy + C_{12}y^2 \quad (A.18)$$

$$a_{2x} = A_1 + A_2x + A_3y + A_4x^2 + A_5xy + A_6y^2 -$$

$$\beta \left[ \frac{C_1x^2}{4\alpha_1} + \frac{C_1y^2}{4} + \frac{C_2x^3}{12\alpha_1} + \frac{C_2xy^2}{4} + \frac{C_3x^2y}{4\alpha_1} + \frac{C_3y^3}{12} + \right.$$

$$\left. \frac{C_4x^4}{24\alpha_1} + \frac{C_4x^2y^2}{4} + \frac{C_5x^3y}{12\alpha_1} + \frac{C_5xy^3}{12} + \frac{C_6x^2y^2}{4\alpha_1} + \frac{C_6y^4}{24} \right] \quad (A.19)$$

$$a_{2y} = A_7 + A_8x + A_9y + A_{10}x^2 + A_{11}xy + A_{12}y^2 -$$

$$\beta \left[ \frac{C_7y^2}{4\alpha_1} + \frac{C_7x^2}{4} + \frac{C_8x^3}{12} + \frac{C_8xy^2}{4\alpha_1} + \frac{C_9x^2y}{4} + \frac{C_9y^3}{12\alpha_1} + \right.$$

$$\left. \frac{C_{10}x^4}{24} + \frac{C_{10}x^2y^2}{4\alpha_1} + \frac{C_{11}x^3y}{12} + \frac{C_{11}xy^3}{12\alpha_1} + \frac{C_{12}x^2y^2}{4} + \frac{C_{12}y^4}{24\alpha_1} \right] \quad (A.20)$$

Where:

$C_i$  and  $A_i$  — unknown coefficients.

Solution of the unknown coefficients is achieved by applying finite displacement boundary conditions to  $a_0$  and zero displacement boundary conditions to  $a_1$  and  $a_2$  (Equations - A.9 and A.10). The displacement boundary conditions are given in Table A.3A.

x	y	$u_y$	$u_x$
0	0	U2	U1
$x_2$	0	U4	U3
$x_3$	$y_3$	U6	U5
$x_2 / 2$	0	U8	U7
$(x_2 + x_3) / 2$	$y_3 / 2$	U10	U9
$x_3 / 2$	$y_3 / 2$	U12	U11

Table A.3A Finite Displacement Boundary Conditions

After applying the boundary conditions, the shape functions can be expressed as

$$a_x = a_{0x} + \omega^2 a_{2x} \quad (A.21)$$

$$a_y = a_{0y} + \omega^2 a_{2y} \quad (A.22)$$

The strain-displacement relationship can be expressed as

$$e = bU \quad (A.23)$$

Where:

$$e^T = \{ e_{xx}, e_{yy}, e_{xy} \} \quad (A.24)$$

$$e_{xx} = \frac{\partial u_x}{\partial x} = \frac{\partial}{\partial x} (a_{0x} + \omega^2 a_{2x}) U = (b_{0xx} + \omega^2 b_{2xx}) U \quad (A.25)$$

$$e_{yy} = \frac{\partial u_y}{\partial y} = \frac{\partial}{\partial y} (a_{0y} + \omega^2 a_{2y}) U = (b_{0yy} + \omega^2 b_{2yy}) U \quad (A.26)$$

$$\begin{aligned} e_{xy} &= \frac{\partial u_x}{\partial y} + \frac{\partial u_y}{\partial x} = \left( \frac{\partial a_{0x}}{\partial y} + \frac{\partial a_{0y}}{\partial x} \right) U + \omega^2 \left( \frac{\partial a_{2x}}{\partial y} + \frac{\partial a_{2y}}{\partial x} \right) U \\ &= (b_{0xy} + \omega^2 b_{2xy}) U \end{aligned} \quad (A.27)$$

The element stiffness matrix can be expressed as

$$K = K_0 + \omega^2 K_2 + \omega^4 K_4 \quad (A.28)$$

Where:

$$K_0 = \int_V b_0^T \chi b_0 dV \quad (A.29)$$

$$K_2 = \int_V b_0^T \chi b_2 dV + \int_V b_2^T \chi b_0 dV \quad (A.30)$$

$$K_4 = \int_V b_2^T \chi b_2 dV \quad (A.31)$$

Where  $\chi$  is the stress-strain matrix

$$\chi = \frac{E}{1 - \mu^2} \begin{bmatrix} 1 & \mu & 0 \\ \mu & 1 & 0 \\ 0 & 0 & \frac{1 - \mu}{2} \end{bmatrix} \quad (A.32)$$

The mass matrix can be expressed as

$$M_x = M_{0x} + \omega^2 M_{2x} \quad (A.33)$$

$$M_y = M_{0y} + \omega^2 M_{2y} \quad (A.34)$$

Where:

$$M_{0x} = \rho \int_V a_{0x}^T a_{0x} dV \quad (A.35)$$

$$M_{0y} = \rho \int_V a_{0y}^T a_{0y} dV \quad (A.36)$$

$$M_{2x} = \rho \int_V a_{0x}^T a_{2x} dV + \rho \int_V a_{2x}^T a_{0x} dV \quad (A.37)$$

$$M_{2y} = \rho \int_V a_{0y}^T a_{2y} dV + \rho \int_V a_{2y}^T a_{0y} dV \quad (A.38)$$

The symbolic manipulation program MACSYMA (Reference - 24) was used to process Equations A.17 through A.38. The program written by the author to perform these manipulations along with the generated mass and stiffness matrices are given in subsequent sections.

#### A.4 NUMERICAL EXAMPLE AND CONCLUSION

The square plate shown in Figure - A.4A was used as an example to verify the validity of the mass and stiffness matrices.

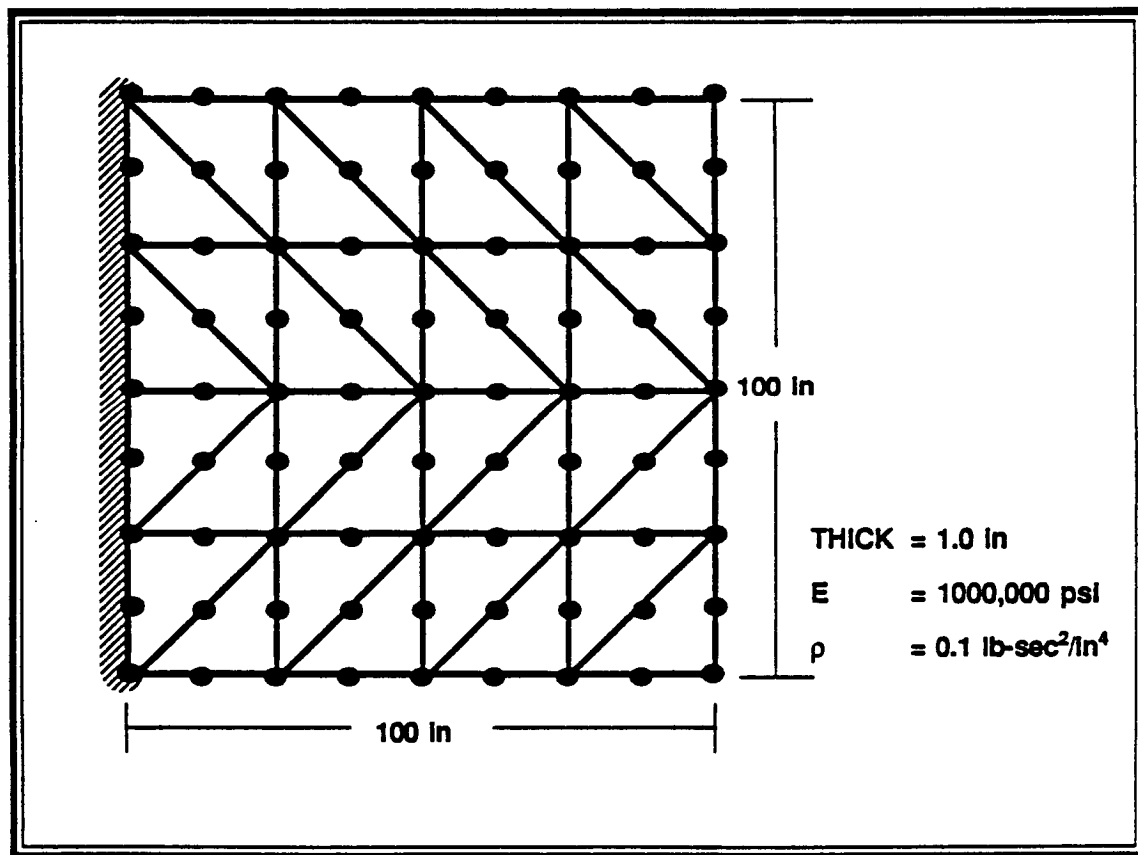


Figure A.4A Square Plate, Thirty-Two-Elements Mesh

The results for three test cases (Two, Eight, and Thirty-Two-Elements Mesh) obtained by Finite Element Method (FEM) and Dynamic Element Method (DEM) are given in Tables A.4A - A.4C. The tables reflect natural frequencies in parametric form and errors with respect to the exact values obtained from 160-Elements mesh.

Where:

$$\Omega_i = \omega_i / \sqrt{E/\rho}$$

$\omega_i$  — Natural frequency for the  $i^{\text{th}}$  mode.

	FEM	DEM	Exact	FEM Error (%)	DEM Error (%)
$\Omega_1$	0.00753001	0.00712904	0.00658513	14.3488283	8.25970035
$\Omega_2$	0.01668734	0.01601567	0.01579494	5.64987587	1.39745335
$\Omega_3$	0.02005333	0.01897272	0.01769073	13.3550221	7.24666178
$\Omega_4$	0.03288674	0.0316876	0.02796497	17.5997648	13.3117728

**Table A.4A** Natural Frequencies and Errors for Two-Elements Mesh

	FEM	DEM	Exact	FEM Error (%)	DEM Error (%)
$\Omega_1$	0.00693487	0.00667841	0.00658513	5.31117941	1.41663465
$\Omega_2$	0.01615449	0.01584605	0.01579494	2.27636742	0.32353648
$\Omega_3$	0.01894837	0.01824761	0.01769073	7.10902168	3.14784692
$\Omega_4$	0.02989933	0.02873055	0.02796497	6.91710108	2.7376658
$\Omega_5$	0.03251454	0.03150893	0.03033699	7.17785144	3.86307253
$\Omega_6$	0.03418327	0.03302366	0.03213664	6.36851169	2.7601476

Table A.4B Natural Frequencies and Errors for Eight-Elements Mesh

	FEM	DEM	Exact	FEM Error (%)	DEM Error (%)
$\Omega_1$	0.00665659	0.00661425	0.00658513	1.08528621	0.44227814
$\Omega_2$	0.01597266	0.01581132	0.01579494	1.12517018	0.10370786
$\Omega_3$	0.01800917	0.01779888	0.01769073	1.80004648	0.61133654
$\Omega_4$	0.02847314	0.02812498	0.02796497	1.81719494	0.57218459
$\Omega_5$	0.03124962	0.03056341	0.03033699	3.00831822	0.74634645
$\Omega_6$	0.03261257	0.03229697	0.03213664	1.48093481	0.49889299

Table A.4C Natural Frequencies and Errors for Thirty Two-Elements Mesh



Figures - A.4B through A.4D display a graphic representation of the errors. Figures - A.4E through A.4H display the error of four selected modes as a function of the number of elements. As shown in the figures, the results from dynamic element method display significantly lower error than the results obtained by the finite element method. It is evident from these graphs that the results obtained from the Eight-Elements mesh by finite dynamic element method fall within the same accuracy bracket as the Thirty-Two-Elements mesh solved by finite element technique. The reduction in the number of elements is equivalent to the reduction in the order of matrices. Therefore, it is significantly more economical to use finite dynamic element method to perform free vibration analysis of complex practical structures.

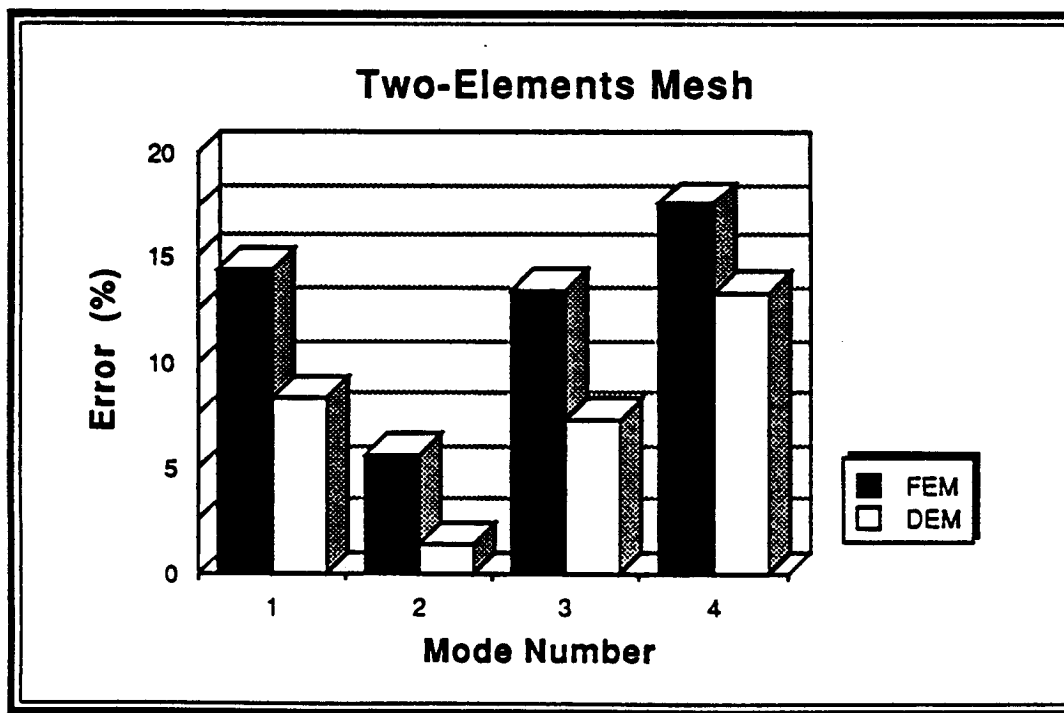


Figure A.4B Two-Elements Mesh Error Graphs

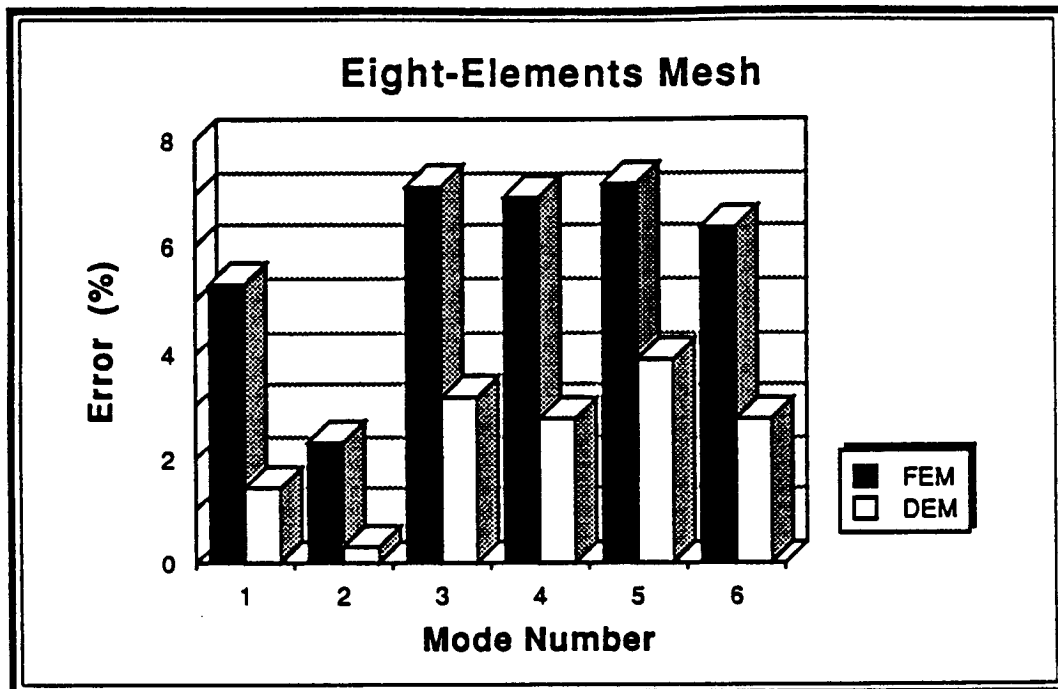


Figure A.4C Eight-Elements Mesh Error Graphs

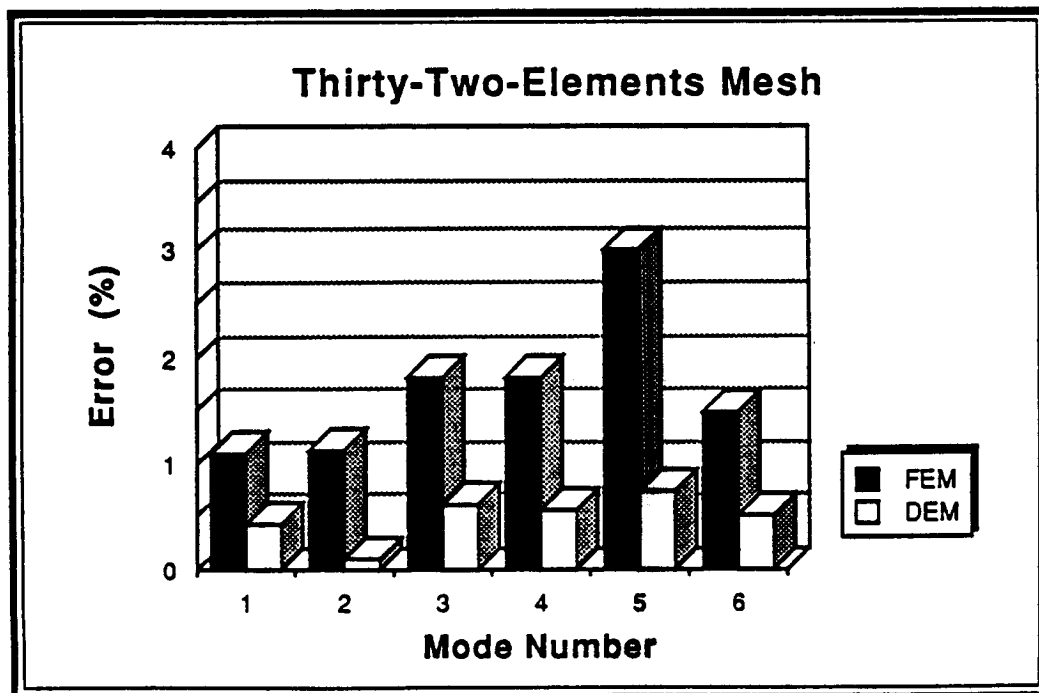


Figure A.4D Thirty Two-Elements Mesh Error Graphs

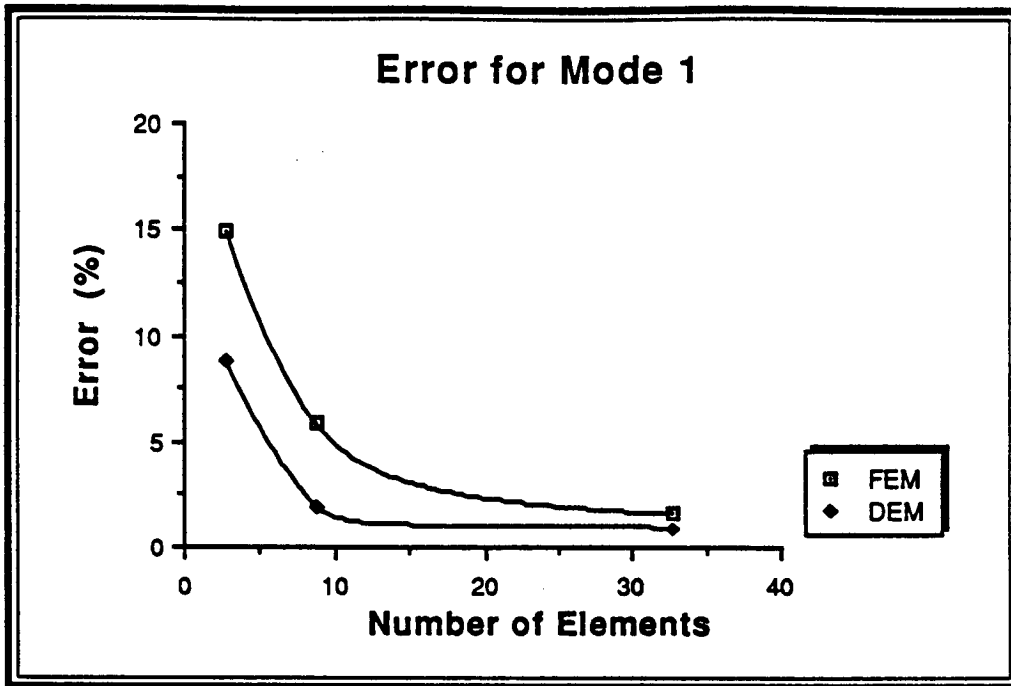


Figure A.4E Error for Mode Number 1

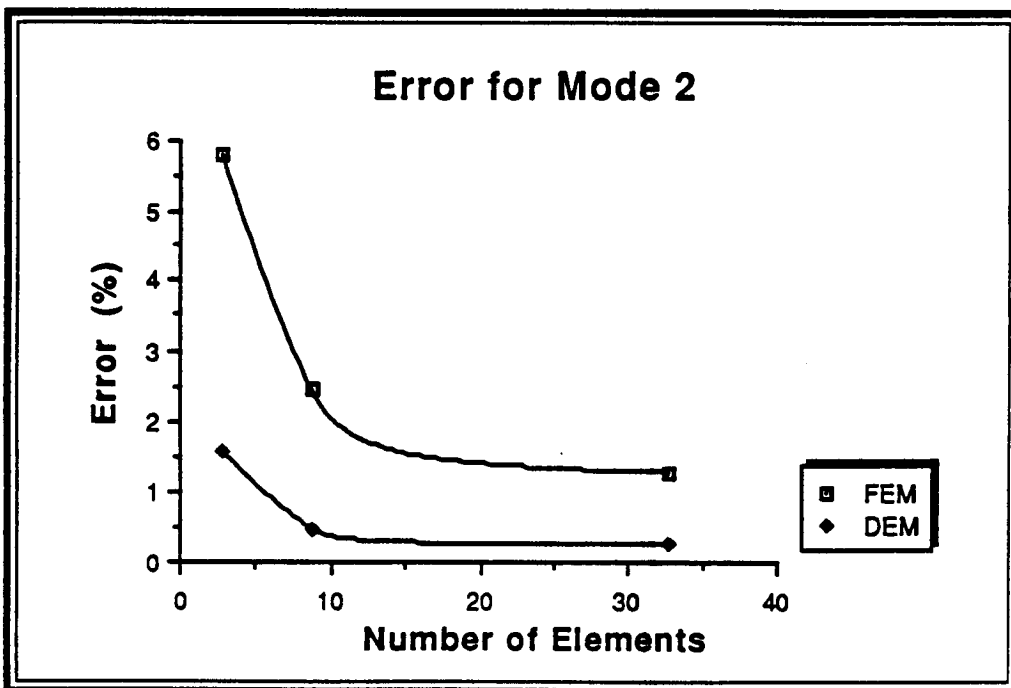


Figure A.4F Error for Mode Number 2

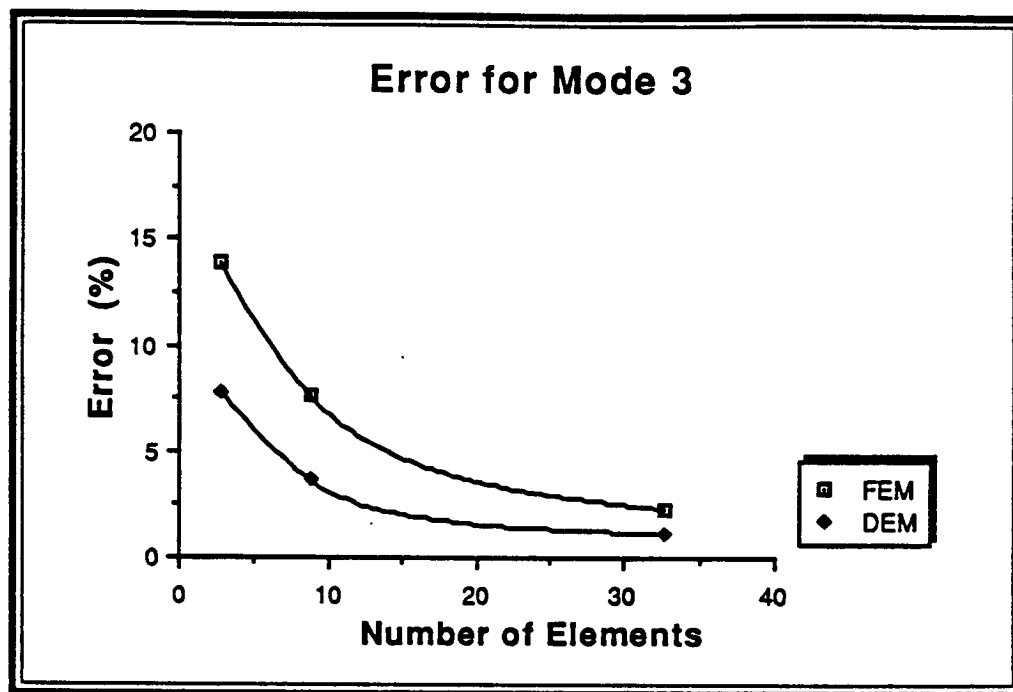


Figure A.4G Error for Mode Number 3

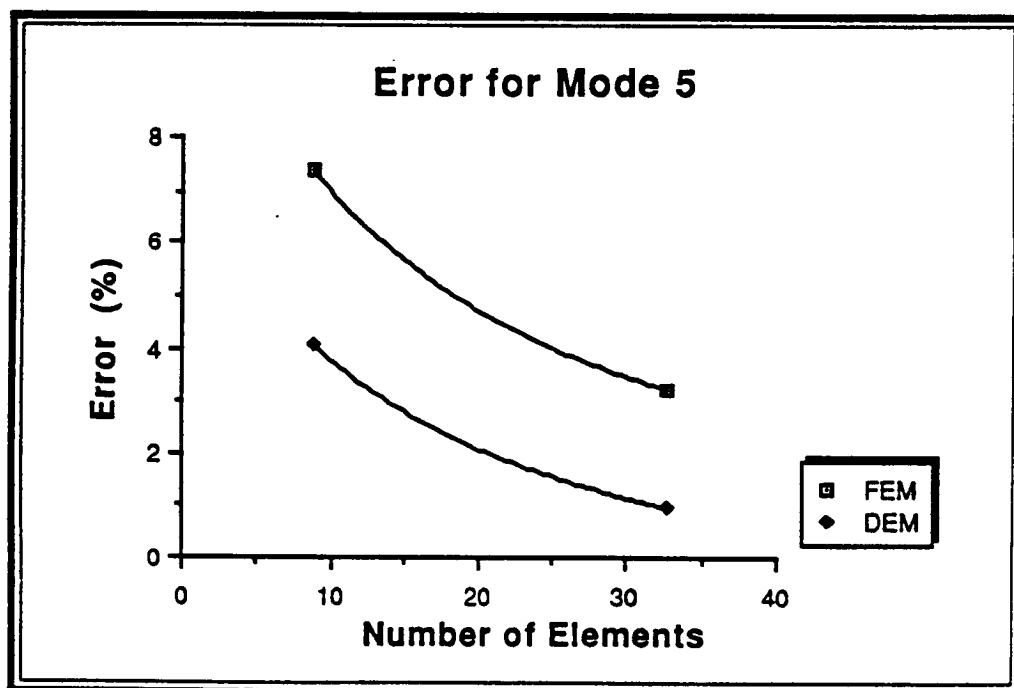


Figure A.4H Error for Mode Number 5

## A.5 LISTING OF THE MACSYMA INPUT PROGRAM

This program was developed to generate the mass and stiffness matrices for the higher order plane-stress finite dynamic triangular element in closed form. The matrices are then coded in FORTRAN language. These matrices are then transformed into subroutine form and implemented into the STARS package for tests and verification. These subroutines are presented in the subsequent sections.

```

/* MACSYMA program listing used to generate Mass and Stiffness matrices for
   Higher Order Plane Triangular Finite Dynamic Element */

/* Find the unknown coefficients ( CC1 - CC6 ) used to define the shape-function
   in the X-direction by applying the displacement boundary conditions */

A0X      : CC1 + CC2*X + CC3*Y + CC4*X^2 + CC5*X*Y + CC6*Y^2$
EQ1      : Subst ( [X=0,      Y=0      ], A0X )$
EQ2      : Subst ( [X=X2,      Y=0      ], A0X )$
EQ3      : Subst ( [X=X3,      Y=Y3     ], A0X )$
EQ4      : Subst ( [X=X2/2,    Y=0      ], A0X )$
EQ5      : Subst ( [X=(X2+X3)/2, Y=Y3/2 ], A0X )$
EQ6      : Subst ( [X=X3/2,    Y=Y3/2 ], A0X )$
Globalsolve : TRUE$
Solve     ( [EQ1=U1, EQ2=U3, EQ3=U5, EQ4=U7, EQ5=U9, EQ6=U11],
            [CC1, CC2, CC3, CC4, CC5, CC6] )$
A0X      : Ev ( A0X )$
A0XX     : Expand ( A0X )$
A0X      : MATRIX ( [Coeff(A0XX,U1)], [Coeff(A0XX,U3)],
                    [Coeff(A0XX,U5)], [Coeff(A0XX,U7)],
                    [Coeff(A0XX,U9)], [Coeff(A0XX,U11)] )$
Display   ( A0X );

```

/\* Find the unknown coefficients ( CC7 - CC12 ) used to define the shape-function in the Y-direction by applying the displacement boundary conditions \*/

```

A0Y      : CC7 + CC8*X + CC9*Y + CC10*X^2 + CC11*X*Y + CC12*Y^2$
EQ1      : Subst ( [X=0,          Y=0    ], A0Y )$
EQ2      : Subst ( [X=X2,          Y=0    ], A0Y )$
EQ3      : Subst ( [X=X3,          Y=Y3   ], A0Y )$
EQ4      : Subst ( [X=X2/2,        Y=0    ], A0Y )$
EQ5      : Subst ( [X=(X2+X3)/2,   Y=Y3/2 ], A0Y )$
EQ6      : Subst ( [X=X3/2,        Y=Y3/2 ], A0Y )$
Globalsolve : TRUE$
Solve     ( [EQ1=U2, EQ2=U4, EQ3=U6, EQ4=U8, EQ5=U10, EQ6=U12],
            [CC7, CC8, CC9, CC10, CC11, CC12] )$
A0Y      : Ev ( A0Y )$
A0YY     : Expand ( A0Y )$
A0Y      : MATRIX ( [Coeff(A0YY,U2)], [Coeff(A0YY,U4)],
                    [Coeff(A0YY,U6)], [Coeff(A0YY,U8)],
                    [Coeff(A0YY,U10)], [Coeff(A0YY,U12)] )$
Display   ( A0Y );
Save      ( [FHA0, 1, USER, [KGUPTA.ALI.MAX]], A0X, A0Y )$
Save      ( [FHC, 1, USER, [KGUPTA.ALI.MAX]],
            CC1, CC2, CC3, CC4, CC5, CC6,
            CC7, CC8, CC9, CC10, CC11, CC12 )$
Kill      ( A0X, A0Y, A0XX, A0YY )$

```

/\* Find the unknown coefficients ( A1 - A6 ) used to define the dynamic correction shape-function in the X-direction by applying zero displacement boundary conditions \*/

```

A2X      : A1 + A2*X + A3*Y + A4*X^2 + A5*X*Y + A6*Y^2 -
            CC1 * ( X^2/(4*AL1)      + Y^2/4      ) +
            CC2 * ( X^3/(12*AL1)     + X*Y^2/4     ) +
            CC3 * ( X^2*Y/(4*AL1)    + Y^3/12      ) +
            CC4 * ( X^4/(24*AL1)     + X^2*Y^2/4   ) +
            CC5 * ( X^3*Y/(12*AL1)   + X*Y^3/12   ) +
            CC6 * ( X^2*Y^2/(4*AL1)  + Y^4/24     ) $
A2X      : Expand ( A2X )$
EQ1      : Subst ( [X=0,          Y=0    ], A2X )$
EQ2      : Subst ( [X=X2,          Y=0    ], A2X )$
EQ3      : Subst ( [X=X3,          Y=Y3   ], A2X )$
EQ4      : Subst ( [X=X2/2,        Y=0    ], A2X )$
EQ5      : Subst ( [X=(X2+X3)/2,   Y=Y3/2 ], A2X )$
EQ6      : Subst ( [X=X3/2,        Y=Y3/2 ], A2X )$

```

```

Globalsolve : TRUE$
Solve       ( [EQ1=0, EQ2=0, EQ3=0, EQ4=0, EQ5=0, EQ6=0],
              [A1, A2, A3, A4, A5, A6] )$
A2X         : Ev ( A2X )$
A2XX        : Expand ( A2X )$
A2X         : Matrix ( [Coeff(A2XX,U1)], [Coeff(A2XX,U3)],
                      [Coeff(A2XX,U5)], [Coeff(A2XX,U7)],
                      [Coeff(A2XX,U9)], [Coeff(A2XX,U11)] )$
Display     ( A2X );

```

/\* Find the unknown coefficients ( A7 - A12 ) used to define the dynamic correction shape-function in the Y-direction by applying zero displacement boundary conditions \*/

```

A2Y         : A7 + A8*X + A9*Y + A10*X^2 + A11*X*Y + A12*Y^2 -
              CC7 * ( Y^2/(4*AL1) + X^2/4 ) +
              CC8 * ( X*Y^2/(4*AL1) + X^3/12 ) +
              CC9 * ( Y^3/(12*AL1) + X^2*Y/4 ) +
              CC10 * ( X^2*Y^2/(4*AL1) + X^4/24 ) +
              CC11 * ( X*Y^3/(12*AL1) + X^3*Y/12 ) +
              CC12 * ( Y^4/(24*AL1) + X^2*Y^2/4 )$
A2Y         : Expand ( A2Y )$
EQ1         : Subst ( [X=0, Y=0 ], A2Y )$
EQ2         : Subst ( [X=X2, Y=0 ], A2Y )$
EQ3         : Subst ( [X=X3, Y=Y3 ], A2Y )$
EQ4         : Subst ( [X=X2/2, Y=0 ], A2Y )$
EQ5         : Subst ( [X=(X2+X3)/2, Y=Y3/2 ], A2Y )$
EQ6         : Subst ( [X=X3/2, Y=Y3/2 ], A2Y )$
Globalsolve : TRUE$
Solve       ( [EQ1=0, EQ2=0, EQ3=0, EQ4=0, EQ5=0, EQ6=0],
              [A7, A8, A9, A10, A11, A12] )$
A2Y         : Ev ( A2Y )$
A2YY        : Expand ( A2Y )$
A2Y         : Matrix ( [Coeff(A2YY,U2)], [Coeff(A2YY,U4)],
                      [Coeff(A2YY,U6)], [Coeff(A2YY,U8)],
                      [Coeff(A2YY,U10)], [Coeff(A2YY,U12)] )$
Display     ( A2Y )$
Save        ( [FHA2, 1, USER, [KGUPTA.ALI.MAX]], A2X, A2Y )$
Kill        ( A2X, A2Y, A2XX, A2YY )$

```

/\* Form the Strain-Displacement Matrix B0 \*/

```

Loadfile ( FHA0, 1, USER, [KGUPTA.ALI.MAX] )$
EX        : A0X[1,1] * U1 + A0X[2,1] * U3 + A0X[3,1] * U5 +
            A0X[4,1] * U7 + A0X[5,1] * U9 + A0X[6,1] * U11$

```

```

EX      : Expand ( EX )$
EXX     : Diff ( EX, X )$
EY      : A0Y[1,1] * U2 + A0Y[2,1] * U4 + A0Y[3,1] * U6 +
          A0Y[4,1] * U8 + A0Y[5,1] * U10 + A0Y[6,1] * U12$
EY      : Expand ( EY )$
EYY     : Diff ( EY, Y )$
EXY     : Diff ( EX, Y ) + Diff ( EY, X )$
B0      : Matrix ( [Coeff(EXX,U1), Coeff(EYY,U1), Coeff(EXY,U1)],
                  [Coeff(EXX,U2), Coeff(EYY,U2), Coeff(EXY,U2)],
                  [Coeff(EXX,U3), Coeff(EYY,U3), Coeff(EXY,U3)],
                  [Coeff(EXX,U4), Coeff(EYY,U4), Coeff(EXY,U4)],
                  [Coeff(EXX,U5), Coeff(EYY,U5), Coeff(EXY,U5)],
                  [Coeff(EXX,U6), Coeff(EYY,U6), Coeff(EXY,U6)],
                  [Coeff(EXX,U7), Coeff(EYY,U7), Coeff(EXY,U7)],
                  [Coeff(EXX,U8), Coeff(EYY,U8), Coeff(EXY,U8)],
                  [Coeff(EXX,U9), Coeff(EYY,U9), Coeff(EXY,U9)],
                  [Coeff(EXX,U10), Coeff(EYY,U10), Coeff(EXY,U10)],
                  [Coeff(EXX,U11), Coeff(EYY,U11), Coeff(EXY,U11)],
                  [Coeff(EXX,U12), Coeff(EYY,U12), Coeff(EXY,U12)] ) $
Save    ( [FHB0, 1, USER, [KGUPTA.ALI.MAX]], B0 )$
Kill    ( A0X, A0Y, B0 )$

```

/\* Form the Strain-Displacement Matrix B2 \*/

```
Loadfile ( FHA2, 1, USER, [KGUPTA.ALI.MAX] )$
```

```

EX      : A2X[1,1] * U1 + A2X[2,1] * U3 + A2X[3,1] * U5 +
          A2X[4,1] * U7 + A2X[5,1] * U9 + A2X[6,1] * U11$
EX      : Expand ( EX )$
EXX     : Diff ( EX, X )$
EY      : A2Y[1,1] * U2 + A2Y[2,1] * U4 + A2Y[3,1] * U6 +
          A2Y[4,1] * U8 + A2Y[5,1] * U10 + A2Y[6,1] * U12$
EY      : Expand ( EY )$
EYY     : Diff ( EY, Y )$
EXY     : Diff ( EX, Y ) + Diff ( EY, X )$
B2      : Matrix ( [Coeff(EXX,U1), Coeff(EYY,U1), Coeff(EXY,U1)],
                  [Coeff(EXX,U2), Coeff(EYY,U2), Coeff(EXY,U2)],
                  [Coeff(EXX,U3), Coeff(EYY,U3), Coeff(EXY,U3)],
                  [Coeff(EXX,U4), Coeff(EYY,U4), Coeff(EXY,U4)],
                  [Coeff(EXX,U5), Coeff(EYY,U5), Coeff(EXY,U5)],
                  [Coeff(EXX,U6), Coeff(EYY,U6), Coeff(EXY,U6)],
                  [Coeff(EXX,U7), Coeff(EYY,U7), Coeff(EXY,U7)],
                  [Coeff(EXX,U8), Coeff(EYY,U8), Coeff(EXY,U8)],
                  [Coeff(EXX,U9), Coeff(EYY,U9), Coeff(EXY,U9)],
                  [Coeff(EXX,U10), Coeff(EYY,U10), Coeff(EXY,U10)],
                  [Coeff(EXX,U11), Coeff(EYY,U11), Coeff(EXY,U11)],
                  [Coeff(EXX,U12), Coeff(EYY,U12), Coeff(EXY,U12)] )$

```



```

Save      ( [FHB2, 1, USER, [KGUPTA.ALI.MAX]], B2 )$
Kill      ( A2X, A2Y, B2, EX, EY, EXX, EYY, EXY )$

/*      Form the Matrices by integrating over the area      */
LX        : X3*Y/Y3$
UX        : X2 - (X2 - X3) * Y/Y3$
UY        : Y3$

/*      Form Mass matrix M0X      */
Loadfile  ( FHA0, 1, USER, [KGUPTA.ALI.MAX] )$
Loadfile  ( FHA2, 1, USER, [KGUPTA.ALI.MAX] )$
A0XT      : Transpose ( A0X )$
A2XT      : Transpose ( A2X )$
M0X       : A0X . A0XT$
For I:1 Step 1 Thru 6 Do
  For J:I Step 1 Thru 6 Do
    ( INTGX : Integrate ( M0X[I,J], X, LX, UX ),
      INTGY : Integrate ( INTGX, Y, 0, UY ),
      M0X[I,J] : Expand ( INTGY ),
      M0X[J,I] : M0X[I,J] )$
  Display  ( M0X );

/*      Form Mass matrix M2X      */
M02X      : A0X . A2XT$
For I:1 Step 1 Thru 6 Do
  For J:I Step 1 Thru 6 Do
    ( INTGX : Integrate ( M02X[I,J], X, LX, UX ),
      INTGY : Integrate ( INTGX, Y, 0, UY ),
      M02X[I,J] : Expand ( INTGY ),
      M02X[J,I] : M02X[I,J] )$

/*      */
M20X      : A2X . A0XT$
For I:1 Step 1 Thru 6 Do
  For J:I Step 1 Thru 6 Do
    ( INTGX : Integrate ( M20X[I,J], X, LX, UX ),
      INTGY : Integrate ( INTGX, Y, 0, UY ),
      M20X[I,J] : Expand ( INTGY ),
      M20X[J,I] : M20X[I,J] )$
M2X       : M02X + M20X$

```

```

Kill ( A0X, A0XT, A2X, A2XT, M02X, M20X )$
DISPLAY ( M2X );

/*          Form Mass matrix  M0Y          */
A0YT      : Transpose ( A0Y )$
A2YT      : Transpose ( A2Y )$
M0Y       : A0Y . A0YT$
For I:1 Step 1 Thru 6 Do
  For J:I Step 1 Thru 6 Do
    ( INTGX   : Integrate ( M0Y[I,J], X, LX, UX ),
      INTGY   : Integrate ( INTGX,   Y, 0, UY ),
      M0Y[I,J] : Expand ( INTGY ),
      M0Y[J,I] : M0Y[I,J] )$
  DISPLAY ( M0Y );

/*          Form Mass matrix  M2Y          */
M02Y      : A0Y . A2YT$
For I:1 Step 1 Thru 6 Do
  For J:I Step 1 Thru 6 Do
    ( INTGX   : Integrate ( M02Y[I,J], X, LX, UX ),
      INTGY   : Integrate ( INTGX,   Y, 0, UY ),
      M02Y[I,J] : Expand ( INTGY ),
      M02Y[J,I] : M02Y[I,J] )$
  M20Y      : A2Y . A0YT$
  For I:1 Step 1 Thru 6 Do
    For J:I Step 1 Thru 6 Do
      ( INTGX   : Integrate ( M20Y[I,J], X, LX, UX ),
        INTGY   : Integrate ( INTGX,   Y, 0, UY ),
        M20Y[I,J] : Expand ( INTGY ),
        M20Y[J,I] : M20Y[I,J] )$
    M2Y       : M02Y + M20Y$
  DISPLAY    ( M2Y );
Save        ( [FHM, 1, USER, [KGUPTA.ALI.MAX]], M0X, M0Y, M2X, M2Y )$
Kill        ( A0Y, A0YT, A2Y, A2YT, M02Y, M20Y, M0X, M0Y, M2X, M2Y )$
/*          Form Stiffness matrix  K0          */
Loadfile    ( FHB0, 1, USER, [KGUPTA.ALI.MAX] )$
Loadfile    ( FHB2, 1, USER, [KGUPTA.ALI.MAX] )$

```

```

B0T      : Transpose ( B0 )$
B2T      : Transpose ( B2 )$
XI       : Matrix ( [1, NU, 0], [NU, 1, 0], [0, 0, (1-NU)/2] );
TEMP     : B0 . XI$
K0       : TEMP . B0T$
For I:1 Step 1 Thru 12 Do
  For J:I Step 1 Thru 12 Do
    ( INTGX : Integrate ( K0[I,J], X, LX, UX ),
      INTGY : Integrate ( INTGX, Y, 0, UY ),
      K0[I,J] : Expand ( INTGY ),
      K0[J,I] : K0[I,J] )$
  DISPLAY ( K0 );
/*      Form Stiffness matrix K2      */
K02      : TEMP . B2T$
For I:1 Step 1 Thru 12 Do
  For J:I Step 1 Thru 12 Do
    ( INTGX : Integrate ( K02[I,J], X, LX, UX ),
      INTGY : Integrate ( INTGX, Y, 0, UY ),
      K02[I,J] : Expand ( INTGY ),
      K02[J,I] : K02[I,J] )$
  TEMP    : B2 . XI$
  K20     : TEMP . B0T$
  For I:1 Step 1 Thru 12 Do
    For J:I Step 1 Thru 12 Do
      ( INTGX : Integrate ( K20[I,J], X, LX, UX ),
        INTGY : Integrate ( INTGX, Y, 0, UY ),
        K20[I,J] : Expand ( INTGY ),
        K20[J,I] : K20[I,J] )$
    K2      : K02 + K20$
  DISPLAY ( K2 );
Kill     ( B0, B0T, K02, K20 )$
TEMP     : B2 . XI$
Kill     ( B2 )$
/*      Form Stiffness matrix K4      */
K4       : TEMP . B2T$
Kill     ( TEMP, B2T )$

```

For I:1 Step 1 Thru 12 Do

For J:I Step 1 Thru 12 Do

( INTGX : Integrate ( K4[I,J], X, LX, UX ),  
INTGY : Integrate ( INTGX, Y, 0, UY ),  
K4[I,J] : Expand ( INTGY ),  
K4[J,I] : K4[I,J] )\$

DISPLAY ( K4 );

Save ( [FHK, 1, USER, [KGUPTA.ALI.MAX]], K0, K2, K4 )\$

## A.6 LISTING OF THE SUBROUTINE TSHK0

This subroutine is used to generate the stiffness matrix  $K_0$ .

```

SUBROUTINE TSHK0 ( X2, X3, Y3, E, TH, NU, K0 )
C
C
C Form the K0 matrix for plane triangular element.
C
C Arguments:
C
C   X2, X3, Y3      —      Geometry to define the triangle.
C   E               —      Young's modulus.
C   TH              —      Element Thickness.
C   NU              —      Poisson's ratio.
C   K0(12,12)       —      Output stiffness matrix.
C
C
C   IMPLICIT INTEGER ( A - Z )
C
C   REAL    X2, X3, Y3, E, TH, NU, F
C   REAL    K0(12,12)
C
C
C   CALL INIT ( K0, 144 )
C
C   F = E*TH / (1.0 - NU*NU)
C
C
C
C   K0(1,1) = Y3/X2/2.0-NU*X3**2/(X2*Y3)/4.0+X3**2/(X2*Y3)/4.0+NU*X3/Y
1  3/2.0-X3/Y3/2.0-NU*X2/Y3/4.0+X2/Y3/4.0
C   K0(1,2) = -NU*X3/X2/4.0-X3/X2/4.0+NU/4.0+1.0/4.0
C   K0(1,3) = Y3/X2/6.0-NU*X3**2/(X2*Y3)/12.0+X3**2/(X2*Y3)/12.0+NU*X3
1  /Y3/12.0-X3/Y3/12.0
C   K0(1,4) = -NU*X3/X2/12.0-X3/X2/12.0-NU/12.0+1.0/12.0
C   K0(1,5) = NU*X3/Y3/12.0-X3/Y3/12.0-NU*X2/Y3/12.0+X2/Y3/12.0
C   K0(1,6) = NU/6.0
C   K0(1,7) = (-2.0)*Y3/(3.0*X2)+NU*X3**2/(X2*Y3)/3.0-X3**2/(X2*Y3)/3.
1  0-NU*X3/Y3/3.0+X3/Y3/3.0
C   K0(1,8) = NU*X3/X2/3.0+X3/X2/3.0+NU/3.0+(-1.0)/3.0
C   K0(1,11) = -NU*X3/Y3/3.0+X3/Y3/3.0+NU*X2/Y3/3.0-X2/Y3/3.0
C   K0(1,12) = (-2.0)*NU/3.0

```

C

$$\begin{aligned}
K0(2,2) &= -NU*Y3/X2/4.0+Y3/X2/4.0+X3**2/(X2*Y3)/2.0-X3/Y3+X2/Y3/2. \\
K0(2,3) &= -NU*X3/X2/12.0-X3/X2/12.0+NU/6.0 \\
K0(2,4) &= -NU*Y3/X2/12.0+Y3/X2/12.0+X3**2/(X2*Y3)/6.0-X3/Y3/6.0 \\
K0(2,5) &= 1.0/12.0-NU/12.0 \\
K0(2,6) &= X2/Y3/6.0-X3/Y3/6.0 \\
K0(2,7) &= NU*X3/X2/3.0+X3/X2/3.0+(-2.0)*NU/3.0 \\
K0(2,8) &= NU*Y3/X2/3.0-Y3/X2/3.0+(-2.0)*X3**2/(3.0*X2*Y3)+2.0*X3/( \\
1 \quad &3.0*Y3) \\
K0(2,11) &= NU/3.0+(-1.0)/3.0 \\
K0(2,12) &= 2.0*X3/(3.0*Y3)+(-2.0)*X2/(3.0*Y3)
\end{aligned}$$

C

$$\begin{aligned}
K0(3,3) &= Y3/X2/2.0-NU*X3**2/(X2*Y3)/4.0+X3**2/(X2*Y3)/4.0 \\
K0(3,4) &= -NU*X3/X2/4.0-X3/X2/4.0 \\
K0(3,5) &= X3/Y3/12.0-NU*X3/Y3/12.0 \\
K0(3,6) &= -NU/6.0 \\
K0(3,7) &= (-2.0)*Y3/(3.0*X2)+NU*X3**2/(X2*Y3)/3.0-X3**2/(X2*Y3)/3. \\
1 \quad &0-NU*X3/Y3/3.0+X3/Y3/3.0 \\
K0(3,8) &= NU*X3/X2/3.0+X3/X2/3.0+(-2.0)*NU/3.0 \\
K0(3,9) &= NU*X3/Y3/3.0-X3/Y3/3.0 \\
K0(3,10) &= 2.0*NU/3.0
\end{aligned}$$

C

$$\begin{aligned}
K0(4,4) &= -NU*Y3/X2/4.0+Y3/X2/4.0+X3**2/(X2*Y3)/2.0 \\
K0(4,5) &= NU/12.0+(-1.0)/12.0 \\
K0(4,6) &= X3/Y3/6.0 \\
K0(4,7) &= NU*X3/X2/3.0+X3/X2/3.0+NU/3.0+(-1.0)/3.0 \\
K0(4,8) &= NU*Y3/X2/3.0-Y3/X2/3.0+(-2.0)*X3**2/(3.0*X2*Y3)+2.0*X3/( \\
1 \quad &3.0*Y3) \\
K0(4,9) &= 1.0/3.0-NU/3.0 \\
K0(4,10) &= (-2.0)*X3/(3.0*Y3)
\end{aligned}$$

C

$$\begin{aligned}
K0(5,5) &= X2/Y3/4.0-NU*X2/Y3/4.0 \\
K0(5,9) &= NU*X3/Y3/3.0-X3/Y3/3.0 \\
K0(5,10) &= 1.0/3.0-NU/3.0 \\
K0(5,11) &= -NU*X3/Y3/3.0+X3/Y3/3.0+NU*X2/Y3/3.0-X2/Y3/3.0 \\
K0(5,12) &= NU/3.0+(-1.0)/3.0
\end{aligned}$$

C

$$\begin{aligned}
K0(6,6) &= X2/Y3/2.0 \\
K0(6,9) &= 2.0*NU/3.0 \\
K0(6,10) &= (-2.0)*X3/(3.0*Y3) \\
K0(6,11) &= (-2.0)*NU/3.0 \\
K0(6,12) &= 2.0*X3/(3.0*Y3)+(-2.0)*X2/(3.0*Y3)
\end{aligned}$$

C

$$\begin{aligned}
K0(7,7) &= 4.0*Y3/(3.0*X2)+(-2.0)*NU*X3**2/(3.0*X2*Y3)+2.0*X3**2/(3 \\
1 \quad &.0*X2*Y3)+2.0*NU*X3/(3.0*Y3)+(-2.0)*X3/(3.0*Y3)+(-2.0)*NU*X2/(3 \\
2 \quad &.0*Y3)+2.0*X2/(3.0*Y3) \\
K0(7,8) &= (-2.0)*NU*X3/(3.0*X2)+(-2.0)*X3/(3.0*X2)+NU/3.0+1.0/3.0 \\
K0(7,9) &= (-2.0)*NU*X3/(3.0*Y3)+2.0*X3/(3.0*Y3)+2.0*NU*X2/(3.0*Y3) \\
1 \quad &+(-2.0)*X2/(3.0*Y3) \\
K0(7,10) &= (-1.0)/3.0-NU/3.0
\end{aligned}$$

```

      K0(7,11) = 2.0*NU*X3/(3.0*Y3)+(-2.0)*X3/(3.0*Y3)
      K0(7,12) = NU/3.0+1.0/3.0
C
      K0(8,8) = (-2.0)*NU*Y3/(3.0*X2)+2.0*Y3/(3.0*X2)+4.0*X3**2/(3.0*X2*
1      Y3)+(-4.0)*X3/(3.0*Y3)+4.0*X2/(3.0*Y3)
      K0(8,9) = (-1.0)/3.0-NU/3.0
      K0(8,10) = 4.0*X3/(3.0*Y3)+(-4.0)*X2/(3.0*Y3)
      K0(8,11) = NU/3.0+1.0/3.0
      K0(8,12) = (-4.0)*X3/(3.0*Y3)
C
      K0(9,9) = 4.0*Y3/(3.0*X2)+(-2.0)*NU*X3**2/(3.0*X2*Y3)+2.0*X3**2/(3
1      .0*X2*Y3)+2.0*NU*X3/(3.0*Y3)+(-2.0)*X3/(3.0*Y3)+(-2.0)*NU*X2/(3
2      .0*Y3)+2.0*X2/(3.0*Y3)
      K0(9,10) = (-2.0)*NU*X3/(3.0*X2)+(-2.0)*X3/(3.0*X2)+NU/3.0+1.0/3.0
      K0(9,11) = (-4.0)*Y3/(3.0*X2)+2.0*NU*X3**2/(3.0*X2*Y3)+(-2.0)*X3**
1      2/(3.0*X2*Y3)+(-2.0)*NU*X3/(3.0*Y3)+2.0*X3/(3.0*Y3)
      K0(9,12) = 2.0*NU*X3/(3.0*X2)+2.0*X3/(3.0*X2)-NU/3.0+(-1.0)/3.0
C
      K0(10,10) = (-2.0)*NU*Y3/(3.0*X2)+2.0*Y3/(3.0*X2)+4.0*X3**2/(3.0*X
1      2*Y3)+(-4.0)*X3/(3.0*Y3)+4.0*X2/(3.0*Y3)
      K0(10,11) = 2.0*NU*X3/(3.0*X2)+2.0*X3/(3.0*X2)-NU/3.0+(-1.0)/3.0
      K0(10,12) = 2.0*NU*Y3/(3.0*X2)+(-2.0)*Y3/(3.0*X2)+(-4.0)*X3**2/(3.
1      0*X2*Y3)+4.0*X3/(3.0*Y3)
C
      K0(11,11) = 4.0*Y3/(3.0*X2)+(-2.0)*NU*X3**2/(3.0*X2*Y3)+2.0*X3**2/
1      (3.0*X2*Y3)+2.0*NU*X3/(3.0*Y3)+(-2.0)*X3/(3.0*Y3)+(-2.0)*NU*X2/
2      (3.0*Y3)+2.0*X2/(3.0*Y3)
      K0(11,12) = (-2.0)*NU*X3/(3.0*X2)+(-2.0)*X3/(3.0*X2)+NU/3.0+1.0/3.
1      0
C
      K0(12,12) = (-2.0)*NU*Y3/(3.0*X2)+2.0*Y3/(3.0*X2)+4.0*X3**2/(3.0*X
1      2*Y3)+(-4.0)*X3/(3.0*Y3)+4.0*X2/(3.0*Y3)
C
C
C
      DO 100 I = 1, 12
      DO 100 J = I, 12
          K0(I,J) = F * K0(I,J)
          K0(J,I) = K0(I,J)
100  CONTINUE
C
C
C
      RETURN
      END

```

## A7 LISTING OF THE SUBROUTINE TSHK2

This subroutine is used to generate the stiffness matrix  $K_2$ .

```

C
C SUBROUTINE TSHK2 ( X2, X3, Y3, E, RHO, TH, NU, K2 )
C
C Form the K2 matrix for plane triangular element.
C
C Arguments:
C
C   X2, X3, Y3  — Geometry to define the triangle.
C   E           — Young's Modulus.
C   RHO         — Mass density per unit volume.
C   TH          — Element Thickness.
C   NU          — Poisson's Ratio
C   K2(12,12)   — Output mass matrix.
C
C
C IMPLICIT INTEGER ( A - Z )
C
C REAL  X2, X3, Y3, E, RHO, TH, NU, F, BETA, AL1
C REAL  X2TWO, X2THR, X3TWO, X3THR, X3FOR, X3FIV, Y3TWO, Y3THR
C
C REAL  K2(12,12)
C
C
C CALL INIT ( K2, 144 )
C
C AL1    = 2.0 * (1 - NU) / (1 - 2.0*NU)
C BETA   = 2.0 * (1 + NU) * RHO / E
C F      = BETA * E * TH / (1.0 - NU*NU)
C
C X2TWO  = X2 * X2
C X2THR  = X2TWO * X2
C
C X3TWO  = X3 * X3
C X3THR  = X3TWO * X3
C X3FOR  = X3THR * X3
C X3FIV  = X3FOR * X3
C
C Y3TWO  = Y3 * Y3
C Y3THR  = Y3TWO * Y3

```



C  
C  
C

```

K2(1,1) = -X3*Y3THR/X2TWO/45.0+Y3THR/X2/360.0+37.0*NU*X3THR*Y3/(14
1  40.0*X2TWO)-X3THR*Y3/(AL1*X2TWO)/90.0+(-37.0)*X3THR*Y3/(1440.0*
2  X2TWO)+(-13.0)*NU*X3TWO*Y3/(288.0*X2)+X3TWO*Y3/(AL1*X2)/120.0+1
3  3.0*X3TWO*Y3/(288.0*X2)+5.0*NU*X3*Y3/288.0+X3*Y3/AL1/60.0+(-5.0
4  )*X3*Y3/288.0+NU*X2*Y3/480.0-X2*Y3/AL1/240.0-X2*Y3/480.0+29.0*N
5  U*X3FIV/(1440.0*AL1*X2TWO*Y3)+(-29.0)*X3FIV/(1440.0*AL1*X2TWO*Y
6  3)+(-5.0)*NU*X3FOR/(96.0*AL1*X2*Y3)+5.0*X3FOR/(96.0*AL1*X2*Y3)+
7  23.0*NU*X3THR/(720.0*AL1*Y3)+(-23.0)*X3THR/(720.0*AL1*Y3)+NU*X2
8  *X3TWO/(AL1*Y3)/96.0-X2*X3TWO/(AL1*Y3)/96.0+(-13.0)*NU*X2TWO*X3
9  /(1440.0*AL1*Y3)+13.0*X2TWO*X3/(1440.0*AL1*Y3)-NU*X2THR/(AL1*Y3
:  )/720.0+X2THR/(AL1*Y3)/720.0
K2(1,2) = 29.0*NU*X3TWO*Y3TWO/(1440.0*AL1*X2TWO)-NU*X3TWO*Y3TWO/X2
1  TWO/576.0+X3TWO*Y3TWO/(AL1*X2TWO)/180.0+37.0*X3TWO*Y3TWO/(2880.
2  0*X2TWO)+(-19.0)*NU*X3*Y3TWO/(1440.0*AL1*X2)-NU*X3*Y3TWO/X2/360
3  .0-X3*Y3TWO/(AL1*X2)/160.0+(-7.0)*X3*Y3TWO/(720.0*X2)-NU*Y3TWO/
4  AL1/360.0+7.0*NU*Y3TWO/2880.0+Y3TWO/AL1/1440.0-Y3TWO/960.0+(-13
5  .0)*NU*X3FOR/(2880.0*AL1*X2TWO)+5.0*NU*X3FOR/(288.0*X2TWO)+29.0
6  *X3FOR/(2880.0*AL1*X2TWO)+X3FOR/X2TWO/360.0+NU*X3THR/(AL1*X2)/1
7  60.0+(-13.0)*NU*X3THR/(480.0*X2)+(-23.0)*X3THR/(1440.0*AL1*X2)+
8  (-7.0)*X3THR/(1440.0*X2)-NU*X3TWO/AL1/240.0+NU*X3TWO/480.0-X3TW
9  O/480.0+NU*X2*X3/AL1/192.0+NU*X2*X3/192.0+X2*X3/AL1/192.0+X2*X3
:  /192.0-NU*X2TWO/AL1/360.0+7.0*NU*X2TWO/2880.0+X2TWO/AL1/1440.0-
;  X2TWO/960.0
K2(1,3) = -Y3THR/X2/72.0+(-7.0)*NU*X3TWO*Y3/(2880.0*X2)-X3TWO*Y3/(
1  AL1*X2)/120.0+7.0*X3TWO*Y3/(2880.0*X2)+7.0*NU*X3*Y3/2880.0-X3*Y
2  3/AL1/120.0+(-7.0)*X3*Y3/2880.0+NU*X2*Y3/1440.0+X2*Y3/AL1/90.0-
3  X2*Y3/1440.0+3.0*NU*X3FOR/(320.0*AL1*X2*Y3)+(-3.0)*X3FOR/(320.0
4  *AL1*X2*Y3)-NU*X3THR/(AL1*Y3)/480.0+X3THR/(AL1*Y3)/480.0+(-23.0
5  )*NU*X2*X3TWO/(1440.0*AL1*Y3)+23.0*X2*X3TWO/(1440.0*AL1*Y3)+5.0
6  *NU*X2TWO*X3/(576.0*AL1*Y3)+(-5.0)*X2TWO*X3/(576.0*AL1*Y3)
K2(1,4) = 29.0*NU*X3TWO*Y3TWO/(1440.0*AL1*X2TWO)+NU*X3TWO*Y3TWO/X2
1  TWO/576.0+X3TWO*Y3TWO/(AL1*X2TWO)/180.0+(-37.0)*X3TWO*Y3TWO/(28
2  80.0*X2TWO)-NU*X3*Y3TWO/(AL1*X2)/96.0-NU*X3*Y3TWO/X2/180.0+(-7.
3  0)*X3*Y3TWO/(1440.0*AL1*X2)+13.0*X3*Y3TWO/(720.0*X2)-NU*Y3TWO/A
4  L1/1440.0+13.0*NU*Y3TWO/2880.0-Y3TWO/AL1/1440.0+(-13.0)*Y3TWO/2
5  880.0+13.0*NU*X3FOR/(2880.0*AL1*X2TWO)+5.0*NU*X3FOR/(288.0*X2TW
6  O)+(-29.0)*X3FOR/(2880.0*AL1*X2TWO)+X3FOR/X2TWO/360.0+(-19.0)*N
7  U*X3THR/(1440.0*AL1*X2)+7.0*NU*X3THR/(1440.0*X2)+5.0*X3THR/(288
8  .0*AL1*X2)-X3THR/X2/1440.0+NU*X3TWO/AL1/160.0-NU*X3TWO/480.0+X3
9  TWO/AL1/480.0-X3TWO/480.0+23.0*NU*X2*X3/(2880.0*AL1)-NU*X2*X3/9
:  60.0+(-49.0)*X2*X3/(2880.0*AL1)-X2*X3/960.0+(-11.0)*NU*X2TWO/(1
;  440.0*AL1)-NU*X2TWO/960.0+11.0*X2TWO/(1440.0*AL1)+X2TWO/960.0
K2(1,5) = (-17.0)*NU*X3TWO*Y3/(576.0*X2)+17.0*X3TWO*Y3/(576.0*X2)+
1  91.0*NU*X3*Y3/2880.0-X3*Y3/AL1/120.0+(-91.0)*X3*Y3/2880.0-NU*X2
2  *Y3/180.0-X2*Y3/AL1/720.0+X2*Y3/180.0+(-13.0)*NU*X3FOR/(576.0*A
3  L1*X2*Y3)+13.0*X3FOR/(576.0*AL1*X2*Y3)+9.0*NU*X3THR/(160.0*AL1*
4  Y3)+(-9.0)*X3THR/(160.0*AL1*Y3)+(-19.0)*NU*X2*X3TWO/(720.0*AL1*

```

```

5  Y3)+19.0*X2*X3TWO/(720.0*AL1*Y3)+(-41.0)*NU*X2TWO*X3/(2880.0*AL
6  1*Y3)+41.0*X2TWO*X3/(2880.0*AL1*Y3)+NU*X2THR/(AL1*Y3)/144.0-X2T
7  HR/(AL1*Y3)/144.0
      K2(1,6) = -NU*X3*Y3TWO/X2/36.0+NU*Y3TWO/AL1/480.0+11.0*NU*Y3TWO/72
1  0.0-NU*X3THR/(AL1*X2)/72.0+NU*X3TWO/AL1/60.0+NU*X3TWO/40.0+X3TW
2  O/240.0+NU*X2*X3/AL1/120.0-NU*X2*X3/288.0-X2*X3/288.0+(-13.0)*N
3  U*X2TWO/(1440.0*AL1)-NU*X2TWO/1440.0-X2TWO/1440.0
      K2(1,7) = X3*Y3THR/X2TWO/45.0+Y3THR/X2/90.0+(-37.0)*NU*X3THR*Y3/(1
1  440.0*X2TWO)+X3THR*Y3/(AL1*X2TWO)/90.0+37.0*X3THR*Y3/(1440.0*X2
2  TWO)+37.0*NU*X3TWO*Y3/(1440.0*X2)+(-37.0)*X3TWO*Y3/(1440.0*X2)+
3  NU*X3*Y3/288.0-X3*Y3/288.0-NU*X2*Y3/288.0+X2*Y3/288.0+(-29.0)*N
4  U*X3FIV/(1440.0*AL1*X2TWO*Y3)+29.0*X3FIV/(1440.0*AL1*X2TWO*Y3)+
5  NU*X3FOR/(AL1*X2*Y3)/40.0-X3FOR/(AL1*X2*Y3)/40.0-NU*X3THR/(AL1*
6  Y3)/144.0+X3THR/(AL1*Y3)/144.0+NU*X2*X3TWO/(AL1*Y3)/48.0-X2*X3T
7  WO/(AL1*Y3)/48.0+(-7.0)*NU*X2TWO*X3/(288.0*AL1*Y3)+7.0*X2TWO*X3
8  /(288.0*AL1*Y3)+NU*X2THR/(AL1*Y3)/180.0-X2THR/(AL1*Y3)/180.0
      K2(1,8) = (-29.0)*NU*X3TWO*Y3TWO/(720.0*AL1*X2TWO)-X3TWO*Y3TWO/(AL
1  1*X2TWO)/90.0+17.0*NU*X3*Y3TWO/(720.0*AL1*X2)-NU*X3*Y3TWO/X2/12
2  0.0+X3*Y3TWO/(AL1*X2)/90.0-X3*Y3TWO/X2/120.0+NU*Y3TWO/180.0+Y3T
3  WO/180.0+(-5.0)*NU*X3FOR/(144.0*X2TWO)-X3FOR/X2TWO/180.0-NU*X3T
4  HR/(AL1*X2)/720.0+NU*X3THR/X2/45.0-X3THR/(AL1*X2)/720.0+X3THR/X
5  2/180.0-NU*X3TWO/AL1/480.0-X3TWO/AL1/480.0+17.0*NU*X2*X3/(1440.
6  0*AL1)-NU*X2*X3/288.0+17.0*X2*X3/(1440.0*AL1)-X2*X3/288.0-NU*X2
7  TWO/AL1/360.0+NU*X2TWO/480.0-X2TWO/AL1/120.0+X2TWO/288.0
      K2(1,9) = -X3*Y3THR/X2TWO/30.0+Y3THR/X2/90.0+NU*X3THR*Y3/X2TWO/30.
1  0-X3THR*Y3/(AL1*X2TWO)/60.0-X3THR*Y3/X2TWO/30.0-NU*X3TWO*Y3/X2/
2  60.0+X3TWO*Y3/(AL1*X2)/24.0+X3TWO*Y3/X2/60.0+(-29.0)*NU*X3*Y3/1
3  440.0+29.0*X3*Y3/1440.0+NU*X2*Y3/160.0-X2*Y3/AL1/80.0-X2*Y3/160
4  .0+NU*X3FIV/(AL1*X2TWO*Y3)/40.0-X3FIV/(AL1*X2TWO*Y3)/40.0+(-101
5  .0)*NU*X3FOR/(1440.0*AL1*X2*Y3)+101.0*X3FOR/(1440.0*AL1*X2*Y3)+
6  11.0*NU*X3THR/(240.0*AL1*Y3)+(-11.0)*X3THR/(240.0*AL1*Y3)-NU*X2
7  *X3TWO/(AL1*Y3)/160.0+X2*X3TWO/(AL1*Y3)/160.0+NU*X2TWO*X3/(AL1*
8  Y3)/90.0-X2TWO*X3/(AL1*Y3)/90.0-NU*X2THR/(AL1*Y3)/180.0+X2THR/(
9  AL1*Y3)/180.0
      K2(1,10) = X3TWO*Y3TWO/X2TWO/30.0+NU*X3*Y3TWO/(AL1*X2)/80.0+NU*X3*
1  Y3TWO/X2/45.0+X3*Y3TWO/(AL1*X2)/360.0-X3*Y3TWO/X2/30.0-NU*Y3TWO
2  /AL1/360.0-NU*Y3TWO/60.0-Y3TWO/AL1/360.0+Y3TWO/180.0-NU*X3FOR/(
3  AL1*X2TWO)/120.0+X3FOR/(AL1*X2TWO)/40.0+NU*X3THR/(AL1*X2)/36.0+
4  (-17.0)*NU*X3THR/(360.0*X2)-X3THR/(AL1*X2)/20.0-X3THR/X2/120.0+
5  (-7.0)*NU*X3TWO/(480.0*AL1)+NU*X3TWO/120.0+3.0*X3TWO/(160.0*AL1
6  )+X3TWO/120.0+(-31.0)*NU*X2*X3/(1440.0*AL1)+NU*X2*X3/360.0+17.0
7  *X2*X3/(1440.0*AL1)+X2*X3/360.0+NU*X2TWO/AL1/60.0-NU*X2TWO/360.
8  0-X2TWO/AL1/180.0-X2TWO/360.0
      K2(1,11) = X3*Y3THR/X2TWO/30.0-Y3THR/X2/90.0-NU*X3THR*Y3/X2TWO/30.
1  0+X3THR*Y3/(AL1*X2TWO)/60.0+X3THR*Y3/X2TWO/30.0+49.0*NU*X3TWO*Y
2  3/(720.0*X2)-X3TWO*Y3/(AL1*X2)/24.0+(-49.0)*X3TWO*Y3/(720.0*X2)
3  +(-5.0)*NU*X3*Y3/144.0+5.0*X3*Y3/144.0+X2*Y3/AL1/144.0-NU*X3FIV
4  /(AL1*X2TWO*Y3)/40.0+X3FIV/(AL1*X2TWO*Y3)/40.0+53.0*NU*X3FOR/(4
5  80.0*AL1*X2*Y3)+(-53.0)*X3FOR/(480.0*AL1*X2*Y3)-NU*X3THR/(AL1*Y

```

```

6  3)/8.0+X3THR/(AL1*Y3)/8.0+5.0*NU*X2*X3TWO/(288.0*AL1*Y3)+(-5.0)
7  *X2*X3TWO/(288.0*AL1*Y3)+NU*X2TWO*X3/(AL1*Y3)/36.0-X2TWO*X3/(AL
8  1*Y3)/36.0-NU*X2THR/(AL1*Y3)/180.0+X2THR/(AL1*Y3)/180.0
  K2(1,12) = -X3TWO*Y3TWO/X2TWO/30.0-NU*X3*Y3TWO/(AL1*X2)/80.0+NU*X3
1  *Y3TWO/X2/45.0-X3*Y3TWO/(AL1*X2)/360.0+X3*Y3TWO/X2/30.0+NU*Y3TW
2  O/AL1/240.0-NU*Y3TWO/90.0+Y3TWO/AL1/360.0-Y3TWO/180.0+NU*X3FOR/
3  (AL1*X2TWO)/120.0-X3FOR/(AL1*X2TWO)/40.0-NU*X3THR/(AL1*X2)/180.
4  0+17.0*NU*X3THR/(360.0*X2)+X3THR/(AL1*X2)/20.0+X3THR/X2/120.0-N
5  U*X3TWO/AL1/480.0-NU*X3TWO/30.0+(-3.0)*X3TWO/(160.0*AL1)-X3TWO/
6  120.0+(-17.0)*NU*X2*X3/(1440.0*AL1)+(-17.0)*X2*X3/(1440.0*AL1)+
7  NU*X2TWO/AL1/180.0+X2TWO/AL1/180.0

```

C

```

  K2(2,2) = NU*X3*Y3THR/(AL1*X2TWO)/90.0-X3*Y3THR/(AL1*X2TWO)/90.0-N
1  U*Y3THR/(AL1*X2)/720.0+Y3THR/(AL1*X2)/720.0+NU*X3THR*Y3/X2TWO/1
2  80.0+(-37.0)*X3THR*Y3/(720.0*AL1*X2TWO)-X3THR*Y3/X2TWO/180.0-NU
3  *X3TWO*Y3/X2/240.0+13.0*X3TWO*Y3/(144.0*AL1*X2)+X3TWO*Y3/X2/240
4  .0-NU*X3*Y3/120.0+(-5.0)*X3*Y3/(144.0*AL1)+X3*Y3/120.0+NU*X2*Y3
5  /480.0-X2*Y3/AL1/240.0-X2*Y3/480.0+(-29.0)*X3FIV/(720.0*X2TWO*Y
6  3)+5.0*X3FOR/(48.0*X2*Y3)+(-23.0)*X3THR/(360.0*Y3)-X2*X3TWO/Y3/
7  48.0+13.0*X2TWO*X3/(720.0*Y3)+X2THR/Y3/360.0
  K2(2,3) = (-29.0)*NU*X3TWO*Y3TWO/(1440.0*AL1*X2TWO)-NU*X3TWO*Y3TWO
1  /X2TWO/576.0-X3TWO*Y3TWO/(AL1*X2TWO)/180.0+37.0*X3TWO*Y3TWO/(28
2  80.0*X2TWO)+43.0*NU*X3*Y3TWO/(1440.0*AL1*X2)-NU*X3*Y3TWO/X2/480
3  .0+X3*Y3TWO/(AL1*X2)/160.0+(-11.0)*X3*Y3TWO/(1440.0*X2)+(-13.0)
4  *NU*Y3TWO/(1440.0*AL1)-NU*Y3TWO/1440.0-Y3TWO/1440.0+(-13.0)*NU*
5  X3FOR/(2880.0*AL1*X2TWO)+(-5.0)*NU*X3FOR/(288.0*X2TWO)+29.0*X3F
6  OR/(2880.0*AL1*X2TWO)-X3FOR/X2TWO/360.0-NU*X3THR/(AL1*X2)/288.0
7  +47.0*NU*X3THR/(1440.0*X2)+X3THR/(AL1*X2)/480.0+X3THR/X2/480.0-
8  NU*X3TWO/AL1/480.0-X3TWO/AL1/480.0+X3TWO/240.0-NU*X2*X3/AL1/960
9  .0+(-17.0)*NU*X2*X3/576.0-X2*X3/AL1/960.0+(-13.0)*X2*X3/2880.0+
:  NU*X2TWO/AL1/480.0+11.0*NU*X2TWO/720.0
  K2(2,4) = NU*Y3THR/(AL1*X2)/144.0-Y3THR/(AL1*X2)/144.0+NU*X3TWO*Y3
1  /X2/240.0+7.0*X3TWO*Y3/(1440.0*AL1*X2)-X3TWO*Y3/X2/240.0+NU*X3*
2  Y3/240.0+(-7.0)*X3*Y3/(1440.0*AL1)-X3*Y3/240.0-NU*X2*Y3/180.0-X
3  2*Y3/AL1/720.0+X2*Y3/180.0+(-3.0)*X3FOR/(160.0*X2*Y3)+X3THR/Y3/
4  240.0+23.0*X2*X3TWO/(720.0*Y3)+(-5.0)*X2TWO*X3/(288.0*Y3)
  K2(2,5) = NU*X3*Y3TWO/(AL1*X2)/72.0-X3*Y3TWO/(AL1*X2)/72.0+(-11.0)
1  *NU*Y3TWO/(1440.0*AL1)-NU*Y3TWO/960.0+11.0*Y3TWO/(1440.0*AL1)+Y
2  3TWO/960.0+NU*X3THR/X2/144.0-X3THR/X2/144.0-NU*X3TWO/AL1/160.0-
3  NU*X3TWO/120.0+7.0*X3TWO/(480.0*AL1)+X3TWO/120.0-NU*X2*X3/AL1/2
4  88.0-NU*X2*X3/240.0-X2*X3/AL1/288.0+X2*X3/240.0-NU*X2TWO/AL1/14
5  40.0+13.0*NU*X2TWO/2880.0-X2TWO/AL1/1440.0+(-13.0)*X2TWO/2880.0
  K2(2,6) = 17.0*X3TWO*Y3/(288.0*AL1*X2)+NU*X3*Y3/240.0+(-91.0)*X3*Y
1  3/(1440.0*AL1)-X3*Y3/240.0+NU*X2*Y3/1440.0+X2*Y3/AL1/90.0-X2*Y3
2  /1440.0+13.0*X3FOR/(288.0*X2*Y3)+(-9.0)*X3THR/(80.0*Y3)+19.0*X2
3  *X3TWO/(360.0*Y3)+41.0*X2TWO*X3/(1440.0*Y3)-X2THR/Y3/72.0
  K2(2,7) = NU*X3TWO*Y3TWO/X2TWO/288.0+(-37.0)*X3TWO*Y3TWO/(1440.0*X
1  2TWO)-NU*X3*Y3TWO/(AL1*X2)/120.0+7.0*NU*X3*Y3TWO/(1440.0*X2)-X3
2  *Y3TWO/(AL1*X2)/120.0+5.0*X3*Y3TWO/(288.0*X2)+NU*Y3TWO/AL1/180.

```

```

3  0+Y3TWO/AL1/180.0+13.0*NU*X3FOR/(1440.0*AL1*X2TWO)+(-29.0)*X3FO
4  R/(1440.0*AL1*X2TWO)-NU*X3THR/(AL1*X2)/360.0-NU*X3THR/X2/720.0+
5  X3THR/(AL1*X2)/72.0-X3THR/X2/720.0-NU*X3TWO/480.0-X3TWO/480.0-N
6  U*X2*X3/AL1/288.0+17.0*NU*X2*X3/1440.0-X2*X3/AL1/288.0+17.0*X2*
7  X3/1440.0+NU*X2TWO/AL1/240.0-NU*X2TWO/90.0+X2TWO/AL1/360.0-X2TW
8  O/180.0
  K2(2,8) = -NU*X3*Y3THR/(AL1*X2TWO)/90.0+X3*Y3THR/(AL1*X2TWO)/90.0-
1  NU*Y3THR/(AL1*X2)/180.0+Y3THR/(AL1*X2)/180.0-NU*X3THR*Y3/X2TWO/
2  180.0+37.0*X3THR*Y3/(720.0*AL1*X2TWO)+X3THR*Y3/X2TWO/180.0+(-37
3  .0)*X3TWO*Y3/(720.0*AL1*X2)-X3*Y3/AL1/144.0+X2*Y3/AL1/144.0+29.
4  0*X3FIV/(720.0*X2TWO*Y3)-X3FOR/(X2*Y3)/20.0+X3THR/Y3/72.0-X2*X3
5  TWO/Y3/24.0+7.0*X2TWO*X3/(144.0*Y3)-X2THR/Y3/90.0
  K2(2,9) = NU*X3TWO*Y3TWO/(AL1*X2TWO)/20.0+X3TWO*Y3TWO/(AL1*X2TWO)/
1  60.0+(-11.0)*NU*X3*Y3TWO/(180.0*AL1*X2)-NU*X3*Y3TWO/X2/480.0-X3
2  *Y3TWO/(AL1*X2)/180.0+11.0*X3*Y3TWO/(1440.0*X2)+NU*Y3TWO/AL1/60
3  .0-NU*Y3TWO/360.0-Y3TWO/AL1/180.0-Y3TWO/360.0+NU*X3FOR/X2TWO/24
4  .0+X3FOR/X2TWO/120.0+NU*X3THR/(AL1*X2)/90.0+(-4.0)*NU*X3THR/(45
5  .0*X2)-X3THR/(AL1*X2)/36.0-X3THR/X2/90.0+NU*X3TWO/AL1/120.0+17.
6  0*NU*X3TWO/480.0+X3TWO/AL1/120.0+X3TWO/480.0+NU*X2*X3/AL1/360.0
7  +41.0*NU*X2*X3/1440.0+X2*X3/AL1/360.0+(-7.0)*X2*X3/1440.0-NU*X2
8  TWO/AL1/360.0-NU*X2TWO/60.0-X2TWO/AL1/360.0+X2TWO/180.0
  K2(2,10) = NU*X3*Y3THR/(AL1*X2TWO)/60.0-X3*Y3THR/(AL1*X2TWO)/60.0-
1  NU*Y3THR/(AL1*X2)/180.0+Y3THR/(AL1*X2)/180.0+NU*X3THR*Y3/X2TWO/
2  120.0-X3THR*Y3/(AL1*X2TWO)/15.0-X3THR*Y3/X2TWO/120.0-NU*X3TWO*Y
3  3/X2/48.0+X3TWO*Y3/(AL1*X2)/30.0+X3TWO*Y3/X2/48.0+29.0*X3*Y3/(7
4  20.0*AL1)+NU*X2*Y3/160.0-X2*Y3/AL1/80.0-X2*Y3/160.0-X3FIV/(X2TW
5  O*Y3)/20.0+101.0*X3FOR/(720.0*X2*Y3)+(-11.0)*X3THR/(120.0*Y3)+X
6  2*X3TWO/Y3/80.0-X2TWO*X3/Y3/45.0+X2THR/Y3/90.0
  K2(2,11) = -NU*X3TWO*Y3TWO/(AL1*X2TWO)/20.0-X3TWO*Y3TWO/(AL1*X2TWO
1  )/60.0+7.0*NU*X3*Y3TWO/(180.0*AL1*X2)+NU*X3*Y3TWO/X2/480.0+X3*Y
2  3TWO/(AL1*X2)/36.0+(-11.0)*X3*Y3TWO/(1440.0*X2)-NU*Y3TWO/AL1/36
3  0.0+NU*Y3TWO/480.0-Y3TWO/AL1/120.0+Y3TWO/288.0-NU*X3FOR/X2TWO/2
4  4.0-X3FOR/X2TWO/120.0-NU*X3THR/(AL1*X2)/90.0+7.0*NU*X3THR/(90.0
5  *X2)+X3THR/(AL1*X2)/36.0+X3THR/X2/45.0+NU*X3TWO/AL1/240.0+(-13.
6  0)*NU*X3TWO/480.0-X3TWO/AL1/48.0-X3TWO/96.0+(-17.0)*NU*X2*X3/14
7  40.0+(-17.0)*X2*X3/1440.0+NU*X2TWO/180.0+X2TWO/180.0
  K2(2,12) = -NU*X3*Y3THR/(AL1*X2TWO)/60.0+X3*Y3THR/(AL1*X2TWO)/60.0
1  +NU*Y3THR/(AL1*X2)/180.0-Y3THR/(AL1*X2)/180.0-NU*X3THR*Y3/X2TWO
2  /120.0+X3THR*Y3/(AL1*X2TWO)/15.0+X3THR*Y3/X2TWO/120.0+NU*X3TWO*
3  Y3/X2/48.0+(-49.0)*X3TWO*Y3/(360.0*AL1*X2)-X3TWO*Y3/X2/48.0+5.0
4  *X3*Y3/(72.0*AL1)-NU*X2*Y3/288.0+X2*Y3/288.0+X3FIV/(X2TWO*Y3)/2
5  0.0+(-53.0)*X3FOR/(240.0*X2*Y3)+X3THR/Y3/4.0+(-5.0)*X2*X3TWO/(1
6  44.0*Y3)-X2TWO*X3/Y3/18.0+X2THR/Y3/90.0

```

c

```

  K2(3,3) = X3*Y3THR/X2TWO/45.0+(-7.0)*Y3THR/(360.0*X2)+(-37.0)*NU*X
1  3THR*Y3/(1440.0*X2TWO)+X3THR*Y3/(AL1*X2TWO)/90.0+37.0*X3THR*Y3/
2  (1440.0*X2TWO)+23.0*NU*X3TWO*Y3/(720.0*X2)+X3TWO*Y3/(AL1*X2)/12
3  0.0+(-23.0)*X3TWO*Y3/(720.0*X2)-NU*X3*Y3/240.0+X3*Y3/240.0+7.0*
4  X2*Y3/(720.0*AL1)+(-29.0)*NU*X3FIV/(1440.0*AL1*X2TWO*Y3)+29.0*X
5  3FIV/(1440.0*AL1*X2TWO*Y3)-NU*X3FOR/(AL1*X2*Y3)/720.0+X3FOR/(AL

```

```

6 1*X2*Y3)/720.0+NU*X3THR/(AL1*Y3)/120.0-X3THR/(AL1*Y3)/120.0+(-7
7 .0)*NU*X2*X3TWO/(1440.0*AL1*Y3)+7.0*X2*X3TWO/(1440.0*AL1*Y3)
  K2(3,4) = (-29.0)*NU*X3TWO*Y3TWO/(1440.0*AL1*X2TWO)+NU*X3TWO*Y3TWO
1 /X2TWO/576.0-X3TWO*Y3TWO/(AL1*X2TWO)/180.0+(-37.0)*X3TWO*Y3TWO/
2 (2880.0*X2TWO)+13.0*NU*X3*Y3TWO/(480.0*AL1*X2)-NU*X3*Y3TWO/X2/1
3 60.0+7.0*X3*Y3TWO/(1440.0*AL1*X2)+23.0*X3*Y3TWO/(1440.0*X2)-NU*
4 Y3TWO/AL1/240.0+NU*Y3TWO/480.0-Y3TWO/480.0+13.0*NU*X3FOR/(2880.
5 0*AL1*X2TWO)+(-5.0)*NU*X3FOR/(288.0*X2TWO)+(-29.0)*X3FOR/(2880.
6 0*AL1*X2TWO)-X3FOR/X2TWO/360.0-NU*X3THR/(AL1*X2)/288.0+NU*X3THR
7 /X2/1440.0-X3THR/(AL1*X2)/1440.0-X3THR/X2/480.0-NU*X3TWO/AL1/24
8 0.0+NU*X3TWO/120.0+X3TWO/AL1/240.0+(-7.0)*NU*X2*X3/(2880.0*AL1)
9 +(-7.0)*NU*X2*X3/2880.0+(-7.0)*X2*X3/(2880.0*AL1)+(-7.0)*X2*X3/
: 2880.0
  K2(3,5) = (-17.0)*NU*X3TWO*Y3/(576.0*X2)+17.0*X3TWO*Y3/(576.0*X2)+
1 79.0*NU*X3*Y3/2880.0+X3*Y3/AL1/120.0+(-79.0)*X3*Y3/2880.0-NU*X2
2 *Y3/288.0+X2*Y3/AL1/144.0+X2*Y3/288.0+(-13.0)*NU*X3FOR/(576.0*A
3 L1*X2*Y3)+13.0*X3FOR/(576.0*AL1*X2*Y3)+(-23.0)*NU*X3THR/(1440.0
4 *AL1*Y3)+23.0*X3THR/(1440.0*AL1*Y3)+NU*X2*X3TWO/(AL1*Y3)/144.0-
5 X2*X3TWO/(AL1*Y3)/144.0+NU*X2TWO*X3/(AL1*Y3)/192.0-X2TWO*X3/(AL
6 1*Y3)/192.0
  K2(3,6) = -NU*X3*Y3TWO/X2/36.0-NU*Y3TWO/AL1/480.0+NU*Y3TWO/80.0-NU
1 *X3THR/(AL1*X2)/72.0-NU*X3TWO/AL1/120.0-NU*X3TWO/40.0-X3TWO/240
2 .0+7.0*NU*X2*X3/1440.0-X2*X3/288.0-NU*X2TWO/AL1/480.0+NU*X2TWO/
3 80.0
  K2(3,7) = -X3*Y3THR/X2TWO/45.0+Y3THR/X2/30.0+37.0*NU*X3THR*Y3/(144
1 0.0*X2TWO)-X3THR*Y3/(AL1*X2TWO)/90.0+(-37.0)*X3THR*Y3/(1440.0*X
2 2TWO)+(-37.0)*NU*X3TWO*Y3/(720.0*X2)+37.0*X3TWO*Y3/(720.0*X2)+N
3 U*X3*Y3/45.0-X3*Y3/45.0+X2*Y3/AL1/90.0+29.0*NU*X3FIV/(1440.0*AL
4 1*X2TWO*Y3)+(-29.0)*X3FIV/(1440.0*AL1*X2TWO*Y3)+(-37.0)*NU*X3FO
5 R/(1440.0*AL1*X2*Y3)+37.0*X3FOR/(1440.0*AL1*X2*Y3)-NU*X3THR/(AL
6 1*Y3)/120.0+X3THR/(AL1*Y3)/120.0-NU*X2*X3TWO/(AL1*Y3)/720.0+X2*
7 X3TWO/(AL1*Y3)/720.0+NU*X2TWO*X3/(AL1*Y3)/240.0-X2TWO*X3/(AL1*Y
8 3)/240.0
  K2(3,8) = 29.0*NU*X3TWO*Y3TWO/(720.0*AL1*X2TWO)+X3TWO*Y3TWO/(AL1*X
1 2TWO)/90.0+(-41.0)*NU*X3*Y3TWO/(720.0*AL1*X2)-NU*X3*Y3TWO/X2/12
2 0.0-X3*Y3TWO/(AL1*X2)/90.0-X3*Y3TWO/X2/120.0+NU*Y3TWO/AL1/60.0+
3 NU*Y3TWO/360.0+Y3TWO/360.0+5.0*NU*X3FOR/(144.0*X2TWO)+X3FOR/X2T
4 WO/180.0-NU*X3THR/(AL1*X2)/720.0-NU*X3THR/X2/30.0-X3THR/(AL1*X2
5 )/720.0-NU*X3TWO/AL1/480.0-NU*X3TWO/120.0-X3TWO/AL1/480.0+NU*X2
6 *X3/AL1/288.0+(-13.0)*NU*X2*X3/1440.0+X2*X3/AL1/288.0+(-13.0)*X
7 2*X3/1440.0-NU*X2TWO/AL1/180.0+NU*X2TWO/72.0
  K2(3,9) = -X3*Y3THR/X2TWO/30.0+Y3THR/X2/45.0+NU*X3THR*Y3/X2TWO/30.
1 0-X3THR*Y3/(AL1*X2TWO)/60.0-X3THR*Y3/X2TWO/30.0+(-23.0)*NU*X3TW
2 O*Y3/(720.0*X2)-X3TWO*Y3/(AL1*X2)/40.0+23.0*X3TWO*Y3/(720.0*X2)
3 -NU*X3*Y3/720.0+X3*Y3/720.0+(-13.0)*X2*Y3/(720.0*AL1)+NU*X3FIV/
4 (AL1*X2TWO*Y3)/40.0-X3FIV/(AL1*X2TWO*Y3)/46.0+17.0*NU*X3FOR/(48
5 0.0*AL1*X2*Y3)+(-17.0)*X3FOR/(480.0*AL1*X2*Y3)-NU*X3THR/(AL1*Y3
6 )/60.0+X3THR/(AL1*Y3)/60.0+7.0*NU*X2*X3TWO/(1440.0*AL1*Y3)+(-7.
7 0)*X2*X3TWO/(1440.0*AL1*Y3)-NU*X2TWO*X3/(AL1*Y3)/240.0+X2TWO*X3
8 /(AL1*Y3)/240.0

```

$$K2(3,10) = X3TWO*Y3TWO/X2TWO/30.0-NU*X3*Y3TWO/(AL1*X2)/80.0+NU*X3*Y3TWO/X2/45.0-X3*Y3TWO/(AL1*X2)/360.0-X3*Y3TWO/X2/30.0+NU*Y3TWO/AL1/120.0-NU*Y3TWO/90.0+Y3TWO/180.0-NU*X3FOR/(AL1*X2TWO)/120.0+X3FOR/(AL1*X2TWO)/40.0+NU*X3THR/(AL1*X2)/90.0+17.0*NU*X3THR/(360.0*X2)+X3THR/X2/120.0+NU*X3TWO/AL1/96.0-NU*X3TWO/40.0-X3TWO/AL1/160.0+NU*X2*X3/AL1/1440.0+NU*X2*X3/120.0+X2*X3/AL1/1440.0+X2*X3/120.0+NU*X2TWO/AL1/180.0-NU*X2TWO/72.0$$

$$K2(3,11) = X3*Y3THR/X2TWO/30.0-Y3THR/X2/45.0-NU*X3THR*Y3/X2TWO/30.0+X3THR*Y3/(AL1*X2TWO)/60.0+X3THR*Y3/X2TWO/30.0+NU*X3TWO*Y3/X2/12.0+X3TWO*Y3/(AL1*X2)/40.0-X3TWO*Y3/X2/12.0+(-67.0)*NU*X3*Y3/1440.0+67.0*X3*Y3/1440.0+NU*X2*Y3/360.0-X2*Y3/AL1/48.0-X2*Y3/360.0-NU*X3FIV/(AL1*X2TWO*Y3)/40.0+X3FIV/(AL1*X2TWO*Y3)/40.0+7.0*NU*X3FOR/(1440.0*AL1*X2*Y3)+(-7.0)*X3FOR/(1440.0*AL1*X2*Y3)+5.0*NU*X3THR/(144.0*AL1*Y3)+(-5.0)*X3THR/(144.0*AL1*Y3)+NU*X2*X3TWO/(AL1*Y3)/96.0-X2*X3TWO/(AL1*Y3)/96.0-NU*X2TWO*X3/(AL1*Y3)/72.0+X2TWO*X3/(AL1*Y3)/72.0$$

$$K2(3,12) = -X3TWO*Y3TWO/X2TWO/30.0+NU*X3*Y3TWO/(AL1*X2)/80.0+NU*X3*Y3TWO/X2/45.0+X3*Y3TWO/(AL1*X2)/360.0+X3*Y3TWO/X2/30.0+(-7.0)*NU*Y3TWO/(720.0*AL1)-NU*Y3TWO/180.0-Y3TWO/180.0+NU*X3FOR/(AL1*X2TWO)/120.0-X3FOR/(AL1*X2TWO)/40.0+NU*X3THR/(AL1*X2)/90.0+(-17.0)*NU*X3THR/(360.0*X2)-X3THR/X2/120.0+NU*X3TWO/AL1/160.0+NU*X3TWO/20.0+X3TWO/AL1/160.0-NU*X2*X3/AL1/1440.0+NU*X2*X3/36.0-X2*X3/AL1/1440.0+X2*X3/90.0-NU*X2TWO/36.0$$

C

$$K2(4,4) = -NU*X3*Y3THR/(AL1*X2TWO)/90.0+X3*Y3THR/(AL1*X2TWO)/90.0+7.0*NU*Y3THR/(720.0*AL1*X2)+(-7.0)*Y3THR/(720.0*AL1*X2)-NU*X3THR*Y3/X2TWO/180.0+37.0*X3THR*Y3/(720.0*AL1*X2TWO)+X3THR*Y3/X2TWO/180.0-NU*X3TWO*Y3/X2/240.0+(-23.0)*X3TWO*Y3/(360.0*AL1*X2)+X3TWO*Y3/X2/240.0+X3*Y3/AL1/120.0+(-7.0)*NU*X2*Y3/1440.0+7.0*X2*Y3/1440.0+29.0*X3FIV/(720.0*X2TWO*Y3)+X3FOR/(X2*Y3)/360.0-X3THR/Y3/60.0+7.0*X2*X3TWO/(720.0*Y3)$$

$$K2(4,5) = NU*X3*Y3TWO/(AL1*X2)/72.0-X3*Y3TWO/(AL1*X2)/72.0-NU*Y3TWO/AL1/160.0+NU*Y3TWO/960.0+Y3TWO/AL1/160.0-Y3TWO/960.0+NU*X3THR/X2/144.0-X3THR/X2/144.0+NU*X3TWO/AL1/160.0+NU*X3TWO/240.0+(-7.0)*X3TWO/(480.0*AL1)-X3TWO/240.0+(-11.0)*NU*X2*X3/(1440.0*AL1)+X2*X3/AL1/1440.0-NU*X2TWO/AL1/160.0+NU*X2TWO/960.0+X2TWO/AL1/160.0-X2TWO/960.0$$

$$K2(4,6) = 17.0*X3TWO*Y3/(288.0*AL1*X2)-NU*X3*Y3/240.0+(-79.0)*X3*Y3/(1440.0*AL1)+X3*Y3/240.0-NU*X2*Y3/288.0+X2*Y3/AL1/144.0+X2*Y3/288.0+13.0*X3FOR/(288.0*X2*Y3)+23.0*X3THR/(720.0*Y3)-X2*X3TWO/Y3/72.0-X2TWO*X3/Y3/96.0$$

$$K2(4,7) = -NU*X3TWO*Y3TWO/X2TWO/288.0+37.0*X3TWO*Y3TWO/(1440.0*X2TWO)-NU*X3*Y3TWO/(AL1*X2)/120.0+17.0*NU*X3*Y3TWO/(1440.0*X2)-X3*Y3TWO/(AL1*X2)/120.0+(-49.0)*X3*Y3TWO/(1440.0*X2)+NU*Y3TWO/AL1/360.0-NU*Y3TWO/120.0+Y3TWO/AL1/360.0+Y3TWO/120.0+(-13.0)*NU*X3*4/(1440.0*AL1*X2TWO)+29.0*X3FOR/(1440.0*AL1*X2TWO)+NU*X3THR/(AL1*X2)/60.0-NU*X3THR/X2/720.0-X3THR/(AL1*X2)/60.0-X3THR/X2/720.0+NU*X3TWO/AL1/240.0-NU*X3TWO/480.0-X3TWO/AL1/240.0-X3TWO/480.0+(-13.0)*NU*X2*X3/(1440.0*AL1)+NU*X2*X3/288.0+(-13.0)*X2*X3/(1440.0*AL1)+X2*X3/288.0-NU*X2TWO/AL1/144.0+NU*X2TWO/360.0+X2TWO/AL1/144.0$$

```

9  L1/144.0-X2TWO/360.0
   K2(4,8) = NU*X3*Y3THR/(AL1*X2TWO)/90.0-X3*Y3THR/(AL1*X2TWO)/90.0-N
1  U*Y3THR/(AL1*X2)/60.0+Y3THR/(AL1*X2)/60.0+NU*X3THR*Y3/X2TWO/180
2  .0+(-37.0)*X3THR*Y3/(720.0*AL1*X2TWO)-X3THR*Y3/X2TWO/180.0+37.0
3  *X3TWO*Y3/(360.0*AL1*X2)+(-2.0)*X3*Y3/(45.0*AL1)-NU*X2*Y3/180.0
4  +X2*Y3/180.0+(-29.0)*X3FIV/(720.0*X2TWO*Y3)+37.0*X3FOR/(720.0*X
5  2*Y3)+X3THR/Y3/60.0+X2*X3TWO/Y3/360.0-X2TWO*X3/Y3/120.0
   K2(4,9) = NU*X3TWO*Y3TWO/(AL1*X2TWO)/20.0+X3TWO*Y3TWO/(AL1*X2TWO)/
1  60.0+(-11.0)*NU*X3*Y3TWO/(180.0*AL1*X2)+NU*X3*Y3TWO/X2/480.0-X3
2  *Y3TWO/(AL1*X2)/180.0+(-11.0)*X3*Y3TWO/(1440.0*X2)+NU*Y3TWO/AL1
3  /72.0-NU*Y3TWO/240.0-Y3TWO/AL1/360.0+Y3TWO/240.0+NU*X3FOR/X2TWO
4  /24.0+X3FOR/X2TWO/120.0-NU*X3THR/(AL1*X2)/90.0-NU*X3THR/X2/180.
5  0+X3THR/(AL1*X2)/36.0+X3THR/X2/180.0+NU*X3TWO/AL1/80.0+(-7.0)*N
6  U*X3TWO/480.0-X3TWO/AL1/80.0+X3TWO/480.0+NU*X2*X3/AL1/120.0+NU*
7  X2*X3/1440.0+X2*X3/AL1/120.0+X2*X3/1440.0+NU*X2TWO/AL1/144.0-NU
8  *X2TWO/360.0-X2TWO/AL1/144.0+X2TWO/360.0
   K2(4,10) = NU*X3*Y3THR/(AL1*X2TWO)/60.0-X3*Y3THR/(AL1*X2TWO)/60.0-
1  NU*Y3THR/(AL1*X2)/90.0+Y3THR/(AL1*X2)/90.0+NU*X3THR*Y3/X2TWO/12
2  0.0-X3THR*Y3/(AL1*X2TWO)/15.0-X3THR*Y3/X2TWO/120.0+NU*X3TWO*Y3/
3  X2/80.0+23.0*X3TWO*Y3/(360.0*AL1*X2)-X3TWO*Y3/X2/80.0+X3*Y3/AL1
4  /360.0+13.0*NU*X2*Y3/1440.0+(-13.0)*X2*Y3/1440.0-X3FIV/(X2TWO*Y
5  3)/20.0+(-17.0)*X3FOR/(240.0*X2*Y3)+X3THR/Y3/30.0+(-7.0)*X2*X3T
6  WO/(720.0*Y3)+X2TWO*X3/Y3/120.0
   K2(4,11) = -NU*X3TWO*Y3TWO/(AL1*X2TWO)/20.0-X3TWO*Y3TWO/(AL1*X2TWO
1  )/60.0+7.0*NU*X3*Y3TWO/(180.0*AL1*X2)-NU*X3*Y3TWO/X2/480.0+X3*Y
2  3TWO/(AL1*X2)/36.0+11.0*X3*Y3TWO/(1440.0*X2)-NU*Y3TWO/AL1/180.0
3  +7.0*NU*Y3TWO/1440.0-Y3TWO/AL1/180.0+(-7.0)*Y3TWO/1440.0-NU*X3F
4  OR/X2TWO/24.0-X3FOR/X2TWO/120.0+NU*X3THR/(AL1*X2)/90.0-NU*X3THR
5  /X2/180.0-X3THR/(AL1*X2)/36.0+X3THR/X2/180.0-NU*X3TWO/AL1/40.0+
6  NU*X3TWO/160.0+X3TWO/AL1/40.0+X3TWO/160.0+NU*X2*X3/AL1/360.0-NU
7  *X2*X3/1440.0+7.0*X2*X3/(360.0*AL1)-X2*X3/1440.0+NU*X2TWO/AL1/7
8  2.0-X2TWO/AL1/72.0
   K2(4,12) = -NU*X3*Y3THR/(AL1*X2TWO)/60.0+X3*Y3THR/(AL1*X2TWO)/60.0
1  +NU*Y3THR/(AL1*X2)/90.0-Y3THR/(AL1*X2)/90.0-NU*X3THR*Y3/X2TWO/1
2  20.0+X3THR*Y3/(AL1*X2TWO)/15.0+X3THR*Y3/X2TWO/120.0-NU*X3TWO*Y3
3  /X2/80.0-X3TWO*Y3/(AL1*X2)/6.0+X3TWO*Y3/X2/80.0+67.0*X3*Y3/(720
4  .0*AL1)+NU*X2*Y3/96.0-X2*Y3/AL1/180.0-X2*Y3/96.0+X3FIV/(X2TWO*Y
5  3)/20.0+(-7.0)*X3FOR/(720.0*X2*Y3)+(-5.0)*X3THR/(72.0*Y3)-X2*X3
6  TWO/Y3/48.0+X2TWO*X3/Y3/36.0

```

c

```

   K2(5,5) = (-7.0)*NU*X2*Y3/1440.0+7.0*X2*Y3/1440.0+(-17.0)*NU*X2*X3
1  TWO/(240.0*AL1*Y3)+17.0*X2*X3TWO/(240.0*AL1*Y3)+NU*X2TWO*X3/(AL
2  1*Y3)/48.0-X2TWO*X3/(AL1*Y3)/48.0+7.0*NU*X2THR/(720.0*AL1*Y3)+(-
3  7.0)*X2THR/(720.0*AL1*Y3)
   K2(5,6) = -NU*X2*X3/AL1/40.0+NU*X2*X3/80.0-X2*X3/80.0-NU*X2TWO/AL1
1  /240.0+NU*X2TWO/480.0-X2TWO/480.0
   K2(5,7) = 17.0*NU*X3TWO*Y3/(288.0*X2)+(-17.0)*X3TWO*Y3/(288.0*X2)+
1  (-17.0)*NU*X3*Y3/288.0+17.0*X3*Y3/288.0+NU*X2*Y3/96.0-X2*Y3/AL1
2  /180.0-X2*Y3/96.0+13.0*NU*X3FOR/(288.0*AL1*X2*Y3)+(-13.0)*X3FOR
3  /(288.0*AL1*X2*Y3)+(-29.0)*NU*X3THR/(720.0*AL1*Y3)+29.0*X3THR/(

```

```

4 720.0*AL1*Y3)-NU*X2*X3TWO/(AL1*Y3)/180.0+X2*X3TWO/(AL1*Y3)/180.
5 0+(-23.0)*NU*X2TWO*X3/(1440.0*AL1*Y3)+23.0*X2TWO*X3/(1440.0*AL1
6 *Y3)+NU*X2THR/(AL1*Y3)/90.0-X2THR/(AL1*Y3)/90.0
K2(5,8) = -NU*X3*Y3TWO/(AL1*X2)/36.0+X3*Y3TWO/(AL1*X2)/36.0+NU*Y3T
1 WO/AL1/72.0-Y3TWO/AL1/72.0-NU*X3THR/X2/72.0+X3THR/X2/72.0+NU*X3
2 TWO/240.0-X3TWO/240.0+NU*X2*X3/AL1/360.0+X2*X3/AL1/360.0-NU*X2T
3 WO/AL1/180.0+7.0*NU*X2TWO/1440.0-X2TWO/AL1/180.0+(-7.0)*X2TWO/1
4 440.0
K2(5,9) = (-7.0)*NU*X3*Y3/480.0-X3*Y3/AL1/30.0+7.0*X3*Y3/480.0+13.
1 0*NU*X2*Y3/1440.0+(-13.0)*X2*Y3/1440.0+5.0*NU*X3THR/(48.0*AL1*Y
2 3)+(-5.0)*X3THR/(48.0*AL1*Y3)-NU*X2*X3TWO/(AL1*Y3)/30.0+X2*X3TW
3 O/(AL1*Y3)/30.0+NU*X2TWO*X3/(AL1*Y3)/144.0-X2TWO*X3/(AL1*Y3)/14
4 4.0-NU*X2THR/(AL1*Y3)/90.0+X2THR/(AL1*Y3)/90.0
K2(5,10) = NU*Y3TWO/AL1/144.0-NU*Y3TWO/360.0-Y3TWO/AL1/144.0+Y3TWO
1 /360.0-NU*X3TWO/AL1/120.0-NU*X3TWO/48.0+X3TWO/AL1/24.0+X3TWO/48
2 .0+NU*X2*X3/AL1/60.0-X2*X3/AL1/60.0+NU*X2TWO/AL1/72.0-NU*X2TWO/
3 240.0-X2TWO/AL1/360.0+X2TWO/240.0
K2(5,11) = 7.0*NU*X3*Y3/480.0+X3*Y3/AL1/30.0+(-7.0)*X3*Y3/480.0-NU
1 *X2*Y3/180.0+X2*Y3/180.0+(-5.0)*NU*X3THR/(48.0*AL1*Y3)+5.0*X3TH
2 R/(48.0*AL1*Y3)+31.0*NU*X2*X3TWO/(240.0*AL1*Y3)+(-31.0)*X2*X3TW
3 O/(240.0*AL1*Y3)-NU*X2TWO*X3/(AL1*Y3)/360.0+X2TWO*X3/(AL1*Y3)/3
4 60.0-NU*X2THR/(AL1*Y3)/60.0+X2THR/(AL1*Y3)/60.0
K2(5,12) = -NU*Y3TWO/AL1/144.0+NU*Y3TWO/360.0+Y3TWO/AL1/144.0-Y3TW
1 O/360.0+NU*X3TWO/AL1/120.0+NU*X3TWO/48.0-X3TWO/AL1/24.0-X3TWO/4
2 8.0+NU*X2*X3/AL1/60.0-NU*X2*X3/120.0+X2*X3/AL1/60.0+X2*X3/120.0
3 +NU*X2TWO/AL1/360.0-NU*X2TWO/120.0+X2TWO/AL1/360.0+X2TWO/120.0
C
K2(6,6) = 7.0*X2*Y3/(720.0*AL1)+17.0*X2*X3TWO/(120.0*Y3)-X2TWO*X3/
1 Y3/24.0+(-7.0)*X2THR/(360.0*Y3)
K2(6,7) = NU*X3*Y3TWO/X2/18.0-NU*Y3TWO/36.0+NU*X3THR/(AL1*X2)/36.0
1 -NU*X3TWO/AL1/120.0+NU*X2*X3/360.0+X2*X3/360.0+(-7.0)*NU*X2TWO/
2 (720.0*AL1)-NU*X2TWO/180.0-X2TWO/180.0
K2(6,8) = (-17.0)*X3TWO*Y3/(144.0*AL1*X2)+17.0*X3*Y3/(144.0*AL1)+N
1 U*X2*Y3/360.0-X2*Y3/AL1/48.0-X2*Y3/360.0+(-13.0)*X3FOR/(144.0*X
2 2*Y3)+29.0*X3THR/(360.0*Y3)+X2*X3TWO/Y3/90.0+23.0*X2TWO*X3/(720
3 .0*Y3)-X2THR/Y3/45.0
K2(6,9) = NU*Y3TWO/AL1/180.0-NU*Y3TWO/72.0+NU*X3TWO/AL1/24.0+NU*X3
1 TWO/15.0+X3TWO/60.0-NU*X2*X3/30.0+NU*X2TWO/AL1/120.0-NU*X2TWO/9
2 0.0+X2TWO/180.0
K2(6,10) = NU*X3*Y3/60.0+7.0*X3*Y3/(240.0*AL1)-X3*Y3/60.0+(-13.0)*
1 X2*Y3/(720.0*AL1)+(-5.0)*X3THR/(24.0*Y3)+X2*X3TWO/Y3/15.0-X2TWO
2 *X3/Y3/72.0+X2THR/Y3/45.0
K2(6,11) = -NU*Y3TWO/AL1/180.0+NU*Y3TWO/72.0-NU*X3TWO/AL1/24.0-NU*
1 X3TWO/15.0-X3TWO/60.0+NU*X2*X3/AL1/60.0+NU*X2*X3/60.0+X2*X3/60.
2 0+NU*X2TWO/AL1/60.0+NU*X2TWO/360.0+X2TWO/360.0
K2(6,12) = -NU*X3*Y3/60.0+(-7.0)*X3*Y3/(240.0*AL1)+X3*Y3/60.0+X2*Y
1 3/AL1/90.0+5.0*X3THR/(24.0*Y3)+(-31.0)*X2*X3TWO/(120.0*Y3)+X2TW
2 O*X3/Y3/180.0+X2THR/Y3/30.0
C
K2(7,7) = (-2.0)*Y3THR/(45.0*X2)+5.0*NU*X3TWO*Y3/(72.0*X2)+(-5.0)*

```



```

1  X3TWO*Y3/(72.0*X2)+(-5.0)*NU*X3*Y3/72.0+5.0*X3*Y3/72.0+NU*X2*Y3
2  /90.0-X2*Y3/AL1/20.0-X2*Y3/90.0+13.0*NU*X3FOR/(360.0*AL1*X2*Y3)
3  +(-13.0)*X3FOR/(360.0*AL1*X2*Y3)-NU*X3THR/(AL1*Y3)/180.0+X3THR/
4  (AL1*Y3)/180.0+NU*X2*X3TWO/(AL1*Y3)/120.0-X2*X3TWO/(AL1*Y3)/120
5  .0+(-7.0)*NU*X2TWO*X3/(180.0*AL1*Y3)+7.0*X2TWO*X3/(180.0*AL1*Y3
6  )+NU*X2THR/(AL1*Y3)/60.0-X2THR/(AL1*Y3)/60.0
  K2(7,8) = NU*X3*Y3TWO/(AL1*X2)/60.0+NU*X3*Y3TWO/X2/60.0+X3*Y3TWO/(
1  AL1*X2)/60.0+X3*Y3TWO/X2/60.0-NU*Y3TWO/AL1/120.0-NU*Y3TWO/120.0
2  -Y3TWO/AL1/120.0-Y3TWO/120.0+NU*X3THR/(AL1*X2)/360.0+NU*X3THR/X
3  2/360.0+X3THR/(AL1*X2)/360.0+X3THR/X2/360.0+NU*X3TWO/AL1/240.0+
4  NU*X3TWO/240.0+X3TWO/AL1/240.0+X3TWO/240.0+NU*X2*X3/AL1/80.0+NU
5  *X2*X3/80.0+X2*X3/AL1/80.0+X2*X3/80.0+(-7.0)*NU*X2TWO/(720.0*AL
6  1)+(-7.0)*NU*X2TWO/720.0+(-7.0)*X2TWO/(720.0*AL1)+(-7.0)*X2TWO/
7  720.0
  K2(7,9) = X3*Y3THR/X2TWO/15.0-Y3THR/X2/30.0-NU*X3THR*Y3/X2TWO/15.0
1  +X3THR*Y3/(AL1*X2TWO)/30.0+X3THR*Y3/X2TWO/15.0+7.0*NU*X3TWO*Y3/
2  (144.0*X2)-X3TWO*Y3/(AL1*X2)/60.0+(-7.0)*X3TWO*Y3/(144.0*X2)+NU
3  *X3*Y3/180.0-X3*Y3/180.0-NU*X2*Y3/360.0+X2*Y3/AL1/72.0+X2*Y3/36
4  0.0-NU*X3FIV/(AL1*X2TWO*Y3)/20.0+X3FIV/(AL1*X2TWO*Y3)/20.0+5.0*
5  NU*X3FOR/(144.0*AL1*X2*Y3)+(-5.0)*X3FOR/(144.0*AL1*X2*Y3)+NU*X3
6  THR/(AL1*Y3)/36.0-X3THR/(AL1*Y3)/36.0-NU*X2*X3TWO/(AL1*Y3)/144.
7  0+X2*X3TWO/(AL1*Y3)/144.0+NU*X2TWO*X3/(AL1*Y3)/36.0-X2TWO*X3/(A
8  L1*Y3)/36.0-NU*X2THR/(AL1*Y3)/60.0+X2THR/(AL1*Y3)/60.0
  K2(7,10) = -X3TWO*Y3TWO/X2TWO/15.0+(-2.0)*NU*X3*Y3TWO/(45.0*X2)+X3
1  *Y3TWO/X2/15.0-NU*Y3TWO/AL1/720.0+11.0*NU*Y3TWO/360.0-Y3TWO/AL1
2  /720.0-Y3TWO/72.0+NU*X3FOR/(AL1*X2TWO)/60.0-X3FOR/(AL1*X2TWO)/2
3  0.0+(-7.0)*NU*X3THR/(180.0*AL1*X2)+X3THR/(AL1*X2)/20.0-NU*X3TWO
4  /AL1/240.0+NU*X3TWO/240.0-X3TWO/AL1/240.0+X3TWO/240.0+NU*X2*X3/
5  AL1/240.0-NU*X2*X3/90.0+X2*X3/AL1/240.0-X2*X3/90.0+NU*X2TWO/AL1
6  /48.0+7.0*NU*X2TWO/720.0-X2TWO/AL1/720.0+7.0*X2TWO/720.0
  K2(7,11) = -X3*Y3THR/X2TWO/15.0+Y3THR/X2/30.0+NU*X3THR*Y3/X2TWO/15
1  .0-X3THR*Y3/(AL1*X2TWO)/30.0-X3THR*Y3/X2TWO/15.0+(-109.0)*NU*X3
2  TWO*Y3/(720.0*X2)+X3TWO*Y3/(AL1*X2)/60.0+109.0*X3TWO*Y3/(720.0*
3  X2)+7.0*NU*X3*Y3/72.0+(-7.0)*X3*Y3/72.0+(-11.0)*NU*X2*Y3/720.0+
4  11.0*X2*Y3/(360.0*AL1)+11.0*X2*Y3/720.0+NU*X3FIV/(AL1*X2TWO*Y3)
5  /20.0-X3FIV/(AL1*X2TWO*Y3)/20.0+(-83.0)*NU*X3FOR/(720.0*AL1*X2*
6  Y3)+83.0*X3FOR/(720.0*AL1*X2*Y3)+NU*X3THR/(AL1*Y3)/30.0-X3THR/(
7  AL1*Y3)/30.0+(-11.0)*NU*X2*X3TWO/(720.0*AL1*Y3)+11.0*X2*X3TWO/(
8  720.0*AL1*Y3)+17.0*NU*X2TWO*X3/(360.0*AL1*Y3)+(-17.0)*X2TWO*X3/
9  (360.0*AL1*Y3)-NU*X2THR/(AL1*Y3)/60.0+X2THR/(AL1*Y3)/60.0
  K2(7,12) = X3TWO*Y3TWO/X2TWO/15.0+(-2.0)*NU*X3*Y3TWO/(45.0*X2)-X3*
1  Y3TWO/X2/15.0+NU*Y3TWO/AL1/720.0+NU*Y3TWO/72.0+Y3TWO/AL1/720.0+
2  Y3TWO/72.0-NU*X3FOR/(AL1*X2TWO)/60.0+X3FOR/(AL1*X2TWO)/20.0-NU*
3  X3THR/(AL1*X2)/180.0-X3THR/(AL1*X2)/20.0+NU*X3TWO/AL1/240.0-NU*
4  X3TWO/240.0+X3TWO/AL1/240.0-X3TWO/240.0-NU*X2*X3/AL1/240.0+(-7.
5  0)*NU*X2*X3/360.0-X2*X3/AL1/240.0+(-7.0)*X2*X3/360.0+NU*X2TWO/A
6  L1/720.0+NU*X2TWO/72.0+X2TWO/AL1/720.0+X2TWO/72.0

```

c

```

  K2(8,8) = NU*Y3THR/(AL1*X2)/45.0-Y3THR/(AL1*X2)/45.0+(-5.0)*X3TWO*
1  Y3/(36.0*AL1*X2)+5.0*X3*Y3/(36.0*AL1)+NU*X2*Y3/40.0-X2*Y3/AL1/4

```

```

2  5.0-X2*Y3/40.0+(-13.0)*X3FOR/(180.0*X2*Y3)+X3THR/Y3/90.0-X2*X3T
3  WO/Y3/60.0+7.0*X2TWO*X3/(90.0*Y3)-X2THR/Y3/30.0
  K2(8,9) = -NU*X3TWO*Y3TWO/(AL1*X2TWO)/10.0-X3TWO*Y3TWO/(AL1*X2TWO)
1  /30.0+11.0*NU*X3*Y3TWO/(90.0*AL1*X2)+X3*Y3TWO/(AL1*X2)/90.0+(-1
2  3.0)*NU*Y3TWO/(360.0*AL1)-NU*Y3TWO/720.0+Y3TWO/AL1/120.0-Y3TWO/
3  720.0-NU*X3FOR/X2TWO/12.0-X3FOR/X2TWO/60.0+17.0*NU*X3THR/(180.0
4  *X2)+X3THR/X2/180.0+NU*X3TWO/AL1/240.0-NU*X3TWO/240.0+X3TWO/AL1
5  /240.0-X3TWO/240.0-NU*X2*X3/AL1/90.0+NU*X2*X3/240.0-X2*X3/AL1/9
6  0.0+X2*X3/240.0+7.0*NU*X2TWO/(720.0*AL1)-NU*X2TWO/80.0+7.0*X2TW
7  O/(720.0*AL1)+7.0*X2TWO/720.0
  K2(8,10) = -NU*X3*Y3THR/(AL1*X2TWO)/30.0+X3*Y3THR/(AL1*X2TWO)/30.0
1  +NU*Y3THR/(AL1*X2)/60.0-Y3THR/(AL1*X2)/60.0-NU*X3THR*Y3/X2TWO/6
2  0.0+2.0*X3THR*Y3/(15.0*AL1*X2TWO)+X3THR*Y3/X2TWO/60.0+NU*X3TWO*
3  Y3/X2/120.0+(-7.0)*X3TWO*Y3/(72.0*AL1*X2)-X3TWO*Y3/X2/120.0-X3*
4  Y3/AL1/90.0-NU*X2*Y3/144.0+X2*Y3/AL1/180.0+X2*Y3/144.0+X3FIV/(X
5  2TWO*Y3)/10.0+(-5.0)*X3FOR/(72.0*X2*Y3)-X3THR/Y3/18.0+X2*X3TWO/
6  Y3/72.0-X2TWO*X3/Y3/18.0+X2THR/Y3/30.0
  K2(8,11) = NU*X3TWO*Y3TWO/(AL1*X2TWO)/10.0+X3TWO*Y3TWO/(AL1*X2TWO)
1  /30.0+(-7.0)*NU*X3*Y3TWO/(90.0*AL1*X2)-X3*Y3TWO/(AL1*X2)/18.0+N
2  U*Y3TWO/AL1/72.0+NU*Y3TWO/720.0+Y3TWO/AL1/72.0+Y3TWO/720.0+NU*X
3  3FOR/X2TWO/12.0+X3FOR/X2TWO/60.0+(-13.0)*NU*X3THR/(180.0*X2)-X3
4  THR/X2/36.0-NU*X3TWO/AL1/240.0+NU*X3TWO/240.0-X3TWO/AL1/240.0+X
5  3TWO/240.0+(-7.0)*NU*X2*X3/(360.0*AL1)-NU*X2*X3/240.0+(-7.0)*X2
6  *X3/(360.0*AL1)-X2*X3/240.0+NU*X2TWO/AL1/72.0+NU*X2TWO/720.0+X2
7  TWO/AL1/72.0+X2TWO/720.0
  K2(8,12) = NU*X3*Y3THR/(AL1*X2TWO)/30.0-X3*Y3THR/(AL1*X2TWO)/30.0-
1  NU*Y3THR/(AL1*X2)/60.0+Y3THR/(AL1*X2)/60.0+NU*X3THR*Y3/X2TWO/60
2  .0+(-2.0)*X3THR*Y3/(15.0*AL1*X2TWO)-X3THR*Y3/X2TWO/60.0-NU*X3TW
3  O*Y3/X2/120.0+109.0*X3TWO*Y3/(360.0*AL1*X2)+X3TWO*Y3/X2/120.0+(-
4  7.0)*X3*Y3/(36.0*AL1)+(-11.0)*NU*X2*Y3/720.0+11.0*X2*Y3/(360.0
5  *AL1)+11.0*X2*Y3/720.0-X3FIV/(X2TWO*Y3)/10.0+83.0*X3FOR/(360.0*
6  X2*Y3)-X3THR/Y3/15.0+11.0*X2*X3TWO/(360.0*Y3)+(-17.0)*X2TWO*X3/
7  (180.0*Y3)+X2THR/Y3/30.0
C
  K2(9,9) = -Y3THR/X2/30.0+7.0*NU*X3TWO*Y3/(180.0*X2)+X3TWO*Y3/(AL1*
1  X2)/10.0+(-7.0)*X3TWO*Y3/(180.0*X2)-NU*X3*Y3/120.0+X3*Y3/120.0-
2  NU*X2*Y3/180.0+X2*Y3/AL1/90.0+X2*Y3/180.0+(-5.0)*NU*X3FOR/(36.0
3  *AL1*X2*Y3)+5.0*X3FOR/(36.0*AL1*X2*Y3)+NU*X3THR/(AL1*Y3)/60.0-X
4  3THR/(AL1*Y3)/60.0+NU*X2*X3TWO/(AL1*Y3)/90.0-X2*X3TWO/(AL1*Y3)/
5  90.0-NU*X2TWO*X3/(AL1*Y3)/60.0+X2TWO*X3/(AL1*Y3)/60.0+NU*X2THR/
6  (AL1*Y3)/60.0-X2THR/(AL1*Y3)/60.0
  K2(9,10) = 11.0*NU*X3*Y3TWO/(360.0*AL1*X2)-NU*X3*Y3TWO/X2/360.0+X3
1  *Y3TWO/(AL1*X2)/120.0+7.0*X3*Y3TWO/(360.0*X2)-NU*Y3TWO/AL1/48.0
2  +NU*Y3TWO/80.0+Y3TWO/AL1/720.0+(-7.0)*Y3TWO/720.0+7.0*NU*X3THR/
3  (360.0*AL1*X2)+(-41.0)*NU*X3THR/(360.0*X2)+(-5.0)*X3THR/(72.0*A
4  L1*X2)-X3THR/X2/40.0+(-3.0)*NU*X3TWO/(80.0*AL1)+NU*X3TWO/16.0+7
5  .0*X3TWO/(240.0*AL1)-X3TWO/240.0-NU*X2*X3/AL1/360.0-NU*X2*X3/36
6  0.0-X2*X3/AL1/360.0-X2*X3/360.0-NU*X2TWO/AL1/48.0+NU*X2TWO/80.0
7  +X2TWO/AL1/720.0+(-7.0)*X2TWO/720.0
  K2(9,11) = Y3THR/X2/30.0+(-7.0)*NU*X3TWO*Y3/(180.0*X2)-X3TWO*Y3/(A

```

```

1  L1*X2)/10.0+7.0*X3TWO*Y3/(180.0*X2)+7.0*NU*X3*Y3/180.0+X3*Y3/AL
2  1/30.0+(-7.0)*X3*Y3/180.0-NU*X2*Y3/144.0+X2*Y3/AL1/180.0+X2*Y3/
3  144.0+5.0*NU*X3FOR/(36.0*AL1*X2*Y3)+(-5.0)*X3FOR/(36.0*AL1*X2*Y
4  3)+(-8.0)*NU*X3THR/(45.0*AL1*Y3)+8.0*X3THR/(45.0*AL1*Y3)+11.0*N
5  U*X2*X3TWO/(360.0*AL1*Y3)+(-11.0)*X2*X3TWO/(360.0*AL1*Y3)-NU*X2
6  TWO*X3/(AL1*Y3)/40.0+X2TWO*X3/(AL1*Y3)/40.0+NU*X2THR/(AL1*Y3)/6
7  0.0-X2THR/(AL1*Y3)/60.0
      K2(9,12) = (-11.0)*NU*X3*Y3TWO/(360.0*AL1*X2)+NU*X3*Y3TWO/X2/360.0
1  -X3*Y3TWO/(AL1*X2)/120.0+(-7.0)*X3*Y3TWO/(360.0*X2)+NU*Y3TWO/AL
2  1/48.0+7.0*NU*Y3TWO/720.0-Y3TWO/AL1/720.0+7.0*Y3TWO/720.0+(-7.0
3  )*NU*X3THR/(360.0*AL1*X2)+41.0*NU*X3THR/(360.0*X2)+5.0*X3THR/(7
4  2.0*AL1*X2)+X3THR/X2/40.0+(-7.0)*NU*X3TWO/(240.0*AL1)+(-7.0)*NU
5  *X3TWO/48.0+(-7.0)*X3TWO/(240.0*AL1)-X3TWO/80.0+NU*X2*X3/AL1/36
6  0.0+NU*X2*X3/360.0+X2*X3/AL1/360.0+X2*X3/360.0-NU*X2TWO/AL1/720
7  .0+11.0*NU*X2TWO/360.0-X2TWO/AL1/720.0-X2TWO/72.0

```

C

```

      K2(10,10) = NU*Y3THR/(AL1*X2)/60.0-Y3THR/(AL1*X2)/60.0-NU*X3TWO*Y3
1  /X2/20.0+(-7.0)*X3TWO*Y3/(90.0*AL1*X2)+X3TWO*Y3/X2/20.0+X3*Y3/A
2  L1/60.0-NU*X2*Y3/180.0+X2*Y3/AL1/90.0+X2*Y3/180.0+5.0*X3FOR/(18
3  .0*X2*Y3)-X3THR/Y3/30.0-X2*X3TWO/Y3/45.0+X2TWO*X3/Y3/30.0-X2THR
4  /Y3/30.0
      K2(10,11) = (-11.0)*NU*X3*Y3TWO/(360.0*AL1*X2)+NU*X3*Y3TWO/X2/360.
1  0-X3*Y3TWO/(AL1*X2)/120.0+(-7.0)*X3*Y3TWO/(360.0*X2)+7.0*NU*Y3T
2  WO/(720.0*AL1)-NU*Y3TWO/80.0+7.0*Y3TWO/(720.0*AL1)+7.0*Y3TWO/72
3  0.0+(-7.0)*NU*X3THR/(360.0*AL1*X2)+41.0*NU*X3THR/(360.0*X2)+5.0
4  *X3THR/(72.0*AL1*X2)+X3THR/X2/40.0+13.0*NU*X3TWO/(240.0*AL1)+(-
5  7.0)*NU*X3TWO/240.0+(-19.0)*X3TWO/(240.0*AL1)+(-7.0)*X3TWO/240.
6  0+NU*X2*X3/AL1/360.0+NU*X2*X3/360.0+X2*X3/AL1/360.0+X2*X3/360.0
7  +(-13.0)*NU*X2TWO/(360.0*AL1)-NU*X2TWO/720.0+X2TWO/AL1/120.0-X2
8  TWO/720.0
      K2(10,12) = -NU*Y3THR/(AL1*X2)/60.0+Y3THR/(AL1*X2)/60.0+NU*X3TWO*Y
1  3/X2/20.0+7.0*X3TWO*Y3/(90.0*AL1*X2)-X3TWO*Y3/X2/20.0-NU*X3*Y3/
2  60.0+(-7.0)*X3*Y3/(90.0*AL1)+X3*Y3/60.0-NU*X2*Y3/360.0+X2*Y3/AL
3  1/72.0+X2*Y3/360.0+(-5.0)*X3FOR/(18.0*X2*Y3)+16.0*X3THR/(45.0*Y
4  3)+(-11.0)*X2*X3TWO/(180.0*Y3)+X2TWO*X3/Y3/20.0-X2THR/Y3/30.0

```

C

```

      K2(11,11) = -Y3THR/X2/30.0+7.0*NU*X3TWO*Y3/(180.0*X2)+X3TWO*Y3/(AL
1  1*X2)/10.0+(-7.0)*X3TWO*Y3/(180.0*X2)+(-5.0)*NU*X3*Y3/72.0-X3*Y
2  3/AL1/15.0+5.0*X3*Y3/72.0+NU*X2*Y3/40.0-X2*Y3/AL1/45.0-X2*Y3/40
3  .0+(-5.0)*NU*X3FOR/(36.0*AL1*X2*Y3)+5.0*X3FOR/(36.0*AL1*X2*Y3)+
4  61.0*NU*X3THR/(180.0*AL1*Y3)+(-61.0)*X3THR/(180.0*AL1*Y3)+(-31.
5  0)*NU*X2*X3TWO/(180.0*AL1*Y3)+31.0*X2*X3TWO/(180.0*AL1*Y3)-NU*X
6  2TWO*X3/(AL1*Y3)/30.0+X2TWO*X3/(AL1*Y3)/30.0+NU*X2THR/(AL1*Y3)/
7  45.0-X2THR/(AL1*Y3)/45.0
      K2(11,12) = 11.0*NU*X3*Y3TWO/(360.0*AL1*X2)-NU*X3*Y3TWO/X2/360.0+X
1  3*Y3TWO/(AL1*X2)/120.0+7.0*X3*Y3TWO/(360.0*X2)+(-7.0)*NU*Y3TWO/
2  (720.0*AL1)+(-7.0)*NU*Y3TWO/720.0+(-7.0)*Y3TWO/(720.0*AL1)+(-7.
3  0)*Y3TWO/720.0+7.0*NU*X3THR/(360.0*AL1*X2)+(-41.0)*NU*X3THR/(36
4  0.0*X2)+(-5.0)*X3THR/(72.0*AL1*X2)-X3THR/X2/40.0+NU*X3TWO/AL1/8
5  0.0+9.0*NU*X3TWO/80.0+19.0*X3TWO/(240.0*AL1)+11.0*X3TWO/240.0-N
6  U*X2*X3/AL1/360.0-NU*X2*X3/360.0-X2*X3/AL1/360.0-X2*X3/360.0-NU

```

```

7  *X2TWO/AL1/120.0-NU*X2TWO/120.0-X2TWO/AL1/120.0-X2TWO/120.0
C
  K2(12,12) = NU*Y3THR/(AL1*X2)/60.0-Y3THR/(AL1*X2)/60.0-NU*X3TWO*Y3
1  /X2/20.0+(-7.0)*X3TWO*Y3/(90.0*AL1*X2)+X3TWO*Y3/X2/20.0+NU*X3*Y
2  3/30.0+5.0*X3*Y3/(36.0*AL1)-X3*Y3/30.0+NU*X2*Y3/90.0-X2*Y3/AL1/
3  20.0-X2*Y3/90.0+5.0*X3FOR/(18.0*X2*Y3)+(-61.0)*X3THR/(90.0*Y3)+
4  31.0*X2*X3TWO/(90.0*Y3)+X2TWO*X3/Y3/15.0+(-2.0)*X2THR/(45.0*Y3)
C
C
C
  DO 100 I   = 1, 12
  DO 100 J   = I, 12
    K2(I,J)  = F * K2(I,J)
    K2(J,I)  = K2(I,J)
100 CONTINUE
C
C
C
  RETURN
  END

```

## A.8 LISTING OF THE SUBROUTINE TSHK4

This subroutine is used to generate the stiffness matrix  $K_4$ .

```

C
C
C SUBROUTINE TSHK4 ( X2, X3, Y3, E, RHO, TH, NU, K4 )
C
C Form the K4 matrix for plane triangular element.
C
C Arguments:
C
C   X2, X3, Y3   —   Geometry to define the triangle.
C   E            —   Young's Modulus.
C   RHO          —   Mass density per unit volume.
C   TH           —   Element Thickness.
C   NU           —   Poisson's Ratio
C   K4(12,12)    —   Output mass matrix.
C
C
C IMPLICIT INTEGER ( A - Z )
C
C   REAL  X2, X3, Y3, E, RHO, TH, NU, F, BETA, AL1
C   REAL  X2PR2, X2PR3, X2PR4, X2PR5, X3PR2, X3PR3, X3PR4, X3PR5,
C   &     X3PR6, X3PR7, X3PR8, Y3PR2, Y3PR3, Y3PR4, Y3PR5
C
C   REAL  K4(12,12)
C
C
C CALL INIT ( K4, 144 )
C
C   AL1    = 2.0 * (1 - NU) / (1 - 2.0*NU)
C   BETA    = 2.0 * (1 + NU) * RHO / E
C   F      = BETA * BETA * E * TH / (1.0 - NU*NU)
C
C   X2PR2   = X2 * X2
C   X2PR3   = X2PR2 * X2
C   X2PR4   = X2PR3 * X2
C   X2PR5   = X2PR4 * X2
C
C   X3PR2   = X3 * X3
C   X3PR3   = X3PR2 * X3
C   X3PR4   = X3PR3 * X3
C   X3PR5   = X3PR4 * X3

```

X3PR6 = X3PR5 \* X3  
 X3PR7 = X3PR6 \* X3  
 X3PR8 = X3PR7 \* X3

C

Y3PR2 = Y3 \* Y3  
 Y3PR3 = Y3PR2 \* Y3  
 Y3PR4 = Y3PR3 \* Y3  
 Y3PR5 = Y3PR4 \* Y3

C

C

C

K4(1,1) = 43.0\*X3PR2\*Y3PR5/(15120.0\*X2PR3)+(-47.0)\*X3\*Y3PR5/(15120  
 1 .0\*X2PR2)+Y3PR5/X2/864.0+(-3683.0)\*NU\*X3PR4\*Y3PR3/(967680.0\*X2P  
 2 R3)+43.0\*X3PR4\*Y3PR3/(15120.0\*AL1\*X2PR3)+3683.0\*X3PR4\*Y3PR3/(96  
 3 7680.0\*X2PR3)+481.0\*NU\*X3PR3\*Y3PR3/(60480.0\*X2PR2)+(-19.0)\*X3PR  
 4 3\*Y3PR3/(3780.0\*AL1\*X2PR2)+(-481.0)\*X3PR3\*Y3PR3/(60480.0\*X2PR2)  
 5 +(-887.0)\*NU\*X3PR2\*Y3PR3/(161280.0\*X2)+X3PR2\*Y3PR3/(AL1\*X2)/403  
 6 2.0+887.0\*X3PR2\*Y3PR3/(161280.0\*X2)+89.0\*NU\*X3\*Y3PR3/60480.0+16  
 7 9.0\*X3\*Y3PR3/(60480.0\*AL1)+(-89.0)\*X3\*Y3PR3/60480.0+(-211.0)\*NU  
 8 \*X2\*Y3PR3/967680.0+(-151.0)\*X2\*Y3PR3/(120960.0\*AL1)+211.0\*X2\*Y3  
 9 PR3/967680.0+(-3019.0)\*NU\*X3PR6\*Y3/(483840.0\*AL1\*X2PR3)+3019.0\*  
 : X3PR6\*Y3/(483840.0\*AL1\*X2PR3)+43.0\*X3PR6\*Y3/(60480.0\*AL1\*\*2\*X2P  
 ; R3)+1079.0\*NU\*X3PR5\*Y3/(60480.0\*AL1\*X2PR2)+(-1079.0)\*X3PR5\*Y3/(  
 < 60480.0\*AL1\*X2PR2)-X3PR5\*Y3/(AL1\*\*2\*X2PR2)/576.0+(-509.0)\*NU\*X3  
 = PR4\*Y3/(34560.0\*AL1\*X2)+509.0\*X3PR4\*Y3/(34560.0\*AL1\*X2)+29.0\*X3  
 > PR4\*Y3/(80640.0\*AL1\*\*2\*X2)+(-13.0)\*NU\*X3PR3\*Y3/(8960.0\*AL1)+13.  
 ? 0\*X3PR3\*Y3/(8960.0\*AL1)+181.0\*X3PR3\*Y3/(120960.0\*AL1\*\*2)+1223.0  
 @ \*NU\*X2\*X3PR2\*Y3/(161280.0\*AL1)+(-1223.0)\*X2\*X3PR2\*Y3/(161280.0\*  
 1 AL1)+(-29.0)\*X2\*X3PR2\*Y3/(80640.0\*AL1\*\*2)+(-439.0)\*NU\*X2PR2\*X3\*  
 2 Y3/(120960.0\*AL1)+439.0\*X2PR2\*X3\*Y3/(120960.0\*AL1)-X2PR2\*X3\*Y3/  
 3 AL1\*\*2/1260.0+151.0\*NU\*X2PR3\*Y3/(241920.0\*AL1)+(-151.0)\*X2PR3\*Y  
 4 3/(241920.0\*AL1)+211.0\*X2PR3\*Y3/(483840.0\*AL1\*\*2)+(-2699.0)\*NU\*  
 5 X3PR8/(967680.0\*AL1\*\*2\*X2PR3\*Y3)+2699.0\*X3PR8/(967680.0\*AL1\*\*2\*  
 6 X2PR3\*Y3)+17.0\*NU\*X3PR7/(1680.0\*AL1\*\*2\*X2PR2\*Y3)+(-17.0)\*X3PR7/  
 7 (1680.0\*AL1\*\*2\*X2PR2\*Y3)+(-127.0)\*NU\*X3PR6/(11520.0\*AL1\*\*2\*X2\*Y  
 8 3)+127.0\*X3PR6/(11520.0\*AL1\*\*2\*X2\*Y3)+(-491.0)\*NU\*X3PR5/(483840  
 9 .0\*AL1\*\*2\*Y3)+491.0\*X3PR5/(483840.0\*AL1\*\*2\*Y3)+313.0\*NU\*X2\*X3PR  
 : 4/(34560.0\*AL1\*\*2\*Y3)+(-313.0)\*X2\*X3PR4/(34560.0\*AL1\*\*2\*Y3)+(-6  
 ; 1.0)\*NU\*X2PR2\*X3PR3/(17280.0\*AL1\*\*2\*Y3)+61.0\*X2PR2\*X3PR3/(17280  
 < .0\*AL1\*\*2\*Y3)+(-373.0)\*NU\*X2PR3\*X3PR2/(138240.0\*AL1\*\*2\*Y3)+373.  
 = 0\*X2PR3\*X3PR2/(138240.0\*AL1\*\*2\*Y3)+17.0\*NU\*X2PR4\*X3/(6912.0\*AL1  
 > \*\*2\*Y3)+(-17.0)\*X2PR4\*X3/(6912.0\*AL1\*\*2\*Y3)-NU\*X2PR5/(AL1\*\*2\*Y3  
 ? )/1728.0+X2PR5/(AL1\*\*2\*Y3)/1728.0  
 K4(1,2) = (-83.0)\*NU\*X3PR3\*Y3PR4/(60480.0\*AL1\*X2PR3)+(-83.0)\*X3PR3  
 1 \*Y3PR4/(60480.0\*AL1\*X2PR3)+1067.0\*NU\*X3PR2\*Y3PR4/(483840.0\*AL1\*  
 2 X2PR2)+1067.0\*X3PR2\*Y3PR4/(483840.0\*AL1\*X2PR2)+(-241.0)\*NU\*X3\*Y  
 3 3PR4/(241920.0\*AL1\*X2)+(-241.0)\*X3\*Y3PR4/(241920.0\*AL1\*X2)+43.0  
 4 \*NU\*Y3PR4/(483840.0\*AL1)+43.0\*Y3PR4/(483840.0\*AL1)+(-43.0)\*NU\*X  
 5 3PR5\*Y3PR2/(60480.0\*AL1\*\*2\*X2PR3)+(-11.0)\*NU\*X3PR5\*Y3PR2/(17280  
 6 .0\*X2PR3)-X3PR5\*Y3PR2/(AL1\*\*2\*X2PR3)/1512.0+(-83.0)\*X3PR5\*Y3PR2

```

7 /(120960.0*X2PR3)+127.0*NU*X3PR4*Y3PR2/(96768.0*AL1**2*X2PR2)+1
8 19.0*NU*X3PR4*Y3PR2/(69120.0*X2PR2)+767.0*X3PR4*Y3PR2/(483840.0
9 *AL1**2*X2PR2)+701.0*X3PR4*Y3PR2/(483840.0*X2PR2)+13.0*NU*X3PR3
: *Y3PR2/(60480.0*AL1**2*X2)+( -11.0)*NU*X3PR3*Y3PR2/(8640.0*X2)+(
; -47.0)*X3PR3*Y3PR2/(60480.0*AL1**2*X2)+( -17.0)*X3PR3*Y3PR2/(604
< 80.0*X2)+( -37.0)*NU*X3PR2*Y3PR2/(24192.0*AL1**2)+NU*X3PR2*Y3PR2
= /69120.0+( -121.0)*X3PR2*Y3PR2/(241920.0*AL1**2)+( -491.0)*X3PR2*
> Y3PR2/483840.0+431.0*NU*X2*X3*Y3PR2/(483840.0*AL1**2)+71.0*NU*X
? 2*X3*Y3PR2/483840.0+191.0*X2*X3*Y3PR2/(483840.0*AL1**2)+311.0*X
@ 2*X3*Y3PR2/483840.0+( -17.0)*NU*X2PR2*Y3PR2/(120960.0*AL1**2)+NU
1 *X2PR2*Y3PR2/120960.0-X2PR2*Y3PR2/AL1**2/24192.0+( -11.0)*X2PR2*
2 Y3PR2/120960.0-NU*X3PR7/(AL1*X2PR3)/3024.0-X3PR7/(AL1*X2PR3)/30
3 24.0+29.0*NU*X3PR6/(32256.0*AL1*X2PR2)+29.0*X3PR6/(32256.0*AL1*
4 X2PR2)+( -41.0)*NU*X3PR5/(161280.0*AL1*X2)+( -41.0)*X3PR5/(161280
5 .0*AL1*X2)+( -1069.0)*NU*X3PR4/(967680.0*AL1)+( -1069.0)*X3PR4/(9
6 67680.0*AL1)+11.0*NU*X2*X3PR3/(13824.0*AL1)+11.0*X2*X3PR3/(1382
7 4.0*AL1)+NU*X2PR2*X3PR2/AL1/3840.0+X2PR2*X3PR2/AL1/3840.0+( -49.
8 0)*NU*X2PR3*X3/(138240.0*AL1)+( -49.0)*X2PR3*X3/(138240.0*AL1)+4
9 3.0*NU*X2PR4/(483840.0*AL1)+43.0*X2PR4/(483840.0*AL1)
K4(1,3) = 43.0*X3PR2*Y3PR5/(15120.0*X2PR3)+( -43.0)*X3*Y3PR5/(15120
1 .0*X2PR2)+Y3PR5/X2/1008.0+( -3683.0)*NU*X3PR4*Y3PR3/(967680.0*X2
2 PR3)+43.0*X3PR4*Y3PR3/(15120.0*AL1*X2PR3)+3683.0*X3PR4*Y3PR3/(9
3 67680.0*X2PR3)+3683.0*NU*X3PR3*Y3PR3/(483840.0*X2PR2)-X3PR3*Y3P
4 R3/(AL1*X2PR2)/432.0+( -3683.0)*X3PR3*Y3PR3/(483840.0*X2PR2)+( -5
5 33.0)*NU*X3PR2*Y3PR3/(107520.0*X2)-X3PR2*Y3PR3/(AL1*X2)/2240.0+
6 533.0*X3PR2*Y3PR3/(107520.0*X2)+557.0*NU*X3*Y3PR3/483840.0+17.0
7 *X3*Y3PR3/(12096.0*AL1)+( -557.0)*X3*Y3PR3/483840.0+( -11.0)*NU*X
8 2*Y3PR3/96768.0+( -29.0)*X2*Y3PR3/(40320.0*AL1)+11.0*X2*Y3PR3/96
9 768.0+( -3019.0)*NU*X3PR6*Y3/(483840.0*AL1*X2PR3)+3019.0*X3PR6*Y
: 3/(483840.0*AL1*X2PR3)+43.0*X3PR6*Y3/(60480.0*AL1**2*X2PR3)+187
; 9.0*NU*X3PR5*Y3/(161280.0*AL1*X2PR2)+( -1879.0)*X3PR5*Y3/(161280
< .0*AL1*X2PR2)-X3PR5*Y3/(AL1**2*X2PR2)/2240.0+( -1991.0)*NU*X3PR4
= *Y3/(322560.0*AL1*X2)+1991.0*X3PR4*Y3/(322560.0*AL1*X2)+( -71.0)
> *X3PR4*Y3/(80640.0*AL1**2*X2)+( -499.0)*NU*X3PR3*Y3/(241920.0*AL
? 1)+499.0*X3PR3*Y3/(241920.0*AL1)+31.0*X3PR3*Y3/(120960.0*AL1**2
@ )+3637.0*NU*X2*X3PR2*Y3/(967680.0*AL1)+( -3637.0)*X2*X3PR2*Y3/(9
1 67680.0*AL1)+X2*X3PR2*Y3/AL1**2/5376.0+( -23.0)*NU*X2PR2*X3*Y3/(
2 17280.0*AL1)+23.0*X2PR2*X3*Y3/(17280.0*AL1)-X2PR2*X3*Y3/AL1**2/
3 10080.0+NU*X2PR3*Y3/AL1/8064.0-X2PR3*Y3/AL1/8064.0+53.0*X2PR3*Y
4 3/(483840.0*AL1**2)+( -2699.0)*NU*X3PR8/(967680.0*AL1**2*X2PR3*Y
5 3)+2699.0*X3PR8/(967680.0*AL1**2*X2PR3*Y3)+167.0*NU*X3PR7/(3456
6 0.0*AL1**2*X2PR2*Y3)+( -167.0)*X3PR7/(34560.0*AL1**2*X2PR2*Y3)+3
7 7.0*NU*X3PR6/(161280.0*AL1**2*X2*Y3)+( -37.0)*X3PR6/(161280.0*AL
8 1**2*X2*Y3)+( -13.0)*NU*X3PR5/(3456.0*AL1**2*Y3)+13.0*X3PR5/(345
9 6.0*AL1**2*Y3)+73.0*NU*X2*X3PR4/(69120.0*AL1**2*Y3)+( -73.0)*X2*
: X3PR4/(69120.0*AL1**2*Y3)+59.0*NU*X2PR2*X3PR3/(69120.0*AL1**2*Y
; 3)+( -59.0)*X2PR2*X3PR3/(69120.0*AL1**2*Y3)+( -59.0)*NU*X2PR3*X3P
< R2/(138240.0*AL1**2*Y3)+59.0*X2PR3*X3PR2/(138240.0*AL1**2*Y3)+N
= U*X2PR4*X3/(AL1**2*Y3)/161280.0-X2PR4*X3/(AL1**2*Y3)/161280.0
K4(1,4) = (-83.0)*NU*X3PR3*Y3PR4/(60480.0*AL1*X2PR3)+( -83.0)*X3PR3

```

```

1  *Y3PR4/(60480.0*AL1*X2PR3)+71.0*NU*X3PR2*Y3PR4/(32256.0*AL1*X2P
2  R2)+139.0*X3PR2*Y3PR4/(69120.0*AL1*X2PR2)+(-79.0)*NU*X3*Y3PR4/(
3  80640.0*AL1*X2)+(-191.0)*X3*Y3PR4/(241920.0*AL1*X2)+59.0*NU*Y3P
4  R4/(483840.0*AL1)+29.0*Y3PR4/(483840.0*AL1)+(-43.0)*NU*X3PR5*Y3
5  PR2/(60480.0*AL1**2*X2PR3)+(-11.0)*NU*X3PR5*Y3PR2/(17280.0*X2PR
6  3)-X3PR5*Y3PR2/(AL1**2*X2PR3)/1512.0+(-83.0)*X3PR5*Y3PR2/(12096
7  0.0*X2PR3)+649.0*NU*X3PR4*Y3PR2/(483840.0*AL1**2*X2PR2)+73.0*NU
8  *X3PR4*Y3PR2/(161280.0*X2PR2)+47.0*X3PR4*Y3PR2/(32256.0*AL1**2*
9  X2PR2)+131.0*X3PR4*Y3PR2/(483840.0*X2PR2)+NU*X3PR3*Y3PR2/(AL1**
:  2*X2)/8640.0+59.0*NU*X3PR3*Y3PR2/(241920.0*X2)+(-67.0)*X3PR3*Y3
;  PR2/(120960.0*AL1**2*X2)+17.0*X3PR3*Y3PR2/(48384.0*X2)+(-17.0)*
<  NU*X3PR2*Y3PR2/(12096.0*AL1**2)-NU*X3PR2*Y3PR2/8640.0+(-31.0)*X
=  3PR2*Y3PR2/(60480.0*AL1**2)+(-23.0)*X3PR2*Y3PR2/120960.0+403.0*
>  NU*X2*X3*Y3PR2/(483840.0*AL1**2)+13.0*NU*X2*X3*Y3PR2/161280.0+X
?  2*X3*Y3PR2/AL1**2/3584.0+71.0*X2*X3*Y3PR2/483840.0-NU*X2PR2*Y3P
@  R2/AL1**2/6912.0+NU*X2PR2*Y3PR2/69120.0-X2PR2*Y3PR2/AL1**2/1209
1  60.0-X2PR2*Y3PR2/69120.0-NU*X3PR7/(AL1*X2PR3)/3024.0-X3PR7/(AL1
2  *X2PR3)/3024.0+101.0*NU*X3PR6/(483840.0*AL1*X2PR2)+59.0*X3PR6/(
3  161280.0*AL1*X2PR2)+NU*X3PR5/(AL1*X2)/1536.0+53.0*X3PR5/(161280
4  .0*AL1*X2)+(-83.0)*NU*X3PR4/(193536.0*AL1)+(-71.0)*X3PR4/(19353
5  6.0*AL1)+(-17.0)*NU*X2*X3PR3/(96768.0*AL1)-X2*X3PR3/AL1/96768.0
6  +NU*X2PR2*X3PR2/AL1/5376.0+X2PR2*X3PR2/AL1/20160.0+(-13.0)*NU*X
7  2PR3*X3/(193536.0*AL1)+(-41.0)*X2PR3*X3/(967680.0*AL1)-NU*X2PR4
8  /AL1/161280.0+X2PR4/AL1/161280.0
K4(1,5) = (-17.0)*NU*X3PR2*Y3PR3/(46080.0*X2)+13.0*X3PR2*Y3PR3/(50
1  40.0*AL1*X2)+17.0*X3PR2*Y3PR3/(46080.0*X2)+31.0*NU*X3*Y3PR3/806
2  40.0-X3*Y3PR3/AL1/1008.0+(-31.0)*X3*Y3PR3/80640.0+(-53.0)*NU*X2
3  *Y3PR3/967680.0-X2*Y3PR3/AL1/4032.0+53.0*X2*Y3PR3/967680.0+(-54
4  7.0)*NU*X3PR4*Y3/(107520.0*AL1*X2)+547.0*X3PR4*Y3/(107520.0*AL1
5  *X2)+13.0*X3PR4*Y3/(10080.0*AL1**2*X2)+73.0*NU*X3PR3*Y3/(10752.
6  0*AL1)+(-73.0)*X3PR3*Y3/(10752.0*AL1)+(-29.0)*X3PR3*Y3/(20160.0
7  *AL1**2)+(-1307.0)*NU*X2*X3PR2*Y3/(967680.0*AL1)+1307.0*X2*X3PR
8  2*Y3/(967680.0*AL1)-X2*X3PR2*Y3/AL1**2/1344.0+(-25.0)*NU*X2PR2*
9  X3*Y3/(24192.0*AL1)+25.0*X2PR2*X3*Y3/(24192.0*AL1)+19.0*X2PR2*X
:  3*Y3/(40320.0*AL1**2)+29.0*NU*X2PR3*Y3/(80640.0*AL1)+(-29.0)*X2
;  PR3*Y3/(80640.0*AL1)+11.0*X2PR3*Y3/(48384.0*AL1**2)+(-661.0)*NU
<  *X3PR6/(161280.0*AL1**2*X2*Y3)+661.0*X3PR6/(161280.0*AL1**2*X2*
=  Y3)+1357.0*NU*X3PR5/(161280.0*AL1**2*Y3)+(-1357.0)*X3PR5/(16128
>  0.0*AL1**2*Y3)+(-173.0)*NU*X2*X3PR4/(69120.0*AL1**2*Y3)+173.0*X
?  2*X3PR4/(69120.0*AL1**2*Y3)+(-277.0)*NU*X2PR2*X3PR3/(69120.0*AL
@  1**2*Y3)+277.0*X2PR2*X3PR3/(69120.0*AL1**2*Y3)+131.0*NU*X2PR3*X
1  3PR2/(69120.0*AL1**2*Y3)+(-131.0)*X2PR3*X3PR2/(69120.0*AL1**2*Y
2  3)+11.0*NU*X2PR4*X3/(13824.0*AL1**2*Y3)+(-11.0)*X2PR4*X3/(13824
3  .0*AL1**2*Y3)-NU*X2PR5/(AL1**2*Y3)/2016.0+X2PR5/(AL1**2*Y3)/201
4  6.0
K4(1,6) = NU*Y3PR4/AL1/80640.0-NU*X3PR3*Y3PR2/X2/768.0+(-19.0)*X3P
1  R3*Y3PR2/(16128.0*X2)-NU*X3PR2*Y3PR2/AL1**2/26880.0+27.0*NU*X3P
2  R2*Y3PR2/17920.0+149.0*X3PR2*Y3PR2/161280.0+NU*X2*X3*Y3PR2/AL1*
3  *2/13440.0-NU*X2*X3*Y3PR2/3780.0+11.0*X2*X3*Y3PR2/60480.0-NU*X2
4  PR2*Y3PR2/AL1**2/34560.0+29.0*NU*X2PR2*Y3PR2/483840.0+(-37.0)*X

```



```

5  2PR2*Y3PR2/483840.0+(-19.0)*NU*X3PR5/(26880.0*AL1*X2)+(-43.0)*X
6  3PR5/(80640.0*AL1*X2)+53.0*NU*X3PR4/(53760.0*AL1)+25.0*X3PR4/(3
7  2256.0*AL1)+NU*X2*X3PR3/AL1/2160.0+13.0*X2*X3PR3/(60480.0*AL1)-
8  NU*X2PR2*X3PR2/AL1/1152.0-X2PR2*X3PR2/AL1/2304.0+11.0*NU*X2PR3*
9  X3/(69120.0*AL1)+(-11.0)*X2PR3*X3/(96768.0*AL1)+NU*X2PR4/AL1/34
:  560.0+11.0*X2PR4/(120960.0*AL1)
K4(1,7) = (-43.0)*X3PR2*Y3PR5/(7560.0*X2PR3)+X3*Y3PR5/X2PR2/168.0+
1  (-13.0)*Y3PR5/(6048.0*X2)+3683.0*NU*X3PR4*Y3PR3/(483840.0*X2PR3
2  )+(-43.0)*X3PR4*Y3PR3/(7560.0*AL1*X2PR3)+(-3683.0)*X3PR4*Y3PR3/
3  (483840.0*X2PR3)+(-7531.0)*NU*X3PR3*Y3PR3/(483840.0*X2PR2)+37.0
4  *X3PR3*Y3PR3/(5040.0*AL1*X2PR2)+7531.0*X3PR3*Y3PR3/(483840.0*X2
5  PR2)+5309.0*NU*X3PR2*Y3PR3/(483840.0*X2)-X3PR2*Y3PR3/(AL1*X2)/1
6  680.0+(-5309.0)*X3PR2*Y3PR3/(483840.0*X2)+(-307.0)*NU*X3*Y3PR3/
7  96768.0+(-7.0)*X3*Y3PR3/(4320.0*AL1)+307.0*X3*Y3PR3/96768.0+97.
8  0*NU*X2*Y3PR3/241920.0+11.0*X2*Y3PR3/(60480.0*AL1)+(-97.0)*X2*Y
9  3PR3/241920.0+3019.0*NU*X3PR6*Y3/(241920.0*AL1*X2PR3)+(-3019.0)
:  *X3PR6*Y3/(241920.0*AL1*X2PR3)+(-43.0)*X3PR6*Y3/(30240.0*AL1**2
;  *X2PR3)+(-14269.0)*NU*X3PR5*Y3/(483840.0*AL1*X2PR2)+14269.0*X3P
<  R5*Y3/(483840.0*AL1*X2PR2)+11.0*X3PR5*Y3/(5040.0*AL1**2*X2PR2)+
=  10223.0*NU*X3PR4*Y3/(483840.0*AL1*X2)+(-10223.0)*X3PR4*Y3/(4838
>  40.0*AL1*X2)+X3PR4*Y3/(AL1**2*X2)/8064.0+(-5.0)*NU*X3PR3*Y3/(13
?  824.0*AL1)+5.0*X3PR3*Y3/(13824.0*AL1)+(-5.0)*X3PR3*Y3/(12096.0
@  AL1**2)+(-11.0)*NU*X2*X3PR2*Y3/(1792.0*AL1)+11.0*X2*X3PR2*Y3/(1
1  792.0*AL1)-X2*X3PR2*Y3/AL1**2/2880.0+349.0*NU*X2PR2*X3*Y3/(1209
2  60.0*AL1)+(-349.0)*X2PR2*X3*Y3/(120960.0*AL1)-X2PR2*X3*Y3/AL1**
3  2/2520.0+(-13.0)*NU*X2PR3*Y3/(32256.0*AL1)+13.0*X2PR3*Y3/(32256
4  .0*AL1)+13.0*X2PR3*Y3/(24192.0*AL1**2)+2699.0*NU*X3PR8/(483840.
5  0*AL1**2*X2PR3*Y3)+(-2699.0)*X3PR8/(483840.0*AL1**2*X2PR3*Y3)+(-
6  -3617.0)*NU*X3PR7/(241920.0*AL1**2*X2PR2*Y3)+3617.0*X3PR7/(2419
7  20.0*AL1**2*X2PR2*Y3)+13.0*NU*X3PR6/(1260.0*AL1**2*X2*Y3)+(-13.
8  0)*X3PR6/(1260.0*AL1**2*X2*Y3)+107.0*NU*X3PR5/(34560.0*AL1**2*Y
9  3)+(-107.0)*X3PR5/(34560.0*AL1**2*Y3)+(-317.0)*NU*X2*X3PR4/(691
:  20.0*AL1**2*Y3)+317.0*X2*X3PR4/(69120.0*AL1**2*Y3)-NU*X2PR2*X3P
;  R3/(AL1**2*Y3)/34560.0+X2PR2*X3PR3/(AL1**2*Y3)/34560.0+NU*X2PR3
<  *X3PR2/(AL1**2*Y3)/8640.0-X2PR3*X3PR2/(AL1**2*Y3)/8640.0+41.0*N
=  U*X2PR4*X3/(48384.0*AL1**2*Y3)+(-41.0)*X2PR4*X3/(48384.0*AL1**2
>  *Y3)+(-47.0)*NU*X2PR5/(120960.0*AL1**2*Y3)+47.0*X2PR5/(120960.0
?  *AL1**2*Y3)
K4(1,8) = 83.0*NU*X3PR3*Y3PR4/(30240.0*AL1*X2PR3)+83.0*X3PR3*Y3PR4
1  /(30240.0*AL1*X2PR3)+(-533.0)*NU*X3PR2*Y3PR4/(120960.0*AL1*X2PR
2  2)+(-17.0)*X3PR2*Y3PR4/(4032.0*AL1*X2PR2)+11.0*NU*X3*Y3PR4/(576
3  0.0*AL1*X2)+X3*Y3PR4/(AL1*X2)/560.0+(-11.0)*NU*Y3PR4/(60480.0*A
4  L1)-Y3PR4/AL1/6720.0+43.0*NU*X3PR5*Y3PR2/(30240.0*AL1**2*X2PR3)
5  +11.0*NU*X3PR5*Y3PR2/(8640.0*X2PR3)+X3PR5*Y3PR2/(AL1**2*X2PR3)/
6  756.0+83.0*X3PR5*Y3PR2/(60480.0*X2PR3)+(-107.0)*NU*X3PR4*Y3PR2/
7  (40320.0*AL1**2*X2PR2)+(-263.0)*NU*X3PR4*Y3PR2/(120960.0*X2PR2)
8  +(-23.0)*X3PR4*Y3PR2/(7560.0*AL1**2*X2PR2)+(-13.0)*X3PR4*Y3PR2/
9  (7560.0*X2PR2)+(-11.0)*NU*X3PR3*Y3PR2/(30240.0*AL1**2*X2)+23.0*
:  NU*X3PR3*Y3PR2/(20160.0*X2)+23.0*X3PR3*Y3PR2/(17280.0*AL1**2*X2
;  )+31.0*X3PR3*Y3PR2/(60480.0*X2)+145.0*NU*X3PR2*Y3PR2/(48384.0*A

```

```

< L1**2)+(-83.0)*NU*X3PR2*Y3PR2/120960.0+7.0*X3PR2*Y3PR2/(6912.0*
= AL1**2)+(-71.0)*X3PR2*Y3PR2/120960.0+(-47.0)*NU*X2*X3*Y3PR2/(26
> 880.0*AL1**2)+109.0*NU*X2*X3*Y3PR2/241920.0+(-163.0)*X2*X3*Y3PR
? 2/(241920.0*AL1**2)+17.0*X2*X3*Y3PR2/26880.0+17.0*NU*X2PR2*Y3PR
@ 2/(60480.0*AL1**2)-NU*X2PR2*Y3PR2/40320.0+X2PR2*Y3PR2/AL1**2/20
1 160.0+(-13.0)*X2PR2*Y3PR2/120960.0+NU*X3PR7/(AL1*X2PR3)/1512.0+
2 X3PR7/(AL1*X2PR3)/1512.0+(-67.0)*NU*X3PR6/(60480.0*AL1*X2PR2)+(-
3 -17.0)*X3PR6/(13440.0*AL1*X2PR2)-NU*X3PR5/(AL1*X2)/2304.0+5.0*X
4 3PR5/(16128.0*AL1*X2)+673.0*NU*X3PR4/(483840.0*AL1)+73.0*X3PR4/
5 (483840.0*AL1)+(-37.0)*NU*X2*X3PR3/(48384.0*AL1)+5.0*X2*X3PR3/(
6 16128.0*AL1)+89.0*NU*X2PR2*X3PR2/(161280.0*AL1)+X2PR2*X3PR2/AL1
7 /161280.0+(-101.0)*NU*X2PR3*X3/(241920.0*AL1)+(-13.0)*X2PR3*X3/
8 (48384.0*AL1)+29.0*NU*X2PR4/(241920.0*AL1)+23.0*X2PR4/(241920.0
9 *AL1)
K4(1,9) = 43.0*X3*Y3PR5/(30240.0*X2PR2)+(-47.0)*Y3PR5/(60480.0*X2)
1 +(-1117.0)*NU*X3PR3*Y3PR3/(483840.0*X2PR2)+(-43.0)*X3PR3*Y3PR3/
2 (12096.0*AL1*X2PR2)+1117.0*X3PR3*Y3PR3/(483840.0*X2PR2)+1691.0*
3 NU*X3PR2*Y3PR3/(483840.0*X2)+59.0*X3PR2*Y3PR3/(40320.0*AL1*X2)+
4 (-1691.0)*X3PR2*Y3PR3/(483840.0*X2)+(-767.0)*NU*X3*Y3PR3/483840
5 .0+(-37.0)*X3*Y3PR3/(30240.0*AL1)+767.0*X3*Y3PR3/483840.0+41.0*
6 NU*X2*Y3PR3/161280.0+11.0*X2*Y3PR3/(8960.0*AL1)+(-41.0)*X2*Y3PR
7 3/161280.0+1061.0*NU*X3PR5*Y3/(161280.0*AL1*X2PR2)+(-1061.0)*X3
8 PR5*Y3/(161280.0*AL1*X2PR2)+(-43.0)*X3PR5*Y3/(20160.0*AL1**2*X2
9 PR2)+(-311.0)*NU*X3PR4*Y3/(40320.0*AL1*X2)+311.0*X3PR4*Y3/(4032
: 0.0*AL1*X2)+X3PR4*Y3/(AL1**2*X2)/384.0+217.0*NU*X3PR3*Y3/(69120
; .0*AL1)+(-217.0)*X3PR3*Y3/(69120.0*AL1)+47.0*X3PR3*Y3/(60480.0*
< AL1**2)+(-491.0)*NU*X2*X3PR2*Y3/(161280.0*AL1)+491.0*X2*X3PR2*Y
= 3/(161280.0*AL1)+(-5.0)*X2*X3PR2*Y3/(5376.0*AL1**2)+17.0*NU*X2P
> R2*X3*Y3/(7560.0*AL1)+(-17.0)*X2PR2*X3*Y3/(7560.0*AL1)+X2PR2*X3
? *Y3/AL1**2/2520.0+(-11.0)*NU*X2PR3*Y3/(17920.0*AL1)+11.0*X2PR3*
@ Y3/(17920.0*AL1)+(-41.0)*X2PR3*Y3/(80640.0*AL1**2)+913.0*NU*X3P
1 R7/(120960.0*AL1**2*X2PR2*Y3)+(-913.0)*X3PR7/(120960.0*AL1**2*X
2 2PR2*Y3)+(-529.0)*NU*X3PR6/(32256.0*AL1**2*X2*Y3)+529.0*X3PR6/(
3 32256.0*AL1**2*X2*Y3)+269.0*NU*X3PR5/(34560.0*AL1**2*Y3)+(-269.
4 0)*X3PR5/(34560.0*AL1**2*Y3)+49.0*NU*X2*X3PR4/(11520.0*AL1**2*Y
5 3)+(-49.0)*X2*X3PR4/(11520.0*AL1**2*Y3)+(-143.0)*NU*X2PR2*X3PR3
6 /(34560.0*AL1**2*Y3)+143.0*X2PR2*X3PR3/(34560.0*AL1**2*Y3)+11.0
7 *NU*X2PR3*X3PR2/(7680.0*AL1**2*Y3)+(-11.0)*X2PR3*X3PR2/(7680.0*
8 AL1**2*Y3)-NU*X2PR4*X3/(AL1**2*Y3)/1152.0+X2PR4*X3/(AL1**2*Y3)/
9 1152.0+47.0*NU*X2PR5/(120960.0*AL1**2*Y3)+(-47.0)*X2PR5/(120960
: .0*AL1**2*Y3)
K4(1,10) = (-3.0)*NU*X3PR2*Y3PR4/(4480.0*AL1*X2PR2)+(-83.0)*X3PR2*
1 Y3PR4/(120960.0*AL1*X2PR2)+19.0*NU*X3*Y3PR4/(24192.0*AL1*X2)+43
2 .0*X3*Y3PR4/(60480.0*AL1*X2)-NU*Y3PR4/AL1/8064.0+(-13.0)*Y3PR4/
3 (120960.0*AL1)-NU*X3PR4*Y3PR2/(AL1**2*X2PR2)/2880.0+47.0*NU*X3P
4 R4*Y3PR2/(24192.0*X2PR2)-X3PR4*Y3PR2/(AL1**2*X2PR2)/3024.0+83.0
5 *X3PR4*Y3PR2/(40320.0*X2PR2)+11.0*NU*X3PR3*Y3PR2/(24192.0*AL1**
6 2*X2)+(-143.0)*NU*X3PR3*Y3PR2/(60480.0*X2)+X3PR3*Y3PR2/(AL1**2*
7 X2)/1680.0+(-43.0)*X3PR3*Y3PR2/(20160.0*X2)+59.0*NU*X3PR2*Y3PR2
8 /(161280.0*AL1**2)+43.0*NU*X3PR2*Y3PR2/60480.0+(-13.0)*X3PR2*Y3

```

```

9 PR2/(161280.0*AL1**2)+7.0*X3PR2*Y3PR2/8640.0+(-61.0)*NU*X2*X3*Y
: 3PR2/(96768.0*AL1**2)-NU*X2*X3*Y3PR2/3024.0+(-121.0)*X2*X3*Y3PR
; 2/(483840.0*AL1**2)-X2*X3*Y3PR2/1680.0+11.0*NU*X2PR2*Y3PR2/(604
< 80.0*AL1**2)+NU*X2PR2*Y3PR2/120960.0+X2PR2*Y3PR2/AL1**2/15120.0
= +X2PR2*Y3PR2/8064.0+61.0*NU*X3PR6/(60480.0*AL1*X2PR2)+X3PR6/(AL
> 1*X2PR2)/1008.0-NU*X3PR5/(AL1*X2)/840.0-X3PR5/(AL1*X2)/560.0+(-
? 587.0)*NU*X3PR4/(483840.0*AL1)+253.0*X3PR4/(483840.0*AL1)+313.0
@ *NU*X2*X3PR3/(161280.0*AL1)+139.0*X2*X3PR3/(483840.0*AL1)+(-149
1 .0)*NU*X2PR2*X3PR2/(161280.0*AL1)+(-29.0)*X2PR2*X3PR2/(161280.0
2 *AL1)+61.0*NU*X2PR3*X3/(161280.0*AL1)+X2PR3*X3/AL1/3584.0-NU*X2
3 PR4/AL1/10080.0-X2PR4/AL1/8640.0
K4(1,11) = (-43.0)*X3*Y3PR5/(30240.0*X2PR2)+47.0*Y3PR5/(60480.0*X2
1 )+1117.0*NU*X3PR3*Y3PR3/(483840.0*X2PR2)+43.0*X3PR3*Y3PR3/(1209
2 6.0*AL1*X2PR2)+(-1117.0)*X3PR3*Y3PR3/(483840.0*X2PR2)+(-881.0)*
3 NU*X3PR2*Y3PR3/(241920.0*X2)+(-131.0)*X3PR2*Y3PR3/(40320.0*AL1*
4 X2)+881.0*X3PR2*Y3PR3/(241920.0*X2)+121.0*NU*X3*Y3PR3/69120.0+(-
5 -11.0)*X3*Y3PR3/(30240.0*AL1)+(-121.0)*X3*Y3PR3/69120.0+(-13.0)
6 *NU*X2*Y3PR3/48384.0+13.0*X2*Y3PR3/(16128.0*AL1)+13.0*X2*Y3PR3/
7 48384.0+(-1061.0)*NU*X3PR5*Y3/(161280.0*AL1*X2PR2)+1061.0*X3PR5
8 *Y3/(161280.0*AL1*X2PR2)+43.0*X3PR5*Y3/(20160.0*AL1**2*X2PR2)+8
9 69.0*NU*X3PR4*Y3/(69120.0*AL1*X2)+(-869.0)*X3PR4*Y3/(69120.0*AL
: 1*X2)+(-47.0)*X3PR4*Y3/(13440.0*AL1**2*X2)+(-2929.0)*NU*X3PR3*Y
; 3/(483840.0*AL1)+2929.0*X3PR3*Y3/(483840.0*AL1)+(-41.0)*X3PR3*Y
< 3/(60480.0*AL1**2)+(-391.0)*NU*X2*X3PR2*Y3/(483840.0*AL1)+391.0
= *X2*X3PR2*Y3/(483840.0*AL1)+59.0*X2*X3PR2*Y3/(26880.0*AL1**2)+1
> 3.0*NU*X2PR2*X3*Y3/(15120.0*AL1)+(-13.0)*X2PR2*X3*Y3/(15120.0*A
? L1)+17.0*X2PR2*X3*Y3/(40320.0*AL1**2)+(-11.0)*NU*X2PR3*Y3/(1209
@ 60.0*AL1)+11.0*X2PR3*Y3/(120960.0*AL1)+(-97.0)*X2PR3*Y3/(120960
1 .0*AL1**2)+(-913.0)*NU*X3PR7/(120960.0*AL1**2*X2PR2*Y3)+913.0*X
2 3PR7/(120960.0*AL1**2*X2PR2*Y3)+3383.0*NU*X3PR6/(161280.0*AL1**
3 2*X2*Y3)+(-3383.0)*X3PR6/(161280.0*AL1**2*X2*Y3)+(-439.0)*NU*X3
4 PR5/(30240.0*AL1**2*Y3)+439.0*X3PR5/(30240.0*AL1**2*Y3)+(-503.0
5 )*NU*X2*X3PR4/(69120.0*AL1**2*Y3)+503.0*X2*X3PR4/(69120.0*AL1**
6 2*Y3)+25.0*NU*X2PR2*X3PR3/(2304.0*AL1**2*Y3)+(-25.0)*X2PR2*X3PR
7 3/(2304.0*AL1**2*Y3)+(-11.0)*NU*X2PR3*X3PR2/(34560.0*AL1**2*Y3)
8 +11.0*X2PR3*X3PR2/(34560.0*AL1**2*Y3)+(-7.0)*NU*X2PR4*X3/(2160.
9 0*AL1**2*Y3)+7.0*X2PR4*X3/(2160.0*AL1**2*Y3)+13.0*NU*X2PR5/(120
: 96.0*AL1**2*Y3)+(-13.0)*X2PR5/(12096.0*AL1**2*Y3)
K4(1,12) = 3.0*NU*X3PR2*Y3PR4/(4480.0*AL1*X2PR2)+83.0*X3PR2*Y3PR4/
1 (120960.0*AL1*X2PR2)+(-29.0)*NU*X3*Y3PR4/(40320.0*AL1*X2)+(-43.
2 0)*X3*Y3PR4/(60480.0*AL1*X2)+NU*Y3PR4/AL1/12096.0+13.0*Y3PR4/(1
3 20960.0*AL1)+NU*X3PR4*Y3PR2/(AL1**2*X2PR2)/2880.0+(-47.0)*NU*X3
4 PR4*Y3PR2/(24192.0*X2PR2)+X3PR4*Y3PR2/(AL1**2*X2PR2)/3024.0+(-8
5 3.0)*X3PR4*Y3PR2/(40320.0*X2PR2)+(-17.0)*NU*X3PR3*Y3PR2/(40320.
6 0*AL1**2*X2)+43.0*NU*X3PR3*Y3PR2/(12096.0*X2)-X3PR3*Y3PR2/(AL1*
7 *2*X2)/1680.0+11.0*X3PR3*Y3PR2/(4032.0*X2)-NU*X3PR2*Y3PR2/AL1**
8 2/2560.0+(-173.0)*NU*X3PR2*Y3PR2/120960.0+13.0*X3PR2*Y3PR2/(161
9 280.0*AL1**2)+X3PR2*Y3PR2/17280.0+281.0*NU*X2*X3*Y3PR2/(483840.
: 0*AL1**2)-NU*X2*X3*Y3PR2/12096.0+121.0*X2*X3*Y3PR2/(483840.0*AL
; 1**2)+(-61.0)*X2*X3*Y3PR2/60480.0-NU*X2PR2*Y3PR2/AL1**2/6720.0-

```

```

< NU*X2PR2*Y3PR2/15120.0-X2PR2*Y3PR2/AL1**2/15120.0+X2PR2*Y3PR2/6
= 048.0+(-61.0)*NU*X3PR6/(60480.0*AL1*X2PR2)-X3PR6/(AL1*X2PR2)/10
> 08.0+13.0*NU*X3PR5/(6720.0*AL1*X2)+13.0*X3PR5/(6720.0*AL1*X2)+1
? 79.0*NU*X3PR4/(483840.0*AL1)+11.0*X3PR4/(483840.0*AL1)+(-1093.0
@ )*NU*X2*X3PR3/(483840.0*AL1)+(-773.0)*X2*X3PR3/(483840.0*AL1)+N
1 U*X2PR2*X3PR2/AL1/1260.0+X2PR2*X3PR2/AL1/3360.0+73.0*NU*X2PR3*X
2 3/(241920.0*AL1)+121.0*X2PR3*X3/(241920.0*AL1)-NU*X2PR4/AL1/756
3 0.0-X2PR4/AL1/6048.0

```

C

```

K4(2,2) = (-43.0)*NU*X3PR2*Y3PR5/(30240.0*AL1**2*X2PR3)+43.0*X3PR2
1 *Y3PR5/(30240.0*AL1**2*X2PR3)+47.0*NU*X3*Y3PR5/(30240.0*AL1**2*
2 X2PR2)+(-47.0)*X3*Y3PR5/(30240.0*AL1**2*X2PR2)-NU*Y3PR5/(AL1**2
3 *X2)/1728.0+Y3PR5/(AL1**2*X2)/1728.0+(-43.0)*NU*X3PR4*Y3PR3/(30
4 240.0*AL1*X2PR3)+43.0*X3PR4*Y3PR3/(30240.0*AL1*X2PR3)+3683.0*X3
5 PR4*Y3PR3/(483840.0*AL1**2*X2PR3)+19.0*NU*X3PR3*Y3PR3/(7560.0*A
6 L1*X2PR2)+(-19.0)*X3PR3*Y3PR3/(7560.0*AL1*X2PR2)+(-481.0)*X3PR3
7 *Y3PR3/(30240.0*AL1**2*X2PR2)-NU*X3PR2*Y3PR3/(AL1*X2)/8064.0+X3
8 PR2*Y3PR3/(AL1*X2)/8064.0+887.0*X3PR2*Y3PR3/(80640.0*AL1**2*X2)
9 +(-169.0)*NU*X3*Y3PR3/(120960.0*AL1)+169.0*X3*Y3PR3/(120960.0*A
: L1)+(-89.0)*X3*Y3PR3/(30240.0*AL1**2)+151.0*NU*X2*Y3PR3/(241920
; .0*AL1)+(-151.0)*X2*Y3PR3/(241920.0*AL1)+211.0*X2*Y3PR3/(483840
< .0*AL1**2)+(-43.0)*NU*X3PR6*Y3/(120960.0*X2PR3)+3019.0*X3PR6*Y3
= /(241920.0*AL1*X2PR3)+43.0*X3PR6*Y3/(120960.0*X2PR3)+NU*X3PR5*Y
> 3/X2PR2/1152.0+(-1079.0)*X3PR5*Y3/(30240.0*AL1*X2PR2)-X3PR5*Y3/
? X2PR2/1152.0+(-29.0)*NU*X3PR4*Y3/(161280.0*X2)+509.0*X3PR4*Y3/(
@ 17280.0*AL1*X2)+29.0*X3PR4*Y3/(161280.0*X2)+(-181.0)*NU*X3PR3*Y
1 3/241920.0+13.0*X3PR3*Y3/(4480.0*AL1)+181.0*X3PR3*Y3/241920.0+2
2 9.0*NU*X2*X3PR2*Y3/161280.0+(-1223.0)*X2*X3PR2*Y3/(80640.0*AL1)
3 +(-29.0)*X2*X3PR2*Y3/161280.0+NU*X2PR2*X3*Y3/2520.0+439.0*X2PR2
4 *X3*Y3/(60480.0*AL1)-X2PR2*X3*Y3/2520.0+(-211.0)*NU*X2PR3*Y3/96
5 7680.0+(-151.0)*X2PR3*Y3/(120960.0*AL1)+211.0*X2PR3*Y3/967680.0
6 +2699.0*X3PR8/(483840.0*X2PR3*Y3)+(-17.0)*X3PR7/(840.0*X2PR2*Y3
7 )+127.0*X3PR6/(5760.0*X2*Y3)+491.0*X3PR5/(241920.0*Y3)+(-313.0)
8 *X2*X3PR4/(17280.0*Y3)+61.0*X2PR2*X3PR3/(8640.0*Y3)+373.0*X2PR3
9 *X3PR2/(69120.0*Y3)+(-17.0)*X2PR4*X3/(3456.0*Y3)+X2PR5/Y3/864.0
K4(2,3) = (-83.0)*NU*X3PR3*Y3PR4/(60480.0*AL1*X2PR3)+(-83.0)*X3PR3
1 *Y3PR4/(60480.0*AL1*X2PR3)+103.0*NU*X3PR2*Y3PR4/(53760.0*AL1*X2
2 PR2)+1019.0*X3PR2*Y3PR4/(483840.0*AL1*X2PR2)-NU*X3*Y3PR4/(AL1*X
3 2)/1440.0+(-107.0)*X3*Y3PR4/(120960.0*AL1*X2)+NU*Y3PR4/AL1/3456
4 0.0+11.0*Y3PR4/(120960.0*AL1)+(-43.0)*NU*X3PR5*Y3PR2/(60480.0*A
5 L1**2*X2PR3)+(-11.0)*NU*X3PR5*Y3PR2/(17280.0*X2PR3)-X3PR5*Y3PR2
6 /(AL1**2*X2PR3)/1512.0+(-83.0)*X3PR5*Y3PR2/(120960.0*X2PR3)+29.
7 0*NU*X3PR4*Y3PR2/(161280.0*AL1**2*X2PR2)+733.0*NU*X3PR4*Y3PR2/(
8 483840.0*X2PR2)+5.0*X3PR4*Y3PR2/(13824.0*AL1**2*X2PR2)+677.0*X3
9 PR4*Y3PR2/(483840.0*X2PR2)+7.0*NU*X3PR3*Y3PR2/(17280.0*AL1**2*X
: 2)+(-43.0)*NU*X3PR3*Y3PR2/(48384.0*X2)+X3PR3*Y3PR2/(AL1**2*X2)/
; 3360.0+(-53.0)*X3PR3*Y3PR2/(241920.0*X2)+(-11.0)*NU*X3PR2*Y3PR2
< /(48384.0*AL1**2)-NU*X3PR2*Y3PR2/15120.0+(-37.0)*X3PR2*Y3PR2/(2
= 41920.0*AL1**2)+(-29.0)*X3PR2*Y3PR2/30240.0+29.0*NU*X2*X3*Y3PR2
> /(161280.0*AL1**2)+NU*X2*X3*Y3PR2/483840.0+11.0*X2*X3*Y3PR2/(96

```

```

? 768.0*AL1**2)+269.0*X2*X3*Y3PR2/483840.0-NU*X2PR2*Y3PR2/AL1**2/
@ 34560.0+29.0*NU*X2PR2*Y3PR2/483840.0+(-37.0)*X2PR2*Y3PR2/483840
1 .0-NU*X3PR7/(AL1*X2PR3)/3024.0-X3PR7/(AL1*X2PR3)/3024.0+43.0*NU
2 *X3PR6/(96768.0*AL1*X2PR2)+139.0*X3PR6/(483840.0*AL1*X2PR2)+3.0
3 *NU*X3PR5/(17920.0*AL1*X2)+79.0*X3PR5/(161280.0*AL1*X2)+(-65.0)
4 *NU*X3PR4/(193536.0*AL1)+(-11.0)*X3PR4/(27648.0*AL1)+NU*X2*X3PR
5 3/AL1/13824.0-X2*X3PR3/AL1/10752.0-NU*X2PR2*X3PR2/AL1/53760.0+1
6 9.0*X2PR2*X3PR2/(161280.0*AL1)+(-29.0)*NU*X2PR3*X3/(967680.0*AL
7 1)+(-53.0)*X2PR3*X3/(967680.0*AL1)+NU*X2PR4/AL1/80640.0
K4(2,4) = (-43.0)*NU*X3PR2*Y3PR5/(30240.0*AL1**2*X2PR3)+43.0*X3PR2
1 *Y3PR5/(30240.0*AL1**2*X2PR3)+43.0*NU*X3*Y3PR5/(30240.0*AL1**2*
2 X2PR2)+(-43.0)*X3*Y3PR5/(30240.0*AL1**2*X2PR2)-NU*Y3PR5/(AL1**2
3 *X2)/2016.0+Y3PR5/(AL1**2*X2)/2016.0+(-43.0)*NU*X3PR4*Y3PR3/(30
4 240.0*AL1*X2PR3)+43.0*X3PR4*Y3PR3/(30240.0*AL1*X2PR3)+3683.0*X3
5 PR4*Y3PR3/(483840.0*AL1**2*X2PR3)+NU*X3PR3*Y3PR3/(AL1*X2PR2)/86
6 4.0-X3PR3*Y3PR3/(AL1*X2PR2)/864.0+(-3683.0)*X3PR3*Y3PR3/(241920
7 .0*AL1**2*X2PR2)+NU*X3PR2*Y3PR3/(AL1*X2)/4480.0-X3PR2*Y3PR3/(AL
8 1*X2)/4480.0+533.0*X3PR2*Y3PR3/(53760.0*AL1**2*X2)+(-17.0)*NU*X
9 3*Y3PR3/(24192.0*AL1)+17.0*X3*Y3PR3/(24192.0*AL1)+(-557.0)*X3*Y
: 3PR3/(241920.0*AL1**2)+29.0*NU*X2*Y3PR3/(80640.0*AL1)+(-29.0)*X
; 2*Y3PR3/(80640.0*AL1)+11.0*X2*Y3PR3/(48384.0*AL1**2)+(-43.0)*NU
< *X3PR6*Y3/(120960.0*X2PR3)+3019.0*X3PR6*Y3/(241920.0*AL1*X2PR3)
= +43.0*X3PR6*Y3/(120960.0*X2PR3)+NU*X3PR5*Y3/X2PR2/4480.0+(-1879
> .0)*X3PR5*Y3/(80640.0*AL1*X2PR2)-X3PR5*Y3/X2PR2/4480.0+71.0*NU*
? X3PR4*Y3/(161280.0*X2)+1991.0*X3PR4*Y3/(161280.0*AL1*X2)+(-71.0
@ )*X3PR4*Y3/(161280.0*X2)+(-31.0)*NU*X3PR3*Y3/241920.0+499.0*X3P
1 R3*Y3/(120960.0*AL1)+31.0*X3PR3*Y3/241920.0-NU*X2*X3PR2*Y3/1075
2 2.0+(-3637.0)*X2*X3PR2*Y3/(483840.0*AL1)+X2*X3PR2*Y3/10752.0+NU
3 *X2PR2*X3*Y3/20160.0+23.0*X2PR2*X3*Y3/(8640.0*AL1)-X2PR2*X3*Y3/
4 20160.0+(-53.0)*NU*X2PR3*Y3/967680.0-X2PR3*Y3/AL1/4032.0+53.0*X
5 2PR3*Y3/967680.0+2699.0*X3PR8/(483840.0*X2PR3*Y3)+(-167.0)*X3PR
6 7/(17280.0*X2PR2*Y3)+(-37.0)*X3PR6/(80640.0*X2*Y3)+13.0*X3PR5/(
7 1728.0*Y3)+(-73.0)*X2*X3PR4/(34560.0*Y3)+(-59.0)*X2PR2*X3PR3/(3
8 4560.0*Y3)+59.0*X2PR3*X3PR2/(69120.0*Y3)-X2PR4*X3/Y3/80640.0
K4(2,5) = -NU*Y3PR4/AL1/161280.0+Y3PR4/AL1/161280.0-NU*X3PR3*Y3PR2
1 /(AL1**2*X2)/896.0+(-5.0)*X3PR3*Y3PR2/(4032.0*AL1**2*X2)+17.0*N
2 U*X3PR2*Y3PR2/(26880.0*AL1**2)+NU*X3PR2*Y3PR2/53760.0+7.0*X3PR2
3 *Y3PR2/(5760.0*AL1**2)-X3PR2*Y3PR2/53760.0+7.0*NU*X2*X3*Y3PR2/(
4 17280.0*AL1**2)-NU*X2*X3*Y3PR2/26880.0-X2*X3*Y3PR2/AL1**2/24192
5 .0+X2*X3*Y3PR2/26880.0-NU*X2PR2*Y3PR2/AL1**2/6912.0+NU*X2PR2*Y3
6 PR2/69120.0-X2PR2*Y3PR2/AL1**2/120960.0-X2PR2*Y3PR2/69120.0-NU*
7 X3PR5/(AL1*X2)/2240.0+(-5.0)*X3PR5/(8064.0*AL1*X2)+3.0*NU*X3PR4
8 /(4480.0*AL1)+71.0*X3PR4/(80640.0*AL1)+11.0*NU*X2*X3PR3/(120960
9 .0*AL1)+41.0*X2*X3PR3/(120960.0*AL1)-NU*X2PR2*X3PR2/AL1/4608.0-
: X2PR2*X3PR2/AL1/1536.0+(-121.0)*NU*X2PR3*X3/(483840.0*AL1)+11.0
; *X2PR3*X3/(483840.0*AL1)+59.0*NU*X2PR4/(483840.0*AL1)+29.0*X2PR
< 4/(483840.0*AL1)
K4(2,6) = (-13.0)*NU*X3PR2*Y3PR3/(10080.0*AL1*X2)+13.0*X3PR2*Y3PR3
1 /(10080.0*AL1*X2)+17.0*X3PR2*Y3PR3/(23040.0*AL1**2*X2)+NU*X3*Y3
2 PR3/AL1/2016.0-X3*Y3PR3/AL1/2016.0+(-31.0)*X3*Y3PR3/(40320.0*AL

```

```

3 1**2)+NU*X2*Y3PR3/AL1/8064.0-X2*Y3PR3/AL1/8064.0+53.0*X2*Y3PR3/
4 (483840.0*AL1**2)+(-13.0)*NU*X3PR4*Y3/(20160.0*X2)+547.0*X3PR4*
5 Y3/(53760.0*AL1*X2)+13.0*X3PR4*Y3/(20160.0*X2)+29.0*NU*X3PR3*Y3
6 /40320.0+(-73.0)*X3PR3*Y3/(5376.0*AL1)+(-29.0)*X3PR3*Y3/40320.0
7 +NU*X2*X3PR2*Y3/2688.0+1307.0*X2*X3PR2*Y3/(483840.0*AL1)-X2*X3P
8 R2*Y3/2688.0+(-19.0)*NU*X2PR2*X3*Y3/80640.0+25.0*X2PR2*X3*Y3/(1
9 2096.0*AL1)+19.0*X2PR2*X3*Y3/80640.0+(-11.0)*NU*X2PR3*Y3/96768.
: 0+(-29.0)*X2PR3*Y3/(40320.0*AL1)+11.0*X2PR3*Y3/96768.0+661.0*X3
; PR6/(80640.0*X2*Y3)+(-1357.0)*X3PR5/(80640.0*Y3)+173.0*X2*X3PR4
< /(34560.0*Y3)+277.0*X2PR2*X3PR3/(34560.0*Y3)+(-131.0)*X2PR3*X3P
= R2/(34560.0*Y3)+(-11.0)*X2PR4*X3/(6912.0*Y3)+X2PR5/Y3/1008.0
K4(2,7) = 83.0*NU*X3PR3*Y3PR4/(30240.0*AL1*X2PR3)+83.0*X3PR3*Y3PR4
1 /(30240.0*AL1*X2PR3)+(-997.0)*NU*X3PR2*Y3PR4/(241920.0*AL1*X2PR
2 2)+(-149.0)*X3PR2*Y3PR4/(34560.0*AL1*X2PR2)+139.0*NU*X3*Y3PR4/(
3 80640.0*AL1*X2)+149.0*X3*Y3PR4/(80640.0*AL1*X2)-NU*Y3PR4/AL1/75
4 60.0-Y3PR4/AL1/6048.0+43.0*NU*X3PR5*Y3PR2/(30240.0*AL1**2*X2PR3
5 )+11.0*NU*X3PR5*Y3PR2/(8640.0*X2PR3)+X3PR5*Y3PR2/(AL1**2*X2PR3)
6 /756.0+83.0*X3PR5*Y3PR2/(60480.0*X2PR3)+(-361.0)*NU*X3PR4*Y3PR2
7 /(241920.0*AL1**2*X2PR2)+(-29.0)*NU*X3PR4*Y3PR2/(8960.0*X2PR2)+
8 (-157.0)*X3PR4*Y3PR2/(80640.0*AL1**2*X2PR2)+(-689.0)*X3PR4*Y3PR
9 2/(241920.0*X2PR2)+NU*X3PR3*Y3PR2/(AL1**2*X2)/5040.0+527.0*NU*X
: 3PR3*Y3PR2/(241920.0*X2)+5.0*X3PR3*Y3PR2/(6048.0*AL1**2*X2)+13.
; 0*X3PR3*Y3PR2/(26880.0*X2)+(-13.0)*NU*X3PR2*Y3PR2/(24192.0*AL1*
< *2)+NU*X3PR2*Y3PR2/48384.0+(-11.0)*X3PR2*Y3PR2/(17280.0*AL1**2)
= +97.0*X3PR2*Y3PR2/48384.0+5.0*NU*X2*X3*Y3PR2/(6912.0*AL1**2)+(-
> 11.0)*NU*X2*X3*Y3PR2/80640.0+131.0*X2*X3*Y3PR2/(241920.0*AL1**2
? )+(-293.0)*X2*X3*Y3PR2/241920.0-NU*X2PR2*Y3PR2/AL1**2/6720.0-NU
@ *X2PR2*Y3PR2/15120.0-X2PR2*Y3PR2/AL1**2/15120.0+X2PR2*Y3PR2/604
1 8.0+NU*X3PR7/(AL1*X2PR3)/1512.0+X3PR7/(AL1*X2PR3)/1512.0+(-65.0
2 )*NU*X3PR6/(48384.0*AL1*X2PR2)+(-41.0)*X3PR6/(34560.0*AL1*X2PR2
3 )+11.0*NU*X3PR5/(16128.0*AL1*X2)-X3PR5/(AL1*X2)/16128.0+(-227.0
4 )*NU*X3PR4/(483840.0*AL1)+373.0*X3PR4/(483840.0*AL1)+41.0*NU*X2
5 *X3PR3/(48384.0*AL1)+(-11.0)*X2*X3PR3/(48384.0*AL1)+(-43.0)*NU*
6 X2PR2*X3PR2/(161280.0*AL1)+X2PR2*X3PR2/AL1/3584.0+(-47.0)*NU*X2
7 PR3*X3/(241920.0*AL1)+(-83.0)*X2PR3*X3/(241920.0*AL1)+NU*X2PR4/
8 AL1/12096.0+13.0*X2PR4/(120960.0*AL1)
K4(2,8) = 43.0*NU*X3PR2*Y3PR5/(15120.0*AL1**2*X2PR3)+(-43.0)*X3PR2
1 *Y3PR5/(15120.0*AL1**2*X2PR3)-NU*X3*Y3PR5/(AL1**2*X2PR2)/336.0+
2 X3*Y3PR5/(AL1**2*X2PR2)/336.0+13.0*NU*Y3PR5/(12096.0*AL1**2*X2)
3 +(-13.0)*Y3PR5/(12096.0*AL1**2*X2)+43.0*NU*X3PR4*Y3PR3/(15120.0
4 *AL1*X2PR3)+(-43.0)*X3PR4*Y3PR3/(15120.0*AL1*X2PR3)+(-3683.0)*X
5 3PR4*Y3PR3/(241920.0*AL1**2*X2PR3)+(-37.0)*NU*X3PR3*Y3PR3/(1008
6 0.0*AL1*X2PR2)+37.0*X3PR3*Y3PR3/(10080.0*AL1*X2PR2)+7531.0*X3PR
7 3*Y3PR3/(241920.0*AL1**2*X2PR2)+NU*X3PR2*Y3PR3/(AL1*X2)/3360.0-
8 X3PR2*Y3PR3/(AL1*X2)/3360.0+(-5309.0)*X3PR2*Y3PR3/(241920.0*AL1
9 **2*X2)+7.0*NU*X3*Y3PR3/(8640.0*AL1)+(-7.0)*X3*Y3PR3/(8640.0*AL
: 1)+307.0*X3*Y3PR3/(48384.0*AL1**2)+(-11.0)*NU*X2*Y3PR3/(120960.
; 0*AL1)+11.0*X2*Y3PR3/(120960.0*AL1)+(-97.0)*X2*Y3PR3/(120960.0*
< AL1**2)+43.0*NU*X3PR6*Y3/(60480.0*X2PR3)+(-3019.0)*X3PR6*Y3/(12
= 0960.0*AL1*X2PR3)+(-43.0)*X3PR6*Y3/(60480.0*X2PR3)+(-11.0)*NU*X
> 3PR5*Y3/(10080.0*X2PR2)+14269.0*X3PR5*Y3/(241920.0*AL1*X2PR2)+1

```

```

? 1.0*X3PR5*Y3/(10080.0*X2PR2)-NU*X3PR4*Y3/X2/16128.0+(-10223.0)*
@ X3PR4*Y3/(241920.0*AL1*X2)+X3PR4*Y3/X2/16128.0+5.0*NU*X3PR3*Y3/
1 24192.0+5.0*X3PR3*Y3/(6912.0*AL1)+(-5.0)*X3PR3*Y3/24192.0+NU*X2
2 *X3PR2*Y3/5760.0+11.0*X2*X3PR2*Y3/(896.0*AL1)-X2*X3PR2*Y3/5760.
3 0+NU*X2PR2*X3*Y3/5040.0+(-349.0)*X2PR2*X3*Y3/(60480.0*AL1)-X2PR
4 2*X3*Y3/5040.0+(-13.0)*NU*X2PR3*Y3/48384.0+13.0*X2PR3*Y3/(16128
5 .0*AL1)+13.0*X2PR3*Y3/48384.0+(-2699.0)*X3PR8/(241920.0*X2PR3*Y
6 3)+3617.0*X3PR7/(120960.0*X2PR2*Y3)+(-13.0)*X3PR6/(630.0*X2*Y3)
7 +(-107.0)*X3PR5/(17280.0*Y3)+317.0*X2*X3PR4/(34560.0*Y3)+X2PR2*
8 X3PR3*Y3/17280.0-X2PR3*X3PR2*Y3/4320.0+(-41.0)*X2PR4*X3/(24192.
9 0*Y3)+47.0*X2PR5/(60480.0*Y3)
K4(2,9) = -NU*X3PR2*Y3PR4/(AL1*X2PR2)/1440.0+(-41.0)*X3PR2*Y3PR4/(
1 60480.0*AL1*X2PR2)+163.0*NU*X3*Y3PR4/(241920.0*AL1*X2)+181.0*X3
2 *Y3PR4/(241920.0*AL1*X2)-NU*Y3PR4/AL1/10080.0-Y3PR4/AL1/8640.0+
3 2.0*NU*X3PR4*Y3PR2/(945.0*AL1**2*X2PR2)+(-13.0)*NU*X3PR4*Y3PR2/
4 (40320.0*X2PR2)+121.0*X3PR4*Y3PR2/(60480.0*AL1**2*X2PR2)+(-41.0
5 )*X3PR4*Y3PR2/(120960.0*X2PR2)+(-61.0)*NU*X3PR3*Y3PR2/(30240.0*
6 AL1**2*X2)+23.0*NU*X3PR3*Y3PR2/(34560.0*X2)+(-17.0)*X3PR3*Y3PR2
7 /(7560.0*AL1**2*X2)+127.0*X3PR3*Y3PR2/(241920.0*X2)+13.0*NU*X3P
8 R2*Y3PR2/(15120.0*AL1**2)+(-7.0)*NU*X3PR2*Y3PR2/23040.0+23.0*X3
9 PR2*Y3PR2/(30240.0*AL1**2)+23.0*X3PR2*Y3PR2/161280.0+(-11.0)*NU
: *X2*X3*Y3PR2/(15120.0*AL1**2)+(-29.0)*NU*X2*X3*Y3PR2/483840.0-X
: 2*X3*Y3PR2/AL1**2/2160.0+(-71.0)*X2*X3*Y3PR2/161280.0+11.0*NU*X
< 2PR2*Y3PR2/(60480.0*AL1**2)+NU*X2PR2*Y3PR2/120960.0+X2PR2*Y3PR2
= /AL1**2/15120.0+X2PR2*Y3PR2/8064.0+17.0*NU*X3PR6/(17280.0*AL1*X
> 2PR2)+121.0*X3PR6/(120960.0*AL1*X2PR2)-NU*X3PR5/(AL1*X2)/480.0-
? X3PR5/(AL1*X2)/672.0+673.0*NU*X3PR4/(483840.0*AL1)+(-167.0)*X3P
@ R4/(483840.0*AL1)+(-29.0)*NU*X2*X3PR3/(53760.0*AL1)+77.0*X2*X3P
1 R3/(69120.0*AL1)+31.0*NU*X2PR2*X3PR2/(161280.0*AL1)+(-89.0)*X2P
2 R2*X3PR2/(161280.0*AL1)+37.0*NU*X2PR3*X3/(161280.0*AL1)+53.0*X2
3 PR3*X3/(161280.0*AL1)-NU*X2PR4/AL1/8064.0+(-13.0)*X2PR4/(120960
4 .0*AL1)
K4(2,10) = (-43.0)*NU*X3*Y3PR5/(60480.0*AL1**2*X2PR2)+43.0*X3*Y3PR
1 5/(60480.0*AL1**2*X2PR2)+47.0*NU*Y3PR5/(120960.0*AL1**2*X2)+(-4
2 7.0)*Y3PR5/(120960.0*AL1**2*X2)+43.0*NU*X3PR3*Y3PR3/(24192.0*AL
3 1*X2PR2)+(-43.0)*X3PR3*Y3PR3/(24192.0*AL1*X2PR2)+1117.0*X3PR3*Y
4 3PR3/(241920.0*AL1**2*X2PR2)+(-59.0)*NU*X3PR2*Y3PR3/(80640.0*AL
5 1*X2)+59.0*X3PR2*Y3PR3/(80640.0*AL1*X2)+(-1691.0)*X3PR2*Y3PR3/(
6 241920.0*AL1**2*X2)+37.0*NU*X3*Y3PR3/(60480.0*AL1)+(-37.0)*X3*Y
7 3PR3/(60480.0*AL1)+767.0*X3*Y3PR3/(241920.0*AL1**2)+(-11.0)*NU*
8 X2*Y3PR3/(17920.0*AL1)+11.0*X2*Y3PR3/(17920.0*AL1)+(-41.0)*X2*Y
9 3PR3/(80640.0*AL1**2)+43.0*NU*X3PR5*Y3/(40320.0*X2PR2)+(-1061.0
: )*X3PR5*Y3/(80640.0*AL1*X2PR2)+(-43.0)*X3PR5*Y3/(40320.0*X2PR2)
: -NU*X3PR4*Y3/X2/768.0+311.0*X3PR4*Y3/(20160.0*AL1*X2)+X3PR4*Y3/
< X2/768.0+(-47.0)*NU*X3PR3*Y3/120960.0+(-217.0)*X3PR3*Y3/(34560.
= 0*AL1)+47.0*X3PR3*Y3/120960.0+5.0*NU*X2*X3PR2*Y3/10752.0+491.0*
> X2*X3PR2*Y3/(80640.0*AL1)+(-5.0)*X2*X3PR2*Y3/10752.0-NU*X2PR2*X
? 3*Y3/5040.0+(-17.0)*X2PR2*X3*Y3/(3780.0*AL1)+X2PR2*X3*Y3/5040.0
@ +41.0*NU*X2PR3*Y3/161280.0+11.0*X2PR3*Y3/(8960.0*AL1)+(-41.0)*X
1 2PR3*Y3/161280.0+(-913.0)*X3PR7/(60480.0*X2PR2*Y3)+529.0*X3PR6/

```

```

2 (16128.0*X2*Y3)+(-269.0)*X3PR5/(17280.0*Y3)+(-49.0)*X2*X3PR4/(5
3 760.0*Y3)+143.0*X2PR2*X3PR3/(17280.0*Y3)+(-11.0)*X2PR3*X3PR2/(3
4 840.0*Y3)+X2PR4*X3/Y3/576.0+(-47.0)*X2PR5/(60480.0*Y3)
K4(2,11) = NU*X3PR2*Y3PR4/(AL1*X2PR2)/1440.0+41.0*X3PR2*Y3PR4/(604
1 80.0*AL1*X2PR2)+(-19.0)*NU*X3*Y3PR4/(26880.0*AL1*X2)+(-173.0)*X
2 3*Y3PR4/(241920.0*AL1*X2)+29.0*NU*Y3PR4/(241920.0*AL1)+23.0*Y3P
3 R4/(241920.0*AL1)+(-2.0)*NU*X3PR4*Y3PR2/(945.0*AL1**2*X2PR2)+13
4 .0*NU*X3PR4*Y3PR2/(40320.0*X2PR2)+(-121.0)*X3PR4*Y3PR2/(60480.0
5 *AL1**2*X2PR2)+41.0*X3PR4*Y3PR2/(120960.0*X2PR2)+NU*X3PR3*Y3PR2
6 /(AL1**2*X2)/432.0+(-11.0)*NU*X3PR3*Y3PR2/(16128.0*X2)+19.0*X3P
7 R3*Y3PR2/(6048.0*AL1**2*X2)+(-41.0)*X3PR3*Y3PR2/(80640.0*X2)+97
8 .0*NU*X3PR2*Y3PR2/(120960.0*AL1**2)+17.0*NU*X3PR2*Y3PR2/53760.0
9 +(-83.0)*X3PR2*Y3PR2/(120960.0*AL1**2)+(-5.0)*X3PR2*Y3PR2/32256
: .0+(-89.0)*NU*X2*X3*Y3PR2/(60480.0*AL1**2)+41.0*NU*X2*X3*Y3PR2/
; 483840.0+(-11.0)*X2*X3*Y3PR2/(20160.0*AL1**2)+67.0*X2*X3*Y3PR2/
< 161280.0+17.0*NU*X2PR2*Y3PR2/(60480.0*AL1**2)-NU*X2PR2*Y3PR2/40
= 320.0+X2PR2*Y3PR2/AL1**2/20160.0+(-13.0)*X2PR2*Y3PR2/120960.0+(-
> -17.0)*NU*X3PR6/(17280.0*AL1*X2PR2)+(-121.0)*X3PR6/(120960.0*AL
? 1*X2PR2)+13.0*NU*X3PR5/(6720.0*AL1*X2)+13.0*X3PR5/(6720.0*AL1*X
@ 2)+(-73.0)*NU*X3PR4/(483840.0*AL1)+19.0*X3PR4/(96768.0*AL1)+(-6
1 13.0)*NU*X2*X3PR3/(483840.0*AL1)+(-311.0)*X2*X3PR3/(161280.0*AL
2 1)+NU*X2PR2*X3PR2/AL1/20160.0+11.0*X2PR2*X3PR2/(20160.0*AL1)+29
3 .0*NU*X2PR3*X3/(48384.0*AL1)+97.0*X2PR3*X3/(241920.0*AL1)+(-11.
4 0)*NU*X2PR4/(60480.0*AL1)-X2PR4/AL1/6720.0
K4(2,12) = 43.0*NU*X3*Y3PR5/(60480.0*AL1**2*X2PR2)+(-43.0)*X3*Y3PR
1 5/(60480.0*AL1**2*X2PR2)+(-47.0)*NU*Y3PR5/(120960.0*AL1**2*X2)+
2 47.0*Y3PR5/(120960.0*AL1**2*X2)+(-43.0)*NU*X3PR3*Y3PR3/(24192.0
3 *AL1*X2PR2)+43.0*X3PR3*Y3PR3/(24192.0*AL1*X2PR2)+(-1117.0)*X3PR
4 3*Y3PR3/(241920.0*AL1**2*X2PR2)+131.0*NU*X3PR2*Y3PR3/(80640.0*A
5 L1*X2)+(-131.0)*X3PR2*Y3PR3/(80640.0*AL1*X2)+881.0*X3PR2*Y3PR3/
6 (120960.0*AL1**2*X2)+11.0*NU*X3*Y3PR3/(60480.0*AL1)+(-11.0)*X3*
7 Y3PR3/(60480.0*AL1)+(-121.0)*X3*Y3PR3/(34560.0*AL1**2)+(-13.0)*
8 NU*X2*Y3PR3/(32256.0*AL1)+13.0*X2*Y3PR3/(32256.0*AL1)+13.0*X2*Y
9 3PR3/(24192.0*AL1**2)+(-43.0)*NU*X3PR5*Y3/(40320.0*X2PR2)+1061.
: 0*X3PR5*Y3/(80640.0*AL1*X2PR2)+43.0*X3PR5*Y3/(40320.0*X2PR2)+47
; .0*NU*X3PR4*Y3/(26880.0*X2)+(-869.0)*X3PR4*Y3/(34560.0*AL1*X2)+
< (-47.0)*X3PR4*Y3/(26880.0*X2)+41.0*NU*X3PR3*Y3/120960.0+2929.0*
= X3PR3*Y3/(241920.0*AL1)+(-41.0)*X3PR3*Y3/120960.0+(-59.0)*NU*X2
> *X3PR2*Y3/53760.0+391.0*X2*X3PR2*Y3/(241920.0*AL1)+59.0*X2*X3PR
? 2*Y3/53760.0+(-17.0)*NU*X2PR2*X3*Y3/80640.0+(-13.0)*X2PR2*X3*Y3
@ /(7560.0*AL1)+17.0*X2PR2*X3*Y3/80640.0+97.0*NU*X2PR3*Y3/241920.
1 0+11.0*X2PR3*Y3/(60480.0*AL1)+(-97.0)*X2PR3*Y3/241920.0+913.0*X
2 3PR7/(60480.0*X2PR2*Y3)+(-3383.0)*X3PR6/(80640.0*X2*Y3)+439.0*X
3 3PR5/(15120.0*Y3)+503.0*X2*X3PR4/(34560.0*Y3)+(-25.0)*X2PR2*X3P
4 R3/(1152.0*Y3)+11.0*X2PR3*X3PR2/(17280.0*Y3)+7.0*X2PR4*X3/(1080
5 .0*Y3)+(-13.0)*X2PR5/(6048.0*Y3)

```

C

```

K4(3,3) = 43.0*X3PR2*Y3PR5/(15120.0*X2PR3)+(-13.0)*X3*Y3PR5/(5040.
1 0*X2PR2)+Y3PR5/X2/1120.0+(-3683.0)*NU*X3PR4*Y3PR3/(967680.0*X2P
2 R3)+43.0*X3PR4*Y3PR3/(15120.0*AL1*X2PR3)+3683.0*X3PR4*Y3PR3/(96

```



```

3 7680.0*X2PR3)+1759.0*NU*X3PR3*Y3PR3/(241920.0*X2PR2)+X3PR3*Y3PR
4 3/(AL1*X2PR2)/2520.0+(-1759.0)*X3PR3*Y3PR3/(241920.0*X2PR2)+(-3
5 61.0)*NU*X3PR2*Y3PR3/(80640.0*X2)-X3PR2*Y3PR3/(AL1*X2)/1344.0+3
6 61.0*X3PR2*Y3PR3/(80640.0*X2)+NU*X3*Y3PR3/1120.0+5.0*X3*Y3PR3/(
7 12096.0*AL1)-X3*Y3PR3/1120.0-NU*X2*Y3PR3/10080.0+(-47.0)*X2*Y3P
8 R3/(120960.0*AL1)+X2*Y3PR3/10080.0+(-3019.0)*NU*X3PR6*Y3/(48384
9 0.0*AL1*X2PR3)+3019.0*X3PR6*Y3/(483840.0*AL1*X2PR3)+43.0*X3PR6*
: Y3/(60480.0*AL1**2*X2PR3)+1321.0*NU*X3PR5*Y3/(241920.0*AL1*X2PR
; 2)+(-1321.0)*X3PR5*Y3/(241920.0*AL1*X2PR2)+17.0*X3PR5*Y3/(20160
< .0*AL1**2*X2PR2)+649.0*NU*X3PR4*Y3/(483840.0*AL1*X2)+(-649.0)*X
= 3PR4*Y3/(483840.0*AL1*X2)+X3PR4*Y3/(AL1**2*X2)/3840.0+(-503.0)*
> NU*X3PR3*Y3/(241920.0*AL1)+503.0*X3PR3*Y3/(241920.0*AL1)+5.0*X3
? PR3*Y3/(24192.0*AL1**2)+113.0*NU*X2*X3PR2*Y3/(241920.0*AL1)+(-1
@ 13.0)*X2*X3PR2*Y3/(241920.0*AL1)+11.0*X2*X3PR2*Y3/(80640.0*AL1*
1 *2)-NU*X2PR2*X3*Y3/AL1/26880.0+X2PR2*X3*Y3/AL1/26880.0+11.0*X2P
2 R3*Y3/(96768.0*AL1**2)+(-2699.0)*NU*X3PR8/(967680.0*AL1**2*X2PR
3 3*Y3)+2699.0*X3PR8/(967680.0*AL1**2*X2PR3*Y3)+(-11.0)*NU*X3PR7/
4 (24192.0*AL1**2*X2PR2*Y3)+11.0*X3PR7/(24192.0*AL1**2*X2PR2*Y3)+
5 173.0*NU*X3PR6/(120960.0*AL1**2*X2*Y3)+(-173.0)*X3PR6/(120960.0
6 *AL1**2*X2*Y3)+(-11.0)*NU*X3PR5/(69120.0*AL1**2*Y3)+11.0*X3PR5/
7 (69120.0*AL1**2*Y3)-NU*X2*X3PR4/(AL1**2*Y3)/2880.0+X2*X3PR4/(AL
8 1**2*Y3)/2880.0+NU*X2PR2*X3PR3/(AL1**2*Y3)/80640.0-X2PR2*X3PR3/
9 (AL1**2*Y3)/80640.0+(-11.0)*NU*X2PR3*X3PR2/(193536.0*AL1**2*Y3)
: +11.0*X2PR3*X3PR2/(193536.0*AL1**2*Y3)
K4(3,4) = (-83.0)*NU*X3PR3*Y3PR4/(60480.0*AL1*X2PR3)+(-83.0)*X3PR3
1 *Y3PR4/(60480.0*AL1*X2PR3)+185.0*NU*X3PR2*Y3PR4/(96768.0*AL1*X2
2 PR2)+185.0*X3PR2*Y3PR4/(96768.0*AL1*X2PR2)+(-17.0)*NU*X3*Y3PR4/
3 (24192.0*AL1*X2)+(-17.0)*X3*Y3PR4/(24192.0*AL1*X2)+NU*Y3PR4/AL1
4 /13440.0+Y3PR4/AL1/13440.0+(-43.0)*NU*X3PR5*Y3PR2/(60480.0*AL1*
5 *2*X2PR3)+(-11.0)*NU*X3PR5*Y3PR2/(17280.0*X2PR3)-X3PR5*Y3PR2/(A
6 L1**2*X2PR3)/1512.0+(-83.0)*X3PR5*Y3PR2/(120960.0*X2PR3)+101.0*
7 NU*X3PR4*Y3PR2/(483840.0*AL1**2*X2PR2)+17.0*NU*X3PR4*Y3PR2/(691
8 20.0*X2PR2)+113.0*X3PR4*Y3PR2/(483840.0*AL1**2*X2PR2)+107.0*X3P
9 R4*Y3PR2/(483840.0*X2PR2)+47.0*NU*X3PR3*Y3PR2/(120960.0*AL1**2*
: X2)+29.0*NU*X3PR3*Y3PR2/(120960.0*X2)+X3PR3*Y3PR2/(AL1**2*X2)/3
; 456.0+41.0*X3PR3*Y3PR2/(120960.0*X2)+(-11.0)*NU*X3PR2*Y3PR2/(48
< 384.0*AL1**2)+(-29.0)*NU*X3PR2*Y3PR2/483840.0-X3PR2*Y3PR2/AL1**
= 2/8640.0+(-83.0)*X3PR2*Y3PR2/483840.0+83.0*NU*X2*X3*Y3PR2/(4838
> 40.0*AL1**2)+29.0*NU*X2*X3*Y3PR2/483840.0+47.0*X2*X3*Y3PR2/(483
? 840.0*AL1**2)+13.0*X2*X3*Y3PR2/96768.0-NU*X2PR2*Y3PR2/AL1**2/26
@ 880.0+NU*X2PR2*Y3PR2/53760.0-X2PR2*Y3PR2/53760.0-NU*X3PR7/(AL1*
1 X2PR3)/3024.0-X3PR7/(AL1*X2PR3)/3024.0+(-17.0)*NU*X3PR6/(69120.
2 0*AL1*X2PR2)+(-17.0)*X3PR6/(69120.0*AL1*X2PR2)+13.0*NU*X3PR5/(1
3 61280.0*AL1*X2)+13.0*X3PR5/(161280.0*AL1*X2)+(-11.0)*NU*X3PR4/(
4 193536.0*AL1)+(-11.0)*X3PR4/(193536.0*AL1)-NU*X2*X3PR3/AL1/1792
5 0.0-X2*X3PR3/AL1/17920.0+NU*X2PR2*X3PR2/AL1/161280.0+X2PR2*X3PR
6 2/AL1/161280.0+(-11.0)*NU*X2PR3*X3/(193536.0*AL1)+(-11.0)*X2PR3
7 *X3/(193536.0*AL1)
K4(3,5) = (-17.0)*NU*X3PR2*Y3PR3/(46080.0*X2)+13.0*X3PR2*Y3PR3/(50
1 40.0*AL1*X2)+17.0*X3PR2*Y3PR3/(46080.0*X2)+19.0*NU*X3*Y3PR3/537

```

```

2 60.0-X3*Y3PR3/AL1/1260.0+(-19.0)*X3*Y3PR3/53760.0+(-19.0)*NU*X2
3 *Y3PR3/483840.0-X2*Y3PR3/AL1/6720.0+19.0*X2*Y3PR3/483840.0+(-54
4 7.0)*NU*X3PR4*Y3/(107520.0*AL1*X2)+547.0*X3PR4*Y3/(107520.0*AL1
5 *X2)+13.0*X3PR4*Y3/(10080.0*AL1**2*X2)+61.0*NU*X3PR3*Y3/(10752.
6 0*AL1)+(-61.0)*X3PR3*Y3/(10752.0*AL1)+19.0*X3PR3*Y3/(20160.0*AL
7 1**2)+(-839.0)*NU*X2*X3PR2*Y3/(967680.0*AL1)+839.0*X2*X3PR2*Y3/
8 (967680.0*AL1)+X2*X3PR2*Y3/AL1**2/6720.0+(-169.0)*NU*X2PR2*X3*Y
9 3/(241920.0*AL1)+169.0*X2PR2*X3*Y3/(241920.0*AL1)+X2PR2*X3*Y3/A
: L1**2/5760.0+NU*X2PR3*Y3/AL1/13440.0-X2PR3*Y3/AL1/13440.0+19.0*
; X2PR3*Y3/(241920.0*AL1**2)+(-661.0)*NU*X3PR6/(161280.0*AL1**2*X
< 2*Y3)+661.0*X3PR6/(161280.0*AL1**2*X2*Y3)+101.0*NU*X3PR5/(16128
= 0.0*AL1**2*Y3)+(-101.0)*X3PR5/(161280.0*AL1**2*Y3)+173.0*NU*X2*
> X3PR4/(96768.0*AL1**2*Y3)+(-173.0)*X2*X3PR4/(96768.0*AL1**2*Y3)
? +(-73.0)*NU*X2PR2*X3PR3/(161280.0*AL1**2*Y3)+73.0*X2PR2*X3PR3/(
@ 161280.0*AL1**2*Y3)+(-163.0)*NU*X2PR3*X3PR2/(483840.0*AL1**2*Y3
1 )+163.0*X2PR3*X3PR2/(483840.0*AL1**2*Y3)-NU*X2PR4*X3/(AL1**2*Y3
2 )/161280.0+X2PR4*X3/(AL1**2*Y3)/161280.0
K4(3,6) = -NU*Y3PR4/AL1/80640.0-NU*X3PR3*Y3PR2/X2/768.0+(-19.0)*X3
1 PR3*Y3PR2/(16128.0*X2)-NU*X3PR2*Y3PR2/AL1**2/80640.0+191.0*NU*X
2 3PR2*Y3PR2/161280.0+137.0*X3PR2*Y3PR2/161280.0-NU*X2*X3*Y3PR2/6
3 048.0+11.0*X2*X3*Y3PR2/60480.0-NU*X2PR2*Y3PR2/AL1**2/120960.0+N
4 U*X2PR2*Y3PR2/10080.0-X2PR2*Y3PR2/20160.0+(-19.0)*NU*X3PR5/(268
5 80.0*AL1*X2)+(-43.0)*X3PR5/(80640.0*AL1*X2)+(-17.0)*NU*X3PR4/(1
6 61280.0*AL1)-X3PR4/AL1/4608.0+13.0*NU*X2*X3PR3/(60480.0*AL1)+X2
7 *X3PR3/AL1/6048.0-NU*X2PR2*X3PR2/AL1/6720.0-X2PR2*X3PR2/AL1/806
8 40.0+17.0*NU*X2PR3*X3/(483840.0*AL1)+(-19.0)*X2PR3*X3/(483840.0
9 *AL1)-NU*X2PR4/AL1/80640.0
K4(3,7) = (-43.0)*X3PR2*Y3PR5/(7560.0*X2PR3)+41.0*X3*Y3PR5/(7560.0
1 *X2PR2)+(-19.0)*Y3PR5/(10080.0*X2)+3683.0*NU*X3PR4*Y3PR3/(48384
2 0.0*X2PR3)+(-43.0)*X3PR4*Y3PR3/(7560.0*AL1*X2PR3)+(-3683.0)*X3P
3 R4*Y3PR3/(483840.0*X2PR3)+(-7201.0)*NU*X3PR3*Y3PR3/(483840.0*X2
4 PR2)+29.0*X3PR3*Y3PR3/(15120.0*AL1*X2PR2)+7201.0*X3PR3*Y3PR3/(4
5 83840.0*X2PR2)+2407.0*NU*X3PR2*Y3PR3/(241920.0*X2)+X3PR2*Y3PR3/
6 (AL1*X2)/2520.0+(-2407.0)*X3PR2*Y3PR3/(241920.0*X2)+(-611.0)*NU
7 *X3*Y3PR3/241920.0+17.0*X3*Y3PR3/(30240.0*AL1)+611.0*X3*Y3PR3/2
8 41920.0+NU*X2*Y3PR3/4032.0+(-23.0)*X2*Y3PR3/(60480.0*AL1)-X2*Y3
9 PR3/4032.0+3019.0*NU*X3PR6*Y3/(241920.0*AL1*X2PR3)+(-3019.0)*X3
: PR6*Y3/(241920.0*AL1*X2PR3)+(-43.0)*X3PR6*Y3/(30240.0*AL1**2*X2
; PR3)+(-8279.0)*NU*X3PR5*Y3/(483840.0*AL1*X2PR2)+8279.0*X3PR5*Y3
< /(483840.0*AL1*X2PR2)-X3PR5*Y3/(AL1**2*X2PR2)/2520.0+17.0*NU*X3
= PR4*Y3/(3360.0*AL1*X2)+(-17.0)*X3PR4*Y3/(3360.0*AL1*X2)+X3PR4*Y
> 3/(AL1**2*X2)/4480.0+629.0*NU*X3PR3*Y3/(483840.0*AL1)+(-629.0)*
? X3PR3*Y3/(483840.0*AL1)+17.0*X3PR3*Y3/(60480.0*AL1**2)+31.0*NU*
@ X2*X3PR2*Y3/(96768.0*AL1)+(-31.0)*X2*X3PR2*Y3/(96768.0*AL1)+X2*
1 X3PR2*Y3/AL1**2/2880.0+(-23.0)*NU*X2PR2*X3*Y3/(34560.0*AL1)+23.
2 0*X2PR2*X3*Y3/(34560.0*AL1)+NU*X2PR3*Y3/AL1/10080.0-X2PR3*Y3/AL
3 1/10080.0+X2PR3*Y3/AL1**2/3780.0+2699.0*NU*X3PR8/(483840.0*AL1*
4 *2*X2PR3*Y3)+(-2699.0)*X3PR8/(483840.0*AL1**2*X2PR3*Y3)+(-353.0
5 )*NU*X3PR7/(80640.0*AL1**2*X2PR2*Y3)+353.0*X3PR7/(80640.0*AL1**
6 2*X2PR2*Y3)+(-517.0)*NU*X3PR6/(241920.0*AL1**2*X2*Y3)+517.0*X3P

```

```

7  R6/(241920.0*AL1**2*X2*Y3)+151.0*NU*X3PR5/(120960.0*AL1**2*Y3)+
8  (-151.0)*X3PR5/(120960.0*AL1**2*Y3)+73.0*NU*X2*X3PR4/(161280.0*
9  AL1**2*Y3)+(-73.0)*X2*X3PR4/(161280.0*AL1**2*Y3)+NU*X2PR2*X3PR3
:  /(AL1**2*Y3)/30240.0-X2PR2*X3PR3/(AL1**2*Y3)/30240.0+(-83.0)*NU
;  *X2PR3*X3PR2/(241920.0*AL1**2*Y3)+83.0*X2PR3*X3PR2/(241920.0*AL
<  1**2*Y3)
  K4(3,8) = 83.0*NU*X3PR3*Y3PR4/(30240.0*AL1*X2PR3)+83.0*X3PR3*Y3PR4
1  /(30240.0*AL1*X2PR3)+(-463.0)*NU*X3PR2*Y3PR4/(120960.0*AL1*X2PR
2  2)+(-9.0)*X3PR2*Y3PR4/(2240.0*AL1*X2PR2)+23.0*NU*X3*Y3PR4/(1728
3  0.0*AL1*X2)+X3*Y3PR4/(AL1*X2)/630.0-NU*Y3PR4/AL1/15120.0-Y3PR4/
4  AL1/6048.0+43.0*NU*X3PR5*Y3PR2/(30240.0*AL1**2*X2PR3)+11.0*NU*X
5  3PR5*Y3PR2/(8640.0*X2PR3)+X3PR5*Y3PR2/(AL1**2*X2PR3)/756.0+83.0
6  *X3PR5*Y3PR2/(60480.0*X2PR3)+(-47.0)*NU*X3PR4*Y3PR2/(120960.0*A
7  L1**2*X2PR2)+(-71.0)*NU*X3PR4*Y3PR2/(40320.0*X2PR2)-X3PR4*Y3PR2
8  /(AL1**2*X2PR2)/1680.0+(-7.0)*X3PR4*Y3PR2/(4320.0*X2PR2)+(-5.0)
9  *NU*X3PR3*Y3PR2/(6048.0*AL1**2*X2)+23.0*NU*X3PR3*Y3PR2/(30240.0
:  *X2)+(-71.0)*X3PR3*Y3PR2/(120960.0*AL1**2*X2)+X3PR3*Y3PR2/X2/21
;  60.0+107.0*NU*X3PR2*Y3PR2/(241920.0*AL1**2)+(-11.0)*NU*X3PR2*Y3
<  PR2/17280.0+13.0*X3PR2*Y3PR2/(48384.0*AL1**2)+(-71.0)*X3PR2*Y3P
=  R2/120960.0+(-17.0)*NU*X2*X3*Y3PR2/(48384.0*AL1**2)+89.0*NU*X2*
>  X3*Y3PR2/241920.0+(-17.0)*X2*X3*Y3PR2/(80640.0*AL1**2)+47.0*X2*
?  X3*Y3PR2/80640.0+NU*X2PR2*Y3PR2/AL1**2/15120.0+NU*X2PR2*Y3PR2/4
@  8384.0+(-5.0)*X2PR2*Y3PR2/48384.0+NU*X3PR7/(AL1*X2PR3)/1512.0+X
1  3PR7/(AL1*X2PR3)/1512.0-NU*X3PR6/(AL1*X2PR2)/5040.0-X3PR6/(AL1*
2  X2PR2)/24192.0+(-23.0)*NU*X3PR5/(80640.0*AL1*X2)-X3PR5/(AL1*X2)
3  /5376.0+73.0*NU*X3PR4/(483840.0*AL1)+(-83.0)*X3PR4/(483840.0*AL
4  1)+(-5.0)*NU*X2*X3PR3/(16128.0*AL1)+(-23.0)*X2*X3PR3/(241920.0*
5  AL1)+11.0*NU*X2PR2*X3PR2/(161280.0*AL1)+X2PR2*X3PR2/AL1/23040.0
6  -NU*X2PR3*X3/AL1/7560.0-X2PR3*X3/AL1/7560.0
  K4(3,9) = 43.0*X3*Y3PR5/(30240.0*X2PR2)+(-13.0)*Y3PR5/(20160.0*X2)
1  +(-1117.0)*NU*X3PR3*Y3PR3/(483840.0*X2PR2)+(-43.0)*X3PR3*Y3PR3/
2  (12096.0*AL1*X2PR2)+1117.0*X3PR3*Y3PR3/(483840.0*X2PR2)+227.0*N
3  U*X3PR2*Y3PR3/(69120.0*X2)+19.0*X3PR2*Y3PR3/(8064.0*AL1*X2)+(-2
4  27.0)*X3PR2*Y3PR3/(69120.0*X2)+(-337.0)*NU*X3*Y3PR3/241920.0+(-
5  5.0)*X3*Y3PR3/(6048.0*AL1)+337.0*X3*Y3PR3/241920.0+NU*X2*Y3PR3/
6  6720.0+181.0*X2*Y3PR3/(241920.0*AL1)-X2*Y3PR3/6720.0+1061.0*NU*
7  X3PR5*Y3/(161280.0*AL1*X2PR2)+(-1061.0)*X3PR5*Y3/(161280.0*AL1*
8  X2PR2)+(-43.0)*X3PR5*Y3/(20160.0*AL1**2*X2PR2)+(-23.0)*NU*X3PR4
9  *Y3/(2160.0*AL1*X2)+23.0*X3PR4*Y3/(2160.0*AL1*X2)+(-17.0)*X3PR4
:  *Y3/(13440.0*AL1**2*X2)+2579.0*NU*X3PR3*Y3/(483840.0*AL1)+(-257
;  9.0)*X3PR3*Y3/(483840.0*AL1)+(-5.0)*X3PR3*Y3/(12096.0*AL1**2)+(-
<  443.0)*NU*X2*X3PR2*Y3/(241920.0*AL1)+443.0*X2*X3PR2*Y3/(241920
=  .0*AL1)+(-47.0)*X2*X3PR2*Y3/(80640.0*AL1**2)+11.0*NU*X2PR2*X3*Y
>  3/(15120.0*AL1)+(-11.0)*X2PR2*X3*Y3/(15120.0*AL1)-NU*X2PR3*Y3/A
?  L1/10080.0+X2PR3*Y3/AL1/10080.0+(-11.0)*X2PR3*Y3/(48384.0*AL1**
@  2)+913.0*NU*X3PR7/(120960.0*AL1**2*X2PR2*Y3)+(-913.0)*X3PR7/(12
1  0960.0*AL1**2*X2PR2*Y3)+(-29.0)*NU*X3PR6/(13824.0*AL1**2*X2*Y3)
2  +29.0*X3PR6/(13824.0*AL1**2*X2*Y3)+(-83.0)*NU*X3PR5/(48384.0*AL
3  1**2*Y3)+83.0*X3PR5/(48384.0*AL1**2*Y3)+23.0*NU*X2*X3PR4/(26880
4  .0*AL1**2*Y3)+(-23.0)*X2*X3PR4/(26880.0*AL1**2*Y3)+(-17.0)*NU*X

```

```

5 2PR2*X3PR3/(241920.0*AL1**2*Y3)+17.0*X2PR2*X3PR3/(241920.0*AL1*
6 *2*Y3)+157.0*NU*X2PR3*X3PR2/(483840.0*AL1**2*Y3)+(-157.0)*X2PR3
7 *X3PR2/(483840.0*AL1**2*Y3)
K4(3,10) = (-3.0)*NU*X3PR2*Y3PR4/(4480.0*AL1*X2PR2)+(-83.0)*X3PR2*
1 Y3PR4/(120960.0*AL1*X2PR2)+5.0*NU*X3*Y3PR4/(8064.0*AL1*X2)+X3*Y
2 3PR4/(AL1*X2)/1512.0-NU*Y3PR4/AL1/30240.0-Y3PR4/AL1/12096.0-NU*
3 X3PR4*Y3PR2/(AL1**2*X2PR2)/2880.0+47.0*NU*X3PR4*Y3PR2/(24192.0*
4 X2PR2)-X3PR4*Y3PR2/(AL1**2*X2PR2)/3024.0+83.0*X3PR4*Y3PR2/(4032
5 0.0*X2PR2)-NU*X3PR3*Y3PR2/(AL1**2*X2)/13440.0-NU*X3PR3*Y3PR2/X2
6 /560.0-X3PR3*Y3PR2/(AL1**2*X2)/60480.0-X3PR3*Y3PR2/X2/504.0+23.
7 0*NU*X3PR2*Y3PR2/(161280.0*AL1**2)+53.0*NU*X3PR2*Y3PR2/120960.0
8 +X3PR2*Y3PR2/AL1**2/10752.0+89.0*X3PR2*Y3PR2/120960.0+(-37.0)*N
9 U*X2*X3*Y3PR2/(483840.0*AL1**2)-NU*X2*X3*Y3PR2/4032.0+(-5.0)*X2
: *X3*Y3PR2/(96768.0*AL1**2)+(-11.0)*X2*X3*Y3PR2/20160.0+NU*X2PR2
; *Y3PR2/AL1**2/30240.0-NU*X2PR2*Y3PR2/30240.0+X2PR2*Y3PR2/8640.0
< +61.0*NU*X3PR6/(60480.0*AL1*X2PR2)+X3PR6/(AL1*X2PR2)/1008.0+NU*
= X3PR5/(AL1*X2)/4032.0+X3PR5/(AL1*X2)/20160.0+(-143.0)*NU*X3PR4/
> (483840.0*AL1)+X3PR4/AL1/483840.0+13.0*NU*X2*X3PR3/(32256.0*AL1
? )+11.0*X2*X3PR3/(53760.0*AL1)+(-17.0)*NU*X2PR2*X3PR2/(161280.0*
@ AL1)-X2PR2*X3PR2/AL1/17920.0+11.0*NU*X2PR3*X3/(96768.0*AL1)+11.
1 0*X2PR3*X3/(96768.0*AL1)
K4(3,11) = (-43.0)*X3*Y3PR5/(30240.0*X2PR2)+13.0*Y3PR5/(20160.0*X2
1 )+1117.0*NU*X3PR3*Y3PR3/(483840.0*X2PR2)+43.0*X3PR3*Y3PR3/(1209
2 6.0*AL1*X2PR2)+(-1117.0)*X3PR3*Y3PR3/(483840.0*X2PR2)+(-83.0)*N
3 U*X3PR2*Y3PR3/(24192.0*X2)+(-167.0)*X3PR2*Y3PR3/(40320.0*AL1*X2
4 )+83.0*X3PR2*Y3PR3/(24192.0*X2)+23.0*NU*X3*Y3PR3/15120.0+(-23.0
5 )*X3*Y3PR3/(30240.0*AL1)+(-23.0)*X3*Y3PR3/15120.0-NU*X2*Y3PR3/6
6 912.0+43.0*X2*Y3PR3/(48384.0*AL1)+X2*Y3PR3/6912.0+(-1061.0)*NU*
7 X3PR5*Y3/(161280.0*AL1*X2PR2)+1061.0*X3PR5*Y3/(161280.0*AL1*X2P
8 R2)+43.0*X3PR5*Y3/(20160.0*AL1**2*X2PR2)+2501.0*NU*X3PR4*Y3/(16
9 1280.0*AL1*X2)+(-2501.0)*X3PR4*Y3/(161280.0*AL1*X2)+X3PR4*Y3/(A
: L1**2*X2)/2688.0+(-3949.0)*NU*X3PR3*Y3/(483840.0*AL1)+3949.0*X3
; PR3*Y3/(483840.0*AL1)+(-11.0)*X3PR3*Y3/(8640.0*AL1**2)+(-149.0)
< *NU*X2*X3PR2*Y3/(80640.0*AL1)+149.0*X2*X3PR2*Y3/(80640.0*AL1)+
= -19.0)*X2*X3PR2*Y3/(80640.0*AL1**2)+97.0*NU*X2PR2*X3*Y3/(48384.
> 0*AL1)+(-97.0)*X2PR2*X3*Y3/(48384.0*AL1)-X2PR2*X3*Y3/AL1**2/134
? 40.0-NU*X2PR3*Y3/AL1/5040.0+X2PR3*Y3/AL1/5040.0+(-41.0)*X2PR3*Y
@ 3/(120960.0*AL1**2)+(-913.0)*NU*X3PR7/(120960.0*AL1**2*X2PR2*Y3
1 )+913.0*X3PR7/(120960.0*AL1**2*X2PR2*Y3)+3229.0*NU*X3PR6/(48384
2 0.0*AL1**2*X2*Y3)+(-3229.0)*X3PR6/(483840.0*AL1**2*X2*Y3)+13.0*
3 NU*X3PR5/(3456.0*AL1**2*Y3)+(-13.0)*X3PR5/(3456.0*AL1**2*Y3)+(-
4 263.0)*NU*X2*X3PR4/(69120.0*AL1**2*Y3)+263.0*X2*X3PR4/(69120.0*
5 AL1**2*Y3)+(-13.0)*NU*X2PR2*X3PR3/(34560.0*AL1**2*Y3)+13.0*X2PR
6 2*X3PR3/(34560.0*AL1**2*Y3)+29.0*NU*X2PR3*X3PR2/(34560.0*AL1**2
7 *Y3)+(-29.0)*X2PR3*X3PR2/(34560.0*AL1**2*Y3)
K4(3,12) = 3.0*NU*X3PR2*Y3PR4/(4480.0*AL1*X2PR2)+83.0*X3PR2*Y3PR4/
1 (120960.0*AL1*X2PR2)+(-67.0)*NU*X3*Y3PR4/(120960.0*AL1*X2)-X3*Y
2 3PR4/(AL1*X2)/1512.0+NU*Y3PR4/AL1/120960.0+Y3PR4/AL1/12096.0+NU
3 *X3PR4*Y3PR2/(AL1**2*X2PR2)/2880.0+(-47.0)*NU*X3PR4*Y3PR2/(2419
4 2.0*X2PR2)+X3PR4*Y3PR2/(AL1**2*X2PR2)/3024.0+(-83.0)*X3PR4*Y3PR

```

```

5 2/(40320.0*X2PR2)+13.0*NU*X3PR3*Y3PR2/(120960.0*AL1**2*X2)+NU*X
6 3PR3*Y3PR2/X2/336.0+X3PR3*Y3PR2/(AL1**2*X2)/60480.0+13.0*X3PR3*
7 Y3PR2/(5040.0*X2)+(-19.0)*NU*X3PR2*Y3PR2/(161280.0*AL1**2)+(-13
8 .0)*NU*X3PR2*Y3PR2/15120.0-X3PR2*Y3PR2/AL1**2/10752.0+X3PR2*Y3P
9 R2/7560.0+37.0*NU*X2*X3*Y3PR2/(483840.0*AL1**2)-NU*X2*X3*Y3PR2/
: 60480.0+5.0*X2*X3*Y3PR2/(96768.0*AL1**2)+(-11.0)*X2*X3*Y3PR2/12
; 096.0-NU*X2PR2*Y3PR2/AL1**2/40320.0-NU*X2PR2*Y3PR2/6048.0+X2PR2
< *Y3PR2/7560.0+(-61.0)*NU*X3PR6/(60480.0*AL1*X2PR2)-X3PR6/(AL1*X
= 2PR2)/1008.0+NU*X3PR5/(AL1*X2)/2016.0+X3PR5/(AL1*X2)/10080.0+31
> 1.0*NU*X3PR4/(483840.0*AL1)+407.0*X3PR4/(483840.0*AL1)+(-157.0)
? *NU*X2*X3PR3/(483840.0*AL1)+(-61.0)*X2*X3PR3/(483840.0*AL1)+NU*
@ X2PR2*X3PR2/AL1/5040.0-X2PR2*X3PR2/AL1/10080.0+17.0*NU*X2PR3*X3
1 /(241920.0*AL1)+41.0*X2PR3*X3/(241920.0*AL1)

```

c

```

K4(4,4) = (-43.0)*NU*X3PR2*Y3PR5/(30240.0*AL1**2*X2PR3)+43.0*X3PR2
1 *Y3PR5/(30240.0*AL1**2*X2PR3)+13.0*NU*X3*Y3PR5/(10080.0*AL1**2*
2 X2PR2)+(-13.0)*X3*Y3PR5/(10080.0*AL1**2*X2PR2)-NU*Y3PR5/(AL1**2
3 *X2)/2240.0+Y3PR5/(AL1**2*X2)/2240.0+(-43.0)*NU*X3PR4*Y3PR3/(30
4 240.0*AL1*X2PR3)+43.0*X3PR4*Y3PR3/(30240.0*AL1*X2PR3)+3683.0*X3
5 PR4*Y3PR3/(483840.0*AL1**2*X2PR3)-NU*X3PR3*Y3PR3/(AL1*X2PR2)/50
6 40.0+X3PR3*Y3PR3/(AL1*X2PR2)/5040.0+(-1759.0)*X3PR3*Y3PR3/(1209
7 60.0*AL1**2*X2PR2)+NU*X3PR2*Y3PR3/(AL1*X2)/2688.0-X3PR2*Y3PR3/(
8 AL1*X2)/2688.0+361.0*X3PR2*Y3PR3/(40320.0*AL1**2*X2)+(-5.0)*NU*
9 X3*Y3PR3/(24192.0*AL1)+5.0*X3*Y3PR3/(24192.0*AL1)-X3*Y3PR3/AL1*
: *2/560.0+47.0*NU*X2*Y3PR3/(241920.0*AL1)+(-47.0)*X2*Y3PR3/(2419
; 20.0*AL1)+X2*Y3PR3/AL1**2/5040.0+(-43.0)*NU*X3PR6*Y3/(120960.0*
< X2PR3)+3019.0*X3PR6*Y3/(241920.0*AL1*X2PR3)+43.0*X3PR6*Y3/(1209
= 60.0*X2PR3)+(-17.0)*NU*X3PR5*Y3/(40320.0*X2PR2)+(-1321.0)*X3PR5
> *Y3/(120960.0*AL1*X2PR2)+17.0*X3PR5*Y3/(40320.0*X2PR2)-NU*X3PR4
? *Y3/X2/7680.0+(-649.0)*X3PR4*Y3/(241920.0*AL1*X2)+X3PR4*Y3/X2/7
@ 680.0+(-5.0)*NU*X3PR3*Y3/48384.0+503.0*X3PR3*Y3/(120960.0*AL1)+
1 5.0*X3PR3*Y3/48384.0+(-11.0)*NU*X2*X3PR2*Y3/161280.0+(-113.0)*X
2 2*X3PR2*Y3/(120960.0*AL1)+11.0*X2*X3PR2*Y3/161280.0+X2PR2*X3*Y3
3 /AL1/13440.0+(-11.0)*NU*X2PR3*Y3/193536.0+11.0*X2PR3*Y3/193536.
4 0+2699.0*X3PR8/(483840.0*X2PR3*Y3)+11.0*X3PR7/(12096.0*X2PR2*Y3
5 )+(-173.0)*X3PR6/(60480.0*X2*Y3)+11.0*X3PR5/(34560.0*Y3)+X2*X3P
6 R4*Y3/1440.0-X2PR2*X3PR3/Y3/40320.0+11.0*X2PR3*X3PR2/(96768.0*Y
7 3)
K4(4,5) = NU*Y3PR4/AL1/161280.0-Y3PR4/AL1/161280.0-NU*X3PR3*Y3PR2/
1 (AL1**2*X2)/896.0+(-5.0)*X3PR3*Y3PR2/(4032.0*AL1**2*X2)+11.0*NU
2 *X3PR2*Y3PR2/(16128.0*AL1**2)+NU*X3PR2*Y3PR2/161280.0+41.0*X3PR
3 2*Y3PR2/(40320.0*AL1**2)-X3PR2*Y3PR2/161280.0+43.0*NU*X2*X3*Y3P
4 R2/(120960.0*AL1**2)+X2*X3*Y3PR2/AL1**2/120960.0-NU*X2PR2*Y3PR2
5 /AL1**2/8064.0+NU*X2PR2*Y3PR2/241920.0+X2PR2*Y3PR2/AL1**2/40320
6 .0-X2PR2*Y3PR2/241920.0-NU*X3PR5/(AL1*X2)/2240.0+(-5.0)*X3PR5/(
7 8064.0*AL1*X2)+(-11.0)*NU*X3PR4/(40320.0*AL1)+(-13.0)*X3PR4/(80
8 640.0*AL1)+17.0*NU*X2*X3PR3/(120960.0*AL1)+23.0*X2*X3PR3/(12096
9 0.0*AL1)+NU*X2PR2*X3PR2/AL1/17920.0+(-13.0)*X2PR2*X3PR2/(161280
: .0*AL1)+(-37.0)*NU*X2PR3*X3/(483840.0*AL1)-X2PR3*X3/AL1/483840.
; 0+NU*X2PR4/AL1/161280.0-X2PR4/AL1/161280.0

```

```

K4(4,6) = (-13.0)*NU*X3PR2*Y3PR3/(10080.0*AL1*X2)+13.0*X3PR2*Y3PR3
1 /(10080.0*AL1*X2)+17.0*X3PR2*Y3PR3/(23040.0*AL1**2*X2)+NU*X3*Y3
2 PR3/AL1/2520.0-X3*Y3PR3/AL1/2520.0+(-19.0)*X3*Y3PR3/(26880.0*AL
3 1**2)+NU*X2*Y3PR3/AL1/13440.0-X2*Y3PR3/AL1/13440.0+19.0*X2*Y3PR
4 3/(241920.0*AL1**2)+(-13.0)*NU*X3PR4*Y3/(20160.0*X2)+547.0*X3PR
5 4*Y3/(53760.0*AL1*X2)+13.0*X3PR4*Y3/(20160.0*X2)+(-19.0)*NU*X3P
6 R3*Y3/40320.0+(-61.0)*X3PR3*Y3/(5376.0*AL1)+19.0*X3PR3*Y3/40320
7 .0-NU*X2*X3PR2*Y3/13440.0+839.0*X2*X3PR2*Y3/(483840.0*AL1)+X2*X
8 3PR2*Y3/13440.0-NU*X2PR2*X3*Y3/11520.0+169.0*X2PR2*X3*Y3/(12096
9 0.0*AL1)+X2PR2*X3*Y3/11520.0+(-19.0)*NU*X2PR3*Y3/483840.0-X2PR3
: *Y3/AL1/6720.0+19.0*X2PR3*Y3/483840.0+661.0*X3PR6/(80640.0*X2*Y
; 3)+(-101.0)*X3PR5/(80640.0*Y3)+(-173.0)*X2*X3PR4/(48384.0*Y3)+7
< 3.0*X2PR2*X3PR3/(80640.0*Y3)+163.0*X2PR3*X3PR2/(241920.0*Y3)+X2
= PR4*X3/80640.0
K4(4,7) = 83.0*NU*X3PR3*Y3PR4/(30240.0*AL1*X2PR3)+83.0*X3PR3*Y3PR4
1 /(30240.0*AL1*X2PR3)+(-199.0)*NU*X3PR2*Y3PR4/(48384.0*AL1*X2PR2
2 )+(-949.0)*X3PR2*Y3PR4/(241920.0*AL1*X2PR2)+83.0*NU*X3*Y3PR4/(4
3 8384.0*AL1*X2)+353.0*X3*Y3PR4/(241920.0*AL1*X2)+(-13.0)*NU*Y3PR
4 4/(60480.0*AL1)-Y3PR4/AL1/8640.0+43.0*NU*X3PR5*Y3PR2/(30240.0*A
5 L1**2*X2PR3)+11.0*NU*X3PR5*Y3PR2/(8640.0*X2PR3)+X3PR5*Y3PR2/(AL
6 1**2*X2PR3)/756.0+83.0*X3PR5*Y3PR2/(60480.0*X2PR3)+(-25.0)*NU*X
7 3PR4*Y3PR2/(16128.0*AL1**2*X2PR2)+(-169.0)*NU*X3PR4*Y3PR2/(2419
8 20.0*X2PR2)+(-409.0)*X3PR4*Y3PR2/(241920.0*AL1**2*X2PR2)+(-17.0
9 )*X3PR4*Y3PR2/(34560.0*X2PR2)+19.0*NU*X3PR3*Y3PR2/(60480.0*AL1*
: *2*X2)+(-113.0)*NU*X3PR3*Y3PR2/(241920.0*X2)+37.0*X3PR3*Y3PR2/(
; 60480.0*AL1**2*X2)+(-19.0)*X3PR3*Y3PR2/(26880.0*X2)+(-17.0)*NU*
< X3PR2*Y3PR2/(30240.0*AL1**2)+11.0*NU*X3PR2*Y3PR2/60480.0+(-37.0
= )*X3PR2*Y3PR2/(60480.0*AL1**2)+43.0*X3PR2*Y3PR2/120960.0+167.0*
> NU*X2*X3*Y3PR2/(241920.0*AL1**2)+(-17.0)*NU*X2*X3*Y3PR2/120960.
? 0+23.0*X2*X3*Y3PR2/(48384.0*AL1**2)+(-17.0)*X2*X3*Y3PR2/60480.0
@ -NU*X2PR2*Y3PR2/AL1**2/6048.0-NU*X2PR2*Y3PR2/30240.0-X2PR2*Y3PR
1 2/AL1**2/24192.0+X2PR2*Y3PR2/30240.0+NU*X3PR7/(AL1*X2PR3)/1512.
2 0+X3PR7/(AL1*X2PR3)/1512.0+NU*X3PR6/(AL1*X2PR2)/26880.0+(-29.0)
3 *X3PR6/(241920.0*AL1*X2PR2)+(-11.0)*NU*X3PR5/(80640.0*AL1*X2)+(-
4 -19.0)*X3PR5/(80640.0*AL1*X2)+(-23.0)*NU*X3PR4/(69120.0*AL1)-X3
5 PR4/AL1/96768.0+NU*X2*X3PR3/AL1/80640.0+(-7.0)*X2*X3PR3/(34560.
6 0*AL1)+NU*X2PR2*X3PR2/AL1/32256.0+X2PR2*X3PR2/AL1/17920.0-NU*X2
7 PR3*X3/AL1/7560.0-X2PR3*X3/AL1/7560.0
K4(4,8) = 43.0*NU*X3PR2*Y3PR5/(15120.0*AL1**2*X2PR3)+(-43.0)*X3PR2
1 *Y3PR5/(15120.0*AL1**2*X2PR3)+(-41.0)*NU*X3*Y3PR5/(15120.0*AL1*
2 *2*X2PR2)+41.0*X3*Y3PR5/(15120.0*AL1**2*X2PR2)+19.0*NU*Y3PR5/(2
3 0160.0*AL1**2*X2)+(-19.0)*Y3PR5/(20160.0*AL1**2*X2)+43.0*NU*X3P
4 R4*Y3PR3/(15120.0*AL1*X2PR3)+(-43.0)*X3PR4*Y3PR3/(15120.0*AL1*X
5 2PR3)+(-3683.0)*X3PR4*Y3PR3/(241920.0*AL1**2*X2PR3)+(-29.0)*NU*
6 X3PR3*Y3PR3/(30240.0*AL1*X2PR2)+29.0*X3PR3*Y3PR3/(30240.0*AL1*X
7 2PR2)+7201.0*X3PR3*Y3PR3/(241920.0*AL1**2*X2PR2)-NU*X3PR2*Y3PR3
8 /(AL1*X2)/5040.0+X3PR2*Y3PR3/(AL1*X2)/5040.0+(-2407.0)*X3PR2*Y3
9 PR3/(120960.0*AL1**2*X2)+(-17.0)*NU*X3*Y3PR3/(60480.0*AL1)+17.0
: *X3*Y3PR3/(60480.0*AL1)+611.0*X3*Y3PR3/(120960.0*AL1**2)+23.0*N
; U*X2*Y3PR3/(120960.0*AL1)+(-23.0)*X2*Y3PR3/(120960.0*AL1)-X2*Y3

```

```

< PR3/AL1**2/2016.0+43.0*NU*X3PR6*Y3/(60480.0*X2PR3)+(-3019.0)*X3
= PR6*Y3/(120960.0*AL1*X2PR3)+(-43.0)*X3PR6*Y3/(60480.0*X2PR3)+NU
> *X3PR5*Y3/X2PR2/5040.0+8279.0*X3PR5*Y3/(241920.0*AL1*X2PR2)-X3P
? R5*Y3/X2PR2/5040.0-NU*X3PR4*Y3/X2/8960.0+(-17.0)*X3PR4*Y3/(1680
@ .0*AL1*X2)+X3PR4*Y3/X2/8960.0+(-17.0)*NU*X3PR3*Y3/120960.0+(-62
1 9.0)*X3PR3*Y3/(241920.0*AL1)+17.0*X3PR3*Y3/120960.0-NU*X2*X3PR2
2 *Y3/5760.0+(-31.0)*X2*X3PR2*Y3/(48384.0*AL1)+X2*X3PR2*Y3/5760.0
3 +23.0*X2PR2*X3*Y3/(17280.0*AL1)-NU*X2PR3*Y3/7560.0-X2PR3*Y3/AL1
4 /5040.0+X2PR3*Y3/7560.0+(-2699.0)*X3PR8/(241920.0*X2PR3*Y3)+353
5 .0*X3PR7/(40320.0*X2PR2*Y3)+517.0*X3PR6/(120960.0*X2*Y3)+(-151.
6 0)*X3PR5/(60480.0*Y3)+(-73.0)*X2*X3PR4/(80640.0*Y3)-X2PR2*X3PR3
7 /Y3/15120.0+83.0*X2PR3*X3PR2/(120960.0*Y3)
K4(4,9) = -NU*X3PR2*Y3PR4/(AL1*X2PR2)/1440.0+(-41.0)*X3PR2*Y3PR4/(
1 60480.0*AL1*X2PR2)+11.0*NU*X3*Y3PR4/(16128.0*AL1*X2)+31.0*X3*Y3
2 PR4/(48384.0*AL1*X2)+(-13.0)*NU*Y3PR4/(120960.0*AL1)-Y3PR4/AL1/
3 17280.0+2.0*NU*X3PR4*Y3PR2/(945.0*AL1**2*X2PR2)+(-13.0)*NU*X3PR
4 4*Y3PR2/(40320.0*X2PR2)+121.0*X3PR4*Y3PR2/(60480.0*AL1**2*X2PR2
5 )+(-41.0)*X3PR4*Y3PR2/(120960.0*X2PR2)-NU*X3PR3*Y3PR2/(AL1**2*X
6 2)/480.0+NU*X3PR3*Y3PR2/X2/80640.0+(-19.0)*X3PR3*Y3PR2/(10080.0
7 *AL1**2*X2)+(-11.0)*X3PR3*Y3PR2/(241920.0*X2)+107.0*NU*X3PR2*Y3
8 PR2/(120960.0*AL1**2)+11.0*NU*X3PR2*Y3PR2/161280.0+71.0*X3PR2*Y
9 3PR2/(120960.0*AL1**2)+19.0*X3PR2*Y3PR2/161280.0-NU*X2*X3*Y3PR2
: /AL1**2/1440.0+(-19.0)*NU*X2*X3*Y3PR2/483840.0-X2*X3*Y3PR2/AL1*
: *2/2520.0+(-31.0)*X2*X3*Y3PR2/483840.0+23.0*NU*X2PR2*Y3PR2/(120
< 960.0*AL1**2)-NU*X2PR2*Y3PR2/60480.0+X2PR2*Y3PR2/AL1**2/24192.0
= +X2PR2*Y3PR2/60480.0+17.0*NU*X3PR6/(17280.0*AL1*X2PR2)+121.0*X3
> PR6/(120960.0*AL1*X2PR2)-NU*X3PR5/(AL1*X2)/20160.0+X3PR5/(AL1*X
? 2)/6720.0+73.0*NU*X3PR4/(483840.0*AL1)+(-71.0)*X3PR4/(483840.0*
@ AL1)+17.0*NU*X2*X3PR3/(161280.0*AL1)+7.0*X2*X3PR3/(23040.0*AL1)
1 -NU*X2PR2*X3PR2/AL1/32256.0+(-13.0)*X2PR2*X3PR2/(161280.0*AL1)+
2 11.0*NU*X2PR3*X3/(96768.0*AL1)+11.0*X2PR3*X3/(96768.0*AL1)
K4(4,10) = (-43.0)*NU*X3*Y3PR5/(60480.0*AL1**2*X2PR2)+43.0*X3*Y3PR
1 5/(60480.0*AL1**2*X2PR2)+13.0*NU*Y3PR5/(40320.0*AL1**2*X2)+(-13
2 .0)*Y3PR5/(40320.0*AL1**2*X2)+43.0*NU*X3PR3*Y3PR3/(24192.0*AL1*
3 X2PR2)+(-43.0)*X3PR3*Y3PR3/(24192.0*AL1*X2PR2)+1117.0*X3PR3*Y3P
4 R3/(241920.0*AL1**2*X2PR2)+(-19.0)*NU*X3PR2*Y3PR3/(16128.0*AL1*
5 X2)+19.0*X3PR2*Y3PR3/(16128.0*AL1*X2)+(-227.0)*X3PR2*Y3PR3/(345
6 60.0*AL1**2*X2)+5.0*NU*X3*Y3PR3/(12096.0*AL1)+(-5.0)*X3*Y3PR3/(
7 12096.0*AL1)+337.0*X3*Y3PR3/(120960.0*AL1**2)+(-181.0)*NU*X2*Y3
8 PR3/(483840.0*AL1)+181.0*X2*Y3PR3/(483840.0*AL1)-X2*Y3PR3/AL1**
9 2/3360.0+43.0*NU*X3PR5*Y3/(40320.0*X2PR2)+(-1061.0)*X3PR5*Y3/(8
: 0640.0*AL1*X2PR2)+(-43.0)*X3PR5*Y3/(40320.0*X2PR2)+17.0*NU*X3PR
; 4*Y3/(26880.0*X2)+23.0*X3PR4*Y3/(1080.0*AL1*X2)+(-17.0)*X3PR4*Y
< 3/(26880.0*X2)+5.0*NU*X3PR3*Y3/24192.0+(-2579.0)*X3PR3*Y3/(2419
= 20.0*AL1)+(-5.0)*X3PR3*Y3/24192.0+47.0*NU*X2*X3PR2*Y3/161280.0+
> 443.0*X2*X3PR2*Y3/(120960.0*AL1)+(-47.0)*X2*X3PR2*Y3/161280.0+
? (-11.0)*X2PR2*X3*Y3/(7560.0*AL1)+11.0*NU*X2PR3*Y3/96768.0+X2PR3*
@ Y3/AL1/5040.0+(-11.0)*X2PR3*Y3/96768.0+(-913.0)*X3PR7/(60480.0*
1 X2PR2*Y3)+29.0*X3PR6/(6912.0*X2*Y3)+83.0*X3PR5/(24192.0*Y3)+(-2
2 3.0)*X2*X3PR4/(13440.0*Y3)+17.0*X2PR2*X3PR3/(120960.0*Y3)+(-157

```

```

3      .0)*X2PR3*X3PR2/(241920.0*Y3)
K4(4,11) = NU*X3PR2*Y3PR4/(AL1*X2PR2)/1440.0+41.0*X3PR2*Y3PR4/(604
1      80.0*AL1*X2PR2)+(-173.0)*NU*X3*Y3PR4/(241920.0*AL1*X2)+(-7.0)*X
2      3*Y3PR4/(11520.0*AL1*X2)+29.0*NU*Y3PR4/(241920.0*AL1)+11.0*Y3PR
3      4/(241920.0*AL1)+(-2.0)*NU*X3PR4*Y3PR2/(945.0*AL1**2*X2PR2)+13.
4      0*NU*X3PR4*Y3PR2/(40320.0*X2PR2)+(-121.0)*X3PR4*Y3PR2/(60480.0*
5      AL1**2*X2PR2)+41.0*X3PR4*Y3PR2/(120960.0*X2PR2)+NU*X3PR3*Y3PR2/
6      (AL1**2*X2)/420.0-NU*X3PR3*Y3PR2/X2/34560.0+X3PR3*Y3PR2/(AL1**2
7      *X2)/360.0+X3PR3*Y3PR2/X2/16128.0+19.0*NU*X3PR2*Y3PR2/(30240.0*
8      AL1**2)+(-13.0)*NU*X3PR2*Y3PR2/161280.0+(-11.0)*X3PR2*Y3PR2/(30
9      240.0*AL1**2)+(-17.0)*X3PR2*Y3PR2/161280.0+(-41.0)*NU*X2*X3*Y3P
:      R2/(30240.0*AL1**2)+19.0*NU*X2*X3*Y3PR2/483840.0-X2*X3*Y3PR2/AL
;      1**2/2160.0+31.0*X2*X3*Y3PR2/483840.0+17.0*NU*X2PR2*Y3PR2/(6048
<      0.0*AL1**2)+NU*X2PR2*Y3PR2/80640.0-X2PR2*Y3PR2/AL1**2/60480.0-X
=      2PR2*Y3PR2/80640.0+(-17.0)*NU*X3PR6/(17280.0*AL1*X2PR2)+(-121.0
>      )*X3PR6/(120960.0*AL1*X2PR2)-NU*X3PR5/(AL1*X2)/10080.0+X3PR5/(A
?      L1*X2)/3360.0+13.0*NU*X3PR4/(13824.0*AL1)+359.0*X3PR4/(483840.0
@      *AL1)+(-13.0)*NU*X2*X3PR3/(483840.0*AL1)+(-109.0)*X2*X3PR3/(483
1      840.0*AL1)-NU*X2PR2*X3PR2/AL1/4032.0+X2PR2*X3PR2/AL1/20160.0+53
2      .0*NU*X2PR3*X3/(241920.0*AL1)+29.0*X2PR3*X3/(241920.0*AL1)
K4(4,12) = 43.0*NU*X3*Y3PR5/(60480.0*AL1**2*X2PR2)+(-43.0)*X3*Y3PR
1      5/(60480.0*AL1**2*X2PR2)+(-13.0)*NU*Y3PR5/(40320.0*AL1**2*X2)+1
2      3.0*Y3PR5/(40320.0*AL1**2*X2)+(-43.0)*NU*X3PR3*Y3PR3/(24192.0*A
3      L1*X2PR2)+43.0*X3PR3*Y3PR3/(24192.0*AL1*X2PR2)+(-1117.0)*X3PR3*
4      Y3PR3/(241920.0*AL1**2*X2PR2)+167.0*NU*X3PR2*Y3PR3/(80640.0*AL1
5      *X2)+(-167.0)*X3PR2*Y3PR3/(80640.0*AL1*X2)+83.0*X3PR2*Y3PR3/(12
6      096.0*AL1**2*X2)+23.0*NU*X3*Y3PR3/(60480.0*AL1)+(-23.0)*X3*Y3PR
7      3/(60480.0*AL1)+(-23.0)*X3*Y3PR3/(7560.0*AL1**2)+(-43.0)*NU*X2*
8      Y3PR3/(96768.0*AL1)+43.0*X2*Y3PR3/(96768.0*AL1)+X2*Y3PR3/AL1**2
9      /3456.0+(-43.0)*NU*X3PR5*Y3/(40320.0*X2PR2)+1061.0*X3PR5*Y3/(80
:      640.0*AL1*X2PR2)+43.0*X3PR5*Y3/(40320.0*X2PR2)-NU*X3PR4*Y3/X2/5
;      376.0+(-2501.0)*X3PR4*Y3/(80640.0*AL1*X2)+X3PR4*Y3/X2/5376.0+11
<      .0*NU*X3PR3*Y3/17280.0+3949.0*X3PR3*Y3/(241920.0*AL1)+(-11.0)*X
=      3PR3*Y3/17280.0+19.0*NU*X2*X3PR2*Y3/161280.0+149.0*X2*X3PR2*Y3/
>      (40320.0*AL1)+(-19.0)*X2*X3PR2*Y3/161280.0+NU*X2PR2*X3*Y3/26880
?      .0+(-97.0)*X2PR2*X3*Y3/(24192.0*AL1)-X2PR2*X3*Y3/26880.0+41.0*N
@      U*X2PR3*Y3/241920.0+X2PR3*Y3/AL1/2520.0+(-41.0)*X2PR3*Y3/241920
1      .0+913.0*X3PR7/(60480.0*X2PR2*Y3)+(-3229.0)*X3PR6/(241920.0*X2*
2      Y3)+(-13.0)*X3PR5/(1728.0*Y3)+263.0*X2*X3PR4/(34560.0*Y3)+13.0*
3      X2PR2*X3PR3/(17280.0*Y3)+(-29.0)*X2PR3*X3PR2/(17280.0*Y3)

```

C

```

K4(5,5) = (-11.0)*NU*X2*Y3PR3/193536.0+11.0*X2*Y3PR3/193536.0+(-17
1      .0)*NU*X2*X3PR2*Y3/(16128.0*AL1)+17.0*X2*X3PR2*Y3/(16128.0*AL1)
2      +X2*X3PR2*Y3/AL1**2/420.0+19.0*NU*X2PR2*X3*Y3/(80640.0*AL1)+(-1
3      9.0)*X2PR2*X3*Y3/(80640.0*AL1)+X2PR2*X3*Y3/AL1**2/1680.0+47.0*N
4      U*X2PR3*Y3/(241920.0*AL1)+(-47.0)*X2PR3*Y3/(241920.0*AL1)+X2PR3
5      *Y3/AL1**2/5040.0+(-41.0)*NU*X2*X3PR4/(6720.0*AL1**2*Y3)+41.0*X
6      2*X3PR4/(6720.0*AL1**2*Y3)+NU*X2PR2*X3PR3/(AL1**2*Y3)/336.0-X2P
7      R2*X3PR3/(AL1**2*Y3)/336.0+NU*X2PR3*X3PR2/(AL1**2*Y3)/720.0-X2P
8      R3*X3PR2/(AL1**2*Y3)/720.0-NU*X2PR4*X3/(AL1**2*Y3)/2240.0+X2PR4

```



```

9  *X3/(AL1**2*Y3)/2240.0-NU*X2PR5/(AL1**2*Y3)/2240.0+X2PR5/(AL1**
:  2*Y3)/2240.0
K4(5,6) = NU*X2*X3*Y3PR2/AL1**2/40320.0-NU*X2*X3*Y3PR2/80640.0+X2*
1  X3*Y3PR2/80640.0-NU*X2PR2*Y3PR2/AL1**2/26880.0+NU*X2PR2*Y3PR2/5
2  3760.0-X2PR2*Y3PR2/53760.0-NU*X2*X3PR3/AL1/960.0-X2*X3PR3/AL1/9
3  60.0+NU*X2PR2*X3PR2/AL1/6720.0+X2PR2*X3PR2/AL1/6720.0+NU*X2PR3*
4  X3/AL1/6720.0+X2PR3*X3/AL1/6720.0+NU*X2PR4/AL1/13440.0+X2PR4/AL
5  1/13440.0
K4(5,7) = 17.0*NU*X3PR2*Y3PR3/(23040.0*X2)+(-13.0)*X3PR2*Y3PR3/(25
1  20.0*AL1*X2)+(-17.0)*X3PR2*Y3PR3/(23040.0*X2)+(-17.0)*NU*X3*Y3P
2  R3/23040.0+X3*Y3PR3/AL1/560.0+17.0*X3*Y3PR3/23040.0+41.0*NU*X2*
3  Y3PR3/241920.0+X2*Y3PR3/AL1/2520.0+(-41.0)*X2*Y3PR3/241920.0+54
4  7.0*NU*X3PR4*Y3/(53760.0*AL1*X2)+(-547.0)*X3PR4*Y3/(53760.0*AL1
5  *X2)+(-13.0)*X3PR4*Y3/(5040.0*AL1**2*X2)+(-67.0)*NU*X3PR3*Y3/(5
6  376.0*AL1)+67.0*X3PR3*Y3/(5376.0*AL1)+X3PR3*Y3/AL1**2/2016.0+19
7  7.0*NU*X2*X3PR2*Y3/(69120.0*AL1)+(-197.0)*X2*X3PR2*Y3/(69120.0*
8  AL1)+NU*X2PR2*X3*Y3/AL1/756.0-X2PR2*X3*Y3/AL1/756.0+17.0*X2PR2*
9  X3*Y3/(20160.0*AL1**2)+(-43.0)*NU*X2PR3*Y3/(96768.0*AL1)+43.0*X
:  2PR3*Y3/(96768.0*AL1)+X2PR3*Y3/AL1**2/3456.0+661.0*NU*X3PR6/(80
:  640.0*AL1**2*X2*Y3)+(-661.0)*X3PR6/(80640.0*AL1**2*X2*Y3)+(-81.
<  0)*NU*X3PR5/(8960.0*AL1**2*Y3)+81.0*X3PR5/(8960.0*AL1**2*Y3)+11
=  .0*NU*X2*X3PR4/(241920.0*AL1**2*Y3)+(-11.0)*X2*X3PR4/(241920.0*
>  AL1**2*Y3)+179.0*NU*X2PR2*X3PR3/(241920.0*AL1**2*Y3)+(-179.0)*X
?  2PR2*X3PR3/(241920.0*AL1**2*Y3)+47.0*NU*X2PR3*X3PR2/(48384.0*AL
@  1**2*Y3)+(-47.0)*X2PR3*X3PR2/(48384.0*AL1**2*Y3)+(-17.0)*NU*X2P
1  R4*X3/(241920.0*AL1**2*Y3)+17.0*X2PR4*X3/(241920.0*AL1**2*Y3)+(-
2  -13.0)*NU*X2PR5/(40320.0*AL1**2*Y3)+13.0*X2PR5/(40320.0*AL1**2*
3  Y3)
K4(5,8) = NU*X3PR3*Y3PR2/(AL1**2*X2)/448.0+5.0*X3PR3*Y3PR2/(2016.0
1  *AL1**2*X2)+(-53.0)*NU*X3PR2*Y3PR2/(40320.0*AL1**2)-NU*X3PR2*Y3
2  PR2/40320.0-X3PR2*Y3PR2/AL1**2/448.0+X3PR2*Y3PR2/40320.0+(-101.
3  0)*NU*X2*X3*Y3PR2/(120960.0*AL1**2)+X2*X3*Y3PR2/AL1**2/30240.0+
4  17.0*NU*X2PR2*Y3PR2/(60480.0*AL1**2)+NU*X2PR2*Y3PR2/80640.0-X2P
5  R2*Y3PR2/AL1**2/60480.0-X2PR2*Y3PR2/80640.0+NU*X3PR5/(AL1*X2)/1
6  120.0+5.0*X3PR5/(4032.0*AL1*X2)-NU*X3PR4/AL1/2520.0+(-29.0)*X3P
7  R4/(40320.0*AL1)-NU*X2*X3PR3/AL1/4320.0+X2*X3PR3/AL1/15120.0+(-
8  17.0)*NU*X2PR2*X3PR2/(80640.0*AL1)+(-43.0)*X2PR2*X3PR2/(80640.0
9  *AL1)+(-53.0)*NU*X2PR3*X3/(241920.0*AL1)+X2PR3*X3/AL1/34560.0+2
:  9.0*NU*X2PR4/(241920.0*AL1)+11.0*X2PR4/(241920.0*AL1)
K4(5,9) = (-17.0)*NU*X3*Y3PR3/69120.0+13.0*X3*Y3PR3/(10080.0*AL1)+
1  17.0*X3*Y3PR3/69120.0+11.0*NU*X2*Y3PR3/96768.0+X2*Y3PR3/AL1/504
2  0.0+(-11.0)*X2*Y3PR3/96768.0+(-473.0)*NU*X3PR3*Y3/(241920.0*AL1
3  )+473.0*X3PR3*Y3/(241920.0*AL1)+(-13.0)*X3PR3*Y3/(3360.0*AL1**2
4  )+31.0*NU*X2*X3PR2*Y3/(17920.0*AL1)+(-31.0)*X2*X3PR2*Y3/(17920.
5  0*AL1)-X2*X3PR2*Y3/AL1**2/1680.0+11.0*NU*X2PR2*X3*Y3/(241920.0*
6  AL1)+(-11.0)*X2PR2*X3*Y3/(241920.0*AL1)-X2PR2*X3*Y3/AL1**2/1440
7  .0+(-181.0)*NU*X2PR3*Y3/(483840.0*AL1)+181.0*X2PR3*Y3/(483840.0
8  *AL1)-X2PR3*Y3/AL1**2/3360.0+449.0*NU*X3PR5/(40320.0*AL1**2*Y3)
9  +(-449.0)*X3PR5/(40320.0*AL1**2*Y3)+(-269.0)*NU*X2*X3PR4/(40320
:  .0*AL1**2*Y3)+269.0*X2*X3PR4/(40320.0*AL1**2*Y3)-NU*X2PR2*X3PR3

```

```

; /(AL1**2*Y3)/12096.0+X2PR2*X3PR3/(AL1**2*Y3)/12096.0+NU*X2PR3*X
< 3PR2/(AL1**2*Y3)/2880.0-X2PR3*X3PR2/(AL1**2*Y3)/2880.0+NU*X2PR4
= *X3/(AL1**2*Y3)/17280.0-X2PR4*X3/(AL1**2*Y3)/17280.0+13.0*NU*X2
> PR5/(40320.0*AL1**2*Y3)+(-13.0)*X2PR5/(40320.0*AL1**2*Y3)
K4(5,10) = -NU*X3PR2*Y3PR2/AL1**2/1920.0+(-5.0)*X3PR2*Y3PR2/(8064.
1 0*AL1**2)+NU*X2*X3*Y3PR2/AL1**2/40320.0+X2*X3*Y3PR2/AL1**2/4032
2 .0+23.0*NU*X2PR2*Y3PR2/(120960.0*AL1**2)-NU*X2PR2*Y3PR2/60480.0
3 +X2PR2*Y3PR2/AL1**2/24192.0+X2PR2*Y3PR2/60480.0+19.0*NU*X3PR4/(
4 13440.0*AL1)+5.0*X3PR4/(2688.0*AL1)+NU*X2*X3PR3/AL1/20160.0-X2*
5 X3PR3/AL1/1344.0-NU*X2PR2*X3PR2/AL1/2880.0+X2PR2*X3PR2/AL1/2880
6 .0+NU*X2PR3*X3/AL1/4032.0-X2PR3*X3/AL1/20160.0+(-13.0)*NU*X2PR4
7 /(120960.0*AL1)-X2PR4/AL1/17280.0
K4(5,11) = 17.0*NU*X3*Y3PR3/69120.0+(-13.0)*X3*Y3PR3/(10080.0*AL1)
1 +(-17.0)*X3*Y3PR3/69120.0-NU*X2*Y3PR3/7560.0-X2*Y3PR3/AL1/5040.
2 0+X2*Y3PR3/7560.0+473.0*NU*X3PR3*Y3/(241920.0*AL1)+(-473.0)*X3P
3 R3*Y3/(241920.0*AL1)+13.0*X3PR3*Y3/(3360.0*AL1**2)+(-211.0)*NU*
4 X2*X3PR2*Y3/(161280.0*AL1)+211.0*X2*X3PR2*Y3/(161280.0*AL1)-X2*
5 X3PR2*Y3/AL1**2/840.0+31.0*NU*X2PR2*X3*Y3/(241920.0*AL1)+(-31.0
6 )*X2PR2*X3*Y3/(241920.0*AL1)-X2PR2*X3*Y3/AL1**2/720.0+23.0*NU*X
7 2PR3*Y3/(120960.0*AL1)+(-23.0)*X2PR3*Y3/(120960.0*AL1)-X2PR3*Y3
8 /AL1**2/2016.0+(-449.0)*NU*X3PR5/(40320.0*AL1**2*Y3)+449.0*X3PR
9 5/(40320.0*AL1**2*Y3)+271.0*NU*X2*X3PR4/(20160.0*AL1**2*Y3)+(-2
: 71.0)*X2*X3PR4/(20160.0*AL1**2*Y3)+5.0*NU*X2PR2*X3PR3/(6048.0*A
; L1**2*Y3)+(-5.0)*X2PR2*X3PR3/(6048.0*AL1**2*Y3)+(-43.0)*NU*X2PR
< 3*X3PR2/(10080.0*AL1**2*Y3)+43.0*X2PR3*X3PR2/(10080.0*AL1**2*Y3
= )-NU*X2PR4*X3/(AL1**2*Y3)/3024.0+X2PR4*X3/(AL1**2*Y3)/3024.0+19
> .0*NU*X2PR5/(20160.0*AL1**2*Y3)+(-19.0)*X2PR5/(20160.0*AL1**2*Y
? 3)
K4(5,12) = NU*X3PR2*Y3PR2/AL1**2/1920.0+5.0*X3PR2*Y3PR2/(8064.0*AL
1 1**2)+NU*X2*X3*Y3PR2/AL1**2/40320.0+NU*X2*X3*Y3PR2/20160.0-X2*X
2 3*Y3PR2/AL1**2/4032.0-X2*X3*Y3PR2/20160.0-NU*X2PR2*Y3PR2/AL1**2
3 /6048.0-NU*X2PR2*Y3PR2/30240.0-X2PR2*Y3PR2/AL1**2/24192.0+X2PR2
4 *Y3PR2/30240.0+(-19.0)*NU*X3PR4/(13440.0*AL1)+(-5.0)*X3PR4/(268
5 8.0*AL1)+NU*X2*X3PR3/AL1/1008.0+X2*X3PR3/AL1/840.0+23.0*NU*X2PR
6 2*X3PR2/(40320.0*AL1)+31.0*X2PR2*X3PR2/(40320.0*AL1)+NU*X2PR3*X
7 3/AL1/5720.0-X2PR3*X3/AL1/6720.0+(-13.0)*NU*X2PR4/(60480.0*AL1)
8 -X2PR4/AL1/8640.0

```

C

```

K4(6,6) = 11.0*X2*Y3PR3/(96768.0*AL1**2)-NU*X2*X3PR2*Y3/840.0+17.0
1 *X2*X3PR2*Y3/(8064.0*AL1)+X2*X3PR2*Y3/840.0-NU*X2PR2*X3*Y3/3360
2 .0+(-19.0)*X2PR2*X3*Y3/(40320.0*AL1)+X2PR2*X3*Y3/3360.0-NU*X2PR
3 3*Y3/10080.0+(-47.0)*X2PR3*Y3/(120960.0*AL1)+X2PR3*Y3/10080.0+4
4 1.0*X2*X3PR4/(3360.0*Y3)-X2PR2*X3PR3/Y3/168.0-X2PR3*X3PR2/Y3/36
5 0.0+X2PR4*X3/Y3/1120.0+X2PR5/Y3/1120.0
K4(6,7) = NU*X3PR3*Y3PR2/X2/384.0+19.0*X3PR3*Y3PR2/(8064.0*X2)+NU*
1 X3PR2*Y3PR2/AL1**2/20160.0+(-31.0)*NU*X3PR2*Y3PR2/11520.0+(-143
2 .0)*X3PR2*Y3PR2/80640.0+113.0*NU*X2*X3*Y3PR2/241920.0+(-97.0)*X
3 2*X3*Y3PR2/241920.0-NU*X2PR2*Y3PR2/AL1**2/40320.0-NU*X2PR2*Y3PR
4 2/6048.0+X2PR2*Y3PR2/7560.0+19.0*NU*X3PR5/(13440.0*AL1*X2)+43.0
5 *X3PR5/(40320.0*AL1*X2)+(-71.0)*NU*X3PR4/(80640.0*AL1)-X3PR4/AL

```

```

6  1/1792.0+13.0*NU*X2*X3PR3/(60480.0*AL1)-X2*X3PR3/AL1/12096.0-NU
7  *X2PR2*X3PR2/AL1/1440.0-X2PR2*X3PR2/AL1/2688.0+37.0*NU*X2PR3*X3
8  /(241920.0*AL1)+(-23.0)*X2PR3*X3/(241920.0*AL1)+NU*X2PR4/AL1/12
9  0960.0+X2PR4/AL1/12096.0
   K4(6,8) = 13.0*NU*X3PR2*Y3PR3/(5040.0*AL1*X2)+(-13.0)*X3PR2*Y3PR3/
1  (5040.0*AL1*X2)+(-17.0)*X3PR2*Y3PR3/(11520.0*AL1**2*X2)-NU*X3*Y
2  3PR3/AL1/1120.0+X3*Y3PR3/AL1/1120.0+17.0*X3*Y3PR3/(11520.0*AL1*
3  *2)-NU*X2*Y3PR3/AL1/5040.0+X2*Y3PR3/AL1/5040.0+(-41.0)*X2*Y3PR3
4  /(120960.0*AL1**2)+13.0*NU*X3PR4*Y3/(10080.0*X2)+(-547.0)*X3PR4
5  *Y3/(26880.0*AL1*X2)+(-13.0)*X3PR4*Y3/(10080.0*X2)-NU*X3PR3*Y3/
6  4032.0+67.0*X3PR3*Y3/(2688.0*AL1)+X3PR3*Y3/4032.0+(-197.0)*X2*X
7  3PR2*Y3/(34560.0*AL1)+(-17.0)*NU*X2PR2*X3*Y3/40320.0-X2PR2*X3*Y
8  3/AL1/378.0+17.0*X2PR2*X3*Y3/40320.0-NU*X2PR3*Y3/6912.0+43.0*X2
9  PR3*Y3/(48384.0*AL1)+X2PR3*Y3/6912.0+(-661.0)*X3PR6/(40320.0*X2
:  *Y3)+81.0*X3PR5/(4480.0*Y3)+(-11.0)*X2*X3PR4/(120960.0*Y3)+(-17
;  9.0)*X2PR2*X3PR3/(120960.0*Y3)+(-47.0)*X2PR3*X3PR2/(24192.0*Y3)
<  +17.0*X2PR4*X3/(120960.0*Y3)+13.0*X2PR5/(20160.0*Y3)
   K4(6,9) = (-3.0)*NU*X3PR2*Y3PR2/4480.0+(-23.0)*X3PR2*Y3PR2/40320.0
1  +29.0*NU*X2*X3*Y3PR2/80640.0+11.0*X2*X3*Y3PR2/80640.0+NU*X2PR2*
2  Y3PR2/AL1**2/30240.0-NU*X2PR2*Y3PR2/30240.0+X2PR2*Y3PR2/8640.0+
3  NU*X3PR4/AL1/480.0+11.0*X3PR4/(6720.0*AL1)+(-23.0)*NU*X2*X3PR3/
4  (20160.0*AL1)-X2*X3PR3/AL1/2880.0+NU*X2PR2*X3PR2/AL1/1440.0-NU*
5  X2PR3*X3/AL1/5040.0+X2PR3*X3/AL1/10080.0-NU*X2PR4/AL1/30240.0-X
6  2PR4/AL1/12096.0
   K4(6,10) = (-13.0)*NU*X3*Y3PR3/(20160.0*AL1)+13.0*X3*Y3PR3/(20160.
1  0*AL1)+17.0*X3*Y3PR3/(34560.0*AL1**2)-NU*X2*Y3PR3/AL1/10080.0+X
2  2*Y3PR3/AL1/10080.0+(-11.0)*X2*Y3PR3/(48384.0*AL1**2)+13.0*NU*X
3  3PR3*Y3/6720.0+473.0*X3PR3*Y3/(120960.0*AL1)+(-13.0)*X3PR3*Y3/6
4  720.0+NU*X2*X3PR2*Y3/3360.0+(-31.0)*X2*X3PR2*Y3/(8960.0*AL1)-X2
5  *X3PR2*Y3/3360.0+NU*X2PR2*X3*Y3/2880.0+(-11.0)*X2PR2*X3*Y3/(120
6  960.0*AL1)-X2PR2*X3*Y3/2880.0+NU*X2PR3*Y3/6720.0+181.0*X2PR3*Y3
7  /(241920.0*AL1)-X2PR3*Y3/6720.0+(-449.0)*X3PR5/(20160.0*Y3)+269
8  .0*X2*X3PR4/(20160.0*Y3)+X2PR2*X3PR3*Y3/6048.0-X2PR3*X3PR2/Y3/1
9  440.0-X2PR4*X3/Y3/8640.0+(-13.0)*X2PR5/(20160.0*Y3)
   K4(6,11) = 3.0*NU*X3PR2*Y3PR2/4480.0+23.0*X3PR2*Y3PR2/40320.0-NU*X
1  2*X3*Y3PR2/AL1**2/10080.0+(-31.0)*NU*X2*X3*Y3PR2/80640.0-X2*X3*
2  Y3PR2/8960.0+NU*X2PR2*Y3PR2/AL1**2/15120.0+NU*X2PR2*Y3PR2/48384
3  .0+(-5.0)*X2PR2*Y3PR2/48384.0-NU*X3PR4/AL1/480.0+(-11.0)*X3PR4/
4  (6720.0*AL1)+13.0*NU*X2*X3PR3/(10080.0*AL1)+11.0*X2*X3PR3/(1008
5  0.0*AL1)+NU*X2PR2*X3PR2/AL1/1152.0+3.0*X2PR2*X3PR2/(4480.0*AL1)
6  -NU*X2PR3*X3/AL1/3360.0-NU*X2PR4/AL1/15120.0-X2PR4/AL1/6048.0
   K4(6,12) = 13.0*NU*X3*Y3PR3/(20160.0*AL1)+(-13.0)*X3*Y3PR3/(20160.
1  0*AL1)+(-17.0)*X3*Y3PR3/(34560.0*AL1**2)+NU*X2*Y3PR3/AL1/10080.
2  0-X2*Y3PR3/AL1/10080.0+X2*Y3PR3/AL1**2/3780.0+(-13.0)*NU*X3PR3*
3  Y3/6720.0+(-473.0)*X3PR3*Y3/(120960.0*AL1)+13.0*X3PR3*Y3/6720.0
4  +NU*X2*X3PR2*Y3/1680.0+211.0*X2*X3PR2*Y3/(80640.0*AL1)-X2*X3PR2
5  *Y3/1680.0+NU*X2PR2*X3*Y3/1440.0+(-31.0)*X2PR2*X3*Y3/(120960.0*
6  AL1)-X2PR2*X3*Y3/1440.0+NU*X2PR3*Y3/4032.0+(-23.0)*X2PR3*Y3/(60
7  480.0*AL1)-X2PR3*Y3/4032.0+449.0*X3PR5/(20160.0*Y3)+(-271.0)*X2
8  *X3PR4/(10080.0*Y3)+(-5.0)*X2PR2*X3PR3/(3024.0*Y3)+43.0*X2PR3*X

```

9 3PR2/(5040.0\*Y3)+X2PR4\*X3/Y3/1512.0+(-19.0)\*X2PR5/(10080.0\*Y3)

c

```

K4(7,7) = 43.0*X3PR2*Y3PR5/(3780.0*X2PR3)+(-43.0)*X3*Y3PR5/(3780.0
1  *X2PR2)+61.0*Y3PR5/(15120.0*X2)+(-3683.0)*NU*X3PR4*Y3PR3/(24192
2  0.0*X2PR3)+43.0*X3PR4*Y3PR3/(3780.0*AL1*X2PR3)+3683.0*X3PR4*Y3P
3  R3/(241920.0*X2PR3)+3683.0*NU*X3PR3*Y3PR3/(120960.0*X2PR2)-X3PR
4  3*Y3PR3/(AL1*X2PR2)/108.0+(-3683.0)*X3PR3*Y3PR3/(120960.0*X2PR2
5  )+(-5311.0)*NU*X3PR2*Y3PR3/(241920.0*X2)+X3PR2*Y3PR3/(AL1*X2)/5
6  60.0+5311.0*X3PR2*Y3PR3/(241920.0*X2)+407.0*NU*X3*Y3PR3/60480.0
7  +(-59.0)*X3*Y3PR3/(15120.0*AL1)+(-407.0)*X3*Y3PR3/60480.0-NU*X2
8  *Y3PR3/1120.0+X2*Y3PR3/AL1/288.0+X2*Y3PR3/1120.0+(-3019.0)*NU*X
9  3PR6*Y3/(120960.0*AL1*X2PR3)+3019.0*X3PR6*Y3/(120960.0*AL1*X2PR
:  3)+43.0*X3PR6*Y3/(15120.0*AL1**2*X2PR3)+1879.0*NU*X3PR5*Y3/(403
;  20.0*AL1*X2PR2)+(-1879.0)*X3PR5*Y3/(40320.0*AL1*X2PR2)-X3PR5*Y3
<  /(AL1**2*X2PR2)/560.0+(-3223.0)*NU*X3PR4*Y3/(120960.0*AL1*X2)+3
=  223.0*X3PR4*Y3/(120960.0*AL1*X2)+X3PR4*Y3/(AL1**2*X2)/2240.0+23
>  3.0*NU*X3PR3*Y3/(40320.0*AL1)+(-233.0)*X3PR3*Y3/(40320.0*AL1)+(-
?  -59.0)*X3PR3*Y3/(30240.0*AL1**2)+(-149.0)*NU*X2*X3PR2*Y3/(40320
@  .0*AL1)+149.0*X2*X3PR2*Y3/(40320.0*AL1)+X2*X3PR2*Y3/AL1**2/2240
1  .0+353.0*NU*X2PR2*X3*Y3/(120960.0*AL1)+(-353.0)*X2PR2*X3*Y3/(12
2  0960.0*AL1)+(-5.0)*NU*X2PR3*Y3/(6048.0*AL1)+5.0*X2PR3*Y3/(6048.
3  0*AL1)+127.0*X2PR3*Y3/(120960.0*AL1**2)+(-2699.0)*NU*X3PR8/(241
4  920.0*AL1**2*X2PR3*Y3)+2699.0*X3PR8/(241920.0*AL1**2*X2PR3*Y3)+
5  167.0*NU*X3PR7/(8640.0*AL1**2*X2PR2*Y3)+(-167.0)*X3PR7/(8640.0*
6  AL1**2*X2PR2*Y3)+(-437.0)*NU*X3PR6/(60480.0*AL1**2*X2*Y3)+437.0
7  *X3PR6/(60480.0*AL1**2*X2*Y3)+NU*X3PR5/(AL1**2*Y3)/120960.0-X3P
8  R5/(AL1**2*Y3)/120960.0+(-121.0)*NU*X2*X3PR4/(40320.0*AL1**2*Y3
9  )+121.0*X2*X3PR4/(40320.0*AL1**2*Y3)+109.0*NU*X2PR2*X3PR3/(6048
:  0.0*AL1**2*Y3)+(-109.0)*X2PR2*X3PR3/(60480.0*AL1**2*Y3)+(-19.0)
;  *NU*X2PR3*X3PR2/(241920.0*AL1**2*Y3)+19.0*X2PR3*X3PR2/(241920.0
<  *AL1**2*Y3)+13.0*NU*X2PR4*X3/(40320.0*AL1**2*Y3)+(-13.0)*X2PR4*
=  X3/(40320.0*AL1**2*Y3)+(-43.0)*NU*X2PR5/(120960.0*AL1**2*Y3)+43
>  .0*X2PR5/(120960.0*AL1**2*Y3)
K4(7,8) = (-83.0)*NU*X3PR3*Y3PR4/(15120.0*AL1*X2PR3)+(-83.0)*X3PR3
1  *Y3PR4/(15120.0*AL1*X2PR3)+83.0*NU*X3PR2*Y3PR4/(10080.0*AL1*X2*
2  *2)+83.0*X3PR2*Y3PR4/(10080.0*AL1*X2PR2)+(-5.0)*NU*X3*Y3PR4/(15
3  12.0*AL1*X2)+(-5.0)*X3*Y3PR4/(1512.0*AL1*X2)+17.0*NU*Y3PR4/(604
4  80.0*AL1)+17.0*Y3PR4/(60480.0*AL1)+(-43.0)*NU*X3PR5*Y3PR2/(1512
5  0.0*AL1**2*X2PR3)+(-11.0)*NU*X3PR5*Y3PR2/(4320.0*X2PR3)-X3PR5*Y
6  3PR2/(AL1**2*X2PR3)/378.0+(-83.0)*X3PR5*Y3PR2/(30240.0*X2PR3)+2
7  3.0*NU*X3PR4*Y3PR2/(7560.0*AL1**2*X2PR2)+17.0*NU*X3PR4*Y3PR2/(4
8  320.0*X2PR2)+11.0*X3PR4*Y3PR2/(3024.0*AL1**2*X2PR2)+101.0*X3PR4
9  *Y3PR2/(30240.0*X2PR2)-NU*X3PR3*Y3PR2/(AL1**2*X2)/2240.0+(-13.0
:  )*NU*X3PR3*Y3PR2/(6720.0*X2)+(-29.0)*X3PR3*Y3PR2/(20160.0*AL1**
;  2*X2)+(-19.0)*X3PR3*Y3PR2/(20160.0*X2)+127.0*NU*X3PR2*Y3PR2/(12
<  0960.0*AL1**2)+163.0*NU*X3PR2*Y3PR2/120960.0+151.0*X3PR2*Y3PR2/
=  (120960.0*AL1**2)+139.0*X3PR2*Y3PR2/120960.0+(-19.0)*NU*X2*X3*Y
>  3PR2/(13440.0*AL1**2)+(-11.0)*NU*X2*X3*Y3PR2/13440.0+(-41.0)*X2
?  *X3*Y3PR2/(40320.0*AL1**2)+(-7.0)*X2*X3*Y3PR2/5760.0+37.0*NU*X2
@  PR2*Y3PR2/(120960.0*AL1**2)+NU*X2PR2*Y3PR2/120960.0+13.0*X2PR2*
1  Y3PR2/(120960.0*AL1**2)+5.0*X2PR2*Y3PR2/24192.0-NU*X3PR7/(AL1*X

```

```

2  2PR3)/756.0-X3PR7/(AL1*X2PR3)/756.0+79.0*NU*X3PR6/(60480.0*AL1*
3  X2PR2)+79.0*X3PR6/(60480.0*AL1*X2PR2)+(-19.0)*NU*X3PR5/(40320.0
4  *AL1*X2)+(-19.0)*X3PR5/(40320.0*AL1*X2)+41.0*NU*X3PR4/(34560.0*
5  AL1)+41.0*X3PR4/(34560.0*AL1)+(-23.0)*NU*X2*X3PR3/(40320.0*AL1)
6  +(-23.0)*X2*X3PR3/(40320.0*AL1)+NU*X2PR2*X3PR2/AL1/13440.0+X2PR
7  2*X3PR2/AL1/13440.0+(-127.0)*NU*X2PR3*X3/(241920.0*AL1)+(-127.0
8  )*X2PR3*X3/(241920.0*AL1)+13.0*NU*X2PR4/(80640.0*AL1)+13.0*X2PR
9  4/(80640.0*AL1)
K4(7,9) = (-43.0)*X3*Y3PR5/(15120.0*X2PR2)+43.0*Y3PR5/(30240.0*X2)
1  +1117.0*NU*X3PR3*Y3PR3/(241920.0*X2PR2)+43.0*X3PR3*Y3PR3/(6048.
2  0*AL1*X2PR2)+(-1117.0)*X3PR3*Y3PR3/(241920.0*X2PR2)+(-41.0)*NU*
3  X3PR2*Y3PR3/(6048.0*X2)+(-11.0)*X3PR2*Y3PR3/(2880.0*AL1*X2)+41.
4  0*X3PR2*Y3PR3/(6048.0*X2)+23.0*NU*X3*Y3PR3/6912.0+5.0*X3*Y3PR3/
5  (3024.0*AL1)+(-23.0)*X3*Y3PR3/6912.0+(-11.0)*NU*X2*Y3PR3/20160.
6  0+(-113.0)*X2*Y3PR3/(120960.0*AL1)+11.0*X2*Y3PR3/20160.0+(-1061
7  .0)*NU*X3PR5*Y3/(80640.0*AL1*X2PR2)+1061.0*X3PR5*Y3/(80640.0*AL
8  1*X2PR2)+43.0*X3PR5*Y3/(10080.0*AL1**2*X2PR2)+2221.0*NU*X3PR4*Y
9  3/(120960.0*AL1*X2)+(-2221.0)*X3PR4*Y3/(120960.0*AL1*X2)+(-3.0)
:  *X3PR4*Y3/(2240.0*AL1**2*X2)+(-409.0)*NU*X3PR3*Y3/(40320.0*AL1)
;  +409.0*X3PR3*Y3/(40320.0*AL1)+5.0*X3PR3*Y3/(6048.0*AL1**2)+209.
<  0*NU*X2*X3PR2*Y3/(60480.0*AL1)+(-209.0)*X2*X3PR2*Y3/(60480.0*AL
=  1)+(-13.0)*X2*X3PR2*Y3/(8064.0*AL1**2)+(-17.0)*NU*X2PR2*X3*Y3/(
>  15120.0*AL1)+17.0*X2PR2*X3*Y3/(15120.0*AL1)+5.0*NU*X2PR3*Y3/(24
?  192.0*AL1)+(-5.0)*X2PR3*Y3/(24192.0*AL1)+(-109.0)*X2PR3*Y3/(120
@  960.0*AL1**2)+(-913.0)*NU*X3PR7/(60480.0*AL1**2*X2PR2*Y3)+913.0
1  *X3PR7/(60480.0*AL1**2*X2PR2*Y3)+895.0*NU*X3PR6/(48384.0*AL1**2
2  *X2*Y3)+(-895.0)*X3PR6/(48384.0*AL1**2*X2*Y3)+(-587.0)*NU*X3PR5
3  /(120960.0*AL1**2*Y3)+587.0*X3PR5/(120960.0*AL1**2*Y3)+5.0*NU*X
4  2*X3PR4/(2688.0*AL1**2*Y3)+(-5.0)*X2*X3PR4/(2688.0*AL1**2*Y3)+(-
5  17.0)*NU*X2PR2*X3PR3/(7560.0*AL1**2*Y3)+17.0*X2PR2*X3PR3/(7560
6  .0*AL1**2*Y3)+41.0*NU*X2PR3*X3PR2/(48384.0*AL1**2*Y3)+(-41.0)*X
7  2PR3*X3PR2/(48384.0*AL1**2*Y3)+(-41.0)*NU*X2PR4*X3/(120960.0*AL
8  1**2*Y3)+41.0*X2PR4*X3/(120960.0*AL1**2*Y3)+43.0*NU*X2PR5/(1209
9  60.0*AL1**2*Y3)+(-43.0)*X2PR5/(120960.0*AL1**2*Y3)
K4(7,10) = 3.0*NU*X3PR2*Y3PR4/(2240.0*AL1*X2PR2)+83.0*X3PR2*Y3PR4/
1  (60480.0*AL1*X2PR2)+(-17.0)*NU*X3*Y3PR4/(12096.0*AL1*X2)+(-83.0
2  )*X3*Y3PR4/(60480.0*AL1*X2)+NU*Y3PR4/AL1/5760.0+Y3PR4/AL1/5760.
3  0+NU*X3PR4*Y3PR2/(AL1**2*X2PR2)/1440.0+(-47.0)*NU*X3PR4*Y3PR2/(
4  12096.0*X2PR2)+X3PR4*Y3PR2/(AL1**2*X2PR2)/1512.0+(-83.0)*X3PR4*
5  Y3PR2/(20160.0*X2PR2)+(-23.0)*NU*X3PR3*Y3PR2/(60480.0*AL1**2*X2
6  )+251.0*NU*X3PR3*Y3PR2/(60480.0*X2)-X3PR3*Y3PR2/(AL1**2*X2)/172
7  8.0+83.0*X3PR3*Y3PR2/(20160.0*X2)-NU*X3PR2*Y3PR2/AL1**2/26880.0
8  +(-29.0)*NU*X3PR2*Y3PR2/24192.0+13.0*X3PR2*Y3PR2/(80640.0*AL1**
9  2)+(-181.0)*X3PR2*Y3PR2/120960.0+(-5.0)*NU*X2*X3*Y3PR2/(16128.0
:  *AL1**2)+NU*X2*X3*Y3PR2/1728.0+(-59.0)*X2*X3*Y3PR2/(241920.0*AL
;  1**2)+23.0*X2*X3*Y3PR2/20160.0+11.0*NU*X2PR2*Y3PR2/(80640.0*AL1
<  **2)+NU*X2PR2*Y3PR2/40320.0+X2PR2*Y3PR2/AL1**2/26880.0+(-29.0)*
=  X2PR2*Y3PR2/120960.0+(-61.0)*NU*X3PR6/(30240.0*AL1*X2PR2)-X3PR6
>  /(AL1*X2PR2)/504.0+19.0*NU*X3PR5/(20160.0*AL1*X2)+X3PR5/(AL1*X2
?  )/576.0+(-37.0)*NU*X3PR4/(241920.0*AL1)+(-253.0)*X3PR4/(241920.

```

```

@ 0*AL1)+71.0*NU*X2*X3PR3/(80640.0*AL1)+277.0*X2*X3PR3/(241920.0*
1 AL1)-NU*X2PR2*X3PR2/AL1/3360.0-X2PR2*X3PR2/AL1/5040.0+109.0*NU*
2 X2PR3*X3/(241920.0*AL1)+109.0*X2PR3*X3/(241920.0*AL1)-NU*X2PR4/
3 AL1/6912.0+(-43.0)*X2PR4/(241920.0*AL1)
K4(7,11) = 43.0*X3*Y3PR5/(15120.0*X2PR2)+(-43.0)*Y3PR5/(30240.0*X2
1 )+(-1117.0)*NU*X3PR3*Y3PR3/(241920.0*X2PR2)+(-43.0)*X3PR3*Y3PR3
2 /(6048.0*AL1*X2PR2)+1117.0*X3PR3*Y3PR3/(241920.0*X2PR2)+1711.0*
3 NU*X3PR2*Y3PR3/(241920.0*X2)+149.0*X3PR2*Y3PR3/(20160.0*AL1*X2)
4 +(-1711.0)*X3PR2*Y3PR3/(241920.0*X2)+(-73.0)*NU*X3*Y3PR3/20160.
5 0+23.0*X3*Y3PR3/(15120.0*AL1)+73.0*X3*Y3PR3/20160.0+5.0*NU*X2*Y
6 3PR3/8064.0+(-331.0)*X2*Y3PR3/(120960.0*AL1)+(-5.0)*X2*Y3PR3/80
7 64.0+1061.0*NU*X3PR5*Y3/(80640.0*AL1*X2PR2)+(-1061.0)*X3PR5*Y3/
8 (80640.0*AL1*X2PR2)+(-43.0)*X3PR5*Y3/(10080.0*AL1**2*X2PR2)+(-6
9 793.0)*NU*X3PR4*Y3/(241920.0*AL1*X2)+6793.0*X3PR4*Y3/(241920.0*
: AL1*X2)+X3PR4*Y3/(AL1**2*X2)/320.0+961.0*NU*X3PR3*Y3/(60480.0*A
; L1)+(-961.0)*X3PR3*Y3/(60480.0*AL1)+23.0*X3PR3*Y3/(30240.0*AL1*
< *2)+97.0*NU*X2*X3PR2*Y3/(30240.0*AL1)+(-97.0)*X2*X3PR2*Y3/(3024
= 0.0*AL1)+47.0*X2*X3PR2*Y3/(40320.0*AL1**2)+(-1291.0)*NU*X2PR2*X
> 3*Y3/(241920.0*AL1)+1291.0*X2PR2*X3*Y3/(241920.0*AL1)-X2PR2*X3*
? Y3/AL1**2/2240.0+331.0*NU*X2PR3*Y3/(241920.0*AL1)+(-331.0)*X2PR
@ 3*Y3/(241920.0*AL1)+(-5.0)*X2PR3*Y3/(4032.0*AL1**2)+913.0*NU*X3
1 PR7/(60480.0*AL1**2*X2PR2*Y3)+(-913.0)*X3PR7/(60480.0*AL1**2*X2
2 PR2*Y3)+(-6689.0)*NU*X3PR6/(241920.0*AL1**2*X2*Y3)+6689.0*X3PR6
3 /(241920.0*AL1**2*X2*Y3)+577.0*NU*X3PR5/(60480.0*AL1**2*Y3)+(-5
4 77.0)*X3PR5/(60480.0*AL1**2*Y3)+253.0*NU*X2*X3PR4/(48384.0*AL1*
5 *2*Y3)+(-253.0)*X2*X3PR4/(48384.0*AL1**2*Y3)-NU*X2PR2*X3PR3/(AL
6 1**2*Y3)/3360.0+X2PR2*X3PR3/(AL1**2*Y3)/3360.0+(-61.0)*NU*X2PR3
7 *X3PR2/(40320.0*AL1**2*Y3)+61.0*X2PR3*X3PR2/(40320.0*AL1**2*Y3)
8 +(-23.0)*NU*X2PR4*X3/(30240.0*AL1**2*Y3)+23.0*X2PR4*X3/(30240.0
9 *AL1**2*Y3)+43.0*NU*X2PR5/(60480.0*AL1**2*Y3)+(-43.0)*X2PR5/(60
: 480.0*AL1**2*Y3)
K4(7,12) = (-3.0)*NU*X3PR2*Y3PR4/(2240.0*AL1*X2PR2)+(-83.0)*X3PR2*
1 Y3PR4/(60480.0*AL1*X2PR2)+11.0*NU*X3*Y3PR4/(8640.0*AL1*X2)+83.0
2 *X3*Y3PR4/(60480.0*AL1*X2)+(-13.0)*NU*Y3PR4/(120960.0*AL1)-Y3PR
3 4/AL1/5760.0-NU*X3PR4*Y3PR2/(AL1**2*X2PR2)/1440.0+47.0*NU*X3PR4
4 *Y3PR2/(12096.0*X2PR2)-X3PR4*Y3PR2/(AL1**2*X2PR2)/1512.0+83.0*X
5 3PR4*Y3PR2/(20160.0*X2PR2)+19.0*NU*X3PR3*Y3PR2/(60480.0*AL1**2*
6 X2)+(-79.0)*NU*X3PR3*Y3PR2/(12096.0*X2)+X3PR3*Y3PR2/(AL1**2*X2)
7 /1728.0+(-107.0)*X3PR3*Y3PR2/(20160.0*X2)+NU*X3PR2*Y3PR2/AL1**2
8 /26880.0+283.0*NU*X3PR2*Y3PR2/120960.0+(-13.0)*X3PR2*Y3PR2/(806
9 40.0*AL1**2)+(-29.0)*X3PR2*Y3PR2/120960.0+5.0*NU*X2*X3*Y3PR2/(1
: 6128.0*AL1**2)+NU*X2*X3*Y3PR2/20160.0+59.0*X2*X3*Y3PR2/(241920.
; 0*AL1**2)+17.0*X2*X3*Y3PR2/8640.0+(-5.0)*NU*X2PR2*Y3PR2/(48384.
< 0*AL1**2)+NU*X2PR2*Y3PR2/4320.0-X2PR2*Y3PR2/AL1**2/26880.0-X2PR
= 2*Y3PR2/3360.0+61.0*NU*X3PR6/(30240.0*AL1*X2PR2)+X3PR6/(AL1*X2P
> R2)/504.0+(-7.0)*NU*X3PR5/(2880.0*AL1*X2)+(-41.0)*X3PR5/(20160.
? 0*AL1*X2)+157.0*NU*X3PR4/(241920.0*AL1)+(-83.0)*X3PR4/(241920.0
@ *AL1)+(-67.0)*NU*X2*X3PR3/(48384.0*AL1)-X2*X3PR3/AL1/16128.0+31
1 .0*NU*X2PR2*X3PR2/(26880.0*AL1)+13.0*X2PR2*X3PR2/(80640.0*AL1)+
2 NU*X2PR3*X3/AL1/4032.0+13.0*X2PR3*X3/(20160.0*AL1)+(-13.0)*NU*X

```

3 2PR4/(120960.0\*AL1)-X2PR4/AL1/5760.0

c

K4(8,8) = (-43.0)\*NU\*X3PR2\*Y3PR5/(7560.0\*AL1\*\*2\*X2PR3)+43.0\*X3PR2\*  
 1 Y3PR5/(7560.0\*AL1\*\*2\*X2PR3)+43.0\*NU\*X3\*Y3PR5/(7560.0\*AL1\*\*2\*X2P  
 2 R2)+(-43.0)\*X3\*Y3PR5/(7560.0\*AL1\*\*2\*X2PR2)+(-61.0)\*NU\*Y3PR5/(30  
 3 240.0\*AL1\*\*2\*X2)+61.0\*Y3PR5/(30240.0\*AL1\*\*2\*X2)+(-43.0)\*NU\*X3PR  
 4 4\*Y3PR3/(7560.0\*AL1\*X2PR3)+43.0\*X3PR4\*Y3PR3/(7560.0\*AL1\*X2PR3)+  
 5 3683.0\*X3PR4\*Y3PR3/(120960.0\*AL1\*\*2\*X2PR3)+NU\*X3PR3\*Y3PR3/(AL1\*  
 6 X2PR2)/216.0-X3PR3\*Y3PR3/(AL1\*X2PR2)/216.0+(-3683.0)\*X3PR3\*Y3PR  
 7 3/(60480.0\*AL1\*\*2\*X2PR2)-NU\*X3PR2\*Y3PR3/(AL1\*X2)/1120.0+X3PR2\*Y  
 8 3PR3/(AL1\*X2)/1120.0+5311.0\*X3PR2\*Y3PR3/(120960.0\*AL1\*\*2\*X2)+59  
 9 .0\*NU\*X3\*Y3PR3/(30240.0\*AL1)+(-59.0)\*X3\*Y3PR3/(30240.0\*AL1)+(-4  
 : 07.0)\*X3\*Y3PR3/(30240.0\*AL1\*\*2)-NU\*X2\*Y3PR3/AL1/576.0+X2\*Y3PR3/  
 ; AL1/576.0+X2\*Y3PR3/AL1\*\*2/560.0+(-43.0)\*NU\*X3PR6\*Y3/(30240.0\*X2  
 < PR3)+3019.0\*X3PR6\*Y3/(60480.0\*AL1\*X2PR3)+43.0\*X3PR6\*Y3/(30240.0  
 = \*X2PR3)+NU\*X3PR5\*Y3/X2PR2/1120.0+(-1879.0)\*X3PR5\*Y3/(20160.0\*AL  
 > 1\*X2PR2)-X3PR5\*Y3/X2PR2/1120.0-NU\*X3PR4\*Y3/X2/4480.0+3223.0\*X3P  
 ? R4\*Y3/(60480.0\*AL1\*X2)+X3PR4\*Y3/X2/4480.0+59.0\*NU\*X3PR3\*Y3/6048  
 @ 0.0+(-233.0)\*X3PR3\*Y3/(20160.0\*AL1)+(-59.0)\*X3PR3\*Y3/6048.0-NU  
 1 \*X2\*X3PR2\*Y3/4480.0+149.0\*X2\*X3PR2\*Y3/(20160.0\*AL1)+X2\*X3PR2\*Y3  
 2 /4480.0+(-353.0)\*X2PR2\*X3\*Y3/(60480.0\*AL1)+(-127.0)\*NU\*X2PR3\*Y3  
 3 /241920.0+5.0\*X2PR3\*Y3/(3024.0\*AL1)+127.0\*X2PR3\*Y3/241920.0+269  
 4 9.0\*X3PR8/(120960.0\*X2PR3\*Y3)+(-167.0)\*X3PR7/(4320.0\*X2PR2\*Y3)+  
 5 437.0\*X3PR6/(30240.0\*X2\*Y3)-X3PR5\*Y3/60480.0+121.0\*X2\*X3PR4/(20  
 6 160.0\*Y3)+(-109.0)\*X2PR2\*X3PR3/(30240.0\*Y3)+19.0\*X2PR3\*X3PR2/(1  
 7 20960.0\*Y3)+(-13.0)\*X2PR4\*X3/(20160.0\*Y3)+43.0\*X2PR5/(60480.0\*Y  
 8 3)  
 K4(8,9) = NU\*X3PR2\*Y3PR4/(AL1\*X2PR2)/720.0+41.0\*X3PR2\*Y3PR4/(30240  
 1 .0\*AL1\*X2PR2)+(-41.0)\*NU\*X3\*Y3PR4/(30240.0\*AL1\*X2)-X3\*Y3PR4/(AL  
 2 1\*X2)/720.0+NU\*Y3PR4/AL1/5760.0+Y3PR4/AL1/5760.0+(-4.0)\*NU\*X3PR  
 3 4\*Y3PR2/(945.0\*AL1\*\*2\*X2PR2)+13.0\*NU\*X3PR4\*Y3PR2/(20160.0\*X2PR2  
 4 )+(-121.0)\*X3PR4\*Y3PR2/(30240.0\*AL1\*\*2\*X2PR2)+41.0\*X3PR4\*Y3PR2/  
 5 (60480.0\*X2PR2)+31.0\*NU\*X3PR3\*Y3PR2/(7560.0\*AL1\*\*2\*X2)+(-41.0)\*  
 6 NU\*X3PR3\*Y3PR2/(60480.0\*X2)+25.0\*X3PR3\*Y3PR2/(6048.0\*AL1\*\*2\*X2)  
 7 +(-29.0)\*X3PR3\*Y3PR2/(60480.0\*X2)+(-199.0)\*NU\*X3PR2\*Y3PR2/(1209  
 8 60.0\*AL1\*\*2)+NU\*X3PR2\*Y3PR2/3840.0+(-163.0)\*X3PR2\*Y3PR2/(120960  
 9 .0\*AL1\*\*2)+X3PR2\*Y3PR2/16128.0+43.0\*NU\*X2\*X3\*Y3PR2/(30240.0\*AL1  
 : \*\*2)+(-17.0)\*NU\*X2\*X3\*Y3PR2/80640.0+13.0\*X2\*X3\*Y3PR2/(15120.0\*A  
 ; L1\*\*2)+(-67.0)\*X2\*X3\*Y3PR2/241920.0-NU\*X2PR2\*Y3PR2/AL1\*\*2/2688.  
 < 0-NU\*X2PR2\*Y3PR2/80640.0+(-13.0)\*X2PR2\*Y3PR2/(120960.0\*AL1\*\*2)+  
 = X2PR2\*Y3PR2/11520.0+(-17.0)\*NU\*X3PR6/(8640.0\*AL1\*X2PR2)+(-121.0  
 > )\*X3PR6/(60480.0\*AL1\*X2PR2)+43.0\*NU\*X3PR5/(20160.0\*AL1\*X2)+3.0\*  
 ? X3PR5/(2240.0\*AL1\*X2)+(-361.0)\*NU\*X3PR4/(241920.0\*AL1)+(-29.0)\*  
 @ X3PR4/(48384.0\*AL1)+103.0\*NU\*X2\*X3PR3/(80640.0\*AL1)+7.0\*X2\*X3PR  
 1 3/(6912.0\*AL1)-NU\*X2PR2\*X3PR2/AL1/6720.0-X2PR2\*X3PR2/AL1/4032.0  
 2 +109.0\*NU\*X2PR3\*X3/(241920.0\*AL1)+109.0\*X2PR3\*X3/(241920.0\*AL1)  
 3 +(-47.0)\*NU\*X2PR4/(241920.0\*AL1)+(-13.0)\*X2PR4/(80640.0\*AL1)  
 K4(8,10) = 43.0\*NU\*X3\*Y3PR5/(30240.0\*AL1\*\*2\*X2PR2)+(-43.0)\*X3\*Y3PR  
 1 5/(30240.0\*AL1\*\*2\*X2PR2)+(-43.0)\*NU\*Y3PR5/(60480.0\*AL1\*\*2\*X2)+4  
 2 3.0\*Y3PR5/(60480.0\*AL1\*\*2\*X2)+(-43.0)\*NU\*X3PR3\*Y3PR3/(12096.0\*A  
 3 L1\*X2PR2)+43.0\*X3PR3\*Y3PR3/(12096.0\*AL1\*X2PR2)+(-1117.0)\*X3PR3\*

```

4 Y3PR3/(120960.0*AL1**2*X2PR2)+11.0*NU*X3PR2*Y3PR3/(5760.0*AL1*X
5 2)+(-11.0)*X3PR2*Y3PR3/(5760.0*AL1*X2)+41.0*X3PR2*Y3PR3/(3024.0
6 *AL1**2*X2)+(-5.0)*NU*X3*Y3PR3/(6048.0*AL1)+5.0*X3*Y3PR3/(6048.
7 0*AL1)+(-23.0)*X3*Y3PR3/(3456.0*AL1**2)+113.0*NU*X2*Y3PR3/(2419
8 20.0*AL1)+(-113.0)*X2*Y3PR3/(241920.0*AL1)+11.0*X2*Y3PR3/(10080
9 .0*AL1**2)+(-43.0)*NU*X3PR5*Y3/(20160.0*X2PR2)+1061.0*X3PR5*Y3/
: (40320.0*AL1*X2PR2)+43.0*X3PR5*Y3/(20160.0*X2PR2)+3.0*NU*X3PR4*
; Y3/(4480.0*X2)+(-2221.0)*X3PR4*Y3/(60480.0*AL1*X2)+(-3.0)*X3PR4
< *Y3/(4480.0*X2)+(-5.0)*NU*X3PR3*Y3/12096.0+409.0*X3PR3*Y3/(2016
= 0.0*AL1)+5.0*X3PR3*Y3/12096.0+13.0*NU*X2*X3PR2*Y3/16128.0+(-209
> .0)*X2*X3PR2*Y3/(30240.0*AL1)+(-13.0)*X2*X3PR2*Y3/16128.0+17.0*
? X2PR2*X3*Y3/(7560.0*AL1)+109.0*NU*X2PR3*Y3/241920.0+(-5.0)*X2PR
@ 3*Y3/(12096.0*AL1)+(-109.0)*X2PR3*Y3/241920.0+913.0*X3PR7/(3024
1 0.0*X2PR2*Y3)+(-895.0)*X3PR6/(24192.0*X2*Y3)+587.0*X3PR5/(60480
2 .0*Y3)+(-5.0)*X2*X3PR4/(1344.0*Y3)+17.0*X2PR2*X3PR3/(3780.0*Y3)
3 +(-41.0)*X2PR3*X3PR2/(24192.0*Y3)+41.0*X2PR4*X3/(60480.0*Y3)+(-
4 43.0)*X2PR5/(60480.0*Y3)
K4(8,11) = -NU*X3PR2*Y3PR4/(AL1*X2PR2)/720.0+(-41.0)*X3PR2*Y3PR4/(
1 30240.0*AL1*X2PR2)+43.0*NU*X3*Y3PR4/(30240.0*AL1*X2)+X3*Y3PR4/(
2 AL1*X2)/756.0+(-5.0)*NU*Y3PR4/(24192.0*AL1)+(-17.0)*Y3PR4/(1209
3 60.0*AL1)+4.0*NU*X3PR4*Y3PR2/(945.0*AL1**2*X2PR2)+(-13.0)*NU*X3
4 PR4*Y3PR2/(20160.0*X2PR2)+121.0*X3PR4*Y3PR2/(30240.0*AL1**2*X2P
5 R2)+(-41.0)*X3PR4*Y3PR2/(60480.0*X2PR2)+(-71.0)*NU*X3PR3*Y3PR2/
6 (15120.0*AL1**2*X2)+43.0*NU*X3PR3*Y3PR2/(60480.0*X2)+(-179.0)*X
7 3PR3*Y3PR2/(30240.0*AL1**2*X2)+X3PR3*Y3PR2/X2/2240.0+(-37.0)*NU
8 *X3PR2*Y3PR2/(24192.0*AL1**2)-NU*X3PR2*Y3PR2/3840.0+127.0*X3PR2
9 *Y3PR2/(120960.0*AL1**2)-X3PR2*Y3PR2/16128.0+59.0*NU*X2*X3*Y3PR
: 2/(20160.0*AL1**2)+17.0*NU*X2*X3*Y3PR2/80640.0+61.0*X2*X3*Y3PR2
; /(60480.0*AL1**2)+67.0*X2*X3*Y3PR2/241920.0+(-17.0)*NU*X2PR2*Y3
< PR2/(30240.0*AL1**2)-NU*X2PR2*Y3PR2/241920.0-X2PR2*Y3PR2/AL1**2
= /30240.0+(-17.0)*X2PR2*Y3PR2/241920.0+17.0*NU*X3PR6/(8640.0*AL1
> *X2PR2)+121.0*X3PR6/(60480.0*AL1*X2PR2)+(-37.0)*NU*X3PR5/(20160
? .0*AL1*X2)-X3PR5/(AL1*X2)/448.0+(-29.0)*NU*X3PR4/(34560.0*AL1)+
@ 37.0*X3PR4/(241920.0*AL1)+29.0*NU*X2*X3PR3/(48384.0*AL1)+(-5.0)
1 *X2*X3PR3/(6912.0*AL1)+(-3.0)*NU*X2PR2*X3PR2/(8960.0*AL1)+53.0*
2 X2PR2*X3PR2/(80640.0*AL1)+17.0*NU*X2PR3*X3/(20160.0*AL1)+X2PR3*
3 X3/AL1/2240.0+(-5.0)*NU*X2PR4/(24192.0*AL1)+(-17.0)*X2PR4/(1209
4 60.0*AL1)
K4(8,12) = (-43.0)*NU*X3*Y3PR5/(30240.0*AL1**2*X2PR2)+43.0*X3*Y3PR
1 5/(30240.0*AL1**2*X2PR2)+43.0*NU*Y3PR5/(60480.0*AL1**2*X2)+(-43
2 .0)*Y3PR5/(60480.0*AL1**2*X2)+43.0*NU*X3PR3*Y3PR3/(12096.0*AL1*
3 X2PR2)+(-43.0)*X3PR3*Y3PR3/(12096.0*AL1*X2PR2)+1117.0*X3PR3*Y3P
4 R3/(120960.0*AL1**2*X2PR2)+(-149.0)*NU*X3PR2*Y3PR3/(40320.0*AL1
5 *X2)+149.0*X3PR2*Y3PR3/(40320.0*AL1*X2)+(-1711.0)*X3PR2*Y3PR3/(
6 120960.0*AL1**2*X2)+(-23.0)*NU*X3*Y3PR3/(30240.0*AL1)+23.0*X3*Y
7 3PR3/(30240.0*AL1)+73.0*X3*Y3PR3/(10080.0*AL1**2)+331.0*NU*X2*Y
8 3PR3/(241920.0*AL1)+(-331.0)*X2*Y3PR3/(241920.0*AL1)+(-5.0)*X2*
9 Y3PR3/(4032.0*AL1**2)+43.0*NU*X3PR5*Y3/(20160.0*X2PR2)+(-1061.0
: )*X3PR5*Y3/(40320.0*AL1*X2PR2)+(-43.0)*X3PR5*Y3/(20160.0*X2PR2)
; -NU*X3PR4*Y3/X2/640.0+6793.0*X3PR4*Y3/(120960.0*AL1*X2)+X3PR4*Y

```



```

< 3/X2/640.0+(-23.0)*NU*X3PR3*Y3/60480.0+(-961.0)*X3PR3*Y3/(30240
= .0*AL1)+23.0*X3PR3*Y3/60480.0+(-47.0)*NU*X2*X3PR2*Y3/80640.0+(-
> 97.0)*X2*X3PR2*Y3/(15120.0*AL1)+47.0*X2*X3PR2*Y3/80640.0+NU*X2P
? R2*X3*Y3/4480.0+1291.0*X2PR2*X3*Y3/(120960.0*AL1)-X2PR2*X3*Y3/4
@ 480.0+5.0*NU*X2PR3*Y3/8064.0+(-331.0)*X2PR3*Y3/(120960.0*AL1)+(-
1 -5.0)*X2PR3*Y3/8064.0+(-913.0)*X3PR7/(30240.0*X2PR2*Y3)+6689.0*
2 X3PR6/(120960.0*X2*Y3)+(-577.0)*X3PR5/(30240.0*Y3)+(-253.0)*X2*
3 X3PR4/(24192.0*Y3)+X2PR2*X3PR3*Y3/1680.0+61.0*X2PR3*X3PR2/(2016
4 0.0*Y3)+23.0*X2PR4*X3/(15120.0*Y3)+(-43.0)*X2PR5/(30240.0*Y3)

```

C

```

K4(9,9) = 43.0*Y3PR5/(60480.0*X2)+(-23.0)*NU*X3PR2*Y3PR3/(16128.0*
1 X2)+(-43.0)*X3PR2*Y3PR3/(10080.0*AL1*X2)+23.0*X3PR2*Y3PR3/(1612
2 8.0*X2)+NU*X3*Y3PR3/756.0-X3*Y3PR3/756.0+(-17.0)*NU*X2*Y3PR3/40
3 320.0+(-5.0)*X2*Y3PR3/(6048.0*AL1)+17.0*X2*Y3PR3/40320.0+649.0*
4 NU*X3PR4*Y3/(60480.0*AL1*X2)+(-649.0)*X3PR4*Y3/(60480.0*AL1*X2)
5 +43.0*X3PR4*Y3/(6720.0*AL1**2*X2)+(-359.0)*NU*X3PR3*Y3/(40320.0
6 *AL1)+359.0*X3PR3*Y3/(40320.0*AL1)+23.0*NU*X2*X3PR2*Y3/(7560.0*
7 AL1)+(-23.0)*X2*X3PR2*Y3/(7560.0*AL1)+5.0*X2*X3PR2*Y3/(2016.0*A
8 L1**2)+(-31.0)*NU*X2PR2*X3*Y3/(40320.0*AL1)+31.0*X2PR2*X3*Y3/(4
9 0320.0*AL1)+5.0*NU*X2PR3*Y3/(12096.0*AL1)+(-5.0)*X2PR3*Y3/(1209
: 6.0*AL1)+17.0*X2PR3*Y3/(20160.0*AL1**2)+(-55.0)*NU*X3PR6/(2688.
; 0*AL1**2*X2*Y3)+55.0*X3PR6/(2688.0*AL1**2*X2*Y3)+199.0*NU*X3PR5
< /(13440.0*AL1**2*Y3)+(-199.0)*X3PR5/(13440.0*AL1**2*Y3)+(-73.0)
= *NU*X2*X3PR4/(13440.0*AL1**2*Y3)+73.0*X2*X3PR4/(13440.0*AL1**2*
> Y3)+169.0*NU*X2PR2*X3PR3/(60480.0*AL1**2*Y3)+(-169.0)*X2PR2*X3P
? R3/(60480.0*AL1**2*Y3)+(-67.0)*NU*X2PR3*X3PR2/(40320.0*AL1**2*Y
@ 3)+67.0*X2PR3*X3PR2/(40320.0*AL1**2*Y3)+43.0*NU*X2PR4*X3/(12096
1 0.0*AL1**2*Y3)+(-43.0)*X2PR4*X3/(120960.0*AL1**2*Y3)+(-43.0)*NU
2 *X2PR5/(120960.0*AL1**2*Y3)+43.0*X2PR5/(120960.0*AL1**2*Y3)
K4(9,10) = (-41.0)*NU*X3*Y3PR4/(120960.0*AL1*X2)+(-41.0)*X3*Y3PR4/
1 (120960.0*AL1*X2)+43.0*NU*Y3PR4/(241920.0*AL1)+43.0*Y3PR4/(2419
2 20.0*AL1)+25.0*NU*X3PR3*Y3PR2/(24192.0*AL1**2*X2)+17.0*NU*X3PR3
3 *Y3PR2/(17280.0*X2)+121.0*X3PR3*Y3PR2/(120960.0*AL1**2*X2)+41.0
4 *X3PR3*Y3PR2/(40320.0*X2)+(-43.0)*NU*X3PR2*Y3PR2/(80640.0*AL1**
5 2)+(-43.0)*NU*X3PR2*Y3PR2/80640.0+(-43.0)*X3PR2*Y3PR2/(80640.0*
6 AL1**2)+(-43.0)*X3PR2*Y3PR2/80640.0+37.0*NU*X2*X3*Y3PR2/(120960
7 .0*AL1**2)+19.0*NU*X2*X3*Y3PR2/120960.0+5.0*X2*X3*Y3PR2/(24192.
8 0*AL1**2)+31.0*X2*X3*Y3PR2/120960.0+(-41.0)*NU*X2PR2*Y3PR2/(241
9 920.0*AL1**2)+NU*X2PR2*Y3PR2/34560.0-X2PR2*Y3PR2/AL1**2/26880.0
: +(-5.0)*X2PR2*Y3PR2/48384.0+(-121.0)*NU*X3PR5/(40320.0*AL1*X2)+
; (-121.0)*X3PR5/(40320.0*AL1*X2)+43.0*NU*X3PR4/(26880.0*AL1)+43.
< 0*X3PR4/(26880.0*AL1)+(-29.0)*NU*X2*X3PR3/(20160.0*AL1)+(-29.0)
= *X2*X3PR3/(20160.0*AL1)+17.0*NU*X2PR2*X3PR2/(40320.0*AL1)+17.0*
> X2PR2*X3PR2/(40320.0*AL1)+(-17.0)*NU*X2PR3*X3/(40320.0*AL1)+(-1
? 7.0)*X2PR3*X3/(40320.0*AL1)+43.0*NU*X2PR4/(241920.0*AL1)+43.0*X
@ 2PR4/(241920.0*AL1)
K4(9,11) = (-43.0)*Y3PR5/(60480.0*X2)+23.0*NU*X3PR2*Y3PR3/(16128.0
1 *X2)+43.0*X3PR2*Y3PR3/(10080.0*AL1*X2)+(-23.0)*X3PR2*Y3PR3/(161
2 28.0*X2)+(-23.0)*NU*X3*Y3PR3/16128.0-X3*Y3PR3/AL1/1120.0+23.0*X
3 3*Y3PR3/16128.0+109.0*NU*X2*Y3PR3/241920.0+(-5.0)*X2*Y3PR3/(120

```

```

4 96.0*AL1)+(-109.0)*X2*Y3PR3/241920.0+(-649.0)*NU*X3PR4*Y3/(6048
5 0.0*AL1*X2)+649.0*X3PR4*Y3/(60480.0*AL1*X2)+(-43.0)*X3PR4*Y3/(6
6 720.0*AL1**2*X2)+379.0*NU*X3PR3*Y3/(30240.0*AL1)+(-379.0)*X3PR3
7 *Y3/(30240.0*AL1)+3.0*X3PR3*Y3/(1120.0*AL1**2)+(-811.0)*NU*X2*X
8 3PR2*Y3/(241920.0*AL1)+811.0*X2*X3PR2*Y3/(241920.0*AL1)+5.0*X2*
9 X3PR2*Y3/(4032.0*AL1**2)+(-13.0)*NU*X2PR2*X3*Y3/(11520.0*AL1)+1
: 3.0*X2PR2*X3*Y3/(11520.0*AL1)+X2PR2*X3*Y3/AL1**2/3360.0+113.0*N
; U*X2PR3*Y3/(241920.0*AL1)+(-113.0)*X2PR3*Y3/(241920.0*AL1)+11.0
< *X2PR3*Y3/(10080.0*AL1**2)+55.0*NU*X3PR6/(2688.0*AL1**2*X2*Y3)+
= (-55.0)*X3PR6/(2688.0*AL1**2*X2*Y3)+(-73.0)*NU*X3PR5/(2688.0*AL
> 1**2*Y3)+73.0*X3PR5/(2688.0*AL1**2*Y3)+23.0*NU*X2*X3PR4/(4480.0
? *AL1**2*Y3)+(-23.0)*X2*X3PR4/(4480.0*AL1**2*Y3)+151.0*NU*X2PR2*
@ X3PR3/(40320.0*AL1**2*Y3)+(-151.0)*X2PR2*X3PR3/(40320.0*AL1**2*
1 Y3)+(-13.0)*NU*X2PR3*X3PR2/(10080.0*AL1**2*Y3)+13.0*X2PR3*X3PR2
2 /(10080.0*AL1**2*Y3)+NU*X2PR4*X3/(AL1**2*Y3)/1260.0-X2PR4*X3/(A
3 L1**2*Y3)/1260.0+(-43.0)*NU*X2PR5/(60480.0*AL1**2*Y3)+43.0*X2PR
4 5/(60480.0*AL1**2*Y3)
K4(9,12) = 41.0*NU*X3*Y3PR4/(120960.0*AL1*X2)+41.0*X3*Y3PR4/(12096
1 0.0*AL1*X2)-NU*Y3PR4/AL1/6912.0+(-43.0)*Y3PR4/(241920.0*AL1)+(-
2 25.0)*NU*X3PR3*Y3PR2/(24192.0*AL1**2*X2)+(-17.0)*NU*X3PR3*Y3PR2
3 /(17280.0*X2)+(-121.0)*X3PR3*Y3PR2/(120960.0*AL1**2*X2)+(-41.0)
4 *X3PR3*Y3PR2/(40320.0*X2)+NU*X3PR2*Y3PR2/AL1**2/2304.0+19.0*NU*
5 X3PR2*Y3PR2/16128.0+43.0*X3PR2*Y3PR2/(80640.0*AL1**2)+X3PR2*Y3P
6 R2/1280.0+(-37.0)*NU*X2*X3*Y3PR2/(120960.0*AL1**2)+(-5.0)*NU*X2
7 *X3*Y3PR2/24192.0+(-5.0)*X2*X3*Y3PR2/(24192.0*AL1**2)+47.0*X2*X
8 3*Y3PR2/120960.0+11.0*NU*X2PR2*Y3PR2/(80640.0*AL1**2)+NU*X2PR2*
9 Y3PR2/40320.0+X2PR2*Y3PR2/AL1**2/26880.0+(-29.0)*X2PR2*Y3PR2/12
: 0960.0+121.0*NU*X3PR5/(40320.0*AL1*X2)+121.0*X3PR5/(40320.0*AL1
; *X2)+(-43.0)*NU*X3PR4/(11520.0*AL1)+(-173.0)*X3PR4/(80640.0*AL1
< )+NU*X2*X3PR3/AL1/576.0+(-13.0)*X2*X3PR3/(20160.0*AL1)+(-13.0)*
= NU*X2PR2*X3PR2/(11520.0*AL1)+37.0*X2PR2*X3PR2/(80640.0*AL1)-NU*
> X2PR3*X3/AL1/5760.0+(-23.0)*X2PR3*X3/(40320.0*AL1)+NU*X2PR4/AL1
? /5760.0+X2PR4/AL1/5760.0

```

C

```

K4(10,10) = (-43.0)*NU*Y3PR5/(120960.0*AL1**2*X2)+43.0*Y3PR5/(1209
1 60.0*AL1**2*X2)+43.0*NU*X3PR2*Y3PR3/(20160.0*AL1*X2)+(-43.0)*X3
2 PR2*Y3PR3/(20160.0*AL1*X2)+23.0*X3PR2*Y3PR3/(8064.0*AL1**2*X2)-
3 X3*Y3PR3/AL1**2/378.0+5.0*NU*X2*Y3PR3/(12096.0*AL1)+(-5.0)*X2*Y
4 3PR3/(12096.0*AL1)+17.0*X2*Y3PR3/(20160.0*AL1**2)+(-43.0)*NU*X3
5 PR4*Y3/(13440.0*X2)+(-649.0)*X3PR4*Y3/(30240.0*AL1*X2)+43.0*X3*
6 *4*Y3/(13440.0*X2)+359.0*X3PR3*Y3/(20160.0*AL1)+(-5.0)*NU*X2*X3
7 PR2*Y3/4032.0+(-23.0)*X2*X3PR2*Y3/(3780.0*AL1)+5.0*X2*X3PR2*Y3/
8 4032.0+31.0*X2PR2*X3*Y3/(20160.0*AL1)+(-17.0)*NU*X2PR3*Y3/40320
9 .0+(-5.0)*X2PR3*Y3/(6048.0*AL1)+17.0*X2PR3*Y3/40320.0+55.0*X3PR
: 6/(1344.0*X2*Y3)+(-199.0)*X3PR5/(6720.0*Y3)+73.0*X2*X3PR4/(6720
; .0*Y3)+(-169.0)*X2PR2*X3PR3/(30240.0*Y3)+67.0*X2PR3*X3PR2/(2016
< 0.0*Y3)+(-43.0)*X2PR4*X3/(60480.0*Y3)+43.0*X2PR5/(60480.0*Y3)
K4(10,11) = 41.0*NU*X3*Y3PR4/(120960.0*AL1*X2)+41.0*X3*Y3PR4/(1209
1 60.0*AL1*X2)+(-47.0)*NU*Y3PR4/(241920.0*AL1)+(-13.0)*Y3PR4/(806
2 40.0*AL1)+(-25.0)*NU*X3PR3*Y3PR2/(24192.0*AL1**2*X2)+(-17.0)*NU
3 *X3PR3*Y3PR2/(17280.0*X2)+(-121.0)*X3PR3*Y3PR2/(120960.0*AL1**2

```

```

4  *X2)+(-41.0)*X3PR3*Y3PR2/(40320.0*X2)+47.0*NU*X3PR2*Y3PR2/(8064
5  0.0*AL1**2)+47.0*NU*X3PR2*Y3PR2/80640.0+79.0*X3PR2*Y3PR2/(80640
6  .0*AL1**2)+13.0*X3PR2*Y3PR2/26880.0+83.0*NU*X2*X3*Y3PR2/(120960
7  .0*AL1**2)+(-19.0)*NU*X2*X3*Y3PR2/120960.0+11.0*X2*X3*Y3PR2/(12
8  0960.0*AL1**2)+(-31.0)*X2*X3*Y3PR2/120960.0-NU*X2PR2*Y3PR2/AL1*
9  *2/2688.0-NU*X2PR2*Y3PR2/80640.0+(-13.0)*X2PR2*Y3PR2/(120960.0*
:  AL1**2)+X2PR2*Y3PR2/11520.0+121.0*NU*X3PR5/(40320.0*AL1*X2)+121
;  .0*X3PR5/(40320.0*AL1*X2)+(-109.0)*NU*X3PR4/(80640.0*AL1)+(-79.
<  0)*X3PR4/(26880.0*AL1)+(-37.0)*NU*X2*X3PR3/(20160.0*AL1)+11.0*X
=  2*X3PR3/(20160.0*AL1)+101.0*NU*X2PR2*X3PR2/(80640.0*AL1)+(-3.0)
>  *X2PR2*X3PR2/(8960.0*AL1)+(-31.0)*NU*X2PR3*X3/(40320.0*AL1)-X2P
?  R3*X3/AL1/2688.0+NU*X2PR4/AL1/5760.0+X2PR4/AL1/5760.0
K4(10,12) = 43.0*NU*Y3PR5/(120960.0*AL1**2*X2)+(-43.0)*Y3PR5/(1209
1  60.0*AL1**2*X2)+(-43.0)*NU*X3PR2*Y3PR3/(20160.0*AL1*X2)+43.0*X3
2  PR2*Y3PR3/(20160.0*AL1*X2)+(-23.0)*X3PR2*Y3PR3/(8064.0*AL1**2*X
3  2)+NU*X3*Y3PR3/AL1/2240.0-X3*Y3PR3/AL1/2240.0+23.0*X3*Y3PR3/(80
4  64.0*AL1**2)+5.0*NU*X2*Y3PR3/(24192.0*AL1)+(-5.0)*X2*Y3PR3/(241
5  92.0*AL1)+(-109.0)*X2*Y3PR3/(120960.0*AL1**2)+43.0*NU*X3PR4*Y3/
6  (13440.0*X2)+649.0*X3PR4*Y3/(30240.0*AL1*X2)+(-43.0)*X3PR4*Y3/(
7  13440.0*X2)+(-3.0)*NU*X3PR3*Y3/2240.0+(-379.0)*X3PR3*Y3/(15120.
8  0*AL1)+3.0*X3PR3*Y3/2240.0+(-5.0)*NU*X2*X3PR2*Y3/8064.0+811.0*X
9  2*X3PR2*Y3/(120960.0*AL1)+5.0*X2*X3PR2*Y3/8064.0-NU*X2PR2*X3*Y3
:  /6720.0+13.0*X2PR2*X3*Y3/(5760.0*AL1)+X2PR2*X3*Y3/6720.0+(-11.0
;  )*NU*X2PR3*Y3/20160.0+(-113.0)*X2PR3*Y3/(120960.0*AL1)+11.0*X2P
<  R3*Y3/20160.0+(-55.0)*X3PR6/(1344.0*X2*Y3)+73.0*X3PR5/(1344.0*Y
=  3)+(-23.0)*X2*X3PR4/(2240.0*Y3)+(-151.0)*X2PR2*X3PR3/(20160.0*Y
>  3)+13.0*X2PR3*X3PR2/(5040.0*Y3)-X2PR4*X3/Y3/630.0+43.0*X2PR5/(3
?  0240.0*Y3)

```

C

```

K4(11,11) = 43.0*Y3PR5/(60480.0*X2)+(-23.0)*NU*X3PR2*Y3PR3/(16128.
1  0*X2)+(-43.0)*X3PR2*Y3PR3/(10080.0*AL1*X2)+23.0*X3PR2*Y3PR3/(16
2  128.0*X2)+37.0*NU*X3*Y3PR3/24192.0+X3*Y3PR3/AL1/560.0+(-37.0)*X
3  3*Y3PR3/24192.0+(-127.0)*NU*X2*Y3PR3/24192.0+5.0*X2*Y3PR3/(302
4  4.0*AL1)+127.0*X2*Y3PR3/24192.0+649.0*NU*X3PR4*Y3/(60480.0*AL1
5  *X2)+(-649.0)*X3PR4*Y3/(60480.0*AL1*X2)+43.0*X3PR4*Y3/(6720.0*A
6  L1**2*X2)+(-391.0)*NU*X3PR3*Y3/(24192.0*AL1)+391.0*X3PR3*Y3/(24
7  192.0*AL1)+(-3.0)*X3PR3*Y3/(560.0*AL1**2)+71.0*NU*X2*X3PR2*Y3/(
8  17280.0*AL1)+(-71.0)*X2*X3PR2*Y3/(17280.0*AL1)-X2*X3PR2*Y3/AL1*
9  *2/315.0+NU*X2PR2*X3*Y3/AL1/288.0-X2PR2*X3*Y3/AL1/288.0+X2PR2*X
:  3*Y3/AL1**2/840.0-NU*X2PR3*Y3/AL1/576.0+X2PR3*Y3/AL1/576.0+X2PR
;  3*Y3/AL1**2/560.0+(-55.0)*NU*X3PR6/(2688.0*AL1**2*X2*Y3)+55.0*X
<  3PR6/(2688.0*AL1**2*X2*Y3)+177.0*NU*X3PR5/(4480.0*AL1**2*Y3)+(-
=  177.0)*X3PR5/(4480.0*AL1**2*Y3)+(-57.0)*NU*X2*X3PR4/(4480.0*AL1
>  **2*Y3)+57.0*X2*X3PR4/(4480.0*AL1**2*Y3)+(-223.0)*NU*X2PR2*X3PR
?  3/(15120.0*AL1**2*Y3)+223.0*X2PR2*X3PR3/(15120.0*AL1**2*Y3)+11.
@  0*NU*X2PR3*X3PR2/(1680.0*AL1**2*Y3)+(-11.0)*X2PR3*X3PR2/(1680.0
1  *AL1**2*Y3)+107.0*NU*X2PR4*X3/(30240.0*AL1**2*Y3)+(-107.0)*X2PR
2  4*X3/(30240.0*AL1**2*Y3)+(-61.0)*NU*X2PR5/(30240.0*AL1**2*Y3)+6
3  1.0*X2PR5/(30240.0*AL1**2*Y3)
K4(11,12) = (-41.0)*NU*X3*Y3PR4/(120960.0*AL1*X2)+(-41.0)*X3*Y3PR4

```

```

1 /(120960.0*AL1*X2)+13.0*NU*Y3PR4/(80640.0*AL1)+13.0*Y3PR4/(8064
2 0.0*AL1)+25.0*NU*X3PR3*Y3PR2/(24192.0*AL1**2*X2)+17.0*NU*X3PR3*
3 Y3PR2/(17280.0*X2)+121.0*X3PR3*Y3PR2/(120960.0*AL1**2*X2)+41.0*
4 X3PR3*Y3PR2/(40320.0*X2)+(-13.0)*NU*X3PR2*Y3PR2/(26880.0*AL1**2
5 )+(-11.0)*NU*X3PR2*Y3PR2/8960.0+(-79.0)*X3PR2*Y3PR2/(80640.0*AL
6 1**2)+(-59.0)*X3PR2*Y3PR2/80640.0+(-83.0)*NU*X2*X3*Y3PR2/(12096
7 0.0*AL1**2)+5.0*NU*X2*X3*Y3PR2/24192.0+(-11.0)*X2*X3*Y3PR2/(120
8 960.0*AL1**2)+(-47.0)*X2*X3*Y3PR2/120960.0+37.0*NU*X2PR2*Y3PR2/
9 (120960.0*AL1**2)+NU*X2PR2*Y3PR2/120960.0+13.0*X2PR2*Y3PR2/(120
: 960.0*AL1**2)+5.0*X2PR2*Y3PR2/24192.0+(-121.0)*NU*X3PR5/(40320.
; 0*AL1*X2)+(-121.0)*X3PR5/(40320.0*AL1*X2)+281.0*NU*X3PR4/(80640
< .0*AL1)+281.0*X3PR4/(80640.0*AL1)+5.0*NU*X2*X3PR3/(4032.0*AL1)+
= 5.0*X2*X3PR3/(4032.0*AL1)-NU*X2PR2*X3PR2/AL1/630.0-X2PR2*X3PR2/
> AL1/630.0-NU*X2PR3*X3/AL1/1680.0-X2PR3*X3/AL1/1680.0+17.0*NU*X2
? PR4/(60480.0*AL1)+17.0*X2PR4/(60480.0*AL1)

```

C

```

K4(12,12) = (-43.0)*NU*Y3PR5/(120960.0*AL1**2*X2)+43.0*Y3PR5/(1209
1 60.0*AL1**2*X2)+43.0*NU*X3PR2*Y3PR3/(20160.0*AL1*X2)+(-43.0)*X3
2 PR2*Y3PR3/(20160.0*AL1*X2)+23.0*X3PR2*Y3PR3/(8064.0*AL1**2*X2)-
3 NU*X3*Y3PR3/AL1/1120.0+X3*Y3PR3/AL1/1120.0+(-37.0)*X3*Y3PR3/(12
4 096.0*AL1**2)+(-5.0)*NU*X2*Y3PR3/(6048.0*AL1)+5.0*X2*Y3PR3/(604
5 8.0*AL1)+127.0*X2*Y3PR3/(120960.0*AL1**2)+(-43.0)*NU*X3PR4*Y3/(
6 13440.0*X2)+(-649.0)*X3PR4*Y3/(30240.0*AL1*X2)+43.0*X3PR4*Y3/(1
7 3440.0*X2)+3.0*NU*X3PR3*Y3/1120.0+391.0*X3PR3*Y3/(12096.0*AL1)+
8 (-3.0)*X3PR3*Y3/1120.0+NU*X2*X3PR2*Y3/630.0+(-71.0)*X2*X3PR2*Y3
9 /(8640.0*AL1)-X2*X3PR2*Y3/630.0-NU*X2PR2*X3*Y3/1680.0-X2PR2*X3*
: Y3/AL1/144.0+X2PR2*X3*Y3/1680.0-NU*X2PR3*Y3/1120.0+X2PR3*Y3/AL1
; /288.0+X2PR3*Y3/1120.0+55.0*X3PR6/(1344.0*X2*Y3)+(-177.0)*X3PR5
< /(2240.0*Y3)+57.0*X2*X3PR4/(2240.0*Y3)+223.0*X2PR2*X3PR3/(7560.
= 0*Y3)+(-11.0)*X2PR3*X3PR2/(840.0*Y3)+(-107.0)*X2PR4*X3/(15120.0
> *Y3)+61.0*X2PR5/(15120.0*Y3)

```

C

C

C

```

DO 100 I = 1, 12
DO 100 J = I, 12
K4(I,J) = F * K4(I,J)
K4(J,I) = K4(I,J)

```

```

100 CONTINUE

```

C

C

C

```

RETURN
END

```

## A.8 LISTING OF THE SUBROUTINE TSHM0

This subroutine is used to generate the mass matrix  $M_0$ .

```

C
C
C SUBROUTINE TSHM0 ( X2, Y3, RHO, TH, M0 )
C
C Form the M0 matrix for plane triangular element.
C
C Arguments:
C
C   X2, Y3      — Geometry to define the triangle.
C   RHO         — Mass density per unit volume.
C   TH         — Element Thickness.
C   M0(12,12)  — Output mass matrix.
C
C
C IMPLICIT INTEGER ( A - Z )
C
C   REAL  X2, Y3, RHO, TH, F, F1, F2, F3, F4, F5
C
C   REAL  M0(12,12)
C
C
C
C   F = X2 * Y3 * RHO * TH
C   F1 = F / 60.0
C   F2 = -F / 360.0
C   F3 = -F / 90.0
C   F4 = F * 4.0 / 45.0
C   F5 = F * 2.0 / 45.0
C
C   CALL INIT ( M0, 144 )
C
C
C
C
C   M0(1,1) = F1
C   M0(2,2) = F1
C   M0(3,3) = F1
C   M0(4,4) = F1
C   M0(5,5) = F1
C   M0(6,6) = F1
C

```

```

      M0(7,7) = F4
      M0(8,8) = F4
      M0(9,9) = F4
      M0(10,10) = F4
      M0(11,11) = F4
      M0(12,12) = F4
C
      M0(1,3) = F2
      M0(1,5) = F2
      M0(1,9) = F3
      M0(2,4) = F2
      M0(2,6) = F2
      M0(2,10) = F3
      M0(3,5) = F2
      M0(3,11) = F3
      M0(4,6) = F2
      M0(4,12) = F3
      M0(5,7) = F3
      M0(6,8) = F3
      M0(7,9) = F5
      M0(7,11) = F5
      M0(8,10) = F5
      M0(8,12) = F5
      M0(9,11) = F5
      M0(10,12) = F5
C
C
C
      DO 100 I = 2, 12
      DO 100 J = 1, I-1
        M0(I,J) = M0(J,I)
100  CONTINUE
C
C
C
      RETURN
      END

```

## A.10 LISTING OF THE SUBROUTINE TSHM2

This subroutine is used to generate the mass matrix  $M_2$ .

```

SUBROUTINE TSHM2 ( X2, X3, Y3, E, RHO, TH, NU, M2 )
C
C
C Form the M2 matrix for plane triangular element.
C
C Arguments:
C
C   X2, X3, Y3   —   Geometry to define the triangle.
C   E            —   Young's Modulus.
C   RHO          —   Mass density per unit volume.
C   TH           —   Element Thickness.
C   NU           —   Poisson's Ratio
C   M2(12,12)    —   Output mass matrix.
C
C
C IMPLICIT INTEGER ( A - Z )
C
C   REAL  X2, X3, Y3, E, RHO, TH, NU, BETA, AL1, F
C   REAL  X2TWO, X2THR, X3TWO, X3THR, X3FOR, Y3THR
C
C   REAL  M2(12,12), M2X(6,6), M2Y(6,6)
C
C
C CALL INIT ( M2X, 36 )
C CALL INIT ( M2Y, 36 )
C CALL INIT ( M2, 144 )
C
C   AL1   = 2.0 * ( 1 - NU ) / ( 1 - 2.0*NU )
C   BETA  = 2.0 * ( 1 + NU ) * RHO / E
C   F     = RHO * TH * BETA
C
C   X2TWO = X2 * X2
C   X2THR = X2TWO * X2
C
C   X3TWO = X3 * X3
C   X3THR = X3TWO * X3
C   X3FOR = X3THR * X3
C
C   Y3THR = Y3 * Y3 * Y3

```

C  
C  
C
$$M2X(1,1) = (-11.0) \cdot X3TWO \cdot Y3THR / (20160.0 \cdot X2) + X3 \cdot Y3THR / 10080.0 + X2 \cdot Y3THR / 20160.0 + (-11.0) \cdot X3FOR \cdot Y3 / (20160.0 \cdot AL1 \cdot X2) + X3THR \cdot Y3 / AL1 / 1260.0 - X2 \cdot X3TWO \cdot Y3 / AL1 / 3360.0 + X2TWO \cdot X3 \cdot Y3 / AL1 / 2520.0 + X2THR \cdot Y3 / AL1 / 20160.0$$

$$M2X(1,2) = (-11.0) \cdot X3TWO \cdot Y3THR / (20160.0 \cdot X2) + 11.0 \cdot X3 \cdot Y3THR / 20160.0 + (-53.0) \cdot X2 \cdot Y3THR / 120960.0 + (-11.0) \cdot X3FOR \cdot Y3 / (20160.0 \cdot AL1 \cdot X2) + X3THR \cdot Y3 / AL1 / 2016.0 - X2 \cdot X3TWO \cdot Y3 / AL1 / 6720.0 - X2TWO \cdot X3 \cdot Y3 / AL1 / 1680.0 + 31.0 \cdot X2THR \cdot Y3 / (120960.0 \cdot AL1)$$

$$M2X(1,3) = X3TWO \cdot Y3THR / X2 / 840.0 - X3 \cdot Y3THR / 840.0 + 31.0 \cdot X2 \cdot Y3THR / 120960.0 + X3FOR \cdot Y3 / (AL1 \cdot X2) / 840.0 - X3THR \cdot Y3 / AL1 / 420.0 + X2 \cdot X3TWO \cdot Y3 / AL1 / 2016.0 + X2TWO \cdot X3 \cdot Y3 / AL1 / 1680.0 + (-53.0) \cdot X2THR \cdot Y3 / (120960.0 \cdot AL1)$$

$$M2X(1,4) = (-29.0) \cdot X3TWO \cdot Y3THR / (20160.0 \cdot X2) + 41.0 \cdot X3 \cdot Y3THR / 20160.0 + X2 \cdot Y3THR / 5040.0 + (-29.0) \cdot X3FOR \cdot Y3 / (20160.0 \cdot AL1 \cdot X2) + X3THR \cdot Y3 / AL1 / 315.0 - X2 \cdot X3TWO \cdot Y3 / AL1 / 10080.0 - X2TWO \cdot X3 \cdot Y3 / AL1 / 504.0 + 13.0 \cdot X2THR \cdot Y3 / (20160.0 \cdot AL1)$$

$$M2X(1,5) = -X3TWO \cdot Y3THR / X2 / 1120.0 + 19.0 \cdot X3 \cdot Y3THR / 20160.0 + X2 \cdot Y3THR / 3024.0 - X3FOR \cdot Y3 / (AL1 \cdot X2) / 1120.0 + 11.0 \cdot X3THR \cdot Y3 / (5040.0 \cdot AL1) + X2 \cdot X3TWO \cdot Y3 / AL1 / 2016.0 - X2TWO \cdot X3 \cdot Y3 / AL1 / 630.0 + X2THR \cdot Y3 / AL1 / 3024.0$$

$$M2X(1,6) = -X3TWO \cdot Y3THR / X2 / 1120.0 + X3 \cdot Y3THR / 960.0 + 13.0 \cdot X2 \cdot Y3THR / 60.0 - X3FOR \cdot Y3 / (AL1 \cdot X2) / 1120.0 + X3THR \cdot Y3 / AL1 / 1680.0 + X2 \cdot X3TWO \cdot Y3 / AL1 / 1680.0 - X2TWO \cdot X3 \cdot Y3 / AL1 / 1008.0 + X2THR \cdot Y3 / AL1 / 5040.0$$

C

$$M2X(2,2) = (-11.0) \cdot X3TWO \cdot Y3THR / (20160.0 \cdot X2) + X3 \cdot Y3THR / 1008.0 - X2 \cdot Y3THR / 2520.0 + (-11.0) \cdot X3FOR \cdot Y3 / (20160.0 \cdot AL1 \cdot X2) + X3THR \cdot Y3 / AL1 / 5040.0 + X2 \cdot X3TWO \cdot Y3 / AL1 / 2520.0 + X2THR \cdot Y3 / AL1 / 2520.0$$

$$M2X(2,3) = X3TWO \cdot Y3THR / X2 / 840.0 - X3 \cdot Y3THR / 840.0 + 31.0 \cdot X2 \cdot Y3THR / 120960.0 + X3FOR \cdot Y3 / (AL1 \cdot X2) / 840.0 - X2 \cdot X3TWO \cdot Y3 / AL1 / 1440.0 + X2TWO \cdot X3 \cdot Y3 / AL1 / 5040.0 + 31.0 \cdot X2THR \cdot Y3 / (120960.0 \cdot AL1)$$

$$M2X(2,4) = (-29.0) \cdot X3TWO \cdot Y3THR / (20160.0 \cdot X2) + 17.0 \cdot X3 \cdot Y3THR / 20160.0 + X2 \cdot Y3THR / 1260.0 + (-29.0) \cdot X3FOR \cdot Y3 / (20160.0 \cdot AL1 \cdot X2) - X3THR \cdot Y3 / AL1 / 1008.0 + X2 \cdot X3TWO \cdot Y3 / AL1 / 2520.0 + X2THR \cdot Y3 / AL1 / 3360.0$$

$$M2X(2,5) = -X3TWO \cdot Y3THR / X2 / 1120.0 + X3 \cdot Y3THR / 1344.0 + X2 \cdot Y3THR / 1260.0 - X3FOR \cdot Y3 / (AL1 \cdot X2) / 1120.0 + X3THR \cdot Y3 / AL1 / 1680.0 - X2 \cdot X3TWO \cdot Y3 / AL1 / 5040.0 - X2THR \cdot Y3 / AL1 / 2016.0$$

$$M2X(2,6) = -X3TWO \cdot Y3THR / X2 / 1120.0 + 17.0 \cdot X3 \cdot Y3THR / 20160.0 + 23.0 \cdot X2 \cdot Y3THR / 60480.0 - X3FOR \cdot Y3 / (AL1 \cdot X2) / 1120.0 - X3THR \cdot Y3 / AL1 / 1008.0 + 13.0 \cdot X2 \cdot X3TWO \cdot Y3 / (10080.0 \cdot AL1) + X2TWO \cdot X3 \cdot Y3 / AL1 / 2520.0 - X2THR \cdot Y3 / AL1 / 945.0$$

C

$$M2X(3,3) = X2 \cdot Y3THR / 2520.0 + X2 \cdot X3TWO \cdot Y3 / AL1 / 280.0 - X2TWO \cdot X3 \cdot Y3 / AL1 / 840.0 - X2THR \cdot Y3 / AL1 / 2520.0$$

$$M2X(3,4) = -X3TWO \cdot Y3THR / X2 / 420.0 + X3 \cdot Y3THR / 420.0 - X2 \cdot Y3THR / 945.0 - X3FOR \cdot Y3 / (AL1 \cdot X2) / 420.0 + X3THR \cdot Y3 / AL1 / 420.0 - X2 \cdot X3TWO \cdot Y3 / AL1 / 360.0 + X2TWO \cdot X3 \cdot Y3 / AL1 / 2520.0 + 23.0 \cdot X2THR \cdot Y3 / (60480.0 \cdot AL1)$$

$$M2X(3,5) = X3 \cdot Y3THR / 1260.0 - X2 \cdot Y3THR / 2016.0 - X3THR \cdot Y3 / AL1 / 315.0 + X2THR \cdot Y3 / AL1 / 1260.0$$

$$M2X(3,6) = -X3 \cdot Y3THR / 1260.0 + X2 \cdot Y3THR / 3360.0 + X3THR \cdot Y3 / AL1 / 315.0 - X2 \cdot X3TWO \cdot Y3 / AL1 / 210.0 + X2THR \cdot Y3 / AL1 / 1260.0$$



C

$M2X(4,4) = X3TWO*Y3THR/X2/126.0 - X3*Y3THR/126.0 + X2*Y3THR/1890.0 + X3F$   
 1  $OR*Y3/(AL1*X2)/126.0 + (-2.0)*X3THR*Y3/(315.0*AL1) - X2*X3TWO*Y3/AL$   
 2  $1/630.0 - X2THR*Y3/AL1/1512.0$   
 $M2X(4,5) = X3TWO*Y3THR/X2/560.0 + (-17.0)*X3*Y3THR/5040.0 - X2*Y3THR/7$   
 1  $560.0 + X3FOR*Y3/(AL1*X2)/560.0 + X3THR*Y3/AL1/252.0 - X2*X3TWO*Y3/AL$   
 2  $1/420.0 - X2THR*Y3/AL1/3024.0$   
 $M2X(4,6) = X3TWO*Y3THR/X2/560.0 - X3*Y3THR/5040.0 + (-13.0)*X2*Y3THR/7$   
 1  $560.0 + X3FOR*Y3/(AL1*X2)/560.0 + (-2.0)*X3THR*Y3/(315.0*AL1) + 11.0*$   
 2  $X2*X3TWO*Y3/(2520.0*AL1) + X2TWO*X3*Y3/AL1/630.0 + (-13.0)*X2THR*Y3$   
 3  $/(7560.0*AL1)$

C

$M2X(5,5) = -X3*Y3THR/840.0 + X2*Y3THR/1890.0 + X3THR*Y3/AL1/210.0 - X2*X$   
 1  $3TWO*Y3/AL1/630.0 + X2THR*Y3/AL1/1890.0$   
 $M2X(5,6) = -X2*Y3THR/3024.0 + X2*X3TWO*Y3/AL1/630.0 + X2TWO*X3*Y3/AL1/$   
 1  $630.0 - X2THR*Y3/AL1/7560.0$

C

$M2X(6,6) = X3*Y3THR/840.0 - X2*Y3THR/1512.0 - X3THR*Y3/AL1/210.0 + X2*X3$   
 1  $TWO*Y3/AL1/315.0 + X2TWO*X3*Y3/AL1/630.0 + X2THR*Y3/AL1/1890.0$

C

C

C

$M2Y(1,1) = (-11.0)*X3TWO*Y3THR/(20160.0*AL1*X2) + X3*Y3THR/AL1/10080$   
 1  $.0 + X2*Y3THR/AL1/20160.0 + (-11.0)*X3FOR*Y3/(20160.0*X2) + X3THR*Y3/$   
 2  $1260.0 - X2*X3TWO*Y3/3360.0 + X2TWO*X3*Y3/2520.0 + X2THR*Y3/20160.0$   
 $M2Y(1,2) = (-11.0)*X3TWO*Y3THR/(20160.0*AL1*X2) + 11.0*X3*Y3THR/(201$   
 1  $60.0*AL1) + (-53.0)*X2*Y3THR/(120960.0*AL1) + (-11.0)*X3FOR*Y3/(201$   
 2  $60.0*X2) + X3THR*Y3/2016.0 - X2*X3TWO*Y3/6720.0 - X2TWO*X3*Y3/1680.0 +$   
 3  $31.0*X2THR*Y3/120960.0$   
 $M2Y(1,3) = X3TWO*Y3THR/(AL1*X2)/840.0 - X3*Y3THR/AL1/840.0 + 31.0*X2*Y$   
 1  $3THR/(120960.0*AL1) + X3FOR*Y3/X2/840.0 - X3THR*Y3/420.0 + X2*X3TWO*Y$   
 2  $3/2016.0 + X2TWO*X3*Y3/1680.0 + (-53.0)*X2THR*Y3/120960.0$   
 $M2Y(1,4) = (-29.0)*X3TWO*Y3THR/(20160.0*AL1*X2) + 41.0*X3*Y3THR/(201$   
 1  $60.0*AL1) + X2*Y3THR/AL1/5040.0 + (-29.0)*X3FOR*Y3/(20160.0*X2) + X3T$   
 2  $HR*Y3/315.0 - X2*X3TWO*Y3/10080.0 - X2TWO*X3*Y3/504.0 + 13.0*X2THR*Y3$   
 3  $/20160.0$   
 $M2Y(1,5) = -X3TWO*Y3THR/(AL1*X2)/1120.0 + 19.0*X3*Y3THR/(20160.0*AL1$   
 1  $) + X2*Y3THR/AL1/3024.0 - X3FOR*Y3/X2/1120.0 + 11.0*X3THR*Y3/5040.0 + X$   
 2  $2*X3TWO*Y3/2016.0 - X2TWO*X3*Y3/630.0 + X2THR*Y3/3024.0$   
 $M2Y(1,6) = -X3TWO*Y3THR/(AL1*X2)/1120.0 + X3*Y3THR/AL1/960.0 + 13.0*X2$   
 1  $*Y3THR/(20160.0*AL1) - X3FOR*Y3/X2/1120.0 + X3THR*Y3/1680.0 + X2*X3TW$   
 2  $O*Y3/1680.0 - X2TWO*X3*Y3/1008.0 + X2THR*Y3/5040.0$

C

$M2Y(2,2) = (-11.0)*X3TWO*Y3THR/(20160.0*AL1*X2) + X3*Y3THR/AL1/1008.$   
 1  $0 - X2*Y3THR/AL1/2520.0 + (-11.0)*X3FOR*Y3/(20160.0*X2) + X3THR*Y3/50$   
 2  $40.0 + X2*X3TWO*Y3/2520.0 + X2THR*Y3/2520.0$   
 $M2Y(2,3) = X3TWO*Y3THR/(AL1*X2)/840.0 - X3*Y3THR/AL1/840.0 + 31.0*X2*Y$   
 1  $3THR/(120960.0*AL1) + X3FOR*Y3/X2/840.0 - X2*X3TWO*Y3/1440.0 + X2TWO*$   
 2  $X3*Y3/5040.0 + 31.0*X2THR*Y3/120960.0$   
 $M2Y(2,4) = (-29.0)*X3TWO*Y3THR/(20160.0*AL1*X2) + 17.0*X3*Y3THR/(201$

```

1  60.0*AL1)+X2*Y3THR/AL1/1260.0+(-29.0)*X3FOR*Y3/(20160.0*X2)-X3T
2  HR*Y3/1008.0+X2*X3TWO*Y3/2520.0+X2THR*Y3/3360.0
M2Y(2,5) = -X3TWO*Y3THR/(AL1*X2)/1120.0+X3*Y3THR/AL1/1344.0+X2*Y3T
1  HR/AL1/1260.0-X3FOR*Y3/X2/1120.0+X3THR*Y3/1680.0-X2*X3TWO*Y3/50
2  40.0-X2THR*Y3/2016.0
M2Y(2,6) = -X3TWO*Y3THR/(AL1*X2)/1120.0+17.0*X3*Y3THR/(20160.0*AL1
1  )+23.0*X2*Y3THR/(60480.0*AL1)-X3FOR*Y3/X2/1120.0-X3THR*Y3/1008.
2  0+13.0*X2*X3TWO*Y3/10080.0+X2TWO*X3*Y3/2520.0-X2THR*Y3/945.0
C
M2Y(3,3) = X2*Y3THR/AL1/2520.0+X2*X3TWO*Y3/280.0-X2TWO*X3*Y3/840.0
1  -X2THR*Y3/2520.0
M2Y(3,4) = -X3TWO*Y3THR/(AL1*X2)/420.0+X3*Y3THR/AL1/420.0-X2*Y3THR
1  /AL1/945.0-X3FOR*Y3/X2/420.0+X3THR*Y3/420.0-X2*X3TWO*Y3/360.0+X
2  2TWO*X3*Y3/2520.0+23.0*X2THR*Y3/60480.0
M2Y(3,5) = X3*Y3THR/AL1/1260.0-X2*Y3THR/AL1/2016.0-X3THR*Y3/315.0+
1  X2THR*Y3/1260.0
M2Y(3,6) = -X3*Y3THR/AL1/1260.0+X2*Y3THR/AL1/3360.0+X3THR*Y3/315.0
1  -X2*X3TWO*Y3/210.0+X2THR*Y3/1260.0
C
M2Y(4,4) = X3TWO*Y3THR/(AL1*X2)/126.0-X3*Y3THR/AL1/126.0+X2*Y3THR/
1  AL1/1890.0+X3FOR*Y3/X2/126.0+(-2.0)*X3THR*Y3/315.0-X2*X3TWO*Y3/
2  630.0-X2THR*Y3/1512.0
M2Y(4,5) = X3TWO*Y3THR/(AL1*X2)/560.0+(-17.0)*X3*Y3THR/(5040.0*AL1
1  )-X2*Y3THR/AL1/7560.0+X3FOR*Y3/X2/560.0+X3THR*Y3/252.0-X2*X3TWO
2  *Y3/420.0-X2THR*Y3/3024.0
M2Y(4,6) = X3TWO*Y3THR/(AL1*X2)/560.0-X3*Y3THR/AL1/5040.0+(-13.0)*
1  X2*Y3THR/(7560.0*AL1)+X3FOR*Y3/X2/560.0+(-2.0)*X3THR*Y3/315.0+1
2  1.0*X2*X3TWO*Y3/2520.0+X2TWO*X3*Y3/630.0+(-13.0)*X2THR*Y3/7560.
3  0
C
M2Y(5,5) = -X3*Y3THR/AL1/840.0+X2*Y3THR/AL1/1890.0+X3THR*Y3/210.0-
1  X2*X3TWO*Y3/630.0+X2THR*Y3/1890.0
M2Y(5,6) = -X2*Y3THR/AL1/3024.0+X2*X3TWO*Y3/630.0+X2TWO*X3*Y3/630.
1  0-X2THR*Y3/7560.0
C
M2Y(6,6) = X3*Y3THR/AL1/840.0-X2*Y3THR/AL1/1512.0-X3THR*Y3/210.0+X
1  2*X3TWO*Y3/315.0+X2TWO*X3*Y3/630.0+X2THR*Y3/1890.0
C
C
C
IC = 1
C
DO 200 I = 1, 6
  JC = IC
  DO 100 J = 1, 6
    M2(IC,JC) = F * M2X(I,J)
    JC = JC + 2
100  CONTINUE
    IC = IC + 2
200  CONTINUE

```

```
C
C
C
C      IC = 2
C
C      DO 400 I = 1, 6
C          JC = IC
C          DO 300 J = 1, 6
C              M2(IC,JC) = F * M2Y(I,J)
C              JC = JC + 2
300      CONTINUE
C          IC = IC + 2
400  CONTINUE
C
C
C
C      DO 500 I = 2, 12
C          DO 500 J = 1, I-1
C              M2(I,J) = M2(J,I)
500  CONTINUE
C
C
C
C      RETURN
C      END
```

## ***APPENDIX B***

# **NATURAL MODE-SHAPES OF X-29A AIRCRAFT**

## **B.1 SYMMETRIC MODE-SHAPES**

The STARS, GAC, and GVS mode-shapes for the symmetric modes presented in section 3.4.1 along with their corresponding node-lines are given in Figures - B.1.1A-1 through B.1.7A-4. A review of the three sets of results for each mode follows.

### B.1.1 Fuselage First Bending (F1B)

The natural mode-shapes and the corresponding node lines (Figures - B.1.1A-1 through B1.1A-4) agree quite well for all three cases. However, the natural frequency calculated by the STARS is 10.5% higher and the corresponding GAC value is 14% lower than the natural frequency measured by the GVS.

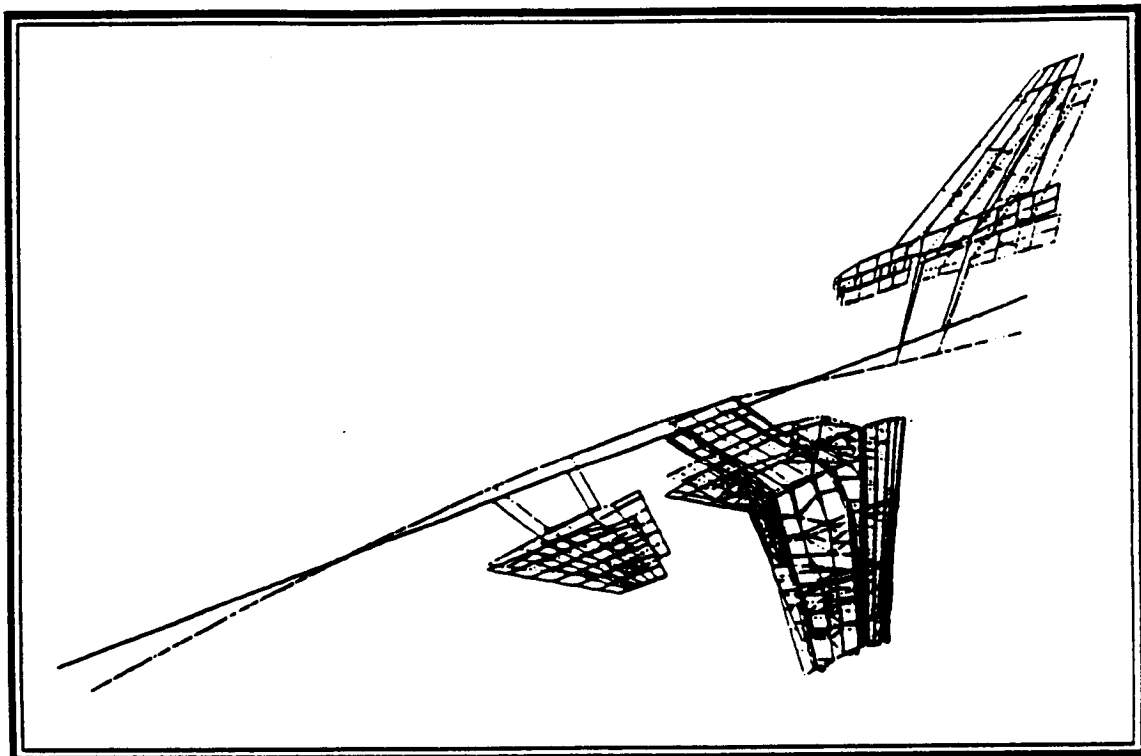
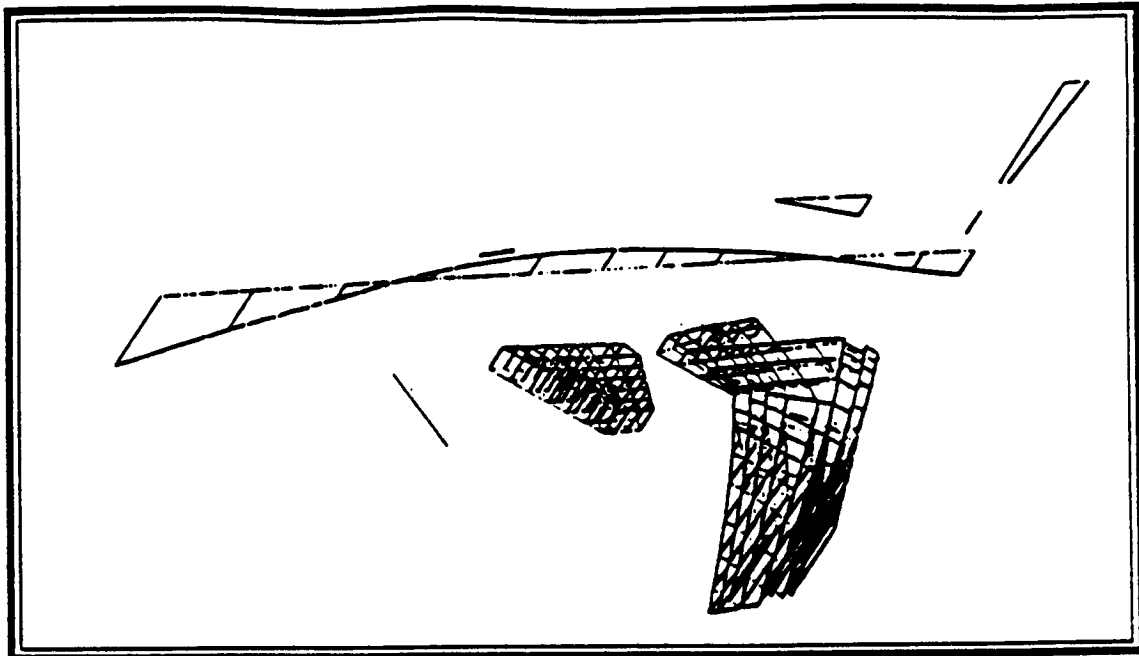
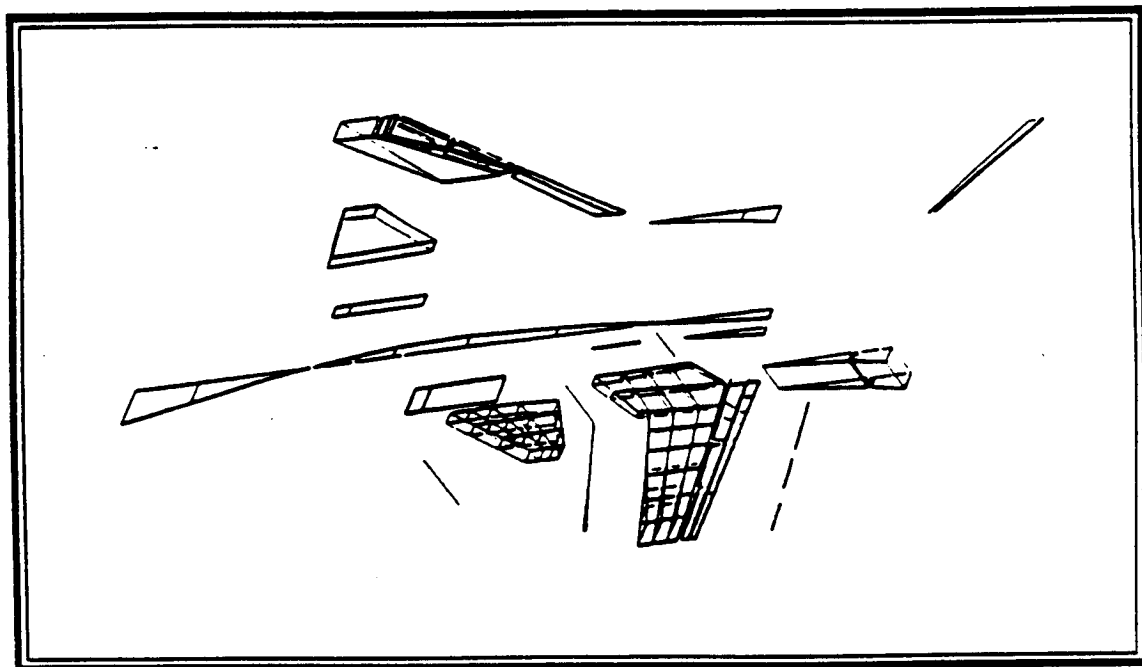


Figure B.1.1A-1 STARS Fuselage First Bending Mode



**Figure B.1.1A-2** GAC Fuselage First Bending Mode



**Figure B.1.1A-3** GVS Fuselage First Bending Mode

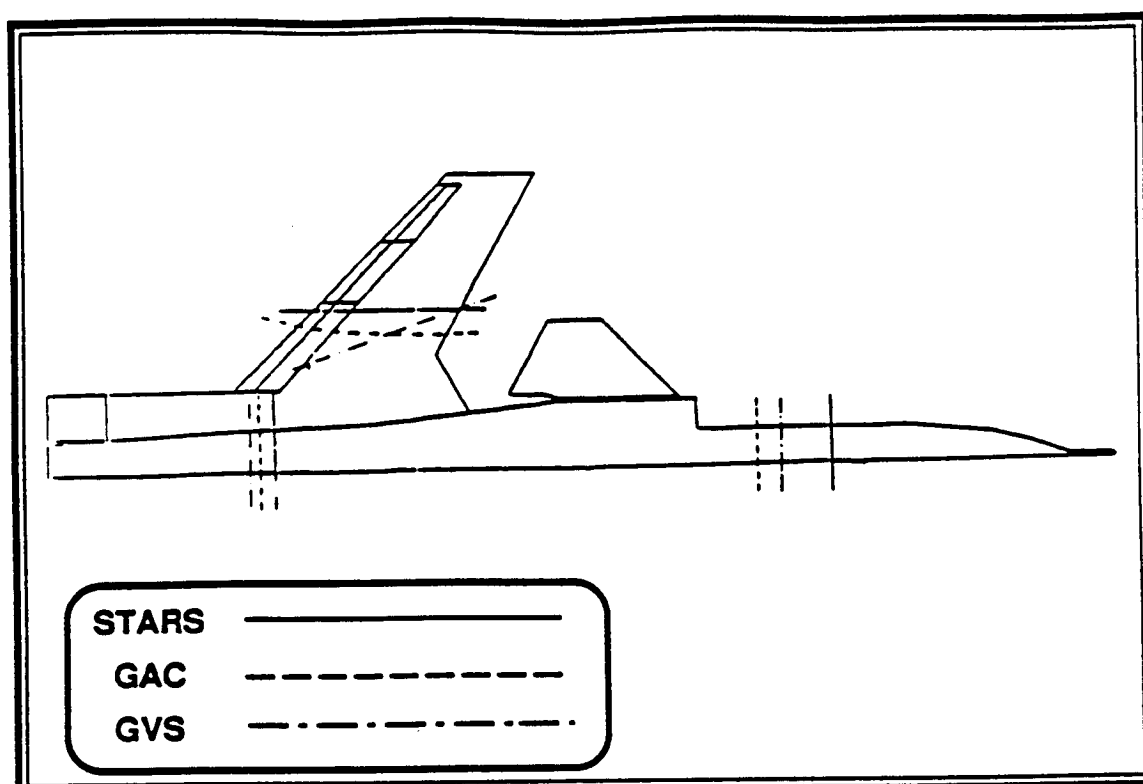


**Figure B.1.1A-4** Fuselage First Bending Node Lines

### **B.1.2 Fuselage Second Bending (F2B)**

Both the STARS and the GAC natural frequencies are significantly lower than the natural frequency measured by the GVS. However, there is good agreement in the outer wing motion (Figures - B.1.2A-1 through B.1.2A-4) among the three sources. The STARS inboard wing node line falls aft, while the GAC node line falls forward of that measured by the GVS. This discrepancy resulted in excessive canard and engine pitching for the GAC case; but this is not evident in either the STARS or the GVS mode-shapes. Also, the relative amplitude of the fuselage calculated by the GAC is very much greater than that calculated by the STARS; as a result, there is gross discrepancy in the generalized mass values

between the two cases.

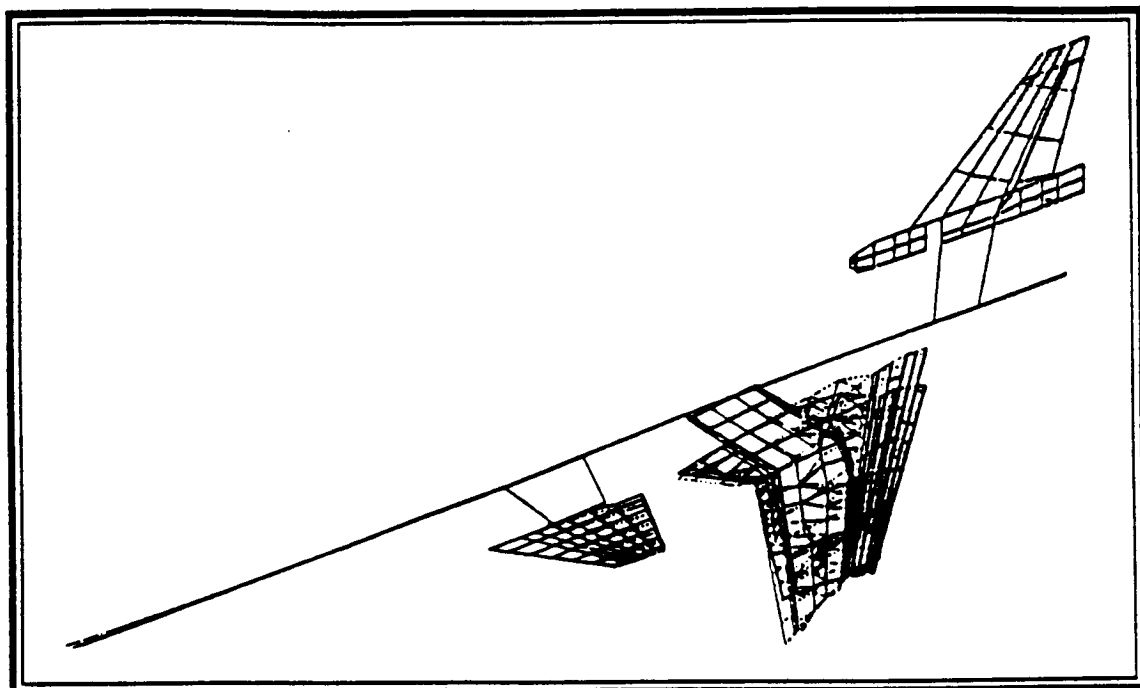


Figure B.1.2A-1 STARS Fuselage Second Bending Mode

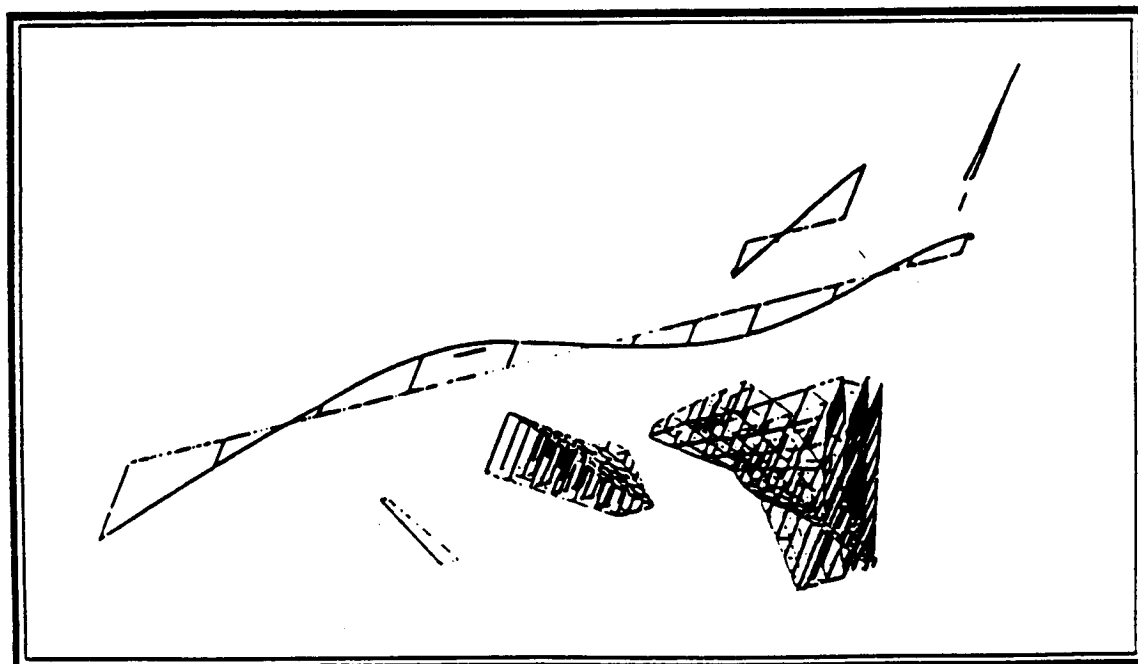


Figure B.1.2A-2 GAC Fuselage Second Bending Mode



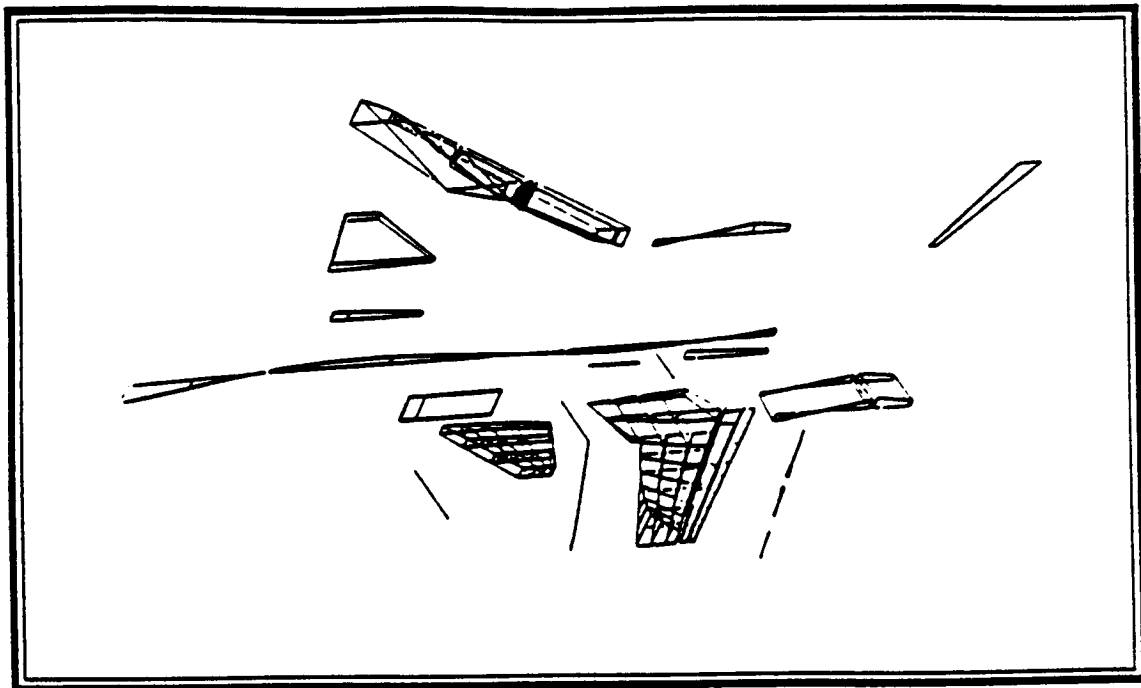


Figure B.1.2A-3 GVS Fuselage Second Bending Mode

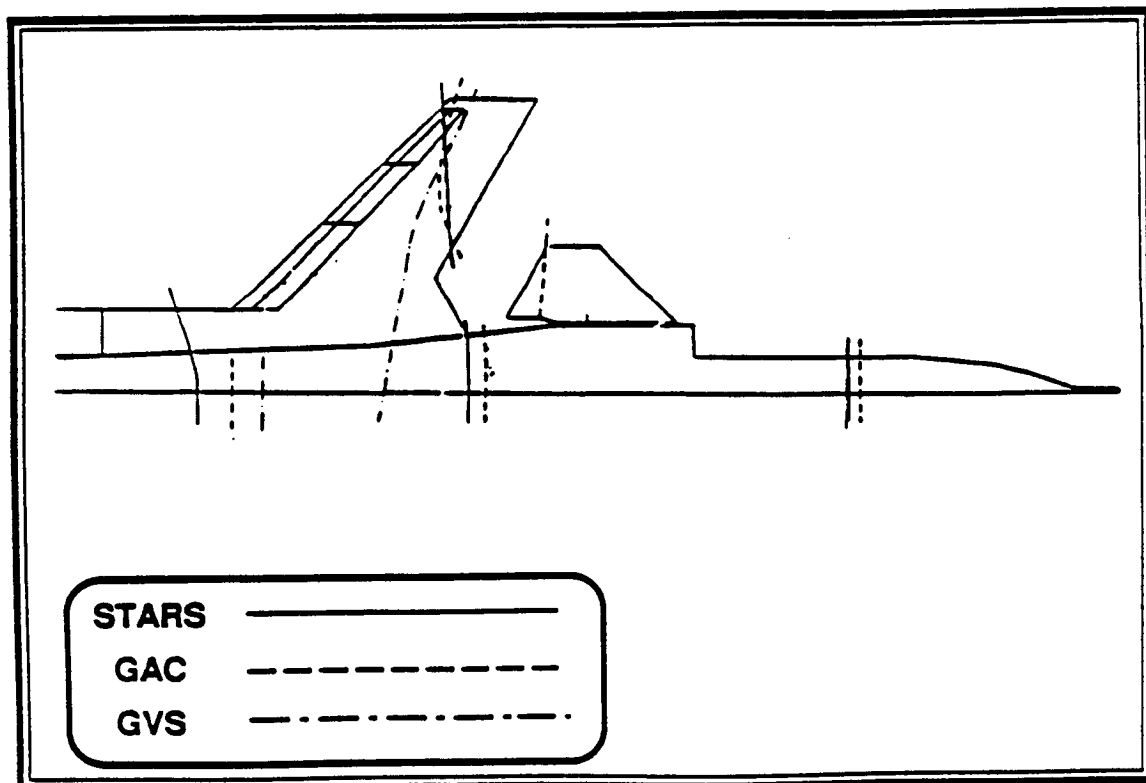
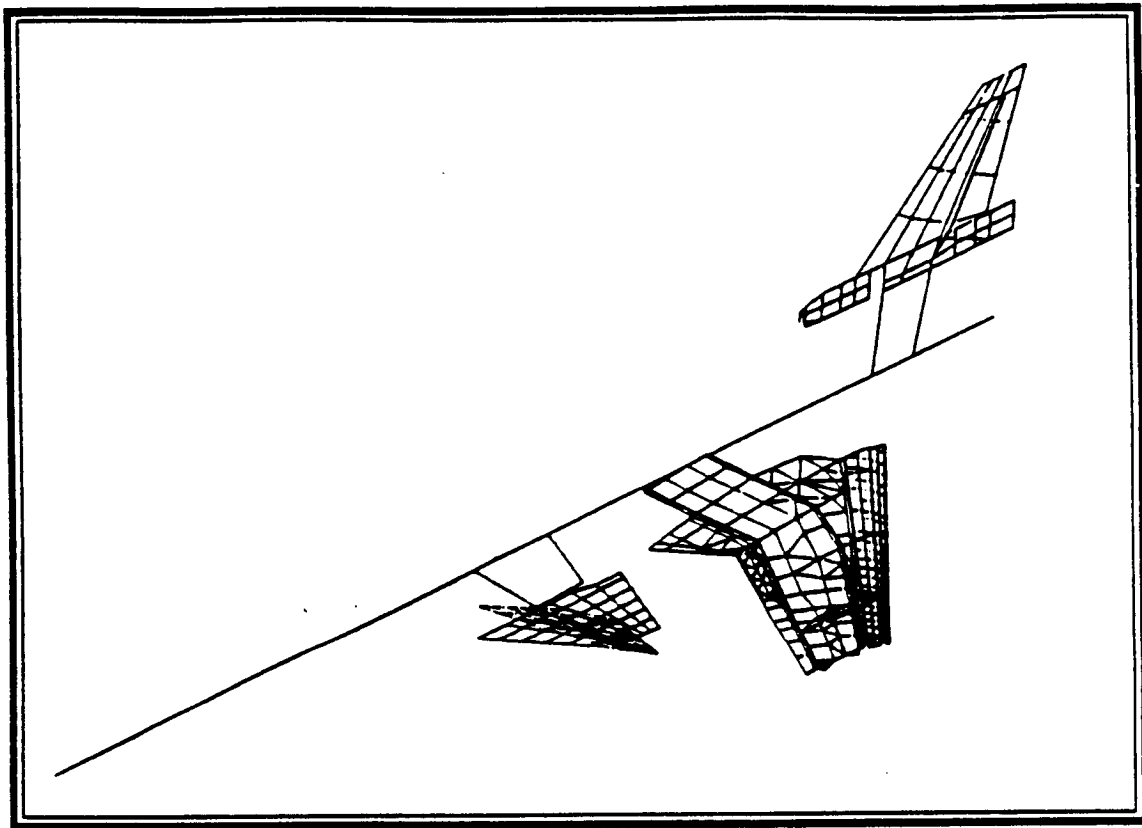


Figure B.1.2A-4 Fuselage Second Bending Node Lines

### B.1.3 Canard Pitch (CP)

The natural frequency, natural mode-shape (Figures - B.1.3A-1 through B.1.3A-4), and the generalized mass derived from all three sources are in good agreement.



**Figure B.1.3A-1 STARS Canard Pitch Mode**

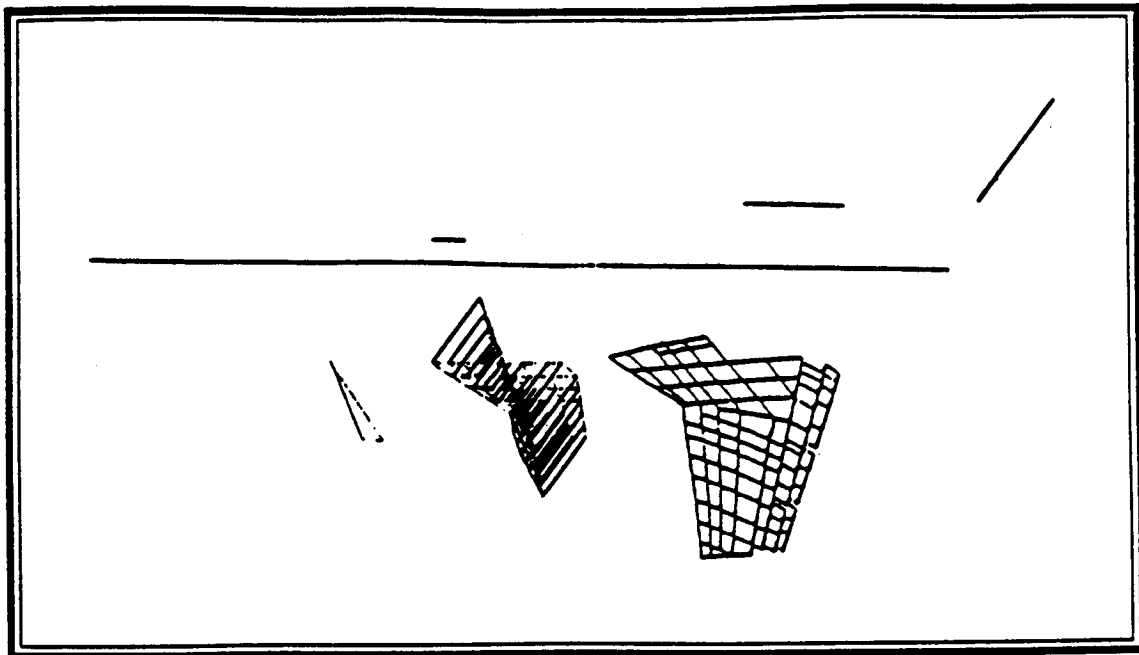


Figure B.1.3A-2 GAC Canard Pitch Mode

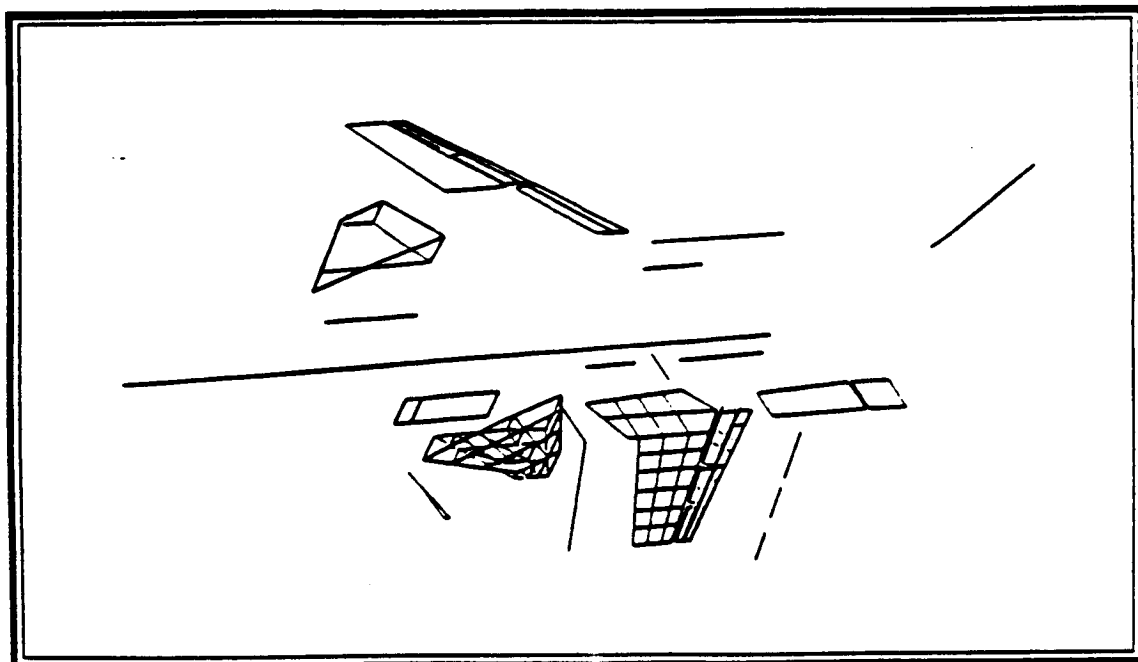


Figure B.1.3A-3 GVS Canard Pitch Mode

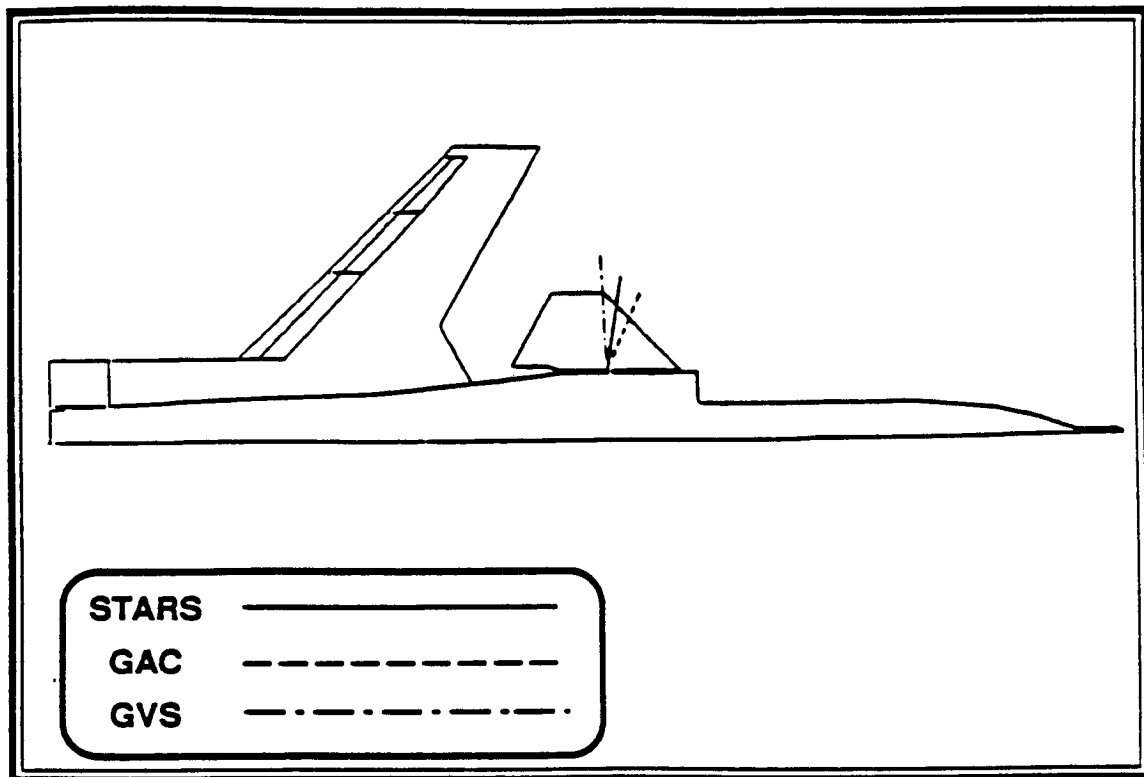


Figure B.1.3A-4 Canard Pitch Node Lines

#### B.1.4 Wing Second Bending (W2B)

There is excellent agreement in the natural frequencies and the natural mode-shapes (Figures - B.1.4A-1 through B.1.4A-4) among the three sources. However, the GAC mode-shape shows a canard pitch node line which is not present in either the STARS or the GVS mode-shapes.

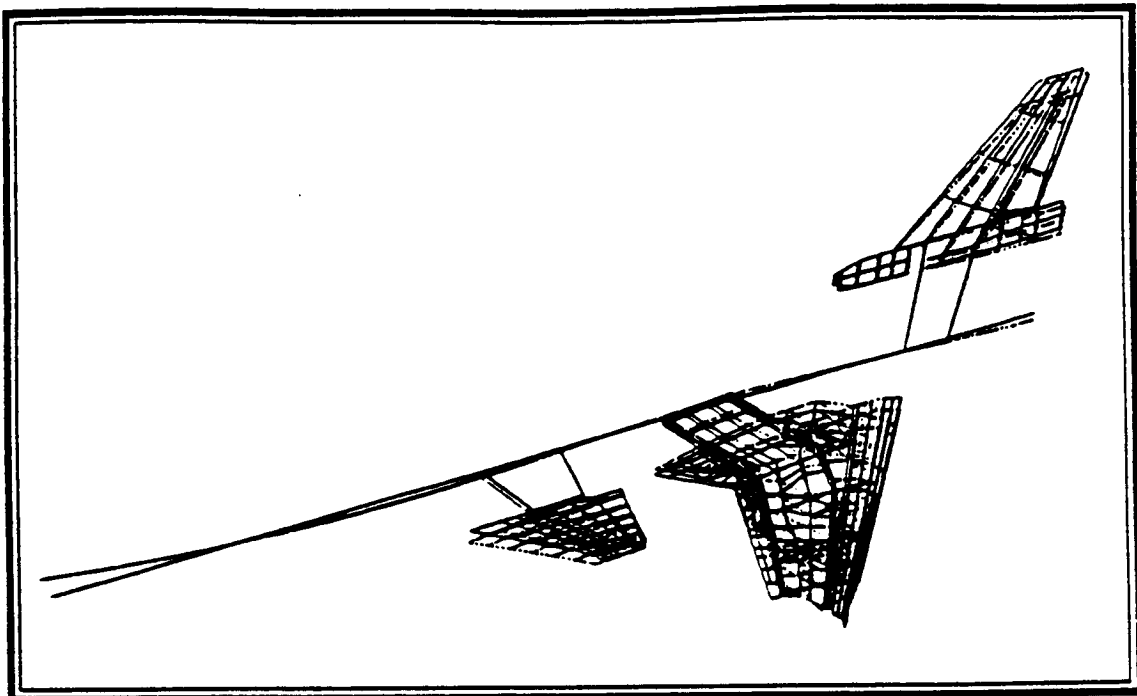


Figure B.1.4A-1 STARS Wing Second Bending Mode

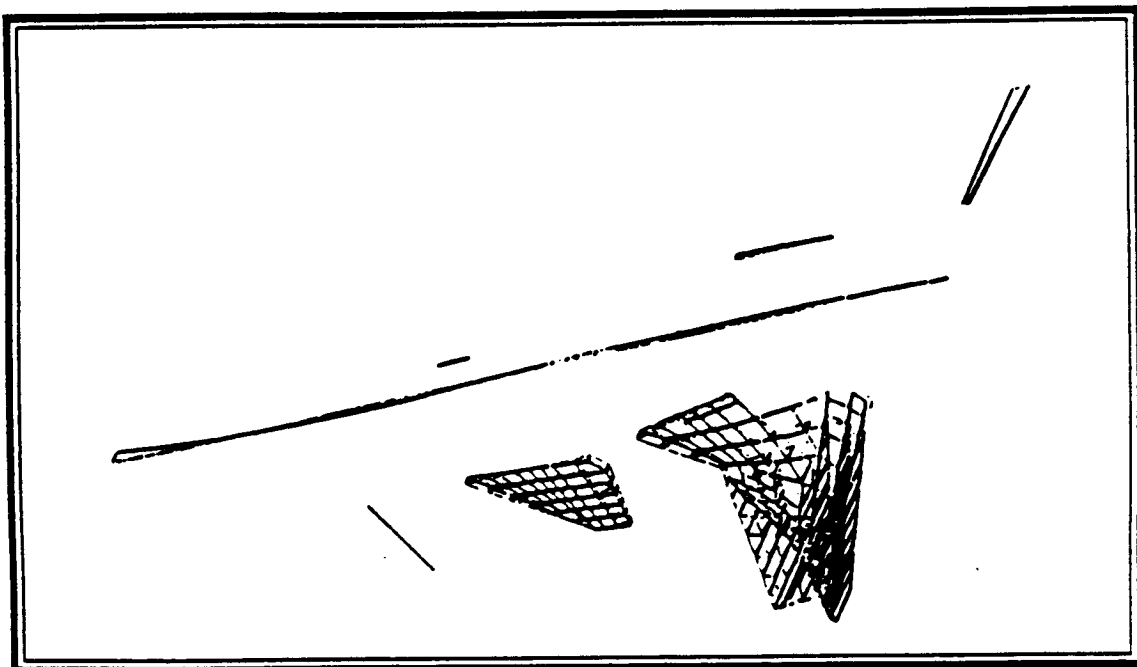


Figure B.1.4A-2 GAC Wing Second Bending Mode

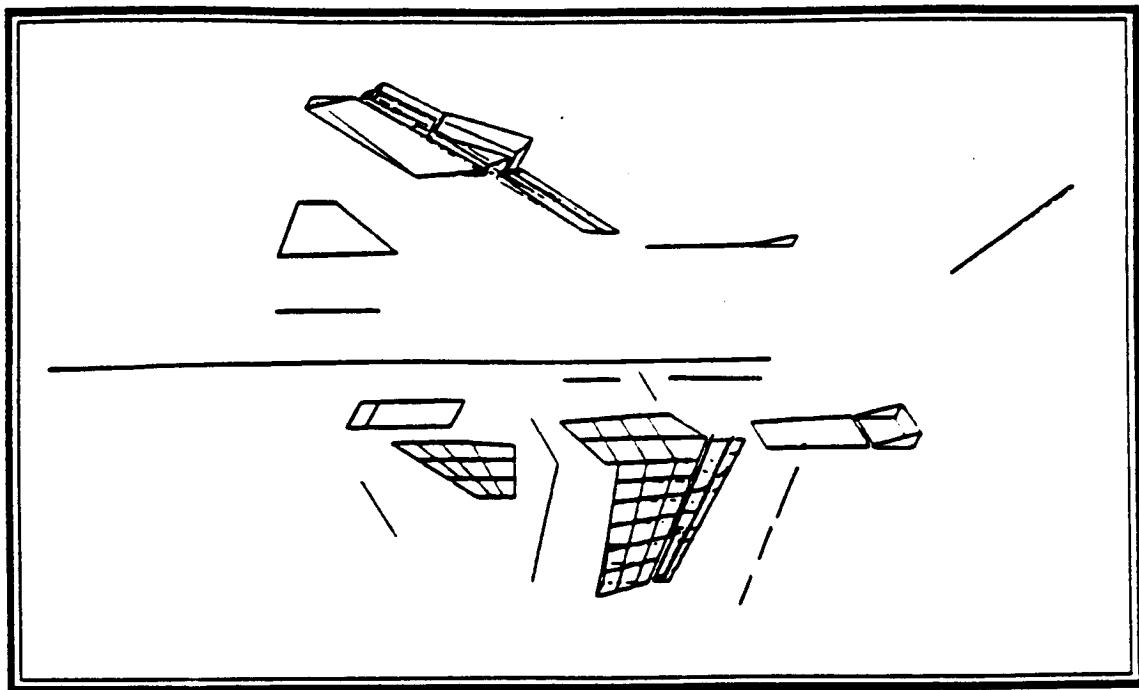


Figure B.1.4A-3 GVS Wing Second Bending Mode

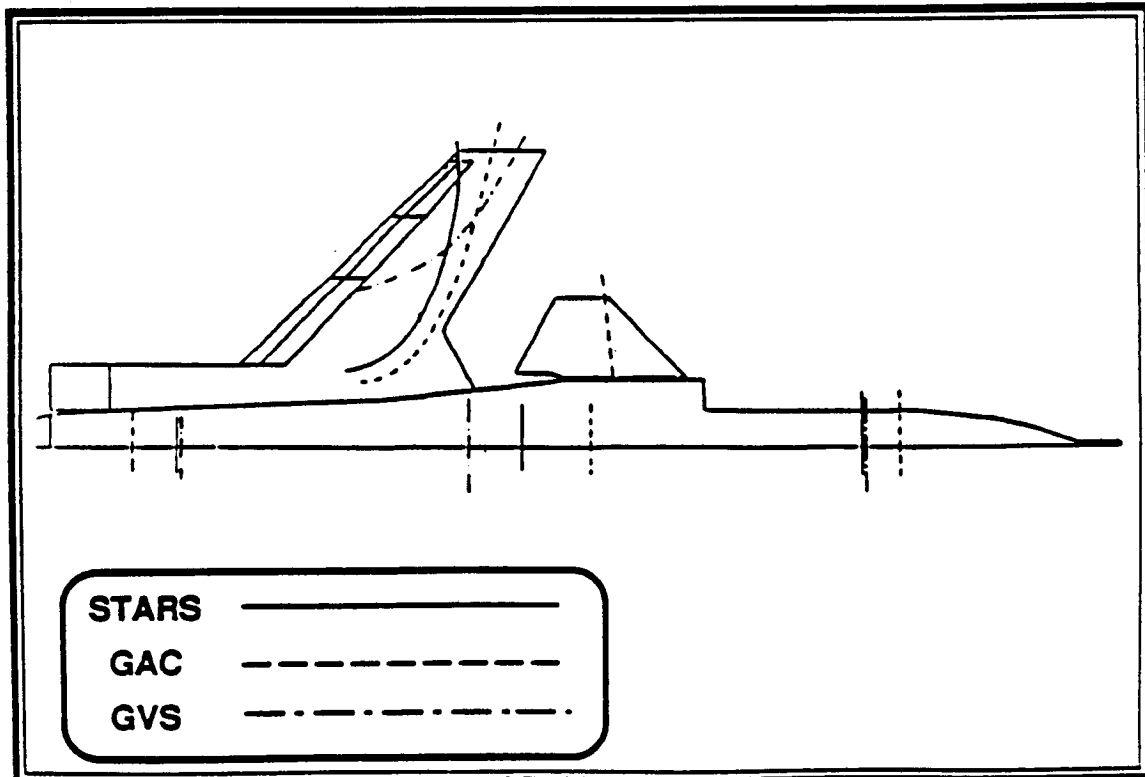


Figure B.1.4A-4 Wing Second Bending Node Lines

### B.1.5 Wing First Torsion (W1T)

Although the STARS calculated natural frequency is somewhat lower than the corresponding GVS value, there is generally good agreement between the STARS and the GVS in the natural mode-shapes and the node lines for the wing structure (Figures - B.1.5A-1 through B.1.5A-4). However, the GAC mode-shape displays significant canard response not indicated by either the STARS or the GVS results.

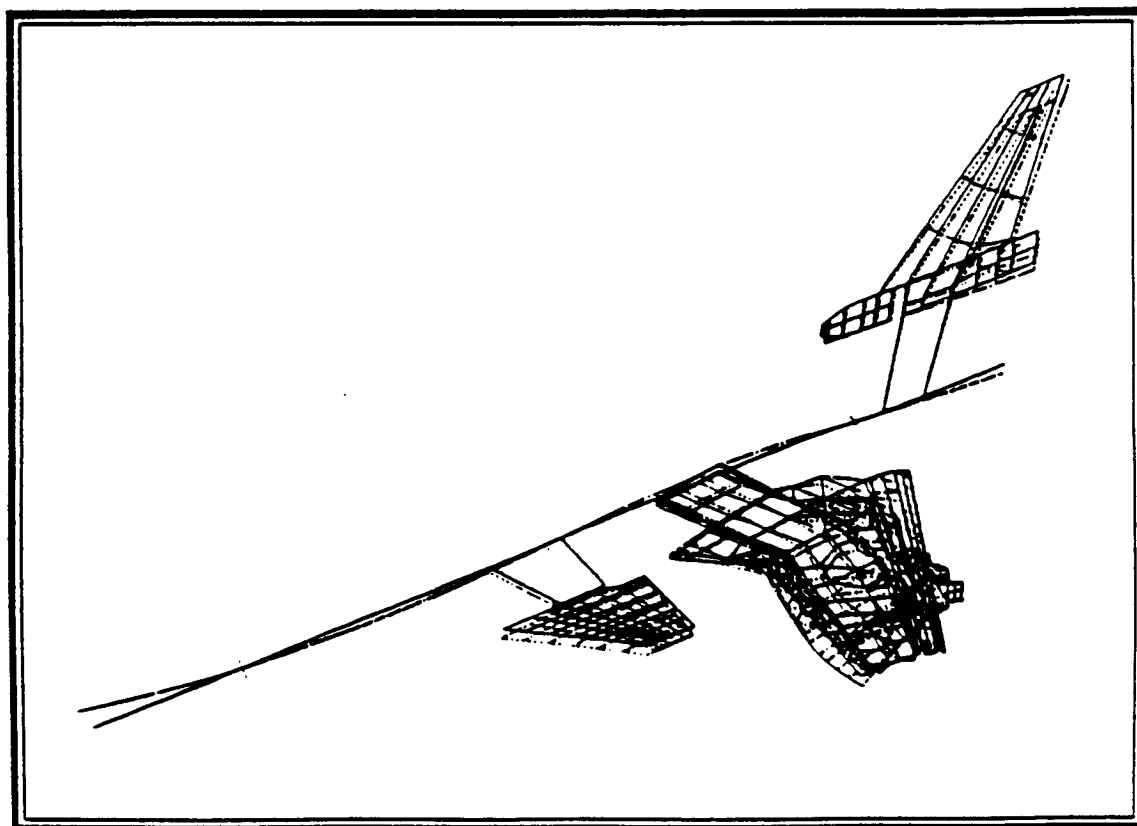


Figure B.1.5A-1 STARS Wing First Torsion Mode

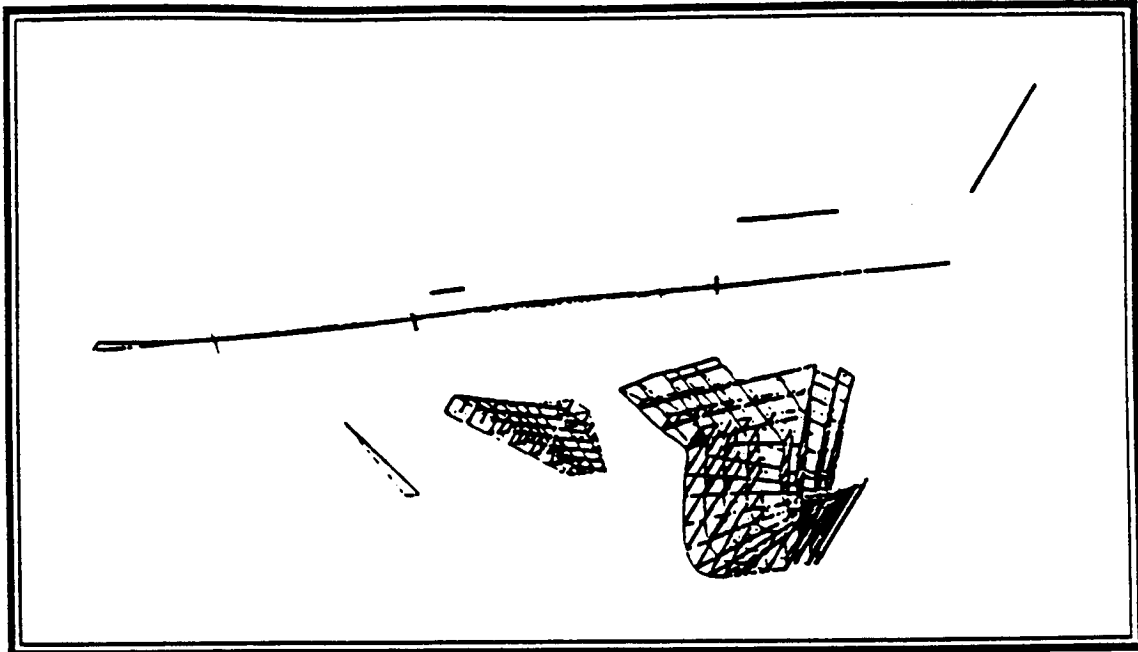


Figure B.1.5A-2 GAC Wing First Torsion Mode

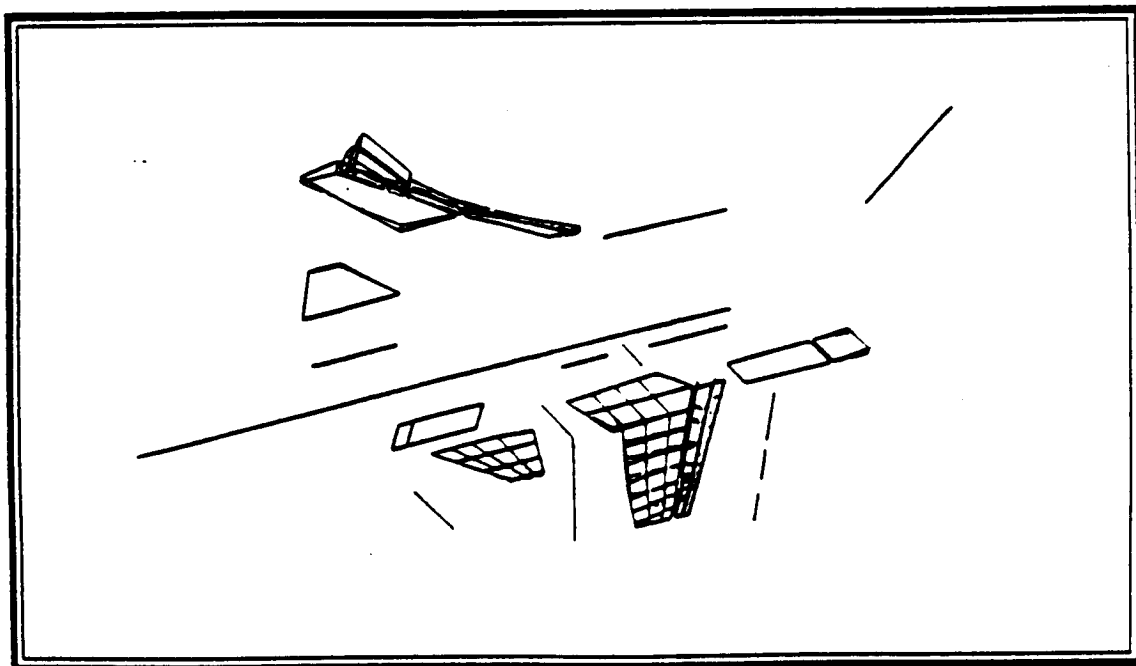


Figure B.1.5A-3 GVS Wing First Torsion Mode



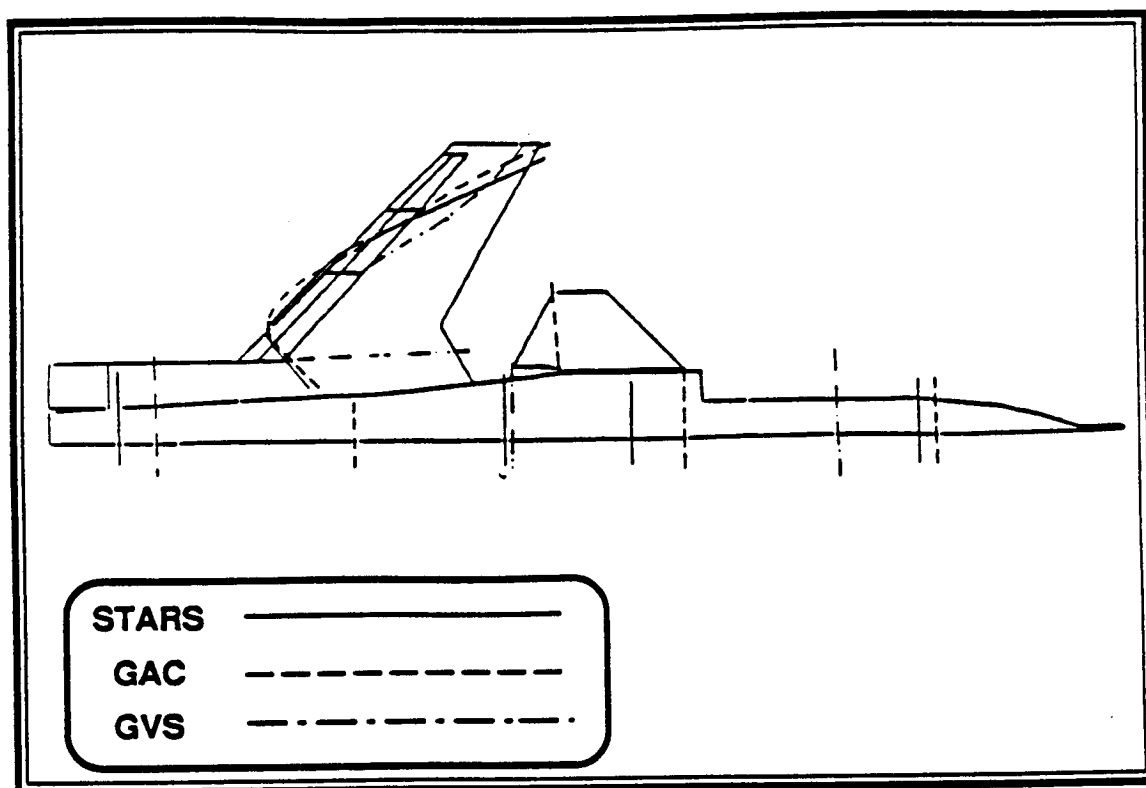


Figure B.1.5A-4 Wing First Torsion Node Lines

### B.1.6 Canard Bending Pitch (CBP)

The natural frequency and generalized mass calculated by the STARS are somewhat higher than those obtained from the GAC or the GVS. The STARS canard node line (Figures - B.1.6A-1 through B.1.6A-4) lies further aft than that in the other two cases. The GAC analysis indicates a wing node line not present in the other two cases. Fuselage node lines from all three sources do not agree very well.

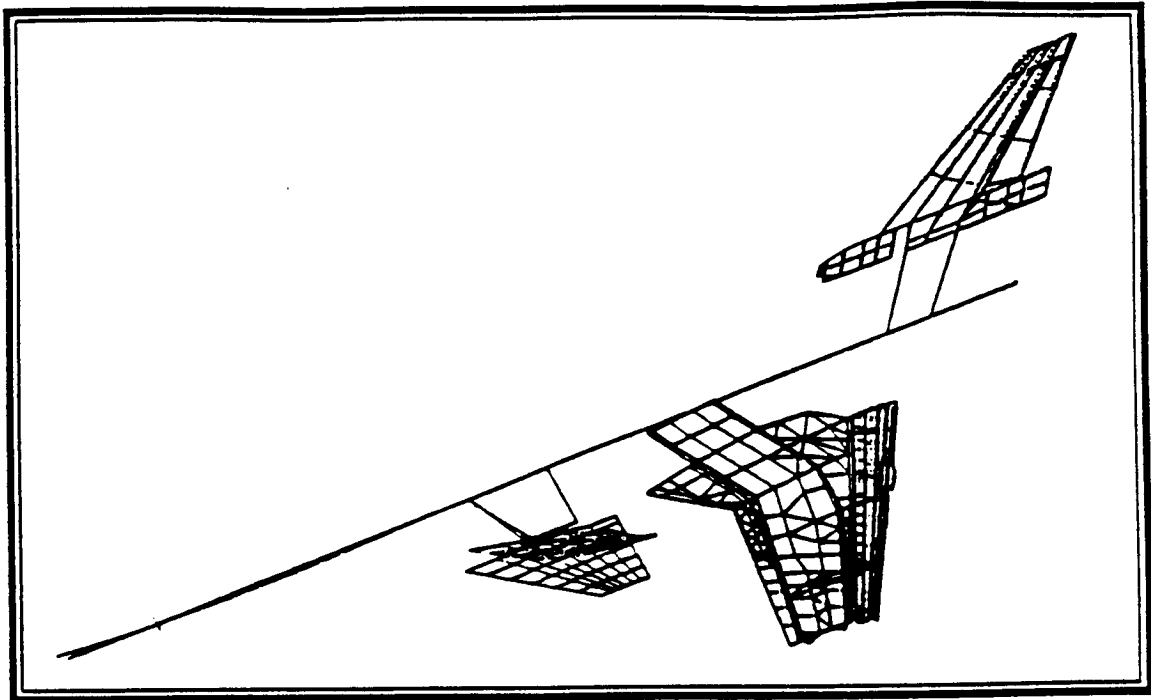


Figure B.1.6A-1 STARS Canard Bending Pitch Mode

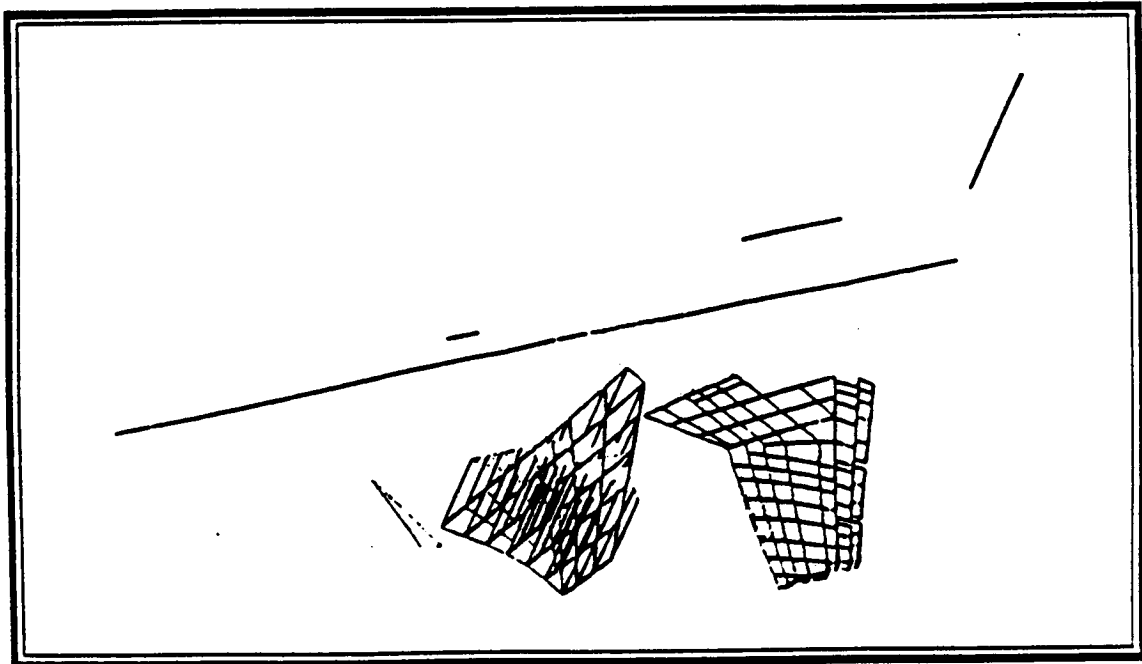


Figure B.1.6A-2 GAC Canard Bending Pitch Mode

The diagram shows a cross-section of a ship's hull. A large, angled structure, possibly a gun turret or radar scanner, is mounted on the deck. The hull has a flat bottom and a slight rise towards the stern. A legend box in the bottom left corner contains the following text:

STARS	_____
GAC	-----
GVS	- . - . - .

238

### B.1.7 Wing Third Bending (W3B)

Very good correspondence exists among all three sources in natural frequency and wing node line (Figures - B.1.7A-1 through B.1.7A-4). The relative amplitude of the fuselage measured by the GVS is much smaller than that calculated by the STARS and the GAC. The reason for this discrepancy may be the lack of fuselage excitation during the GVS. The STARS and the GAC analyses indicate the presence of a node line in the canard; however, there is no such evidence in the GVS results. Relatively large canard motion is obtained from calculated modal data, particularly that calculated by the STARS. But the relative amplitude of the canard obtained by the GVS is almost negligible.

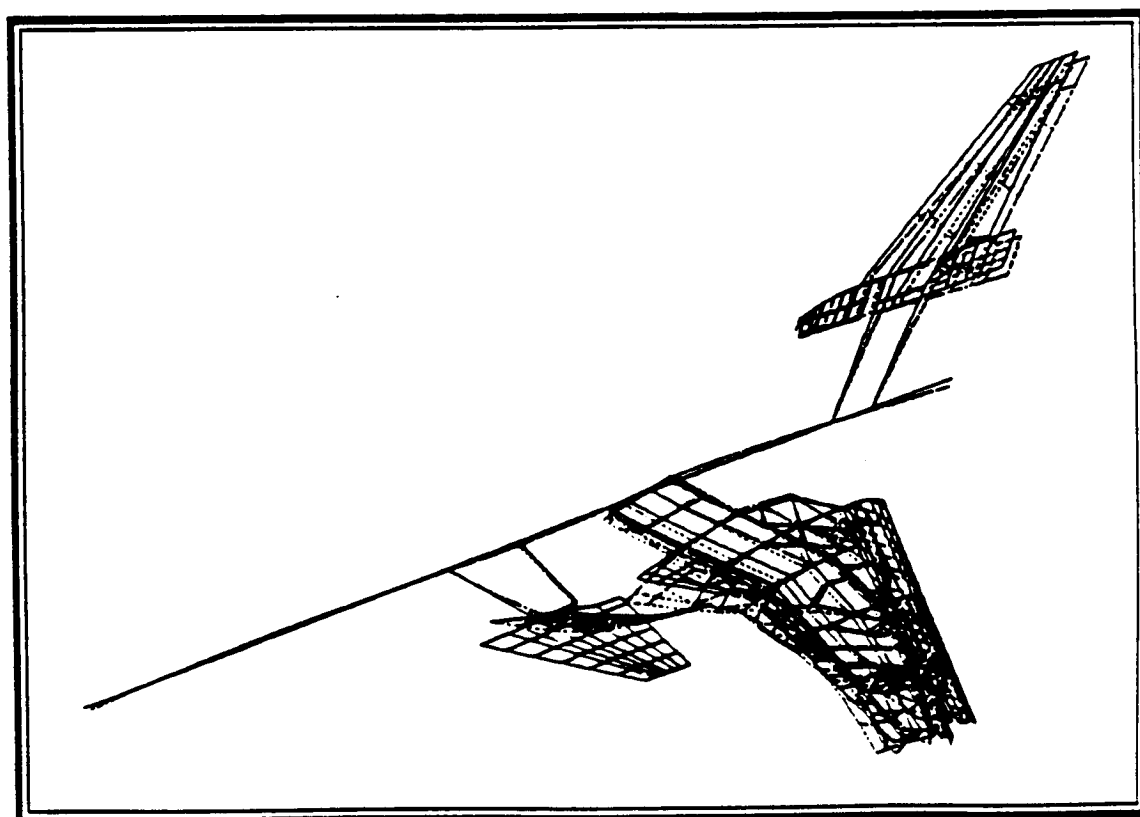


Figure B.1.7A-1 STARS Wing Third Bending Mode

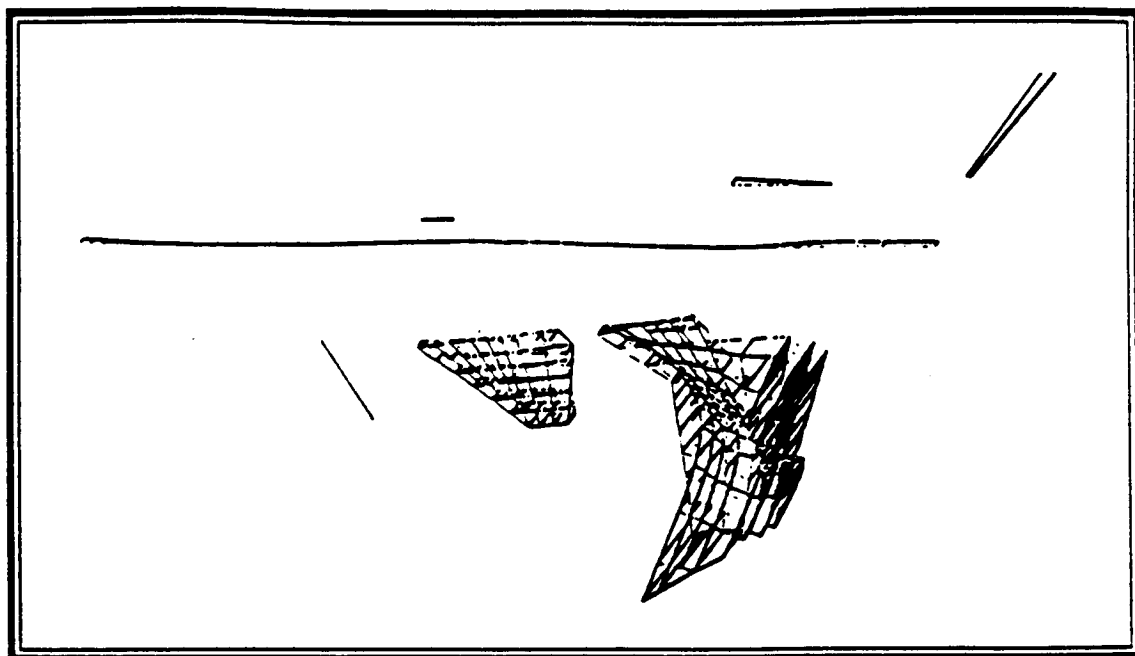


Figure B.1.7A-2 GAC Wing Third Bending Mode

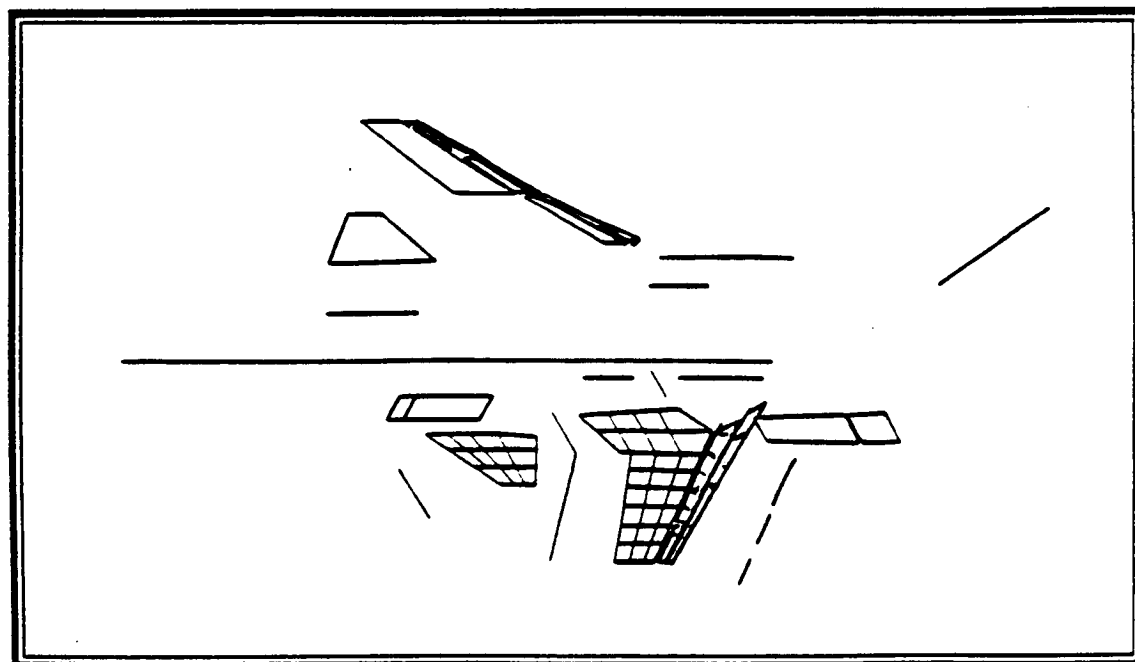


Figure B.1.7A-3 GVS Wing Third Bending Mode

## B.2 ANTI-SYMMETRIC MODE-SHAPES

241

### B.2.1 Vertical Fin First Bending (VF1B)

The STARS natural frequency is 13% higher than the measured natural frequency. Also the generalized mass computed by the STARS is somewhat higher than that of the GVS. However, the corresponding GAC values show better agreement with the measured values. There is good correspondence in the natural mode-shape and the node lines (Figures - B.2.1A-1 through B.2.1A-4) among the three sources.

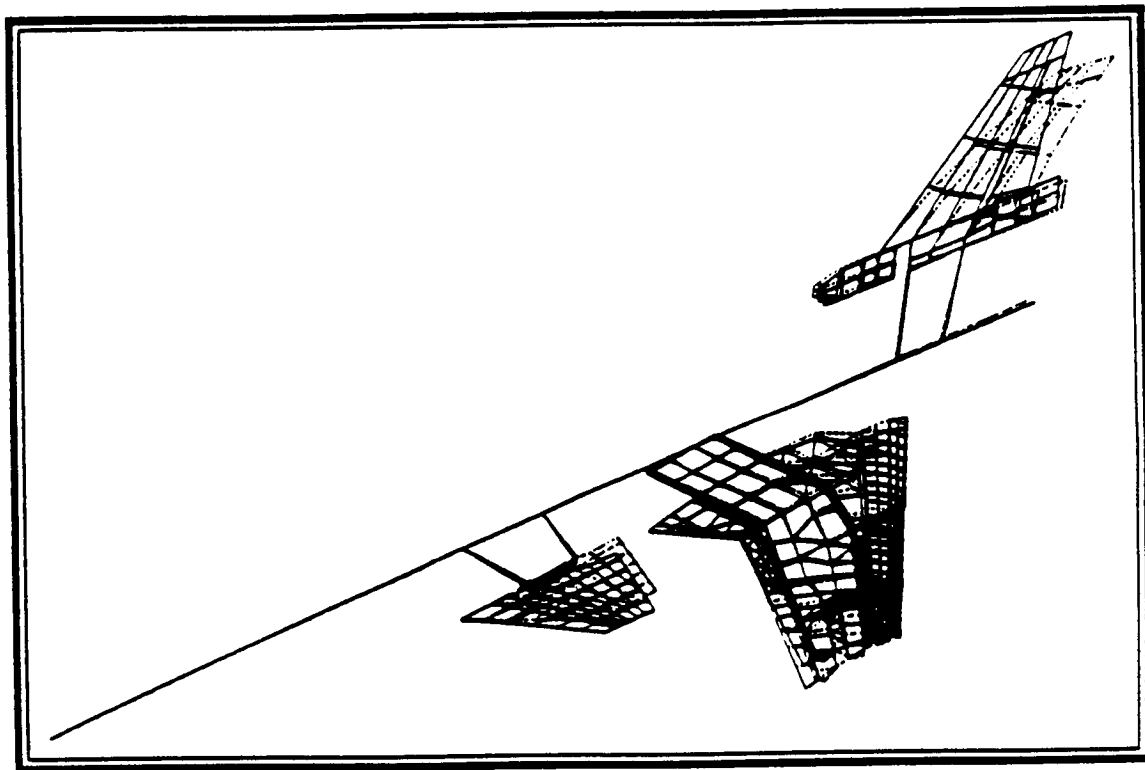


Figure B.2.1A-1 STARS Vertical Fin First Bending Mode

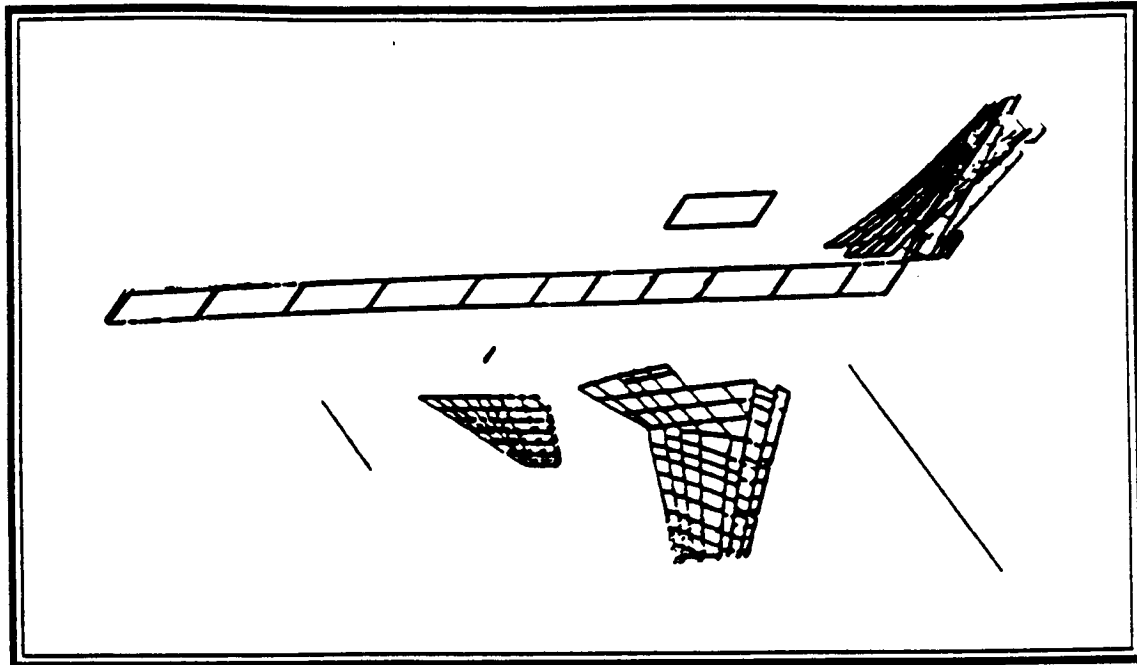


Figure B.2.1A-2 GAC Vertical Fin First Bending Mode

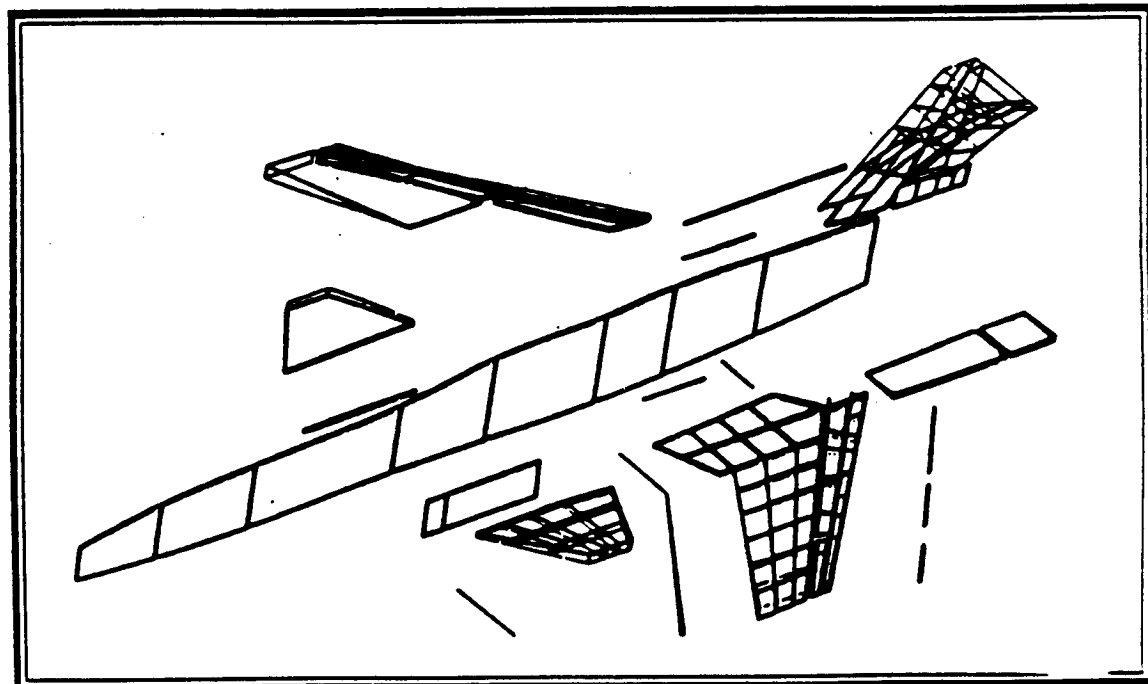


Figure B.2.1A-3 GVS Vertical Fin First Bending Mode



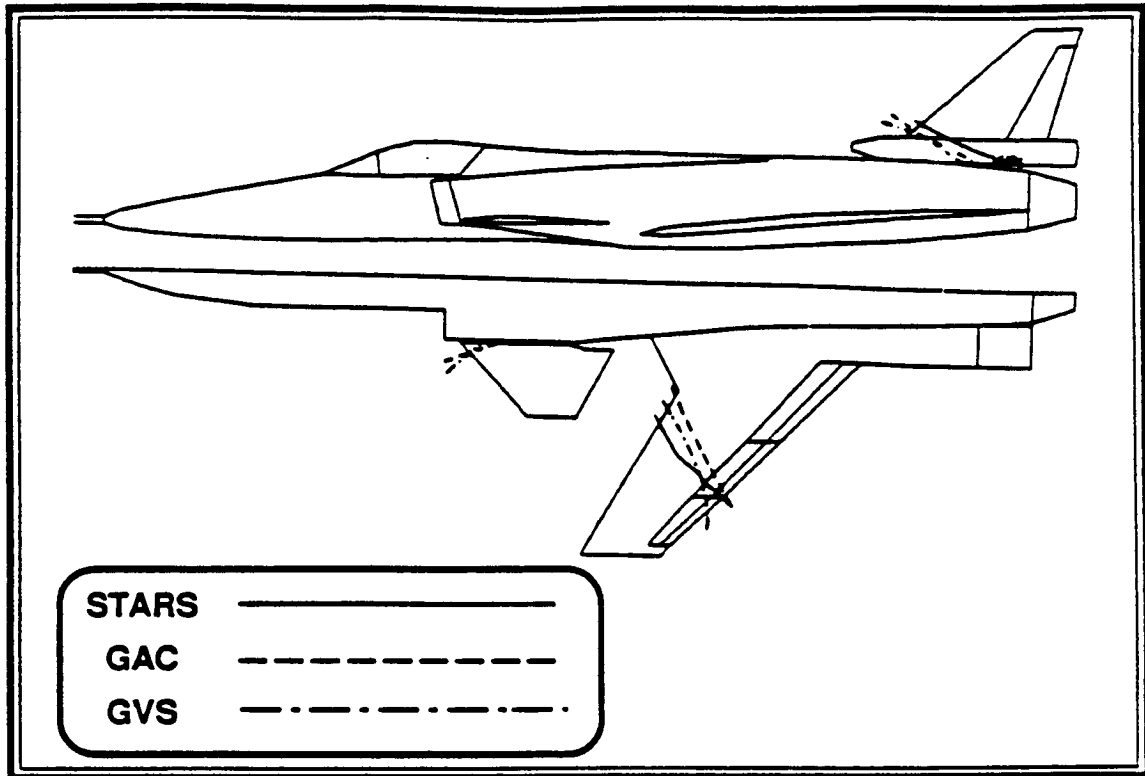


Figure B.2.1A-4 Vertical Fin First Bending Node Lines

### B.2.2 Canard Pitch (CP)

Excellent agreement exists, in general, among all three sources in terms of the natural frequency, the natural mode-shape, and the node lines (Figures - B.2.2A-1 through B.2.2A-4). The node lines on the wing and the vertical tail measured by the GVS were neglected because of their relatively small amplitude. The generalized mass values determined by the three sources do not agree well.

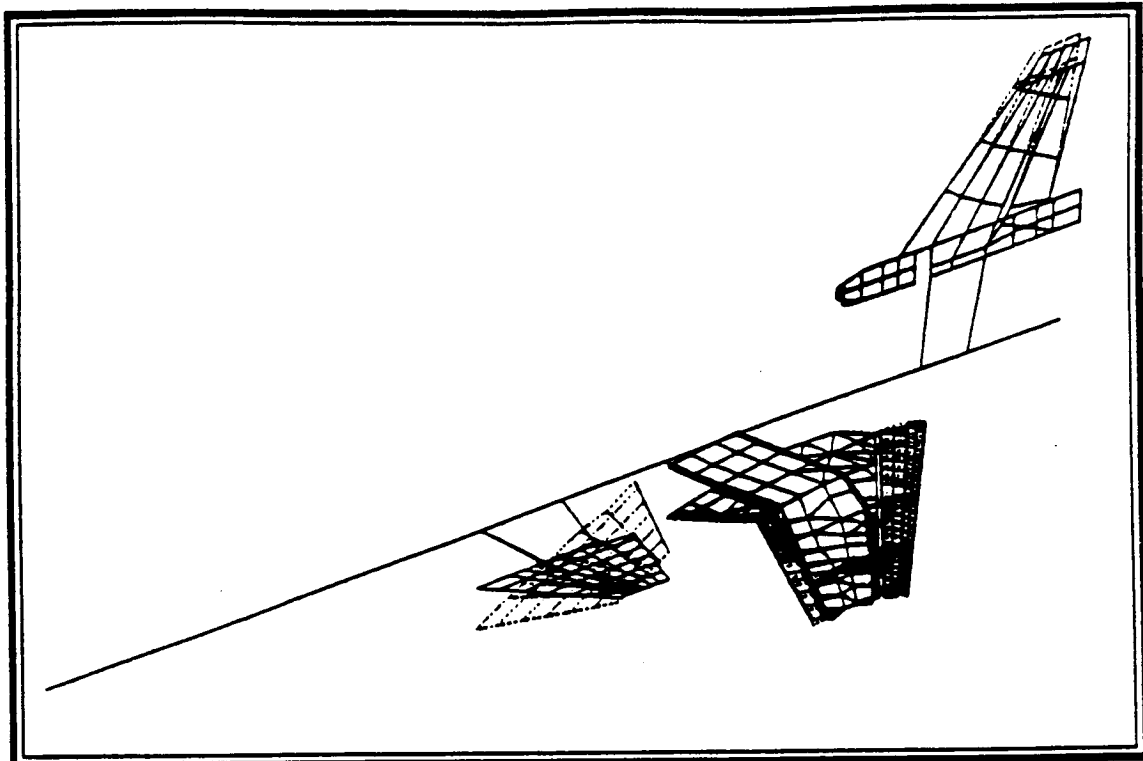


Figure B.2.2A-1 STARS Canard Pitch Mode

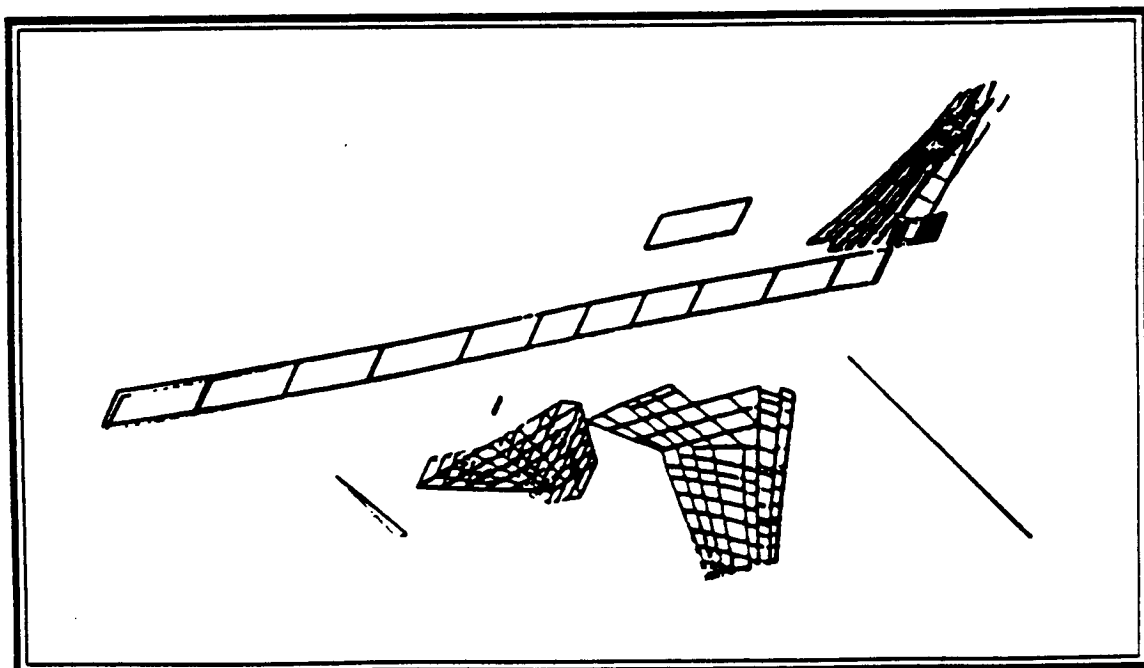


Figure B.2.2A-2 GAC Canard Pitch Mode

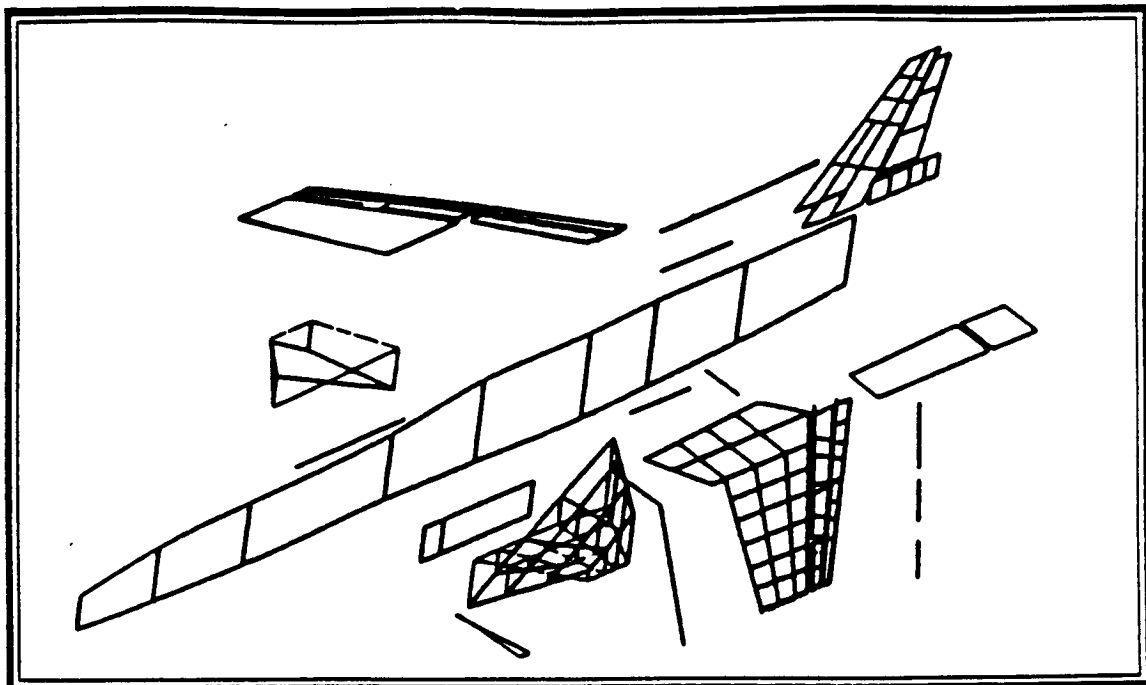


Figure B.2.2A-3 GVS Canard Pitch Mode

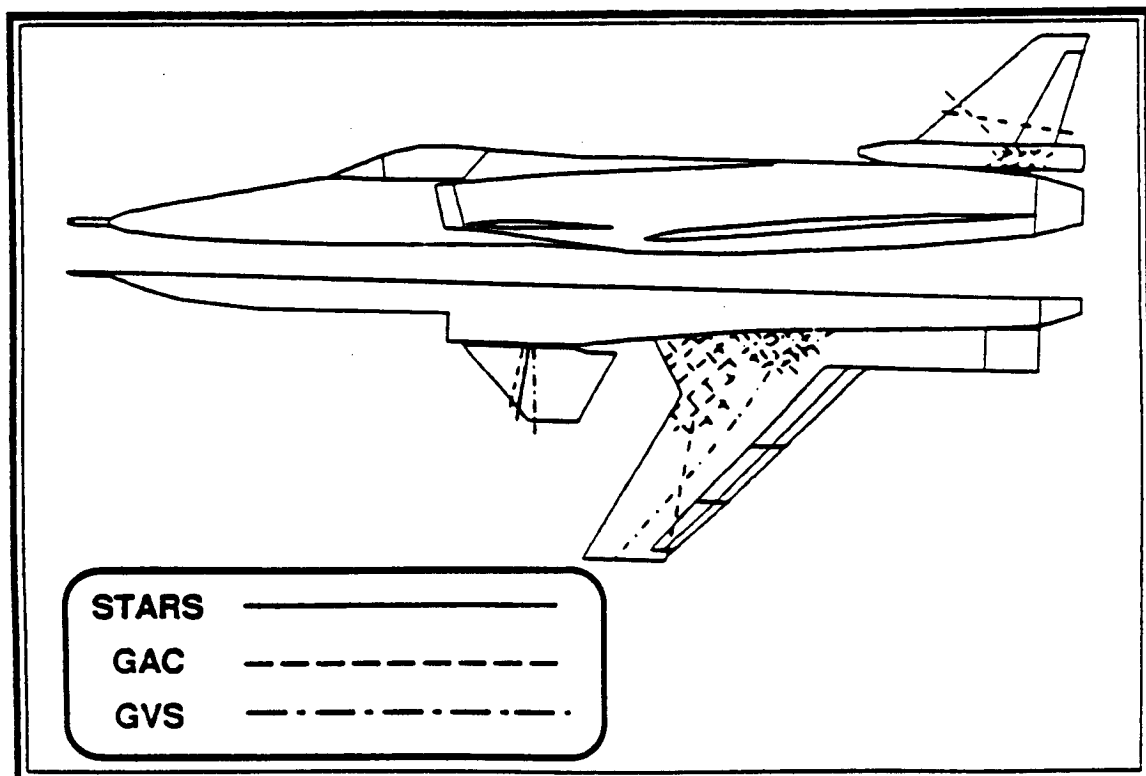


Figure B.2.2A-4 Canard Pitch Node Lines

### B.2.3 Wing First Torsion (W1T)

The natural frequency obtained by the STARS is in good agreement with the GVS value. However, the value obtained by the GAC is on the low side. The generalized mass and the natural mode-shape (Figures - B.2.3A-1 through B.2.3A-4) calculated by the STARS agree better with those obtained by the GVS than with those calculated by the GAC. The node lines obtained by three sources are not in good agreement.

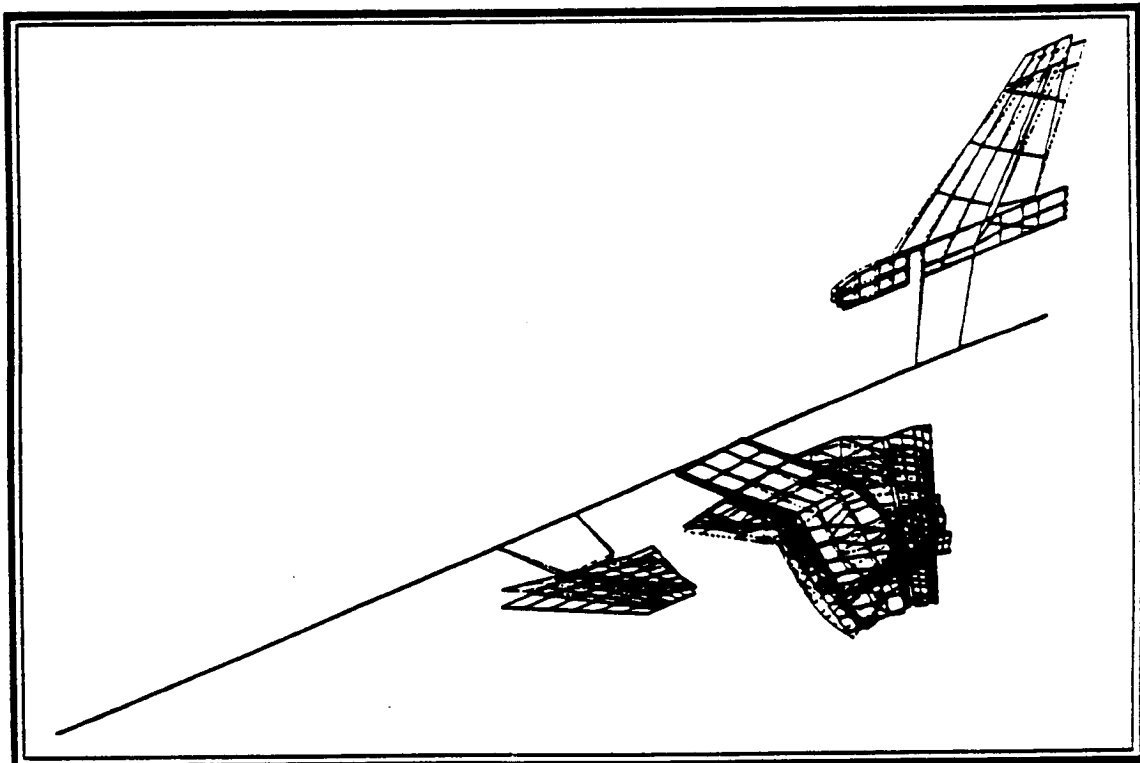


Figure B.2.3A-1 STARS Wing First Torsion Mode

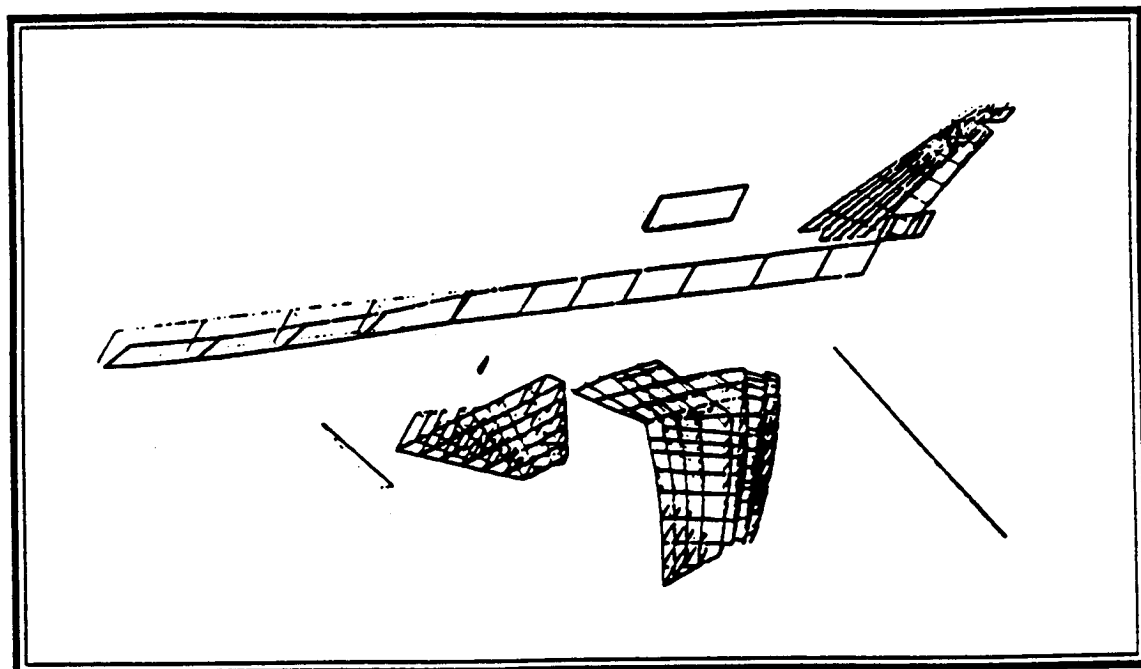


Figure B.2.3A-2 GAC Wing First Torsion Mode

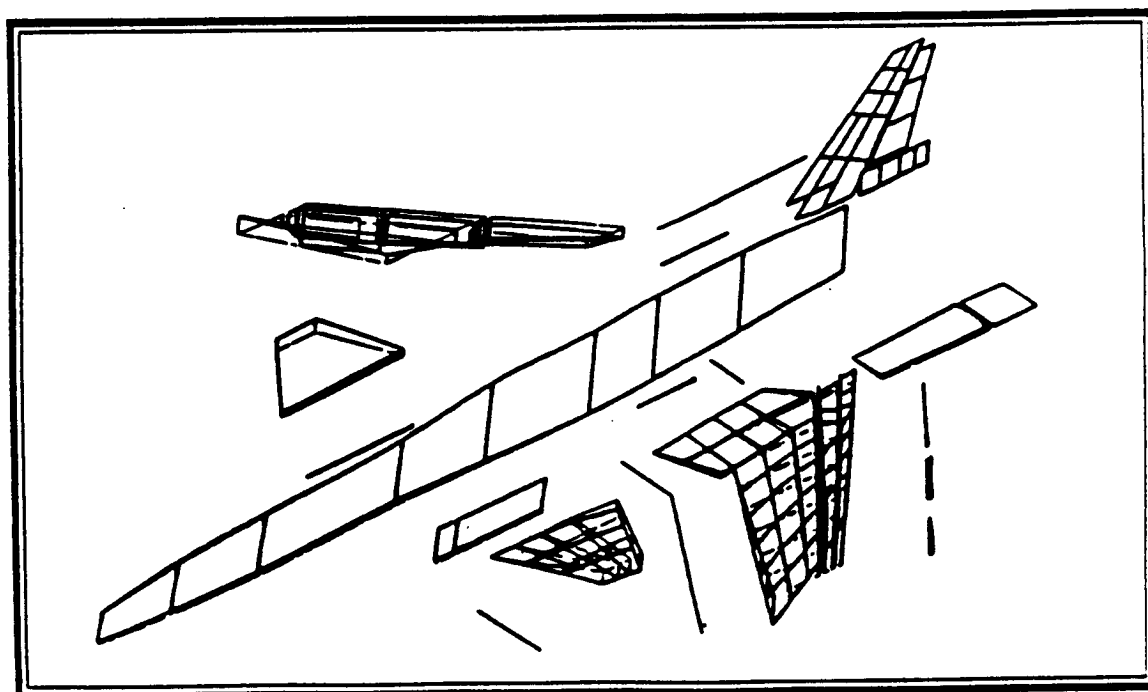


Figure B.2.3A-3 GVS Wing First Torsion Mode

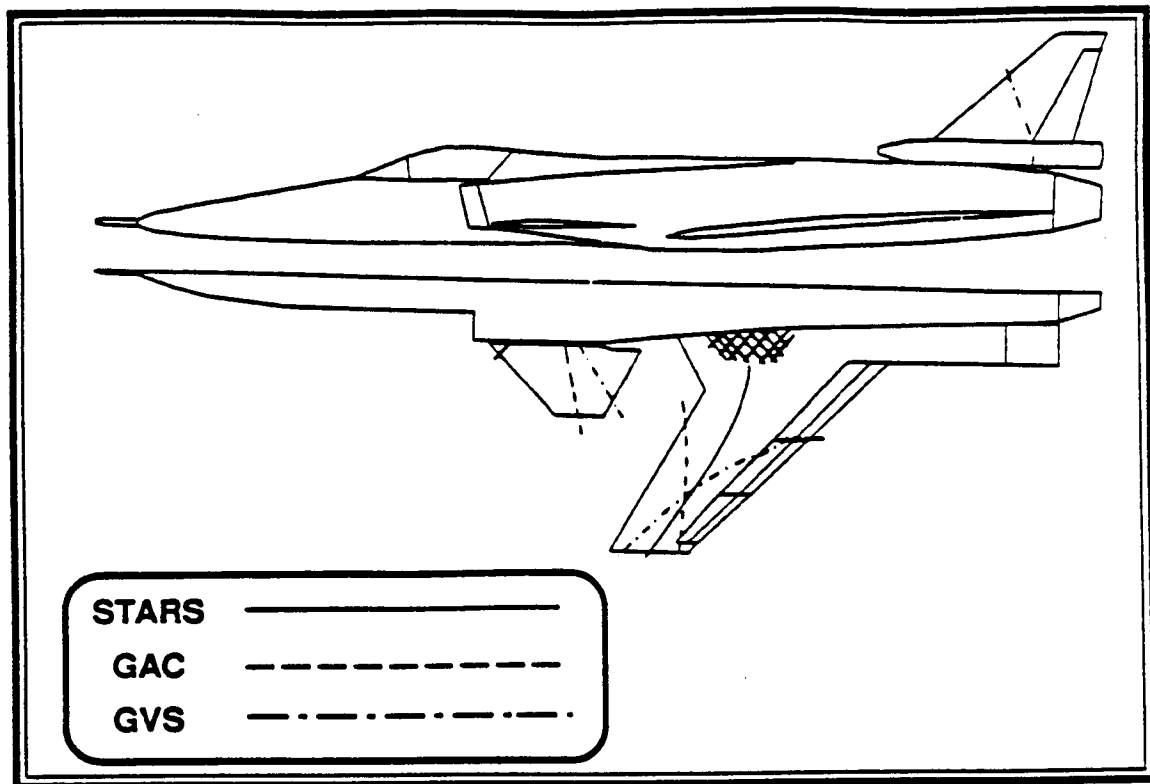


Figure B.2.3A-4 Wing First Torsion Node Lines

#### B.2.4 Wing Second Bending (W2B)

The natural frequencies obtained by the STARS and the GAC agree well with the measured value (STARS: -5.5% ; GAC: +3.3%). There is very good agreement in the generalized mass between the STARS and the GAC. The GAC outer wing natural mode-shape and node lines (Figures - B.2.4A-1 through B.2.4A-4) agree well with those measured by the GVS, but this agreement is not shared by the STARS.

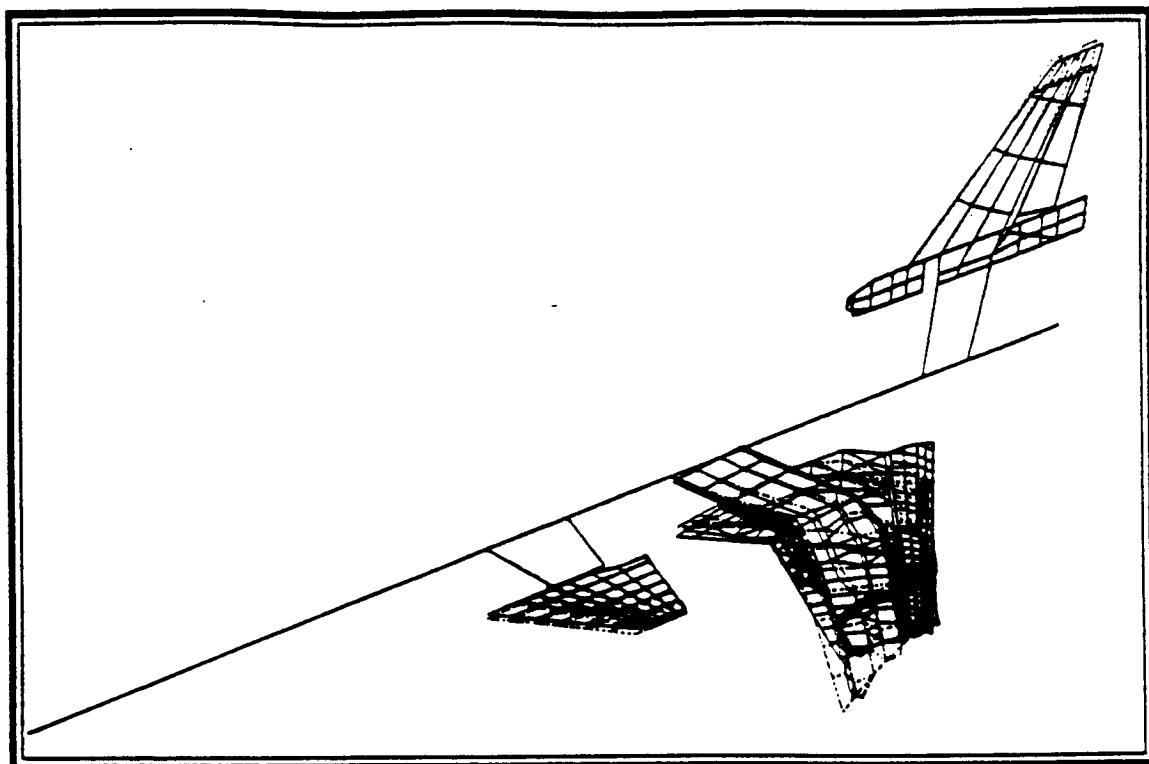


Figure B.2.4A-1 STARS Wing Second Bending Mode

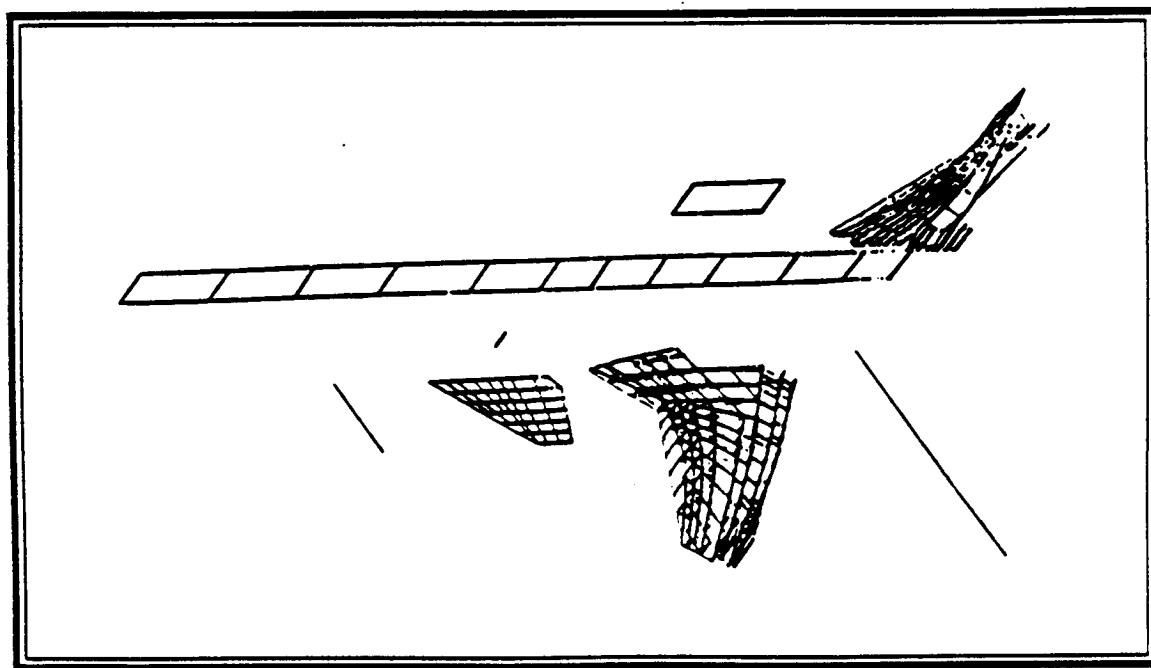


Figure B.2.4A-2 GAC Wing Second Bending Mode

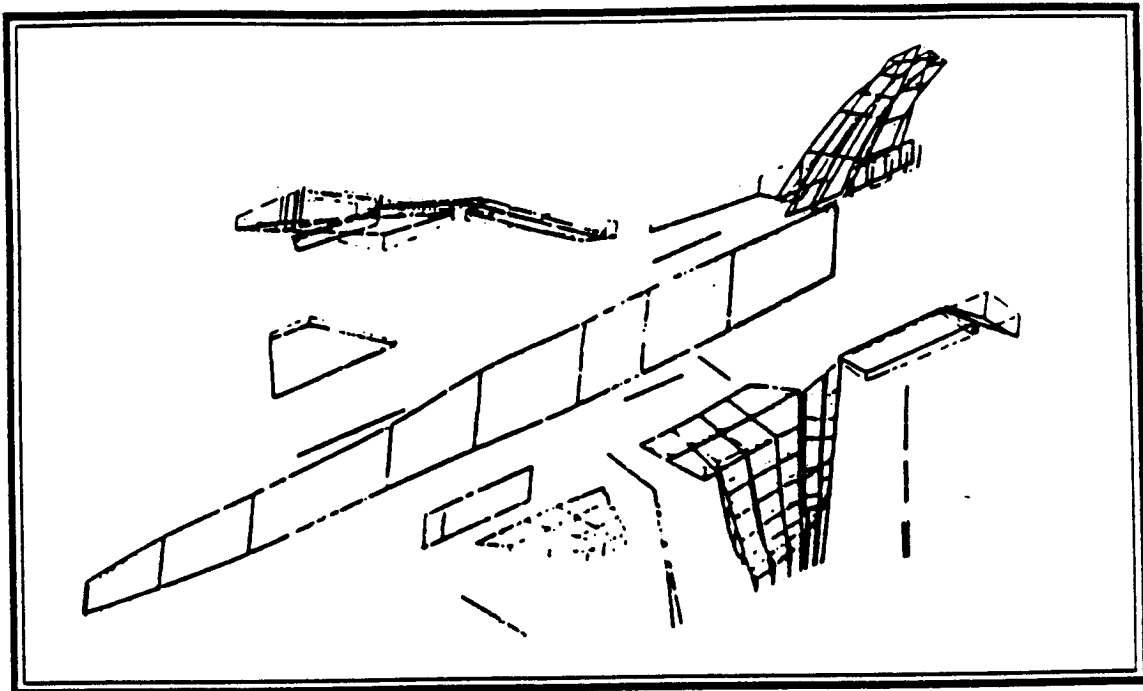


Figure B.2.4A-3 GVS Wing Second Bending Mode

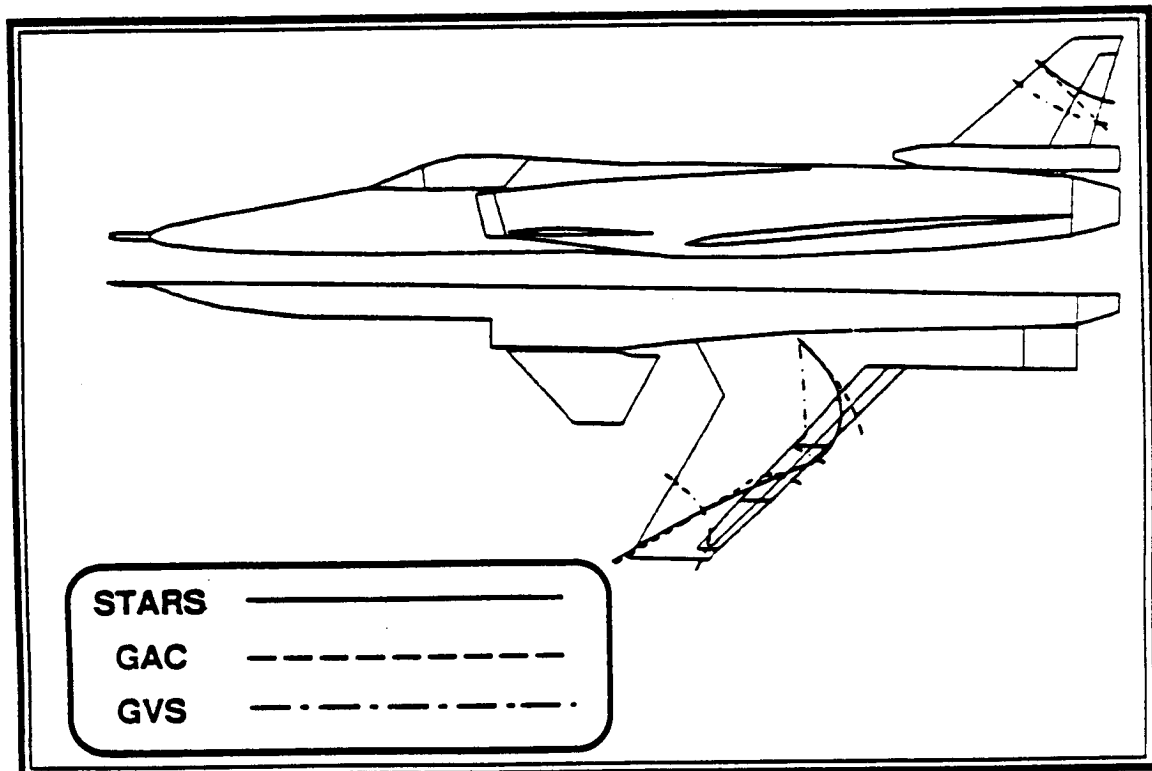


Figure B.2.4A-4 Wing Second Bending Node Lines



### B.2.5 Vertical Fin Second Bending (VF2B)

The STARS natural frequency is 8.0% lower, while the natural frequency measured by the GAC is 11.1% higher than that measured by the GVS. However, another GAC mode, named fin first torsion, shows much better agreement with this GVS mode. The natural mode-shape (Figures - B.2.5A-1 through B.2.5A-4) obtained by the GVS for this mode shows a significant degree of rudder rotation that is not evident in either the STARS or the GAC mode-shapes. The STARS mode-shape shows a classical bending response without rudder rotation coupling.

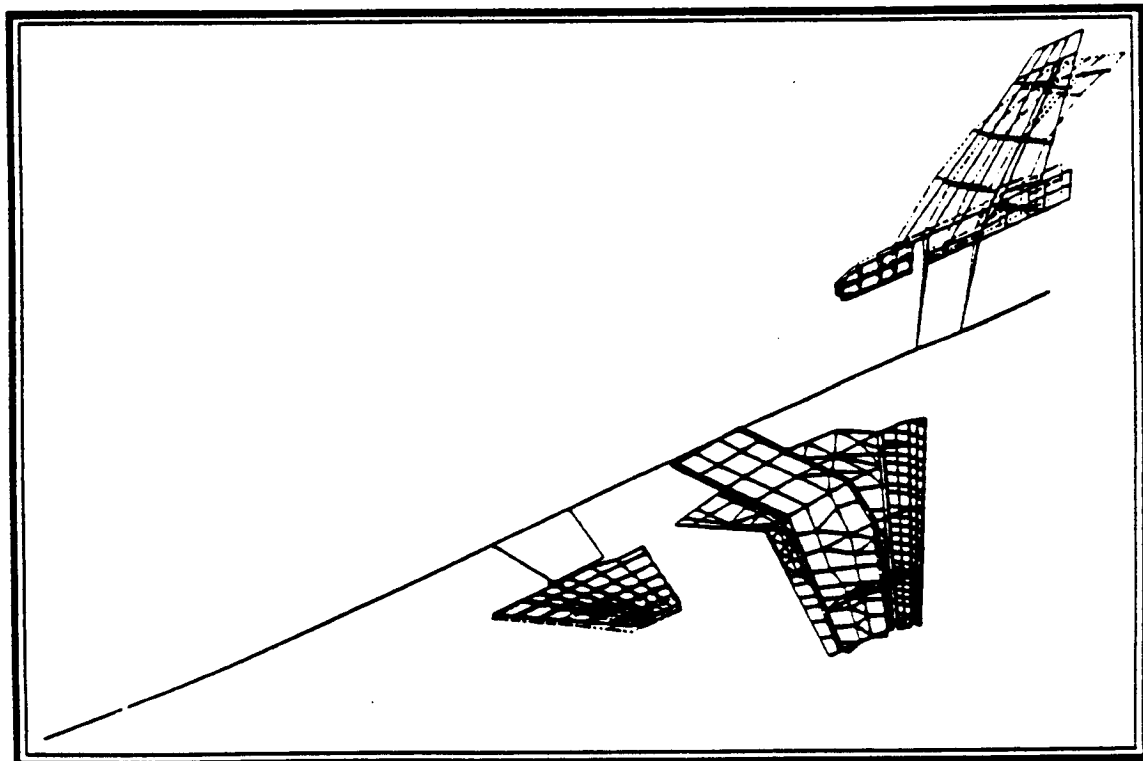
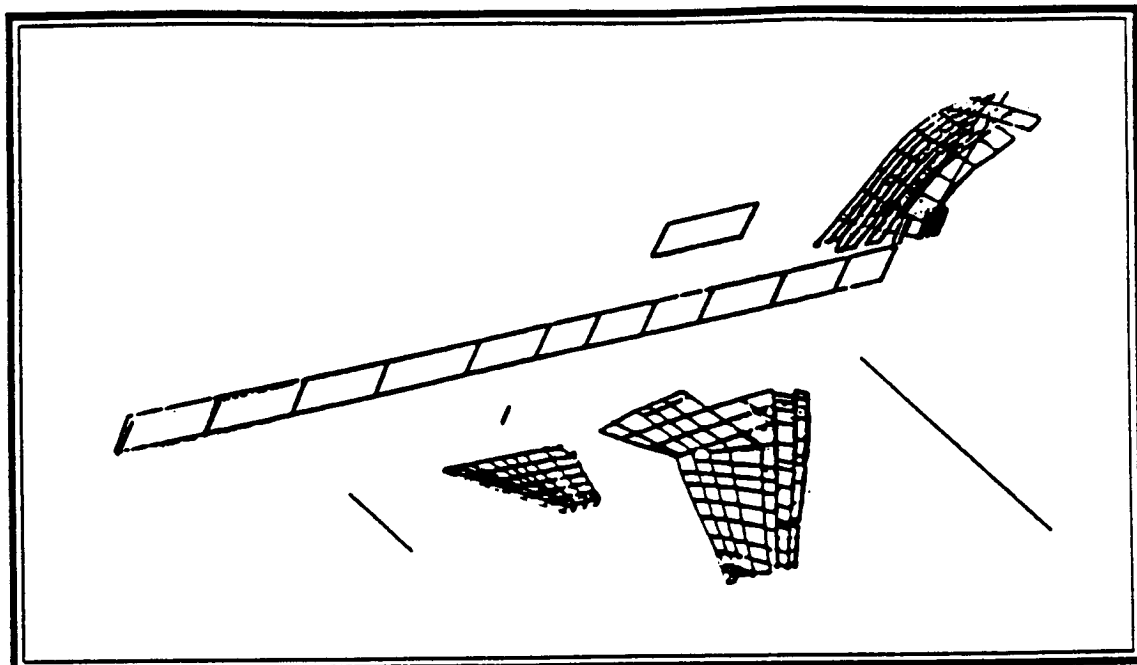
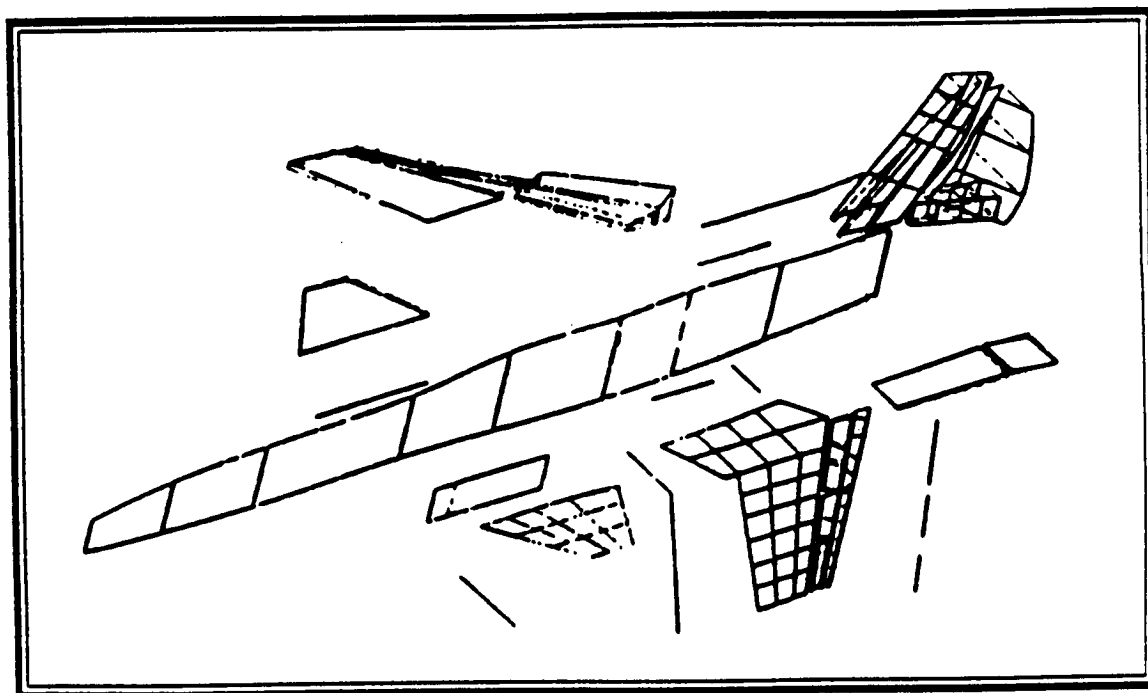


Figure B.2.5A-1 STARS Vertical Fin Second Bending Mode



**Figure B.2.5A-2** GAC Vertical Fin Second Bending Mode



**Figure B.2.5A-3** GVS Vertical Fin Second Bending Mode

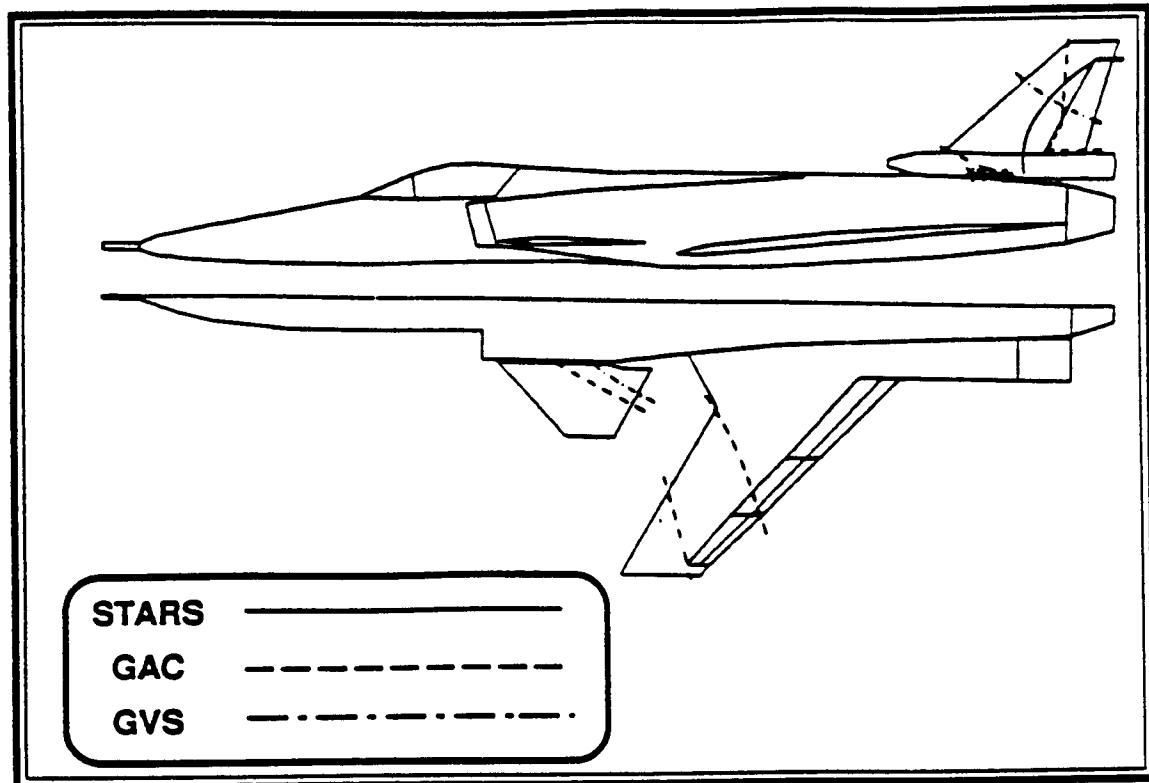


Figure B.2.5A-4 Vertical Fin Second Bending Node Lines

### B.2.6 Wing Third Bending (W3B)

The STARS natural frequency is 11.3% lower, and that obtained by the GAC is 2.1% higher than the GVS natural frequency. The node lines for the STARS and the GVS do not agree well. The natural mode-shape (Figures - B.2.6A-1 through B.2.6A-3) obtained by the STARS is that of the classical wing third bending, but the GVS natural mode-shape is more like that of a combined wing torsion and flaperon rotation. The GAC generalized mass, natural mode-shape, and node lines were not available.

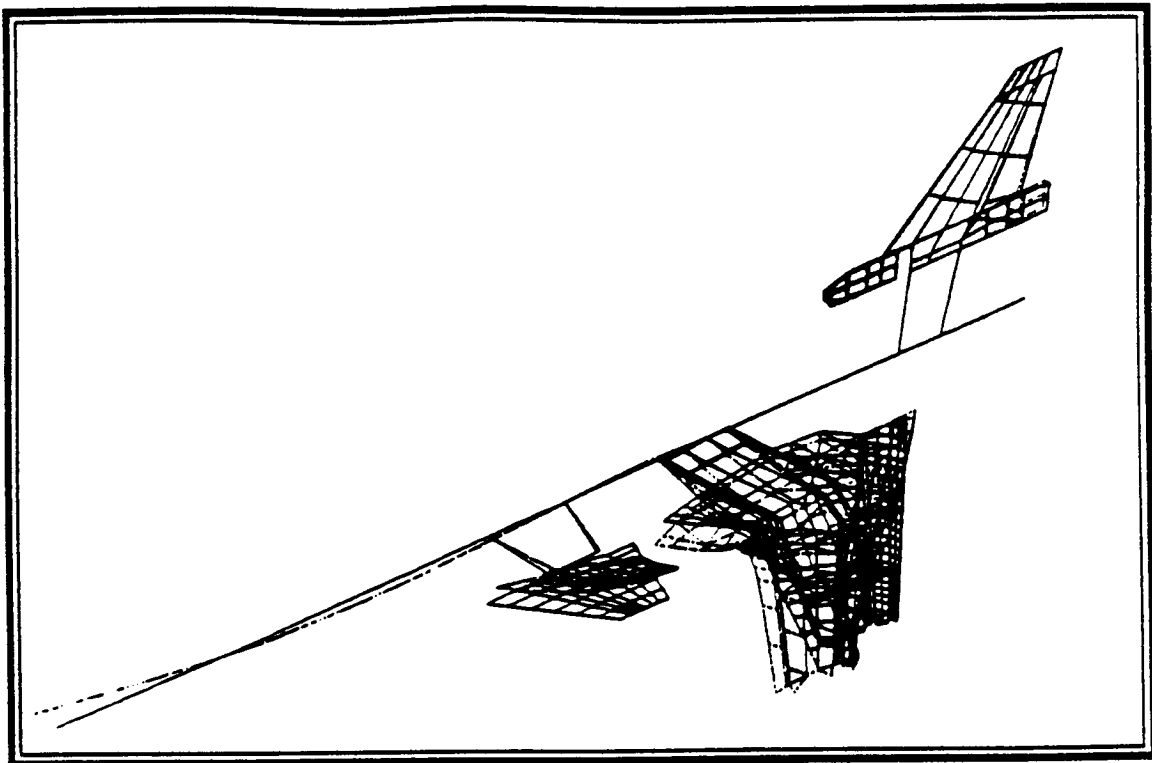


Figure B.2.6A-1 STARS Wing Third Bending Mode

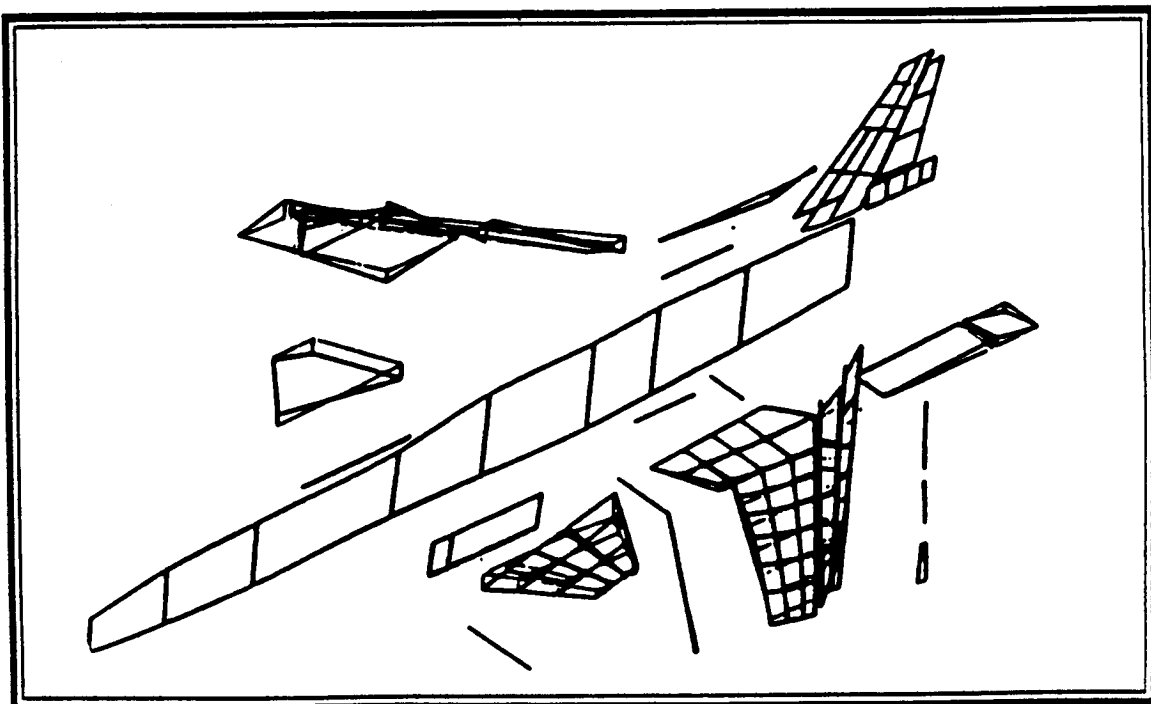


Figure B.2.6A-2 GVS Wing Third Bending Mode

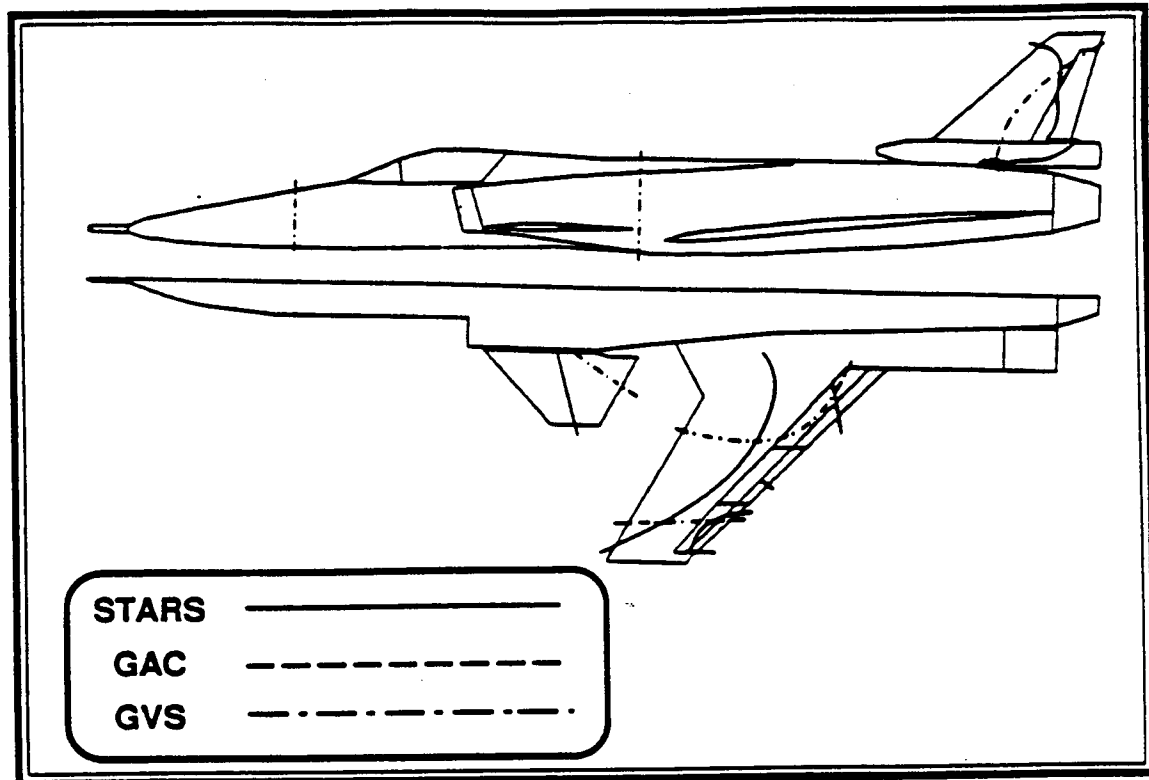
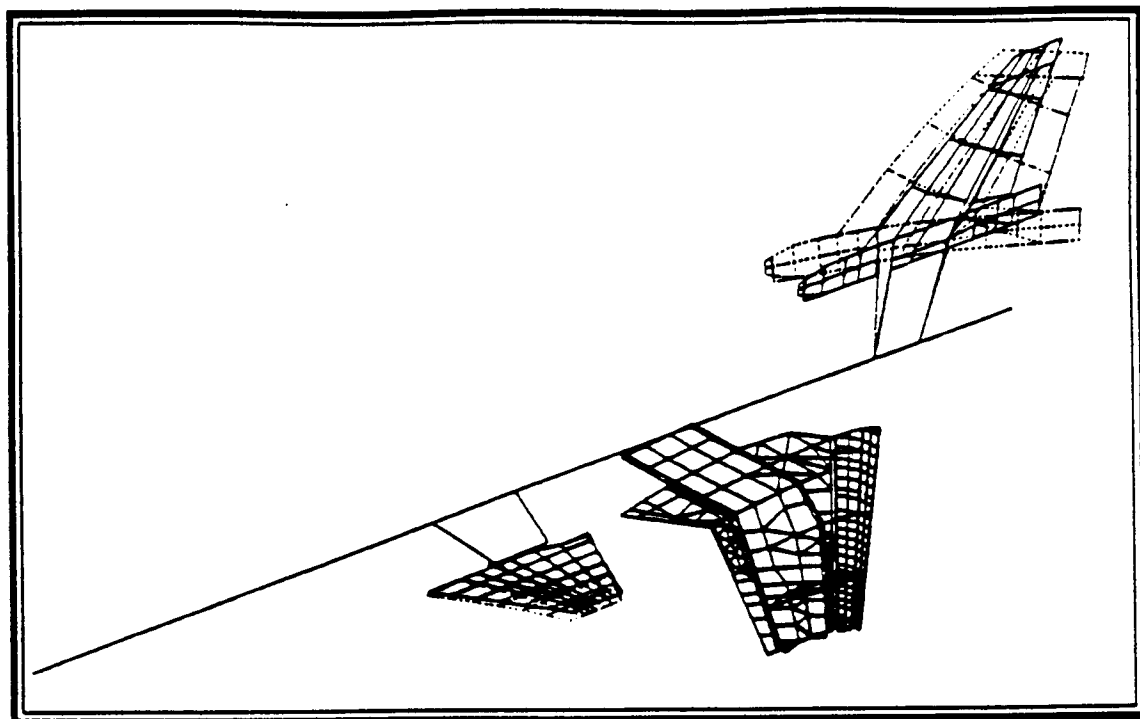


Figure B.2.6A-3 Wing Third Bending Node Lines

### B.2.7 Vertical Fin First Torsion (VF1T)

The STARS natural frequency is 2.1% lower, and the natural frequency obtained by the GAC is 11.8% lower than the GVS value. There is good agreement in the natural mode-shape and node lines (Figures - B.2.7A-1 through B.2.7A-4) among the three sources.



**Figure B.2.7A-1** STARS Vertical Fin First Torsion Mode

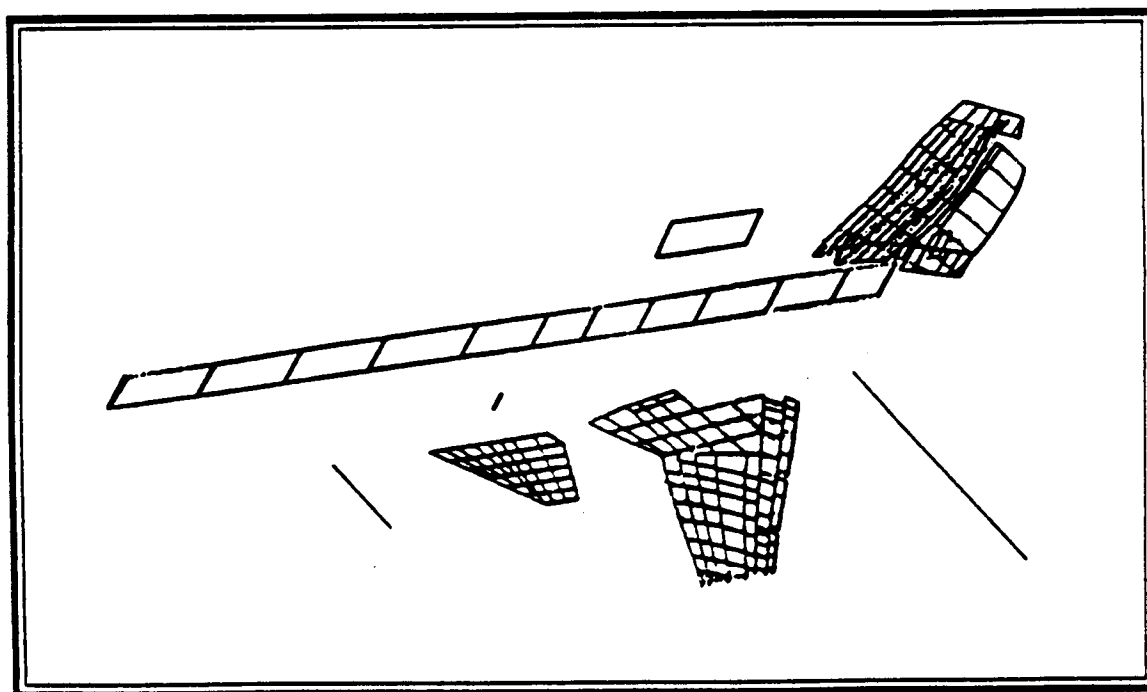


**Figure B.2.7A-2** GAC Vertical Fin First Torsion Mode

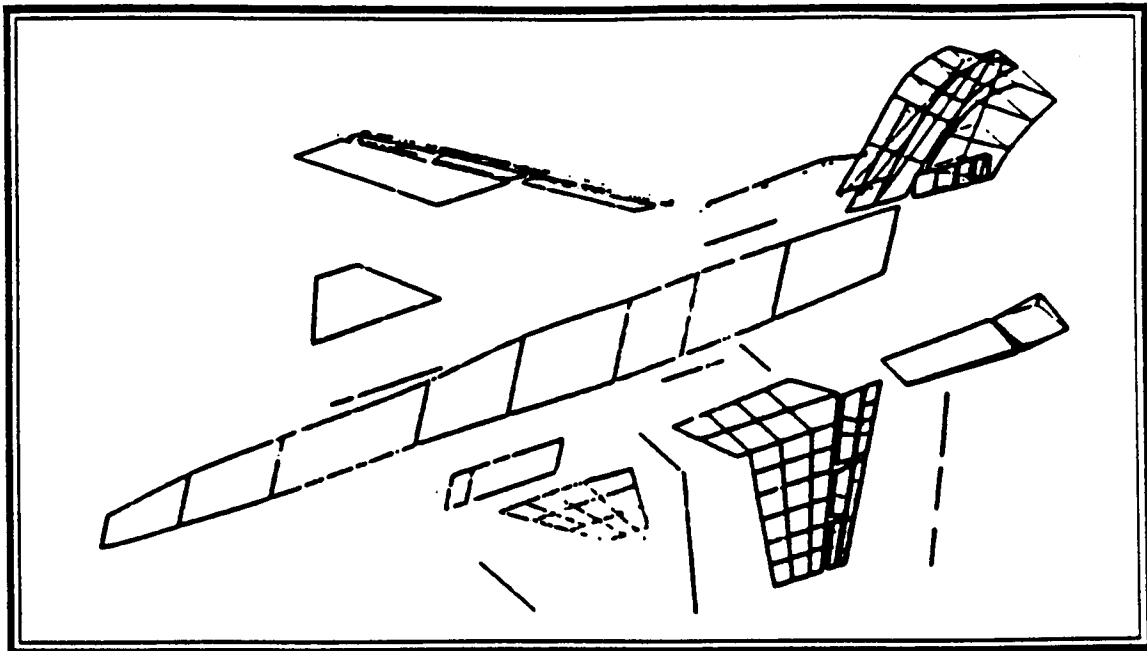


Figure B.2.7A-3 GVS Vertical Fin First Torsion Mode

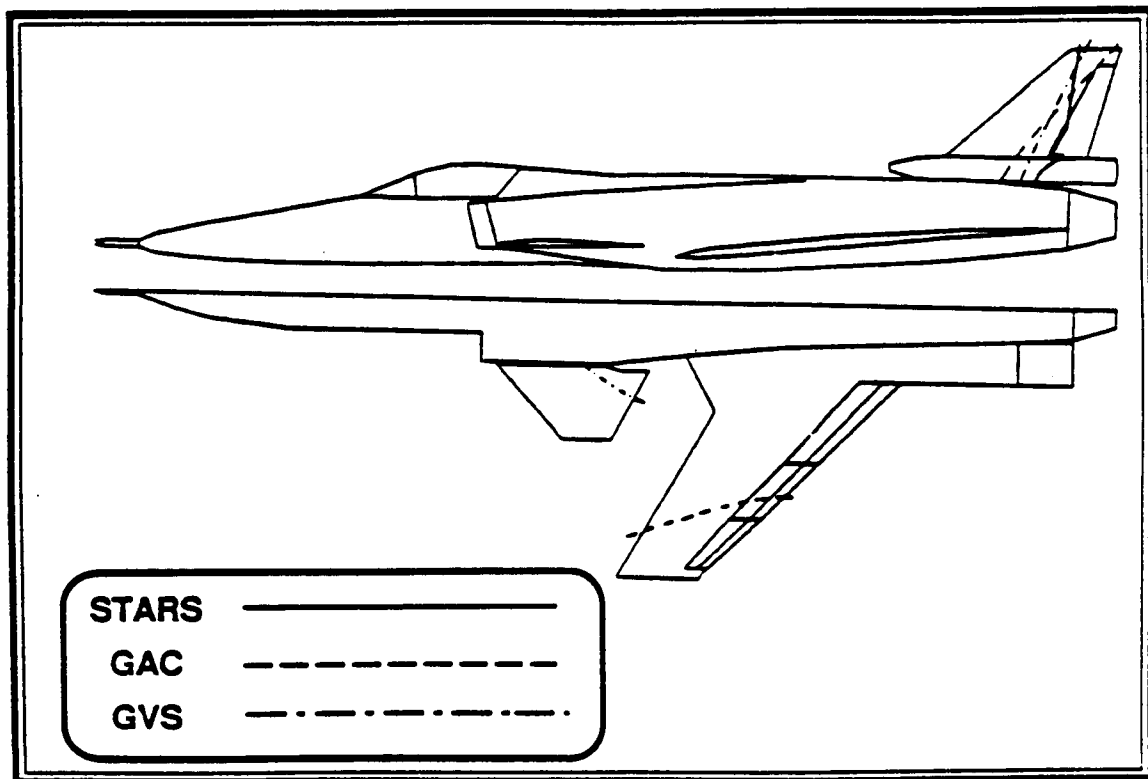


Figure B.2.7A-4 Vertical Fin First Torsion Node Lines

### B.2.8 Inboard Flap Torsion (IFT)

The STARS natural frequency agrees well with the measured value ( $-0.3\%$ ), but the natural frequency obtained by the GAC is on the high side ( $+17.6\%$ ). The STARS natural mode-shape and node lines (Figures - B.2.8A-1 through B.2.8A-3) do not agree well with the GVS results. The GAC generalized mass, natural mode-shape, and node lines were not available.

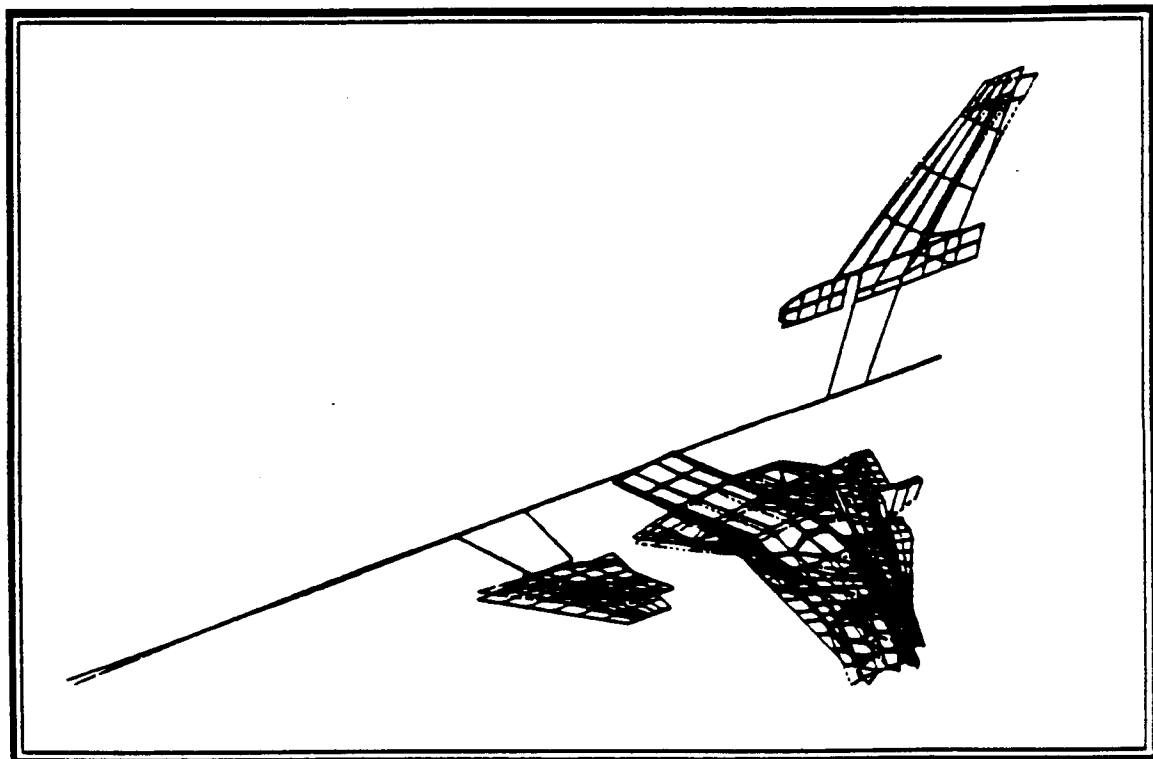


Figure B.2.8A-1 STARS Inboard Flap Torsion Mode



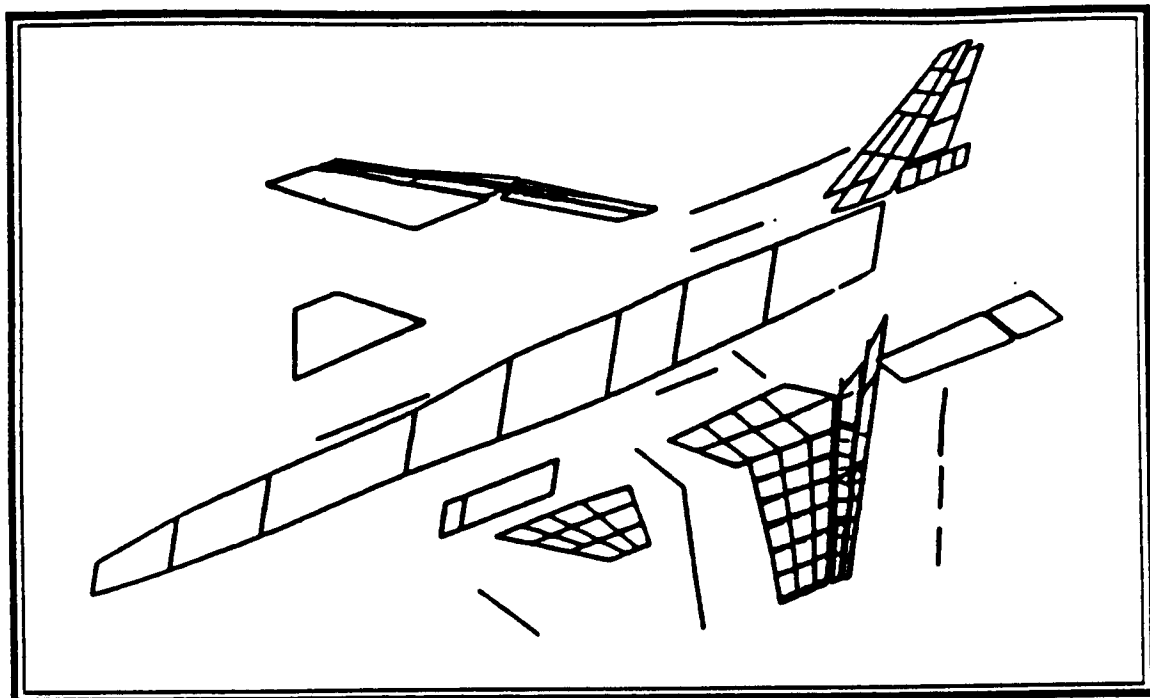


Figure B.2.8A-2 GVS Inboard Flap Torsion Mode

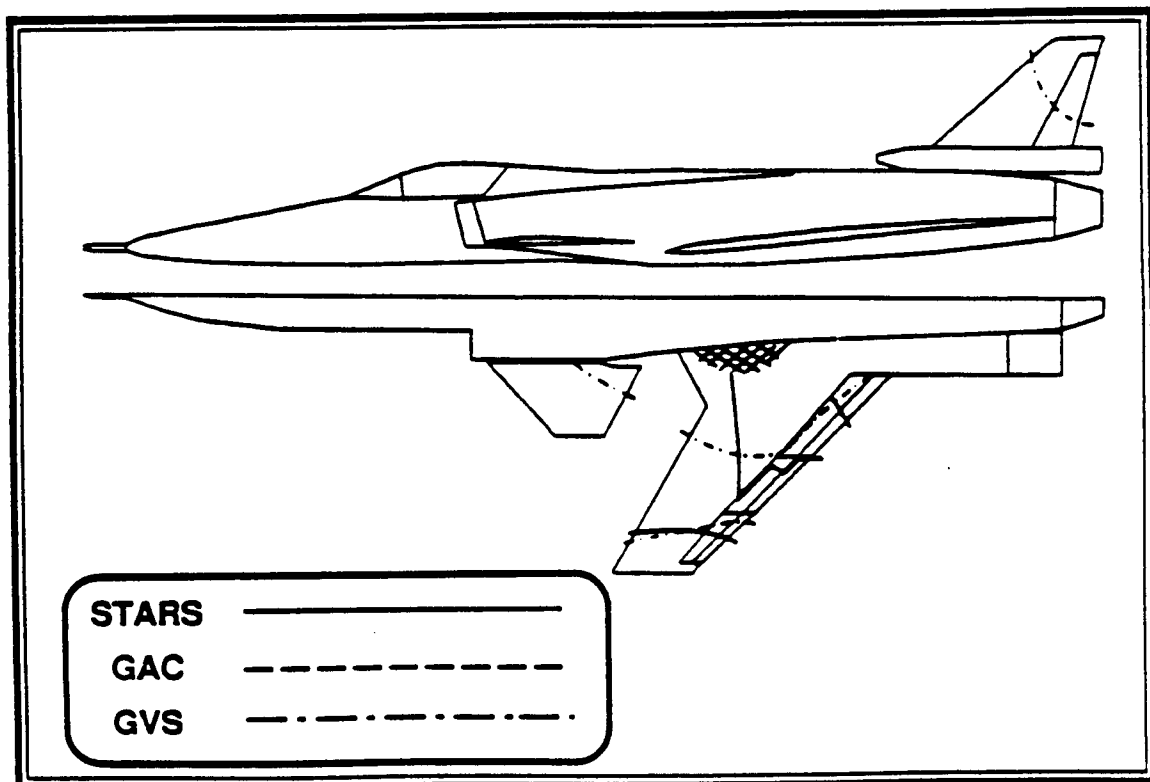


Figure B.2.8A-3 Inboard Flap Torsion Node Lines

## ***REFERENCES***

- 1) Krone, N. S. Jr., "Divergence Elimination With Advanced Composites," AIAA paper 75-1009, August 1975 .
- 2) X-29A SYMPOSIUM, "Initial Flight Results," NASA-Ames Research Center, Dryden Flight Research Center, September 17-19, 1985.
- 3) Moore, M., Feri, D., "X-29 FSW Aerodynamic Overview," AIAA paper 83-1834, July 1983 .
- 4) Pearcey, H. H., "Shock-Induced Separation and Its Prevention by Design and Boundary Layer Control," Boundary Layer and Flow control, Vol. 2, G. V. Lachman, ed., Pergamon Press, 1961, pp. 1166-1344.
- 5) Grafron, S. B., Gilbert, W. P., "High-Angle-of-Attack Characteristics of FSW Fighter Configurations," AIAA paper 82-1322, August 1982.

- 6) Gupta, K. K., "STARS - A General Purpose Finite Element Computer Program for Analysis of Engineering Structures," NASA Reference Publication 1129, October 1984.
- 7) Gupta, K. K., "Development of a Unified Numerical Procedure for Free Vibration Analysis of Structures," Int. J. Numerical Methods in Engineering, Vol.17, pp. 187-198, 1981.
- 8) Hassig, H. J., "An Approximate True Damping Solution of the Flutter Equation by Determinant Iteration," Journal of Aircraft, Vol. 8, No. 11, November 1971.
- 9) GIESING, J. P., KALMAN, T. P., RODDEN, W. P., "Subsonic Unsteady Aerodynamics for General Configuration," Part 1, Vol. 1, Air Force: 17-12 71/150.
- 10) Wilkinson, J. H., "The Algebraic Eigenvalue Problem," Clarendon Press, Oxford, pp. 515-568, 1965.
- 11) Wilkinson, K., "An Automated Procedure for Flutter and Strength Analysis and Optimization of Aerospace Vehicles," AFFDL-TR-75-137, Vols. I and II, December 1975.
- 12) Brockman, R. A., "Modification of the Structural Optimization Code in FASTOP," UDR-TR-77-51, University of Dayton Research Institute, Dayton, Ohio, September 1977.
- 13) Brockman, R. A., "Automated Conversion of NASTRAN Finite Element Data for the FASTOP Program," UDRI-TM-77-02, University of Dayton Research Institute, Dayton, Ohio, March 1977.

- 14) Brockman, R. A., "Modification of the Flutter Optimization Code in FASTOP," UDR-TR-77-60, University of Dayton Research Institute, Dayton, Ohio, October 1977.
- 15) Markowitz, J., & Isackson, G., "FASTOP-3: A Strength, Deflection, and Flutter Optimization Program for Metallic and Composite Structure," AFWAL-tr-78-50, Vols. I and II, May 1978.
- 16) Taylor, R. F., Miller, K. L., and Brockman, R. A., "A Procedure for Flutter Analysis of FASTOP-3 Compatible Mathematical Models," AFWAL-tr-81-3063, Vol. I, June, 1981.
- 17) Harris, T. M., "In-House Evaluation of FASTEX," AFWAL-TM-81-131-FIBR, Flight Dynamics Laboratory, Wright-Patterson Air Force, Ohio, July 1981.
- 18) Taylor, R. F., Miller, K. L., and Brockman, R. A., "A Procedure for Flutter Analysis of FASTOP-3 Compatible Mathematical Models," AFWAL-tr-80-3063, Vol. II, May, 1981.
- 19) Taylor, R. F., "Improvements to the FASTEX Flutter Analysis Computer Code," UDR-TR-87-14, University of Dayton Research Institute, Dayton, Ohio, July 1987.
- 20) Freed, N., Carosso, K., Newman, D. "MATHLIB Reference Manual," MATHLIB Version 9.0, HARVEY MUDD College, Jan, 1984.
- 21) Gupta, K. K., "On a Finite Dynamic Element Method for Free Vibration Analysis of Structures," Comput. Meth. Appl. Mech. Eng., 9, 105-120, 1976.

- 22) Przemieniecki, J. S., "Theory of Matrix Structural Analysis," McGraw-Hill, New York, 1968.
- 23) Gupta, K. K., "Numerical Formulation for a Higher Order Plane Finite Dynamic Element," Int. J. Numerical Methods in Engineering, Vol. 20, pp. 1407-1414, 1984.
- 24) Bogen, R., "MACSYMA Reference Manual," Mathlab Group, Massachusetts Institute of Technology, Cambridge, Massachusetts, 1980.